

# **Evaluation of Effects of HRHF Response Spectra on SSCs**

**Revision 3**

**Non-Proprietary**

**December 2017**

**Copyright © 2017**

**Korea Electric Power Corporation &  
Korea Hydro & Nuclear Power Co., Ltd  
All Rights Reserved**

**REVISION HISTORY**

| Revision | Date          | Section(s) or Page(s)                             | Description  |
|----------|---------------|---|--|
| 0        | November 2014 | All   | First Issue  |
| 1        | February 2015 | 1, 5, 17, 19, 24, 55, 111~116                     | The descriptions of HRHF evaluation for EDGB/DFOT room are added.  |
| 2        | February 2017 | Page 1  | The description of FE model identicalness between HRHF and CSDRS seismic analyses is added by the Action Item 3-81_3.7.2_#9.   |
|          |               | Pages 2, 5  | The description of conservativeness regarding derivation of the coherency matrix is deleted, and the descriptions of details considered for HRHF seismic analyses of NI and EDBG/DFOT room are added by the 3.7_3.8 Audit Tracking List_July 6 2016. |
|          |               | Pages 18, 19                                      | The description of design results of RCB internal structures and EDGB are added by the 3.7_3.8 Audit Tracking List_July 6 2016.  |
|          |               | Pages vi, 8, 9, 14, 37~38, 41                     | The descriptions and tables related to V/A and AD/V <sup>2</sup> are deleted by the response to RAI 253-8300, Question 03.07.01-7, Rev.1.  |
|          |               | Pages 11, 94                                      | The detailed description of generating the target PSD and related figure are added and revised by the response to RAI 182-8160, Question 03.07.01-1, Rev.1.  |
|          |               | Page 13   | The expression of equivalent stationary duration is changed and the description of discrete form of the Fourier spectrum is added by the response to RAI 182-8160, Question 03.07.01-3, Rev.2.   |
|          |               | Pages vi, 16, 17, 49~59                           | A table for the soil layers and the properties used in the HRHF SSI model is added with its description by the response to RAI 182-8160, Question 03.07.01-4, Rev.1.   |
|          |               | Pages vi, 43~46                                   | Tables for the numerical values of the HRHF RS-compatible time histories are added by the response to RAI 182-8160, Question 03.07.01-2, Rev.2.  |
|          |               | Pages viii, 106                                   | The expression "generic" is changed to "low-strain" by the response to RAI 182-8160, Question 03.07.01-4, Rev.1.   |
|          |               | Pages 21~23, 26, 138                              | The descriptions and figure of HRHF evaluation for the safety related equipment are added by the response to RAI 344-8407, Question 03.10-7 and 9.   |
|          |               | Pages vi, 69                                      | Table 6-9 is changed to summarize potentially HF sensitive components by the response to RAI 344-8407, Question 03.10-8.   |
| 3        | December 2017 | Pages 7, 11, 20                                   | The editorial errors are corrected to clearly describe the sentences by the response to RAI 249-8323, Question 03.08.01-16.  |
|          |               | Page 13   | The equation and equation number are corrected to incorporate the response to RAI 182-8160, Question 03.07.01-3, Rev.2.  |
|          |               | Page 16   | The descriptions of the site profiles are revised by the response to RAI 252-8299, Question 03.07.02-9, Rev.2.   |
|          |               | Pages v, vi, 17, 18, C1~C230                      | The descriptions, tables, and figures related to the additional incoherence SSI analyses performed by the response to RAI 183-8197, Question 03.07.02-1, Rev.1.  |
|          |               | Pages v, vii, viii, xi, 19~23, 25, 70~77, 146~150 | The detailed descriptions, tables, and figures for HRHF evaluations of piping systems in accordance with the scope of the graded approach including ASME Class 1 and 2 piping are added by the response to RAI 311-8278, Question 03.12-9, Rev.2.    |

This document was prepared for the design certification application to the U.S. Nuclear Regulatory Commission and contains technological information that constitutes intellectual property of Korea Hydro & Nuclear Power Co., Ltd. Copying, using, or distributing the information in this document in whole or in part is permitted only to the U.S. Nuclear Regulatory Commission and its contractors for the purpose of reviewing design certification application materials. Other uses are strictly prohibited without the written permission of Korea Electric Power Corporation and Korea Hydro & Nuclear Power Co., Ltd.

## **ABSTRACT**

This technical report summarizes the methodology and results of the evaluation for the effects of hard rock high frequency (HRHF) input ground motion on structures, systems, and components (SSCs) of the APR1400 standard plant.

The seismic analysis and design of the APR1400 standard plant are based on certified seismic design response spectra. The spectra are based on U.S. Nuclear Regulatory Commission (NRC) Regulatory Guide 1.60 with an enhancement in the high frequency range. However, many of the envelope response spectra of the central and eastern United States rock sites show higher amplitudes at higher frequencies than the certified seismic design response spectra. Response spectra with these characteristics are referred to as HRHF ground motion response spectra.

Based on the 2011 EPRI report "Evaluation of Seismic Hazard at Central and Eastern US Nuclear Power Plant Sites", the APR1400 HRHF response spectra are determined as the 0.8-fractile, 5%-damped, horizontal composite envelope ground motion response spectra for central and eastern United States hard rock sites. The APR1400 HRHF response spectra exceed the certified seismic design response spectra for frequencies above approximately 10 Hz. However, in general, as presented in EPRI Draft White Paper, "Considerations for NPP Equipment and Structures Subjected to Response Levels Caused by High Frequency Ground Motions", the high frequency input ground motion is regarded as non-damaging.

Confirmation of nondamage from high frequency seismic input motion is needed for the APR1400 structures and equipment qualified by seismic analyses for the design-basis certified seismic design response spectra. The building structures, reactor pressure vessel and internals, primary component supports, primary loop nozzles, piping, and equipment are included in the evaluation of the APR1400 standard plant for HRHF seismic responses to demonstrate that the seismic responses of the SSCs to the high frequency input ground motion are non-damaging. In the evaluation, effects of spatial incoherence of ground motion on the seismic responses of the structures due to the high frequency input ground motion are considered.



## **TABLE OF CONTENTS**

|          |   |           |
|----------|---|-----------|
| <b>1</b> | <b>INTRODUCTION .....</b>   | <b>1</b>  |
| <b>2</b> | <b>INCOHERENT SSI ANALYSIS METHODOLOGY AND PROCEDURE .....</b>                  | <b>2</b>  |
| 2.1      | Analysis Methodology .....  | 2         |
| 2.2      | Site Response Analysis .....  | 4         |
| 2.3      | SSI Analysis .....  | 4         |
| <b>3</b> | <b>SEISMIC INPUT .....</b>  | <b>6</b>  |
| 3.1      | EPRI GMRS for CEUS Rock Sites .....   | 6         |
| 3.2      | HRHF Response Spectra for APR1400 .....   | 6         |
| 3.3      | Generation of HRHF Response-spectrum-compatible Time Histories .....            | 7         |
| 3.3.1    | Ground Motion Time Histories .....  | 7         |
| 3.3.2    | Response Spectrum and Power Spectral Density Enveloping Requirements .....      | 8         |
| 3.3.3    | Selection of Initial Seed Motion Time Histories .....                           | 8         |
| 3.4      | Method for Generation Spectrum-compatible Time Histories .....                  | 9         |
| 3.4.1    | Analytical Background .....   | 10        |
| 3.4.2    | Analytical Procedure .....  | 10        |
| 3.5      | Developing HRHF Response Spectrum-compatible PSDs .....                         | 11        |
| 3.5.1    | HRHF Response Spectrum-compatible Target PSDs .....                             | 11        |
| 3.5.2    | Minimum Required Target PSDs .....  | 12        |
| 3.5.3    | Calculation of Time History PSDs .....  | 12        |
| 3.6      | Generation Results .....  | 13        |
| <b>4</b> | <b>GROUND MOTION COHERENCY FUNCTIONS.....</b>                                   | <b>15</b> |
| <b>5</b> | <b>ANALYSIS RESULTS .....</b>   | <b>16</b> |
| 5.1      | Site Response Analysis .....  | 16        |
| 5.2      | INCOH Analysis Results .....  | 16        |
| 5.3      | SSI Analysis .....  | 17        |
| 5.4      | Comparison of Incoherent-motion SSI Analysis Results Using 7 and 12 Modes ..... | 17        |
| 5.5      | Comparison of ISRS Based on CSDRS and HRHF Response Spectra .....               | 17        |
| 5.6      | Convergence of Coherency Mode Expansion .....                                   | 17        |
| <b>6</b> | <b>EVALUATION .....</b>   | <b>19</b> |
| 6.1      | Building Structures .....   | 19        |
| 6.2      | Reactor Coolant System .....  | 20        |
| 6.2.1    | Reactor Vessel Internals and Core .....   | 20        |
| 6.2.2    | RCS Component Supports, Nozzles, and Loop Pipings .....                         | 21        |
| 6.3      | Piping Systems .....  | 21        |

|  |   |           |
|--|---|-----------|
| 6.4  | Safety-related Equipment .....                      | 22        |
| 6.4.1  | Evaluation Process Steps and Description .....      | 23        |
| 6.4.1.1  | Potentially High-frequency Sensitive Equipment..... | 23        |
| 6.4.1.1.1  | Use of Existing Qualification Data .....            | 23        |
| 6.4.1.1.2  | Screening Test .....                                | 24        |
| 6.4.1.2  | Items Not Potentially HF Sensitive .....            | 24        |
| <b>7</b>   | <b>CONCLUSION .....</b>                             | <b>25</b> |
| <b>8</b>   | <b>REFERENCES .....</b>                             | <b>26</b> |
| <b>APPENDIX A APR1400 HRHF RESPONSE SPECTRA FOR 2, 3, 4, 5, 7, AND 10%<br/>DAMPING RATIOS.....</b>   |   | <b>A1</b> |
| <b>APPENDIX B COMPARISON OF INCOHERENT-MOTION SSI ANALYSIS RESULTS<br/>USING 7 AND 12 MODES.....</b> |   | <b>B1</b> |
| <b>APPENDIX C INVESTIGATION OF SPATIAL COHERENCY MODE EXPANSION<br/>CONVERGENCE.....</b>             |   | <b>C1</b> |

**LIST OF TABLES**

|            |  |    |
|------------|--|----|
| Table 2-1  | Shear-modulus-degradation and Damping-value Variation Curves for Rock Considered for HRHF .....                  | 29 |
| Table 3-1  | 5%-damped HRHF Horizontal Target Response Spectrum .....   | 30 |
| Table 3-2  | 5%-damped HRHF Vertical Target Response Spectrum .....   | 32 |
| Table 3-3  | V/H Ratios for CEUS Rock Site Conditions .....   | 34 |
| Table 3-4  | Scale Factors for Horizontal Response Spectra Damping Ratios Relative to 5%-damped Response Spectrum, CEUS ..... | 35 |
| Table 3-5  | Deleted.....   | 38 |
| Table 3-6  | Deleted.....   | 39 |
| Table 3-7  | Target PSD Compatible with APR1400 HRHF Response Spectra – Horizontal .....                                      | 40 |
| Table 3-8  | Target PSD Compatible with APR1400 HRHF Response Spectra – Vertical.....   | 41 |
| Table 3-9  | Deleted.....   | 42 |
| Table 3-10 | Cross-correlation Coefficients of HRHF Response-Spectrum-Compatible Time History Pairs.....                      | 43 |
| Table 3-11 | Stationary Duration of Generated Time Histories .....  | 44 |
| Table 3-12 | Maximum Acceleration (A), Velocity (V), and Displacement (D) of Generated Time Histories .....                   | 45 |
| Table 3-13 | Number of Points of the Response Spectra below each HRHF DRS .....   | 46 |
| Table 3-14 | The Lowest Percentage below the HRHF DRS.....  | 47 |
| Table 4-1  | EPRI (2007) Empirical Plane-Wave Coherency Function for Horizontal Seismic Ground Motions for Hard Rock .....    | 48 |
| Table 4-2  | EPRI (2007) Empirical Plane-Wave Coherency Function for Vertical Seismic Ground Motions for Hard Rock.....       | 49 |
| Table 5-1  | Soil Layers and Properties of SSI Model for HRHF Seismic Input Motions .....                                     | 50 |
| Table 5-2  | INCOH Results - Horizontal.....  | 54 |
| Table 5-3  | INCOH Results - Vertical .....   | 57 |
| Table 5-4  | Frequencies of Analysis – Incoherent.....  | 60 |
| Table 6-1  | Comparison of Design Force and Moment for PSW .....  | 61 |
| Table 6-2  | Comparison of Design Force and Moment for IRWST .....  | 62 |
| Table 6-3  | Comparison of Design Force and Moment for SSW .....  | 63 |
| Table 6-4  | Comparison of Design Force and Moment for Containment Structure .....  | 65 |
| Table 6-5  | Comparison of Equivalent Accelerations for Auxiliary Building .....  | 66 |
| Table 6-6  | Comparison of Equivalent Accelerations for EDGB/DFOT room .....  | 67 |
| Table 6-7  | Comparison of Design Force and Moment for RCS Component Supports.....  | 68 |
| Table 6-8  | Comparison of Design Force and Moment RCS Component Nozzles.....   | 69 |
| Table 6-9  | Comparison of Design Force and Moment for Reactor Coolant System Loop Piping .....                               | 70 |

|            |   |    |
|------------|---|----|
| Table 6-10 | Comparison of Stress Analysis Results for Class 1 Piping Systems..... | 72 |
| Table 6-11 | Comparison of Stress Analysis Results for Class 2 Piping Systems..... | 73 |
| Table 6-12 | Comparison of Design Moment for Surge Line .....                      | 74 |
| Table 6-13 | Potentially HF Sensitive Component .....                              | 77 |

---

## **LIST OF FIGURES**

|             |  |     |
|-------------|--|-----|
| Figure 2-1  | Shear-modulus-degradation and Damping-value Variation Curves for Rock Considered for HRHF .....                                    | 78  |
| Figure 3-1  | 5%-Damped Maximum and Fractile Hard Rock Composite Envelope Spectra Developed for 60 Existing CEUS Nuclear Power Plant Sites.....  | 79  |
| Figure 3-2  | APR1400 HRHF Response Spectrum for 5% Damping Ratio - Horizontal.....  | 80  |
| Figure 3-3  | APR1400 HRHF Response Spectrum for 5% Damping Ratio - Vertical .....   | 81  |
| Figure 3-4  | V/H Response Spectra Ratios (0.2 – 0.5g) .....   | 82  |
| Figure 3-5  | APR1400 HRHF Response Spectra for 2, 3, 4, 5, 7, and 10% Damping Ratios - Horizontal.....  | 83  |
| Figure 3-6  | APR1400 HRHF Response Spectra for 2, 3, 4, 5, 7, and 10% Damping Ratios - Vertical .....   | 84  |
| Figure 3-7  | APR1400 HRHF Response Spectrum vs CSDRS for 5% Damping Ratio - Horizontal.....   | 85  |
| Figure 3-8  | APR1400 HRHF Response Spectrum vs CSDRS for 5% Damping Ratio - Vertical.....   | 86  |
| Figure 3-9  | Recorded Nahanni, Canada, Earthquake at Mackenzie Station #3 – 270 Component Seed Motion .....                                     | 87  |
| Figure 3-10 | Recorded Nahanni, Canada, Earthquake at Mackenzie Station #3 – 360 Component Seed Motion .....                                     | 88  |
| Figure 3-11 | Recorded Nahanni, Canada, Earthquake at Mackenzie Station #3 – VT Component Seed Motion .....                                      | 89  |
| Figure 3-12 | Response Spectra of Nahanni Earthquake Mackenzie Station #3 Recorded Motion Scaled to PGA of 0.46g – 270 Component.....            | 90  |
| Figure 3-13 | Response Spectra of Nahanni Earthquake Mackenzie Station #3 Recorded Motion Scaled to PGA of 0.46g – 360 Component.....            | 91  |
| Figure 3-14 | Response Spectra of Nahanni Earthquake Mackenzie Station #3 Recorded Motion Scaled to PGA of 0.46g – VT Component .....            | 92  |
| Figure 3-15 | Intensity Envelope Function.....   | 93  |
| Figure 3-16 | Comparison of 2%-Damped Ensemble of 30 Time-History Response Spectra and Ensemble-Median Response Spectrum - Horizontal.....       | 94  |
| Figure 3-17 | Comparison of 2%-Damped Ensemble of 30 Time-History Response Spectra and Ensemble-Median Response Spectrum - Vertical.....         | 95  |
| Figure 3-18 | Comparison of 2%-Damped Ensemble of Median Response Spectra and APR1400 HRHF Horizontal Target Response Spectrum - Horizontal..... | 96  |
| Figure 3-19 | Comparison of 2%-Damped Ensemble of Median Response Spectra and APR1400 HRHF Vertical Target Response Spectrum - Vertical.....     | 97  |
| Figure 3-20 | Computed PSDs for the Generated 30 Time History Ensemble - Horizontal.....   | 98  |
| Figure 3-21 | Computed PSDs for the Generated 30 Time History Ensemble - Vertical .....  | 99  |
| Figure 3-22 | Smoothed Ensemble-Mean and Piecewise Log-Log Linear PSD Obtained from the Generated 30 Time History Ensemble - Horizontal .....    | 100 |
| Figure 3-23 | Smoothed Ensemble-Mean and Piecewise Log-Log Linear PSD Obtained from  |     |

|             |  |     |
|-------------|--|-----|
|             | the Generated 30 Time History Ensemble - Vertical.....   | 101 |
| Figure 3-24 | Comparison of the Horizontal Target PSD Compatible with APR1400 HRHF Horizontal Response Spectra with the SRP 3.7.1 PSDs for CEUS Rock Sites ..... | 102 |
| Figure 3-25 | Target and Minimum Required PSDs - Horizontal.....   | 103 |
| Figure 3-26 | Target and Minimum Required PSDs - Vertical .....  | 104 |
| Figure 3-27 | Procedure for Determining Equivalent Stationary Duration.....  | 105 |
| Figure 3-28 | Acceleration, Velocity, and Displacement of H1H.....   | 106 |
| Figure 3-29 | Comparison of Response Spectra of H1H and HRHF Horizontal Target Response Spectra.....   | 107 |
| Figure 3-30 | Acceleration, Velocity, and Displacement of H2H.....   | 108 |
| Figure 3-31 | Comparison of Response Spectra of H2H and HRHF Horizontal Target Response Spectra.....   | 109 |
| Figure 3-32 | Acceleration, Velocity, and Displacement of VTH.....   | 110 |
| Figure 3-33 | Comparison of Response Spectra of VTH and HRHF Vertical Target Response Spectra.....   | 111 |
| Figure 4-1  | Amplitude of Empirical Plane-Wave Spatial-Coherency Function for Horizontal and Vertical Ground Motion Components for Hard Rock .....              | 112 |
| Figure 5-1  | Shear-Wave-Velocity Profile of the Pinyon Flat Array Site .....  | 113 |
| Figure 5-2  | Shear-Wave-Velocity Profiles of APR1400 Low-strain Sites S8 and S9 .....   | 114 |
| Figure 5-3  | Horizontal Site Response Transfer Function for the APR1400 Generic Site Profile S8.....  | 115 |
| Figure 5-4  | Horizontal Site Response Transfer Function for the APR1400 Generic Site Profile S9.....  | 116 |
| Figure 5-5  | Comparison of ISRS Based on CSDRS and HRHF Response Spectra - Containment Structure at El. 78'-0" .....  | 117 |
| Figure 5-6  | Comparison of ISRS Based on CSDRS and HRHF Response Spectra - Containment Structure at El. 160'-0" .....   | 118 |
| Figure 5-7  | Comparison of ISRS Based on CSDRS and HRHF Response Spectra - Containment Structure at El. 332'-0" .....   | 119 |
| Figure 5-8  | Comparison ISRS Based on of CSDRS and HRHF Response Spectra – Primary Shield Wall at El. 78'-0".....   | 120 |
| Figure 5-9  | Comparison of ISRS Based on CSDRS and HRHF Response Spectra – Primary Shield Wall at El. 156'-0".....  | 121 |
| Figure 5-10 | Comparison of ISRS Based on CSDRS and HRHF Response Spectra – Primary Shield Wall at El. 191'-0".....  | 122 |
| Figure 5-11 | Comparison of ISRS Based on CSDRS and HRHF Response Spectra – Secondary Shield Wall at El. 78'-0" .....  | 123 |
| Figure 5-12 | Comparison of ISRS Based on CSDRS and HRHF Response Spectra – Secondary Shield Wall at El. 156'-0" .....   | 124 |
| Figure 5-13 | Comparison of ISRS Based on CSDRS and HRHF Response Spectra – Secondary Shield Wall at El. 191'-0" .....   | 125 |
| Figure 5-14 | Comparison of ISRS Based on CSDRS and HRHF Response Spectra – Auxiliary  |     |

|             |   |     |
|-------------|---|-----|
|             | Building Shearwall at El. 55'-0" .....  | 126 |
| Figure 5-15 | Comparison of ISRS Based on CSDRS and HRHF Response Spectra – Auxiliary Building Shearwall at El. 156'-0" .....                 | 127 |
| Figure 5-16 | Comparison of ISRS Based on CSDRS and HRHF Response Spectra – Auxiliary Building Shearwall at El. 213'-6" .....                 | 128 |
| Figure 5-17 | Comparison of ISRS Based on CSDRS and HRHF Response Spectra – Auxiliary Building Slabs at El. 55'-0", 156'-0" and 213'-6" ..... | 129 |
| Figure 5-18 | Comparison of ISRS Based on CSDRS and HRHF Response Spectra – DFOT Room Wall at El. 63'-0" .....                                | 130 |
| Figure 5-19 | Comparison of ISRS Based on CSDRS and HRHF Response Spectra – DFOT Room Wall at El. 100'-0" .....                               | 131 |
| Figure 5-20 | Comparison of ISRS Based on CSDRS and HRHF Response Spectra – EDGB Wall at El. 100'-0" .....                                    | 132 |
| Figure 5-21 | Comparison of ISRS Based on CSDRS and HRHF Response Spectra – EDGB Wall at El. 135'-0" .....                                    | 133 |
| Figure 5-22 | Comparison of ISRS Based on CSDRS and HRHF Response Spectra – DFOT Room Slabs .....   | 134 |
| Figure 5-23 | Comparison of ISRS Based on CSDRS and HRHF Response Spectra – EDGB Slabs .....  | 135 |
| Figure 6-1  | Arrangement of RCS .....  | 136 |
| Figure 6-2  | Reactor Coolant System Component Supports.....  | 137 |
| Figure 6-3  | Reactor Coolant System Component Nozzles .....  | 138 |
| Figure 6-4  | RV Supports.....  | 139 |
| Figure 6-5  | SG Support (No.1) .....   | 140 |
| Figure 6-6  | RCP Support (1A) .....  | 141 |
| Figure 6-7  | PZR Supports .....  | 142 |
| Figure 6-8  | RV Nozzle .....   | 143 |
| Figure 6-9  | SG Nozzle.....  | 144 |
| Figure 6-10 | RCP Nozzle .....  | 145 |
| Figure 6-11 | Reactor Coolant System Loop Piping Section/End Locations and Coordinate Systems .....   | 146 |
| Figure 6-12 | High-Frequency Screening Process.....   | 149 |
| Figure 6-13 | Location of Surge Line Loads .....  | 150 |

**ACRONYMS AND ABBREVIATIONS**

|         |   |
|---------|---|
| AB      | auxiliary building                        |
| APR1400 | Advanced Power Reactor 1400               |
| BLPB    | branch line pipe break                    |
| CESMD   | center for engineering strong motion data |
| CEUS    | central eastern United States             |
| COL     | combined license                          |
| CSDRS   | certified seismic design response spectra |
| DFOT    | diesel fuel oil tank                      |
| EDGB    | emergency diesel generator building       |
| EPRI    | Electric Power Research Institute         |
| E-W     | east-west                                 |
| GMRS    | ground motion response spectra            |
| HRHF    | hard rock high frequency                  |
| ISRS    | in-structure response spectra             |
| ISG     | interim staff guidance                    |
| KEPCO   | Korea Electric Power Corporation          |
| KHNP    | Korea Hydro & Nuclear Power Co., Ltd.     |
| NI      | nuclear island                            |
| N-S     | north-south                               |
| PGA     | peak ground acceleration                  |
| POSRV   | pilot-operated safety relief valve        |
| PSD     | power spectral density                    |
| PZR     | pressurizer                               |
| RCB     | reactor containment building              |
| RCP     | reactor coolant pump                      |
| RCS     | reactor coolant system                    |
| RG      | regulatory guide                          |
| RPV     | reactor pressure vessel                   |
| RV      | reactor vessel                            |
| RVI     | reactor vessel internals                  |
| SG      | steam generator                           |
| SRP     | standard review plan                      |
| SRSS    | square-root-of-the-sum-of-squares         |
| SSCs    | structures, systems, and components       |
| SSE     | safe shutdown earthquake                  |
| SSI     | soil-structure interaction                |
| WUS     | western United States                     |



## 1 INTRODUCTION

This technical report presents the evaluation of the effects of hard rock high frequency (HRHF) input ground motion on structures, systems, and components (SSCs) of the APR1400 standard plant. The technical report also describes the soil-structure-interaction (SSI) analysis of the nuclear island (NI) structures including the effects of spatial incoherence of seismic ground motions. The analysis procedure for incorporating spatial incoherence of seismic input ground motion in the SSI analysis is the same as the conventional SSI analysis procedure for coherent input ground motion. The analysis is performed using the computer program SASSI, with modifications to allow the program to incorporate the spatial incoherence of ground motion in the input ground motion to the analysis.

The response spectra used in this evaluation are developed for central eastern United States (CEUS) hard rock sites. In this report, such response spectra are also called the HRHF response spectra. The HRHF response spectra have spectral amplitudes higher than the amplitudes of the certified seismic design response spectra (CSDRS) in the high frequency range from approximately 10 to 100 Hz. However, by including the effects of spatial incoherence of seismic ground motions in the seismic SSI analysis, seismic responses such as in-structure response spectra (ISRS) in the high frequency are reduced.

Since the reactor containment building (RCB) and the auxiliary building (AB) share a common basemat, the seismic SSI analysis is performed with the combined NI structures (i.e., the combined RCB and AB supported on a common basemat foundation). The incoherent-motion SSI analysis is performed using the analysis methodology described in Subsection 2.1 with the SASSI computer program. The direct method (or flexible volume method) of the SASSI substructuring methodology is used in the SSI analysis.

In addition, evaluations of the APR1400 SSCs are performed to demonstrate that the seismic responses obtained from the design-basis SSI analysis envelop the corresponding responses obtained from the incoherent-motion SSI analysis or that the seismic responses obtained from the incoherent-motion SSI analysis are non-damaging.

Apart from the combined NI structures, the seismic SSI analysis is also performed with the emergency diesel generator building (EDGB) and the diesel fuel oil tank (DFOT) room considering coherent and incoherent ground motion effects.

The FE models including material properties and damping values used for HRHF seismic analyses are identical to those FE models for CSDRS seismic analyses.

This technical report consists of eight sections. Section 1 provides an introduction and background information. Section 2 describes the methodology of the incoherent SSI analysis. Section 3 describes the methodology for generating HRHF-response-spectrum-compatible ground motion time histories and the results generated. Section 4 describes the ground motion coherency functions used in the incoherent-motion SSI analysis. Section 5 compares the ISRS generated from the seismic input of CSDRS (Reference 1) and HRHF response spectra (Reference 2). Section 6 describes the evaluation of the effects of HRHF response spectra on SSCs of the APR1400 standard plant. Section 7 contains the conclusions from the evaluation. Section 8 lists the references cited in the report.

## 2 INCOHERENT SSI ANALYSIS METHODOLOGY AND PROCEDURE

### 2.1 Analysis Methodology

The incoherent-motion SSI analysis determines the maximum seismic response of the APR1400 NI structures and EDGB/DFOT room, taking into account the effects of spatial incoherence of seismic ground motions. The conventional SSI analysis methodology for coherent input ground motion, utilizing the computer program SASSI (Reference 3), is modified to allow the program to incorporate the spatial incoherence of ground motion in the input ground motion to the analysis.

The seismic SSI analysis using SASSI assumes that the seismic motions input to the structure SSI system are coherent motions. These input motions result from vertically propagating plane seismic shear (S) waves for the horizontal input motion and plane seismic compression (P) waves for the vertical input motion. For a horizontally layered free-field soil/rock medium, the idealized plane-wave input ground motions can be derived from horizontal and vertical free-field site response analyses using a one-dimensional elastic wave propagation theory. These analyses are generally performed using the equivalent-linear, free-field site response analysis computer program SHAKE (Reference 4 and 5). The free-field input ground motions derived from a one-dimensional elastic wave propagation theory are spatially coherent vertically propagating plane-wave input ground motions. Such motions are used for the conventional SSI analysis without taking into account spatial incoherence of seismic motions.

To incorporate spatial incoherence in the input ground motions for the SSI analysis using SASSI, the methodology developed by Tseng and Lilhanand as described in Electric Power Research Institute (EPRI) Report TR-102631 (Reference 6), is used in the industry.

Following the methodology described in EPRI Report TR-102631, for each of the two horizontal (north-south [N-S] and East-West [E-W]) and vertical components of input ground motion, the “plane-wave coherency function”  $\gamma_{pw}(f, \xi)$  for hard rock described in Section 4 is used to construct a “spatial coherency matrix”  $[\gamma]$  for each frequency,  $f_j$ ,  $j = 1, 2, 3, \dots, m$ , selected for the SASSI response analysis. The set of frequencies  $f_j$ ,  $j = 1, 2, 3, \dots, m$  is designated as the SASSI calculated frequencies. The matrix  $[\gamma]$  to be constructed is generated for the spatial locations of the nodal points on the ground surface of the SASSI finite element model used to model the excavated soil/rock volume. Thus, the matrix  $[\gamma]$  is a function of frequency  $f_j$  only, i.e.,  $[\gamma] = [\gamma(f_j)]$ , since the spatial separations of the nodal-point locations have been explicitly represented by the elements in the matrix. Each coefficient in this matrix expresses the spatial coherency of the co-directional input ground motions at any two nodal points lying on each horizontal plane of the SASSI finite element mesh, which is used to model the excavated soil/rock volume that corresponds to the embedded portion of the NI structure complex below grade.

Since the coherency functions for characterizing the spatial coherency of seismic motions at different depths are not available, the coherency matrix  $[\gamma] = [\gamma(f_j)]$  derived for motions on a horizontal ground surface is assumed to be the same for motions on all other horizontal planes at different depths. As a result of this assumption, motions for different horizontal planes at different depths are fully coherent with depth. That is, the variation of input ground motions with depth are fully correlated in the form of vertically propagating plane-wave motions that are derivable from the one-dimensional soil column site response analyses.

The coherency matrix  $[\gamma] = [\gamma(f_j)]$  is a symmetrical full matrix with real-valued matrix coefficients with the unit of power (motion-amplitude squared). To incorporate the incoherency of motion into the input ground motion vector for SSI analysis, the square root of the coherency matrix  $[\gamma(f_j)]$  is determined. To do this, the coherency matrix  $[\gamma]$  is decomposed into two identical but complimentary matrices so that their product gives the coherency matrix  $[\gamma]$ . To achieve decomposition, it is convenient to decompose the matrix  $[\gamma]$  for each calculated frequency  $f_j$  into its eigenvalues (principal coherency wave-numbers),  $\lambda_i^2$ ,

and associated eigenvectors (principal coherency mode shapes),  $\{\phi_i\}$ ,  $i = 1, 2, 3, \dots, n$ , where the number  $n$  is the total number of nodal points that lie on each horizontal plane of the finite element model mesh used to model the excavated soil/rock volume of the NI structural foundation below grade (i.e.,  $[\gamma] = [\phi]^T [\lambda^2] [\phi]$ ). The matrix  $[\phi]$  contains in its columns all eigen-vectors  $\{\phi_i\}$ ,  $i = 1, 2, 3, \dots, n$ , and  $[\phi]^T$  is the transpose of  $[\phi]$ . The matrix  $[\lambda^2]$  is a diagonal matrix containing on its diagonal terms the eigen-values  $\lambda_i^2$ ,  $i = 1, 2, 3, \dots, n$ .

Since the eigenvectors of the coherency matrix  $[\gamma]$  are mutually orthogonal to each other, the square root of the coherency matrix  $[\gamma]$  can be expressed as the product of  $[\lambda]$  and  $[\phi]$ , in which the diagonal matrix  $[\lambda]$  contains on its diagonal terms the square root of the eigenvalues, namely,  $\lambda_i$ . Due to orthogonality of the eigenvectors, construction of the spatially incoherent input ground motion vectors can be carried out independently for each principal coherency mode. In other words, the product  $\lambda_i \{\phi_i\}$  for each principal coherency mode  $i$ ,  $i = 1, 2, 3, \dots, n$ , can be used independently to modify the spatially coherent, co-directional input ground motion vector for each horizontal plane.

The assumption of vertically propagating plane waves for the coherent seismic input motion implies that the spatially coherent, co-directional, seismic input motions for each horizontal plane have identical motion amplitudes and phase angles. Using the product  $\lambda_i \{\phi_i\}$  to modify the spatially coherent seismic input motions, the identical spatially coherent seismic input motion amplitudes on each horizontal plane are modified to their corresponding non-identical spatially incoherent seismic input motion amplitudes on each horizontal plane. This modification preserves the phase angles associated with the spatially coherent seismic input motions.

By modifying the spatially coherent seismic input motions using the product  $\lambda_i \{\phi_i\}$  for each principal coherency mode, the SSI analysis for the spatially incoherent seismic input motions constructed for each principal coherency mode is carried out independently in the same manner as the SSI analysis for the conventional, spatially coherent, seismic input motion. The contributions to the SSI response parameters of interest from different principal coherency modes are then combined using the square-root-of-the-sum-of-squares (SRSS) combination rule, which implicitly assumes that the responses of all principal coherency modes are mutually statistically independent (i.e., the phase angles of all principal coherency modes are uncorrelated).

Correlation studies for validating the SSI analysis methodology with spatially incoherent seismic input motions developed as described above have been made as reported in EPRI Report TR-102631. These studies considered the problems of the SSI response of a flexible structure on a rigid base supported on the surface of an elastic halfspace that was subjected to excitation of a spatially incoherent (random) seismic input motion. These were the same problems studied by Luco and Mita with their analytical solutions (References 7 and 8). The results of the correlation studies, as published in the EPRI report (Reference 6), indicate that to capture the global SSI response due to spatially incoherent seismic input motions adequately, it is only necessary to include a few lower principal coherency modes of the coherency matrix. For each horizontal seismic input, only the first (horizontal translation) and second (twisting) modes are sufficient to capture the global SSI response of the problems studied due to the horizontal incoherent ground motion input. Likewise, for the vertical seismic input, only the first (vertical translation), second (rocking about one horizontal axis), and third (rocking about the other orthogonal horizontal axis) modes are sufficient to capture the global SSI response due to the vertical incoherent ground motion input.

For the incoherent SSI analysis to be carried out for the APR1400 NI structure complex, for each of the two horizontal directions, a minimum of two principal coherency modes, namely, the first (horizontal translation) and second (twisting about the vertical axis) modes, need to be included in the horizontal SSI analysis. For the vertical direction, a minimum of three principal coherency modes, namely, the first (vertical translation), second, and third (rocking about the two orthogonal horizontal axes) modes need to be included in the vertical SSI analysis. Additional parametric studies are to be carried out to demonstrate that inclusion of more principal coherency modes, in addition to those described previously, does not

change the SSI response significantly.

## 2.2 Site Response Analysis

The procedure used for performing the free-field site response analysis is described below.

- (1) Select the soil profile from Reference 9 consistent with the hard rock coherency functions considered.
- (2) Perform two horizontal (H1H and H2H) site response analyses with equivalent linear iterations on non-linear soil properties using SHAKE (Reference 4 and 5) to determine strain-compatible soil properties. The H1H and H2H ground motion time histories for the SSE are input motion at El. 98'-6" (ground surface). The shear-modulus-degradation and damping-value variation curves considered for rock are from Reference 4 and 5, and are shown in Table 2-1 and Figure 2-1.
- (3) Compute the averaged strain-compatible soil properties by averaging the two horizontal strain-compatible soil properties obtained from SHAKE in Step (2) for use as horizontal free-field soil properties in the SASSI soil model for the SSI analysis.
- (4) Using the averaged strain-compatible soils obtained from Step (3), perform horizontal (H1H and H2H) SHAKE analyses with no iterations on soil properties to determine horizontal free-field soil response motions at other elevations and transfer functions.
- (5) For vertical site response analyses, use the low-strain compression wave velocities. If the low-strain compression wave velocity is less than 4800 fps, then 4800 fps is used since the groundwater table is at the surface (El. 98'-6") unless this causes Poisson's Ratio to exceed 0.48, in which case a compression wave velocity corresponding to a Poisson's Ratio of 0.48 is used due to limitations in SASSI.

## 2.3 SSI Analysis

Using the SSI analysis methodology and the associated modified SSI analysis computer program SASSI and the associated INCOH program module (Reference 6) for incorporating the spatial incoherence of seismic ground motion, the SSI analysis of the APR1400 NI structures incorporating effects of spatial incoherence of input ground motion is performed for each frequency selected for the SASSI analysis following the analysis steps described below:

- (1) Based on the finite element mesh for the horizontal plane on the ground surface of the finite element model for the excavated soil/rock volume, generate the horizontal and vertical incoherent ground-motion coherency matrices using INCOH and the horizontal and vertical plane-wave coherency functions for hard rock sites as described in Section 4 of this report.
- (2) Perform an eigenvalue analysis of each horizontal and vertical incoherent ground-motion coherency matrix using INCOH to generate the eigenvalues (principal coherency wave-numbers),  $\lambda_i^2$ , and associated eigenvectors (principal coherency mode shapes),  $\{\phi_i\}$ ,  $i = 1, 2, 3, \dots, n$ ; where  $n$  is the total number of nodal points on the horizontal plane on the ground surface of the finite element mesh used to model the excavated soil/rock volume.
- (3) For each principal coherency mode  $i$ , compute the product  $\lambda_i\{\phi_i\}$  and incorporate the product into the horizontal or vertical coherent ground-motion vector, as appropriate, for the " $n$ " nodal points lying on each horizontal plane of the finite element mesh used in modeling the excavated soil/rock volume. This step generates an incoherent seismic input ground-motion vector for each principal coherency mode  $i$  to be included in the incoherent-motion SSI analysis,  $i = 1, 2, \dots, m$ , and  $m \ll n$ .

- (4) Using the incoherent ground-motion vector generated in Step (3) for each principal coherency mode  $i$  for each of the two horizontal or vertical seismic input ground motion, input the incoherent ground-motion load vector to ACS-SASSI to perform a horizontal or vertical SASSI analysis to generate the seismic response transfer functions for all seismic response parameters of interest. Such response parameters may include absolute accelerations, relative displacements, member forces and moments, and in-structure response spectral values, at all designated structure locations.
- (5) For each principal coherency mode  $i$  included in the analysis of Step (4), perform convolution of the computed seismic response transfer functions with the Fourier spectrum of the prescribed HRHF response spectrum-compatible seismic input time history to generate corresponding frequency-response functions. The resulting frequency response functions are then inverse Fourier-transformed back to the time domain to produce the response time-histories.
- (6) For each principal coherency mode  $i$  included in the analysis in Step (5), generate the maximum response values from the time histories of seismic response parameters of interest.
- (7) For each seismic response parameter of interest, combine the maximum response contributions from all principal coherency modes included in the analysis using the SRSS combination rule.

Steps (3) through (6) described above need to be repeated as many times as the total number of principal coherency modes,  $m$ , included in the seismic SSI analysis. As described previously, the minimum number of modes included in the incoherency SSI analysis of the NI structures is seven, which include two ( $m = 2$ ) for each of the horizontal N-S and E-W seismic inputs and three ( $m = 3$ ) for the vertical seismic input.

For EDGB and DFOT room, SSI analyses are also performed on a combined finite element model of EDGB and DFOT room of APR1400 to determine the seismic responses resulting from the incoherent HRHF seismic input motion. For analyses considering incoherent ground motion effects, the hard rock coherency functions developed by Norm Abrahamson (Reference 5) and the SASSI-SRSS approach (Reference 29) are employed in generating ISRS using ACS-SASSI. The method involves calculation of transfer functions corresponding to each of the principal coherency modes, which are then combined using the SRSS rule. The final transfer function is then used to calculate the ISRS. Studies are performed to compare the ISRS generated using the SASSI-SRSS approach and the ISRS generated using the SASSI-INCOH approach to confirm that ISRS generated using both approach are very similar and comparable (Appendix C.4 of Reference 31). Case studies are performed to confirm adequacy of the number of frequencies and modes used for incoherent analyses and fifty principal modes of the coherency matrix are assumed to be sufficient.

### 3 SEISMIC INPUT

In this section the seismic design spectra for the APR1400 and high frequency ground motion response spectra (GMRS) are described.

#### 3.1 EPRI GMRS for CEUS Rock Sites

Following the issuance of NRC RG 1.208 “A Performance-Based Approach to Define the Site-Specific Earthquake Ground Motion” in March 2007, EPRI undertook seismic hazard studies in 2008 and 2011 for the existing CEUS nuclear power plant sites.

The first EPRI study was documented in an EPRI report published in August 2008. This report, “Assessment of Seismic Hazard at 34 U.S. Nuclear Power Plant Sites” (Reference 10), presents the results of seismic hazard assessment for 34 existing U.S. nuclear power plant sites located in the CEUS. The study was performed using the NRC RG 1.208 methodology and guidelines and incorporated the 1989 EPRI seismic source characterization model with updated seismic source characterization information through 2003. The 5%-damped GMRS for 28 of the 34 sites studied were computed and compared with the NRC RG 1.60 design response spectra anchored to a peak ground acceleration (PGA) value of 0.3g. The comparisons indicate that the GMRS for 7 of the 28 sites developed have GMRS exceeding the RG 1.60 design response spectra anchored to 0.3g in the high frequency range of 8 Hz to 50 Hz and higher.

The second EPRI study was documented in the EPRI report, “Evaluation of Seismic Hazard at Central and Eastern US Nuclear Power Plant Sites” (Reference 11). This report presents the results of seismic hazard evaluations performed for 60 U.S. nuclear power plant sites located in CEUS. The 60 sites studied include the 34 sites that were studied in the first EPRI study (Reference 10). This study, like the first EPRI study in 2008, was performed using the methodology and guidelines of NRC RG 1.208 but instead of the 1989 EPRI seismic source characterization model used in the first study, it incorporated the updated 2008 U.S. Geological Survey seismic source characterization model (Reference 12).

The site-specific GMRS for all 60 sites were computed considering their site-specific site conditions. The 60 site conditions were categorized into five site categories, labelled Site 1 through Site 5. The 5%-damped GMRS for all 60 sites were calculated again for each of the 60 sites by assuming that each site condition of all 60 sites was represented by one of the generic site categories (Sites 1 through 5) plus a hard rock category. The computed GMRS were then enveloped and the maximum (enveloped) and 0.95, 0.9, 0.8, 0.7, 0.6, and 0.5 fractiles of the “composite envelope spectra” were computed. These spectra represent that, if any of the 5 generic site conditions (Sites 1 through 5 or rock) exists at a specific plant site, the 0.9-fractile “composite envelop spectrum” will encompass 90 percent of the GMRS computed for the 60 nuclear power plant sites studied. The maximum and fractile “composite envelope spectra” for the CEUS nuclear power plant sites developed in this study are useful for comparison with the CSDRS used for the standard plant design to assess the approximate percentage of sites in the CEUS that will be covered by the CSDRS.

The details of the CSDRS and the CSDRS-compatible design time histories are provided in the technical report APR1400-E-S-NR-14001-P (Reference 13).

#### 3.2 HRHF Response Spectra for APR1400

In the second EPRI study (Reference 11) described above, the maximum and fractile GMRS for the 60 CEUS nuclear power plant sites were developed, assuming that they are all hard rock sites. These 5%-damped maximum and fractile hard rock horizontal “composite envelope GMRS” are shown in Figure 3-1. The fractile GMRS shown in Figure 3-1 provide a rational basis for determining a suitable HRHF response spectra for applicable to the APR1400. The APR1400 has selected a goal of 0.8-fractile for non-exceedance probability. Thus the 0.8-fractile horizontal “composite envelope GMRS” for the CEUS hard

rock sites is selected as the 5%-damped horizontal target HRHF response spectrum for application to the APR1400 standard plant design as shown in Figure 3-2.

The 5%-damped vertical target HRHF response spectrum is generated from the 5%-damped HRHF horizontal target response spectrum by multiplying the vertical/horizontal (V/H) ratios for CEUS rock sites recommended in NUREG/CR-6728 (Reference 14). The V/H ratios for the 0.2 to 0.5g range of the peak rock-outcrop horizontal acceleration are used. For all needed frequencies not listed in NUREG/CR-6728, the ratios used follow a log-log amplitude-frequency linear interpolation. The resulting 5%-damped vertical HRHF target response spectrum generated are plotted along with the 5%-damped HRHF horizontal target response spectrum in Figure 3-3.

The digitized values of the HRHF horizontal and vertical target response spectra are given in Table 3-1 and 3-2. The V/H ratios are given in Table 3-3 and plotted in Figure 3-4.

The horizontal HRHF response spectra for damping ratios other than 5% (namely, 2%, 3%, 7%, and 10% damping ratios, which are not available from the EPRI study) are generated from the 5%-damped HRHF horizontal response spectrum by multiplying the 5%-damped spectral values by the spectral ratios for the CEUS rock sites given in Table 3-4 of Appendix C of SRP 3.7.1 (Reference 15). For spectral frequencies not listed in Table 3-4 of this report, the ratios that were used follow a log-log amplitude-frequency linear interpolation. The horizontal HRHF response spectrum for a 4% damping ratio, for which the spectral ratios are not available in Table 3-4 of this report, is generated by interpolating between the spectral values for 3% and 5% damping ratios on a log scale for the damping ratio and a linear scale for the spectral acceleration.

The vertical HRHF response spectra for 2%, 3%, 4%, 7%, and 10% damping ratios are generated by multiplying the V/H ratios for the CEUS rock site conditions given in Table 3-3 by the corresponding HRHF horizontal response spectra.

The resulting horizontal and vertical HRHF response spectra for 2%, 3%, 4%, 5%, 7%, and 10% damping ratios developed in the manner described above are shown in Figures 3-5 and 3-6, respectively. The spectrum curves shown in these two figures are the HRHF horizontal and vertical response spectra selected for the APR1400. The numerical values of the HRHF horizontal and vertical response spectra selected are listed in Tables A-1 and A-2 in Appendix A of this report.

Comparisons of the HRHF response spectra with the CSDRS for 5% damping are shown in Figures 3-7 and 3-8 for the horizontal and vertical directions, respectively.

### 3.3 Generation of HRHF Response-spectrum-compatible Time Histories

The basic guidelines and criteria to be used for generating a set of three-component design time histories compatible with the HRHF target response spectra follow the guidelines and criteria in NRC SRP Section 3.7.1, for Option 1 ("single time history option"). Since the HRHF response-spectrum-compatible design time histories are to be used for the evaluation of the APR1400 standard plant design, which involves the plant SSCs with different damping ratios, the recommended approach for generating the spectrum-compatible design time history is Option 1, Approach 1. The requirements of Option 1, Approach 1, are summarized below.

#### 3.3.1 Ground Motion Time Histories

The guidelines and criteria in SRP Section 3.7.1, for Option 1, Approach 1, and the desirable spectrum-compatible design time histories are as follows:

- (1) Design time histories to be generated are based on recorded seed motion time histories.

- (2) The set of time histories should consist of time histories in three mutually orthogonal directions - two horizontal and one vertical.
- (3) The time interval of time history digitization,  $t$ , shall be less than  $1/(2 f_n)$  where  $f_n$  is the highest frequency of interest. For the APR1400, the interval of time history digitization shall be 0.005 second, which corresponds to a  $f_n$  of 100 Hz.
- (4) The minimum acceptable strong-motion duration, which is defined as the time required for the Arias Intensity to rise from 5 to 75 percent, should be 6 seconds.
- (5) The three time histories (two horizontal and one vertical) shall be statistically independent from one another. The criterion for statistical independence shall be based on the cross-correlation coefficients computed for any pairs of time histories and these calculated coefficients shall be less than 0.16.

### 3.3.2 Response Spectrum and Power Spectral Density Enveloping Requirements

In accordance with the guidelines and criteria for Option 1 Approach 1, the response spectrum and power spectral density (PSD) enveloping requirements for design time histories are as follows:

- (1) The response spectra from the time history must envelop the target HRHF response spectra for all damping values used in the seismic response analysis.
- (2) For each applicable damping value, the response spectrum of the time history shall envelop the target response spectrum with no more than five points falling below the target spectrum by no more than 10 percent of the target spectral values.
- (3) In checking spectrum-enveloping, the set of frequencies at which the response spectra are to be calculated shall be the standard set of 92 frequencies from 0.2 Hz to 80 Hz as specified in SRP 3.7.1 Table 3.7.1-1.
- (4) The PSD of the time history shall adequately match a target PSD, which is compatible with the target design response spectra. For design response spectra other than the NRC RG 1.60 response spectra, the response spectrum-compatible target PSDs should be generated. In generating the target PSDs, the guidelines and procedures provided in Appendix B to SRP 3.7.1 can be used.
- (5) The time history PSDF shall generally envelop the minimum required target PSD, which is set at 80 percent of the target PSD, in the frequency range between 0.3 Hz and 80 Hz.

### 3.3.3 Selection of Initial Seed Motion Time Histories

To comply with the SRP 3.7.1 guidelines, design time histories should be generated from the recorded, actual earthquake ground motion called "seed motion". The selection guidelines of a set of recorded time histories to be used as the seed motion for the generation of the HRHF response spectrum-compatible design time histories are follows:

- (1) The three component seed motion time histories, two horizontal and one vertical, should come from the same earthquake event and recording station.
- (2) The scaled seed motions should provide a reasonably close match to the target response spectra over the amplified frequency range of the target response spectra to select seed motions that require the least amount of modifications to match the target spectra.



- (3) The seed motions should have a reasonable duration of 20 seconds and a strong-motion duration greater than 6 seconds as characterized by and Arias Intensity from 5 to 75 percent. Long-duration seed motions can be truncated to duration of between 20 and 24 seconds.
- (4) The seed motions with a PGA value greater than 0.10g are more desirable because they require a scale factor of less than 3.0 to bring them to the 0.3g target PGA value.
- (5) Seed motions from an earthquake of magnitude  $M$  greater than or equal to 6.5 and less than or equal to 7.3 are more desirable because they tend to generate motions that are sufficiently strong.
- (6) Seed motions at recording sites at a distance greater than or equal to 10 but less than or equal to 50 km from the earthquake epicenter are more desirable because they contain distinctive phases of P and S waves and have sufficiently high PGA amplitudes greater than 0.1 g.
- (7) Seed motions with broadband and high frequency motion contents are more desirable than those having narrow-band and low frequency motion contents.
- (8) Recorded motions from the CEUS rock sites, when available, are more desirable than recorded motions from the CEUS soil sites or western United States (WUS) soil or rock sites because they should have more high frequency motion contents.
- (9) The cross-correlation coefficient computed for any pair of the three component time histories of seed motions should be less than 0.16. The modification of seed motion time histories to match the target spectra generally does not change cross-correlation coefficients of the seed motion significantly.

For generation of the horizontal and vertical HRHF response spectrum-compatible time histories, the initial seed motion time histories are selected from the catalog of recorded actual earthquake ground motion time histories for the CEUS rock sites presented in Appendix B of NUREG/CR 6728 (Reference 14).

Based on the selection guidelines described above, a set of three component earthquake motion time histories from magnitude 6.8 Nahanni, Canada, earthquake of December 23, 1985 recorded at Station #3, Mackenzie, Northwest Territories, Canada, is selected as the initial seed time histories. This recording is selected from the catalog of NRC time histories presented on Page B-50 of Appendix B in NUREG/CR 6728. The recording station is located about 16 km from the epicenter of the earthquake. The digitized data of the recording are obtained from the center for engineering strong motion data (CESMD) website (Reference 17). The recorded motion consists of time histories for two horizontal (designated as 270 and 360) and one vertical (designated as VT) components. The digitized data of the recorded time history of each component have 3,819 points digitized at 0.005-second time increments giving a total record duration of 19.09 seconds. The plots of acceleration and integrated velocity and displacement time histories of the recorded motion for each component are shown in Figures 3-9 through 3-11 for the 270, 360, and VT components, respectively.

Comparisons of the time history response spectra for the recorded motion scaled to the target PGA value of 0.46g and the corresponding APR1400 HRHF horizontal and vertical target response spectra are shown in Figures 3-12 through 3-14 for the 270, 360, and VT components, respectively. As shown in these comparisons, the recorded time histories scaled to the target PGA value of 0.46g have time history response spectra match the target response spectra over a relatively wide frequency band.

### 3.4 Method for Generation Spectrum-compatible Time Histories

Two methods have generally been adopted for the generation of response-spectrum-compatible time

histories: (a) the time domain time history adjustment method and (b) the frequency domain time history adjustment method. To generate a time history that is compatible with a set of multiple damping target response spectra based on a recorded actual earthquake seed motion time history, the time domain time history adjustment method is usually adopted because it preserves the motion characteristics of the recorded seed motion.

### **3.4.1 Analytical Background**

The method for generating a design time history with response spectra closely matching a family of target response spectra of multiple damping values is the time domain time history adjustment method. This method was originally developed by Kaul (Reference 20) for matching a single damping target spectrum. It was extended later by Lilhanand and Tseng (References 21 and 22) for matching multiple damping target response spectra. The extended method by Lilhanand and Tseng is implemented into the computer program SYNQKE-R, PC Version 1.0 (Reference 23).

The time domain time history generation method begins with the use of an appropriately selected initial seed motion time history. The seed motion time history is selected to be consistent with the pertinent earthquake source, path, site parameters and the guidelines described previously in Section 3.3.2. Using the time domain time history generation method, the initial time history is modified (adjusted) in an iterative manner to match the time history response spectral values to the target spectral values within a prescribed tolerance. For each selected frequency for which the spectral values of multiple damping are to be matched, only localized adjustment with a wavelet is made to the time history over a short duration centered around the time when the maximum (i.e., spectral) response values occur. As a result, the iterative time history modifications produce not only a close match to the target response spectra but also only small localized perturbations to the initial time history; thus, the final modified time history closely resembles the motion characteristics of the initial seed time history.

### **3.4.2 Analytical Procedure**

For generating a set of three component design time histories matching the APR1400 HRHF target response spectra, the recommended seed motion time histories recorded from the 1985 Nahanni, Canada, earthquake, as described in Section 3.3.3 are to be used as the initial set of time histories. These initial time histories are first adjusted by (a) scaling to have a maximum acceleration of 0.46g, (b) adding trailing zeros to make the time histories with 4,096 points with a total duration of 20.475 seconds, and (c) modulating the time histories by an intensity envelope function,  $g(t)$  as shown in Figure 3-15. The adjusted initial time histories are then used for time history modifications using the computer program SYNQKE-R.

The SYNQKE-R adjusts the initial time history by automated iterations. For each cycle of iteration, the time history response spectra are compared with the target response spectra of corresponding damping values and the necessary time history adjustments to achieve spectrum-matching for the cycle are automatically solved. By repeating this iteration process and constantly monitoring the convergence to within the SRP spectrum-enveloping guidelines, a final modified time history that which has response spectra closely matching with the target multiple damping response spectra and satisfying the SRP spectrum-enveloping guidelines is obtained.

The final modified acceleration time histories, H1H, H2H, and VTH, are integrated to obtain their integrated velocity and displacement time histories. From these results, baseline corrections are performed, as necessary, to minimize the residual velocity and displacement values and, at the same time, produce the desirable time history intensity envelopes and integrated maximum velocity (V) and displacement (D) values, giving the baseline-corrected acceleration time histories.

Time history response spectra of the baseline-corrected time histories are then computed and compared with the target spectra to provide reasonable assurance that the SRP spectrum-enveloping guidelines are

still satisfied; otherwise, further time history modifications and baseline corrections are performed until the guidelines are satisfied.

### 3.5 Developing HRHF Response Spectrum-compatible PSDs

To check the adequacy of the power spectral density (PSD) of each generated response spectrum-compatible time history, horizontal and vertical target PSDs that are compatible with the horizontal and vertical HRHF target response spectra for the APR1400 are needed. The development of the horizontal and vertical target PSDs compatible with the APR1400 horizontal and vertical HRHF response spectra is described below.

#### 3.5.1 HRHF Response Spectrum-compatible Target PSDs

The development of the APR1400-HRHF response spectrum-compatible target PSDs in the frequency range of 0.3 to 80 Hz, the time history simulation method described in NUREG/CR-5347 (Reference 24) is used. Applying this method for developing the target PSD involves the following steps:

- (1) Initial target PSDs compatible with the APR1400 HRHF response spectra are developed from the 2%-damped APR1400 HRHF response spectra using a "PSD-to-response spectrum peak factor", as a function of frequency developed from the random vibration theory. The peak factor, which relates the target PSD value to the 2%-damped target response spectral value, is a function of frequency and non-exceedance probability of the target response spectra. The initial time history is then modified iteratively by adjusting the initial time history PSD at each frequency using the square of the ratio of the 2%-damped time history response spectral value to the 2%-damped target response spectral value. In this step, the computer program SIMQKE (Reference 25) developed by Gasparini, D. A. and Vanmarcke, E. H., at Department of Civil Engineering, Massachusetts Institute of Technology Publication No. R76-4, November 1976 is utilized to obtain the initial target PSDs compatible with the APR1400 HRHF response spectra.
- (2) Using the initial target PSDs developed in Step (1), the computer program SIMQKE, which implements the procedure in Equations (7), (8), and (9) of Appendix B of NUREG/CR-5347, is utilized to generate an ensemble of 30 time histories, each of which has the same initial target PSDs developed in Step (1) and a randomly phase angle sampled between 0 and  $2\pi$ , for each of APR1400 HRHF response spectra. An ensemble of 30 artificial time histories is generated using a frequency domain response spectrum-compatible time history generation method developed by Gasparini and Vanmarcke and implemented in SIMQKE (Reference 25). Each time history 30 time history ensemble has a total duration of 20.475 seconds and is modulated by the intensity envelope function shown in Figure 3-15. Each time history generated has a 2%-damped time history response spectrum compatible with the 2%-damped horizontal APR1400 HRHF response spectra.

The 2%-damped time history response spectra for the ensemble of 30 artificial time histories are computed based on which 2%-damped "ensemble-median" time history response spectrum is derived. This spectrum for the ensemble of 30 artificial time histories is shown in Figure 3-16 for the horizontal motion and in Figure 3-17 for the vertical motion. The 2%-damped horizontal and vertical "ensemble-median" time history response spectra are then compared with the 2%-damped horizontal and vertical target HRHF response spectra. These comparisons are shown in Figures 3-18 and 3-19.

As indicated in Figures 3-18 and 3-19, the ensemble-median time history response spectra derived from the generated horizontal and vertical 30 time history ensembles compared closely with the horizontal and vertical target horizontal and vertical APR1400 HRHF response spectra. The good comparisons indicate that the ensembles of the 30 generated time histories are compatible with the horizontal and vertical target HRHF response spectra and are therefore

representative time history ensembles from which the target PSDs compatible with the horizontal and vertical target APR1400 HRHF response spectra can be developed.

- (3) The PSD of each individual time history in each 30 time history ensemble is computed. Because each time history in the ensemble is intensity modulated and is therefore a non-stationary motion, an equivalent stationary duration for the motion must be determined for use in computing the PSD of the individual time history. The PSDs computed for the 30 time history ensemble are shown in Figure 3-20 for the horizontal motion and in Figure 3-21 for the vertical motion.
- (4) The “ensemble-average” or “ensemble-mean” PSDs obtained from the horizontal and vertical 30 time history PSDs computed in Step (2) and shown in Figures 3-20 and 3-21 are smoothed in accordance with the PSD smoothing procedure recommended in NUREG/CR-5347 (Reference 24). To simplify the representation of the target PSDs shown in Figures 3-20 and 3-21, the smoothed ensemble-mean PSDs obtained from the PSDs of the 30 time history ensembles are segmentally smoothed using log-log amplitude frequency linear functions for seven frequency bands, namely, (a)  $0.3 < f \leq 1.5$  Hz, (b)  $1.5 < f \leq 4.0$  Hz, (c)  $4.0 < f \leq 19$  Hz, (d)  $19 < f \leq 40$  Hz, (e)  $40 < f \leq 55$  Hz, (f)  $55 < f \leq 70$  Hz, and (g)  $70 < f \leq 80$  Hz.

The resulting horizontal and vertical, piecewise log-log linear, ensemble-mean PSDs generated for the seven frequency bands are the target PSDs compatible with the APR1400 HRHF horizontal and vertical response spectra for the frequency range  $0.3 \leq f \leq 80$  Hz and are tabulated in Tables 3-7 and 3-8. The smoothed ensemble-mean PSDs and the piecewise log-log linear smoothed PSDs are shown in Figures 3-22 and 3-23 for the horizontal and vertical motions, respectively. The horizontal target PSD is compared with the PSDs for the CEUS rock sites for magnitudes of 6 to 7 with epicentral distances of  $R = 0$  to 100 km as given in Table 1 of SRP 3.7.1, Appendix B, in Figure 3-24. As shown in this figure, the horizontal target PSD generated to be compatible with the APR1400 HRHF horizontal response spectra envelops the PSDs given in Table 1 in SRP 3.7.1, Appendix B, for magnitudes of  $M = 6$  to 7 and epicentral distances of  $R = 0$  to 100 km.

The target PSDs given in Tables 3-7 and 3-8, which are designated in this report as  $S_H(f)$  and  $S_V(f)$ , respectively, are the target PSDs for checking adequacy of the PSDs as functions of frequency of the generated horizontal and vertical HRHF response spectrum-compatible design time histories.

### 3.5.2 Minimum Required Target PSDs

The minimum required horizontal and vertical target PSDs, designated as  $\bar{S}_H(f)$  and  $\bar{S}_V(f)$ , for checking power adequacy of the horizontal and vertical time histories are obtained as 80 percent of the target PSD,  $S_H(f)$  and  $S_V(f)$ , given in Section 3.5.1:

$$\bar{S}_H(f) = 0.8 \times S_H(f); \quad \bar{S}_V(f) = 0.8 \times S_V(f) \quad (3-1)$$

The horizontal and vertical target and minimum required target PSDs are shown in Figures 3-25 and 3-26. The minimum required target PSDs shown in these figures are used to compare the PSDs of the generated horizontal and vertical HRHF response spectrum-compatible time histories to demonstrate adequacy in power density contents.

### 3.5.3 Calculation of Time History PSDs

To obtain the PSDs of the generated spectrum-compatible time histories for comparison with the minimum required horizontal and vertical target PSDs, the following calculation steps are used for each acceleration time history  $a_i(t)$ ,  $i = H1H, H2H, VTH$ .

- (1) Calculate the (equivalent stationary) strong-motion duration  $T_{s-e}^i$  for the time history  $a_i(t)$  using the following equations:

$$E_i(t_p^i) = \int_0^{t_p^i} a_i^2(t) dt; \quad i = \text{H1H, H2H, VTH} \quad (3-2)$$

$$T_{s-e}^i = \frac{t_{p2}^i - t_{p1}^i}{p_2 - p_1} \quad (3-3)$$

Where  $P_1$  and  $P_2$ ,  $P_1 < P_2$ , are the ratio of the cumulative energies  $E_i(t_{p1}^i)$  and  $E_i(t_{p2}^i)$  to the total cumulative energy of the entire time history; and where  $t_{p1}^i$  and  $t_{p2}^i$ ,  $t_{p1}^i < t_{p2}^i$ , are the times at which the ratios  $P_1$  and  $P_2$  are reached. The ratios  $P_1$  and  $P_2$ , and the corresponding over the duration  $t_s^i = t_{p2}^i - t_{p1}^i$  can best be fitted by a straight line (i.e., constant energy buildup) having a constant slope  $S = [E_i(t_{p2}^i) - E_i(t_{p1}^i)] / (t_{p2}^i - t_{p1}^i)$ . The equivalent stationary duration  $T_{s-e}^i$  for the entire time history as determined from Eq. (3-3) is the duration over which the total energy of the time history is built up from  $P_1=0\%$  to  $p_2=100\%$  with the constant slope  $S$ . This procedure of calculating  $T_{s-e}^i$  is illustrated in Figure 3-27.

- (2) Compute the one-sided PSD,  $S_i(f)$  of the time history  $a_i(t)$  using the following equations:

$$S_i(f) = \frac{2|A_i(f)|^2}{T_s^i} \quad (3-4)$$

Where  $|A_i(f)|$  is the amplitude of the Fourier spectrum obtained from the following equation:

$$A_i(f) = \int_0^{T_i} a_i(t) e^{-2\pi f t} dt \quad (3-5)$$

Where  $T_i$  is the total duration of the time history  $a_i(t)$ .

This discrete form of the mathematical Equation (3-5) is computed using the following discrete equation:

$$|A_i(\omega_n)| = \Delta t \left| \sum_{j=0}^{N-1} a_i(t_j) e^{-2\pi i(nj/N)} \right| \quad (3-6)$$

Where  $\omega_n = n\Delta\omega = 2\pi n\Delta f = \frac{2\pi n}{(N\Delta t)}$ ;  $n = 0, 1, \dots, N/2$  and  $t_j = j\Delta t$ ,  $j = 0, 1, \dots, N-1$ .

- (3) Smooth the time history PSD  $S_i(f)$  using the moving average technique over a  $\pm 20$  percent frequency bandwidth centered at the frequency  $f$ , in accordance with the guidelines in NUREG/CR-5347 (Reference 24), to give the smoothed time history PSD  $\tilde{S}_i(f)$ .

The smoothed time history PSD,  $\tilde{S}_i(f)$ , obtained from step (c) above is then compared with the minimum required target PSD,  $\tilde{S}_i(f)$ , to check the adequacy of the power content of the generated time history.

### 3.6 Generation Results

The acceleration time histories generated using the procedure described in Section 3.4 consist of two horizontal (H1H and H2H) and one vertical (VTH) components. Time histories H1H, H2H, and VTH are applied in the horizontal E-W, horizontal N-S, and vertical directions, respectively. The time interval of time history digitization,  $\Delta t$ , is 0.005 second, which corresponds to the highest frequency of interest of 100 Hz.

The horizontal H1H acceleration time history is plotted along with the integrated velocity and

displacement time histories in Figure 3-28. The comparison of the time history response spectra with the corresponding horizontal target HRHF response spectra for the corresponding damping values are shown in Figure 3-29. Similar results for the horizontal H2H time history are shown in Figures 3-30 and 3-31. Similar results for the vertical time history VTH are shown in Figures 3-32 and 3-33.

To show the statistical independence of the set of time histories, the cross-correlation coefficients of pairs of the HRHF response spectrum-compatible time histories are given in Table 3-10. The values all are below 0.16, thus satisfying the SRP Section 3.7.1 (Reference 15) threshold for statistical independence.

#### 4 GROUND MOTION COHERENCY FUNCTIONS

Spatial coherency, or simply coherency, of ground motion, designated with the symbol  $\gamma$ , is a measure of the degree of cross-correlation (similarity) between the two motions within a specific frequency band. It is defined mathematically as the normalized cross-power spectral density function of frequency ( $f$ ) of co-directional ground motion time histories at two stations on a horizontal ground surface separated by a distance  $\xi$ . Thus, coherency  $\gamma$  is a function of motion frequency  $f$  and separation distance between two stations on the horizontal ground surface (i.e.,  $\gamma \equiv \gamma(f, \xi)$ ). The function  $\gamma(f, \xi)$  is by definition a complex-valued function whose complex conjugate is anti-symmetrical with respect to the origin ( $f, \xi = (0, 0)$ ) (i.e., the function  $\gamma(f, \xi)$  is a Hermitian function).

Coherency function has an amplitude  $|\gamma(f, \xi)|$  varying between 0 and 1. For the extreme case in which the coherency is 0 at all frequencies, the co-directional motions at the two ground surface stations are statistically independent from each other. For the other extreme case in which the coherency has the value equal to 1 at all frequencies, the co-directional motions at the two ground stations are completely correlated (i.e., the two motions are identical to each other except by a scalar factor).

The empirical coherency functions for characterizing spatial coherency of seismic ground motions are derived from statistical analyses of amplitudes of coherency functions computed from earthquake data recorded from many instrument arrays and from many recordings of past earthquakes. Such functions reflect the statistical averages of the amplitudes of coherency functions derived from the recorded instrument-array data. Thus, the empirical coherency functions derived from statistical analyses of recorded earthquake data are real-valued functions of frequency and distance.

The coherency functions generally used for characterizing spatial coherence (or incoherence) of co-directional free field seismic motions at any two stations on the ground surface of hard rock sites are empirically derived, horizontal and vertical, "plane-wave coherency functions", designated by the symbol  $\gamma_{pw}(f, \xi)$ . These coherency functions were developed by Abrahamson based on the recorded Pinyon Flat array data and published in the EPRI report "Hard-Rock Coherency Functions Based on the Pinyon Flat Array Data," (Reference 26). In accordance with the guidance of ISG-01 (Reference 27), these coherency functions are acceptable to the NRC for application to hard rock sites. The mathematical expressions of these horizontal and vertical "plane-wave coherency functions" for hard rock are tabulated in Tables 4-1 and 4-2, respectively. The amplitudes of these functions, plotted as functions of frequency  $f$  and separation distance  $\xi$ , are shown in Figure 4-1 for both the horizontal and vertical components of ground motion.

## 5 ANALYSIS RESULTS

In this section, results of incoherent-input-motion SSI analysis performed for the seismic input motion of the HRHF response spectra are discussed (Reference 28 and 31).

### 5.1 Site Response Analysis

For the APR1400 NI structures and EDGB/DFOT room, the incoherent-input-motion SSI analysis with the HRHF-response-spectra-compatible seismic input motion is performed for the generic hard rock sites. The shear-wave-velocity profile of the Pinyon Flat Array site (the recorded data of this site provide the bases for developing the coherency functions for hard rock sites) is shown in Figure 5-1. Excluding the 5-m-thick softer surface layers, one can find from this shear-wave-velocity profile that the site has an average shear wave velocity of about 5,000 ft/sec for the top 50-m depth and about 9,800 ft/sec below the depth of 50 m.

Of the eight (8) generic site-shear-wave-velocity profiles S1 through S4 and S6 through S9 selected for design of the APR1400, the site profiles that can be classified as hard rock sites that have shear-wave-velocity profiles of the order or higher than that of the Pinyon Flat Array site are S8 and S9. Both S8 and S9 have site shear-wave-velocity profiles of the same order as the profile of Pinyon Flat site, as shown in Figure 5-2. For the site profile S8, the depth of bedrock where the rock shear-wave velocity ( $V_s$ ) equal to 9,200 ft/sec is reached is at the depth of 61 m (200 ft). Whereas for S9, the bedrock where  $V_s = 9,200$  ft/sec is reached is at the depth of 30.5 m (100 ft).

The horizontal site response analyses performed for S8 and S9 give the horizontal site response amplification (transfer) functions from the bedrock where  $V_s = 9,200$  ft/sec to the ground surface, as shown in Figures 5-3 and 5-4, respectively. Comparing the site response transfer functions shown in Figures 5-3 and 5-4 with the horizontal HRHF response spectra shown in Figure 3-2, one can readily see that the generic site profile S9, which has the peak amplification of the site at higher frequency, is more critical when subjected to the horizontal HRHF seismic input motion than the site profile S8. Thus, from the controlling-seismic-response-motion-point-of-view, site profile S9 is the controlling case for the incoherent-motion SSI analysis performed with the HRHF-response-spectra-compatible seismic input motion input. Thus, the incoherent-motion SSI analysis of the APR1400 NI structures and EDGB/DFOT room, subjected to the seismic input of APR1400 HRHF-response-spectra-compatible seismic input motion, is performed for the generic S9 site profile. The soil layers, and their associated properties, used in the SSI model for HRHF seismic input motions are presented in Table 5-1.

### 5.2 INCOH Analysis Results

The INCOH program module computes the coherency matrix of the finite element mesh of the excavated soil volume on the ground surface and performs an eigenvalue analysis of the coherency matrix for each selected frequency for the SASSI analysis. Tables 5-2 and 5-3 present INCOH analysis results in terms of the eigenvalues and the participation factors of the first 15 principal coherency modes for selected representative frequencies 1, 10, 20, 30, 40, and 50, Hz. The participation factors shown in these tables are defined as, for mode  $j$ :

$$\begin{aligned} Z_j &= \lambda_j \times [\sum \phi_i]^2 & i=1, 2 \dots \text{number of nodes} \\ XX_j &= \lambda_j \times [\sum \phi_i (Y_i - Y_o)]^2 & i=1, 2 \dots \text{number of nodes} \\ YY_j &= \lambda_j \times [\sum \phi_i (X_i - X_o)]^2 & i=1, 2 \dots \text{number of nodes} \\ ZZ_j &= XX_j + YY_j \end{aligned}$$



$\lambda$  = square root of eigenvalues

$\phi$  = eigenvector

$(X_o, Y_o) = (0.0, 0.0)$  (center of RCB)

The participation factors shown for each principal coherency mode are a measure of contribution of each principal coherency mode to the horizontal or vertical translation ( $Z_j$ ) and torsion ( $ZZ_j$  about the vertical Z-axis) or rocking ( $XX_j$  for rocking about the X-axis or  $YY_j$  for rocking about the Y-axis) rotation of the foundation.

Based on the INCOH principal coherency mode-shape plots, Mode 1 is a translational mode in X, Y, or Z direction. Modes 2 and 3 are torsional modes (when applied to the horizontal analysis) or are rocking modes (when applied to the vertical analysis). The mode-shape plot for each mode also shows the amount of spatial distortion in the mode shape, which increases as the frequency increases.

### 5.3 SSI Analysis

The incoherent-motion SSI analysis is performed using the methodology described in Section 2. Table 5-4 lists the SASSI calculated frequencies, i.e., the frequencies selected, for the incoherent-motion SSI analysis of the APR1400 NI structures.

### 5.4 Comparison of Incoherent-motion SSI Analysis Results Using 7 and 12 Modes

Comparison of incoherent-input-motion SSI analysis results obtained from the SRSS of the responses of Modes 1-7 versus the results of the SRSS of the responses of Modes 1-12 are provided in Appendix B.

### 5.5 Comparison of ISRS Based on CSDRS and HRHF Response Spectra

To show the significance of the HRHF response spectra, the seismic responses resulting from the coherent CSDRS compatible seismic input motion and the corresponding responses resulting from the incoherent HRHF-response-spectra compatible seismic input motion are compared. Figures 5-5 through 5-17 show such comparisons of the 5%-damped ISRS generated at a number of locations in the NI structures. As shown in these comparisons, there are some exceedances of the CSDRS-based ISRS, most of the exceedances occur in the frequency range above 10 Hz. The comparisons shown in Figures 5-5 through 5-17 are typical of the response comparisons found throughout the NI structures.

Figures 5-18 through 5-23 provide broadened (+/- 15%) ISRS from the coherent CSDRS, coherent and incoherent HRHF response spectra for the 5% spectral damping. The calculation procedures for the ISRS from the CSDRS and the HRHF seismic input motion can be found in References 30 and 31, respectively. ISRS plots of the walls are compared for each of the three direction (E-W, N-S, and vertical), whereas those of the slabs are compared for the vertical direction only. As shown in these comparisons, there are some exceedances of the CSDRS-based ISRS, and most of the exceedances occur in the frequency range above 10~20 Hz.

The exceedances of CSDRS-based ISRS by HRHF-based ISRS are addressed in this report as part of the sampling evaluation to confirm that high frequency seismic response has a marginal effect on the equivalent piping, and structures qualified by analysis for ISRS developed from the APR1400 CSDRS seismic input.

### 5.6 Convergence of Coherency Mode Expansion

Additional incoherence SSI analyses are performed for the additional coherency Modes 13 through 16 to demonstrate the convergence of results and to provide the technical justification for the selection of the

appropriate number of modes to be used to capture the incoherent-motion and structural responses. A supplementary study is performed in advance to confirm that the accumulative effect of spatial coherency modes higher than the 16 modes is insignificant. More details about the spatial coherency mode expansion convergence are provided in Appendix C.

---

## 6 EVALUATION

This section describes the results of evaluations of the SSCs subjected to the seismic response demands of the HRHF response spectra. The HRHF response spectra for the following SSCs are evaluated:

- Building structures
  - RCB internal structure
  - RCB containment structure
  - Auxiliary building
  - EDGB/DFOT room
- Reactor coolant system
  - Reactor vessel internals and core
  - Reactor coolant system supports
  - Reactor coolant system component nozzles and loop pipings
- Piping systems
- Safety-related equipment

### 6.1 Building Structures

Maintaining the structural integrity of the NI buildings is important to plant safety. The RCB internal structure, RCB containment structure and auxiliary building are evaluated for the effect of high frequency input ground motion.

The evaluation consists of comparisons of the responses from high frequency input ground motion to those obtained from the APR1400 CSDRS for the building structures.

The comparisons are performed to demonstrate that seismic responses from the CSDRS envelop those from the high frequency input motion. The NI structures are considered to be qualified for the high frequency input ground motion if the seismic responses from the CSDRS envelop those from the high frequency input motion.

To evaluate an effect on the RCB internal structures (i.e., PSW, IRWST, and SSW), seismic forces and moments of these structures are compared as shown in Tables 6-1, 6-2, and 6-3. Although the comparisons of forces and moments from high frequency input motion are greater than the CSDRS, the design results of the RCB internal structures are not affected by the seismic responses from the HRHF seismic input. Since the design margin of the RCB internal structures for CSDRS input motion covers the exceeded forces and moments, the arrangements of rebar are not changed due to seismic responses from the HRHF seismic input. The maximum stress of the rebar in the RCB internal structures occurs at the SSW, and the value is 51.49 ksi which is less than the allowable stress of 54 ksi.

Comparisons of the RCB containment structures are presented in Table 6-4. The comparisons of the containment structures show that seismic forces and moments resulting from the CSDRS input motion are greater than forces and moments obtained from high frequency input ground motion.

Equivalent accelerations of auxiliary building to seismic response story forces are evaluated for comparison of equivalent accelerations from the CSDRS and HRHF response spectra. The comparisons for the auxiliary building are presented in Table 6-5. Equivalent accelerations from CSDRS input ground motion envelop those from the HRHF except the vertical acceleration of Fuel Handling Area 3 (EL. 195'-0" to 213'-0"). The effect due to the increment of equivalent acceleration in the global z direction can be absorbed in the design of the shear walls because each wall member has stiffness enough to resist the additional seismic load due to high frequency seismic input in the axial direction.

Equivalent accelerations of EDGB/DFOT room are also compared in Table 6-6 for the CSDRS and HRHF response spectra. Although some of the equivalent accelerations from HRHF input motion are greater than those from the CSDRS, the design results of the EDGB are not affected by the seismic responses from the HRHF seismic input. Since the provided reinforcement of the EDGB for the CSDRS is greater than the required reinforcement for the HRHF, the arrangements of rebar are not changed. The design critical section which has a lowest provided/required rebar ratio of 1.10 occurs at EL. 100'-0" to 135'-0" center wall of the EDGB due to the CSDRS seismic input. The critical section location is maintained for the HRHF seismic input and the provided/required rebar ratio is 1.02 which is still greater than the design limit of 1.00.

## **6.2 Reactor Coolant System**

The reactor vessel internals (RVI) support the core which is important to safety. The RVI consists of complicated components whose natural frequencies are in the relatively high frequency range. The RCS component supports are evaluated because they provide the support for the RCS components to maintain their intended safety-related functions. The nozzles are evaluated because piping failures generally occur at high stress locations such as at nozzles of a component and they represent the sensitivity of the reactor coolant loop piping to high frequency excitation. For selected items, the HRHF response is evaluated by comparing the design loads with the loads obtained from the HRHF incoherent analysis. It is concluded that the supports, nozzles, and loop pipings are acceptable for the HRHF seismic loads if the design loads from the CSDRS envelop those from the HRHF input ground motion.

### **6.2.1 Reactor Vessel Internals and Core**

The RVI and core were selected because they are important to safety and their analyses are representative of major primary components. Because the natural frequencies of the RVI components are in the relatively high frequency range, the RVI may be sensitive to high frequency excitation.

Detailed analyses were performed to obtain the responses of the RVI and core to HRHF loads. The RVI HRHF analysis was done using the HRHF excitation of the reactor vessel (RV) obtained from the response of the RCB and RCS to HRHF loads. Then, the response of the core was calculated using the detailed core model and the core plate motion obtained from the RVI analysis.

The time history analyses of the RVI and core were performed for each HRHF mode, and the responses of all modes were combined for the resultant response. The maximum response of each mode was used for the combination. The broadening of the input excitation was also considered for the RVI and core analyses by frequency variation as implemented for the CSDRS loads.

The RVI resultant responses of HRHF loads were compared with those of the CSDRS loads. Most forces and moments of the RVI components for HRHF loads were calculated to be less than those for the CSDRS loads. It was already determined that the structural integrities of the RVI and core are maintained for the CSDRS loads. The evaluations were performed for RVI components such as the core support barrel flange and cylinder because the forces and moments on the components from HRHF loads exceeded those from CSDRS loads. The results of the evaluations showed that the increases in component loads due to HRHF loads were insignificant for the structural integrity of the components.

The core resultant responses of HRHF loads were compared with those of the CSDRS loads. The resultant responses for the comparison were grid impact forces. Since the natural frequency of the fuel assembly is in the relatively low range, the core responses for the HRHF loads were predicted to be less than those of the CSDRS loads. The resultant grid impact forces of the HRHF loads were calculated to be less than those of the CSDRS loads. No grid impact of the fuel assemblies occurs for all the modes except the first mode.

Therefore, the effects of HRHF loads on the structural integrity of the RVI and core are insignificant.

### **6.2.2 RCS Component Supports, Nozzles, and Loop Pippings**

The RCS structural supports support RCS components during normal operation and transients and during SSE and design basis accident conditions. RCS component supports are necessary to preserve the safety function of the RCS components. The arrangement of the RCS, including acronyms of the components, is shown in Figure 6-1. A comparison of the support loads on the RCS supports is provided in Table 6-7. The design loads for the RCS supports and nozzles are bounding at all locations.

The RV is supported by four vertical columns located under the vessel inlet nozzles. The columns are designed to be flexible in the horizontal direction to allow horizontal thermal expansion during heat-up and cool-down. They also support the reactor vessel in the vertical direction.

The steam generator (SG) is supported at the bottom by a sliding base bolted to an integrally attached conical skirt. The sliding base rests on low friction bearings, which allows unrestrained thermal expansion of the RCS. Two keyways in the sliding base mate with embedded keys to guide the movement of the steam generator during expansion and contraction of the RCS and to limit the movement of the bottom of the steam generator during SSE and branch line pipe break (BLPB) events.

The reactor coolant pump (RCP) supports consist of four vertical columns, four horizontal columns and two horizontal snubbers.

The pressurizer (PZR) is supported by a cylindrical skirt which is welded to the pressurizer and bolted to the building structure. Four keys welded to the upper shell of the pressurizer provide additional restraint for an SSE, pressurizer pilot-operated safety and relief valve (POSRV) actuation and BLPB conditions. The component supports of the RCS are shown in Figure 6-2.

The RCS component nozzles of the RV, SG, and RCP are included in the evaluation since a component nozzle has greater potential for failure than at other locations and the cold leg, hot leg, and crossover leg are relatively sensitive to high frequencies when compared with other components.

The locations and acronyms of the RCS component nozzles are shown in Figure 6-3. A comparison of the component nozzle loads with the design basis loads is provided in Table 6-8. Table 6-8 shows that the nozzle design loads envelop the loads from the HRHF incoherent analysis at all locations.

The section locations and coordinate systems for RCS loop piping force and moment are shown in Figure 6-11. A comparison of the loop piping forces and moments with the design basis loads is provided in Table 6-9. Table 6-9 shows that the loop piping design loads envelop the loads from the HRHF incoherent analysis at all locations.

## **6.3 Piping Systems**

Since piping lines and piping supports throughout the plant are designed according to the relevant guidelines, a stress analysis of a sample of lines is representative of all lines in the plant. Evaluating the susceptibility to excitation caused by high frequency seismic input requires the following factors to be present:

- The local HRHF-based ISRS need to have exceedances relative to the CSDRS-based ISRS in the high frequency range.
- The system must have modes or natural frequencies in the high frequency range.
- The system layout must include valves or other concentrated masses that would require closely spaced supports and therefore, cause high local natural frequencies. This generally yields significant cumulative mass in the high frequency range.

ASME Class 1, 2, and 3 piping systems are required to be evaluated for the HRHF-based ISRS.

A graded approach is taken to the scope of piping systems and components design. Therefore, the piping systems within the scope of the graded approach are evaluated for the HRHF seismic response spectra. The combined license (COL) applicant is to evaluate the HRHF response spectra for piping systems other than those within the scope of the graded approach.

Comparisons of ASME Code Section III Division 1 stresses calculated the most highly stressed location in the direct vessel injection line, shutdown cooling line, main steam and main feedwater piping located inside containment and in the main steam valve house for CSDRS and HRHF response spectra are listed in Table 6-10 and 6-11 for ASME Class 1 and 2 piping systems.

The maximum surge line loads obtained from the HRHF seismic input are compared with the design loads determined from the results of the CSDRS seismic input. Because the design loads from CSDRS seismic input envelop the surge line loads from the HRHF seismic input (refer to Table 6-12), a stress evaluation is not performed.

#### **6.4 Safety-related Equipment**

In some situations, the site specific spectra may exceed the certified design spectra in the high-frequency range. As a result of the high frequency ground motion, the seismic input to SSCs may also contain high-frequency excitations. The vast majority of prior existing seismic qualification tests used input frequencies up to only 33 Hz. The use of these prior testing results should be justified by demonstrating that the frequency content of the PSD of the test waveform is sufficient.

Safety-related equipment is evaluated for the effect of high frequency input motion to demonstrate their safety-related functionality.

For the evaluation of the equipment and components functionality for those cases where the GMRS/FIRS-based ISRS exceed the CSDRS-based ISRS below 50 Hz, further equipment and component functionality evaluations are needed. The screening process is applied for identification and evaluation of high-frequency sensitive mechanical and electrical equipment/components. If a new test is planned for the qualification of equipment and components, the RRS that is generated to meet GMRS/FIRS-based ISRS as well as the CSDRS-based ISRS are applied.

Evaluation process for evaluating equipment and components that are screened in is described in this report with a basis for the criteria used for each screening step that is used to identify equipment/components with potential to HF sensitivity. The method of generating the RRS at the location of support or attachment point within a structure or a cabinet that will be used in the evaluation is described.

The HRHF evaluations of the safety equipment shall be performed and the seismic qualification test/analysis will be performed for the components to envelop the in-structure response spectra resulting from the entire set of certified seismic design response spectra (CSDRS), including ground motions for the specific sites with high frequency content.

### 6.4.1 Evaluation Process Steps and Description

Identification and evaluation process of HF sensitive mechanical and electrical equipment and components are performed for safety-related equipment and components before performing seismic qualification. Refer to Figure 6-11 for the High Frequency Screening Process.

#### 6.4.1.1 Potentially High-frequency Sensitive Equipment

Safety-related equipment and components that have been undergone prior qualification testing/analysis are classified to either HF sensitive or HF insensitive. The potentially HF sensitive equipment and components are evaluated for the HF sensitivity.

The concern with potentially HF-sensitive components is related to the functionality of the devices when subjected to HF motions. Concerns over functionality of components due to HF motions have been focused on:

- 1) devices that have inadvertently changed state, permanently or temporarily (i.e., chattered) or had their output signals affected as a result of vibratory motions. This group is characterized as having bi-stable contacts or other mechanisms loaded by springs and/or electromagnetic forces which can be actuated/moved by inertial forces. Bi-stable devices such as relays, contactors, switches, potentiometers and similar devices, and those components whose output signal or settings (set-points) could be changed by HF vibratory motion are observed from seismic qualification tests and operating experience during which HF impact excitation (and likely high accelerations) caused relays to actuate resulting in inadvertent actions. From the industry experience, relays, contact devices, pressure transducers, and potentiometer are observed to be sensitive to high frequency motion.
- 2) non-ductile components such as ceramic insulators and cast iron components that have failed due to HF shock-type loads. The latter group of devices has been screened by either avoiding use of brittle materials, or by seismic and operational qualification testing of components (such as breakers and switchgear) whose operation involves impact loads and also requires potentially brittle insulating materials.

Non-ductile components and internal parts include those made of such materials as cast iron and ceramics. Standard commercial components which require non-ductile parts for function (e.g., circuit breakers) will be tested in accordance with traditional test standards; components otherwise fabricated of brittle materials should be avoided or justified on a case-by-case basis.

Based on the above considerations, the component types suggested in Table 6-13 are considered potentially sensitive to HF motions and should be screened following the procedures and criteria provided in this report. For all safety-related equipment that is designed to have part(s) of its assembly with components classified to be potentially sensitive to HF motions are to be evaluated for the adequacy in accordance with the procedures described in this report. List of HF sensitive equipment is provided to Technical Report APR1400-E-X-NR-14001-P, "Equipment Qualification Program", Table 3, "Equipment Qualification Equipment List". The items potential to HF sensitivity listed in Table 6-13 shall be verified for its applicability of evaluation in accordance with site specific condition and/or equipment supplier's design characteristics.

HF insensitive equipment and components are also evaluated for the adequacy of the qualification in terms of their natural frequency. Detail evaluation process for HF insensitive equipment is described in 6.4.1.2.

##### 6.4.1.1.1 Use of Existing Qualification Data

Safety-related equipment and components have been seismically qualified in accordance with IEEE Standard 344 random multi-frequency type test. Input motions containing additional HF content which is

greater than specified for low frequency (LF) design motions were included in seismic testing either intentionally or unintentionally. Also HF content has been combined with seismic test motions for some equipment to demonstrate equipment intended function for concurrent seismic and non-seismic loads (e.g. hydrodynamic loads) during a seismic event. In order to define HF sensitivity vulnerability, test result could be confirmed to envelop the RRS generated for both HRHF-based ISRS and CSDRS-based ISRS including proper margins. However, proper frequency contents with sufficient energy which were used for input to the shaking table shall be demonstrated to allow use of existing test data.

#### **6.4.1.1.2 Screening Test**

HF vibration screening tests can be conducted to identify any HF sensitivities or abnormalities of the components in case when only the RRS based on CSDRS-based ISRS are confirmed to be satisfied. A high frequency screening test can also be used to demonstrate lack of component sensitivity to high frequency vibration. The procedures for screening test prepared by the equipment manufacturer shall be reviewed to identify the adequacy of the criteria used for the test. The RRS for the screening test shall be used to envelop HRHF based ISRS. Upper limit for the HF screening evaluation is set to 50 Hz since majority of HRHF based ISRS show this limit is appropriate. However, if there is any ISRS that shows HF content above 50 Hz, this frequency content will also be evaluated.

#### **6.4.1.2 Items Not Potentially HF Sensitive**

In case that items are not potentially sensitive to HF, the confirmation that the natural frequency of the equipment or components is at the region where CSDRS-based ISRS exceedance occurs is required. When the natural frequency is at the CSDRS exceedance region, the higher seismic load based on the HRHF-based ISRS is imposed to the equipment compared to the CSDRS-based ISRS. Therefore, additional evaluation to ensure that HRHF-based ISRS does not affect any structural integrity and functional requirement is required although the equipment is potentially classified to be insensitive to HF. The method of additional evaluation could be evaluating the existing data to envelop the RRS that is prepared for HRHF-based ISRS including margins, conduct screening test if necessary or any analysis to verify acceptability.



## 7 CONCLUSION

Evaluations are performed for portions of structures, components, piping, and systems for the HRHF seismic response. The sample that was evaluated consists of the following:

- Building structures
  - RCB internal structure
  - RCB containment structure
  - Auxiliary building
  - EDGB/DFOT room
- Reactor coolant system
  - Reactor vessel internals and core
  - Reactor coolant system supports
  - Reactor coolant system component nozzles and loop pipings
- Piping systems
- Safety-related equipment

The evaluation of the building structures is performed through a comparison of the seismic responses obtained from HRHF incoherent analysis to those obtained from the design-basis seismic analysis. It is concluded that the existing design for nuclear island structures based on the CSDRS includes the seismic responses considering HRHF input ground motion.

For selected items of the reactor coolant system, the HRHF seismic responses are evaluated by comparing the design loads obtained from design-basis seismic analysis with the loads from the HRHF incoherent analysis. It is concluded that the supports and nozzles including loop pipings are acceptable for the HRHF seismic loads and the design loads from the CSDRS envelop those from the HRHF input ground motion.

The evaluations for HRHF seismic response on ASME Class 1 and 2 piping systems are performed within the scope of the graded approach. Although seismic input response spectra of HRHF in high frequency range are greater than CSDRS, the piping stress results based on ASME Code are within the allowable stresses for both CSDRS and HRHF response spectra. And surge line loads obtained from CSDRS seismic input envelop the loads from HRHF seismic input. Therefore, it is concluded that graded approach piping systems are acceptable for the HRHF seismic loading.

The evaluations for HRHF input ground motion on safety-related equipment are to be accomplished by the COL applicant.

## 8 REFERENCES

1. APR1400 Document No. 1-300-C305-001, "Artificial Time History Generation," Rev. 5, KEPCO Engineering & Construction Company, Inc. and KHNP, December 2016.
2. APR1400 Document No. 1-300-C305-002, "HRHF Time History Generation," Rev. 2, KEPCO Engineering & Construction Company, Inc. and KHNP, June 2016.
3. J. Lysmer, et al., "SASSI – A System for Analysis of Soil-Structure Interaction," Report No. UCB/GT/81-02, Department of Civil Engineering, University of California, Berkeley, April 1981.
4. P. B. Schnabel, J. Lysmer, and H. B. Seed, "SHAKE: A Computer Program for Earthquake Response Analysis of Horizontally Layered Sites," Report No. UCB/EERC-72/12, Earthquake Engineering Research Center, University of California, Berkeley, December 1972.
5. "SHAKE: A Computer Program for Conducting Equivalent Linear Seismic Response Analysis of Horizontally Layered Soil Deposits, Version 1.3," User's and Theoretical Manual, Rev. 4, Paul C. Rizzo Associates, Inc. September 2012.
6. EPRI TR-102631, "Soil-Structure Interaction Analysis Incorporating Spatial Incoherence of Ground Motions," Electric Power Research Institute, October 1997.
7. J. E. Luco and A. Mita, "Response of Circular Foundation to Spatially Random Ground Motion," Journal of Engineering Mechanics, American Society of Civil Engineer, Vol. 113, No. 1, January 1987.
8. J. E. Luco and A. Mita, "Response of Structures to Spatially Random Ground Motion," Proceedings, Third U. S. National Conference on Earthquake Engineering, Charleston, South Carolina, 1986.
9. APR1400 Document No. 9-310-C455-001, "Seismic Analysis Report, Reactor Containment Building Seismic Analysis," Rev. 1, KEPCO Engineering & Construction Company, Inc. and KHNP, May 2013.
10. EPRI TR-1016736, "Assessment of Seismic Hazard at 34 U.S. Nuclear Plant Sites," Electric Power Research Institute, August 2008.
11. EPRI TR-1023389, "Evaluation of Seismic Hazards at Central and Eastern US Nuclear Power Sites," Electric Power Research Institute, June 2011.
12. Mark D. Petersen, et al., "Documentation for the 2008 Update of the United States National Seismic Hazard Maps," U.S. Geological Survey Open-File Report 2008-1128, 2008.
13. APR1400-E-S-NR-14001-P, "Seismic Design Bases," Rev. 1, KHNP, February 2017.
14. NUREG/CR-6728, "Technical Basis for Revision of Regulatory Guidance on Design Ground Motions: Hazard- and Risk-consistent Ground Motion Spectra Guidelines," U.S. Nuclear Regulatory Commission, October 2001.
15. NUREG-0800, Standard Review Plan, Section 3.7.1, "Seismic Design Parameters," Draft Rev. 4, U.S. Nuclear Regulatory Commission, December 2012.
16. Regulatory Guide 1.208, "A Performance-Based Approach to Define the Site-Specific Earthquake Ground Motion," U.S. Nuclear Regulatory Commission, March 2007.

17. Center for Engineering Strong Motion Data (CESMD), (<http://strongmotioncenter.org/>).
18. NUREG-0003, "Statistical Studies of Vertical and Horizontal Earthquake Spectra," U.S. Nuclear Regulatory Commission, January 1976.
19. Regulatory Guide 1.60, "Design Response Spectra for Seismic Design of Nuclear Power Plants," Rev. 1, U.S. Nuclear Regulatory Commission, December 1973.
20. M. K. Kaul, "Spectrum-Consistent Time-History Generation," Journal of the Engineering Mechanics Division, American Society of Civil Engineer, Vol. 104, No. EM4, pp. 781-788, August 1978.
21. K. Lilhanand, K and W. S. Tseng, "Generation of Synthetic Time Histories Compatible with Multiple-Damping Design Response Spectra," SMiRT-9, Lausanne, K2/10, 1987.
22. K. Lilhanand, K and W. S. Tseng, "Development and Application of Realistic Earthquake Time Histories Compatible with Multiple-Damping Design Spectra," Proceedings of 9th World Conference on Earthquake Engineering, Tokyo-Kyoto, Japan, August 1988.
23. Computer Program, "SYNQKE-R," PC Version 1.0, "User's and Theoretical Manual," Rev. 1, Paul C. Rizzo Associates, Inc., December 2009.
24. NUREG/CR-5347, "Recommendations for Resolutions of Public Comments on USI A-40, 'Seismic Design Criteria'," Brookhaven National Laboratory, Prepared for U.S. Nuclear Regulatory Commission, June 1989.
25. D. A. Gasparini and E. H. Vanmarcke, "SIMQKE – A Program for Artificial Motion Generation, User's Manual and Documentation; Simulated Earthquake Motions Compatible with Prescribed Response Spectra," Department of Civil Engineering, Massachusetts Institute of Technology, Publication No. R76-4, November 1976.
26. EPRI TR-1015110, "Effects of Spatial Incoherence on Seismic Ground Motions," Electric Power Research Institute, November 2007.
27. Interim Staff Guidance (ISG) 01, "Seismic Issues Associated with High Frequency Ground Motion in Design Certification and Combined License Applications," U.S. Nuclear Regulatory Commission, May 2008.
28. APR1400 Document No. 1-310-C305-002, "Seismic Analysis of NI Structures Using Incoherent Ground Motion," Rev. 0, KEPCO Engineering & Construction Company, Inc. and KHNP, July 2013.
29. Ghiocel Predictive Technologies, Inc., "ACS SASSI Version 3.0 Including Options A, AA and FS," User Manuals, Revision 1, Pittsford, NY, October 2014.
30. APR1400 Document No. 1-350-C305-001, "Emergency D/G BLDG Seismic Analysis," Rev. 6, KEPCO Engineering & Construction Company, Inc. and KHNP, January 2017.
31. APR1400 Document No. 1-350-C305-002, "Seismic Analysis of EDGB Using Incoherent Ground Motion," Rev. 1, KEPCO Engineering & Construction Company, Inc. and KHNP, February 2015.
32. Regulatory Guide 1.100, "Seismic Qualification of Electrical and Active Mechanical Equipment and Functional Qualification of Active Mechanical Equipment for Nuclear Power Plants," Rev. 3, U.S. Nuclear Regulatory Commission, September 2009.

- 33. EPRI TR-1015108, "Program on Technology Innovation: The Effects of High-Frequency Ground Motion on Structures, Components, and Equipment in Nuclear Power Plants," Electric Power Research Institute, June 2007.
- 34. EPRI TR-1015109, "Program on Technology Innovation: Seismic Screening of Components Sensitive to High-Frequency Vibratory Motions," Electric Power Research Institute, October 2007.
- 35. APR1400-E-X-NR-14001-P, "Equipment Qualification Program," Rev. 1, KHNP, February 2017.

Table 2-1

Shear-modulus-degradation and Damping-value Variation Curves for Rock Considered for HRHF

(a) G/Gmax

| Uniform shear strain, $\gamma$ (%) | G/Gmax |
|------------------------------------|--------|
| 0.0001                             | 1.0    |
| 0.0003                             | 1.0    |
| 0.001                              | 0.9875 |
| 0.003                              | 0.9525 |
| 0.01                               | 0.900  |
| 0.03                               | 0.810  |
| 0.1                                | 0.725  |
| 1.0                                | 0.550  |

(b) Damping Ratio

| Uniform shear strain, $\gamma$ (%) | Damping Ratio (%) |
|------------------------------------|-------------------|
| 0.0001                             | 0.40              |
| 0.001                              | 0.80              |
| 0.01                               | 1.50              |
| 0.1                                | 3.00              |
| 1.0                                | 4.60              |

Table 3-1 (1 of 2)

5%-damped HRHF Horizontal Target Response Spectrum

| 5% - Damped Horizontal Response Spectrum |        |                |        |
|--|--------|----------------|--------|
| Frequency (Hz)                           | Sa (g) | Frequency (Hz) | Sa (g) |
| 0.10                                     | 0.0144 | 8.00           | 0.8200 |
| 0.13                                     | 0.0225 | 8.50           | 0.8398 |
| 0.15                                     | 0.0323 | 9.00           | 0.8589 |
| 0.20                                     | 0.0431 | 9.50           | 0.8823 |
| 0.25                                     | 0.0539 | 10.00          | 0.9050 |
| 0.30                                     | 0.0647 | 10.50          | 0.9263 |
| 0.40                                     | 0.0862 | 11.00          | 0.9471 |
| 0.50                                     | 0.1078 | 11.50          | 0.9674 |
| 0.60                                     | 0.1271 | 12.00          | 0.9873 |
| 0.70                                     | 0.1452 | 12.50          | 1.0067 |
| 0.80                                     | 0.1622 | 13.00          | 1.0245 |
| 0.90                                     | 0.1780 | 13.50          | 1.0420 |
| 1.00                                     | 0.1960 | 14.00          | 1.0591 |
| 1.10                                     | 0.2153 | 14.50          | 1.0759 |
| 1.20                                     | 0.2346 | 15.00          | 1.0924 |
| 1.25                                     | 0.2442 | 16.00          | 1.1150 |
| 1.30                                     | 0.2535 | 17.00          | 1.1367 |
| 1.40                                     | 0.2720 | 18.00          | 1.1575 |
| 1.50                                     | 0.2905 | 20.00          | 1.1969 |
| 1.60                                     | 0.3056 | 22.00          | 1.2168 |
| 1.70                                     | 0.3205 | 25.00          | 1.2441 |
| 1.80                                     | 0.3351 | 28.00          | 1.2376 |
| 1.90                                     | 0.3497 | 30.00          | 1.2336 |
| 2.00                                     | 0.3640 | 31.00          | 1.2274 |
| 2.10                                     | 0.3747 | 34.00          | 1.2102 |
| 2.20                                     | 0.3852 | 35.00          | 1.2048 |
| 2.30                                     | 0.3955 | 37.00          | 1.1866 |
| 2.40                                     | 0.4056 | 40.00          | 1.1615 |
| 2.50                                     | 0.4156 | 43.00          | 1.1262 |
| 2.60                                     | 0.4288 | 45.00          | 1.1046 |
| 2.70                                     | 0.4420 | 46.00          | 1.0896 |
| 2.80                                     | 0.4550 | 49.00          | 1.0476 |
| 2.90                                     | 0.4679 | 50.00          | 1.0345 |
| 3.00                                     | 0.4808 | 52.00          | 0.9970 |
| 3.15                                     | 0.4961 | 55.00          | 0.9458 |

Table 3-1 (2 of 2)

| 5% - Damped Horizontal Response Spectrum |        |                |        |
|--|--------|----------------|--------|
| Frequency (Hz)                           | Sa (g) | Frequency (Hz) | Sa (g) |
| 3.30                                     | 0.5111 | 58.00          | 0.8997 |
| 3.45                                     | 0.5259 | 60.00          | 0.8715 |
| 3.60                                     | 0.5405 | 61.00          | 0.8530 |
| 3.80                                     | 0.5596 | 64.00          | 0.8015 |
| 4.00                                     | 0.5783 | 65.00          | 0.7856 |
| 4.20                                     | 0.5942 | 67.00          | 0.7553 |
| 4.40                                     | 0.6097 | 70.00          | 0.7136 |
| 4.60                                     | 0.6249 | 73.00          | 0.6726 |
| 4.80                                     | 0.6398 | 75.00          | 0.6474 |
| 5.00                                     | 0.6545 | 76.00          | 0.6354 |
| 5.25                                     | 0.6711 | 79.00          | 0.6017 |
| 5.50                                     | 0.6873 | 80.00          | 0.5911 |
| 5.75                                     | 0.7032 | 82.00          | 0.5733 |
| 6.00                                     | 0.7187 | 85.00          | 0.5483 |
| 6.25                                     | 0.7328 | 88.00          | 0.5251 |
| 6.50                                     | 0.7467 | 90.00          | 0.5107 |
| 6.75                                     | 0.7603 | 91.00          | 0.5055 |
| 7.00                                     | 0.7736 | 94.00          | 0.4904 |
| 7.25                                     | 0.7855 | 97.00          | 0.4763 |
| 7.50                                     | 0.7972 | 100.00         | 0.4630 |
| 7.75                                     | 0.8087 |                |        |

Table 3-2 (1 of 2)

5%-damped HRHF Vertical Target Response Spectrum

| 5% - Damped Vertical Response Spectrum |        |                |        |
|--|--------|----------------|--------|
| Frequency (Hz)                         | Sa (g) | Frequency (Hz) | Sa (g) |
| 0.10                                   | 0.0108 | 8.00           | 0.6150 |
| 0.13                                   | 0.0169 | 8.50           | 0.6298 |
| 0.15                                   | 0.0242 | 9.00           | 0.6442 |
| 0.20                                   | 0.0323 | 9.50           | 0.6617 |
| 0.25                                   | 0.0404 | 10.00          | 0.6788 |
| 0.30                                   | 0.0485 | 10.50          | 0.6989 |
| 0.40                                   | 0.0647 | 11.00          | 0.7187 |
| 0.50                                   | 0.0809 | 11.50          | 0.7381 |
| 0.60                                   | 0.0953 | 12.00          | 0.7572 |
| 0.70                                   | 0.1089 | 12.50          | 0.7759 |
| 0.80                                   | 0.1217 | 13.00          | 0.7935 |
| 0.90                                   | 0.1335 | 13.50          | 0.8108 |
| 1.00                                   | 0.1470 | 14.00          | 0.8278 |
| 1.10                                   | 0.1615 | 14.50          | 0.8445 |
| 1.20                                   | 0.1759 | 15.00          | 0.8610 |
| 1.25                                   | 0.1832 | 16.00          | 0.8858 |
| 1.30                                   | 0.1901 | 17.00          | 0.9097 |
| 1.40                                   | 0.2040 | 18.00          | 0.9329 |
| 1.50                                   | 0.2179 | 20.00          | 0.9882 |
| 1.60                                   | 0.2292 | 22.00          | 1.0335 |
| 1.70                                   | 0.2403 | 25.00          | 1.0948 |
| 1.80                                   | 0.2514 | 28.00          | 1.1322 |
| 1.90                                   | 0.2622 | 30.00          | 1.1556 |
| 2.00                                   | 0.2730 | 31.00          | 1.1628 |
| 2.10                                   | 0.2810 | 34.00          | 1.1881 |
| 2.20                                   | 0.2889 | 35.00          | 1.1963 |
| 2.30                                   | 0.2966 | 37.00          | 1.2040 |
| 2.40                                   | 0.3042 | 40.00          | 1.2199 |
| 2.50                                   | 0.3117 | 43.00          | 1.2198 |
| 2.60                                   | 0.3216 | 45.00          | 1.2177 |
| 2.70                                   | 0.3315 | 46.00          | 1.2114 |
| 2.80                                   | 0.3413 | 49.00          | 1.1765 |
| 2.90                                   | 0.3510 | 50.00          | 1.1632 |
| 3.00                                   | 0.3606 | 52.00          | 1.1238 |



Table 3-2 (2 of 2)

| 5% - Damped Vertical Response Spectrum |        |                |        |
|--|--------|----------------|--------|
| Frequency (Hz)                         | Sa (g) | Frequency (Hz) | Sa (g) |
| 3.15                                   | 0.3721 | 55.00          | 1.0698 |
| 3.30                                   | 0.3833 | 58.00          | 1.0210 |
| 3.45                                   | 0.3944 | 60.00          | 0.9910 |
| 3.60                                   | 0.4054 | 61.00          | 0.9710 |
| 3.80                                   | 0.4197 | 64.00          | 0.9116 |
| 4.00                                   | 0.4337 | 65.00          | 0.8922 |
| 4.20                                   | 0.4456 | 67.00          | 0.8553 |
| 4.40                                   | 0.4573 | 70.00          | 0.8046 |
| 4.60                                   | 0.4687 | 73.00          | 0.7553 |
| 4.80                                   | 0.4799 | 75.00          | 0.7251 |
| 5.00                                   | 0.4909 | 76.00          | 0.7077 |
| 5.25                                   | 0.5033 | 79.00          | 0.6594 |
| 5.50                                   | 0.5155 | 80.00          | 0.6444 |
| 5.75                                   | 0.5274 | 82.00          | 0.6185 |
| 6.00                                   | 0.5390 | 85.00          | 0.5827 |
| 6.25                                   | 0.5496 | 88.00          | 0.5500 |
| 6.50                                   | 0.5600 | 90.00          | 0.5299 |
| 6.75                                   | 0.5702 | 91.00          | 0.5221 |
| 7.00                                   | 0.5802 | 94.00          | 0.4998 |
| 7.25                                   | 0.5892 | 97.00          | 0.4808 |
| 7.50                                   | 0.5979 | 100.00         | 0.4630 |
| 7.75                                   | 0.6065 |                |        |

Table 3-3

V/H Ratios for CEUS Rock Site Conditions

| <b>Table 4-5 (FROM NUREG/CR-6728 OCTOBER 2001)<br/>RECOMMENDED V/H RATIOS FOR CEUS ROCK SITE CONDITIONS</b> |                          |                                |                          |
|---|--------------------------|--------------------------------|--------------------------|
| <b>Frequency (Hz)</b>   | <b>0.2g<sup>1)</sup></b> | <b>0.2 - 0.5g<sup>1)</sup></b> | <b>0.5g<sup>1)</sup></b> |
| 0.10  | 0.67                     | 0.75                           | 0.90                     |
| 10.00   | 0.67                     | 0.75                           | 0.90                     |
| 18.75   | 0.70                     | 0.81                           | 1.01                     |
| 22.06   | 0.73                     | 0.85                           | 1.08                     |
| 25.00   | 0.75                     | 0.88                           | 1.12                     |
| 31.25   | 0.77                     | 0.95                           | 1.25                     |
| 37.50   | 0.81                     | 1.02 <sup>2)</sup>             | 1.37                     |
| 41.67   | 0.84                     | 1.07                           | 1.44                     |
| 46.88   | 0.85                     | 1.12                           | 1.50                     |
| 62.50   | 0.90                     | 1.14                           | 1.52                     |
| 75.00   | 0.89                     | 1.12                           | 1.48                     |
| 93.75   | 0.81                     | 1.02                           | 1.33                     |
| 100.0   | 0.78                     | 1.00                           | 1.30                     |

Notes

- 1) Range in rock outcrop horizontal component peak acceleration.
- 2) The original Table had 1.00. 1.02 was used to make the curves smoother.

Table 3-4 (1 of 3)

Scale Factors for Horizontal Response Spectra Damping Ratios Relative to 5%-damped Response Spectrum, CEUS

| Scale Factors for Horizontal Response Spectra<br>Damping Ratios (0.5 - 80 Hz) Relative to<br>5% - Damped Response Spectrum, CEUS |               |               |               |                |
|--|---------------|---------------|---------------|----------------|
| Frequency (Hz)   | 2%<br>Damping | 3%<br>Damping | 7%<br>Damping | 10%<br>Damping |
| 0.50   | 1.1588        | 1.0835        | 0.9620        | 0.9500         |
| 0.60   | 1.2038        | 1.1113        | 0.9381        | 0.8927         |
| 0.70   | 1.2299        | 1.1263        | 0.9263        | 0.8651         |
| 0.80   | 1.2487        | 1.1369        | 0.9190        | 0.8480         |
| 0.90   | 1.2631        | 1.1445        | 0.9137        | 0.8359         |
| 1.00   | 1.2749        | 1.1503        | 0.9096        | 0.8266         |
| 1.10   | 1.2836        | 1.1546        | 0.9062        | 0.8193         |
| 1.20   | 1.2889        | 1.1571        | 0.9045        | 0.8147         |
| 1.30   | 1.2914        | 1.1587        | 0.9038        | 0.8121         |
| 1.40   | 1.2941        | 1.1603        | 0.9027        | 0.8096         |
| 1.50   | 1.2991        | 1.1623        | 0.9022        | 0.8084         |
| 1.60   | 1.3060        | 1.1657        | 0.9008        | 0.8059         |
| 1.70   | 1.3099        | 1.1675        | 0.9000        | 0.8041         |
| 1.80   | 1.3145        | 1.1699        | 0.8986        | 0.8017         |
| 1.90   | 1.3173        | 1.1720        | 0.8973        | 0.7993         |
| 2.00   | 1.3215        | 1.1745        | 0.8964        | 0.7980         |
| 2.10   | 1.3287        | 1.1785        | 0.8943        | 0.7947         |
| 2.20   | 1.3355        | 1.1816        | 0.8923        | 0.7912         |
| 2.30   | 1.3388        | 1.1828        | 0.8916        | 0.7902         |
| 2.40   | 1.3400        | 1.1831        | 0.8919        | 0.7908         |
| 2.50   | 1.3391        | 1.1825        | 0.8920        | 0.7909         |
| 2.60   | 1.3392        | 1.1829        | 0.8914        | 0.7902         |
| 2.70   | 1.3392        | 1.1827        | 0.8916        | 0.7902         |
| 2.80   | 1.3386        | 1.1820        | 0.8919        | 0.7908         |
| 2.90   | 1.3354        | 1.1796        | 0.8931        | 0.7925         |
| 3.00   | 1.3330        | 1.1781        | 0.8944        | 0.7945         |
| 3.15   | 1.3330        | 1.1777        | 0.8951        | 0.7959         |
| 3.30   | 1.3341        | 1.1779        | 0.8953        | 0.7964         |
| 3.45   | 1.3309        | 1.1764        | 0.8954        | 0.7965         |
| 3.60   | 1.3279        | 1.1748        | 0.8962        | 0.7980         |

Table 3-4 (2 of 3)

| Scale Factors for Horizontal Response Spectra<br>Damping Ratios (0.5 - 80 Hz) Relative to<br>5% - Damped Response Spectrum, CEUS |               |               |               |                |
|--|---------------|---------------|---------------|----------------|
| Frequency (Hz)   | 2%<br>Damping | 3%<br>Damping | 7%<br>Damping | 10%<br>Damping |
| 3.80   | 1.3238        | 1.1721        | 0.8979        | 0.8004         |
| 4.00   | 1.3238        | 1.1719        | 0.8985        | 0.8014         |
| 4.20   | 1.3238        | 1.1717        | 0.8989        | 0.8016         |
| 4.40   | 1.3308        | 1.1752        | 0.8973        | 0.7989         |
| 4.60   | 1.3357        | 1.1773        | 0.8960        | 0.7964         |
| 4.80   | 1.3387        | 1.1791        | 0.8948        | 0.7938         |
| 5.00   | 1.3427        | 1.1813        | 0.8938        | 0.7915         |
| 5.25   | 1.3512        | 1.1853        | 0.8925        | 0.7889         |
| 5.50   | 1.3596        | 1.1892        | 0.8906        | 0.7852         |
| 5.75   | 1.3726        | 1.1961        | 0.8874        | 0.7804         |
| 6.00   | 1.3800        | 1.2002        | 0.8847        | 0.7764         |
| 6.25   | 1.3856        | 1.2024        | 0.8839        | 0.7751         |
| 6.50   | 1.3838        | 1.2010        | 0.8844        | 0.7760         |
| 6.75   | 1.3815        | 1.1995        | 0.8849        | 0.7775         |
| 7.00   | 1.3776        | 1.1973        | 0.8862        | 0.7800         |
| 7.25   | 1.3723        | 1.1945        | 0.8878        | 0.7835         |
| 7.50   | 1.3662        | 1.1917        | 0.8892        | 0.7867         |
| 7.75   | 1.3605        | 1.1887        | 0.8907        | 0.7895         |
| 8.00   | 1.3574        | 1.1863        | 0.8921        | 0.7921         |
| 8.50   | 1.3566        | 1.1857        | 0.8931        | 0.7940         |
| 9.00   | 1.3600        | 1.1877        | 0.8928        | 0.7942         |
| 9.50   | 1.3625        | 1.1892        | 0.8932        | 0.7953         |
| 10.00  | 1.3653        | 1.1906        | 0.8942        | 0.7972         |
| 10.50  | 1.3668        | 1.1911        | 0.8951        | 0.7993         |
| 11.00  | 1.3690        | 1.1920        | 0.8951        | 0.7994         |
| 11.50  | 1.3735        | 1.1941        | 0.8947        | 0.7989         |
| 12.00  | 1.3761        | 1.1953        | 0.8945        | 0.7988         |
| 12.50  | 1.3758        | 1.1952        | 0.8948        | 0.7994         |
| 13.00  | 1.3758        | 1.1946        | 0.8958        | 0.8011         |
| 13.50  | 1.3722        | 1.1924        | 0.8966        | 0.8029         |
| 14.00  | 1.3682        | 1.1900        | 0.8977        | 0.8049         |
| 14.50  | 1.3622        | 1.1868        | 0.8982        | 0.8058         |

Table 3-4 (3 of 3)

| Scale Factors for Horizontal Response Spectra<br>Damping Ratios (0.5 - 80 Hz) Relative to<br>5% - Damped Response Spectrum, CEUS |               |               |               |                |
|--|---------------|---------------|---------------|----------------|
| Frequency (Hz)   | 2%<br>Damping | 3%<br>Damping | 7%<br>Damping | 10%<br>Damping |
| 15.00  | 1.3614        | 1.1866        | 0.8978        | 0.8053         |
| 16.00  | 1.3583        | 1.1845        | 0.8992        | 0.8079         |
| 17.00  | 1.3536        | 1.1819        | 0.9003        | 0.8098         |
| 18.00  | 1.3501        | 1.1801        | 0.9018        | 0.8127         |
| 20.00  | 1.3490        | 1.1796        | 0.9022        | 0.8135         |
| 22.00  | 1.3456        | 1.1781        | 0.9025        | 0.8142         |
| 25.00  | 1.3413        | 1.1759        | 0.9040        | 0.8168         |
| 28.00  | 1.3402        | 1.1755        | 0.9039        | 0.8166         |
| 31.00  | 1.3412        | 1.1764        | 0.9037        | 0.8165         |
| 34.00  | 1.3386        | 1.1745        | 0.9054        | 0.8196         |
| 40.00  | 1.3344        | 1.1723        | 0.9066        | 0.8219         |
| 45.00  | 1.3240        | 1.1671        | 0.9095        | 0.8274         |
| 50.00  | 1.3089        | 1.1592        | 0.9134        | 0.8350         |
| 55.00  | 1.2851        | 1.1465        | 0.9201        | 0.8473         |
| 60.00  | 1.2566        | 1.1316        | 0.9279        | 0.8621         |
| 65.00  | 1.2289        | 1.1171        | 0.9359        | 0.8771         |
| 70.00  | 1.1980        | 1.1009        | 0.9449        | 0.8944         |
| 75.00  | 1.1670        | 1.0847        | 0.9540        | 0.9119         |
| 80.00  | 1.1361        | 1.0691        | 0.9621        | 0.9274         |

Table 3-5

Deleted

Table 3-6

Deleted

Table 3-7

Target PSD Compatible with APR1400 HRHF Response Spectra – Horizontal

| Frequency ( $f$ ) Range<br>$f$ (Hz or cps) | Piecewise Linear Target PSD<br>$S_H (f)$ ( $\text{in}^2/\text{sec}^4/\text{cps}$ ) |
|--|--|
| $0.3 < f \leq 1.5 \text{ Hz}$              | $S_0(f) = 2\pi \times 6.85 (0.3/f)^{-0.4}$   |
| $1.5 < f \leq 4.0 \text{ Hz}$              | $S_0(f) = 2\pi \times 13.04 (1.5/f)^{-0.2}$  |
| $4.0 < f \leq 19 \text{ Hz}$               | $S_0(f) = 2\pi \times 15.86 (4.0/f)^{0.25}$  |
| $19 < f \leq 40 \text{ Hz}$                | $S_0(f) = 2\pi \times 10.75 (19.0/f)^{1.1}$  |
| $40 < f \leq 55 \text{ Hz}$                | $S_0(f) = 2\pi \times 4.75 (40.0/f)^{2.3}$   |
| $55 < f \leq 70 \text{ Hz}$                | $S_0(f) = 2\pi \times 2.28 (55.0/f)^{4.5}$   |
| $70 < f \leq 80 \text{ Hz}$                | $S_0(f) = 2\pi \times 0.76 (70.0/f)^{7.1}$   |



Table 3-8

Target PSD Compatible with APR1400 HRHF Response Spectra – Vertical

| Frequency ( $f$ ) Range<br>$f$ (Hz or cps) | Piecewise Linear Target PSD<br>$S_v(f)$ ( $\text{in}^2/\text{sec}^4/\text{cps}$ ) |
|--|---|
| $0.3 < f \leq 1.5 \text{ Hz}$              | $S_0(f) = 2\pi \times 3.44 (0.3/f)^{-0.5}$  |
| $1.5 < f \leq 4.0 \text{ Hz}$              | $S_0(f) = 2\pi \times 7.69 (1.5/f)^{-0.1}$  |
| $4.0 < f \leq 19 \text{ Hz}$               | $S_0(f) = 2\pi \times 8.49 (4.0/f)^{0.15}$  |
| $19 < f \leq 40 \text{ Hz}$                | $S_0(f) = 2\pi \times 6.72 (19.0/f)^{0.3}$  |
| $40 < f \leq 55 \text{ Hz}$                | $S_0(f) = 2\pi \times 5.38 (40.0/f)^{1.5}$  |
| $55 < f \leq 70 \text{ Hz}$                | $S_0(f) = 2\pi \times 3.34 (55.0/f)^{3.9}$  |
| $70 < f \leq 80 \text{ Hz}$                | $S_0(f) = 2\pi \times 1.31 (70.0/f)^{6.2}$  |

Table 3-9

Deleted

Table 3-10

Cross-correlation Coefficients of HRHF Response-Spectrum-Compatible Time History Pairs

| Components | Cross-Correlation Coefficient |
|------------|-------------------------------|
| H1H × H2H  | 0.028                         |
| H2H × VTH  | 0.036                         |
| VTH × H1H  | 0.031                         |

Table 3-11

Stationary Duration of Generated Time Histories

| <b>Components</b> | <b>Ts' (5-75%)<br/>(sec)</b> |
|-------------------|------------------------------|
| H1H               | 6.090                        |
| H2H               | 6.400                        |
| VTH               | 6.505                        |

Table 3-12

Maximum Acceleration (A), Velocity (V), and Displacement (D) of Generated Time Histories

| Components | A<br>(g) | V<br>(in/sec) | D<br>(in) |
|------------|----------|---------------|-----------|
| H1H        | 0.463    | 8.86          | 3.63      |
| H2H        | 0.463    | 10.50         | 3.51      |
| VTH        | 0.463    | 9.94          | 4.16      |

Table 3-13

Number of Points of the Response Spectra below each HRHF DRS

| Damping | Component |     |     |
|---------|-----------|-----|-----|
|         | H1H       | H2H | VTH |
| 2%      | 0         | 1   | 3   |
| 3%      | 2         | 4   | 1   |
| 4%      | 1         | 5   | 2   |
| 5%      | 0         | 4   | 3   |
| 7%      | 0         | 0   | 2   |
| 10%     | 4         | 3   | 2   |

Table 3-14

The Lowest Percentage below the HRHF DRS

| Damping | Component |         |         |
|---------|-----------|---------|---------|
|         | H1H (%)   | H2H (%) | VTH (%) |
| 2%      | 1.02      | -0.77   | -2.94   |
| 3%      | -1.85     | -4.02   | -1.49   |
| 4%      | -0.67     | -1.84   | -1.61   |
| 5%      | 1.56      | -3.02   | -2.01   |
| 7%      | 0.76      | 0.33    | -0.89   |
| 10%     | -1.94     | -1.09   | -4.40   |

Table 4-1

EPRI (2007) Empirical Plane-Wave Coherency Function for Horizontal Seismic Ground Motions for Hard Rock

The EPRI (2007) empirical plane-wave coherency function for horizontal component of seismic ground motions for hard rock (Reference 6) is given as follows:

$$\gamma_{pw}(f, \xi) = \left[ 1 + \left( \frac{f \tanh(a_3 \xi)}{a_1 f_c(\xi)} \right)^{n_1(\xi)} \right]^{-1/2} \left[ 1 + \left( \frac{f \tanh(a_3 \xi)}{a_2} \right)^{n_2} \right]^{-1/2}$$

where  $f$  = frequency in Hz, and  $\xi$  = separation distance in meter.

The coefficients in the function for the horizontal component of ground motion are listed in the following table:

| Coefficient | Horizontal Component  |
|-------------|---|
| $a_1$       | 1.0   |
| $a_2$       | 40  |
| $a_3$       | 0.4   |
| $n_1(\xi)$  | $3.80 - 0.040 \cdot \ln(\xi + 1) + 0.0105 \cdot [\ln(\xi + 1) - 3.6]^2$ |
| $n_2$       | 16.4  |
| $f_c(\xi)$  | $27.9 - 4.82 \cdot \ln(\xi + 1) + 1.24 \cdot [\ln(\xi + 1) - 3.6]^2$    |



Table 4-2

EPRI (2007) Empirical Plane-Wave Coherency Function for Vertical Seismic Ground Motions for Hard Rock

The equation for the EPRI (2007) plane-wave coherency function for vertical component of seismic ground motions for hard rock (Reference 6) is the same as that for the horizontal motion given in Table 4-1, i.e.,

$$\gamma_{pw}(f, \xi) = \left[ 1 + \left( \frac{f \tanh(a_3 \xi)}{a_1 f_c(\xi)} \right)^{n_1(\xi)} \right]^{-1/2} \left[ 1 + \left( \frac{f \tanh(a_3 \xi)}{a_2} \right)^{n_2} \right]^{-1/2}$$

where  $f$  = frequency in Hz, and  $\xi$  = separation distance in meter.

The coefficients in the function for the vertical component of ground motion are listed in the table below.

| Coefficient | Vertical Component  |
|-------------|---|
| $a_1$       | 1.0   |
| $a_2$       | 200   |
| $a_3$       | 0.4   |
| $n_1(\xi)$  | $2.03 + 0.41 \cdot \ln(\xi + 1) - 0.078 \cdot [\ln(\xi + 1) - 3.6]^2$ |
| $n_2$       | 10  |
| $f_c(\xi)$  | $29.2 - 5.20 \cdot \ln(\xi + 1) + 1.45 \cdot [\ln(\xi + 1) - 3.6]^2$  |

Table 5-1 (1 of 4)

Soil Layers and Properties of SSI Model for HRHF Seismic Input Motions

| Soil Type | Layer No. | Thick. (ft) | $\gamma^{(1)}$ (k/ft <sup>3</sup> ) | Damp. | Vs (ft/s) | Vp (ft/s) | $\rho^{(2)}$ |
|-----------|-----------|-------------|-------------------------------------|-------|-----------|-----------|--------------|
| Rock      | 1         | 5           | 0.145                               | 0.004 | 4,692     | 9,315     | 0.33         |
|           | 2         | 5           | 0.145                               | 0.006 | 4,707     | 9,348     | 0.33         |
|           | 3         | 5           | 0.145                               | 0.007 | 4,711     | 9,382     | 0.33         |
|           | 4         | 5           | 0.145                               | 0.008 | 4,720     | 9,415     | 0.33         |
|           | 5         | 5           | 0.145                               | 0.008 | 4,731     | 9,448     | 0.33         |
|           | 6         | 5           | 0.145                               | 0.008 | 4,737     | 9,481     | 0.33         |
|           | 7         | 5           | 0.145                               | 0.009 | 4,743     | 9,513     | 0.33         |
|           | 8         | 5           | 0.145                               | 0.009 | 4,750     | 9,546     | 0.34         |
|           | 9         | 5           | 0.145                               | 0.010 | 4,758     | 9,578     | 0.34         |
|           | 10        | 5           | 0.145                               | 0.010 | 4,767     | 9,610     | 0.34         |
|           | 11        | 5           | 0.145                               | 0.010 | 4,775     | 9,642     | 0.34         |
|           | 12        | 5           | 0.145                               | 0.010 | 4,785     | 9,674     | 0.34         |
|           | 13        | 5           | 0.145                               | 0.011 | 4,795     | 9,706     | 0.34         |
|           | 14        | 5           | 0.145                               | 0.011 | 4,807     | 9,737     | 0.34         |
|           | 15        | 5           | 0.145                               | 0.011 | 4,818     | 9,768     | 0.34         |
|           | 16        | 5           | 0.145                               | 0.011 | 4,830     | 9,799     | 0.34         |
|           | 17        | 5           | 0.145                               | 0.011 | 4,843     | 9,830     | 0.34         |
|           | 18        | 5           | 0.145                               | 0.011 | 4,855     | 9,861     | 0.34         |
|           | 19        | 5           | 0.145                               | 0.011 | 4,868     | 9,892     | 0.34         |
|           | 20        | 5           | 0.145                               | 0.011 | 4,882     | 9,922     | 0.34         |
|           | 21        | 5           | 0.155                               | 0.010 | 9,200     | 18,264    | 0.33         |
|           | 22        | 5           | 0.155                               | 0.010 | 9,200     | 18,264    | 0.33         |
|           | 23        | 5           | 0.155                               | 0.010 | 9,200     | 18,264    | 0.33         |
|           | 24        | 5           | 0.155                               | 0.010 | 9,200     | 18,264    | 0.33         |
|           | 25        | 5           | 0.155                               | 0.010 | 9,200     | 18,264    | 0.33         |
|           | 26        | 5           | 0.155                               | 0.010 | 9,200     | 18,264    | 0.33         |

Table 5-1 (2 of 4)

| Soil Type       | Layer No. | Thick. (ft) | $\gamma^{(1)}$<br>(k/ft <sup>3</sup> ) | Damp. | Vs<br>(ft/s) | Vp<br>(ft/s) | $\rho^{(2)}$ |
|-----------------|-----------|-------------|--|-------|--------------|--------------|--------------|
| Rock<br>(cont.) | 27        | 5           | 0.155                                  | 0.010 | 9,200        | 18,264       | 0.33         |
|                 | 28        | 5           | 0.155                                  | 0.010 | 9,200        | 18,264       | 0.33         |
|                 | 29        | 5           | 0.155                                  | 0.010 | 9,200        | 18,264       | 0.33         |
|                 | 30        | 5           | 0.155                                  | 0.010 | 9,200        | 18,264       | 0.33         |
|                 | 31        | 5           | 0.155                                  | 0.010 | 9,200        | 18,264       | 0.33         |
|                 | 32        | 5           | 0.155                                  | 0.010 | 9,200        | 18,264       | 0.33         |
|                 | 33        | 5           | 0.155                                  | 0.010 | 9,200        | 18,264       | 0.33         |
|                 | 34        | 5           | 0.155                                  | 0.010 | 9,200        | 18,264       | 0.33         |
|                 | 35        | 5           | 0.155                                  | 0.010 | 9,200        | 18,264       | 0.33         |
|                 | 36        | 5           | 0.155                                  | 0.010 | 9,200        | 18,264       | 0.33         |
|                 | 37        | 5           | 0.155                                  | 0.010 | 9,200        | 18,264       | 0.33         |
|                 | 38        | 5           | 0.155                                  | 0.010 | 9,200        | 18,264       | 0.33         |
|                 | 39        | 5           | 0.155                                  | 0.010 | 9,200        | 18,264       | 0.33         |
|                 | 40        | 5           | 0.155                                  | 0.010 | 9,200        | 18,264       | 0.33         |
|                 | 41        | 10          | 0.155                                  | 0.010 | 9,200        | 18,264       | 0.33         |
|                 | 42        | 10          | 0.155                                  | 0.010 | 9,200        | 18,264       | 0.33         |
|                 | 43        | 10          | 0.155                                  | 0.010 | 9,200        | 18,264       | 0.33         |
|                 | 44        | 10          | 0.155                                  | 0.010 | 9,200        | 18,264       | 0.33         |
|                 | 45        | 10          | 0.155                                  | 0.010 | 9,200        | 18,264       | 0.33         |
|                 | 46        | 10          | 0.155                                  | 0.010 | 9,200        | 18,264       | 0.33         |
|                 | 47        | 10          | 0.155                                  | 0.010 | 9,200        | 18,264       | 0.33         |
|                 | 48        | 10          | 0.155                                  | 0.010 | 9,200        | 18,264       | 0.33         |
|                 | 49        | 10          | 0.155                                  | 0.010 | 9,200        | 18,264       | 0.33         |
|                 | 50        | 10          | 0.155                                  | 0.010 | 9,200        | 18,264       | 0.33         |
|                 | 51        | 10          | 0.155                                  | 0.010 | 9,200        | 18,264       | 0.33         |
|                 | 52        | 10          | 0.155                                  | 0.010 | 9,200        | 18,264       | 0.33         |

Table 5-1 (3 of 4)

| Soil Type       | Layer No. | Thick. (ft) | $\gamma^{(1)}$<br>(k/ft <sup>3</sup> ) | Damp. | Vs<br>(ft/s) | Vp<br>(ft/s) | $\rho^{(2)}$ |
|-----------------|-----------|-------------|--|-------|--------------|--------------|--------------|
| Rock<br>(cont.) | 53        | 10          | 0.155                                  | 0.010 | 9,200        | 18,264       | 0.33         |
|                 | 54        | 10          | 0.155                                  | 0.010 | 9,200        | 18,264       | 0.33         |
|                 | 55        | 10          | 0.155                                  | 0.010 | 9,200        | 18,264       | 0.33         |
|                 | 56        | 10          | 0.155                                  | 0.010 | 9,200        | 18,264       | 0.33         |
|                 | 57        | 10          | 0.155                                  | 0.010 | 9,200        | 18,264       | 0.33         |
|                 | 58        | 10          | 0.155                                  | 0.010 | 9,200        | 18,264       | 0.33         |
|                 | 59        | 10          | 0.155                                  | 0.010 | 9,200        | 18,264       | 0.33         |
|                 | 60        | 10          | 0.155                                  | 0.010 | 9,200        | 18,264       | 0.33         |
|                 | 61        | 10          | 0.155                                  | 0.010 | 9,200        | 18,264       | 0.33         |
|                 | 62        | 10          | 0.155                                  | 0.010 | 9,200        | 18,264       | 0.33         |
|                 | 63        | 10          | 0.155                                  | 0.010 | 9,200        | 18,264       | 0.33         |
|                 | 64        | 10          | 0.155                                  | 0.010 | 9,200        | 18,264       | 0.33         |
|                 | 65        | 10          | 0.155                                  | 0.010 | 9,200        | 18,264       | 0.33         |
|                 | 66        | 10          | 0.155                                  | 0.010 | 9,200        | 18,264       | 0.33         |
|                 | 67        | 10          | 0.155                                  | 0.010 | 9,200        | 18,264       | 0.33         |
|                 | 68        | 10          | 0.155                                  | 0.010 | 9,200        | 18,264       | 0.33         |
|                 | 69        | 10          | 0.155                                  | 0.010 | 9,200        | 18,264       | 0.33         |
|                 | 70        | 10          | 0.155                                  | 0.010 | 9,200        | 18,264       | 0.33         |
|                 | 71        | 20          | 0.155                                  | 0.010 | 9,200        | 18,264       | 0.33         |
|                 | 72        | 20          | 0.155                                  | 0.010 | 9,200        | 18,264       | 0.33         |
|                 | 73        | 20          | 0.155                                  | 0.010 | 9,200        | 18,264       | 0.33         |
|                 | 74        | 20          | 0.155                                  | 0.010 | 9,200        | 18,264       | 0.33         |
|                 | 75        | 20          | 0.155                                  | 0.010 | 9,200        | 18,264       | 0.33         |
|                 | 76        | 20          | 0.155                                  | 0.010 | 9,200        | 18,264       | 0.33         |
|                 | 77        | 20          | 0.155                                  | 0.010 | 9,200        | 18,264       | 0.33         |
|                 | 78        | 20          | 0.155                                  | 0.010 | 9,200        | 18,264       | 0.33         |

Table 5-1 (4 of 4)

| Soil Type    | Layer No. | Thick. (ft) | $\gamma^{1)}$ (k/ft <sup>3</sup> ) | Damp. | Vs (ft/s) | Vp (ft/s) | $\rho^{2)}$ |
|--------------|-----------|-------------|------------------------------------|-------|-----------|-----------|-------------|
| Rock (cont.) | 79        | 20          | 0.155                              | 0.010 | 9,200     | 18,264    | 0.33        |
|              | 80        | 20          | 0.155                              | 0.010 | 9,200     | 18,264    | 0.33        |
|              | 81        | 20          | 0.155                              | 0.010 | 9,200     | 18,264    | 0.33        |
|              | 82        | 20          | 0.155                              | 0.010 | 9,200     | 18,264    | 0.33        |
|              | 83        | 20          | 0.155                              | 0.010 | 9,200     | 18,264    | 0.33        |
|              | 84        | 20          | 0.155                              | 0.010 | 9,200     | 18,264    | 0.33        |
|              | 85        | 20          | 0.155                              | 0.010 | 9,200     | 18,264    | 0.33        |
|              | 86        | 20          | 0.155                              | 0.010 | 9,200     | 18,264    | 0.33        |
|              | 87        | 20          | 0.155                              | 0.010 | 9,200     | 18,264    | 0.33        |
|              | 88        | 20          | 0.155                              | 0.010 | 9,200     | 18,264    | 0.33        |
|              | 89        | 20          | 0.155                              | 0.010 | 9,200     | 18,264    | 0.33        |
|              | 90        | 20          | 0.155                              | 0.010 | 9,200     | 18,264    | 0.33        |
|              | 91        | 20          | 0.155                              | 0.010 | 9,200     | 18,264    | 0.33        |
|              | 92        | 20          | 0.155                              | 0.010 | 9,200     | 18,264    | 0.33        |
|              | 93        | 20          | 0.155                              | 0.010 | 9,200     | 18,264    | 0.33        |
|              | 94        | 20          | 0.155                              | 0.010 | 9,200     | 18,264    | 0.33        |
|              | 95        | 20          | 0.155                              | 0.010 | 9,200     | 18,264    | 0.33        |
|              | 96        | —           | 0.155                              | 0.004 | 9,200     | 18,264    | 0.33        |

#### Notes

- 1) Unit weight density of soil/rock
- 2) Poisson's Ratio

Table 5-2 (1 of 3)

INCOH Results - Horizontal

(a) Horizontal, Frequency = 1.0 Hz

| MODE        | EIGEN-VALUE | PARTICIPATION FACTOR |          |          |          | CUMULATIVE PERCENT |        |        |        |
|-------------|-------------|----------------------|----------|----------|----------|--------------------|--------|--------|--------|
|             |             | Z                    | XX       | YY       | ZZ       | Z                  | XX     | YY     | ZZ     |
| 1           | 1.32E+03    | 48061.97             | 845.571  | 3847.529 | 4693.099 | 100                | 0.218  | 0.792  | 0.538  |
| 2           | 1.19E-01    | 0                    | 608.961  | 480683.6 | 481292.5 | 100                | 0.376  | 99.789 | 55.685 |
| 3           | 1.03E-01    | 0                    | 385241   | 475.733  | 385716.7 | 100                | 99.874 | 99.887 | 99.881 |
| 4           | 1.65E-02    | 3.09E-09             | 0.10187  | 0.17263  | 0.27449  | 100                | 99.874 | 99.887 | 99.881 |
| 5           | 1.52E-02    | 3.98E-07             | 0.01013  | 0.98738  | 0.99751  | 100                | 99.874 | 99.887 | 99.881 |
| 6           | 9.11E-03    | 6.12E-09             | 0.04332  | 3.17799  | 3.22131  | 100                | 99.874 | 99.888 | 99.882 |
| 7           | 2.46E-03    | 3.58E-15             | 339.4706 | 0.16315  | 339.6338 | 100                | 99.962 | 99.888 | 99.921 |
| 8           | 2.17E-03    | 7.45E-11             | 0.00572  | 417.828  | 417.8337 | 100                | 99.962 | 99.974 | 99.968 |
| 9           | 1.37E-03    | 4.56E-12             | 0.36757  | 120.4476 | 120.8152 | 100                | 99.962 | 99.998 | 99.982 |
| 10          | 1.19E-03    | 3.87E-16             | 140.4027 | 0.06179  | 140.4645 | 100                | 99.998 | 99.998 | 99.998 |
| 11          | 6.47E-04    | 1.31E-11             | 0.00349  | 0.00007  | 0.00356  | 100                | 99.998 | 99.998 | 99.998 |
| 12          | 6.30E-04    | 2.92E-10             | 0.00015  | 0.01408  | 0.01423  | 100                | 99.998 | 99.998 | 99.998 |
| 13          | 3.98E-04    | 3.96E-13             | 0.1725   | 0.00204  | 0.17454  | 100                | 99.998 | 99.998 | 99.998 |
| 14          | 3.65E-04    | 1.20E-12             | 0.00014  | 0.09677  | 0.09691  | 100                | 99.998 | 99.998 | 99.998 |
| 15          | 3.29E-04    | 9.30E-11             | 0.00066  | 0.04859  | 0.04926  | 100                | 99.998 | 99.998 | 99.998 |
| SUMMATIONS: |             | 4.81E+04             | 3.87E+05 | 4.86E+05 | 8.73E+05 |                    |        |        |        |
| TOTAL:      |             | 4.81E+04             | 3.87E+05 | 4.86E+05 | 8.73E+05 |                    |        |        |        |

(b) Horizontal, Frequency = 10.0 Hz

| MODE        | EIGEN-VALUE | PARTICIPATION FACTOR |          |          |          | CUMULATIVE PERCENT |        |        |        |
|-------------|-------------|----------------------|----------|----------|----------|--------------------|--------|--------|--------|
|             |             | Z                    | XX       | YY       | ZZ       | Z                  | XX     | YY     | ZZ     |
| 1           | 8.49E+02    | 38353.26             | 676.061  | 10109.89 | 10785.95 | 99.909             | 0.006  | 0.069  | 0.041  |
| 2           | 1.18E+02    | 0.685                | 17544.28 | 14377796 | 14395340 | 99.911             | 0.153  | 97.891 | 54.116 |
| 3           | 1.05E+02    | 0.001                | 11652642 | 13795.07 | 11666437 | 99.911             | 97.887 | 97.984 | 97.941 |
| 4           | 4.31E+01    | 5.19E-02             | 1595.096 | 116.399  | 1711.495 | 99.911             | 97.901 | 97.985 | 97.947 |
| 5           | 3.71E+01    | 3.02E+01             | 0.17102  | 1722.088 | 1722.259 | 99.99              | 97.901 | 97.997 | 97.954 |
| 6           | 3.02E+01    | 3.00E+00             | 25.73267 | 1516.082 | 1541.815 | 99.998             | 97.901 | 98.007 | 97.96  |
| 7           | 1.71E+01    | 3.46E-04             | 137619.2 | 34.4095  | 137653.6 | 99.998             | 99.055 | 98.007 | 98.477 |
| 8           | 1.56E+01    | 1.59E-01             | 9.94344  | 188827.7 | 188837.7 | 99.998             | 99.055 | 99.292 | 99.186 |
| 9           | 1.21E+01    | 7.54E-03             | 149.2213 | 90549.32 | 90698.55 | 99.998             | 99.056 | 99.908 | 99.527 |
| 10          | 1.04E+01    | 1.04E-05             | 99660.82 | 13.56101 | 99674.38 | 99.998             | 99.892 | 99.908 | 99.901 |
| 11          | 7.51E+00    | 5.87E-02             | 5.65581  | 2.02354  | 7.67936  | 99.998             | 99.892 | 99.908 | 99.901 |
| 12          | 7.45E+00    | 2.52E-01             | 2.61073  | 22.00585 | 24.61659 | 99.999             | 99.892 | 99.909 | 99.901 |
| 13          | 5.38E+00    | 1.26E-03             | 1571.751 | 6.7957   | 1578.547 | 99.999             | 99.906 | 99.909 | 99.907 |
| 14          | 4.61E+00    | 5.93E-02             | 0.00347  | 55.45493 | 55.4584  | 99.999             | 99.906 | 99.909 | 99.907 |
| 15          | 4.29E+00    | 3.06E-01             | 0.01206  | 166.68   | 166.692  | 100                | 99.906 | 99.91  | 99.908 |
| SUMMATIONS: |             | 3.84E+04             | 1.19E+07 | 1.47E+07 | 2.66E+07 |                    |        |        |        |
| TOTAL:      |             | 3.84E+04             | 1.19E+07 | 1.47E+07 | 2.66E+07 |                    |        |        |        |

Table 5-2 (2 of 3)

(c) Horizontal, Frequency = 20.0 Hz

| MODE        | EIGEN-VALUE | PARTICIPATION FACTOR |          |          |          | CUMULATIVE PERCENT |        |        |        |
|-------------|-------------|----------------------|----------|----------|----------|--------------------|--------|--------|--------|
|             |             | Z                    | XX       | YY       | ZZ       | Z                  | XX     | YY     | ZZ     |
| 1           | 3.45E+02    | 24243.5              | 421.141  | 14959.23 | 15380.37 | 99.578             | 0.004  | 0.118  | 0.067  |
| 2           | 9.16E+01    | 3.127                | 16674.5  | 11820376 | 11837051 | 99.591             | 0.165  | 93.484 | 51.479 |
| 3           | 8.32E+01    | 0.005                | 9641401  | 13762.49 | 9655163  | 99.591             | 93.198 | 93.593 | 93.415 |
| 4           | 4.93E+01    | 1.41E-01             | 22240.69 | 551.8312 | 22792.52 | 99.592             | 93.413 | 93.597 | 93.514 |
| 5           | 4.37E+01    | 6.23E+01             | 2.28481  | 9021.694 | 9023.979 | 99.848             | 93.413 | 93.669 | 93.554 |
| 6           | 3.95E+01    | 2.71E+01             | 70.33661 | 5225.4   | 5295.737 | 99.959             | 93.413 | 93.71  | 93.577 |
| 7           | 2.94E+01    | 7.26E-03             | 307366.5 | 1042.449 | 308408.9 | 99.959             | 96.379 | 93.718 | 94.916 |
| 8           | 2.82E+01    | 1.59E+00             | 277.442  | 422869.1 | 423146.5 | 99.965             | 96.382 | 97.058 | 96.754 |
| 9           | 2.52E+01    | 3.54E-02             | 670.9175 | 267245.5 | 267916.4 | 99.966             | 96.389 | 99.169 | 97.918 |
| 10          | 2.17E+01    | 1.98E-03             | 280548.9 | 54.21946 | 280603.1 | 99.966             | 99.096 | 99.17  | 99.136 |
| 11          | 1.97E+01    | 5.60E-04             | 0.04116  | 114.2055 | 114.2466 | 99.966             | 99.096 | 99.171 | 99.137 |
| 12          | 1.85E+01    | 1.67E+00             | 20.42441 | 0.16167  | 20.58607 | 99.972             | 99.096 | 99.171 | 99.137 |
| 13          | 1.61E+01    | 1.65E-02             | 10391.48 | 208.9352 | 10600.41 | 99.972             | 99.196 | 99.172 | 99.183 |
| 14          | 1.51E+01    | 3.54E-01             | 49.40599 | 855.1659 | 904.5719 | 99.974             | 99.197 | 99.179 | 99.187 |
| 15          | 1.40E+01    | 3.56E+00             | 2.92242  | 8049.306 | 8052.229 | 99.989             | 99.197 | 99.243 | 99.222 |
| SUMMATIONS: |             | 2.43E+04             | 1.03E+07 | 1.26E+07 | 2.28E+07 |                    |        |        |        |
| TOTAL:      |             | 2.43E+04             | 1.04E+07 | 1.27E+07 | 2.30E+07 |                    |        |        |        |

(d) Horizontal, Frequency = 30.0 Hz

| MODE        | EIGEN-VALUE | PARTICIPATION FACTOR |          |          |          | CUMULATIVE PERCENT |        |        |        |
|-------------|-------------|----------------------|----------|----------|----------|--------------------|--------|--------|--------|
|             |             | Z                    | XX       | YY       | ZZ       | Z                  | XX     | YY     | ZZ     |
| 1           | 1.76E+02    | 17249.8              | 280.135  | 12872.75 | 13152.89 | 99.448             | 0.004  | 0.135  | 0.076  |
| 2           | 5.25E+01    | 3.381                | 12679.5  | 8747486  | 8760166  | 99.468             | 0.165  | 91.601 | 50.393 |
| 3           | 4.80E+01    | 0.006                | 7130020  | 10787.74 | 7140808  | 99.468             | 91.037 | 91.713 | 91.408 |
| 4           | 3.08E+01    | 1.38E-01             | 33579.95 | 650.4098 | 34230.36 | 99.469             | 91.465 | 91.72  | 91.605 |
| 5           | 2.77E+01    | 4.60E+01             | 13.12859 | 10151.77 | 10164.9  | 99.734             | 91.465 | 91.826 | 91.663 |
| 6           | 2.54E+01    | 3.40E+01             | 54.64258 | 6985.28  | 7039.922 | 99.929             | 91.466 | 91.899 | 91.704 |
| 7           | 2.01E+01    | 7.33E-03             | 286975.5 | 2660.039 | 289635.5 | 99.929             | 95.123 | 91.927 | 93.367 |
| 8           | 1.95E+01    | 1.87E+00             | 1144.612 | 394361.1 | 395505.7 | 99.94              | 95.138 | 96.051 | 95.639 |
| 9           | 1.80E+01    | 2.15E-02             | 1044.081 | 244658.8 | 245702.9 | 99.94              | 95.151 | 98.609 | 97.05  |
| 10          | 1.56E+01    | 6.60E-03             | 268501.6 | 112.2362 | 268613.9 | 99.94              | 98.573 | 98.61  | 98.593 |
| 11          | 1.50E+01    | 4.22E-03             | 61.45854 | 208.6349 | 270.0934 | 99.94              | 98.574 | 98.612 | 98.595 |
| 12          | 1.38E+01    | 1.47E+00             | 89.87461 | 74.23937 | 164.114  | 99.949             | 98.575 | 98.613 | 98.596 |
| 13          | 1.27E+01    | 1.54E-02             | 7592.504 | 488.354  | 8080.858 | 99.949             | 98.672 | 98.618 | 98.642 |
| 14          | 1.21E+01    | 2.66E-01             | 274.1223 | 1796.424 | 2070.546 | 99.95              | 98.675 | 98.637 | 98.654 |
| 15          | 1.15E+01    | 1.69E+00             | 34.11959 | 22236.7  | 22270.82 | 99.96              | 98.676 | 98.869 | 98.782 |
| SUMMATIONS: |             | 1.73E+04             | 7.74E+06 | 9.46E+06 | 1.72E+07 |                    |        |        |        |
| TOTAL:      |             | 1.73E+04             | 7.85E+06 | 9.56E+06 | 1.74E+07 |                    |        |        |        |

Table 5-2 (3 of 3)

(e) Horizontal, Frequency = 40.0 Hz

| MODE        | EIGEN-VALUE | PARTICIPATION FACTOR |          |          |          | CUMULATIVE PERCENT |        |        |        |
|-------------|-------------|----------------------|----------|----------|----------|--------------------|--------|--------|--------|
|             |             | Z                    | XX       | YY       | ZZ       | Z                  | XX     | YY     | ZZ     |
| 1           | 7.67E+01    | 11390.36             | 151.134  | 9336.098 | 9487.232 | 99.347             | 0.003  | 0.142  | 0.079  |
| 2           | 2.48E+01    | 2.922                | 7797.281 | 5907077  | 5914874  | 99.373             | 0.147  | 89.842 | 49.379 |
| 3           | 2.28E+01    | 0.006                | 4799486  | 6899.612 | 4806386  | 99.373             | 88.824 | 89.947 | 89.44  |
| 4           | 1.55E+01    | 1.18E-01             | 42363.47 | 608.5324 | 42972.01 | 99.374             | 89.607 | 89.956 | 89.798 |
| 5           | 1.42E+01    | 2.79E+01             | 58.15663 | 8934.379 | 8992.535 | 99.617             | 89.608 | 90.092 | 89.873 |
| 6           | 1.32E+01    | 3.24E+01             | 10.63865 | 10543.48 | 10554.12 | 99.899             | 89.608 | 90.252 | 89.961 |
| 7           | 1.09E+01    | 4.11E-03             | 235312.7 | 3903.791 | 239216.5 | 99.899             | 93.956 | 90.311 | 91.955 |
| 8           | 1.07E+01    | 1.83E+00             | 2105.876 | 350399.7 | 352505.6 | 99.915             | 93.995 | 95.632 | 94.893 |
| 9           | 1.02E+01    | 8.69E-03             | 1516.173 | 148936.8 | 150452.9 | 99.915             | 94.023 | 97.893 | 96.147 |
| 10          | 8.86E+00    | 2.69E-03             | 9001.319 | 58.45551 | 9059.774 | 99.915             | 94.189 | 97.894 | 96.223 |
| 11          | 8.83E+00    | 2.26E-02             | 205859.9 | 316.4389 | 206176.3 | 99.916             | 97.993 | 97.899 | 97.941 |
| 12          | 8.16E+00    | 1.00E+00             | 348.5914 | 808.735  | 1157.326 | 99.924             | 97.999 | 97.911 | 97.951 |
| 13          | 7.80E+00    | 8.84E-03             | 457.7878 | 1194.363 | 1652.151 | 99.924             | 98.008 | 97.93  | 97.965 |
| 14          | 7.48E+00    | 6.33E-04             | 625.9269 | 12080.11 | 12706.04 | 99.924             | 98.019 | 98.113 | 98.071 |
| 15          | 7.34E+00    | 6.44E-01             | 70.1689  | 12100.52 | 12170.69 | 99.93              | 98.02  | 98.297 | 98.172 |
| SUMMATIONS: |             | 1.15E+04             | 5.31E+06 | 6.47E+06 | 1.18E+07 |                    |        |        |        |
| TOTAL:      |             | 1.15E+04             | 5.41E+06 | 6.59E+06 | 1.20E+07 |                    |        |        |        |

(f) Horizontal, Frequency = 50.0 Hz

| MODE        | EIGEN-VALUE | PARTICIPATION FACTOR |          |          |          | CUMULATIVE PERCENT |        |        |        |
|-------------|-------------|----------------------|----------|----------|----------|--------------------|--------|--------|--------|
|             |             | Z                    | XX       | YY       | ZZ       | Z                  | XX     | YY     | ZZ     |
| 1           | 1.33E+01    | 4702.325             | 0.008    | 5499.483 | 5499.491 | 98.658             | 0      | 0.175  | 0.096  |
| 2           | 5.73E+00    | 1.908                | 601.091  | 2366881  | 2367483  | 98.698             | 0.023  | 75.488 | 41.333 |
| 3           | 5.39E+00    | 0.007                | 1835093  | 691.137  | 1835785  | 98.698             | 70.648 | 75.51  | 73.31  |
| 4           | 4.50E+00    | 1.14E+01             | 631.1243 | 206988.9 | 207620   | 98.938             | 70.672 | 82.096 | 76.926 |
| 5           | 4.32E+00    | 1.87E+01             | 9094.787 | 26202.92 | 35297.71 | 99.331             | 71.022 | 82.93  | 77.541 |
| 6           | 4.24E+00    | 5.17E-01             | 217061.4 | 0.6329   | 217062   | 99.342             | 79.376 | 82.93  | 81.322 |
| 7           | 3.81E+00    | 4.76E+00             | 111065.1 | 66511.31 | 177576.4 | 99.441             | 83.651 | 85.047 | 84.415 |
| 8           | 3.74E+00    | 3.96E+00             | 22954.7  | 120507.3 | 143462   | 99.524             | 84.534 | 88.881 | 86.914 |
| 9           | 3.62E+00    | 2.85E+00             | 15328.51 | 23069.01 | 38397.52 | 99.584             | 85.124 | 89.615 | 87.583 |
| 10          | 3.57E+00    | 1.67E+00             | 138.1512 | 3509.923 | 3648.074 | 99.619             | 85.129 | 89.727 | 87.646 |
| 11          | 3.55E+00    | 1.47E+00             | 38846.49 | 47584.58 | 86431.07 | 99.65              | 86.624 | 91.241 | 89.152 |
| 12          | 3.51E+00    | 3.79E-06             | 43742.92 | 95.53992 | 43838.46 | 99.65              | 88.308 | 91.244 | 89.915 |
| 13          | 3.41E+00    | 4.43E-03             | 2716.295 | 1414.086 | 4130.38  | 99.65              | 88.412 | 91.289 | 89.987 |
| 14          | 3.36E+00    | 3.07E-01             | 4668.249 | 48284.76 | 52953.01 | 99.657             | 88.592 | 92.825 | 90.909 |
| 15          | 3.33E+00    | 7.77E-01             | 5830.066 | 802.9065 | 6632.973 | 99.673             | 88.816 | 92.851 | 91.025 |
| SUMMATIONS: |             | 4.75E+03             | 2.31E+06 | 2.92E+06 | 5.23E+06 |                    |        |        |        |
| TOTAL:      |             | 4.77E+03             | 2.60E+06 | 3.14E+06 | 5.74E+06 |                    |        |        |        |



Table 5-3 (1 of 3)

INCOH Results - Vertical

(a) Vertical, Frequency = 1.0 Hz

| MODE   | EIGEN-VALUE | PARTICIPATION FACTOR |          |          |          | CUMULATIVE PERCENT |        |        |        |
|--------|-------------|----------------------|----------|----------|----------|--------------------|--------|--------|--------|
|        |             | Z                    | XX       | YY       | ZZ       | Z                  | XX     | YY     | ZZ     |
| 1      | 1.32E+03    | 48062.11             | 845.576  | 3846.043 | 4691.619 | 100                | 0.292  | 1.057  | 0.718  |
| 2      | 6.71E-02    | 0                    | 451.067  | 359653.9 | 360105   | 100                | 0.447  | 99.874 | 55.797 |
| 3      | 5.83E-02    | 0                    | 288372.1 | 351.57   | 288723.7 | 100                | 99.944 | 99.971 | 99.959 |
| 4      | 1.05E-02    | 8.53E-10             | 1.02633  | 0.17069  | 1.19702  | 100                | 99.945 | 99.971 | 99.959 |
| 5      | 9.49E-03    | 9.96E-08             | 0.02217  | 1.47512  | 1.49729  | 100                | 99.945 | 99.971 | 99.959 |
| 6      | 5.17E-03    | 1.32E-09             | 0.01024  | 4.41502  | 4.42525  | 100                | 99.945 | 99.972 | 99.96  |
| 7      | 4.41E-04    | 6.68E-14             | 154.1602 | 1.12339  | 155.2836 | 100                | 99.998 | 99.973 | 99.984 |
| 8      | 2.58E-04    | 6.05E-17             | 0        | 0.00108  | 0.00108  | 100                | 99.998 | 99.973 | 99.984 |
| 9      | 2.56E-04    | 8.67E-13             | 0.00001  | 14.58438 | 14.58439 | 100                | 99.998 | 99.977 | 99.986 |
| 10     | 2.56E-04    | 3.96E-18             | 0        | 0.00007  | 0.00007  | 100                | 99.998 | 99.977 | 99.986 |
| 11     | 2.56E-04    | 1.89E-16             | 0        | 0.00317  | 0.00317  | 100                | 99.998 | 99.977 | 99.986 |
| 12     | 2.56E-04    | 1.43E-18             | 0        | 0.00002  | 0.00002  | 100                | 99.998 | 99.977 | 99.986 |
| 13     | 2.56E-04    | 8.64E-17             | 0        | 0.00143  | 0.00143  | 100                | 99.998 | 99.977 | 99.986 |
| 14     | 2.56E-04    | 5.52E-18             | 0        | 0.00009  | 0.00009  | 100                | 99.998 | 99.977 | 99.986 |
| 15     | 2.56E-04    | 1.28E-22             | 0        | 0        | 0        | 100                | 99.998 | 99.977 | 99.986 |
| SUM:   |             | 4.81E+04             | 2.90E+05 | 3.64E+05 | 6.54E+05 |                    |        |        |        |
| TOTAL: |             | 4.81E+04             | 2.90E+05 | 3.64E+05 | 6.54E+05 |                    |        |        |        |

(b) Vertical, Frequency = 10.0 Hz

| MODE   | EIGEN-VALUE | PARTICIPATION FACTOR |          |          |          | CUMULATIVE PERCENT |        |        |        |
|--------|-------------|----------------------|----------|----------|----------|--------------------|--------|--------|--------|
|        |             | Z                    | XX       | YY       | ZZ       | Z                  | XX     | YY     | ZZ     |
| 1      | 8.24E+02    | 37738.77             | 664.723  | 11113.02 | 11777.75 | 99.882             | 0.005  | 0.073  | 0.043  |
| 2      | 1.27E+02    | 0.877                | 17897.76 | 14977162 | 14995059 | 99.884             | 0.15   | 98.241 | 54.336 |
| 3      | 1.12E+02    | 0.001                | 12127285 | 14013.46 | 12141299 | 99.884             | 98.252 | 98.333 | 98.297 |
| 4      | 4.36E+01    | 5.47E-02             | 926.2077 | 92.4951  | 1018.703 | 99.884             | 98.259 | 98.334 | 98.3   |
| 5      | 3.67E+01    | 3.89E+01             | 0.38246  | 1468.329 | 1468.712 | 99.987             | 98.259 | 98.343 | 98.306 |
| 6      | 2.95E+01    | 3.91E+00             | 21.71158 | 1546.521 | 1568.233 | 99.998             | 98.259 | 98.353 | 98.311 |
| 7      | 1.55E+01    | 2.83E-04             | 120804.6 | 18.65786 | 120823.3 | 99.998             | 99.237 | 98.353 | 98.749 |
| 8      | 1.39E+01    | 1.66E-01             | 20.05946 | 160854.8 | 160874.9 | 99.998             | 99.237 | 99.408 | 99.331 |
| 9      | 1.03E+01    | 7.14E-03             | 119.6594 | 81873.05 | 81992.71 | 99.998             | 99.238 | 99.944 | 99.628 |
| 10     | 8.87E+00    | 4.32E-06             | 86044.06 | 12.3334  | 86056.39 | 99.998             | 99.934 | 99.945 | 99.94  |
| 11     | 6.04E+00    | 3.06E-01             | 0.00406  | 29.04362 | 29.04767 | 99.999             | 99.934 | 99.945 | 99.94  |
| 12     | 5.93E+00    | 9.37E-03             | 11.8822  | 1.38529  | 13.26748 | 99.999             | 99.934 | 99.945 | 99.94  |
| 13     | 4.15E+00    | 9.64E-04             | 1033.033 | 3.2689   | 1036.302 | 99.999             | 99.942 | 99.945 | 99.944 |
| 14     | 3.42E+00    | 6.03E-02             | 0.02454  | 28.12761 | 28.15215 | 99.999             | 99.942 | 99.945 | 99.944 |
| 15     | 3.18E+00    | 2.62E-01             | 0.10925  | 93.42087 | 93.53012 | 100                | 99.942 | 99.946 | 99.944 |
| SUM:   |             | 3.78E+04             | 1.24E+07 | 1.52E+07 | 2.76E+07 |                    |        |        |        |
| TOTAL: |             | 3.78E+04             | 1.24E+07 | 1.53E+07 | 2.76E+07 |                    |        |        |        |

Table 5-3 (2 of 3)

(c) Vertical, Frequency = 20.0 Hz

| MODE        | EIGEN-VALUE | PARTICIPATION FACTOR |          |          |          | CUMULATIVE PERCENT |        |        |        |
|-------------|-------------|----------------------|----------|----------|----------|--------------------|--------|--------|--------|
|             |             | Z                    | XX       | YY       | ZZ       | Z                  | XX     | YY     | ZZ     |
| 1           | 3.42E+02    | 23991.18             | 424.111  | 20335.2  | 20759.31 | 99.33              | 0.004  | 0.149  | 0.084  |
| 2           | 1.07E+02    | 5.079                | 17678.86 | 12816477 | 12834156 | 99.351             | 0.162  | 93.951 | 51.747 |
| 3           | 9.69E+01    | 0.008                | 10462583 | 14462.53 | 10477045 | 99.351             | 93.755 | 94.057 | 93.921 |
| 4           | 5.61E+01    | 1.73E-01             | 18190.24 | 500.2161 | 18690.46 | 99.351             | 93.918 | 94.061 | 93.997 |
| 5           | 4.87E+01    | 9.57E+01             | 0.00317  | 8705.818 | 8705.821 | 99.747             | 93.918 | 94.124 | 94.032 |
| 6           | 4.38E+01    | 4.71E+01             | 75.09215 | 7136.58  | 7211.672 | 99.943             | 93.919 | 94.177 | 94.061 |
| 7           | 3.15E+01    | 1.17E-02             | 310698.2 | 513.9933 | 311212.2 | 99.943             | 96.698 | 94.18  | 95.313 |
| 8           | 2.99E+01    | 2.45E+00             | 55.22288 | 419091.3 | 419146.5 | 99.953             | 96.699 | 97.248 | 97.001 |
| 9           | 2.61E+01    | 5.46E-02             | 530.1361 | 289011.2 | 289541.3 | 99.953             | 96.703 | 99.363 | 98.166 |
| 10          | 2.24E+01    | 1.51E-03             | 288354.7 | 37.11927 | 288391.8 | 99.953             | 99.283 | 99.363 | 99.327 |
| 11          | 1.96E+01    | 5.46E-05             | 28.72722 | 64.58576 | 93.31298 | 99.953             | 99.283 | 99.364 | 99.327 |
| 12          | 1.87E+01    | 2.59E+00             | 7.67512  | 38.16717 | 45.84228 | 99.964             | 99.283 | 99.364 | 99.328 |
| 13          | 1.56E+01    | 2.29E-02             | 10446.72 | 125.9579 | 10572.68 | 99.964             | 99.377 | 99.365 | 99.37  |
| 14          | 1.44E+01    | 5.76E-01             | 12.90948 | 563.8406 | 576.7501 | 99.966             | 99.377 | 99.369 | 99.372 |
| 15          | 1.33E+01    | 5.69E+00             | 0.18258  | 3235.971 | 3236.154 | 99.99              | 99.377 | 99.393 | 99.386 |
| SUMMATIONS: |             | 2.42E+04             | 1.11E+07 | 1.36E+07 | 2.47E+07 |                    |        |        |        |
| TOTAL:      |             | 2.42E+04             | 1.12E+07 | 1.37E+07 | 2.48E+07 |                    |        |        |        |

(d) Vertical, Frequency = 30.0 Hz

| MODE        | EIGEN-VALUE | PARTICIPATION FACTOR |          |          |          | CUMULATIVE PERCENT |        |        |        |
|-------------|-------------|----------------------|----------|----------|----------|--------------------|--------|--------|--------|
|             |             | Z                    | XX       | YY       | ZZ       | Z                  | XX     | YY     | ZZ     |
| 1           | 1.84E+02    | 17444.11             | 297.76   | 22148.32 | 22446.08 | 98.928             | 0.003  | 0.202  | 0.113  |
| 2           | 6.95E+01    | 7.461                | 15005.49 | 9992415  | 10007420 | 98.97              | 0.17   | 91.46  | 50.309 |
| 3           | 6.35E+01    | 0.012                | 8163067  | 12707.01 | 8175774  | 98.971             | 91.004 | 91.576 | 91.318 |
| 4           | 4.08E+01    | 2.03E-01             | 34686.3  | 716.9716 | 35403.28 | 98.972             | 91.39  | 91.582 | 91.495 |
| 5           | 3.61E+01    | 7.81E+01             | 2.8711   | 11335.66 | 11338.54 | 99.415             | 91.39  | 91.686 | 91.552 |
| 6           | 3.31E+01    | 7.96E+01             | 84.04466 | 12003.42 | 12087.47 | 99.866             | 91.391 | 91.795 | 91.613 |
| 7           | 2.58E+01    | 2.03E-02             | 329165.8 | 1838.513 | 331004.3 | 99.866             | 95.053 | 91.812 | 93.273 |
| 8           | 2.49E+01    | 3.99E+00             | 566.9417 | 428165.7 | 428732.6 | 99.889             | 95.06  | 95.722 | 95.424 |
| 9           | 2.26E+01    | 4.20E-02             | 946.0785 | 333234.9 | 334180.9 | 99.889             | 95.07  | 98.766 | 97.1   |
| 10          | 1.95E+01    | 6.80E-03             | 323814.6 | 77.98925 | 323892.6 | 99.889             | 98.673 | 98.766 | 98.724 |
| 11          | 1.82E+01    | 4.12E-03             | 7.59452  | 210.9296 | 218.5241 | 99.889             | 98.673 | 98.768 | 98.726 |
| 12          | 1.70E+01    | 3.14E+00             | 50.96982 | 0.00006  | 50.96988 | 99.907             | 98.674 | 98.768 | 98.726 |
| 13          | 1.52E+01    | 3.51E-02             | 12722.14 | 331.4841 | 13053.62 | 99.907             | 98.816 | 98.771 | 98.791 |
| 14          | 1.43E+01    | 7.41E-01             | 112.281  | 1098.638 | 1210.919 | 99.912             | 98.817 | 98.781 | 98.797 |
| 15          | 1.33E+01    | 5.63E+00             | 19.97653 | 19787.79 | 19807.76 | 99.944             | 98.817 | 98.962 | 98.897 |
| SUMMATIONS: |             | 1.76E+04             | 8.88E+06 | 1.08E+07 | 1.97E+07 |                    |        |        |        |
| TOTAL:      |             | 1.76E+04             | 8.99E+06 | 1.10E+07 | 1.99E+07 |                    |        |        |        |

Table 5-3 (3 of 3)

(e) Vertical, Frequency = 40.0 Hz

| MODE        | EIGEN-VALUE | PARTICIPATION FACTOR |          |          |          | CUMULATIVE PERCENT |        |        |        |
|-------------|-------------|----------------------|----------|----------|----------|--------------------|--------|--------|--------|
|             |             | Z                    | XX       | YY       | ZZ       | Z                  | XX     | YY     | ZZ     |
| 1           | 1.16E+02    | 13805.98             | 222.552  | 22082.7  | 22305.25 | 98.628             | 0.003  | 0.242  | 0.134  |
| 2           | 4.85E+01    | 8.661                | 12812.7  | 8179456  | 8192269  | 98.69              | 0.174  | 89.864 | 49.398 |
| 3           | 4.45E+01    | 0.016                | 6676960  | 11135.2  | 6688095  | 98.69              | 89.166 | 89.986 | 89.616 |
| 4           | 3.00E+01    | 2.09E-01             | 44925.49 | 803.7979 | 45729.29 | 98.691             | 89.764 | 89.995 | 89.891 |
| 5           | 2.69E+01    | 6.05E+01             | 12.31138 | 11582.21 | 11594.52 | 99.123             | 89.764 | 90.121 | 89.96  |
| 6           | 2.48E+01    | 9.44E+01             | 79.78685 | 15753.87 | 15833.66 | 99.798             | 89.766 | 90.294 | 90.056 |
| 7           | 2.01E+01    | 2.22E-02             | 314982   | 3241.511 | 318223.5 | 99.798             | 93.964 | 90.33  | 91.969 |
| 8           | 1.95E+01    | 4.73E+00             | 1243.398 | 399492.8 | 400736.2 | 99.832             | 93.98  | 94.707 | 94.379 |
| 9           | 1.81E+01    | 2.24E-02             | 1291.82  | 329026.8 | 330318.6 | 99.832             | 93.997 | 98.312 | 96.365 |
| 10          | 1.56E+01    | 1.42E-02             | 318230.3 | 126.7995 | 318357.1 | 99.832             | 98.239 | 98.313 | 98.28  |
| 11          | 1.50E+01    | 1.05E-02             | 244.6884 | 301.6312 | 546.3196 | 99.832             | 98.242 | 98.317 | 98.283 |
| 12          | 1.39E+01    | 3.06E+00             | 110.616  | 20.03252 | 130.6486 | 99.854             | 98.244 | 98.317 | 98.284 |
| 13          | 1.28E+01    | 3.67E-02             | 10857.81 | 508.9235 | 11366.73 | 99.854             | 98.388 | 98.322 | 98.352 |
| 14          | 1.21E+01    | 7.33E-01             | 265.7582 | 1502.36  | 1768.118 | 99.859             | 98.392 | 98.339 | 98.363 |
| 15          | 1.14E+01    | 3.39E+00             | 50.28389 | 28135.76 | 28186.04 | 99.884             | 98.393 | 98.647 | 98.532 |
| SUMMATIONS: |             | 1.40E+04             | 7.38E+06 | 9.00E+06 | 1.64E+07 |                    |        |        |        |
| TOTAL:      |             | 1.40E+04             | 7.50E+06 | 9.13E+06 | 1.66E+07 |                    |        |        |        |

(f) Vertical, Frequency = 50.0 Hz

| MODE        | EIGEN-VALUE | PARTICIPATION FACTOR |          |          |          | CUMULATIVE PERCENT |        |        |        |
|-------------|-------------|----------------------|----------|----------|----------|--------------------|--------|--------|--------|
|             |             | Z                    | XX       | YY       | ZZ       | Z                  | XX     | YY     | ZZ     |
| 1           | 8.12E+01    | 11499.51             | 172.608  | 21637.13 | 21809.74 | 98.377             | 0.003  | 0.275  | 0.152  |
| 2           | 3.62E+01    | 9.373                | 11145.86 | 6961925  | 6973071  | 98.457             | 0.175  | 88.672 | 48.719 |
| 3           | 3.33E+01    | 0.018                | 5676524  | 9896.435 | 5686420  | 98.457             | 87.75  | 88.798 | 88.325 |
| 4           | 2.32E+01    | 2.09E-01             | 51733.97 | 838.5909 | 52572.56 | 98.459             | 88.548 | 88.809 | 88.691 |
| 5           | 2.10E+01    | 4.82E+01             | 28.4533  | 11121.76 | 11150.21 | 98.871             | 88.549 | 88.95  | 88.769 |
| 6           | 1.93E+01    | 1.01E+02             | 71.88129 | 18820.82 | 18892.7  | 99.735             | 88.55  | 89.189 | 88.9   |
| 7           | 1.60E+01    | 2.21E-02             | 297344.3 | 4367.455 | 301711.8 | 99.736             | 93.137 | 89.244 | 91.002 |
| 8           | 1.56E+01    | 5.15E+00             | 1819.41  | 371469.7 | 373289.1 | 99.78              | 93.165 | 93.961 | 93.602 |
| 9           | 1.47E+01    | 9.21E-03             | 1578.926 | 314107   | 315685.9 | 99.78              | 93.19  | 97.949 | 95.8   |
| 10          | 1.27E+01    | 2.36E-02             | 304740.2 | 188.415  | 304928.6 | 99.78              | 97.891 | 97.952 | 97.924 |
| 11          | 1.24E+01    | 1.48E-02             | 1429.911 | 327.2047 | 1757.116 | 99.78              | 97.913 | 97.956 | 97.936 |
| 12          | 1.15E+01    | 2.87E+00             | 182.4033 | 59.20523 | 241.6086 | 99.805             | 97.916 | 97.956 | 97.938 |
| 13          | 1.07E+01    | 3.55E-02             | 8270.616 | 656.3473 | 8926.964 | 99.805             | 98.043 | 97.965 | 98     |
| 14          | 1.02E+01    | 6.68E-01             | 419.3389 | 1934.856 | 2354.195 | 99.811             | 98.05  | 97.989 | 98.017 |
| 15          | 9.73E+00    | 2.47E+00             | 60.431   | 29117.52 | 29177.95 | 99.832             | 98.051 | 98.359 | 98.22  |
| SUMMATIONS: |             | 1.17E+04             | 6.36E+06 | 7.75E+06 | 1.41E+07 |                    |        |        |        |
| TOTAL:      |             | 1.17E+04             | 6.48E+06 | 7.88E+06 | 1.44E+07 |                    |        |        |        |

Table 5-4

Frequencies of Analysis – Incoherent

| No. | SASSI Freq. No.   | Frequency f (Hz) | No. | SASSI Freq. No.    | Frequency f (Hz) | No. | SASSI Freq. No. | Frequency f (Hz) |
|-----|-------------------|------------------|-----|--------------------|------------------|-----|-----------------|------------------|
| 1   | 1                 | 0.0122           | 31  | 1004               | 12.256           | 61  | 3066            | 37.427           |
| 2   | 28                | 0.3418           | 32  | 1054               | 12.866           | 62  | 3156            | 38.525           |
| 3   | 54                | 0.6592           | 33  | 1104               | 13.477           | 63  | 3246            | 39.624           |
| 4   | 104               | 1.2695           | 34  | 1154               | 14.087           | 64  | 3336            | 40.723           |
| 5   | 154               | 1.8799           | 35  | 1204               | 14.697           | 65  | 3426            | 41.821           |
| 6   | 187               | 2.2827           | 36  | 1254               | 15.308           | 66  | 3516            | 42.920           |
| 7   | 229               | 2.7954           | 37  | 1304               | 15.918           | 67  | 3606            | 44.019           |
| 8   | 279               | 3.4058           | 38  | 1354               | 16.528           | 68  | 3696            | 45.117           |
| 9   | 304               | 3.7109           | 39  | 1404               | 17.139           | 69  | 3786            | 46.216           |
| 10  | 354               | 4.3213           | 40  | 1500 <sup>2)</sup> | 18.311           | 70  | 3878            | 47.339           |
| 11  | 379 <sup>1)</sup> | 4.6265           | 41  | 1596               | 19.482           | 71  | 3966            | 48.413           |
| 12  | 404               | 4.9316           | 42  | 1692               | 20.654           | 72  | 4056            | 49.512           |
| 13  | 429               | 5.2368           | 43  | 1740               | 21.240           | 73  | 4146            | 50.610           |
| 14  | 454               | 5.5420           | 44  | 1788               | 21.826           | 74  | 4219            | 51.501           |
| 15  | 479               | 5.8472           | 45  | 1836               | 22.412           | 75  | 4342            | 53.003           |
| 16  | 504               | 6.1523           | 46  | 1884               | 22.998           | 76  | 4465            | 54.504           |
| 17  | 529               | 6.4575           | 47  | 1932               | 23.584           | 77  | 4588            | 56.006           |
| 18  | 554               | 6.7627           | 48  | 1980               | 24.170           | 78  | 4834            | 59.009           |
| 19  | 579               | 7.0679           | 49  | 2028               | 24.756           | 79  | 4957            | 60.510           |
| 20  | 604               | 7.3730           | 50  | 2076               | 25.342           | 80  | 5079            | 62.000           |
| 21  | 629               | 7.6782           | 51  | 2166               | 26.440           | 81  | 5202            | 63.501           |
| 22  | 654               | 7.9834           | 52  | 2256               | 27.539           | 82  | 5325            | 65.002           |
| 23  | 679               | 8.2886           | 53  | 2346               | 28.638           | 83  | 5448            | 66.504           |
| 24  | 704               | 8.5938           | 54  | 2438               | 29.761           | 84  | 5571            | 68.005           |
| 25  | 754               | 9.2041           | 55  | 2526               | 30.835           | 85  | 5694            | 69.507           |
| 26  | 804               | 9.8145           | 56  | 2616               | 31.934           | 86  | 5817            | 71.008           |
| 27  | 854               | 10.4248          | 57  | 2706               | 33.032           |     |                 |                  |
| 28  | 904               | 11.0352          | 58  | 2796               | 34.131           |     |                 |                  |
| 29  | 954               | 11.6455          | 59  | 2886               | 35.229           |     |                 |                  |
| 30  | 979               | 11.9507          | 60  | 2976 <sup>3)</sup> | 36.328           |     |                 |                  |

## Notes:

- 1) 379 was removed for Mode 3, X-input, uncracked case, because it was an unstable frequency.
- 2) 1500 was removed for Modes 8 and 9, X-input, uncracked case, because it was an unstable frequency.
- 3) 2976 was removed for Mode 8, Y-input, uncracked case, because it was an unstable frequency.

Table 6-1

Comparison of Design Force and Moment for PSW

Unit: kips/ft, kips-ft/ft

| Location   | CSDRS             |                   |              |                    | HRHF Response Spectra |                   |         |               |
|------------|-------------------|-------------------|--------------|--------------------|-----------------------|-------------------|---------|---------------|
| North Wall | $M\phi^{1)}$      | $M\theta^{2)}$    | $N\phi^{3)}$ | $N\theta^{4)}$     | $M\phi$               | $M\theta$         | $N\phi$ | $N\theta$     |
|            | 157.9<br>(-195.9) | 111.3<br>(-77.9)  | 26.5         | 60.0               | 163.7<br>(-138.3)     | 44.5<br>(-62.6)   | 28.5    | 66.8          |
|            | $Q\phi^{5)}$      | $Q\theta^{6)}$    | $QT^{7)}$    | $M\phi\theta^{8)}$ | $Q\phi$               | $Q\theta$         | $QT$    | $M\phi\theta$ |
|            | -74.8             | -89.2             | 127.4        | -117.6             | -77.3                 | -92.4             | 144.3   | -133.3        |
| East Wall  | $M\phi$           | $M\theta$         | $N\phi$      | $N\theta$          | $M\phi$               | $M\theta$         | $N\phi$ | $N\theta$     |
|            | 680.7<br>(-616.1) | 352.1<br>(-351.4) | 108.8        | 184.5              | 695.0<br>(-630.4)     | 419.2<br>(-423.0) | 120.9   | 221.7         |
|            | $Q\phi$           | $Q\theta$         | $QT$         | $M\phi\theta$      | $Q\phi$               | $Q\theta$         | $QT$    | $M\phi\theta$ |
|            | -139.7            | -135.2            | 99.6         | -213.9             | -150.2                | -158.0            | 105.2   | -230.6        |
| East Wall  | $M\phi$           | $M\theta$         | $N\phi$      | $N\theta$          | $M\phi$               | $M\theta$         | $N\phi$ | $N\theta$     |
|            | 162.4<br>(-144.2) | 46.6<br>(-64.0)   | 33.0         | 50.6               | 182.2<br>(-146.8)     | 55.4<br>(-63.4)   | 36.2    | 57.0          |
|            | $Q\phi$           | $Q\theta$         | $QT$         | $M\phi\theta$      | $Q\phi$               | $Q\theta$         | $QT$    | $M\phi\theta$ |
|            | -76.3             | -74.5             | 108.5        | -106.3             | -78.5                 | 80.4              | 122.8   | -124.0        |

Notes:

- 1)  $M\phi$  - Meridional Moment around Horizontal Axis
- 2)  $M\theta$  - Hoop Moment around Vertical Axis
- 3)  $N\phi$  - Meridional Axial Force (+ : Tension, - : Compression)
- 4)  $N\theta$  - Hoop Axial Force (+ : Tension, - : Compression)
- 5)  $Q\phi$  - Meridional Transverse Shear Force
- 6)  $Q\theta$  - Hoop Transverse Shear Force
- 7)  $QT$  - Tangential Shear Force (In-plane Shear Force)
- 8)  $M\phi\theta$  - Torsion Moment

Table 6-2

Comparison of Design Force and Moment for IRWST

Unit: kips/ft, kips-ft/ft

| Location   | CSDRS           |                |              |                    | HRHF Response Spectra |                |         |               |
|------------|-----------------|----------------|--------------|--------------------|-----------------------|----------------|---------|---------------|
| Top Slab   | $M\phi^{1)}$    | $M\theta^{2)}$ | $N\phi^{3)}$ | $N\theta^{4)}$     | $M\phi$               | $M\theta$      | $N\phi$ | $N\theta$     |
|            | 60.2<br>(-19.7) | 12.6<br>(-9.3) | 45.5         | 15.4               | 60.2<br>(-20.1)       | 12.5<br>(-9.2) | 50.0    | 17.5          |
|            | $Q\phi^{5)}$    | $Q\theta^{6)}$ | $QT^{7)}$    | $M\phi\theta^{8)}$ | $Q\phi$               | $Q\theta$      | $QT$    | $M\phi\theta$ |
|            | 17.5            | 15.7           | 16.3         | -5.6               | 19.1                  | 17.1           | 19.6    | -5.6          |
| Outer wall | $M\phi$         | $M\theta$      | $N\phi$      | $N\theta$          | $M\phi$               | $M\theta$      | $N\phi$ | $N\theta$     |
|            | 50.3<br>(-51.7) | 11.6<br>(-7.5) | -65.3        | 70.2               | 50.3<br>(-51.7)       | 11.6<br>(-7.5) | -65.3   | 70.2          |
|            | $Q\phi$         | $Q\theta$      | $QT$         | $M\phi\theta$      | $Q\phi$               | $Q\theta$      | $QT$    | $M\phi\theta$ |
|            | 47.8            | 3.7            | 10.5         | -4.0               | 47.8                  | 4.4            | 11.7    | -4.0          |

Notes:

- 1)  $M\phi$  - Meridional Moment around Horizontal Axis
- 2)  $M\theta$  - Hoop Moment around Vertical Axis
- 3)  $N\phi$  - Meridional Axial Force (+ : Tension, - : Compression)
- 4)  $N\theta$  - Hoop Axial Force (+ : Tension, - : Compression)
- 5)  $Q\phi$  - Meridional Transverse Shear Force
- 6)  $Q\theta$  - Hoop Transverse Shear Force
- 7)  $QT$  - Tangential Shear Force (In-plane Shear Force)
- 8)  $M\phi\theta$  - Torsion Moment

Table 6-3 (1 of 2)

Comparison of Design Force and Moment for SSW

Unit: kips/ft, kips-ft/ft

| Location            | CSDRS               |                    |                      |                       | HRHF Response Spectra |                   |                      |                       |
|---------------------|---------------------|--------------------|----------------------|-----------------------|-----------------------|-------------------|----------------------|-----------------------|
| SSW <sup>(9)</sup>  | Mφ <sup>1)</sup>    | Mθ <sup>2)</sup>   | Nφ <sup>3)</sup>     | Nθ <sup>4)</sup>      | Mφ                    | Mθ                | Nφ                   | Nθ                    |
|                     | 130.9<br>(-119.8)   | 240.3<br>(-130.3)  | 88.4                 | 154.4                 | 136.5<br>(-125.4)     | 265.9<br>(-155.7) | 90.8                 | 159.6                 |
|                     | Qφ <sup>5)</sup>    | Qθ <sup>6)</sup>   | QT <sup>7)</sup>     | Mφθ <sup>8)</sup>     | Qφ                    | Qθ                | QT                   | Mφθ                   |
|                     | -35.3               | 54.0               | -128.2               | -71.2                 | -36.5                 | 59.1              | -136.1               | -78.3                 |
| RFP <sup>(10)</sup> | Mφ                  | Mθ                 | Nφ                   | Nθ                    | Mφ                    | Mθ                | Nφ                   | Nθ                    |
|                     | 1521.6<br>(-1304.2) | 949.7<br>(-1038.2) | 215.6                | 344.1                 | 1389.5<br>(-1165.9)   | 897.3<br>(-978.6) | 222.4                | 319.7                 |
|                     | Qφ                  | Qθ                 | QT                   | Mφθ                   | Qφ                    | Qθ                | QT                   | Mφθ                   |
|                     | 232.5               | 415.5              | -158.8               | 673.6                 | 213.8                 | 377.2             | -165.8               | 633.4                 |
| RFP <sup>(11)</sup> | Mφ                  | Mθ                 | Nφ                   | Nθ                    | Mφ                    | Mθ                | Nφ                   | Nθ                    |
|                     | 89.1<br>(-74.3)     | 306.8<br>(-255.6)  | 40.4                 | 365.6                 | 105.7<br>(-90.6)      | 295.7<br>(-244.5) | 43.7                 | 366.3                 |
|                     | Qφ                  | Qθ                 | QT                   | Mφθ                   | Qφ                    | Qθ                | QT                   | Mφθ                   |
|                     | 32.7                | -72.3              | -108.9               | 53.5                  | 31.5                  | -71.0             | -105.7               | 51.7                  |
| SG <sup>(12)</sup>  | Mφ                  | Mθ                 | Nφ                   | Nθ                    | Mφ                    | Mθ                | Nφ                   | Nθ                    |
|                     | 430.3<br>(-335.7)   | 492.3<br>(-407.3)  | 399.2                | 199.4                 | 407.5<br>(-313.6)     | 513.1<br>(-421.7) | 379.6                | 208.6                 |
|                     | Qφ                  | Qθ                 | QT                   | Mφθ                   | Qφ                    | Qθ                | QT                   | Mφθ                   |
|                     | 114.1               | 92.2               | 61.7(g)<br>-111.4(h) | -220.2(g)<br>280.3(h) | 111.7                 | 92.3              | 58.1(g)<br>-108.3(h) | -221.5(g)<br>275.1(h) |

Table 6-3 (2 of 2)

| Location            | CSDRS             |                   |   |  | HRHF Response Spectra |                   |  |  |
|---------------------|-------------------|-------------------|---|--|-----------------------|-------------------|--|--|
| SG <sup>(13)</sup>  | M $\phi$          | M $\theta$        | N $\phi$                                      | N $\theta$                                       | M $\phi$              | M $\theta$        | N $\phi$                                       | N $\theta$                                       |
|                     | 743.5<br>(-685.3) | 703.4<br>(-603.5) | 85.1  | 211.5  | 895.1<br>(-784.0)     | 610.1<br>(-713.0) | 20.5   | 168.7  |
|                     | Q $\phi$          | Q $\theta$        | QT  | M $\phi\theta$                                   | Q $\phi$              | Q $\theta$        | QT   | M $\phi\theta$                                   |
|                     | -171.4            | -149.5            | 57.2 <sup>(15)</sup><br>116.5 <sup>(16)</sup> | -446.0 <sup>(15)</sup><br>-324.0 <sup>(16)</sup> | -158.9                | -140.5            | 71.7 <sup>(15)</sup><br>-131.6 <sup>(16)</sup> | -362.4 <sup>(15)</sup><br>-346.9 <sup>(16)</sup> |
| PZR <sup>(14)</sup> | M $\phi$          | M $\theta$        | N $\phi$                                      | N $\theta$                                       | M $\phi$              | M $\theta$        | N $\phi$                                       | N $\theta$                                       |
|                     | 21.2<br>(-15.7)   | 178.8<br>(-244.7) | 173.7   | 89.6   | 21.5<br>(-16.5)       | 197.5<br>(-205.0) | 177.9  | 169.2  |
|                     | Q $\phi$          | Q $\theta$        | QT  | M $\phi\theta$                                   | Q $\phi$              | Q $\theta$        | QT   | M $\phi\theta$                                   |
|                     | -1.2              | -92.3             | 135.7 <sup>(15)</sup><br>95.2 <sup>(16)</sup> | 16.3 <sup>(15)</sup><br>-69.7 <sup>(16)</sup>    | -1.3                  | -96.3             | 138.9 <sup>(15)</sup><br>118.7 <sup>(16)</sup> | -17.1 <sup>(15)</sup><br>-26.6 <sup>(16)</sup>   |

Notes:

- 1) M $\phi$  - Meridional Moment around Horizontal Axis
- 2) M $\theta$  - Hoop Moment around Vertical Axis
- 3) N $\phi$  - Meridional Axial Force (+ : Tension, - : Compression)
- 4) N $\theta$  - Hoop Axial Force (+ : Tension, - : Compression)
- 5) Q $\phi$  - Meridional Transverse Shear Force
- 6) Q $\theta$  - Hoop Transverse Shear Force
- 7) QT - Tangential Shear Force (In-plane Shear Force)
- 8) M $\phi\theta$  - Torsion Moment
- 9) Secondary Shield Wall (Thickness 4 feet)
- 10) South/North Wall of Refueling pool (Thickness 6 feet 2 inches)
- 11) West Wall of Refueling pool (Thickness 5 feet)
- 12) Circular Wall of Steam Generator (S/G) Enclosure (Thickness 4 feet)
- 13) Straight Wall of Steam Generator (S/G) Enclosure (Thickness 5 feet)
- 14) Pressurizer (PZR) Enclosure Wall (Thickness 2 feet 9 inches)
- 15) These forces are considered with N $\phi$  and M $\phi$  when designing vertical re-bar
- 16) These forces are considered with N $\theta$  and M $\theta$  when designing horizontal re-bar



Table 6-4

Comparison of Design Force and Moment for Containment Structure

| Location | Elevation   |          | CSDRS               |                        |                       |                          | HRHF Response Spectra |                        |                       |                          |
|----------|-------------|----------|---------------------|------------------------|-----------------------|--------------------------|-----------------------|------------------------|-----------------------|--------------------------|
|          | Bottom (ft) | Top (ft) | $N_{\phi}$ (kip/ft) | $M_{\phi}$ (kip-ft/ft) | $N_{\theta}$ (kip/ft) | $M_{\theta}$ (kip-ft/ft) | $N_{\phi}$ (kip/ft)   | $M_{\phi}$ (kip-ft/ft) | $N_{\theta}$ (kip/ft) | $M_{\theta}$ (kip-ft/ft) |
| RCB-1    | 78'-0"      | 103'-0"  | 694.33              | 254.56                 | 306.00                | 50.42                    | 462.93                | 167.78                 | 212.05                | 34.27                    |
| RCB-2    | 103'-0"     | 143'-0"  | 598.84              | 64.69                  | 300.47                | 40.56                    | 400.43                | 44.94                  | 209.42                | 38.69                    |
| RCB-3    | 143'-0"     | 157'-6"  | 503.42              | 158.60                 | 280.95                | 85.44                    | 342.62                | 112.57                 | 203.42                | 51.43                    |
| RCB-4    | 157'-6"     | 197'-6"  | 471.44              | 117.51                 | 272.82                | 47.37                    | 317.36                | 79.04                  | 191.96                | 31.65                    |
| RCB-5    | 197'-6"     | 228'-0"  | 305.13              | 55.19                  | 221.56                | 52.64                    | 216.83                | 36.39                  | 148.83                | 28.71                    |
| RCB-6    | 228'-0"     | 254'-6"  | 272.38              | 126.76                 | 223.21                | 144.11                   | 196.83                | 94.80                  | 156.34                | 95.69                    |

Notes:

- 1)  $N_{\phi}$  - Meridional Force
- 2)  $M_{\phi}$  - Meridional Moment
- 3)  $N_{\theta}$  - Hoop Force
- 4)  $M_{\theta}$  - Hoop Moment

Table 6-5

Comparison of Equivalent Accelerations for Auxiliary Building

| Location  | Elevation (ft) |         | CSDRS      |            |            | HRHF Response Spectra |            |            |
|-----------|----------------|---------|------------|------------|------------|-----------------------|------------|------------|
|           | Bottom         | Top     | Acc. X (g) | Acc. Y (g) | Acc. Z (g) | Acc. X (g)            | Acc. Y (g) | Acc. Z (g) |
| AB-FHA: 1 | 213'-6"        | 226'-6" | 1.39       | 1.84       | 0.75       | 1.04                  | 1.50       | 0.73       |
| AB-FHA: 2 | 213'-0"        | 213'-6" | 1.60       | 1.05       | 0.61       | 1.02                  | 0.83       | 0.44       |
| AB-FHA: 3 | 195'-0"        | 213'-0" | 1.33       | 1.27       | 0.34       | 0.86                  | 0.96       | 0.47       |
| AB-MCR: 1 | 195'-0"        | 213'-0" | 1.48       | 1.12       | 0.77       | 1.34                  | 0.90       | 0.61       |
| AB: 1     | 174'-0"        | 195'-0" | 1.00       | 1.07       | 0.49       | 0.58                  | 0.69       | 0.39       |
| AB: 2     | 156'-0"        | 174'-0" | 0.71       | 0.96       | 0.51       | 0.54                  | 0.69       | 0.42       |
| AB: 3     | 137'-6"        | 156'-0" | 0.60       | 0.77       | 0.50       | 0.45                  | 0.46       | 0.41       |
| AB: 4     | 120'-0"        | 137'-6" | 0.62       | 0.71       | 0.45       | 0.39                  | 0.50       | 0.41       |
| AB: 5     | 98'-6"         | 120'-0" | 0.51       | 0.64       | 0.42       | 0.33                  | 0.45       | 0.33       |
| AB: 6     | 77'-0"         | 98'-6"  | 0.33       | 0.47       | 0.34       | 0.25                  | 0.33       | 0.30       |
| AB: 7     | 67'-0"         | 77'-0"  | 0.27       | 0.31       | 0.31       | 0.23                  | 0.27       | 0.27       |
| AB: 8     | 55'-0"         | 67'-0"  | 0.26       | 0.26       | 0.31       | 0.23                  | 0.23       | 0.24       |

Table 6-6

Comparison of Equivalent Accelerations for EDGB/DFOT room

| Location  | Elevation (ft) | CSDRS      |            |            | HRHF Response Spectra |            |            |
|-----------|----------------|------------|------------|------------|-----------------------|------------|------------|
|           |                | Acc. X (g) | Acc. Y (g) | Acc. Z (g) | Acc. X (g)            | Acc. Y (g) | Acc. Z (g) |
| DFOT Room | 63             | 0.48       | 0.37       | 0.38       | 0.53                  | 0.60       | 0.46       |
| DFOT Room | 100            | 0.81       | 0.90       | 0.45       | 0.53                  | 0.65       | 0.72       |
| EDGB      | 100            | 0.59       | 0.49       | 0.33       | 0.60                  | 0.48       | 0.35       |
| EDGB      | 135            | 0.82       | 0.82       | 0.45       | 0.86                  | 0.74       | 0.56       |

Table 6-7

## Comparison of Design Force and Moment for RCS Component Supports

| Load Interface <sup>3)</sup> |     | Description                     | HRHF <sup>1),2)</sup> | Design Loads <sup>2)</sup> |
|------------------------------|-----|---------------------------------|-----------------------|----------------------------|
| RV                           | H   | Upper Lateral Support           | 1160                  | 3190                       |
|                              | Fa  | Column Base                     | 11                    | 30                         |
|                              | Fb  |                                 | 946                   | 1900                       |
|                              | Fc  |                                 | 288                   | 390                        |
|                              | Ma  |                                 | 250                   | 400                        |
|                              | Mb  |                                 | 632                   | 970                        |
|                              | Mc  |                                 | 115                   | 280                        |
| SG                           | Y1  | Sliding Vertical Pad            | 620                   | 880                        |
|                              | Y2  |                                 | 1146                  | 1610                       |
|                              | Y3  |                                 | 820                   | 1170                       |
|                              | Y4  |                                 | 1201                  | 1610                       |
|                              | Z11 | Lower Key                       | 737                   | 950                        |
|                              | Z12 |                                 | 737                   | 950                        |
|                              | X   | Snubber Assembly (per Snubber)  | 1055                  | 1910                       |
|                              | S   |                                 | 228                   | 400                        |
|                              | Z1  | Upper Key                       | 1048                  | 1500                       |
|                              | Z2  |                                 | 1048                  | 1500                       |
| RCP                          | V1  | Vertical Column Support         | 134                   | 200                        |
|                              | V2  |                                 | 134                   | 200                        |
|                              | V3  |                                 | 134                   | 200                        |
|                              | V4  |                                 | 134                   | 200                        |
|                              | R1  | Lower Horizontal Column Support | 98                    | 150                        |
|                              | R2  |                                 | 98                    | 150                        |
|                              | R3  | Upper Horizontal Column Support | 220                   | 410                        |
|                              | R4  |                                 | 220                   | 410                        |
|                              | P   | Snubber (Pair)                  | 502                   | 810                        |
| PZR                          | Fv  | Skirt Flange                    | 258                   | 380                        |
|                              | Fh  |                                 | 314                   | 410                        |
|                              | Mt  |                                 | 1160                  | 1750                       |
|                              | Mb  |                                 | 6224                  | 8880                       |
|                              | Fk  | Key                             | 389                   | 570                        |

Notes : 1) The maximum loads from HRHF seismic analyses are as-calculated values.

2) Units are [kips] for forces and [ft-kips] for moments.

3) For load designation, refer to Figures 6-4 ~ 6-7.

Table 6-8

Comparison of Design Force and Moment RCS Component Nozzles

| Location   | Case <sup>1)</sup> | Nozzle Loads <sup>2),3)</sup> |     |     |      |      |      |
|------------|--------------------|-------------------------------|-----|-----|------|------|------|
|            |                    | Fa                            | Fb  | Fc  | Ma   | Mb   | Mc   |
| RV Inlet   | HRHF               | 131                           | 41  | 120 | 250  | 164  | 186  |
|            | Design Loads       | 180                           | 80  | 170 | 530  | 480  | 340  |
| RV outlet  | HRHF               | 725                           | 324 | 85  | 218  | 553  | 1907 |
|            | Design Loads       | 1500                          | 540 | 340 | 680  | 2600 | 3700 |
| SG Inlet   | HRHF               | 759                           | 84  | 237 | 375  | 2339 | 571  |
|            | Design Loads       | 1500                          | 360 | 480 | 1600 | 3400 | 1800 |
| SG outlet  | HRHF               | 22                            | 95  | 21  | 286  | 162  | 380  |
|            | Design Loads       | 30                            | 130 | 40  | 390  | 230  | 490  |
| RCP Inlet  | HRHF               | 27                            | 71  | 75  | 129  | 262  | 296  |
|            | Design Loads       | 40                            | 90  | 100 | 190  | 370  | 410  |
| RCP outlet | HRHF               | 171                           | 38  | 10  | 105  | 135  | 547  |
|            | Design Loads       | 240                           | 70  | 20  | 130  | 210  | 880  |

Notes:

- 1) The maximum loads from HRHF seismic analyses are as-calculated values.
- 2) Units are [kips] for forces and [ft-kips] for moments.
- 3) For load designation, refer to Figures 6-8 ~ 6-10

Table 6-9

Comparison of Design Force and Moment for Reactor Coolant System Loop Piping

TS

Table 6-9 (Cont'd)

Comparison of Design Force and Moment for Reactor Coolant System Loop Piping

TS

Table 6-10

Comparison of Stress Analysis Results for Class 1 Piping Systems

TS



Table 6-11

Comparison of Stress Analysis Results for Class 2 Piping Systems

TS

Table 6-12

Comparison of Design Moment for Surge Line

TS

Table 6-12 (Cont'd)

Comparison of Design Moment for Surge Line

TS

Table 6-12 (Cont'd)

Comparison of Design Moment for Surge Line

TS

Table 6-13

Potentially HF Sensitive Component

- Electro-mechanical relays (e.g., control relays, time delay relays, protective relays)
- Electro-mechanical contactors (e.g., Motor Control Center(MCC) starter)
- Circuit breakers (e.g., molded case and power breaker – low and medium voltage)
- Auxiliary contacts (e.g., for Molded Case Circuit Breaker (MCCBs), fused disconnects, contactors/starters)
- Control switches (e.g., benchboard panel, operator switches)
- Transfer switches (e.g., low and medium voltage switches with instrumentation)
- Process switches and sensors (e.g., pressure/diff. pressure, temperature, level, limit/position, and flow)
- Potentiometers
- Digital solid-state devices (mounting and connections only)
- microprocessors-based components
- Connectors and connections (including circuit board connections for digital and analog equipment)
- Unrestrained components

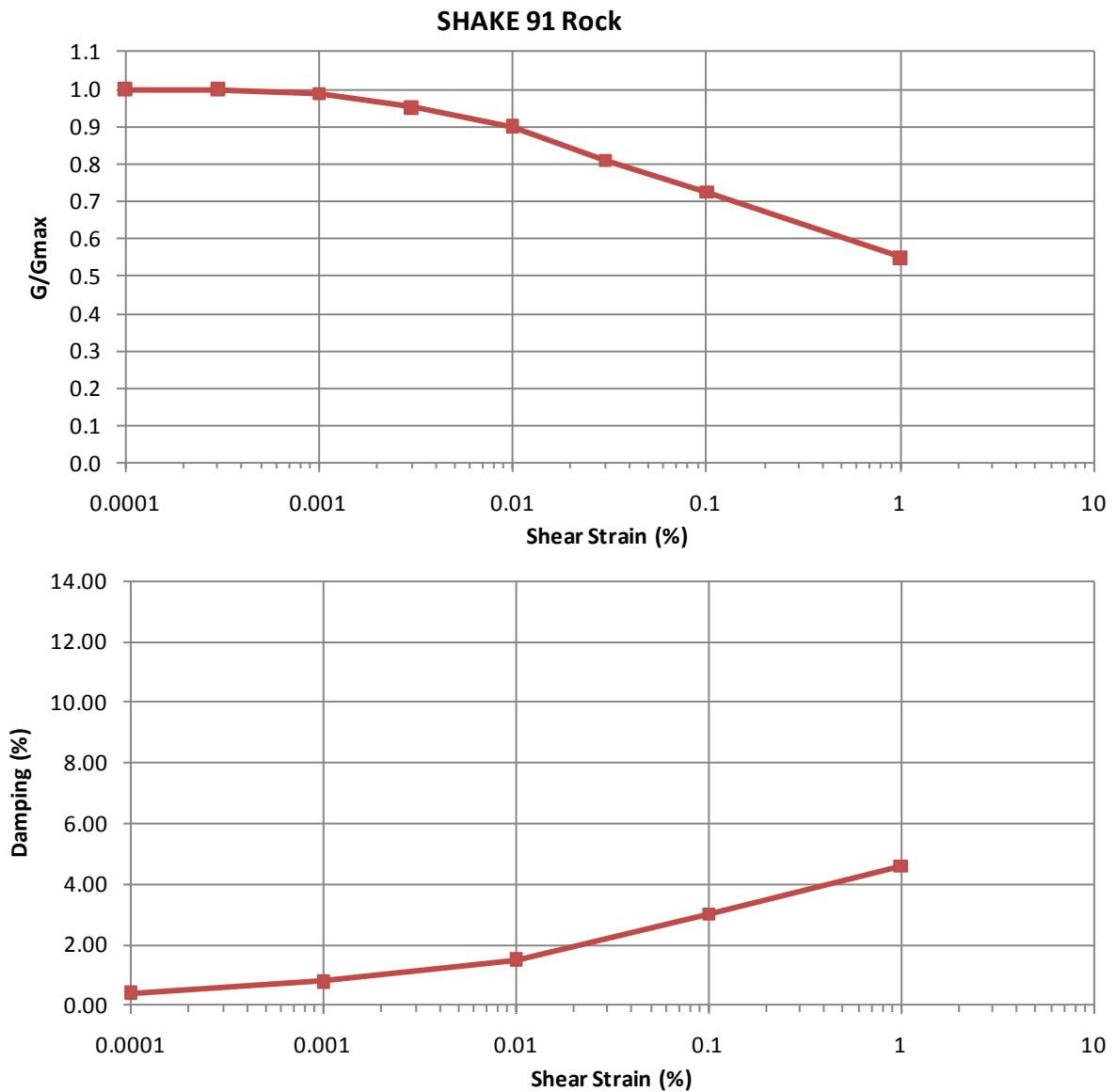


**Figure 2-1 Shear-modulus-degradation and Damping-value Variation Curves for Rock Considered for HRHF**

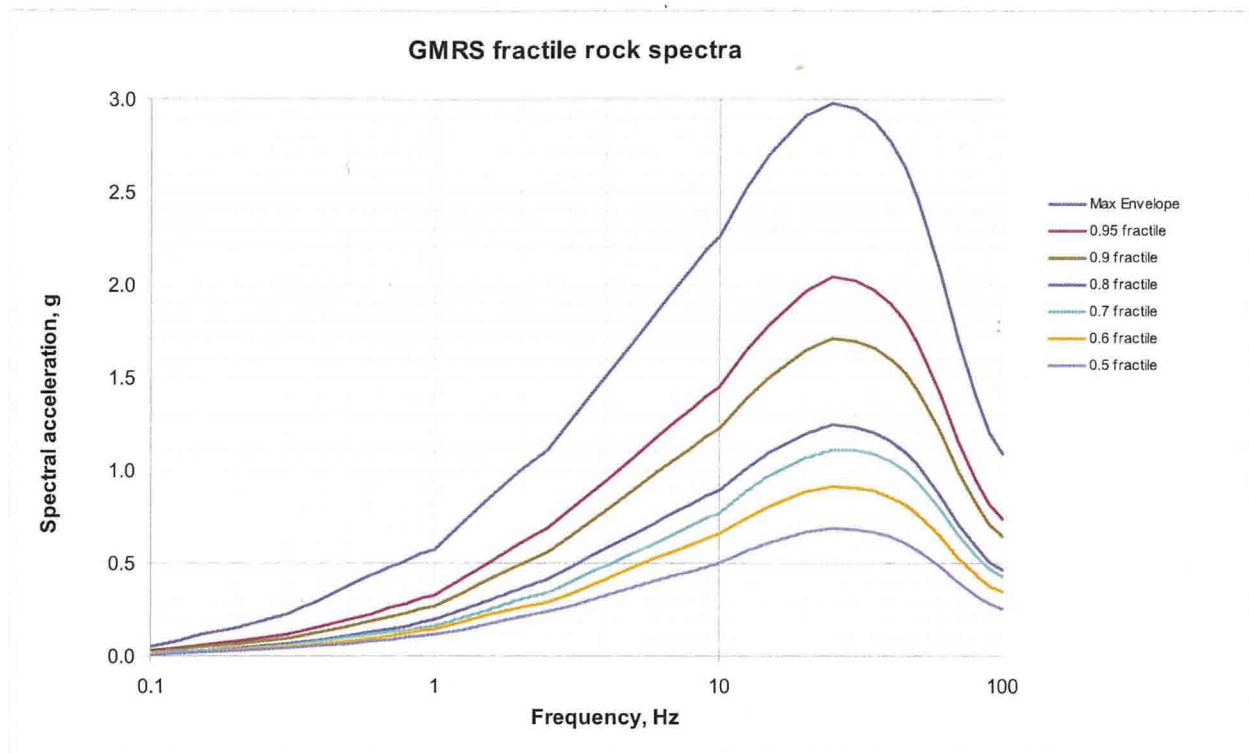


**Figure 3-1 5%-Damped Maximum and Fractile Hard Rock Composite Envelope Spectra  
Developed for 60 Existing CEUS Nuclear Power Plant Sites**

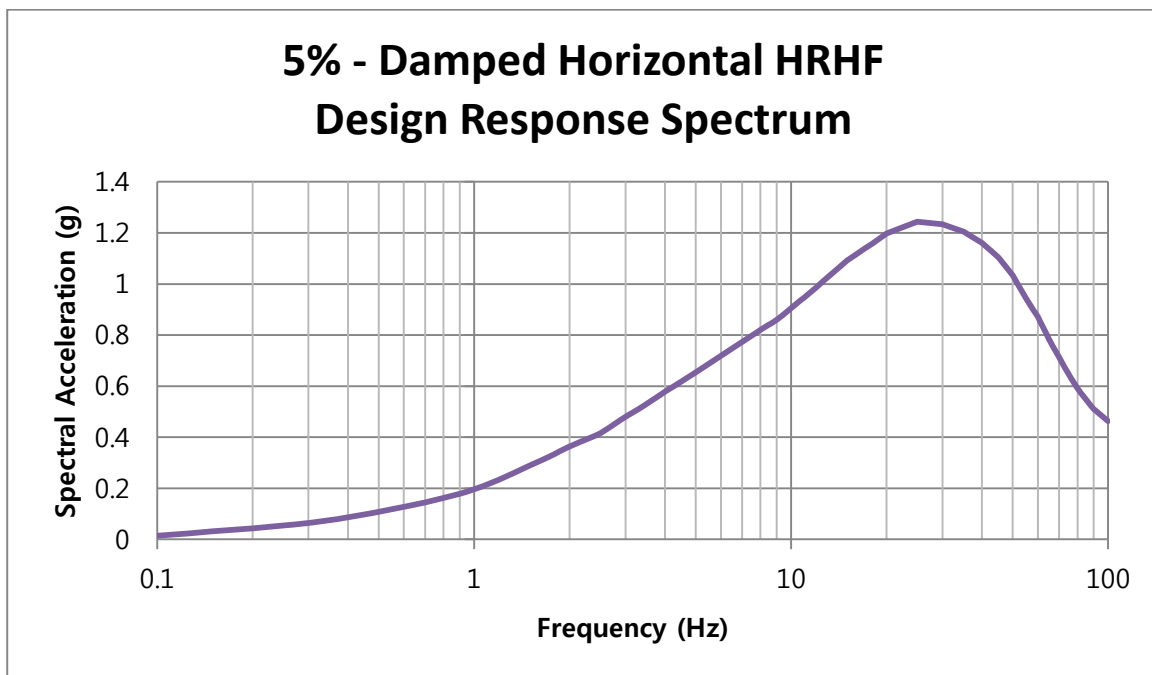


**Figure 3-2 APR1400 HRHF Response Spectrum for 5% Damping Ratio - Horizontal**



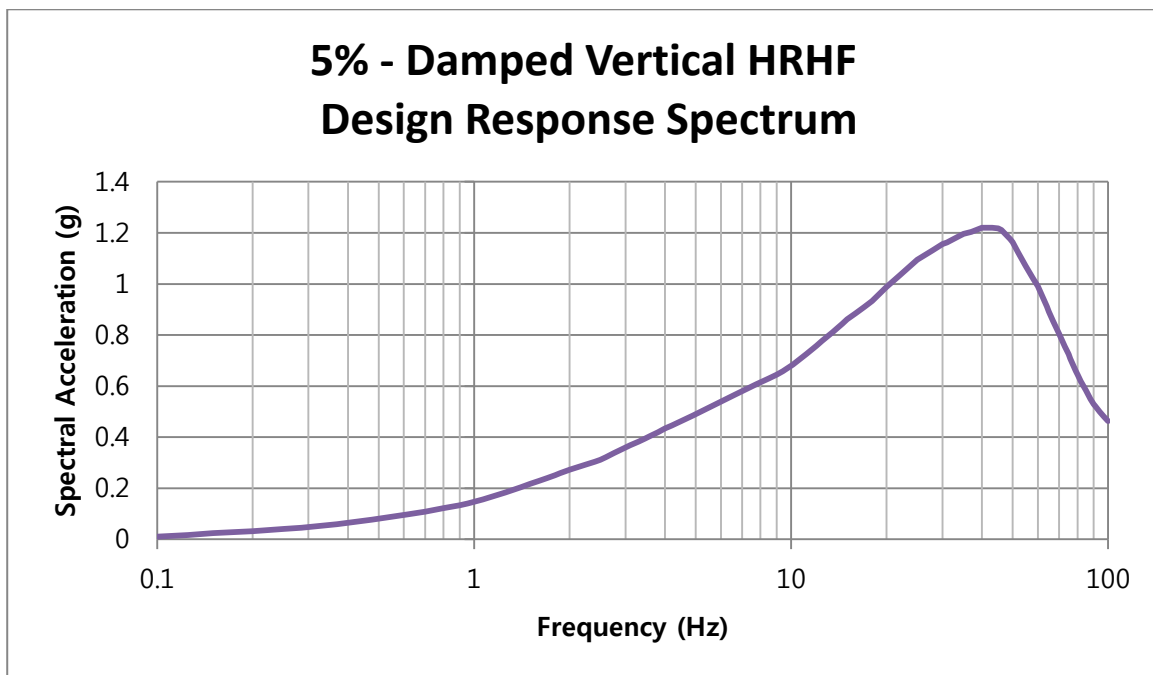


**Figure 3-3 APR1400 HRHF Response Spectrum for 5% Damping Ratio - Vertical**

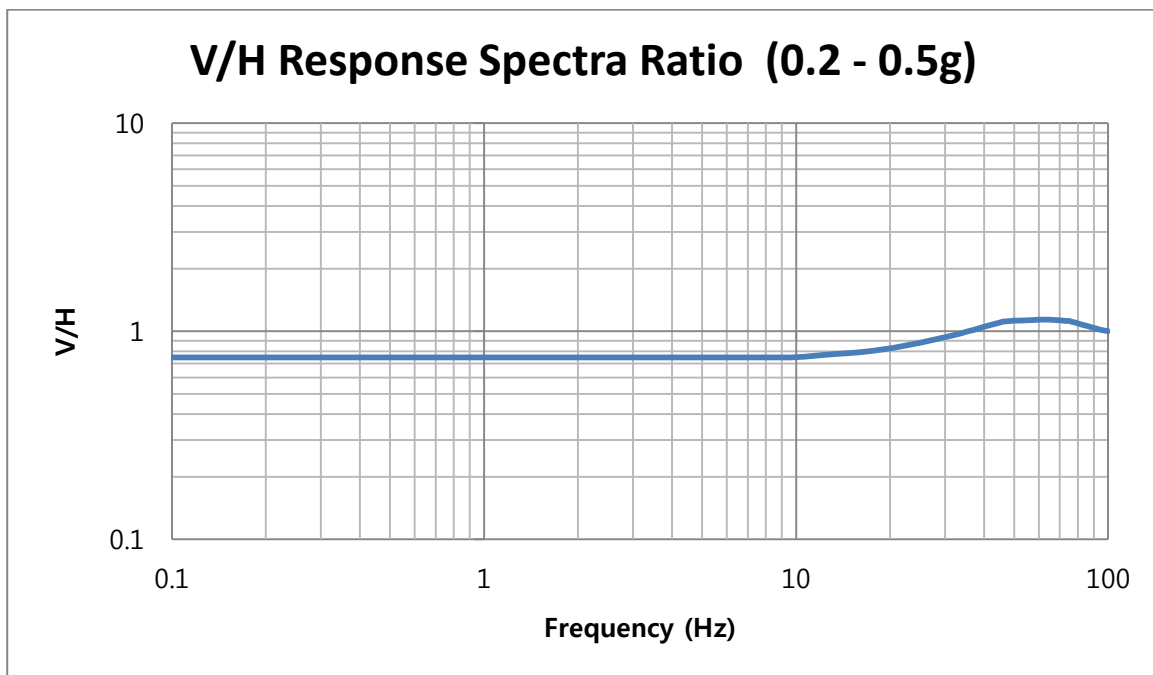


**Figure 3-4 V/H Response Spectra Ratios (0.2 – 0.5g)**

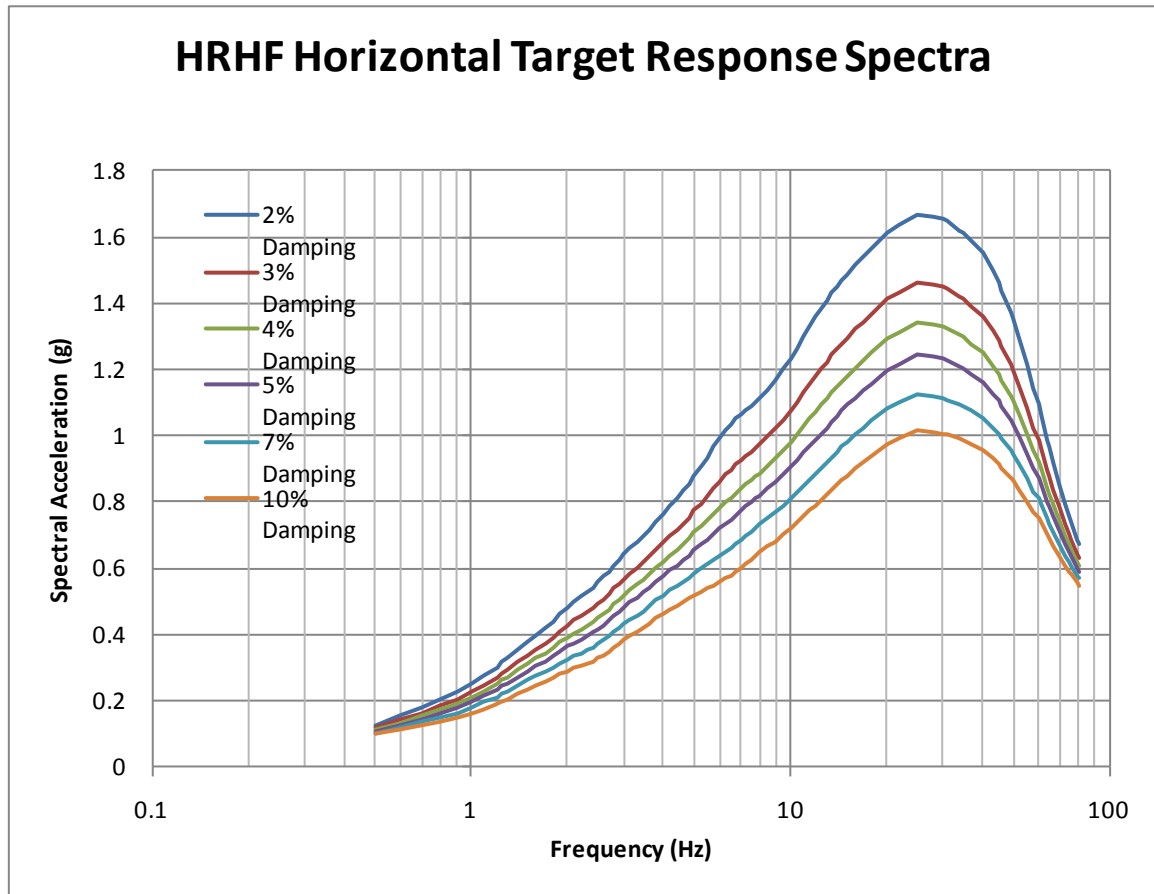
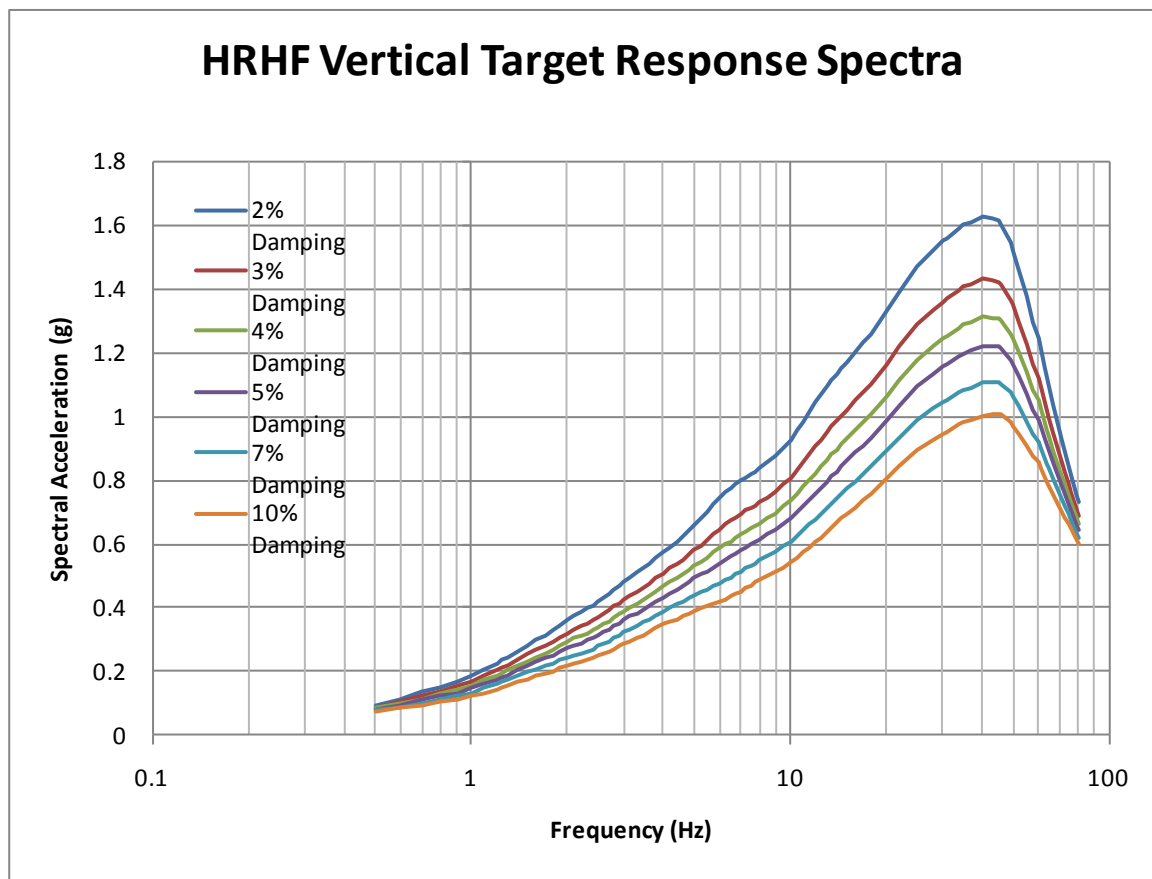


Figure 3-5 APR1400 HRHF Response Spectra for 2, 3, 4, 5, 7, and 10% Damping Ratios - Horizontal



**Figure 3-6 APR1400 HRHF Response Spectra for 2, 3, 4, 5, 7, and 10% Damping Ratios - Vertical**

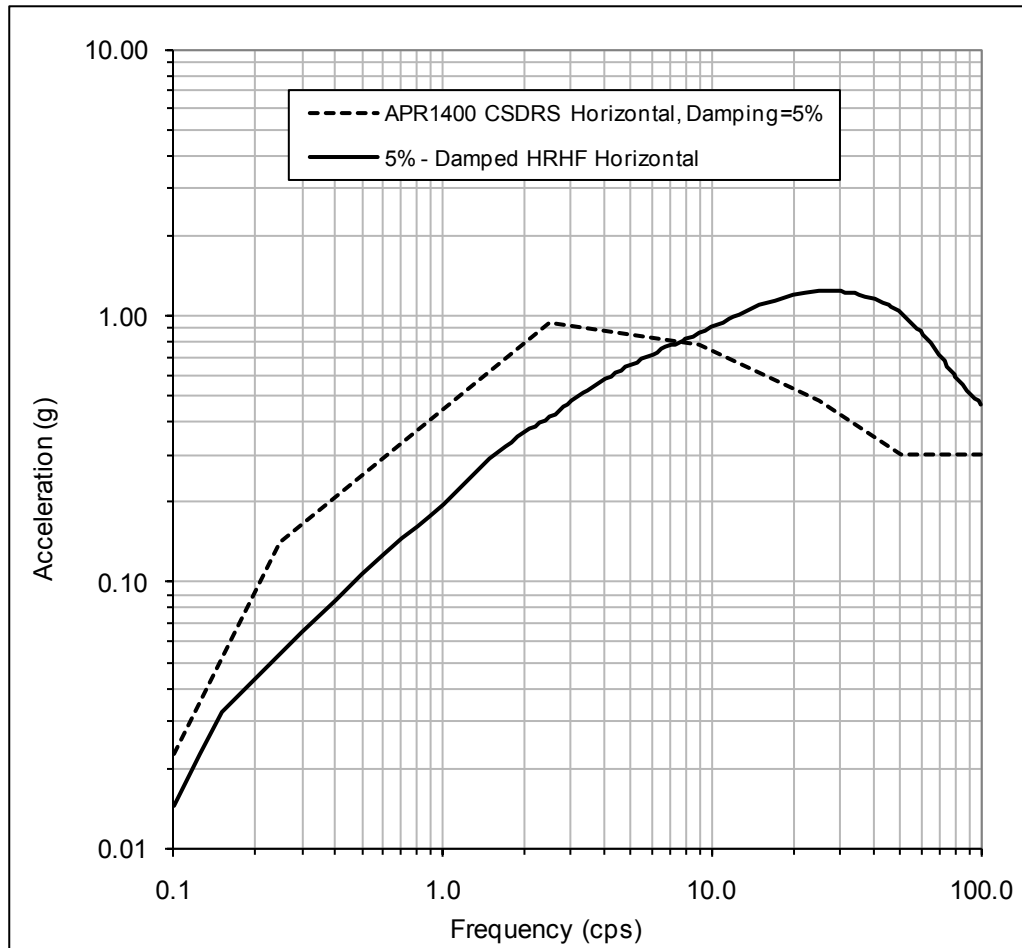


Figure 3-7 APR1400 HRHF Response Spectrum vs CSDRS for 5% Damping Ratio - Horizontal

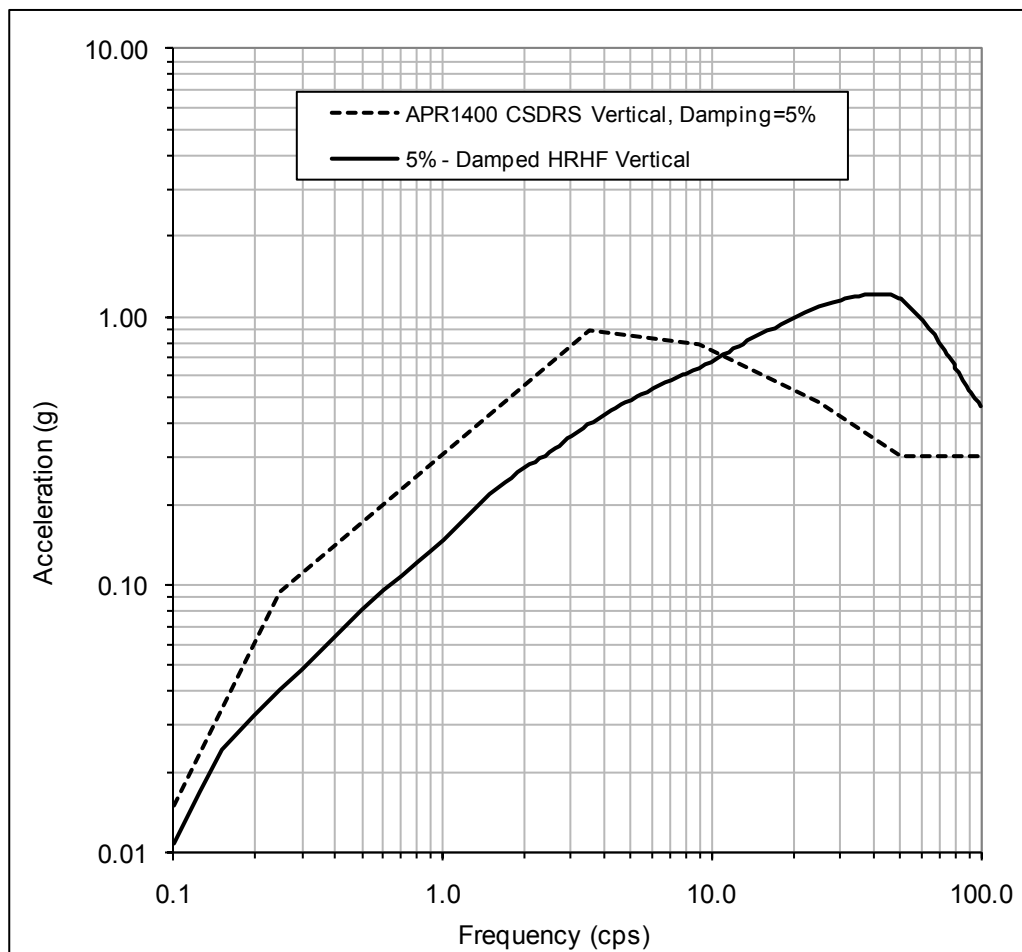
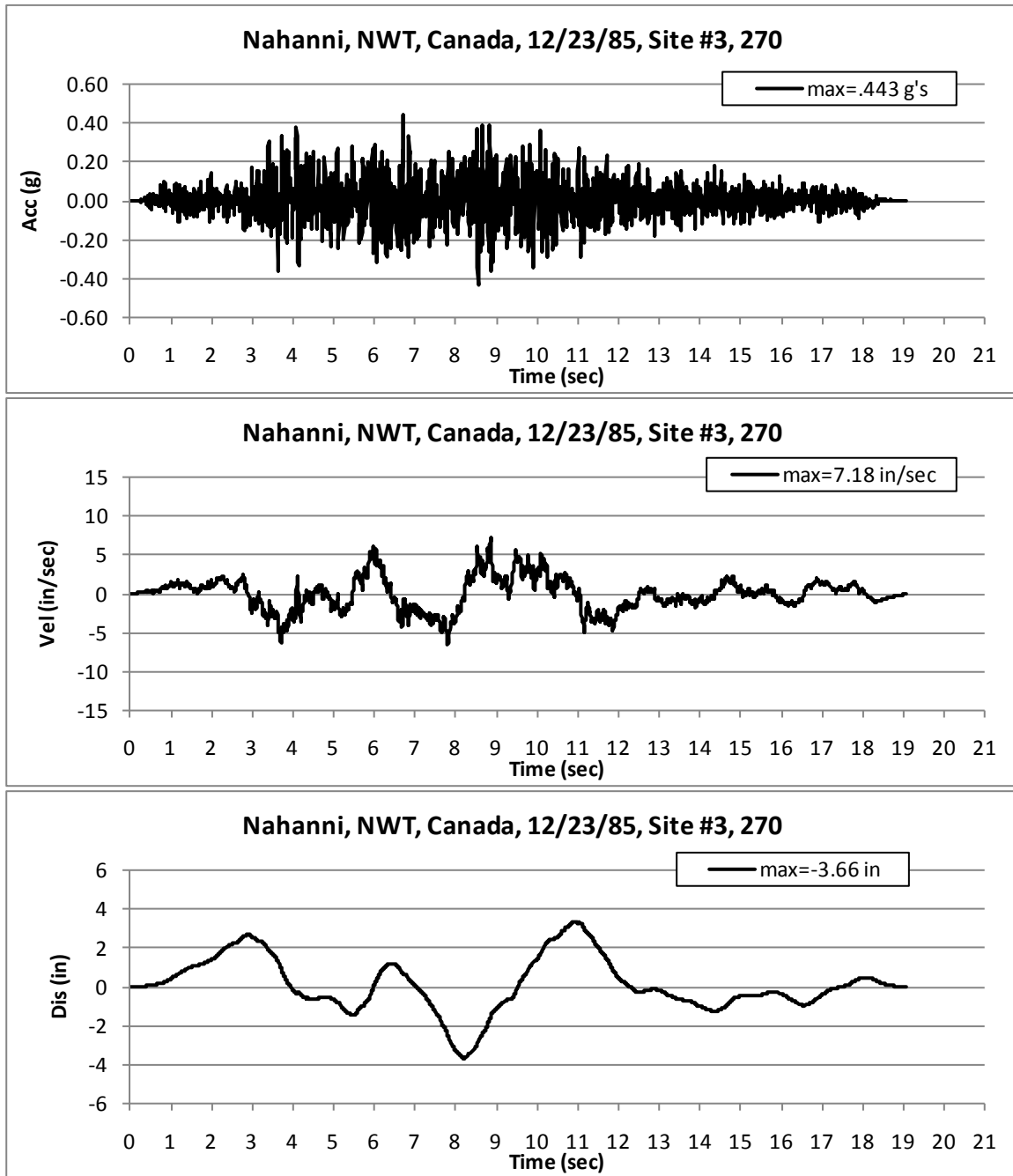
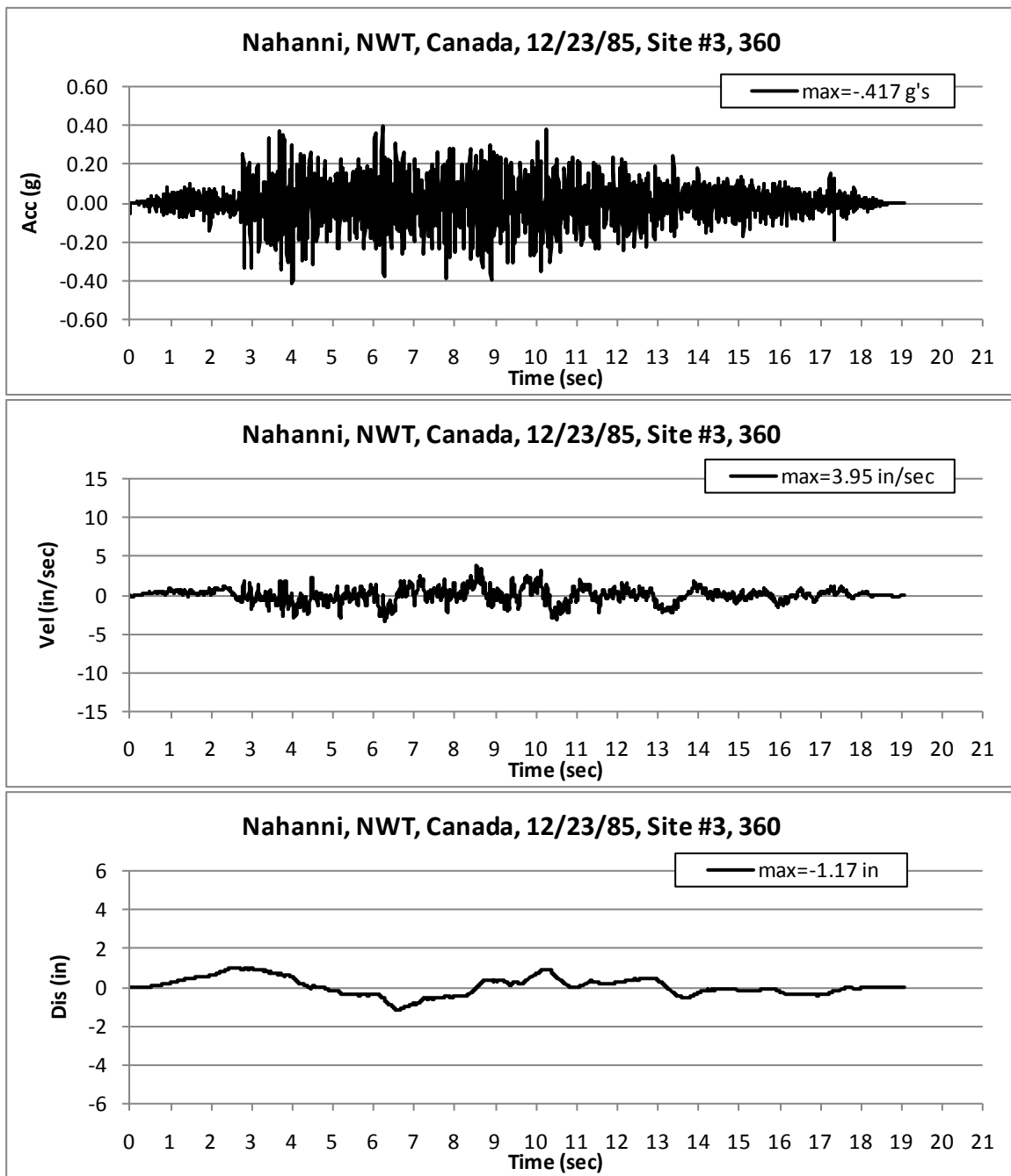


Figure 3-8 APR1400 HRHF Response Spectrum vs CSDRS for 5% Damping Ratio - Vertical

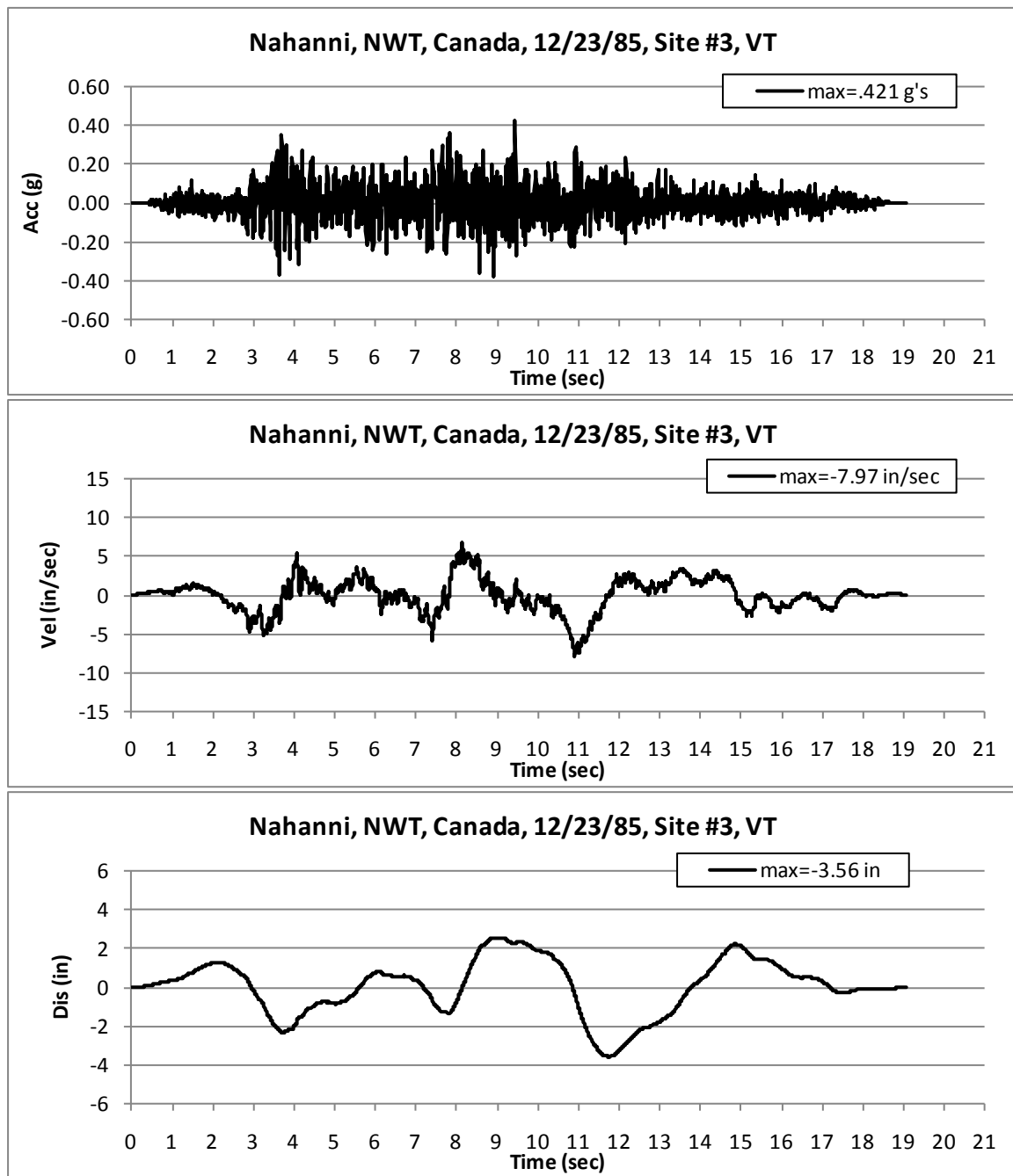


**Figure 3-9 Recorded Nahanni, Canada, Earthquake at Mackenzie Station #3 – 270 Component Seed Motion**

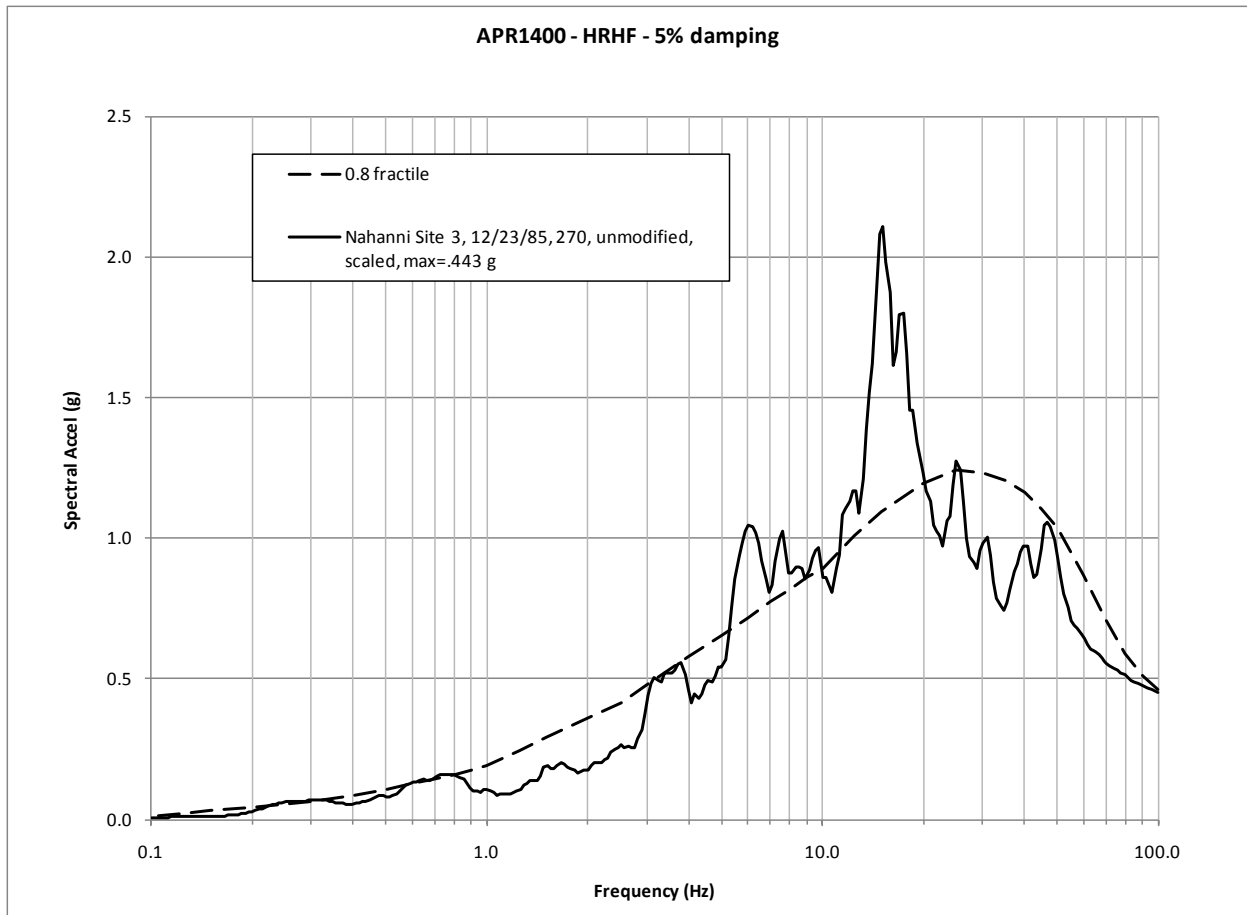


**Figure 3-10** Recorded Nahanni, Canada, Earthquake at Mackenzie Station #3 – 360 Component Seed Motion

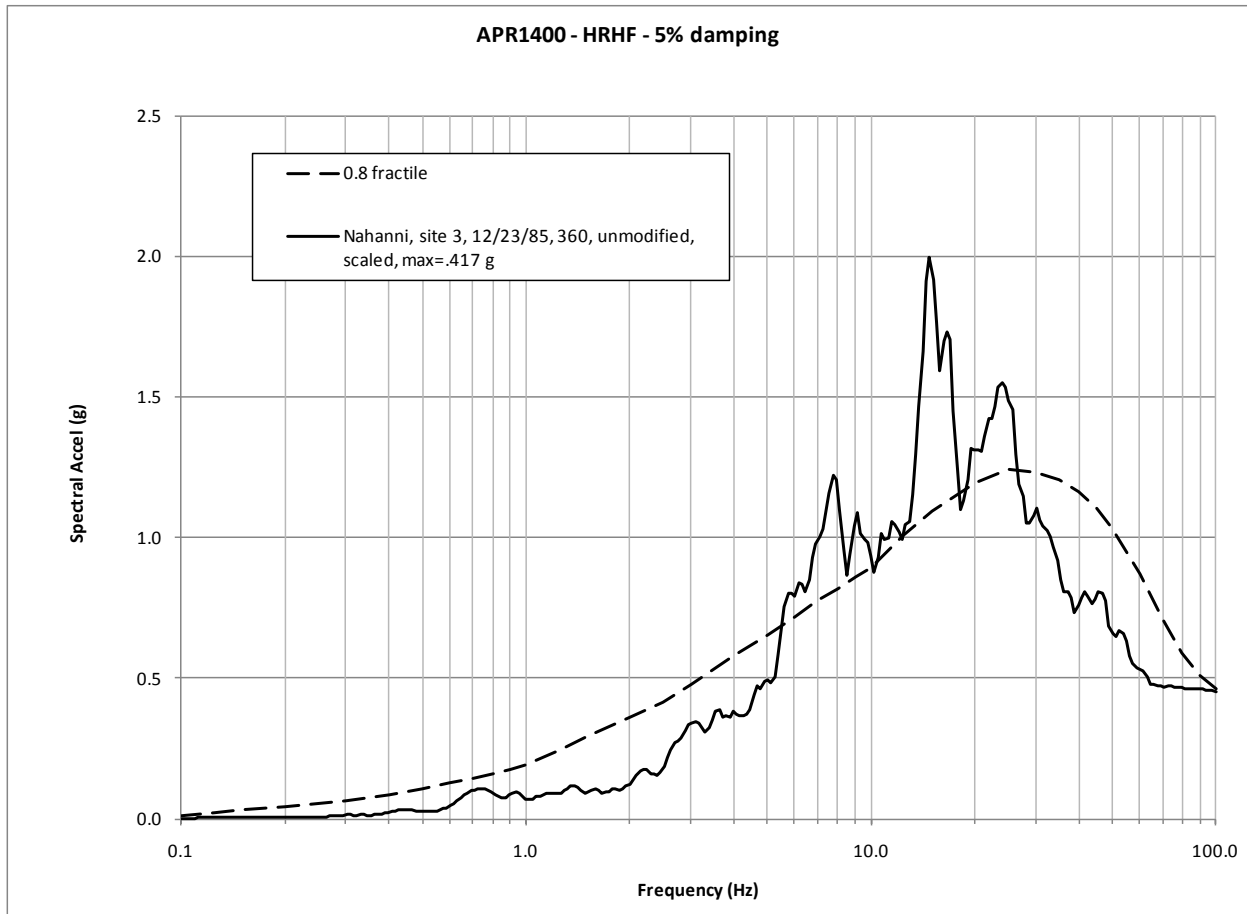




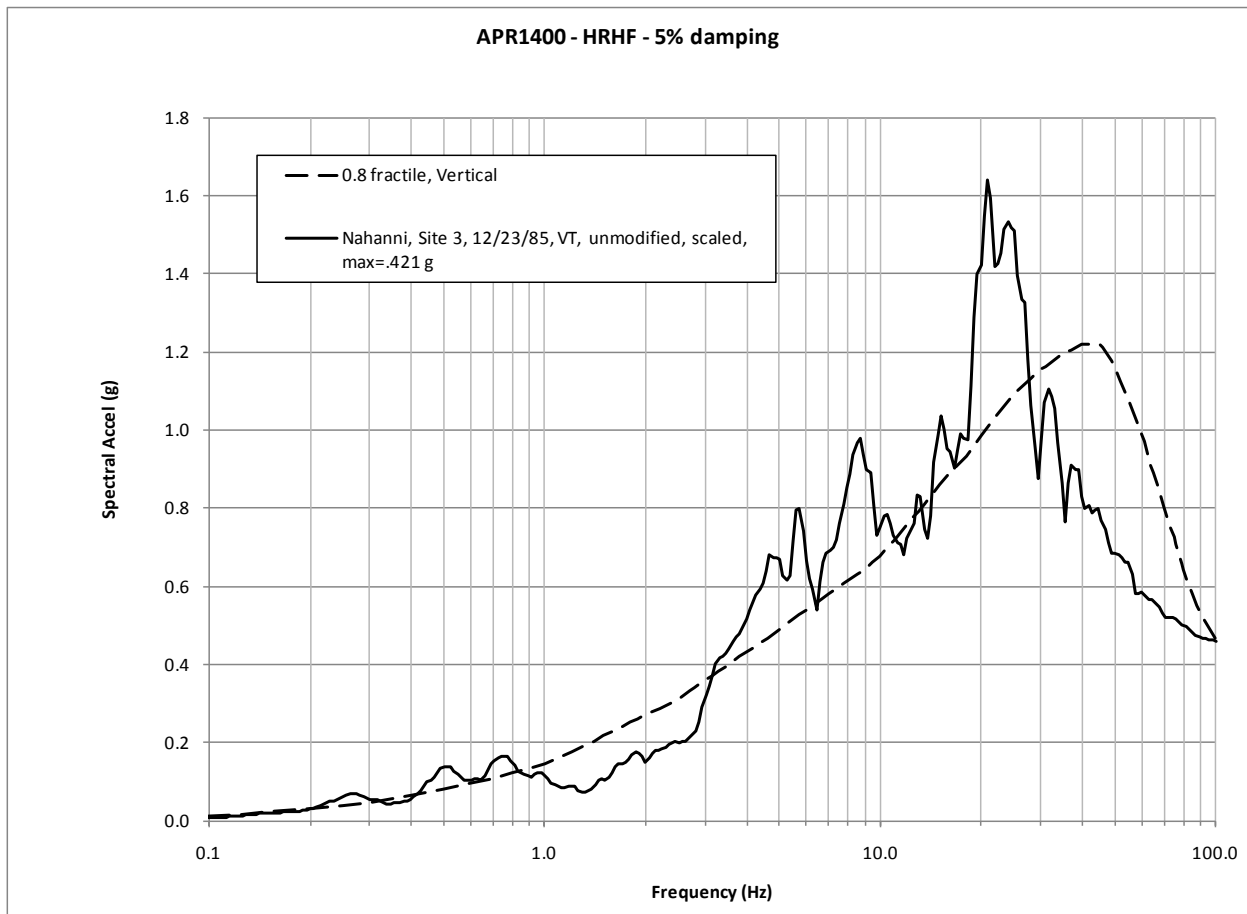
**Figure 3-11 Recorded Nahanni, Canada, Earthquake at Mackenzie Station #3 – VT Component Seed Motion**



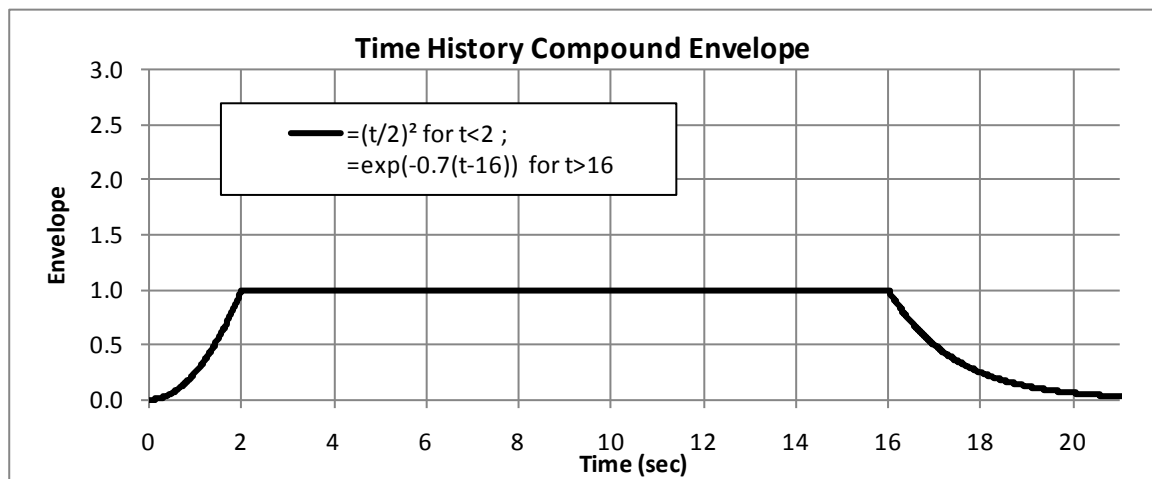
**Figure 3-12 Response Spectra of Nahanni Earthquake Mackenzie Station #3 Recorded Motion Scaled to PGA of 0.46g – 270 Component**



**Figure 3-13 Response Spectra of Nahanni Earthquake Mackenzie Station #3 Recorded Motion Scaled to PGA of 0.46g – 360 Component**



**Figure 3-14 Response Spectra of Nahanni Earthquake Mackenzie Station #3 Recorded Motion Scaled to PGA of 0.46g – VT Component**

**Figure 3-15 Intensity Envelope Function**

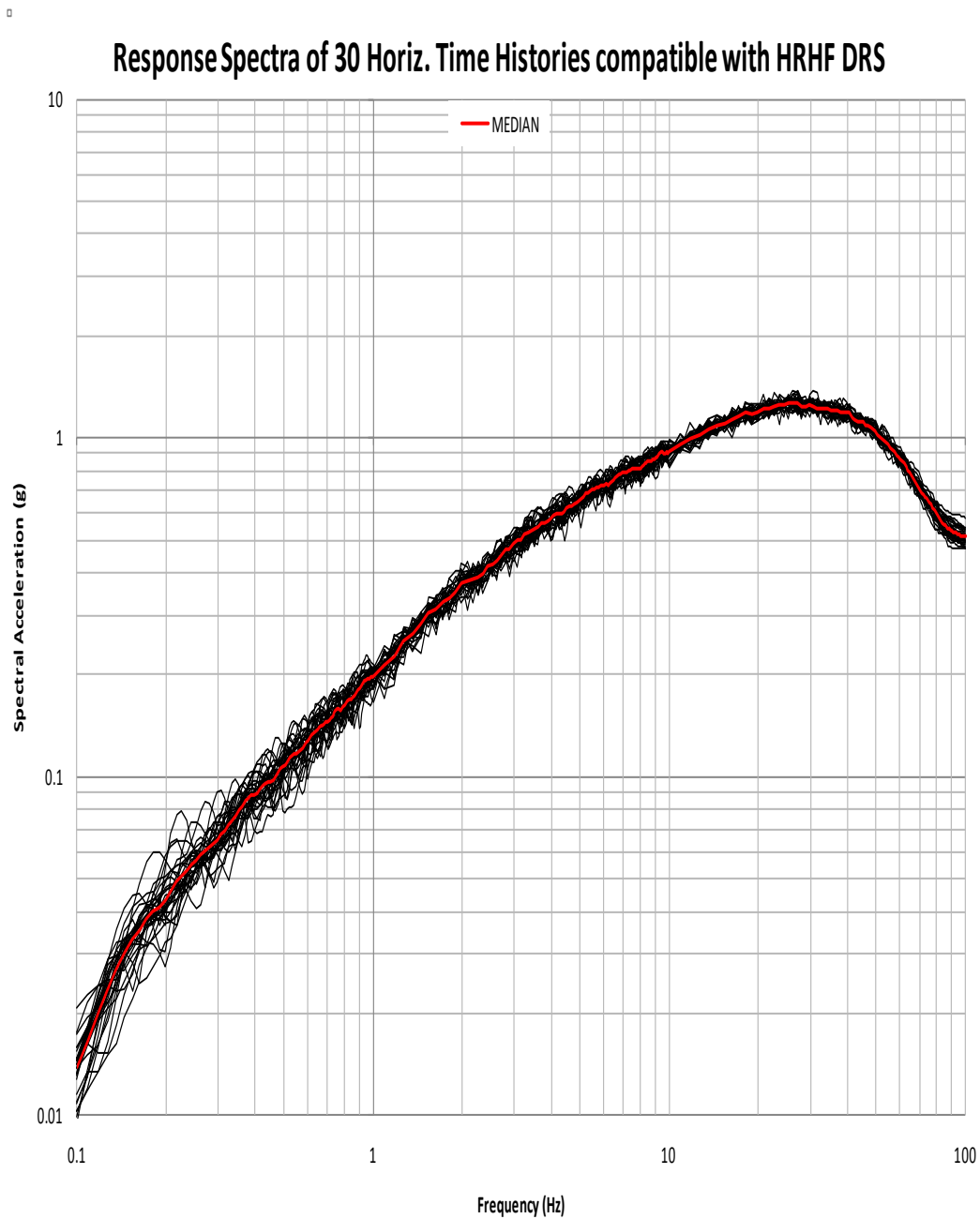


**Figure 3-16 Comparison of 2%-Damped Ensemble of 30 Time-History Response Spectra and Ensemble-Median Response Spectrum - Horizontal**

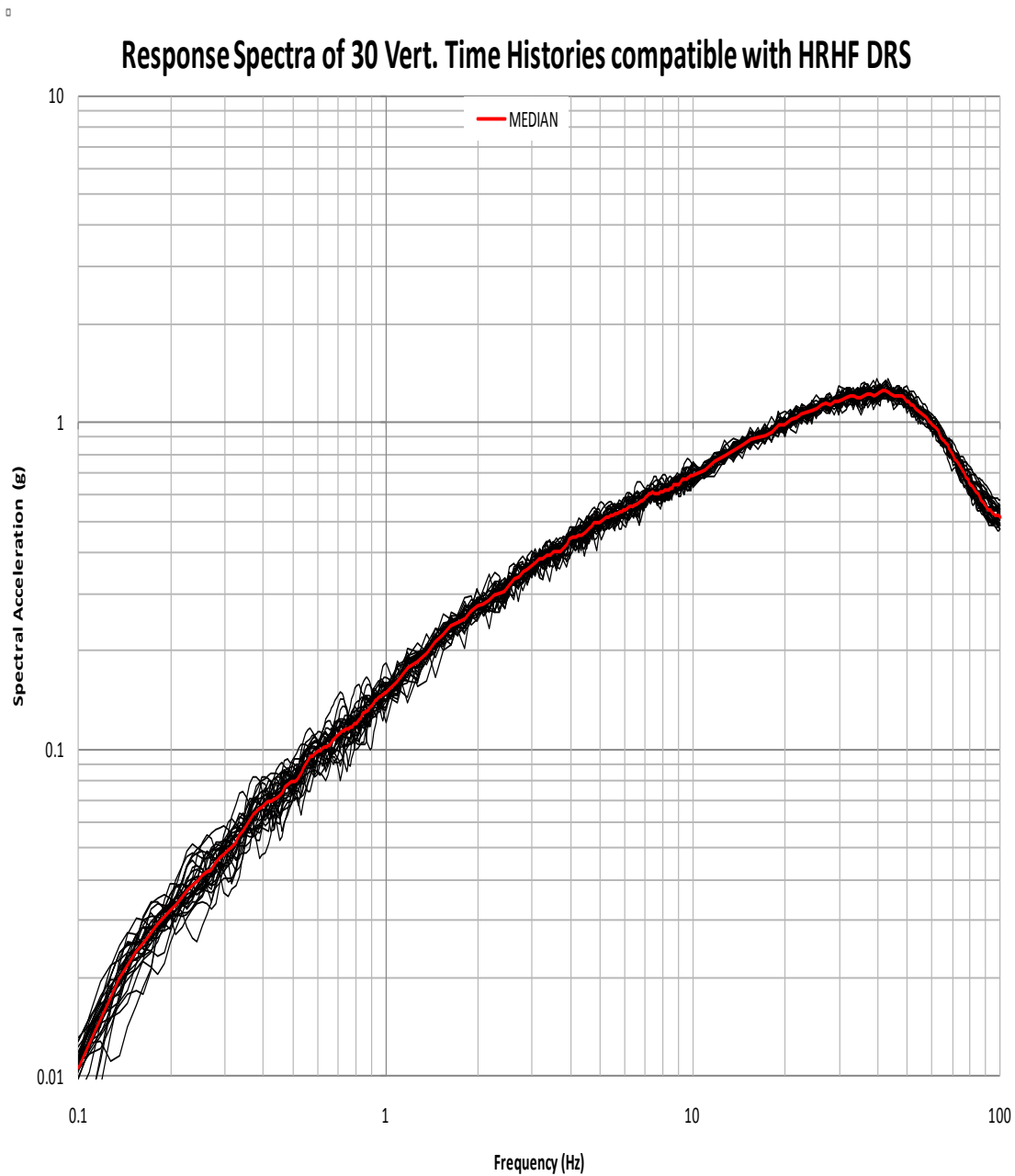


**Figure 3-17 Comparison of 2%-Damped Ensemble of 30 Time-History Response Spectra and Ensemble-Median Response Spectrum - Vertical**

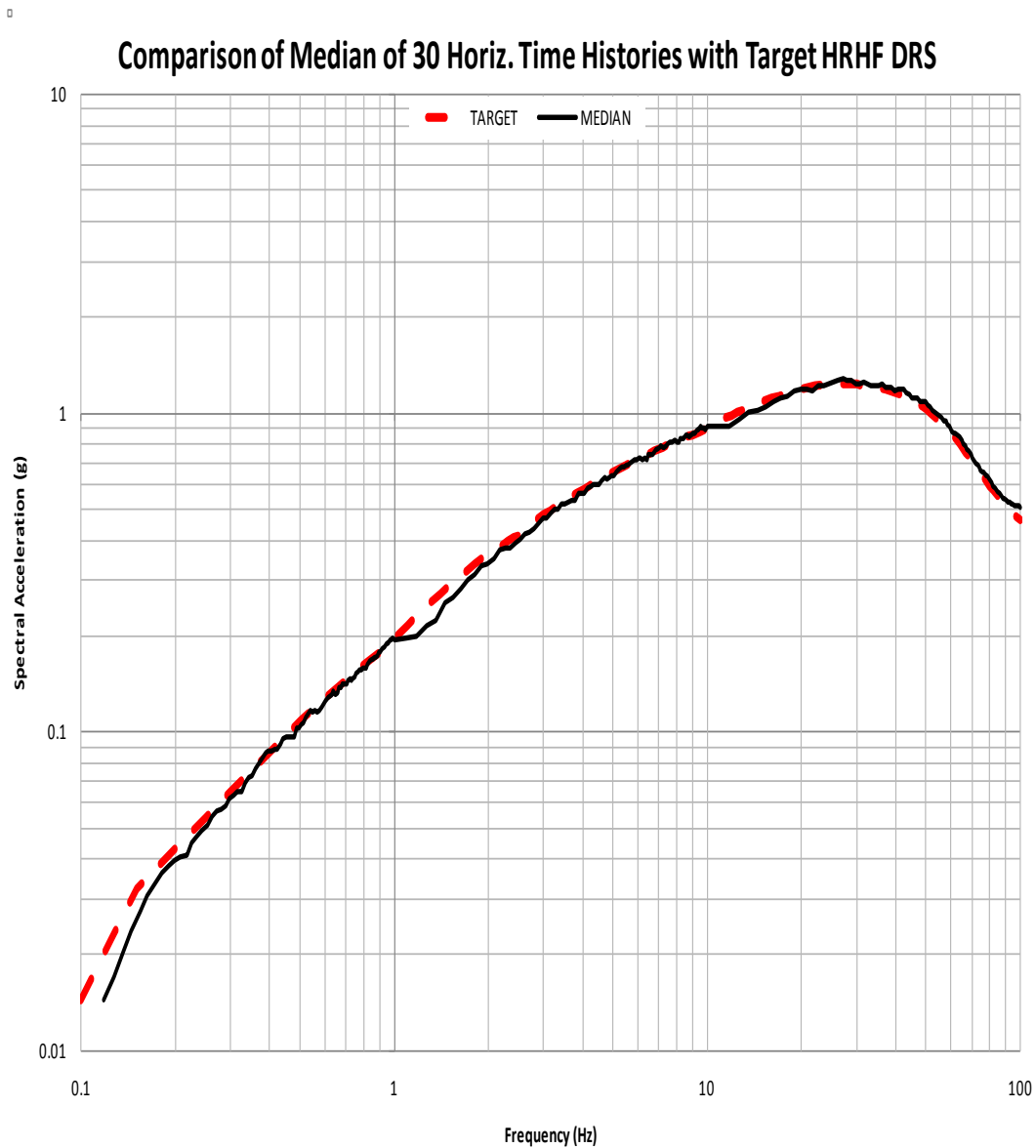


**Figure 3-18 Comparison of 2%-Damped Ensemble of Median Response Spectra and APR1400 HRHF Horizontal Target Response Spectrum - Horizontal**



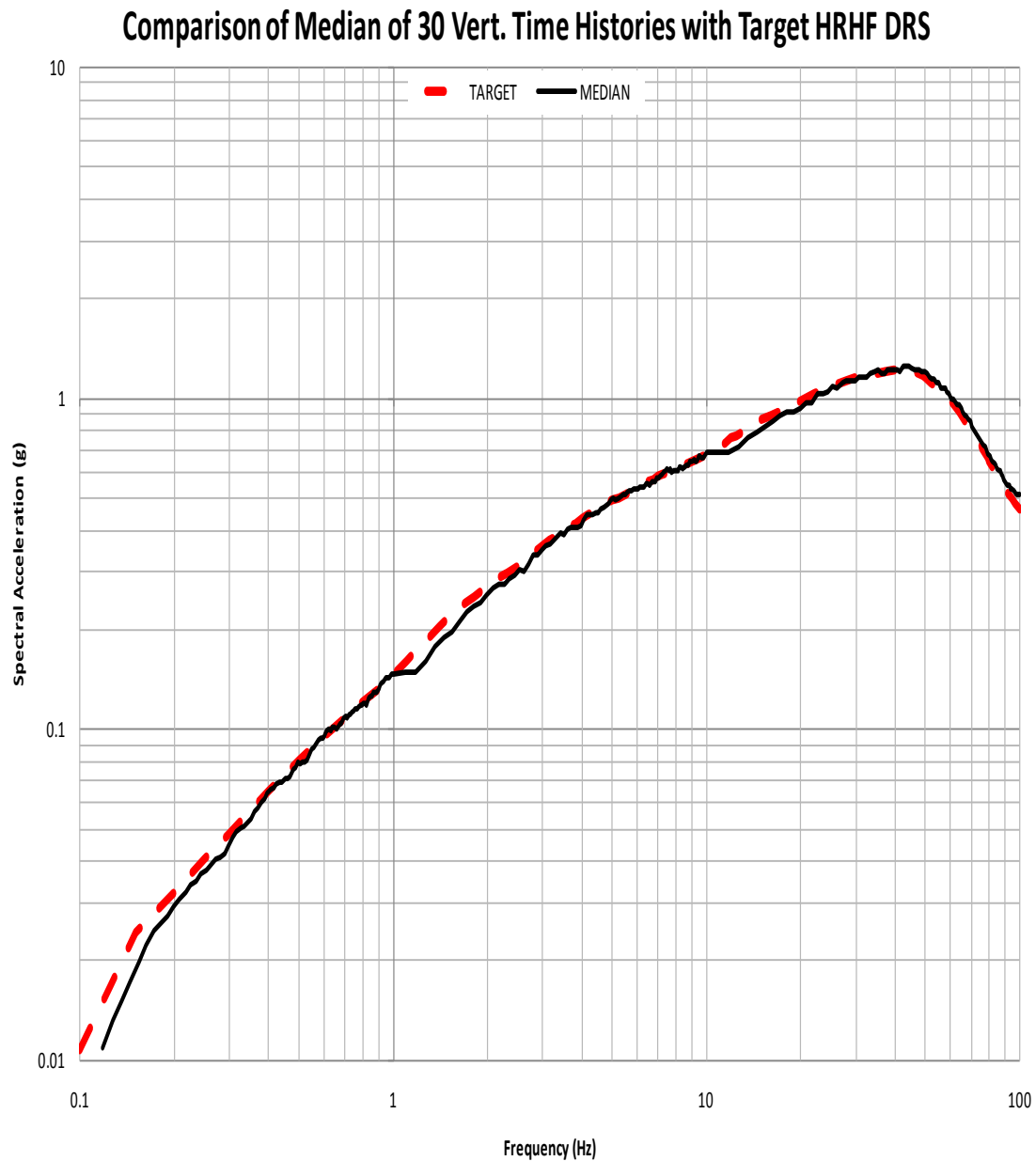


**Figure 3-19 Comparison of 2%-Damped Ensemble of Median Response Spectra and APR1400 HRHF Vertical Target Response Spectrum - Vertical**

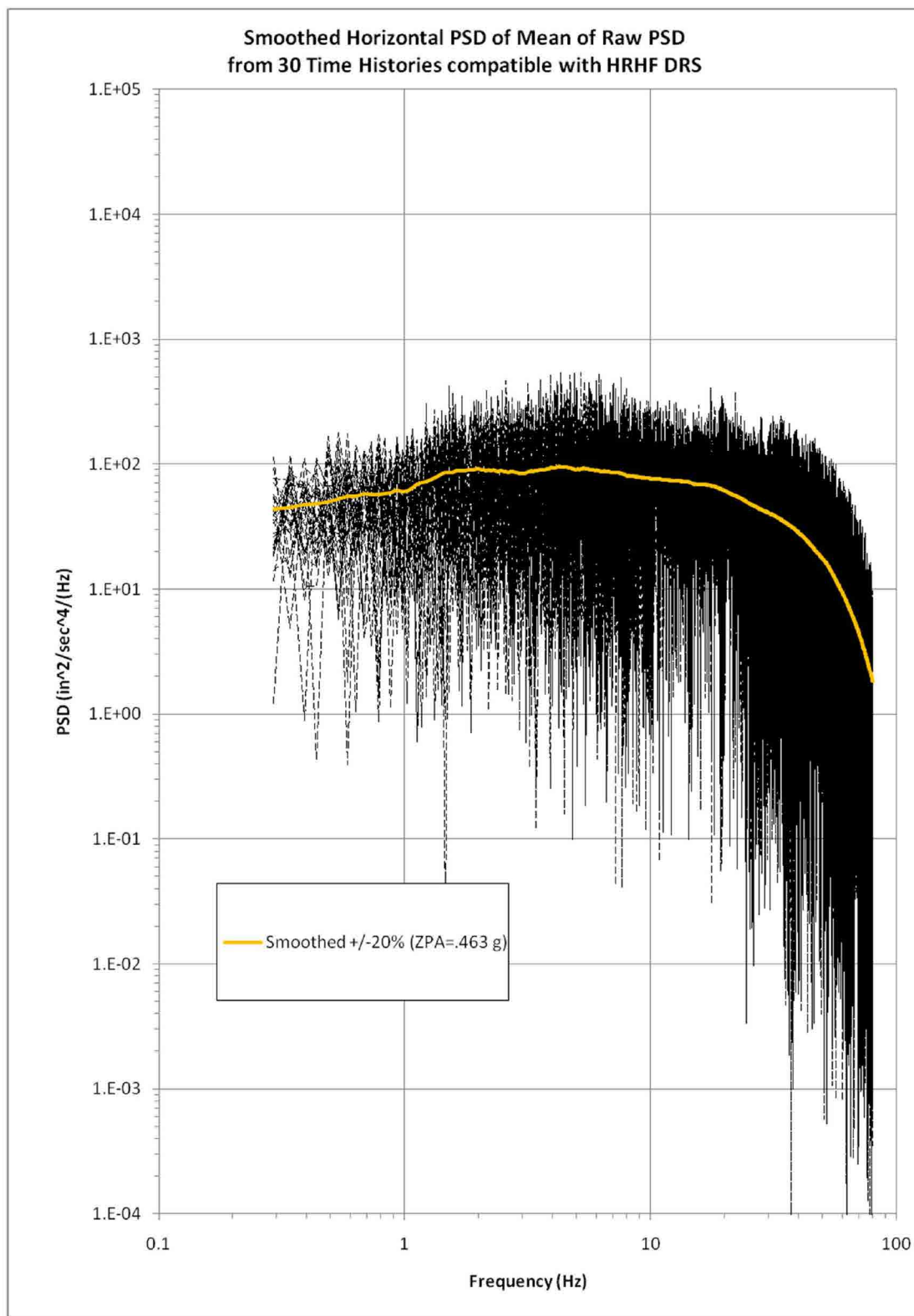


Figure 3-20 Computed PSDs for the Generated 30 Time History Ensemble - Horizontal

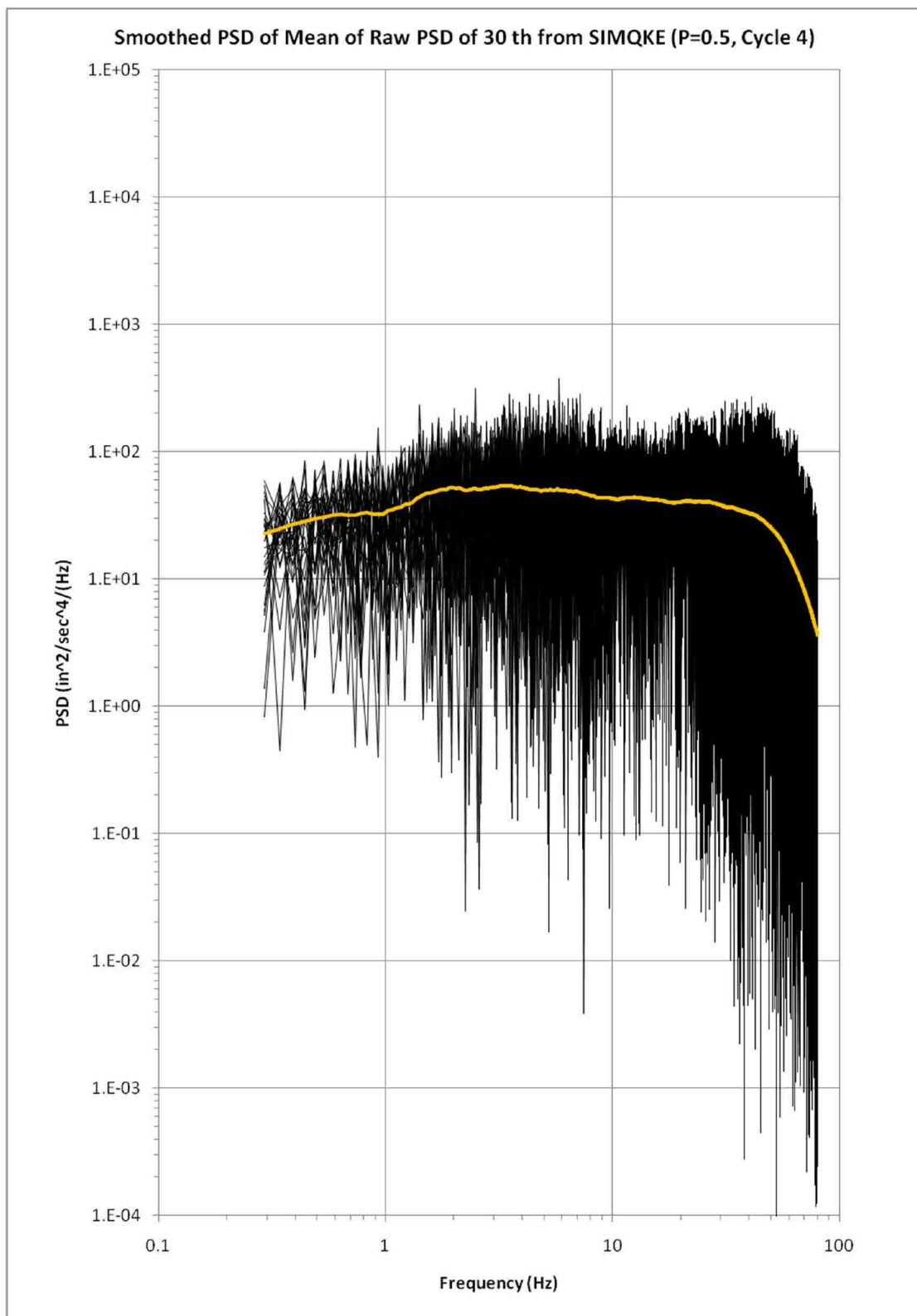
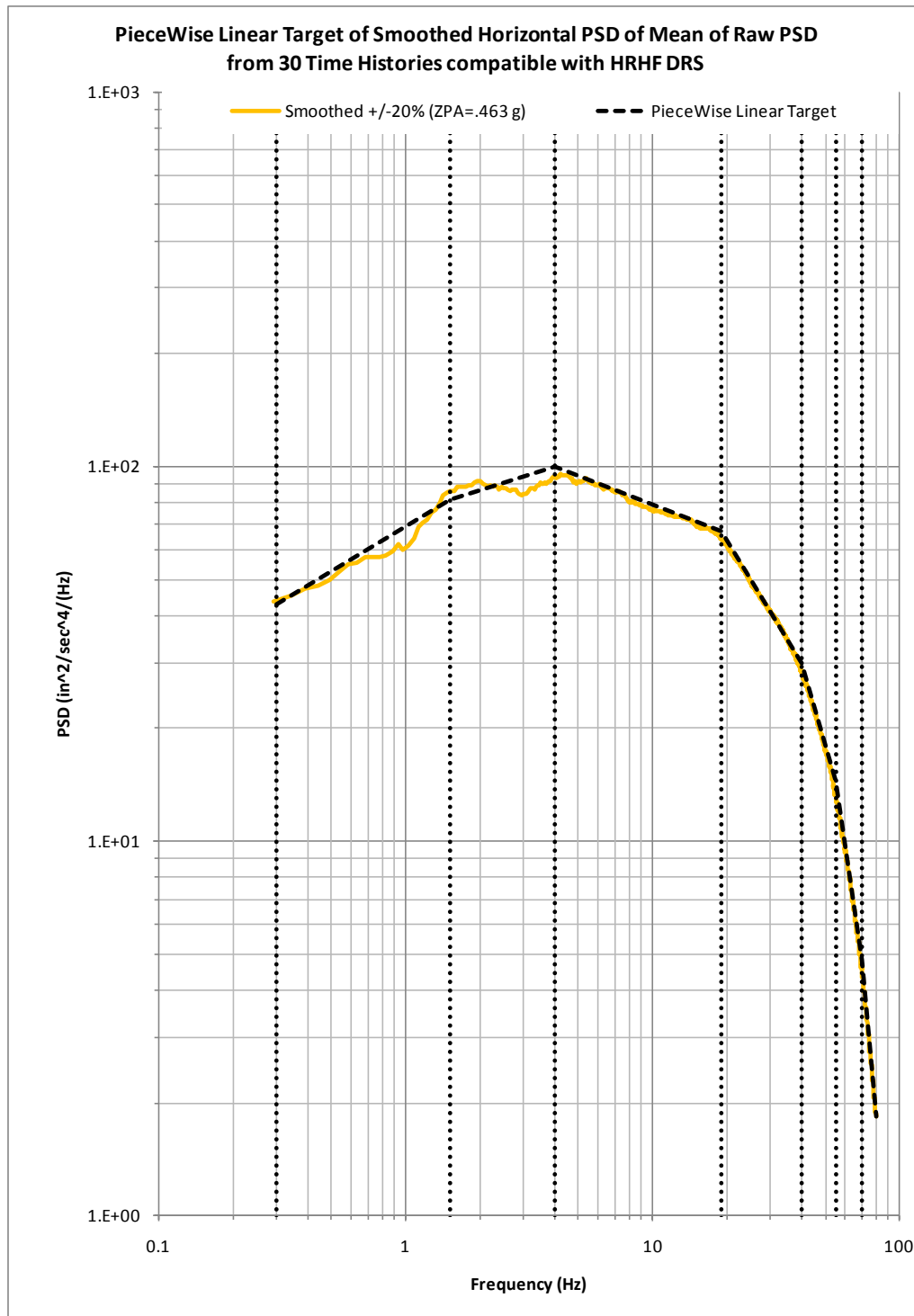
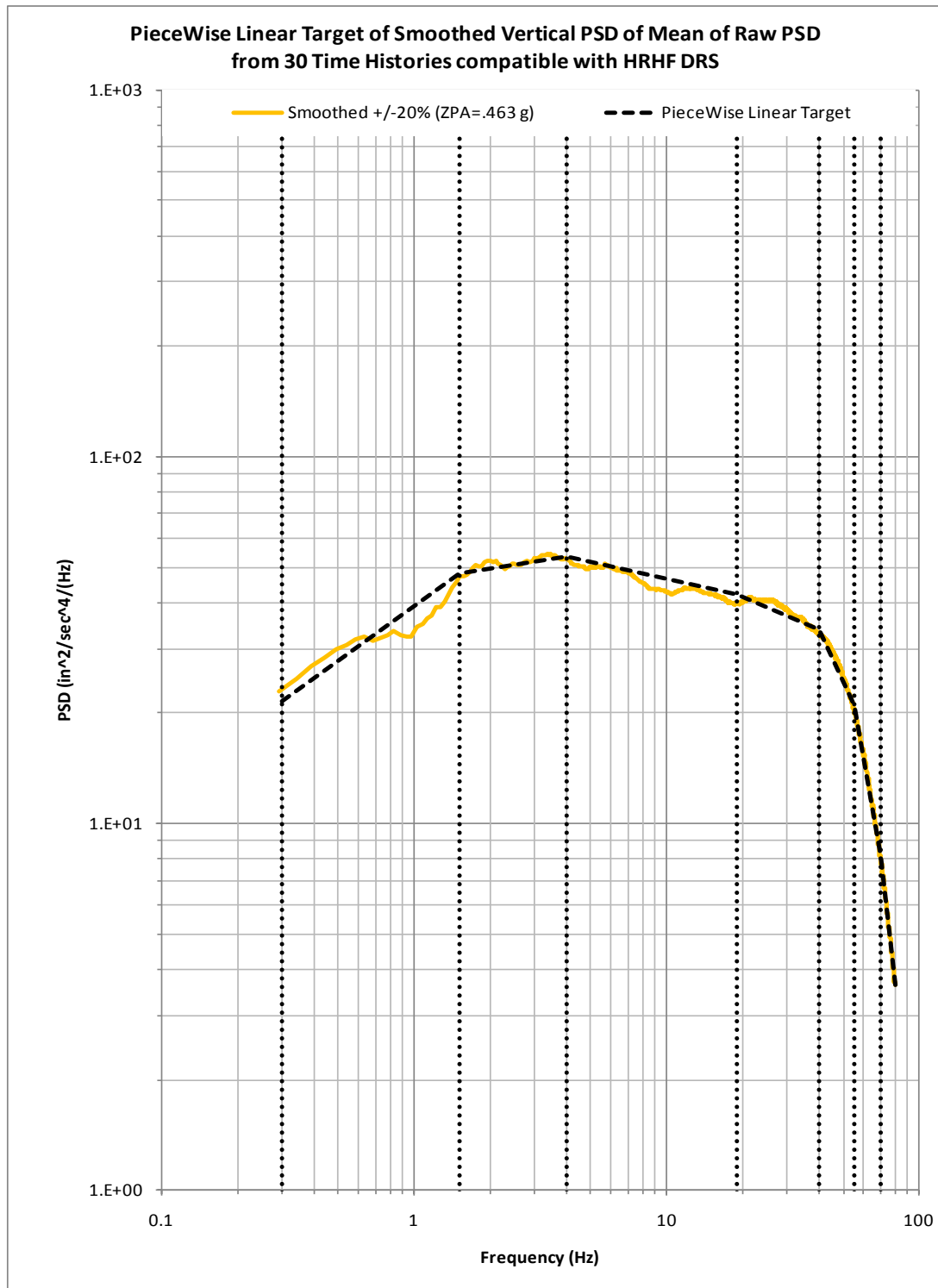


Figure 3-21 Computed PSDs for the Generated 30 Time History Ensemble - Vertical



**Figure 3-22 Smoothed Ensemble-Mean and Piecewise Log-Log Linear PSD Obtained from the Generated 30 Time History Ensemble - Horizontal**



**Figure 3-23 Smoothed Ensemble-Mean and Piecewise Log-Log Linear PSD Obtained from the Generated 30 Time History Ensemble - Vertical**

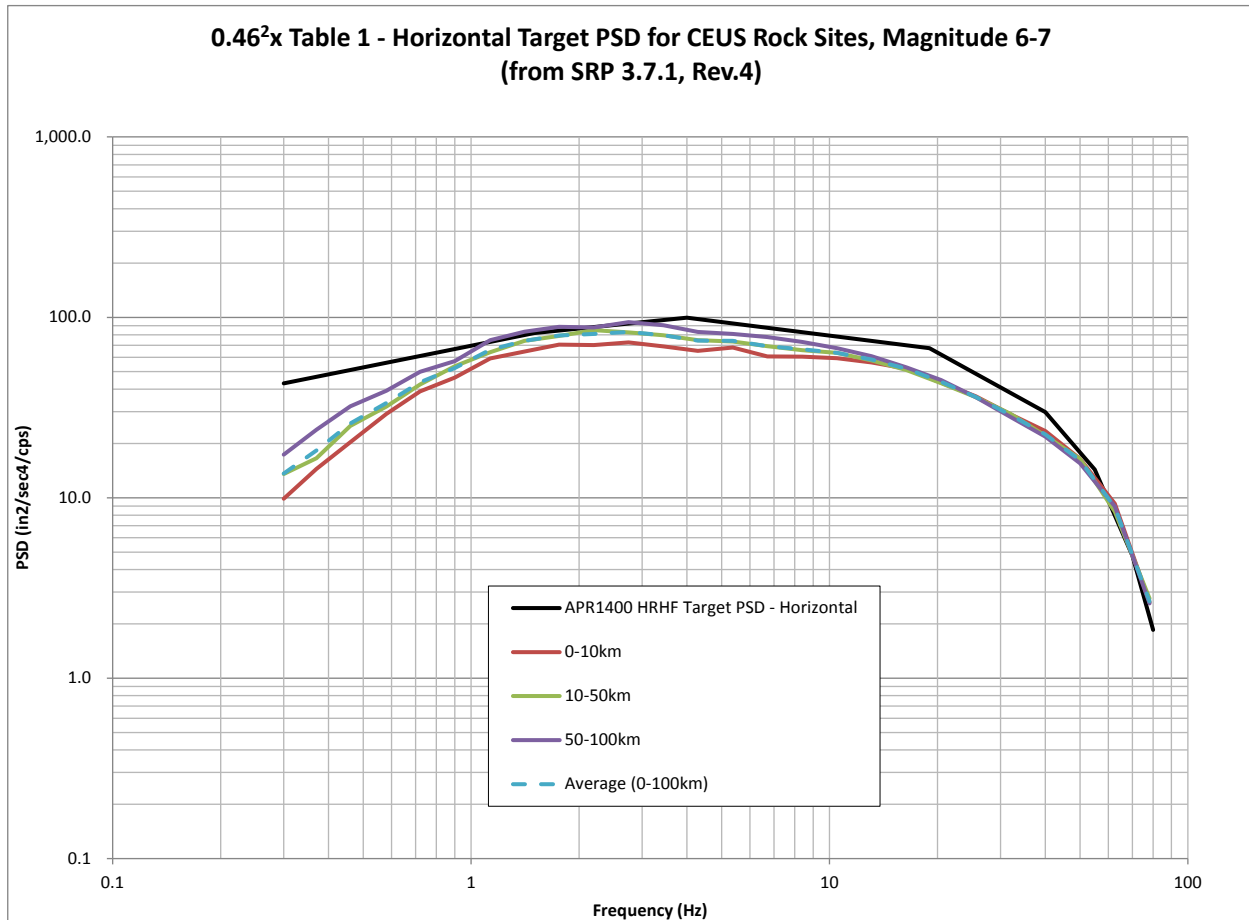


**Figure 3-24 Comparison of the Horizontal Target PSD Compatible with APR1400 HRHF Horizontal Response Spectra with the SRP 3.7.1 PSDs for CEUS Rock Sites**

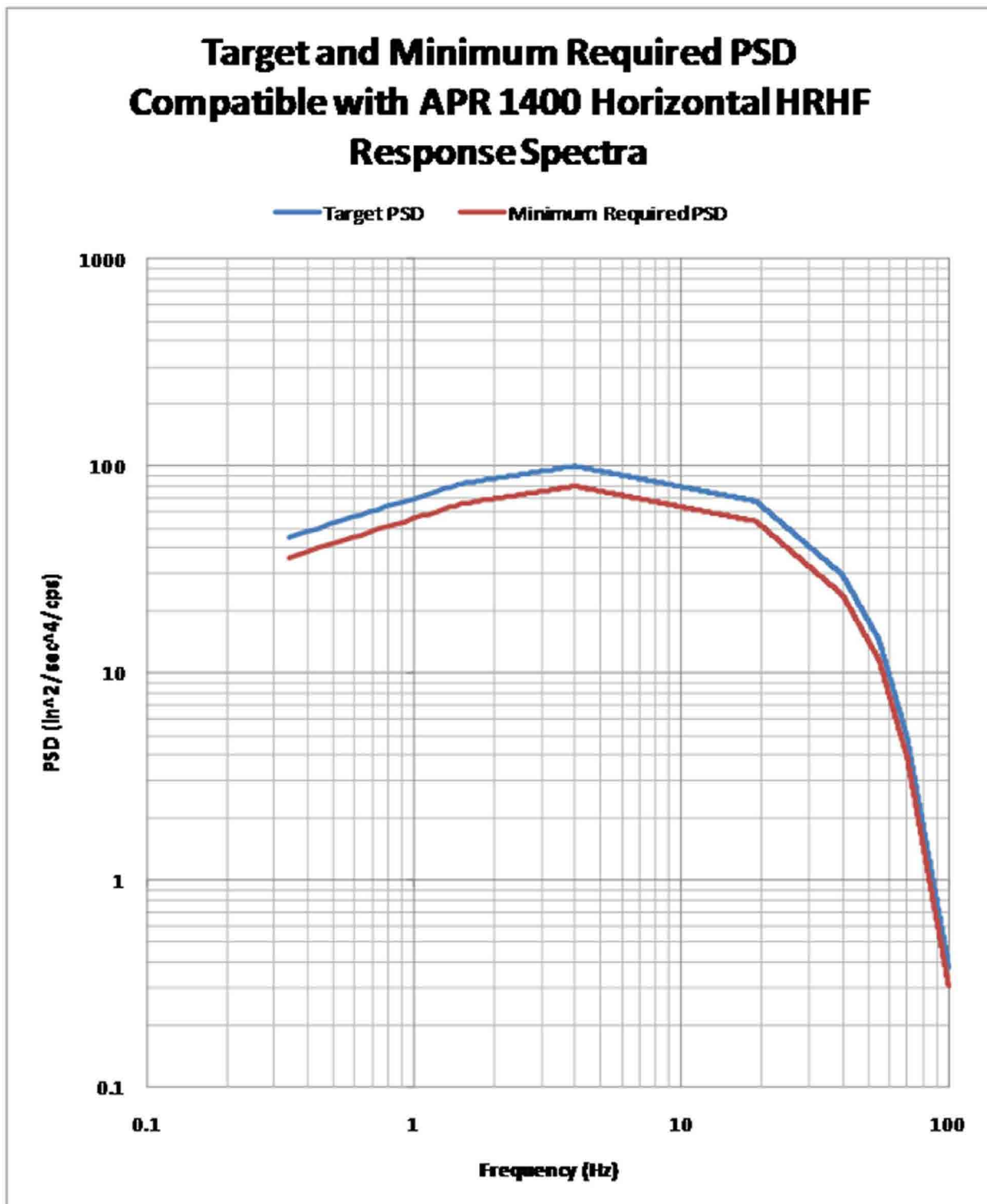


Figure 3-25 Target and Minimum Required PSDs - Horizontal

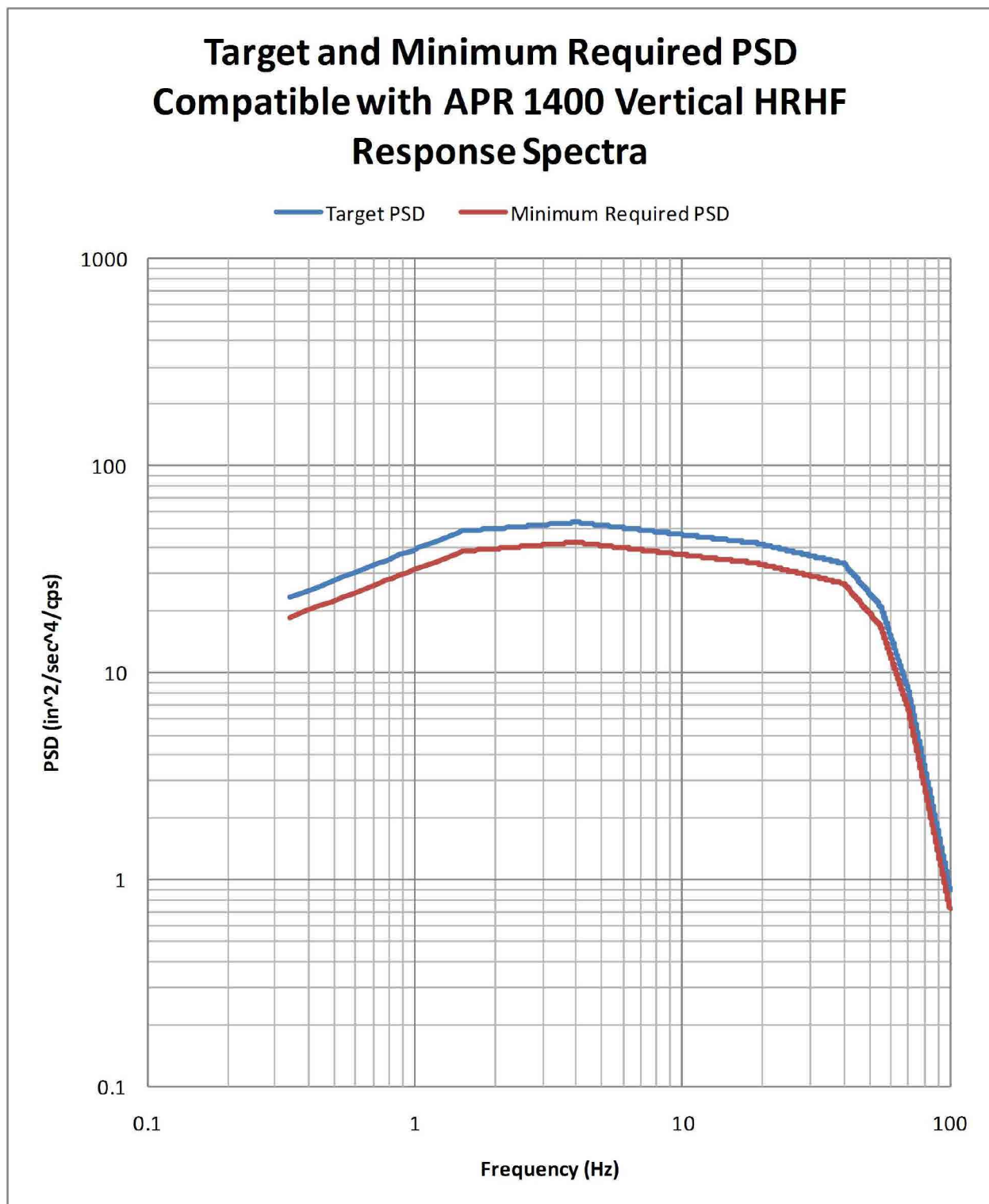
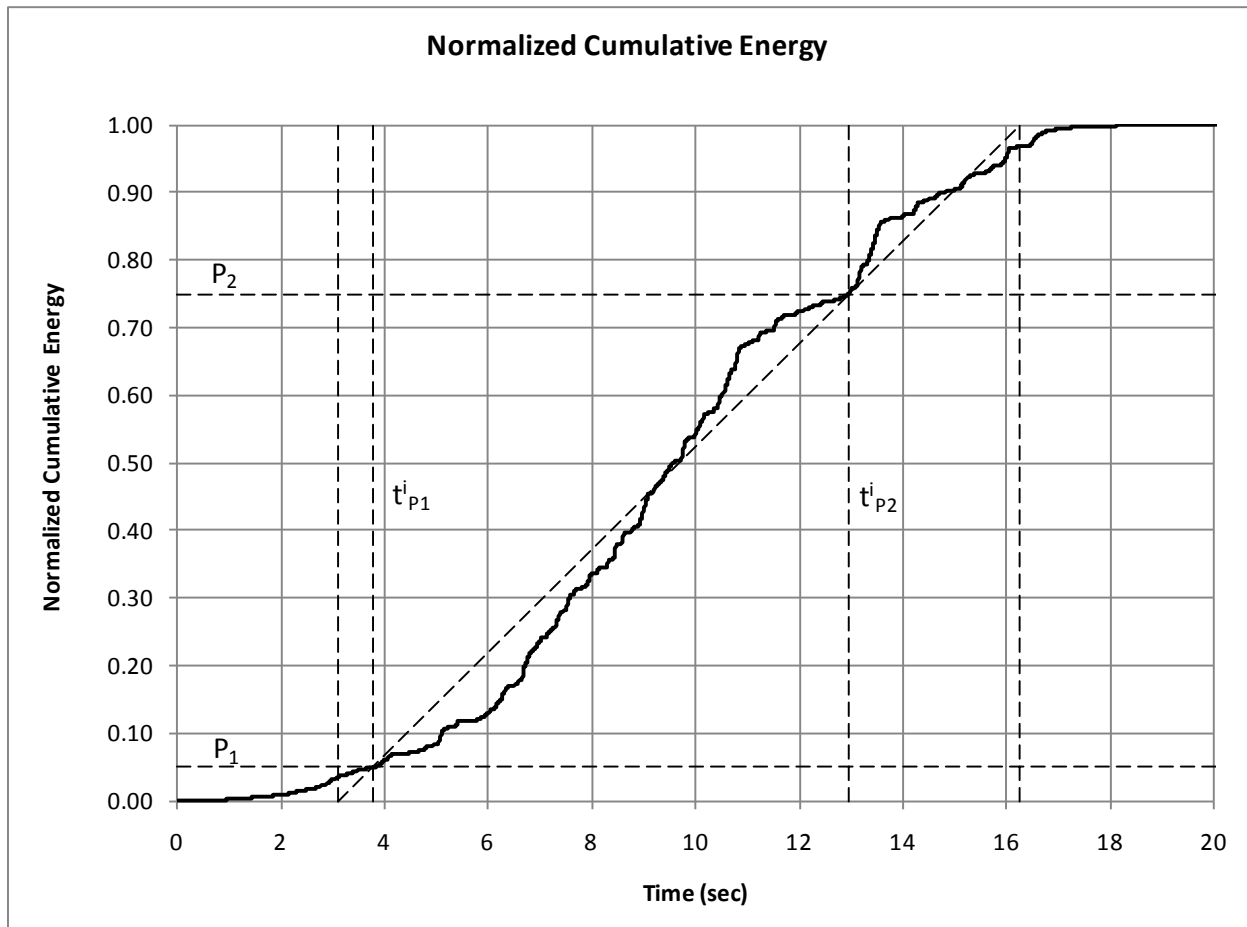
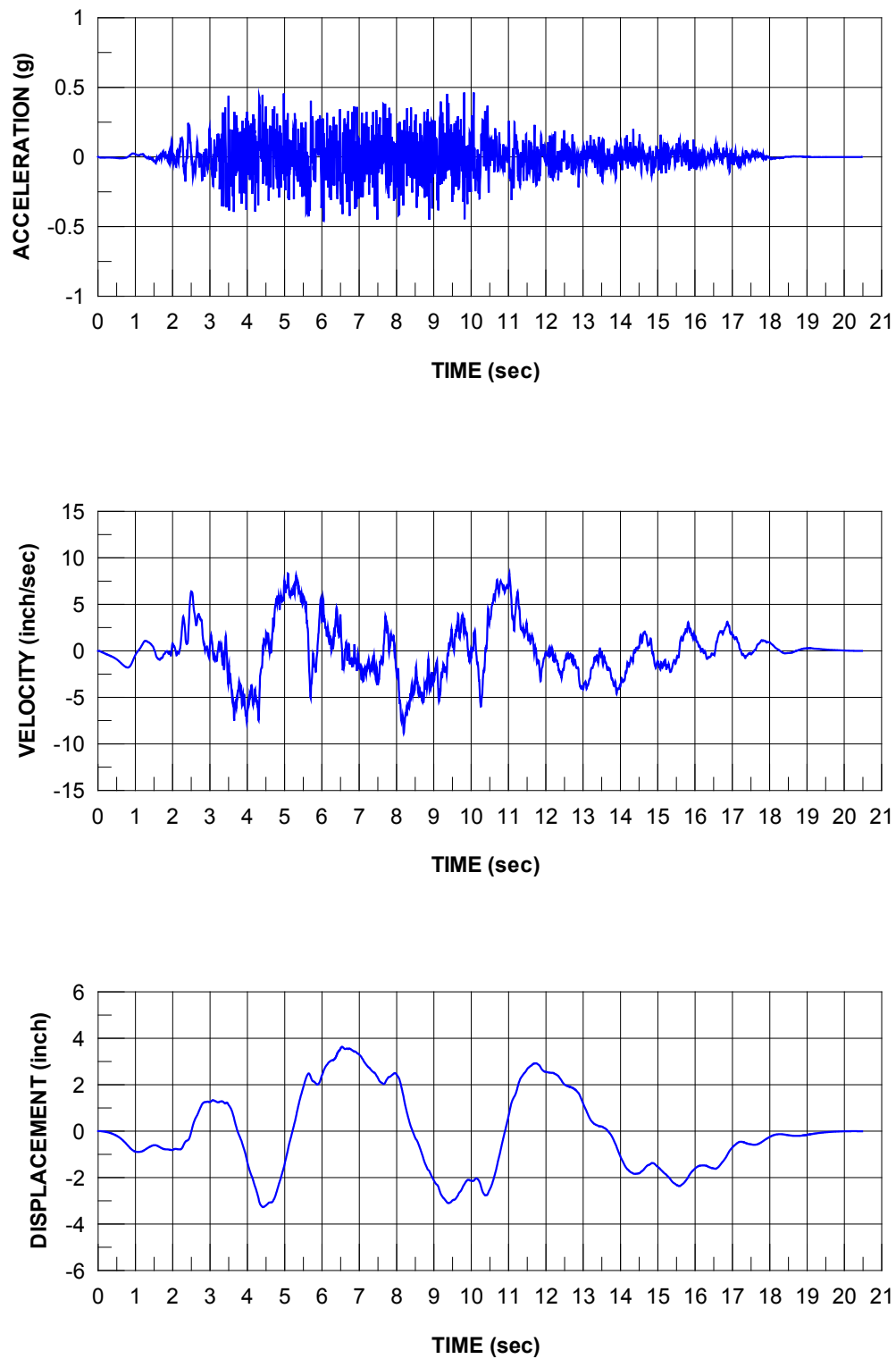


Figure 3-26 Target and Minimum Required PSDs - Vertical





**Figure 3-27 Procedure for Determining Equivalent Stationary Duration**

**Figure 3-28 Acceleration, Velocity, and Displacement of H1H**

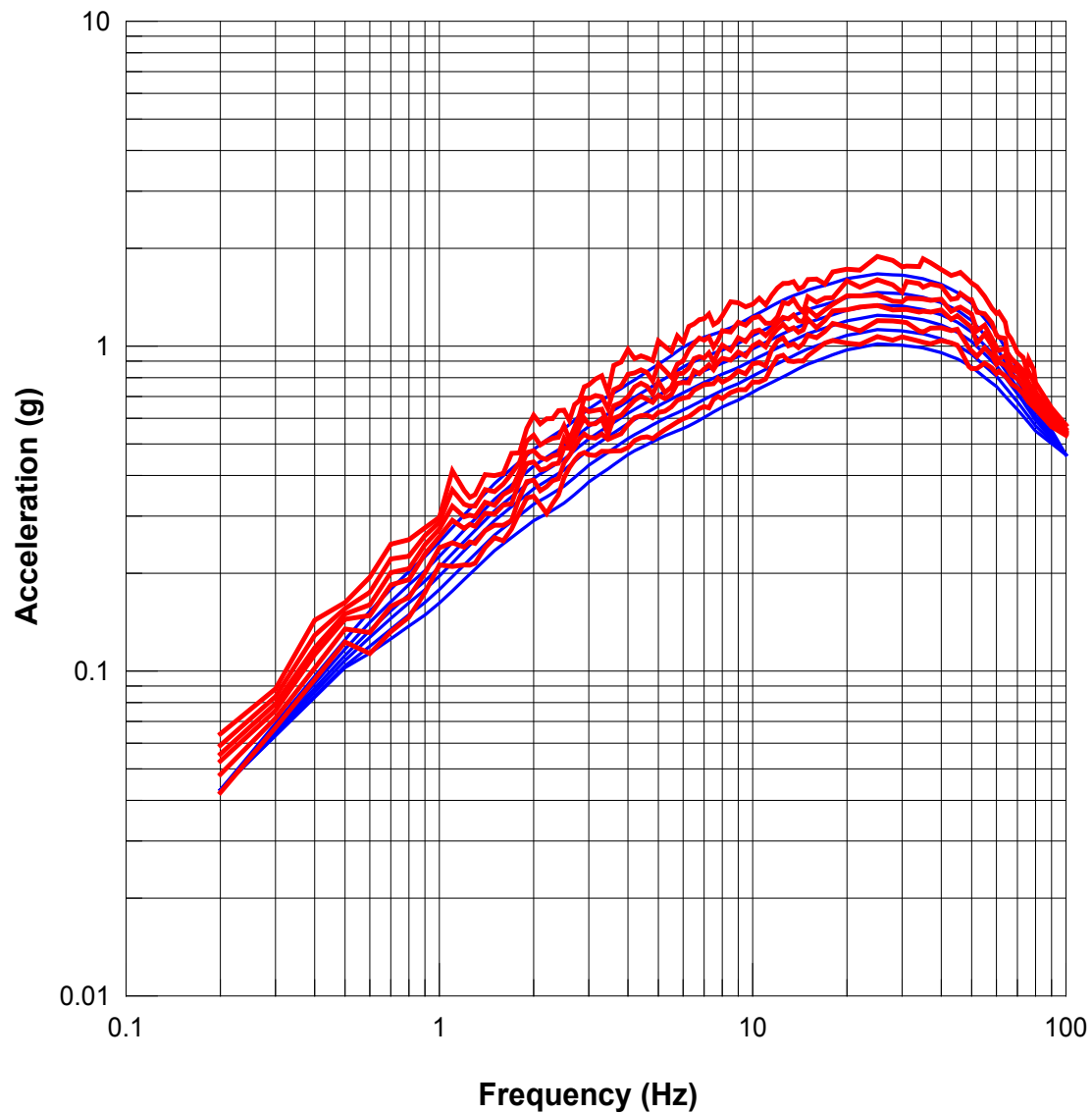


**Figure 3-29 Comparison of Response Spectra of H1H and HRHF Horizontal Target Response Spectra**

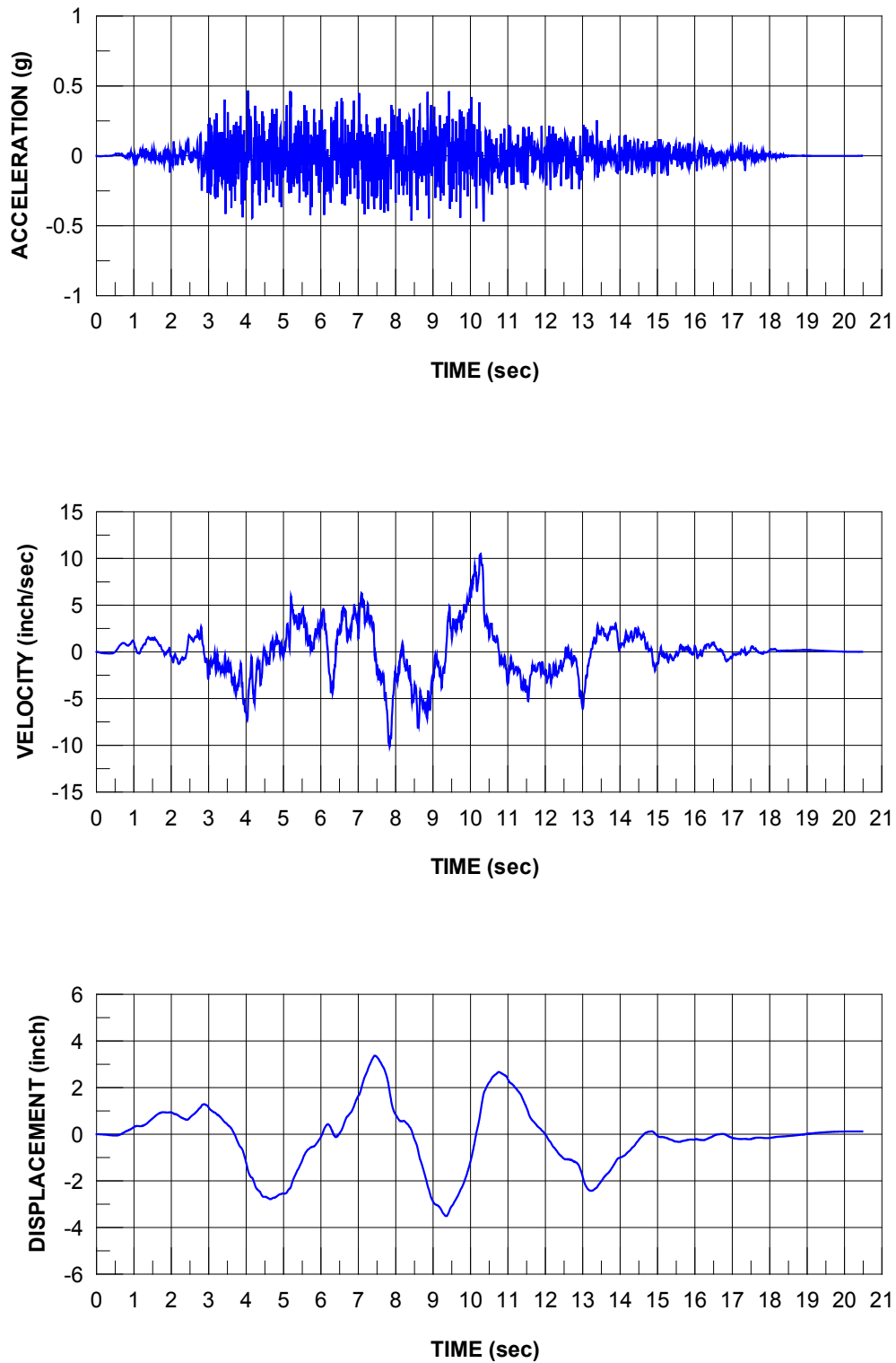
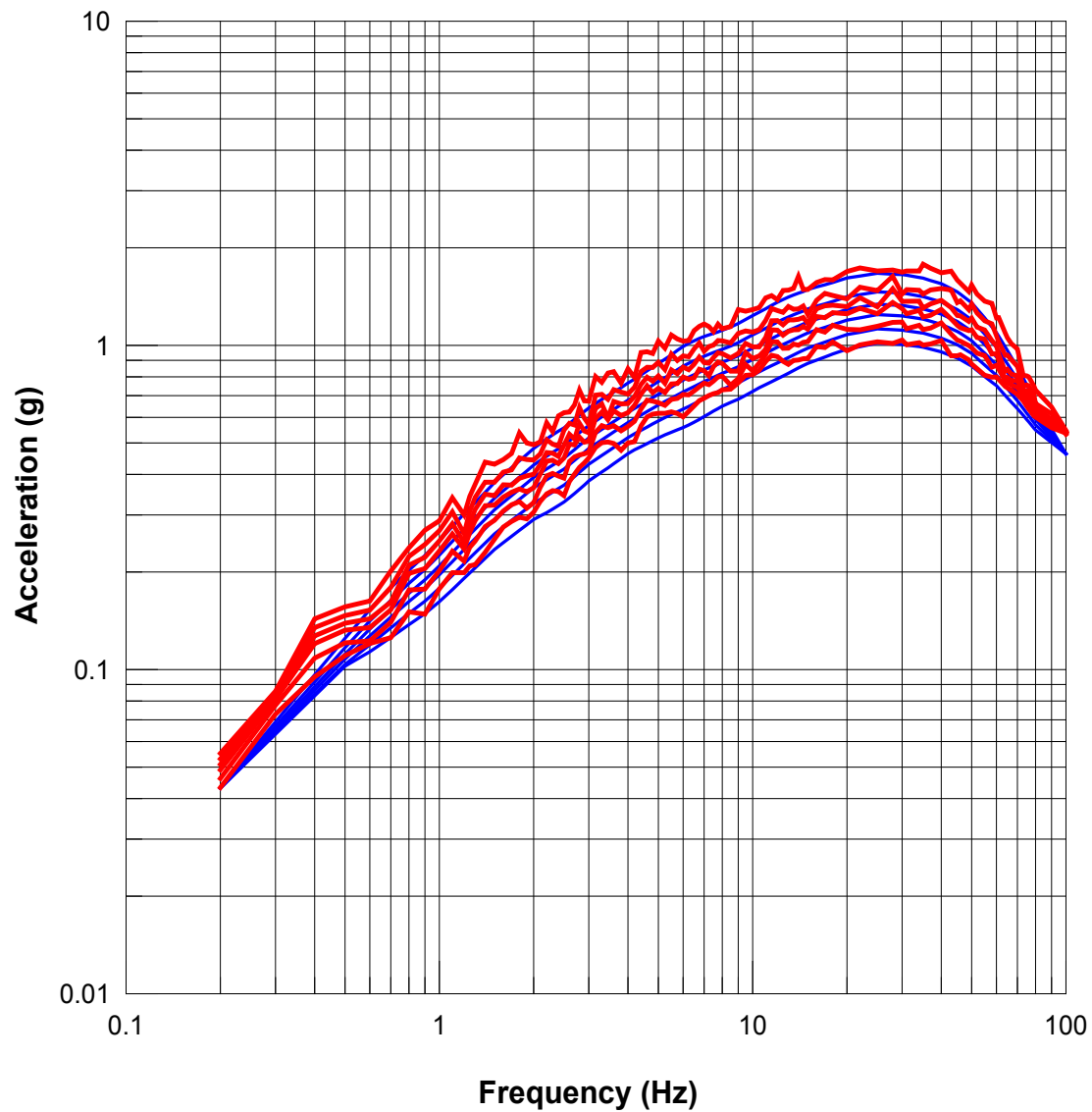


Figure 3-30 Acceleration, Velocity, and Displacement of H2H



**Figure 3-31 Comparison of Response Spectra of H2H and HRHF Horizontal Target Response Spectra**

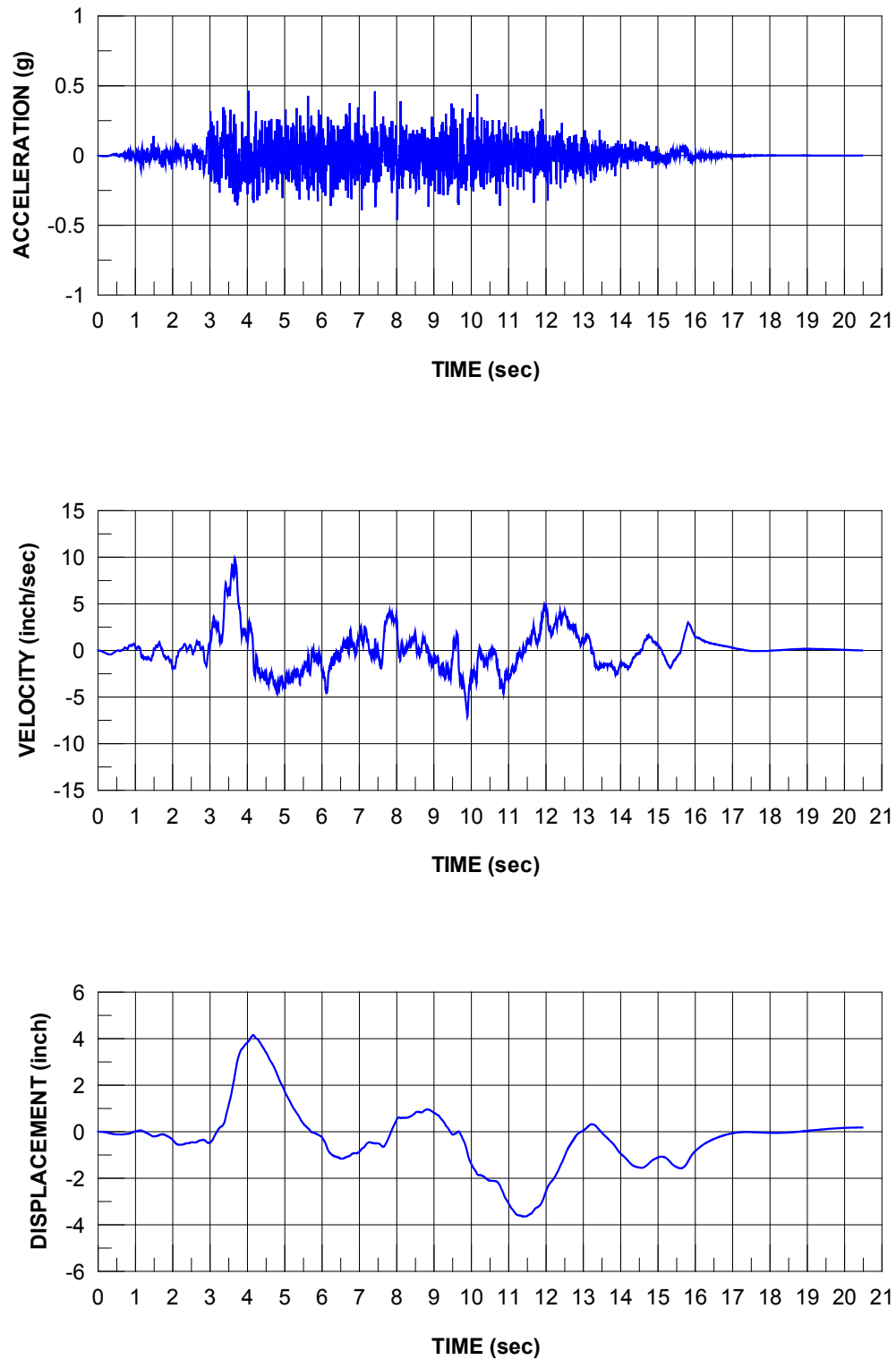
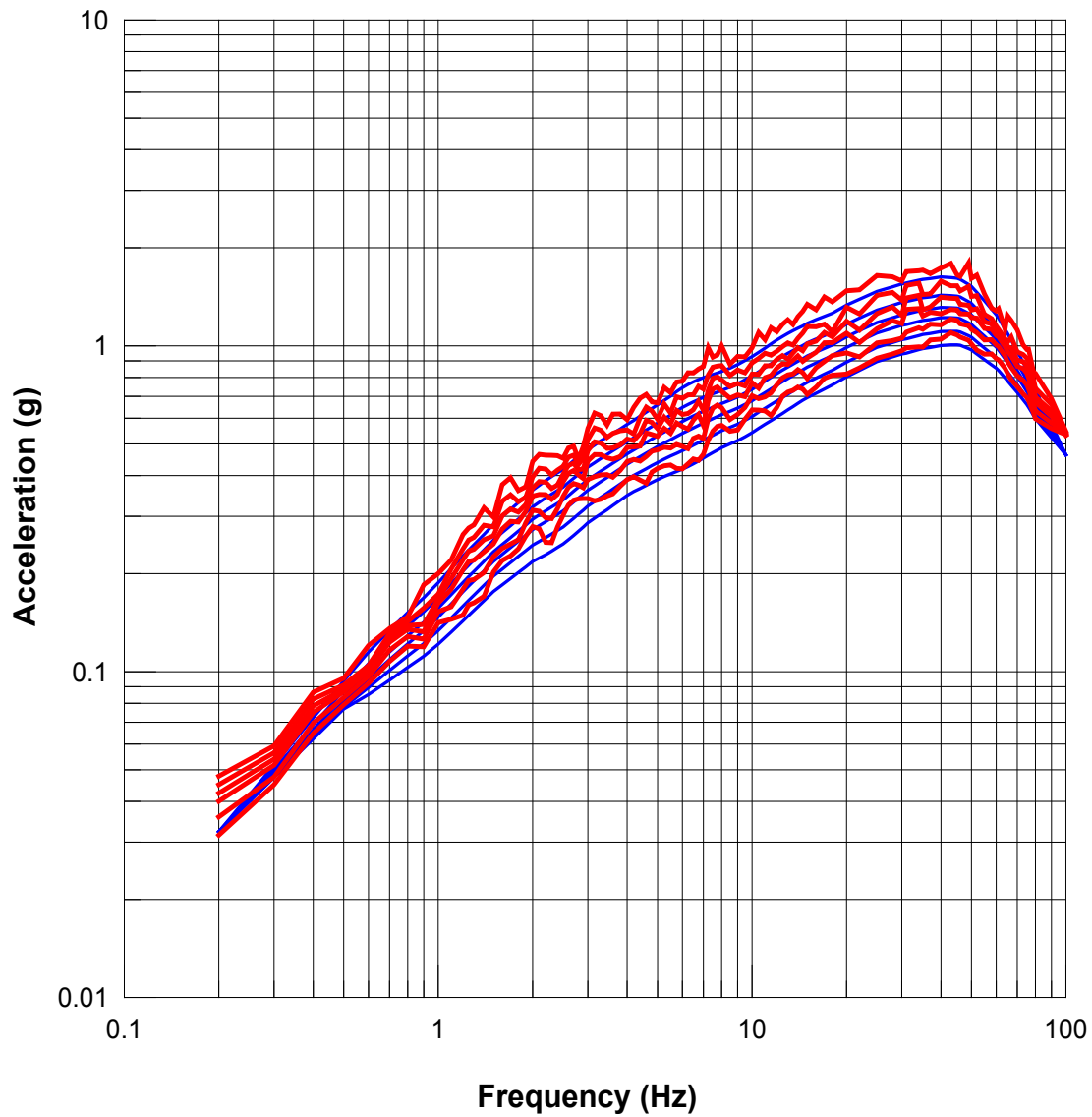
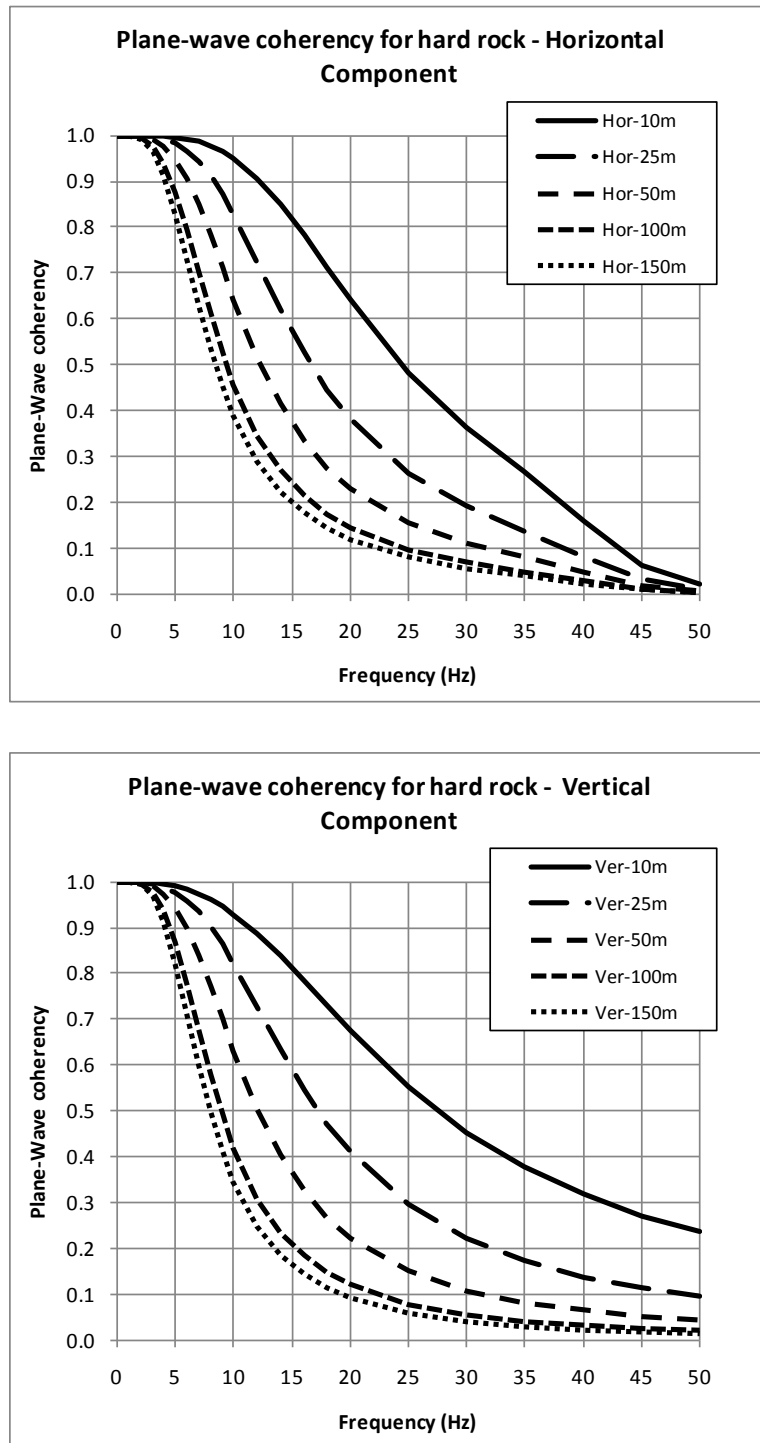


Figure 3-32 Acceleration, Velocity, and Displacement of VTH



**Figure 3-33 Comparison of Response Spectra of VTH and HRHF Vertical Target Response Spectra**



**Figure 4-1 Amplitude of Empirical Plane-Wave Spatial-Coherency Function for Horizontal and Vertical Ground Motion Components for Hard Rock**



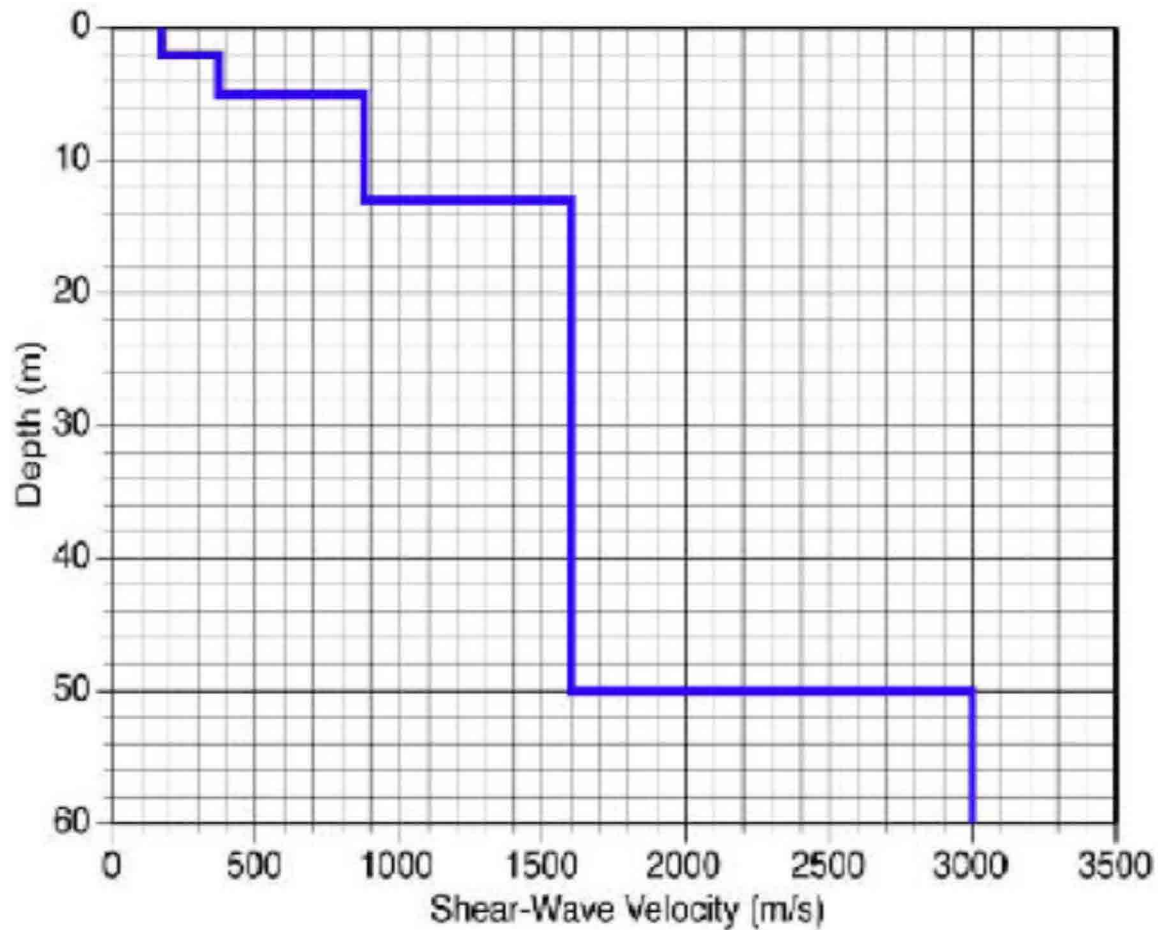
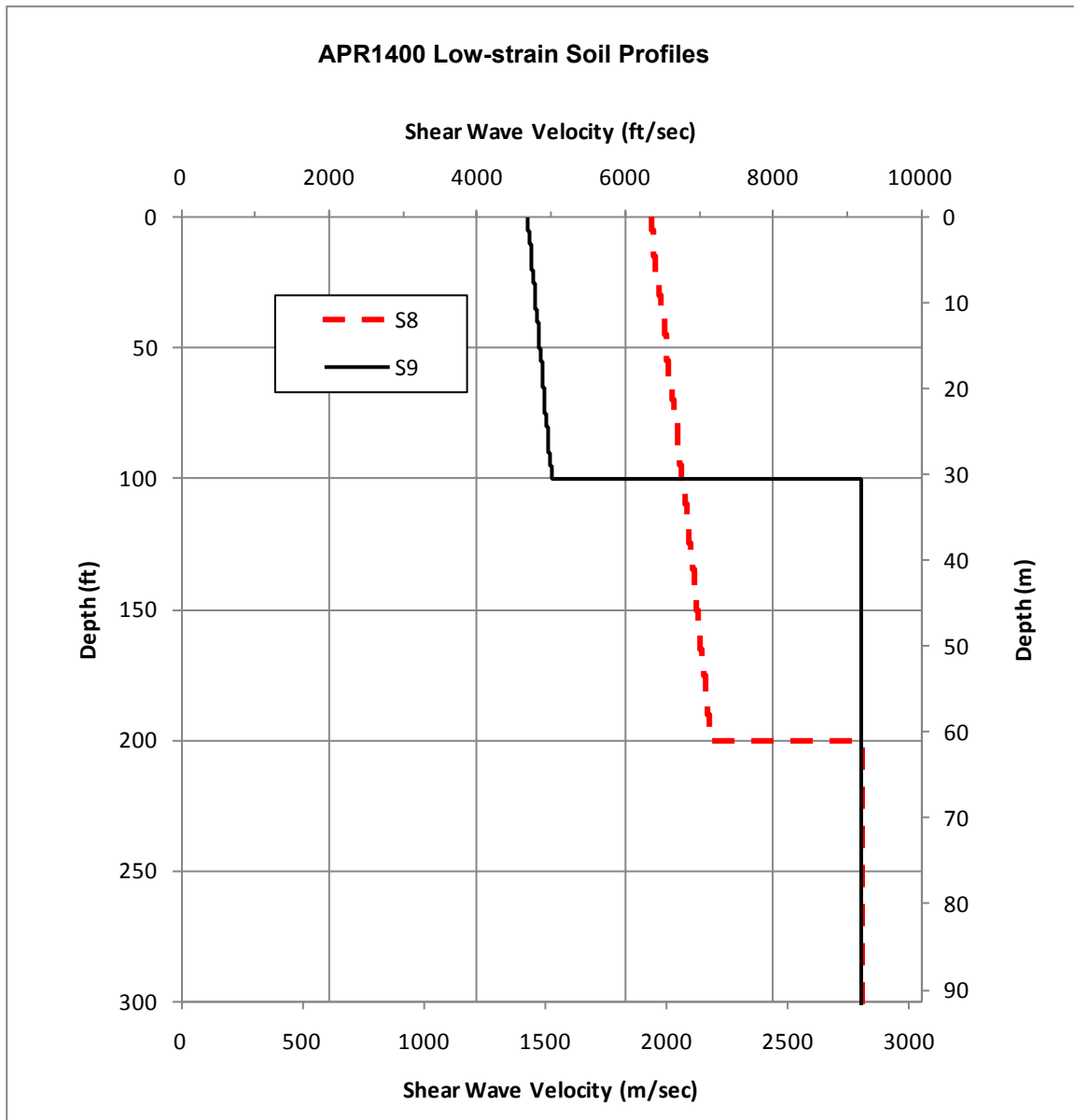
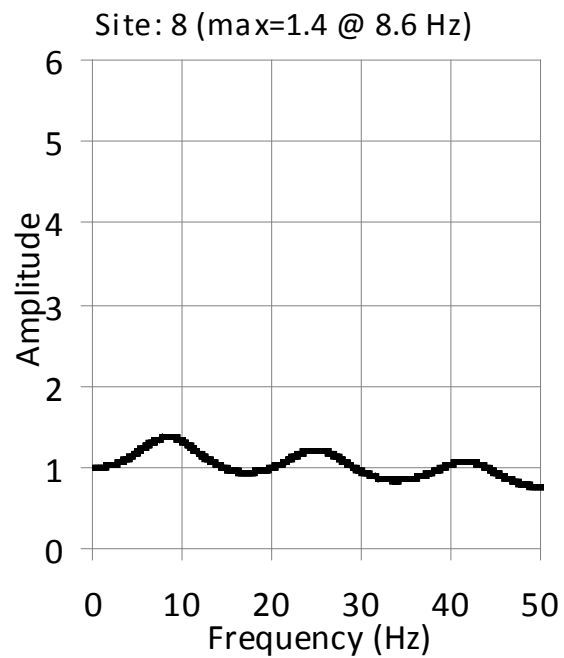


Figure 5-1 Shear-Wave-Velocity Profile of the Pinyon Flat Array Site



**Figure 5-2 Shear-Wave-Velocity Profiles of APR1400 Low-strain Sites S8 and S9**



**Figure 5-3 Horizontal Site Response Transfer Function for the APR1400 Generic Site Profile S8**

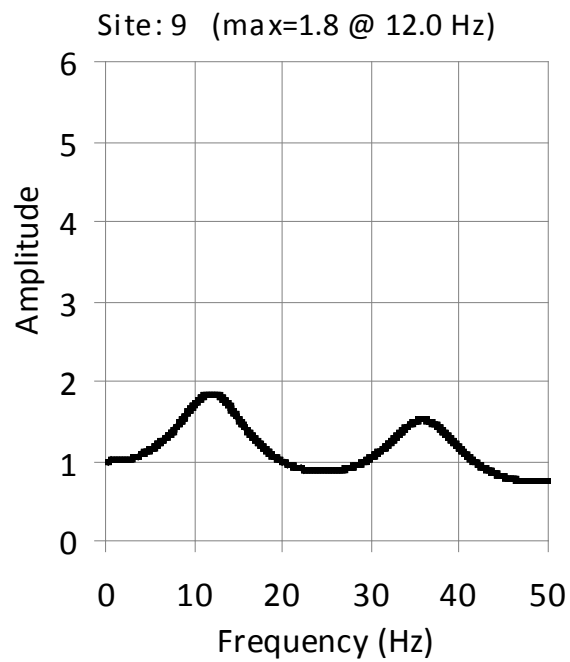


**Figure 5-4 Horizontal Site Response Transfer Function for the APR1400 Generic Site Profile S9**

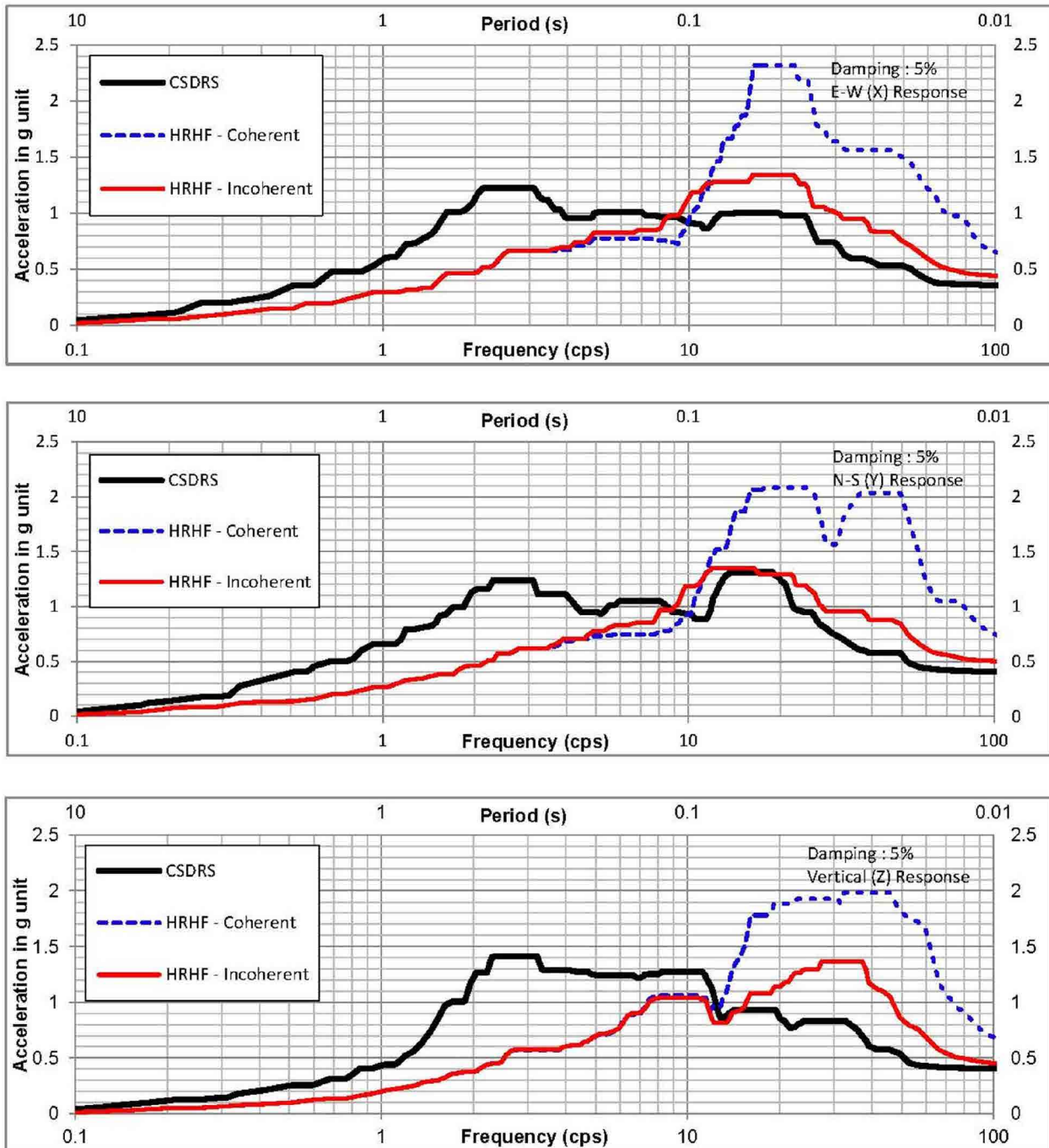


**Figure 5-5 Comparison of ISRS Based on CSDRS and HRHF Response Spectra - Containment Structure at El. 78'-0"**

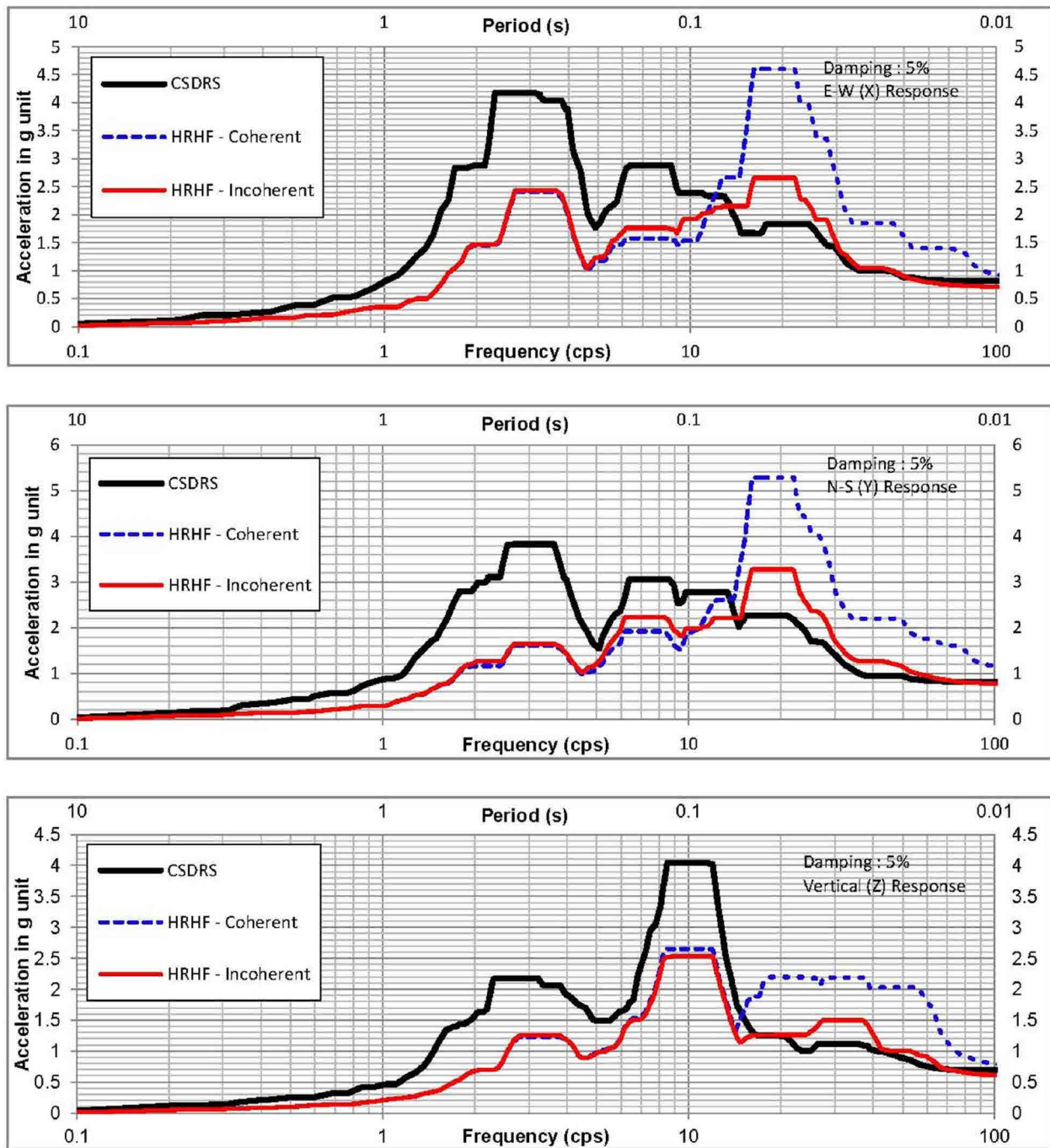


**Figure 5-6 Comparison of ISRS Based on CSDRS and HRHF Response Spectra - Containment Structure at El. 160'-0"**

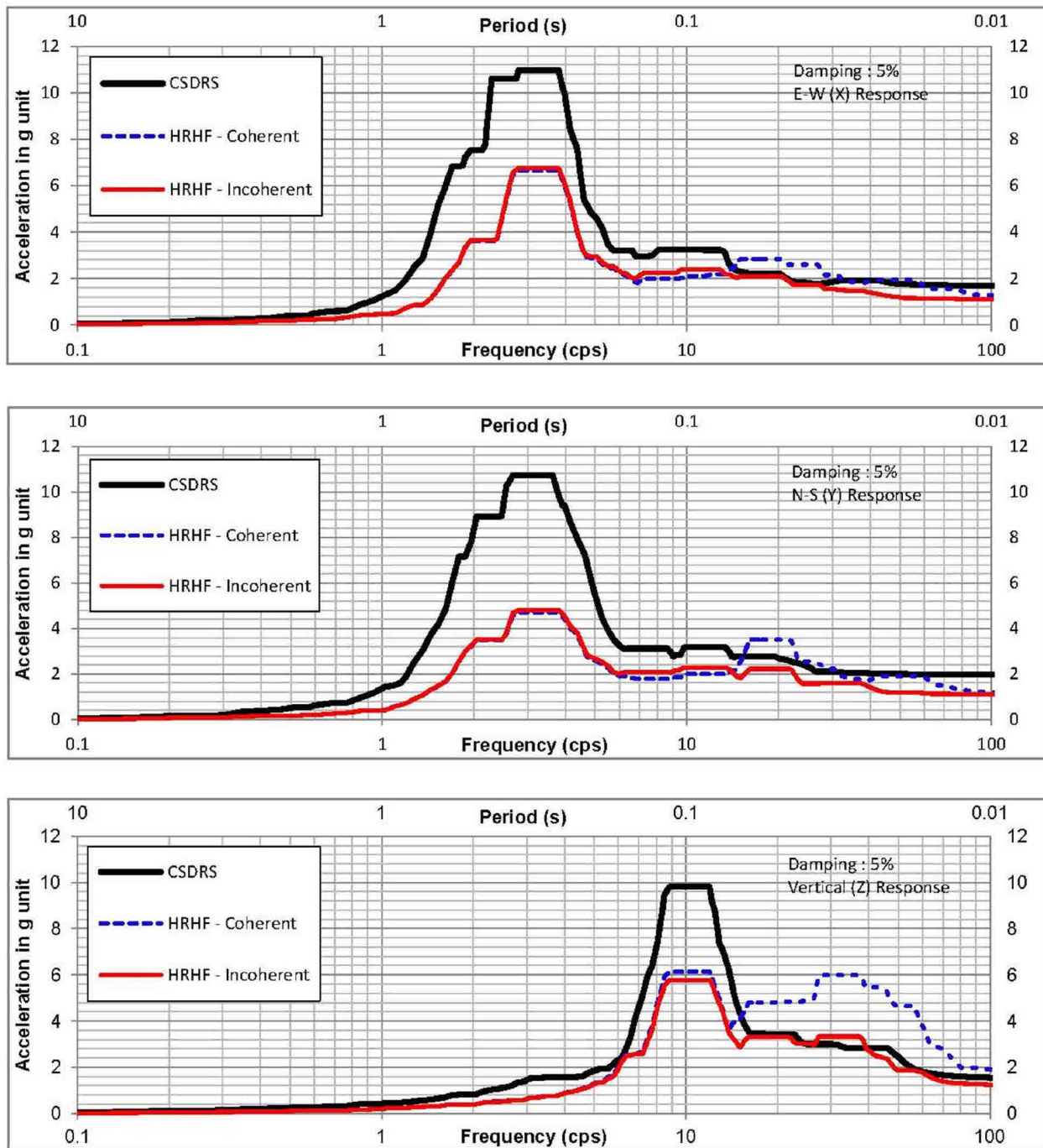


**Figure 5-7 Comparison of ISRS Based on CSDRS and HRHF Response Spectra - Containment Structure at El. 332'-0"**



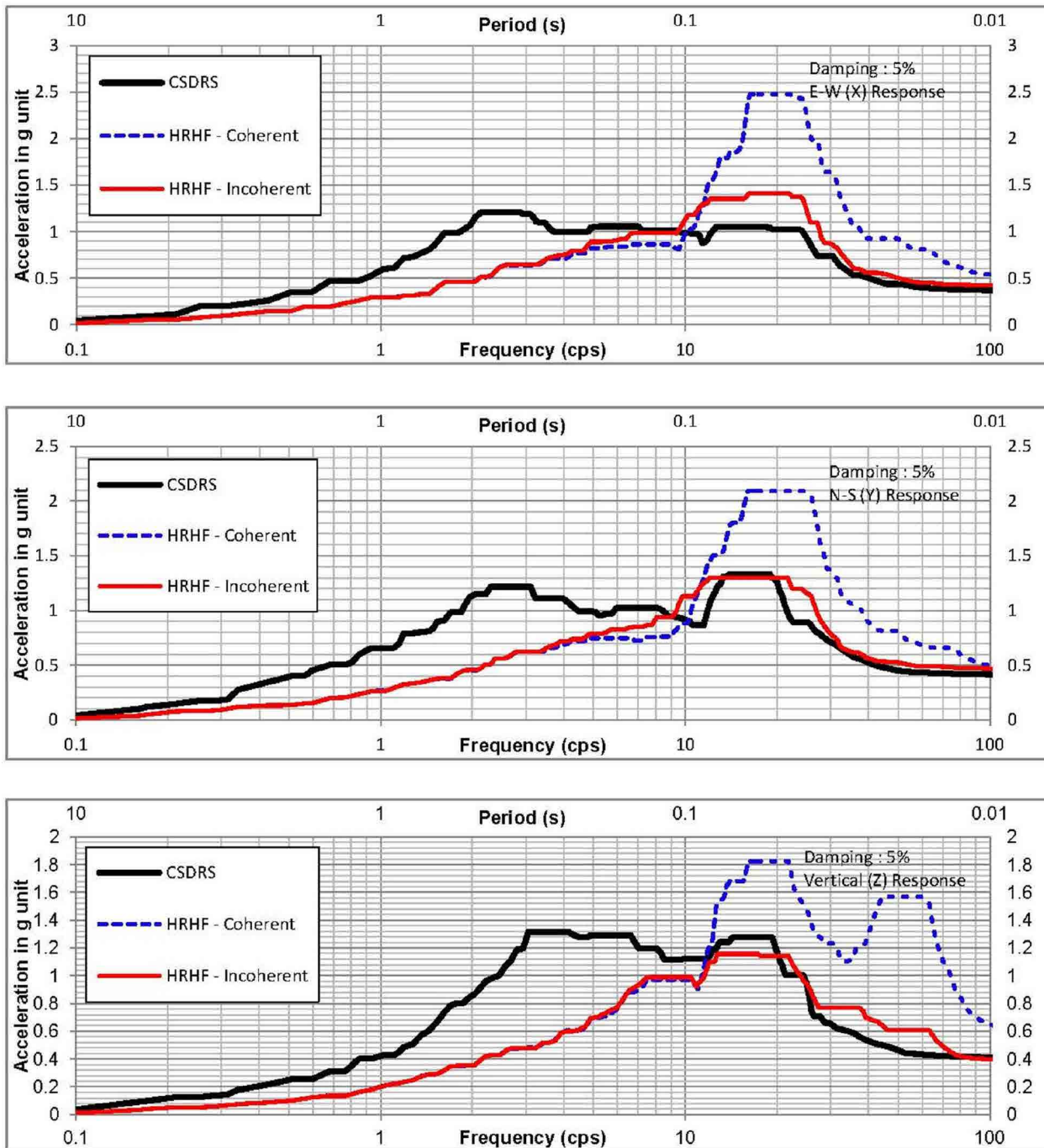


**Figure 5-8 Comparison ISRS Based on of CSDRS and HRHF Response Spectra – Primary Shield Wall at El. 78'-0"**



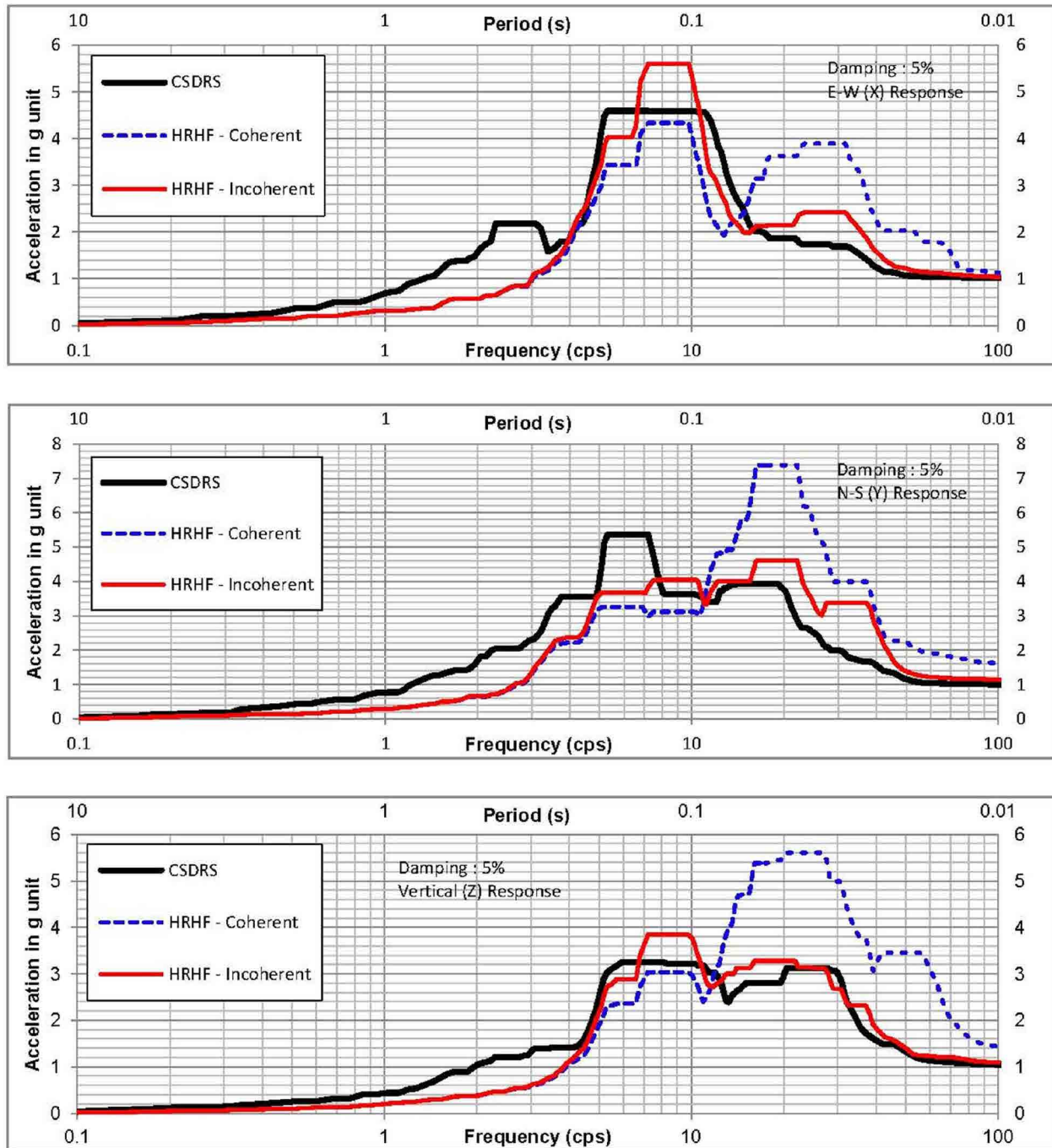


**Figure 5-9 Comparison of ISRS Based on CSDRS and HRHF Response Spectra – Primary Shield Wall at El. 156'-0"**

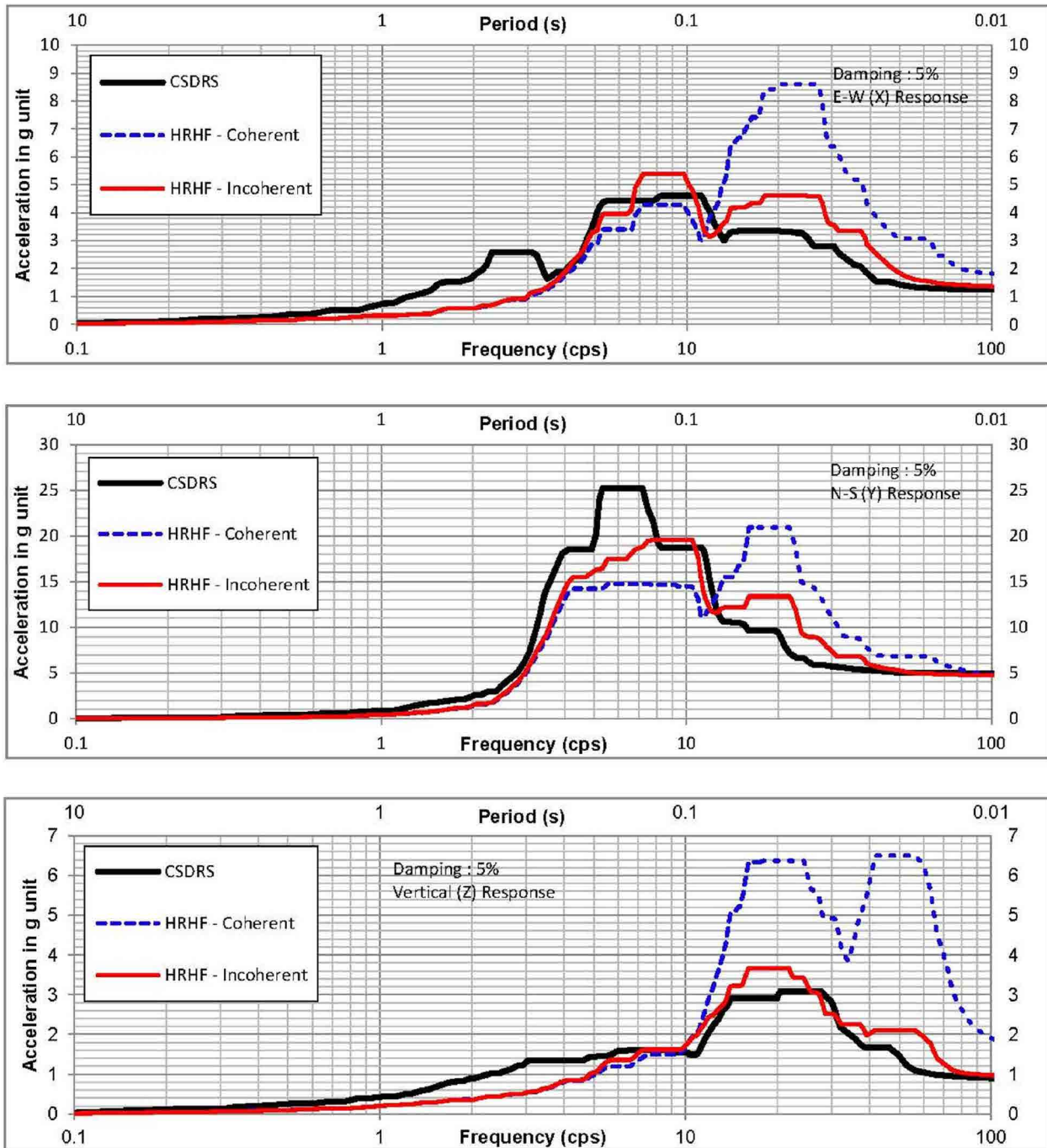
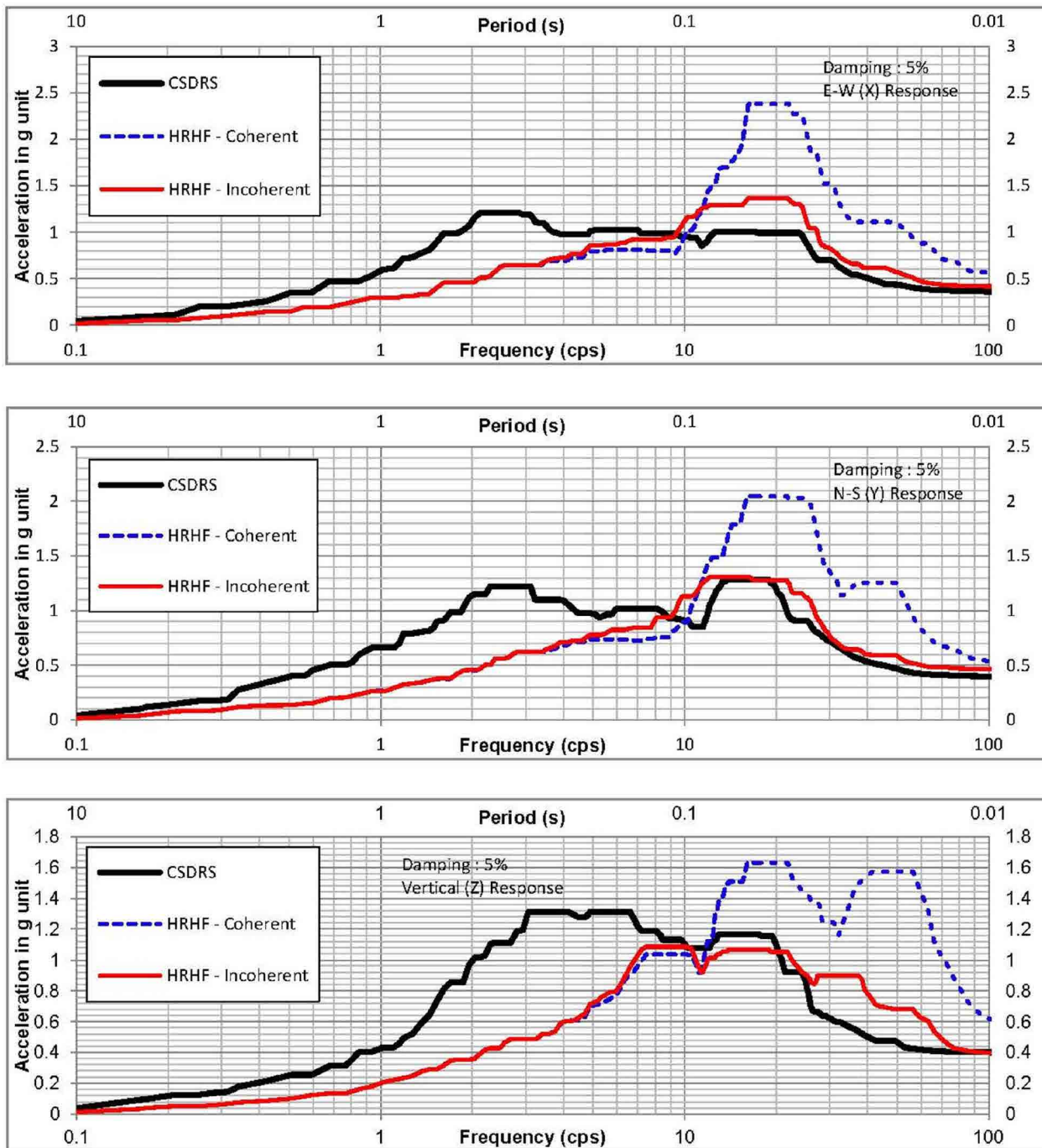
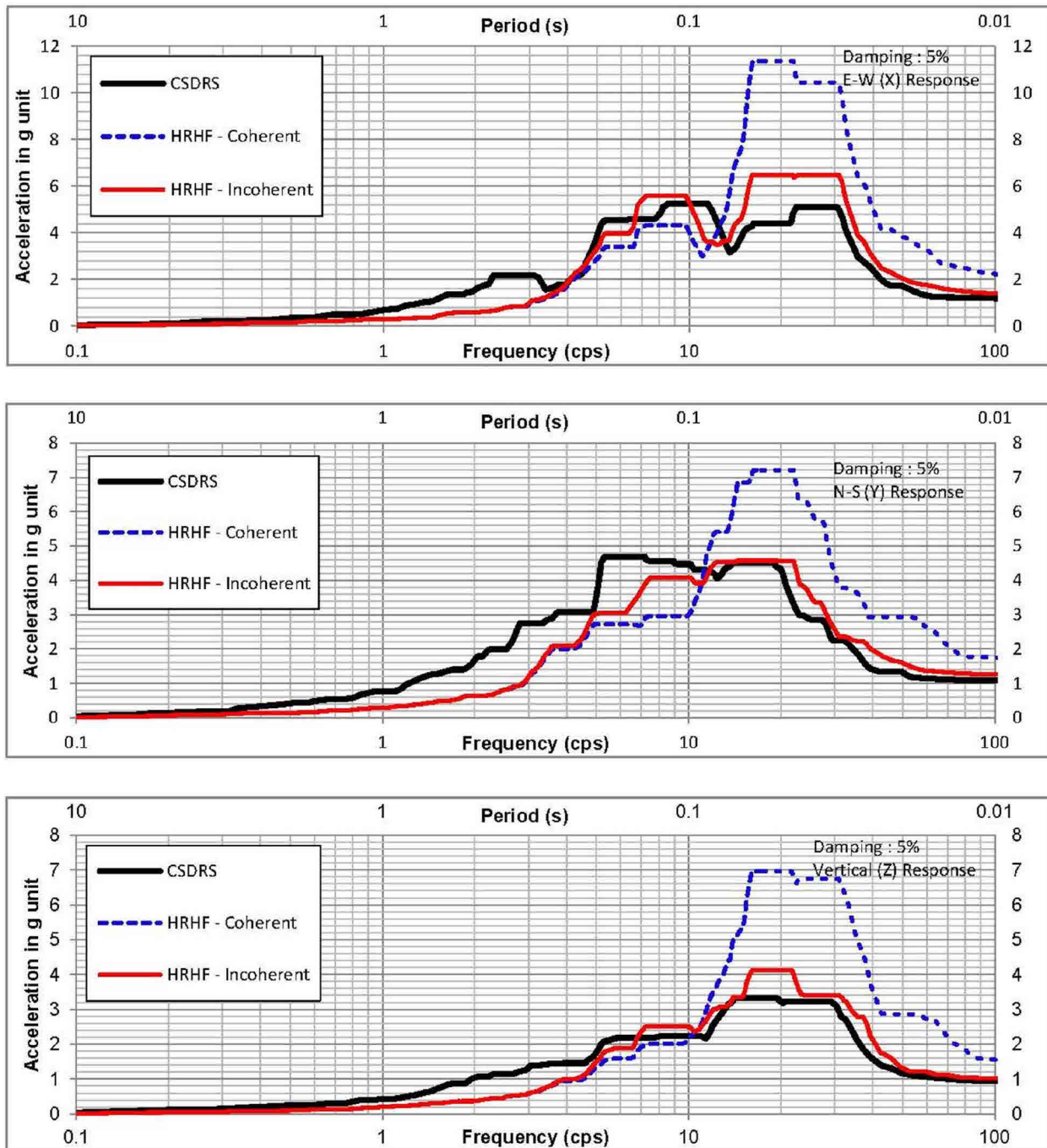


Figure 5-10 Comparison of ISRS Based on CSDRS and HRHF Response Spectra – Primary Shield Wall at El. 191'-0"



**Figure 5-11 Comparison of ISRS Based on CSDRS and HRHF Response Spectra – Secondary Shield Wall at El. 78'-0"**



**Figure 5-12 Comparison of ISRS Based on CSDRS and HRHF Response Spectra – Secondary Shield Wall at El. 156'-0"**



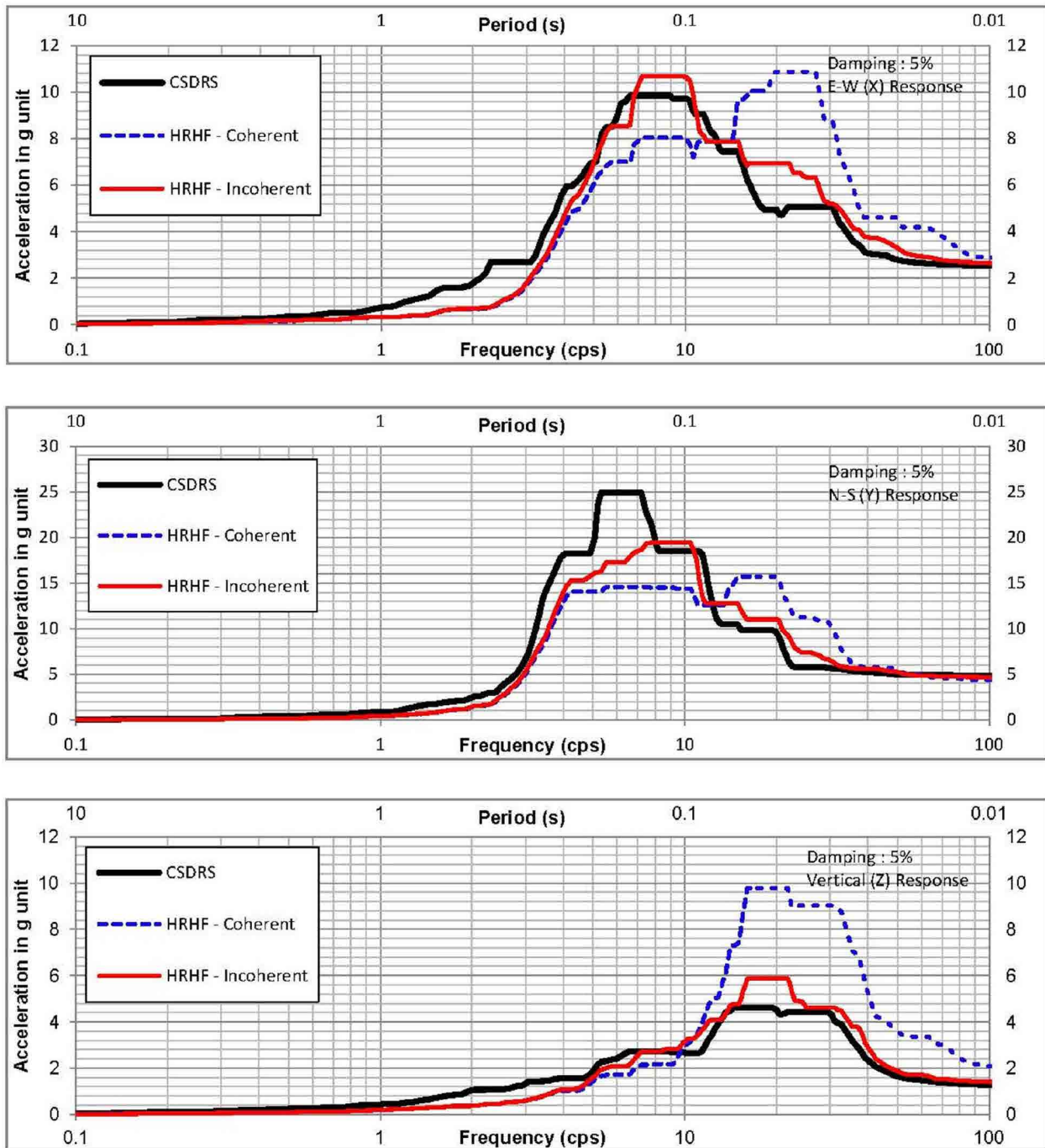
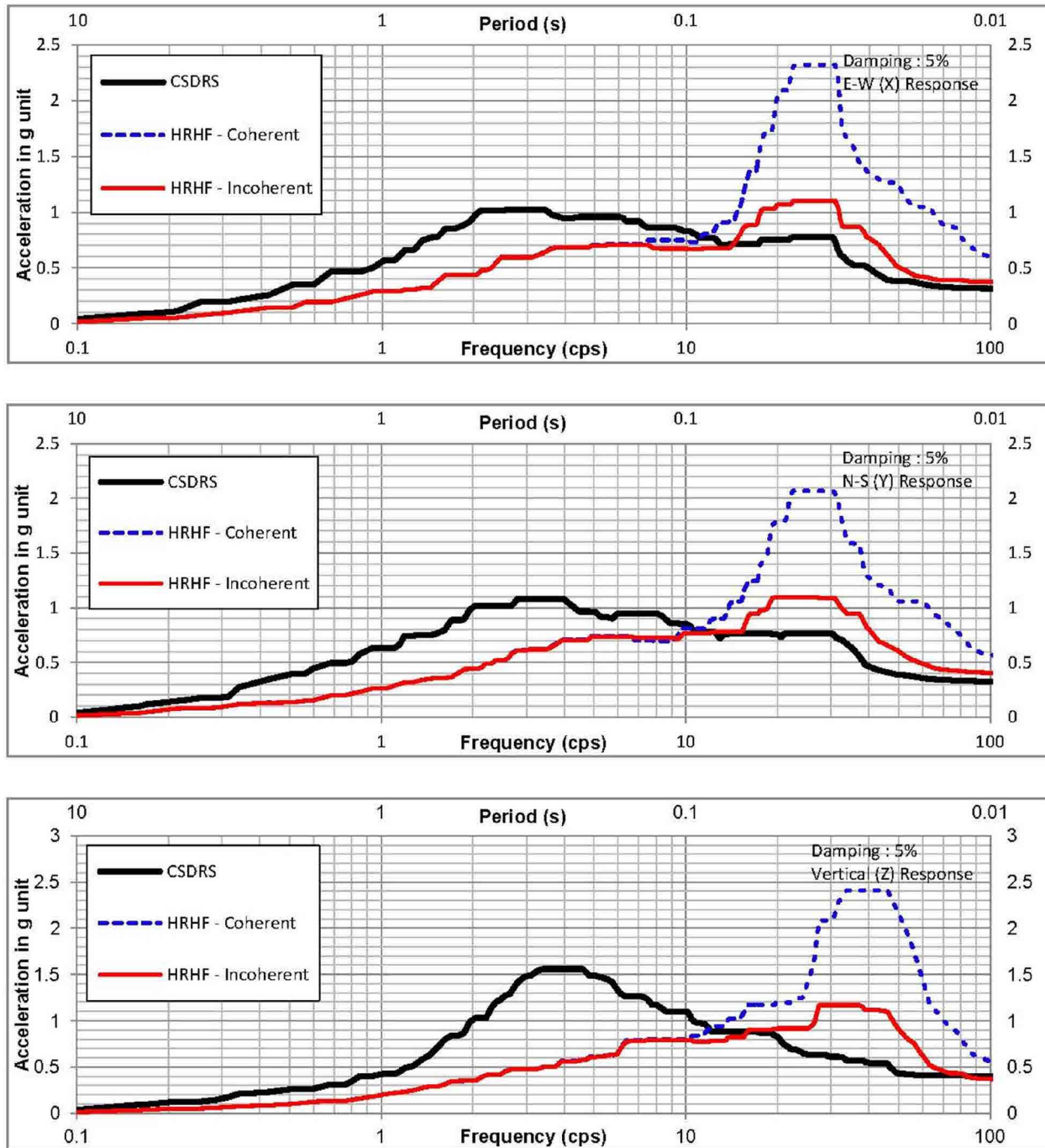
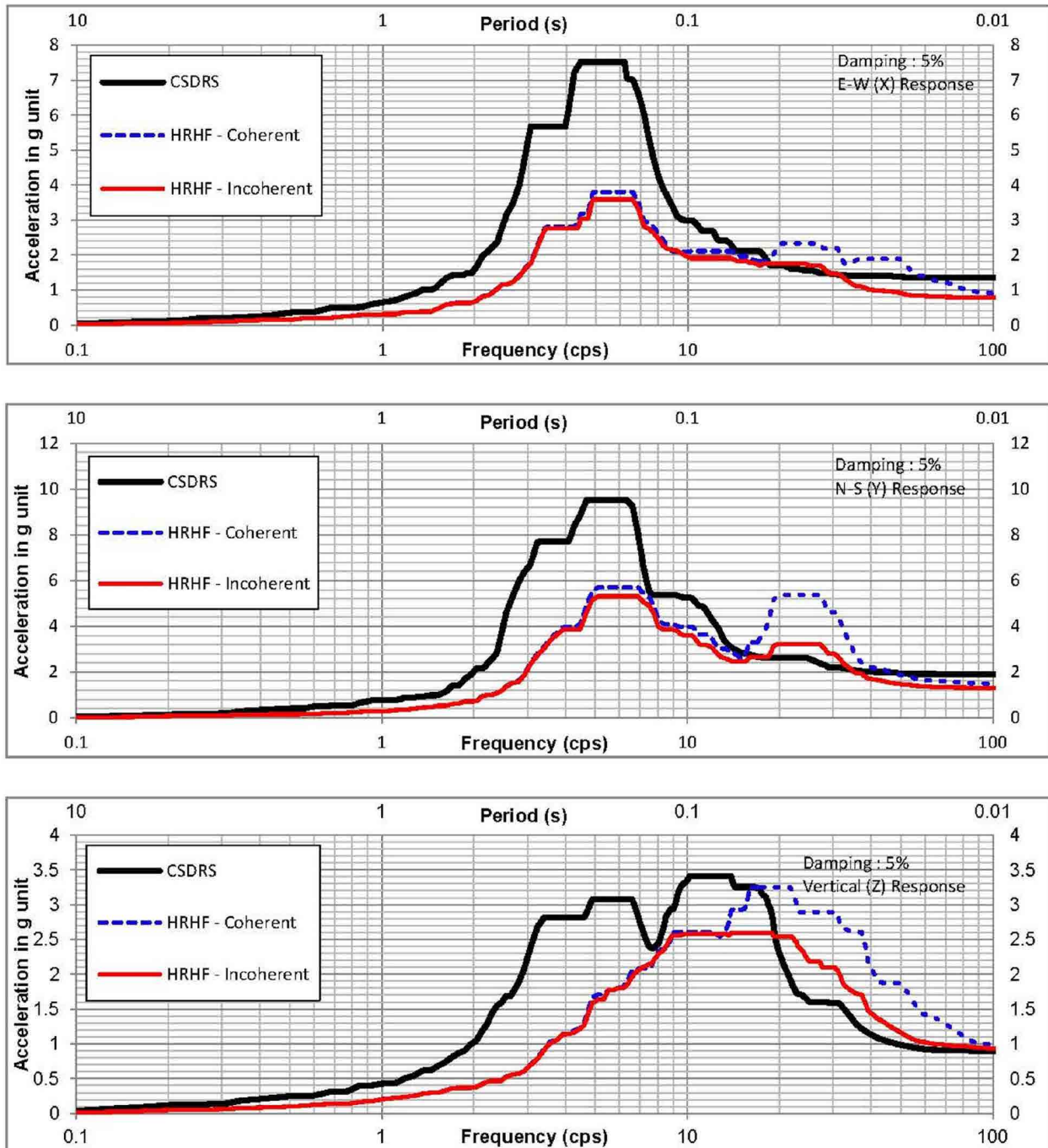


Figure 5-13 Comparison of ISRS Based on CSDRS and HRHF Response Spectra – Secondary Shield Wall at El. 191'-0"



**Figure 5-14 Comparison of ISRS Based on CSDRS and HRHF Response Spectra – Auxiliary Building Shearwall at El. 55'-0"**



**Figure 5-15 Comparison of ISRS Based on CSDRS and HRHF Response Spectra – Auxiliary Building Shearwall at El. 156'-0"**

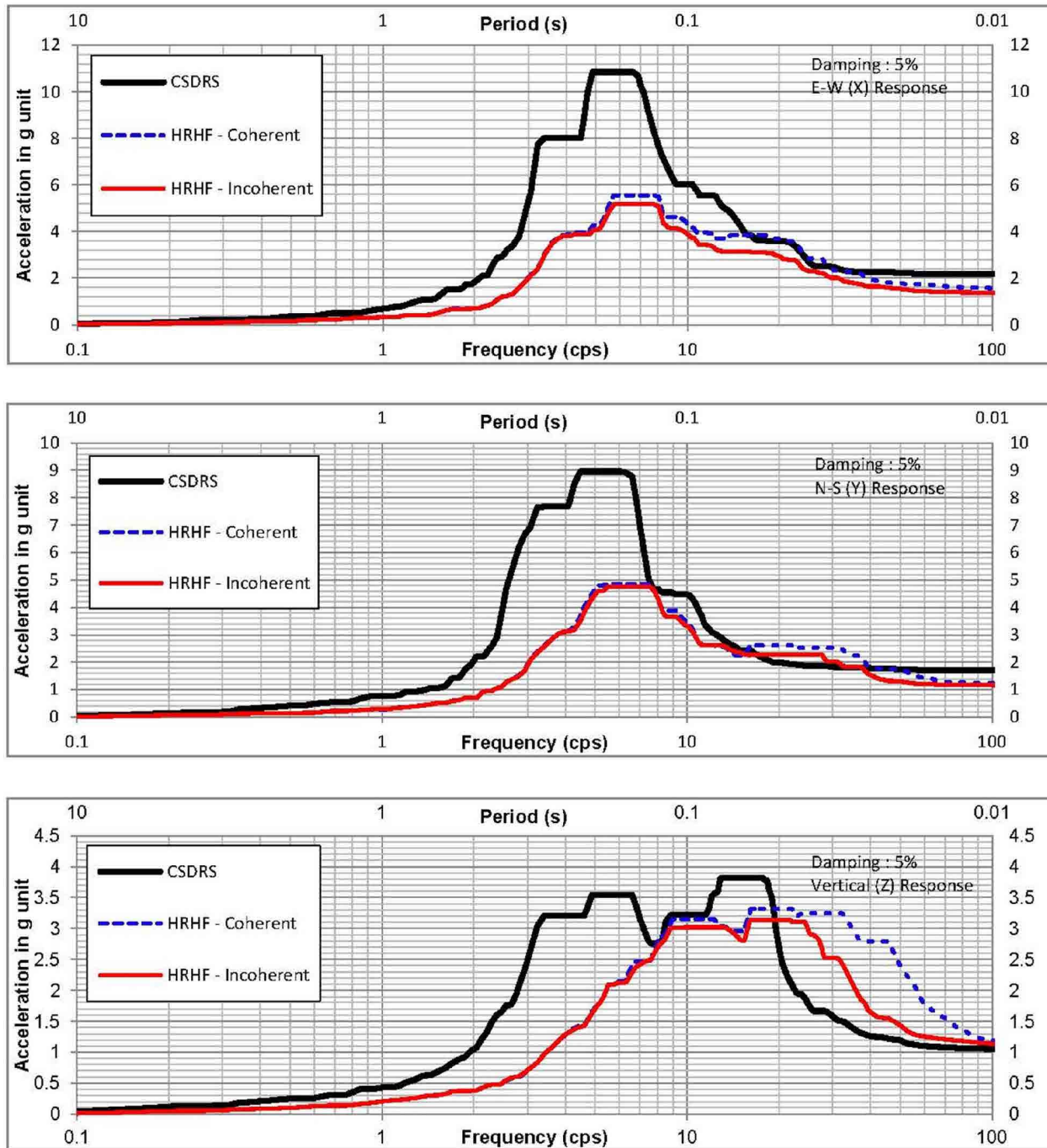


**Figure 5-16 Comparison of ISRS Based on CSDRS and HRHF Response Spectra – Auxiliary Building Shearwall at El. 213'-6"**



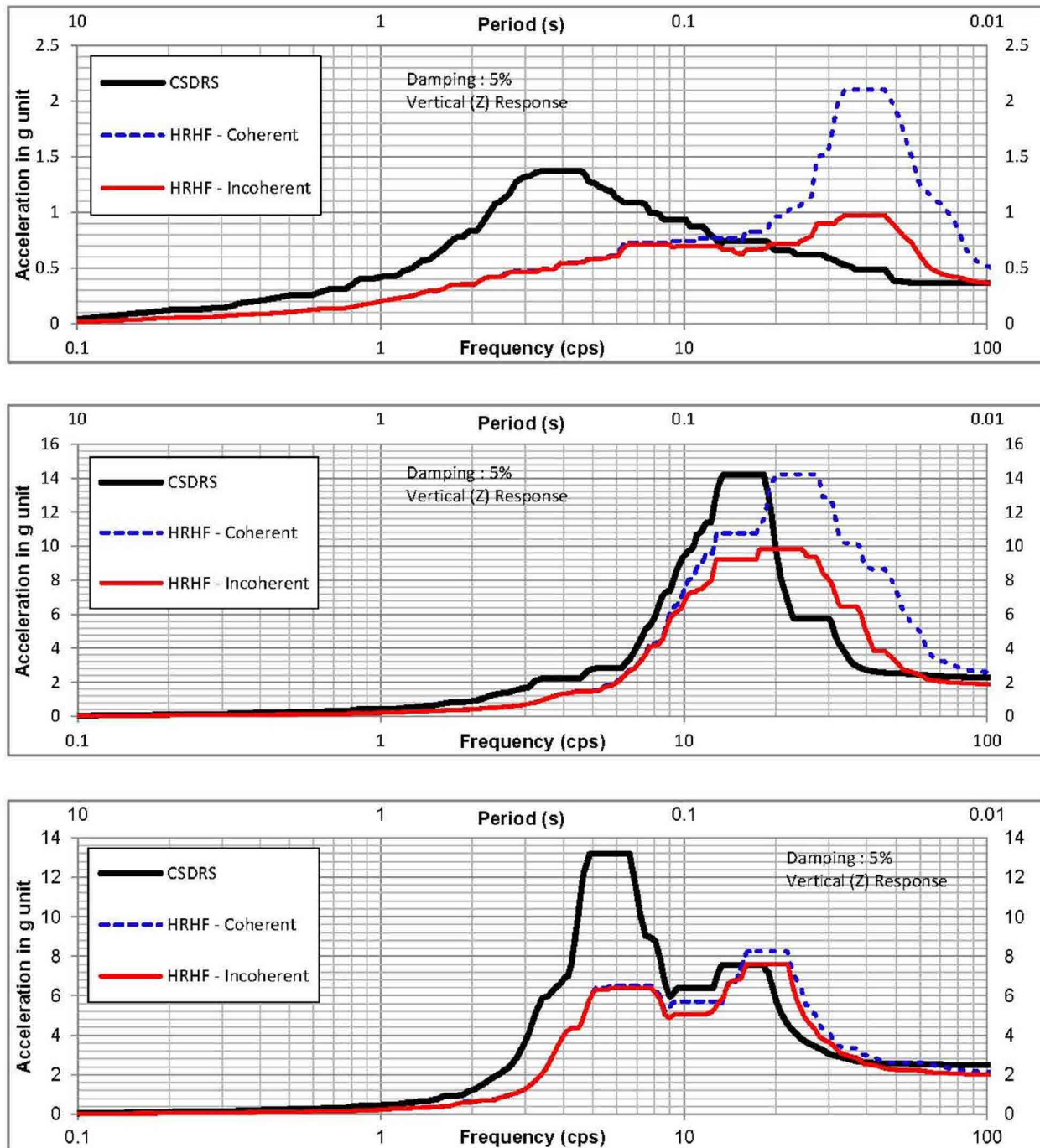
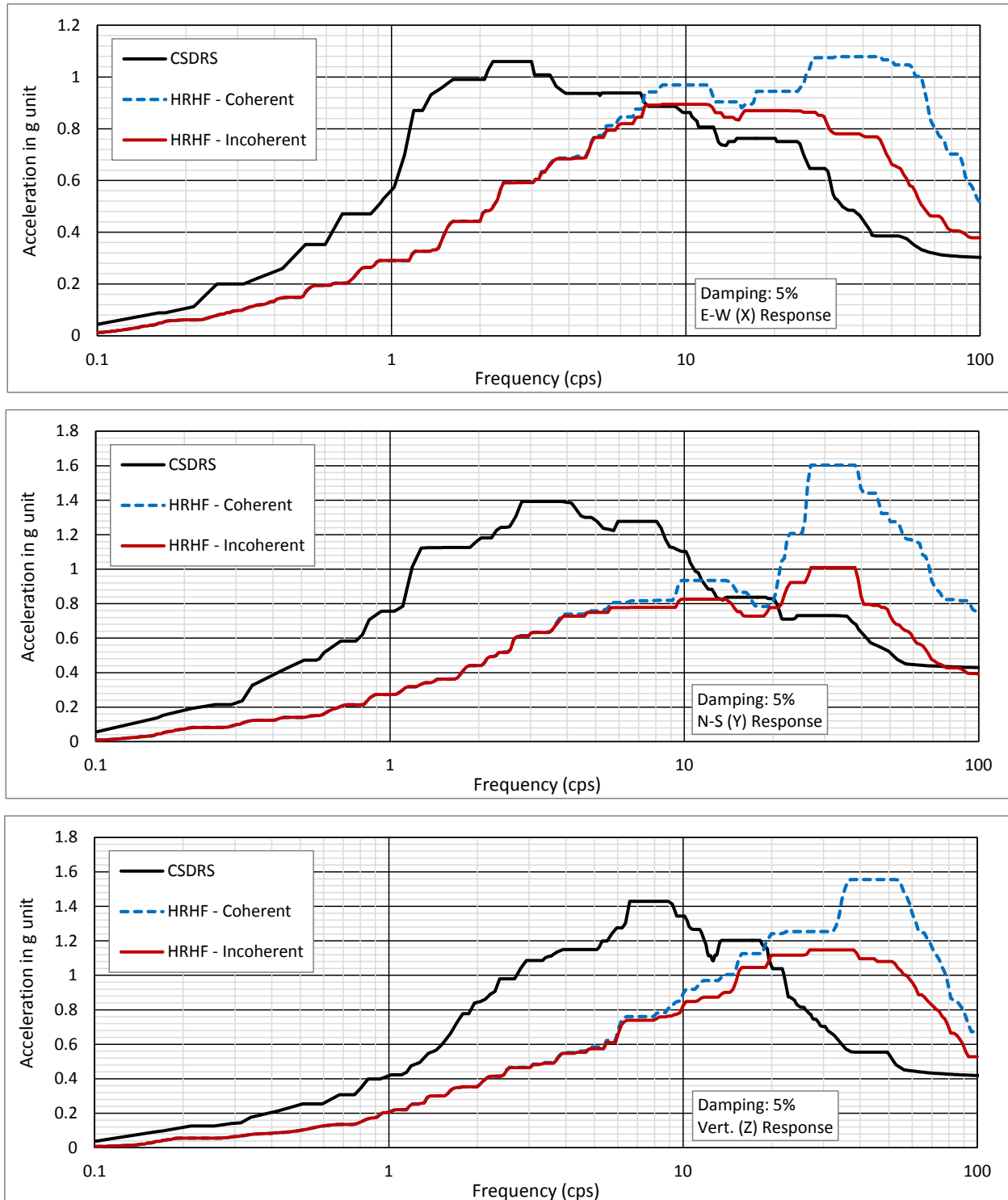
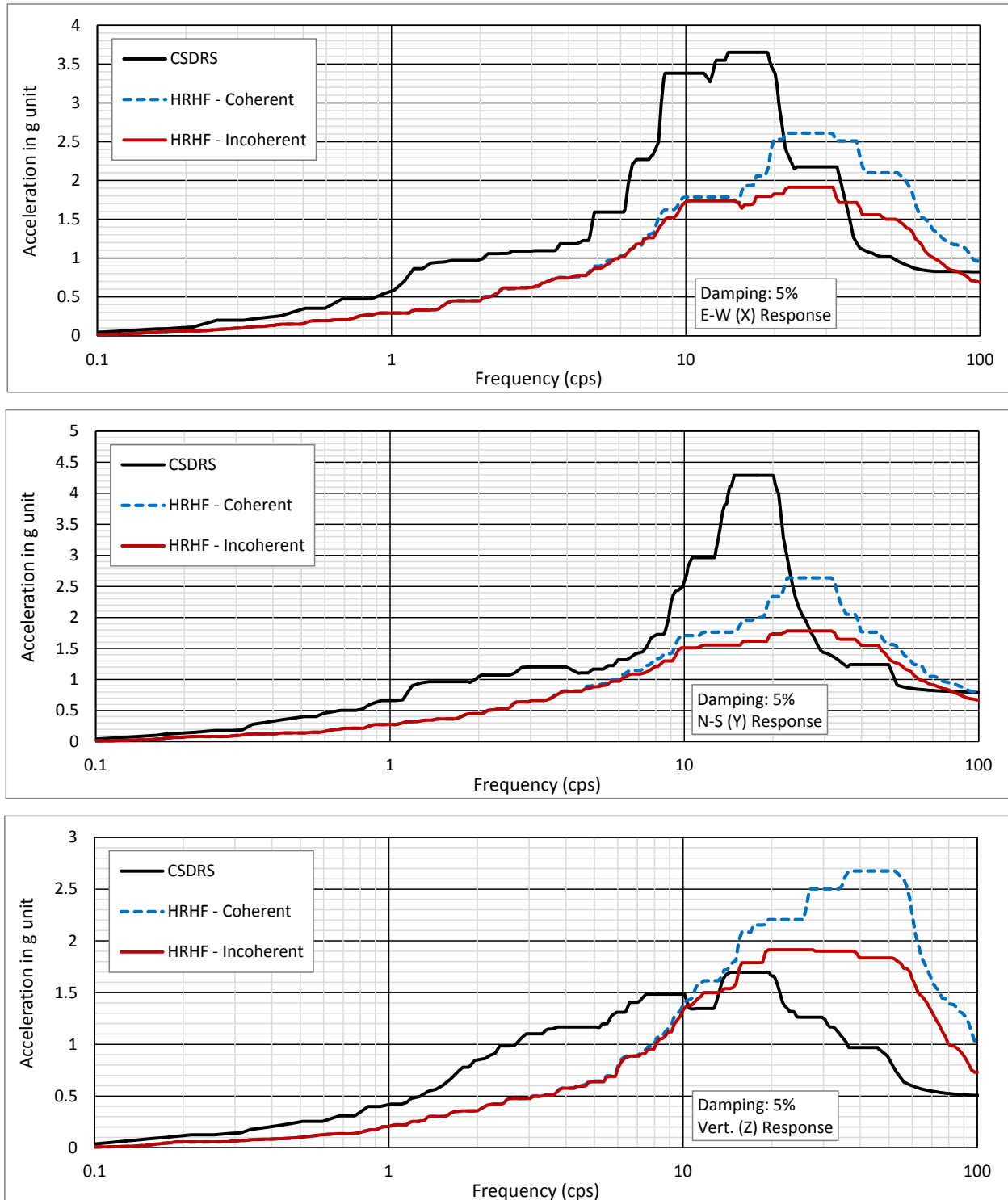


Figure 5-17 Comparison of ISRS Based on CSDRS and HRHF Response Spectra – Auxiliary Building Slabs at El. 55'-0", 156'-0" and 213'-6"



**Figure 5-18 Comparison of ISRS Based on CSDRS and HRHF Response Spectra – DFOT Room Wall at El. 63'-0"**



**Figure 5-19 Comparison of ISRS Based on CSDRS and HRHF Response Spectra – DFOT Room Wall at El. 100'-0"**

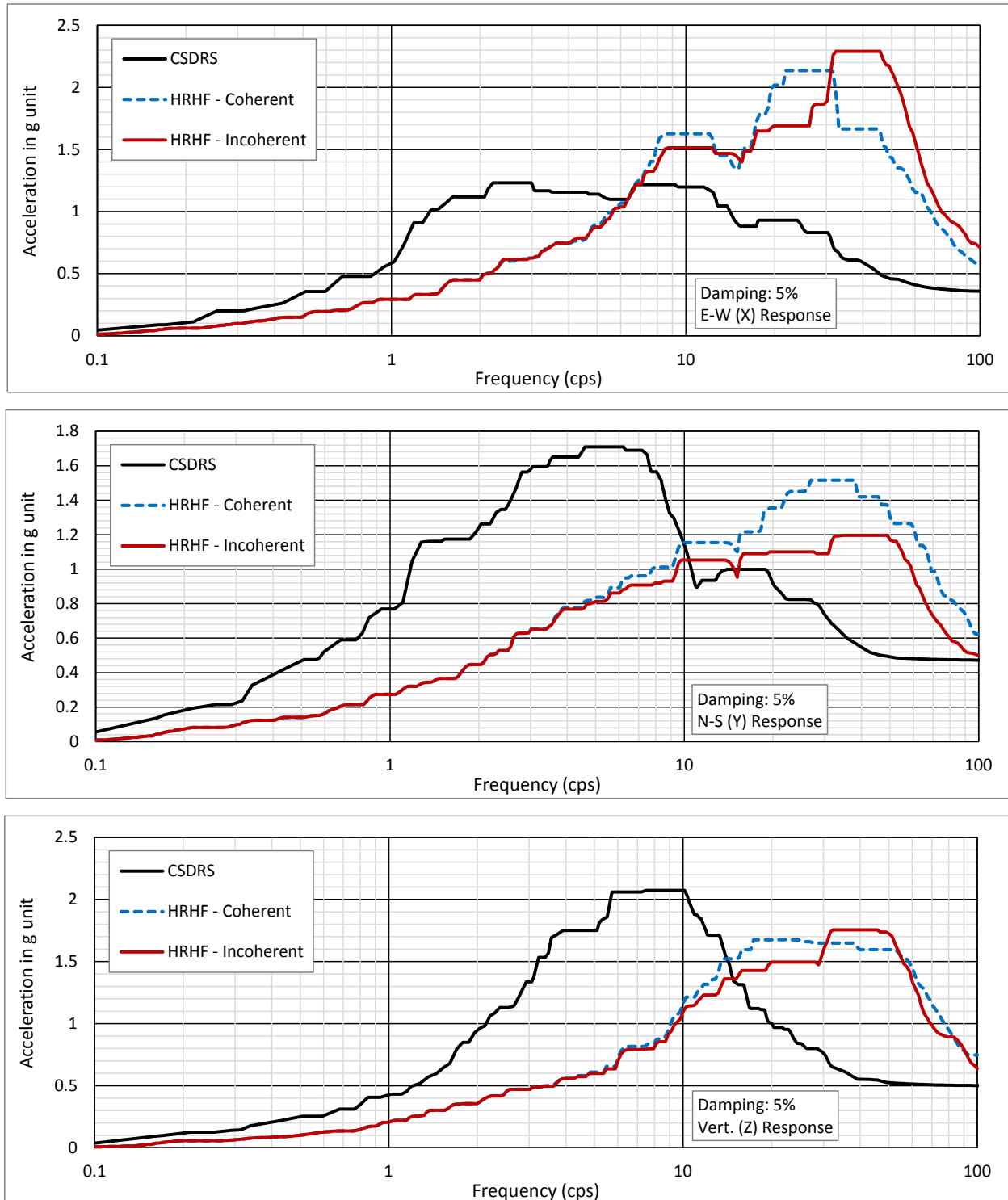


**Figure 5-20 Comparison of ISRS Based on CSDRS and HRHF Response Spectra – EDGB Wall at El. 100'-0"**

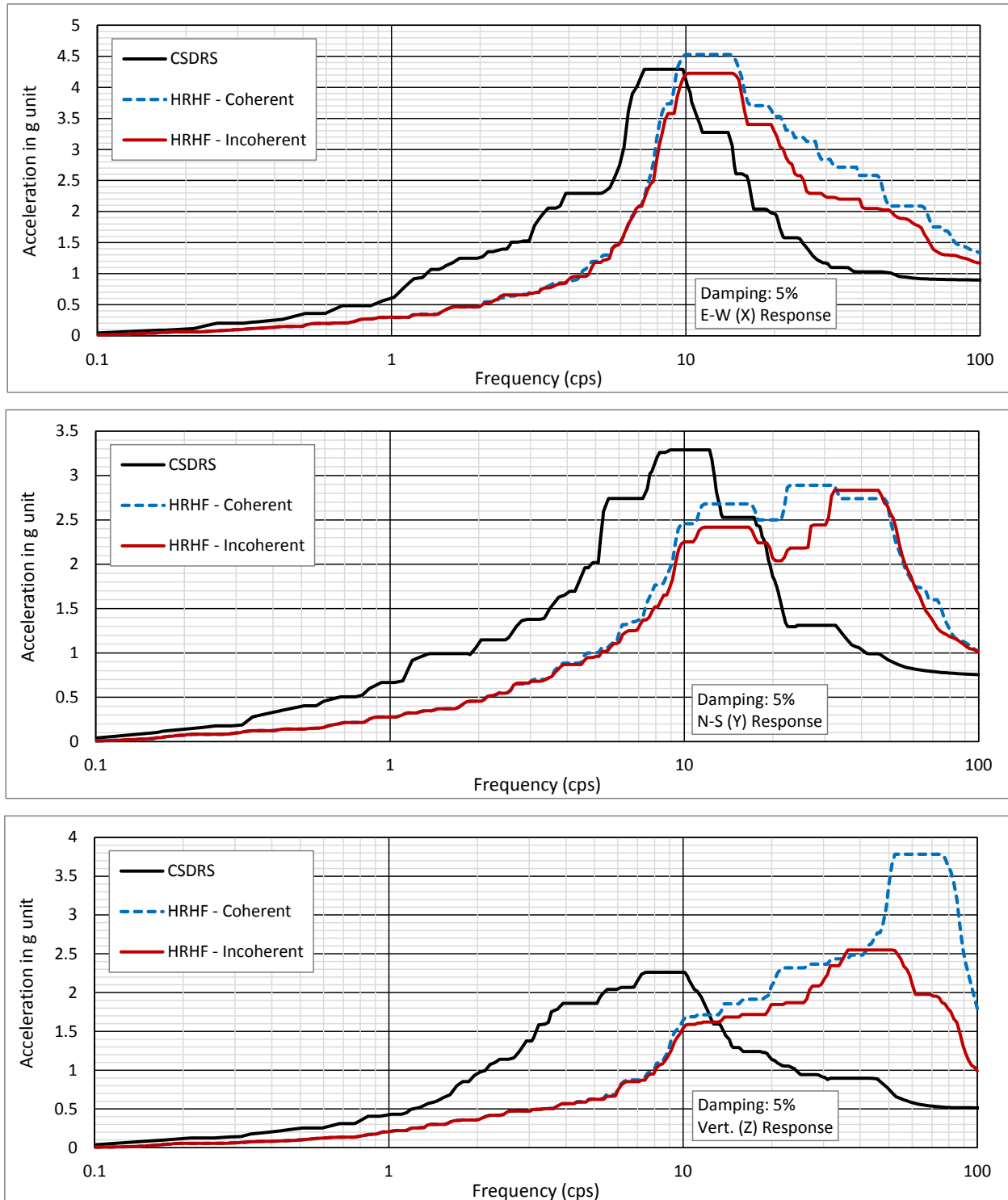
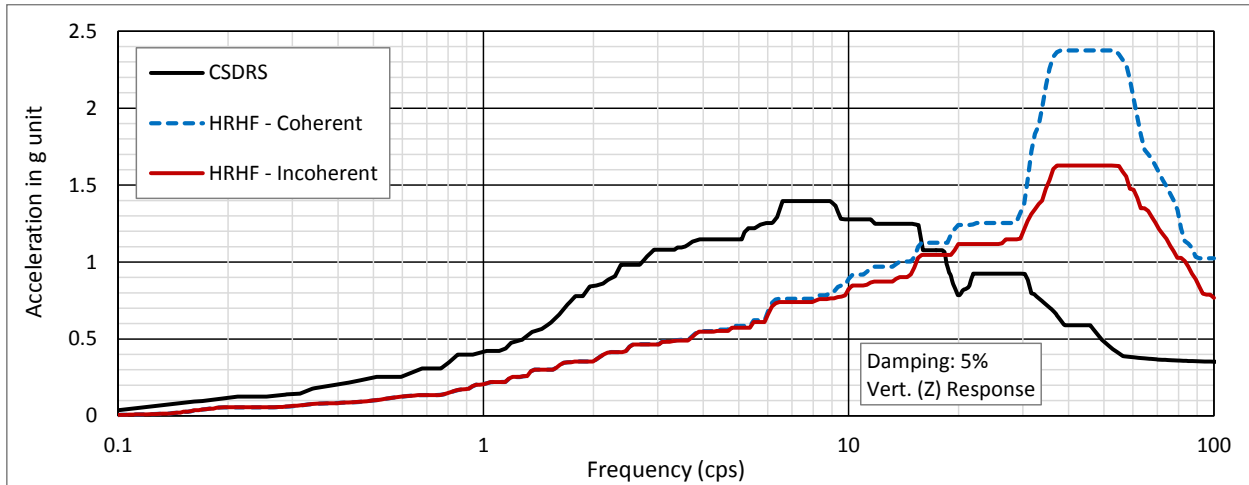
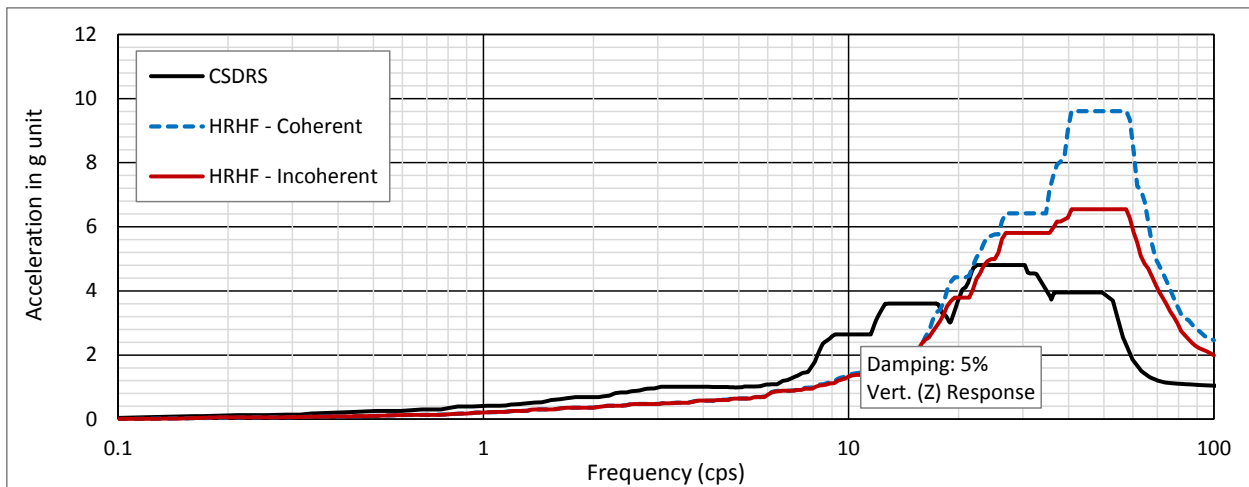


**Figure 5-21 Comparison of ISRS Based on CSDRS and HRHF Response Spectra – EDGB Wall at El. 135'-0"**

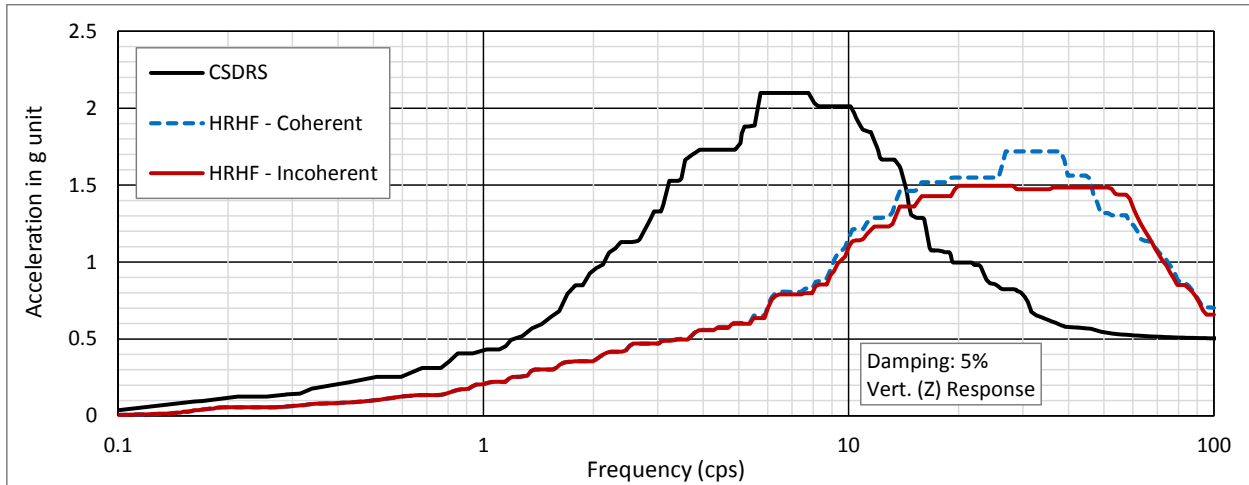


(a) El. 63'-0"

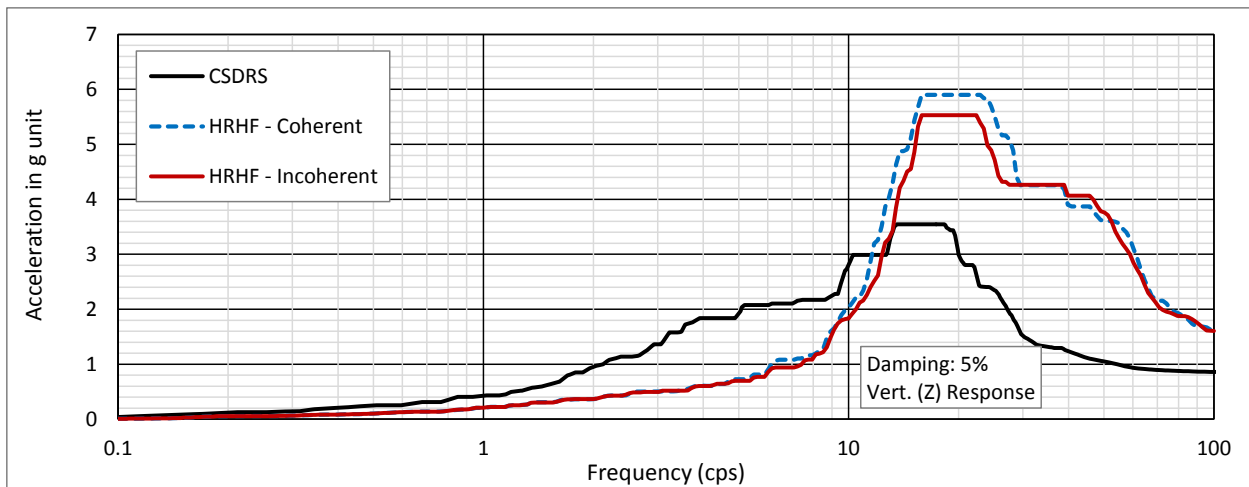


(a) El. 100'-0"

Figure 5-22 Comparison of ISRS Based on CSDRS and HRHF Response Spectra – DFOT Room Slabs



(a) El. 100'-0"



(a) El. 135'-0"

Figure 5-23 Comparison of ISRS Based on CSDRS and HRHF Response Spectra – EDGB Slabs

TS

**Figure 6-1 Arrangement of RCS**



TS

**Figure 6-2 Reactor Coolant System Component Supports**

TS

**Figure 6-3 Reactor Coolant System Component Nozzles**

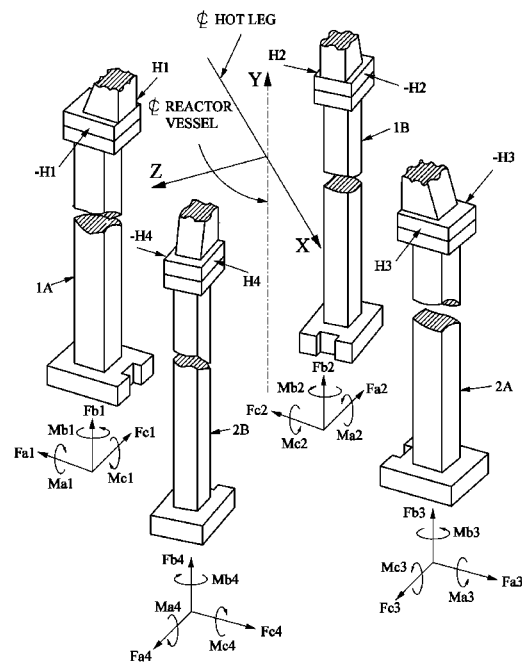


Figure 6-4 RV Supports

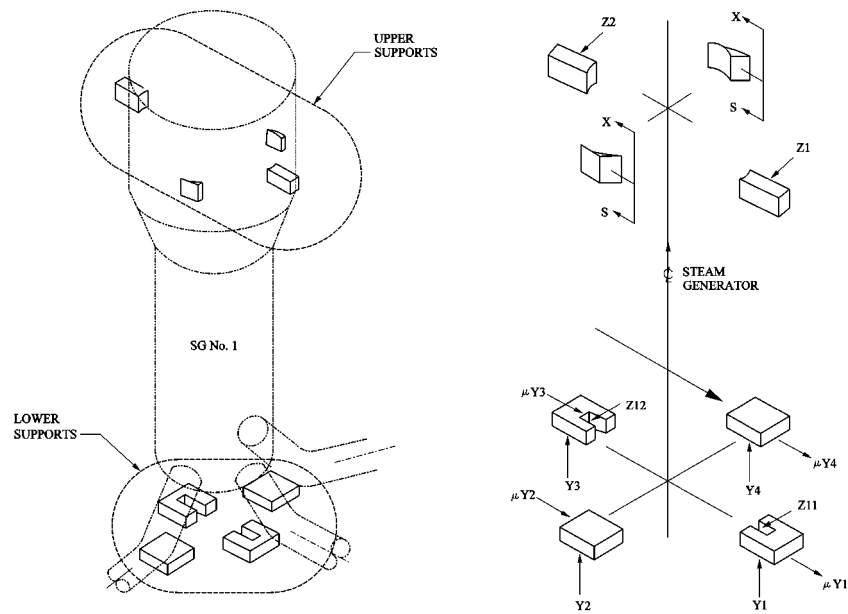


Figure 6-5 SG Support (No.1)

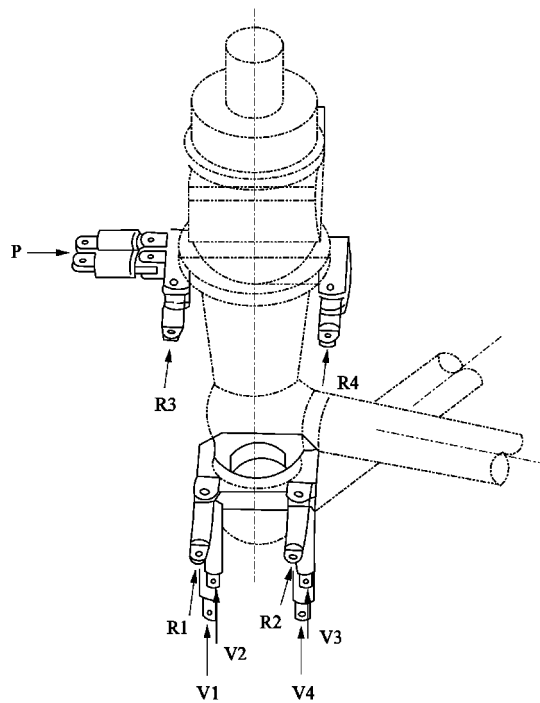


Figure 6-6 RCP Support (1A)

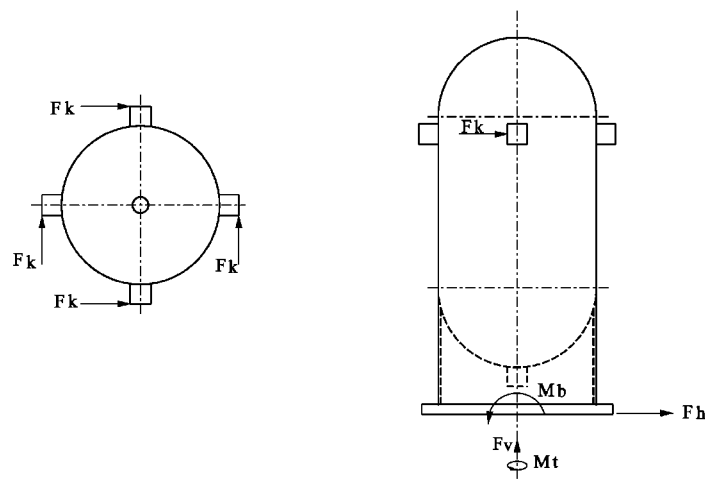


Figure 6-7 PZR Supports

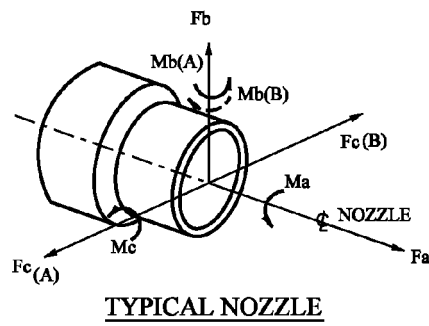


Figure 6-8 RV Nozzle

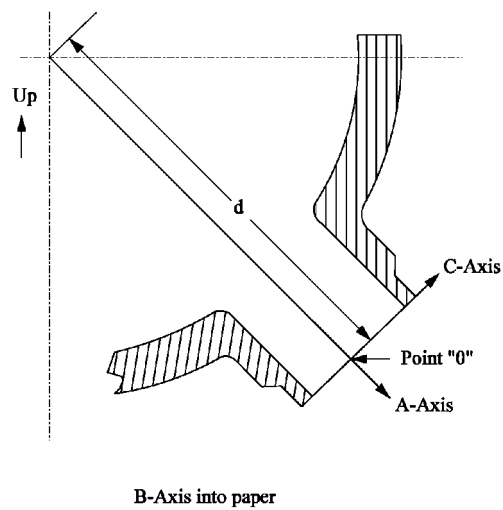


Figure 6-9 SG Nozzle



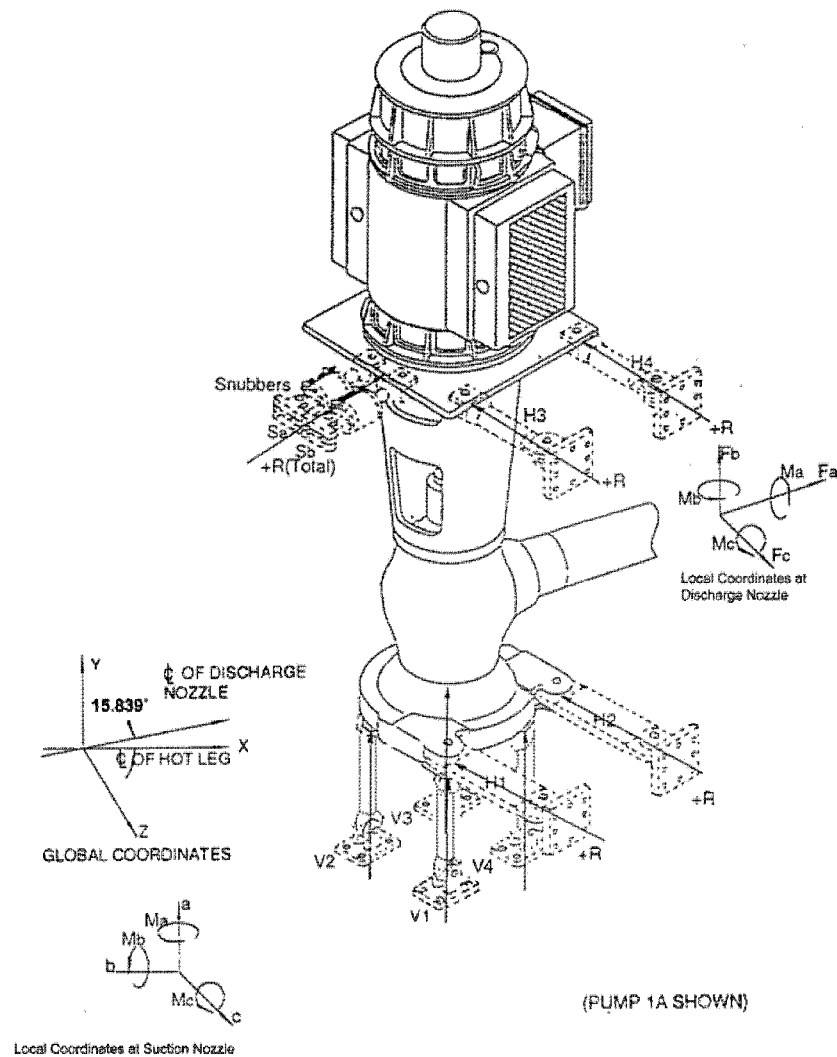
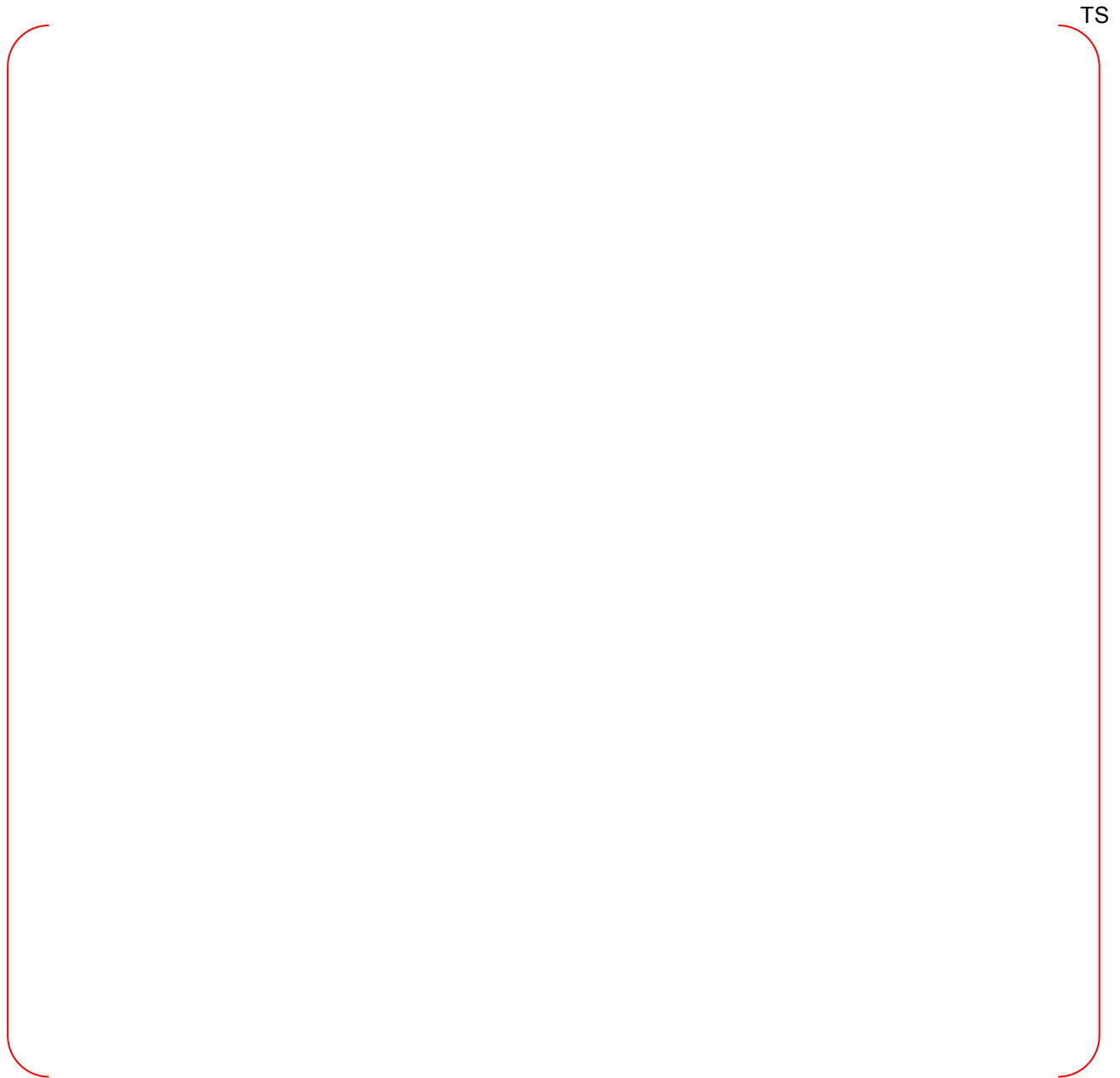


Figure 6-10 RCP Nozzle



**Figure 6-11 Reactor Coolant System Loop Piping Section/End Locations and Coordinate Systems**



**Figure 6-11 Reactor Coolant System Loop Piping Section/End Locations and Coordinate Systems (Cont'd)**



**Figure 6-11 Reactor Coolant System Loop Piping Section/End Locations and Coordinate Systems (Cont'd)**

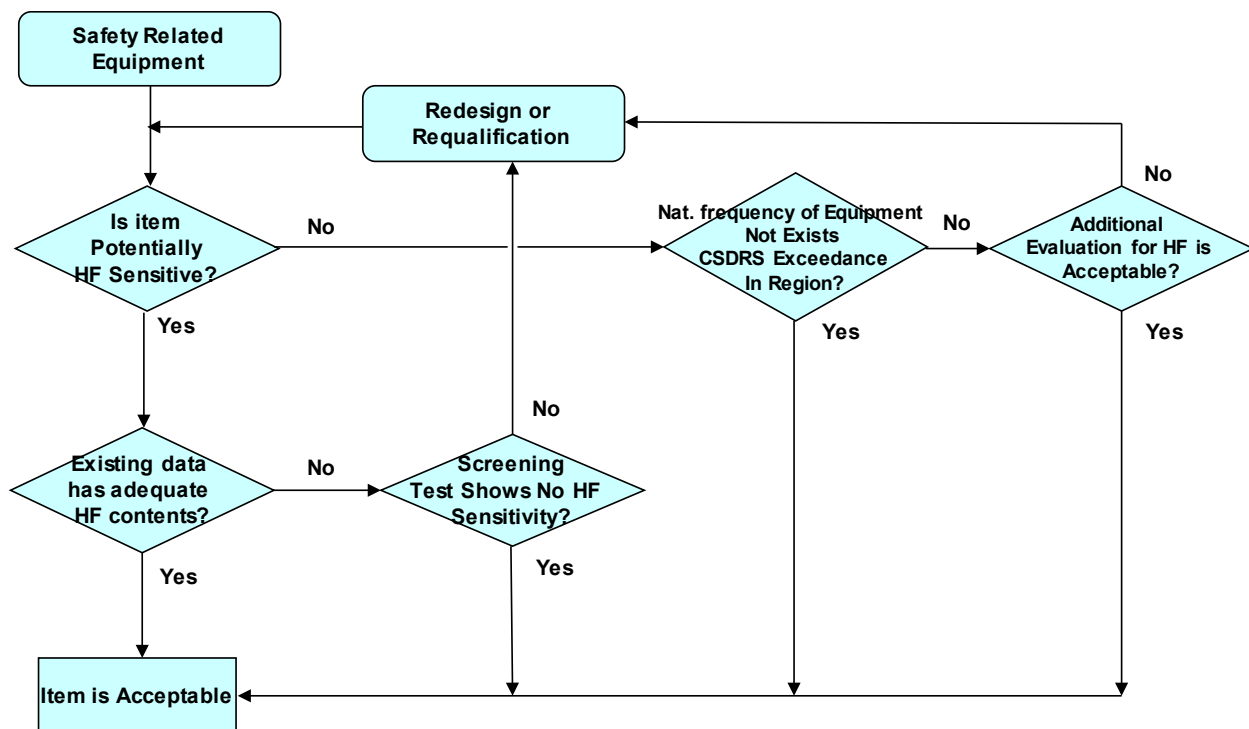


Figure 6-12 High-Frequency Screening Process



**Figure 6-13 Location of Surge Line Loads**

# **APPENDIX A**

## **APR1400 HRHF RESPONSE SPECTRA**

### **FOR 2, 3, 4, 5, 7, AND 10%**

### **DAMPING RATIOS**

Page intentionally blank



Table A-1 (1 of 3)

HRHF Horizontal Target Response Spectrum for 2, 3, 4, 5, 7 and 10% Damping Ratios

| HRHF Horizontal Target Response Spectra (g) |            |            |            |            |            |             |
|---|------------|------------|------------|------------|------------|-------------|
| Frequency (Hz)                              | 2% Damping | 3% Damping | 4% Damping | 5% Damping | 7% Damping | 10% Damping |
| 0.5   | 0.1249     | 0.1168     | 0.1117     | 0.1078     | 0.1037     | 0.1024      |
| 0.6   | 0.1530     | 0.1412     | 0.1333     | 0.1271     | 0.1192     | 0.1135      |
| 0.7   | 0.1786     | 0.1635     | 0.1532     | 0.1452     | 0.1345     | 0.1256      |
| 0.8   | 0.2025     | 0.1844     | 0.1719     | 0.1622     | 0.1491     | 0.1375      |
| 0.9   | 0.2248     | 0.2037     | 0.1892     | 0.1780     | 0.1626     | 0.1488      |
| 1   | 0.2499     | 0.2255     | 0.2089     | 0.1960     | 0.1783     | 0.1620      |
| 1.1   | 0.2764     | 0.2486     | 0.2298     | 0.2153     | 0.1951     | 0.1764      |
| 1.2   | 0.3023     | 0.2714     | 0.2507     | 0.2346     | 0.2122     | 0.1911      |
| 1.25  | 0.3151     | 0.2828     | 0.2610     | 0.2442     | 0.2208     | 0.1986      |
| 1.3   | 0.3274     | 0.2937     | 0.2711     | 0.2535     | 0.2291     | 0.2059      |
| 1.4   | 0.3520     | 0.3156     | 0.2911     | 0.2720     | 0.2456     | 0.2202      |
| 1.5   | 0.3774     | 0.3376     | 0.3111     | 0.2905     | 0.2621     | 0.2348      |
| 1.6   | 0.3991     | 0.3562     | 0.3277     | 0.3056     | 0.2753     | 0.2463      |
| 1.7   | 0.4198     | 0.3741     | 0.3439     | 0.3205     | 0.2884     | 0.2577      |
| 1.8   | 0.4405     | 0.3921     | 0.3600     | 0.3351     | 0.3012     | 0.2687      |
| 1.9   | 0.4606     | 0.4098     | 0.3759     | 0.3497     | 0.3137     | 0.2795      |
| 2   | 0.4810     | 0.4275     | 0.3917     | 0.3640     | 0.3263     | 0.2905      |
| 2.1   | 0.4979     | 0.4416     | 0.4039     | 0.3747     | 0.3351     | 0.2978      |
| 2.2   | 0.5144     | 0.4552     | 0.4158     | 0.3852     | 0.3437     | 0.3048      |
| 2.3   | 0.5295     | 0.4678     | 0.4271     | 0.3955     | 0.3526     | 0.3125      |
| 2.4   | 0.5436     | 0.4799     | 0.4381     | 0.4056     | 0.3618     | 0.3208      |
| 2.5   | 0.5565     | 0.4914     | 0.4487     | 0.4156     | 0.3707     | 0.3287      |
| 2.6   | 0.5743     | 0.5073     | 0.4631     | 0.4288     | 0.3823     | 0.3389      |
| 2.7   | 0.5919     | 0.5227     | 0.4772     | 0.4420     | 0.3941     | 0.3492      |
| 2.8   | 0.6091     | 0.5378     | 0.4912     | 0.4550     | 0.4058     | 0.3598      |
| 2.9   | 0.6249     | 0.5520     | 0.5047     | 0.4679     | 0.4179     | 0.3708      |
| 3   | 0.6409     | 0.5664     | 0.5182     | 0.4808     | 0.4300     | 0.3820      |
| 3.15  | 0.6613     | 0.5843     | 0.5346     | 0.4961     | 0.4441     | 0.3948      |
| 3.3   | 0.6819     | 0.6021     | 0.5509     | 0.5111     | 0.4576     | 0.4071      |
| 3.45  | 0.7000     | 0.6187     | 0.5664     | 0.5259     | 0.4709     | 0.4189      |
| 3.6   | 0.7177     | 0.6350     | 0.5818     | 0.5405     | 0.4844     | 0.4313      |
| 3.8   | 0.7408     | 0.6559     | 0.6016     | 0.5596     | 0.5024     | 0.4479      |
| 4   | 0.7656     | 0.6777     | 0.6217     | 0.5783     | 0.5196     | 0.4634      |
| 4.2   | 0.7866     | 0.6962     | 0.6387     | 0.5942     | 0.5341     | 0.4763      |
| 4.4   | 0.8114     | 0.7165     | 0.6564     | 0.6097     | 0.5471     | 0.4871      |

Table A-1 (2 of 3)

| HRHF Horizontal Target Response Spectra (g) |            |            |            |            |            |             |
|---|------------|------------|------------|------------|------------|-------------|
| Frequency (Hz)                              | 2% Damping | 3% Damping | 4% Damping | 5% Damping | 7% Damping | 10% Damping |
| 4.6   | 0.8347     | 0.7357     | 0.6733     | 0.6249     | 0.5599     | 0.4977      |
| 4.8   | 0.8566     | 0.7544     | 0.6899     | 0.6398     | 0.5725     | 0.5079      |
| 5   | 0.8788     | 0.7732     | 0.7063     | 0.6545     | 0.5850     | 0.5180      |
| 5.25  | 0.9068     | 0.7954     | 0.7254     | 0.6711     | 0.5990     | 0.5294      |
| 5.5   | 0.9345     | 0.8174     | 0.7441     | 0.6873     | 0.6121     | 0.5397      |
| 5.75  | 0.9652     | 0.8411     | 0.7634     | 0.7032     | 0.6240     | 0.5488      |
| 6   | 0.9918     | 0.8626     | 0.7816     | 0.7187     | 0.6358     | 0.5580      |
| 6.25  | 1.0154     | 0.8812     | 0.7976     | 0.7328     | 0.6478     | 0.5680      |
| 6.5   | 1.0333     | 0.8968     | 0.8123     | 0.7467     | 0.6604     | 0.5794      |
| 6.75  | 1.0503     | 0.9120     | 0.8265     | 0.7603     | 0.6728     | 0.5911      |
| 7   | 1.0657     | 0.9262     | 0.8403     | 0.7736     | 0.6856     | 0.6034      |
| 7.25  | 1.0780     | 0.9383     | 0.8523     | 0.7855     | 0.6974     | 0.6155      |
| 7.5   | 1.0892     | 0.9501     | 0.8640     | 0.7972     | 0.7089     | 0.6272      |
| 7.75  | 1.1003     | 0.9613     | 0.8754     | 0.8087     | 0.7203     | 0.6385      |
| 8   | 1.1131     | 0.9728     | 0.8867     | 0.8200     | 0.7315     | 0.6495      |
| 8.5   | 1.1393     | 0.9957     | 0.9079     | 0.8398     | 0.7500     | 0.6668      |
| 9   | 1.1681     | 1.0201     | 0.9293     | 0.8589     | 0.7668     | 0.6821      |
| 9.5   | 1.2021     | 1.0492     | 0.9552     | 0.8823     | 0.7880     | 0.7017      |
| 10  | 1.2356     | 1.0775     | 0.9803     | 0.9050     | 0.8093     | 0.7215      |
| 10.5  | 1.2661     | 1.1033     | 1.0036     | 0.9263     | 0.8291     | 0.7404      |
| 11  | 1.2966     | 1.1290     | 1.0266     | 0.9471     | 0.8478     | 0.7571      |
| 11.5  | 1.3288     | 1.1552     | 1.0495     | 0.9674     | 0.8656     | 0.7729      |
| 12  | 1.3586     | 1.1801     | 1.0715     | 0.9873     | 0.8831     | 0.7886      |
| 12.5  | 1.3850     | 1.2032     | 1.0925     | 1.0067     | 0.9008     | 0.8048      |
| 13  | 1.4096     | 1.2239     | 1.1116     | 1.0245     | 0.9178     | 0.8208      |
| 13.5  | 1.4299     | 1.2425     | 1.1296     | 1.0420     | 0.9343     | 0.8366      |
| 14  | 1.4491     | 1.2604     | 1.1471     | 1.0591     | 0.9508     | 0.8525      |
| 14.5  | 1.4656     | 1.2769     | 1.1637     | 1.0759     | 0.9664     | 0.8670      |
| 15  | 1.4872     | 1.2962     | 1.1814     | 1.0924     | 0.9808     | 0.8797      |
| 16  | 1.5145     | 1.3207     | 1.2049     | 1.1150     | 1.0026     | 0.9008      |
| 17  | 1.5386     | 1.3435     | 1.2270     | 1.1367     | 1.0234     | 0.9205      |
| 18  | 1.5628     | 1.3660     | 1.2486     | 1.1575     | 1.0438     | 0.9407      |
| 20  | 1.6146     | 1.4119     | 1.2908     | 1.1969     | 1.0798     | 0.9737      |
| 22  | 1.6374     | 1.4336     | 1.3115     | 1.2168     | 1.0982     | 0.9907      |
| 25  | 1.6687     | 1.4629     | 1.3397     | 1.2441     | 1.1247     | 1.0162      |
| 28  | 1.6586     | 1.4548     | 1.3324     | 1.2376     | 1.1186     | 1.0106      |
| 30  | 1.6541     | 1.4508     | 1.3285     | 1.2336     | 1.1149     | 1.0073      |

Table A-1 (3 of 3)

| HRHF Horizontal Target Response Spectra (g) |            |            |            |            |            |             |
|---|------------|------------|------------|------------|------------|-------------|
| Frequency (Hz)                              | 2% Damping | 3% Damping | 4% Damping | 5% Damping | 7% Damping | 10% Damping |
| 31  | 1.6462     | 1.4439     | 1.3220     | 1.2274     | 1.1092     | 1.0022      |
| 34  | 1.6199     | 1.4213     | 1.3024     | 1.2102     | 1.0957     | 0.9919      |
| 35  | 1.6118     | 1.4146     | 1.2964     | 1.2048     | 1.0911     | 0.9879      |
| 37  | 1.5858     | 1.3923     | 1.2765     | 1.1866     | 1.0751     | 0.9740      |
| 40  | 1.5499     | 1.3616     | 1.2489     | 1.1615     | 1.0530     | 0.9546      |
| 43  | 1.4956     | 1.3166     | 1.2094     | 1.1262     | 1.0230     | 0.9294      |
| 45  | 1.4625     | 1.2892     | 1.1852     | 1.1046     | 1.0046     | 0.9139      |
| 46  | 1.4392     | 1.2699     | 1.1683     | 1.0896     | 0.9919     | 0.9033      |
| 49  | 1.3742     | 1.2160     | 1.1211     | 1.0476     | 0.9561     | 0.8732      |
| 50  | 1.3541     | 1.1992     | 1.1064     | 1.0345     | 0.9449     | 0.8638      |
| 52  | 1.2952     | 1.1505     | 1.0641     | 0.9970     | 0.9134     | 0.8375      |
| 55  | 1.2155     | 1.0844     | 1.0063     | 0.9458     | 0.8702     | 0.8014      |
| 58  | 1.1405     | 1.0233     | 0.9537     | 0.8997     | 0.8321     | 0.7704      |
| 60  | 1.0951     | 0.9862     | 0.9216     | 0.8715     | 0.8087     | 0.7513      |
| 61  | 1.0670     | 0.9627     | 0.9009     | 0.8530     | 0.7929     | 0.7380      |
| 64  | 0.9892     | 0.8976     | 0.8435     | 0.8015     | 0.7489     | 0.7007      |
| 65  | 0.9654     | 0.8776     | 0.8258     | 0.7856     | 0.7352     | 0.6890      |
| 67  | 0.9186     | 0.8387     | 0.7917     | 0.7553     | 0.7097     | 0.6678      |
| 70  | 0.8549     | 0.7856     | 0.7451     | 0.7136     | 0.6743     | 0.6382      |
| 73  | 0.7930     | 0.7338     | 0.6993     | 0.6726     | 0.6393     | 0.6087      |
| 75  | 0.7556     | 0.7023     | 0.6714     | 0.6474     | 0.6176     | 0.5904      |
| 76  | 0.7374     | 0.6872     | 0.6580     | 0.6354     | 0.6072     | 0.5814      |
| 79  | 0.6872     | 0.6451     | 0.6207     | 0.6017     | 0.5779     | 0.5562      |
| 80  | 0.6715     | 0.6319     | 0.6089     | 0.5911     | 0.5687     | 0.5482      |

Table A-2 (1 of 3)

HRHF Vertical Target Response Spectrum for 2, 3, 4, 5, 7, and 10% Damping Ratios

| HRHF Vertical Target Response Spectra (g) |      |            |            |            |            |            |             |
|---|------|------------|------------|------------|------------|------------|-------------|
| Frequency (Hz)                            | V/H  | 2% Damping | 3% Damping | 4% Damping | 5% Damping | 7% Damping | 10% Damping |
| 0.5                                       | 0.75 | 0.0937     | 0.0876     | 0.0838     | 0.0809     | 0.0778     | 0.0768      |
| 0.6                                       | 0.75 | 0.1148     | 0.1059     | 0.1000     | 0.0953     | 0.0894     | 0.0851      |
| 0.7                                       | 0.75 | 0.1339     | 0.1227     | 0.1149     | 0.1089     | 0.1009     | 0.0942      |
| 0.8                                       | 0.75 | 0.1519     | 0.1383     | 0.1289     | 0.1217     | 0.1118     | 0.1032      |
| 0.9                                       | 0.75 | 0.1686     | 0.1528     | 0.1419     | 0.1335     | 0.1220     | 0.1116      |
| 1   | 0.75 | 0.1874     | 0.1691     | 0.1567     | 0.1470     | 0.1337     | 0.1215      |
| 1.1                                       | 0.75 | 0.2073     | 0.1864     | 0.1724     | 0.1615     | 0.1463     | 0.1323      |
| 1.2                                       | 0.75 | 0.2268     | 0.2036     | 0.1880     | 0.1759     | 0.1591     | 0.1433      |
| 1.25                                      | 0.75 | 0.2363     | 0.2121     | 0.1958     | 0.1832     | 0.1656     | 0.1490      |
| 1.3                                       | 0.75 | 0.2455     | 0.2203     | 0.2033     | 0.1901     | 0.1718     | 0.1544      |
| 1.4                                       | 0.75 | 0.2640     | 0.2367     | 0.2183     | 0.2040     | 0.1842     | 0.1652      |
| 1.5                                       | 0.75 | 0.2830     | 0.2532     | 0.2333     | 0.2179     | 0.1966     | 0.1761      |
| 1.6                                       | 0.75 | 0.2993     | 0.2672     | 0.2458     | 0.2292     | 0.2064     | 0.1847      |
| 1.7                                       | 0.75 | 0.3148     | 0.2806     | 0.2579     | 0.2403     | 0.2163     | 0.1933      |
| 1.8                                       | 0.75 | 0.3304     | 0.2941     | 0.2700     | 0.2514     | 0.2259     | 0.2015      |
| 1.9                                       | 0.75 | 0.3454     | 0.3073     | 0.2819     | 0.2622     | 0.2353     | 0.2096      |
| 2   | 0.75 | 0.3608     | 0.3206     | 0.2938     | 0.2730     | 0.2447     | 0.2179      |
| 2.1                                       | 0.75 | 0.3734     | 0.3312     | 0.3029     | 0.2810     | 0.2513     | 0.2233      |
| 2.2                                       | 0.75 | 0.3858     | 0.3414     | 0.3118     | 0.2889     | 0.2578     | 0.2286      |
| 2.3                                       | 0.75 | 0.3971     | 0.3509     | 0.3203     | 0.2966     | 0.2645     | 0.2344      |
| 2.4                                       | 0.75 | 0.4077     | 0.3599     | 0.3286     | 0.3042     | 0.2713     | 0.2406      |
| 2.5                                       | 0.75 | 0.4174     | 0.3686     | 0.3365     | 0.3117     | 0.2780     | 0.2465      |
| 2.6                                       | 0.75 | 0.4307     | 0.3805     | 0.3473     | 0.3216     | 0.2867     | 0.2541      |
| 2.7                                       | 0.75 | 0.4439     | 0.3920     | 0.3579     | 0.3315     | 0.2955     | 0.2619      |
| 2.8                                       | 0.75 | 0.4568     | 0.4034     | 0.3684     | 0.3413     | 0.3044     | 0.2699      |
| 2.9                                       | 0.75 | 0.4687     | 0.4140     | 0.3785     | 0.3510     | 0.3134     | 0.2781      |
| 3   | 0.75 | 0.4807     | 0.4248     | 0.3887     | 0.3606     | 0.3225     | 0.2865      |
| 3.15                                      | 0.75 | 0.4960     | 0.4382     | 0.4010     | 0.3721     | 0.3330     | 0.2961      |
| 3.3                                       | 0.75 | 0.5114     | 0.4515     | 0.4131     | 0.3833     | 0.3432     | 0.3053      |
| 3.45                                      | 0.75 | 0.5250     | 0.4640     | 0.4248     | 0.3944     | 0.3532     | 0.3142      |
| 3.6                                       | 0.75 | 0.5383     | 0.4762     | 0.4363     | 0.4054     | 0.3633     | 0.3235      |
| 3.8                                       | 0.75 | 0.5556     | 0.4919     | 0.4512     | 0.4197     | 0.3768     | 0.3359      |

Table A-2 (2 of 3)

| HRHF Vertical Target Response Spectra (g) |        |               |               |               |               |               |                |
|---|--------|---------------|---------------|---------------|---------------|---------------|----------------|
| Frequency<br>(Hz)                         | V/H    | 2%<br>Damping | 3%<br>Damping | 4%<br>Damping | 5%<br>Damping | 7%<br>Damping | 10%<br>Damping |
| 4   | 0.75   | 0.5742        | 0.5083        | 0.4663        | 0.4337        | 0.3897        | 0.3476         |
| 4.2                                       | 0.75   | 0.5899        | 0.5221        | 0.4790        | 0.4456        | 0.4006        | 0.3572         |
| 4.4                                       | 0.75   | 0.6085        | 0.5374        | 0.4923        | 0.4573        | 0.4103        | 0.3653         |
| 4.6                                       | 0.75   | 0.6260        | 0.5518        | 0.5050        | 0.4687        | 0.4199        | 0.3733         |
| 4.8                                       | 0.75   | 0.6424        | 0.5658        | 0.5174        | 0.4799        | 0.4294        | 0.3809         |
| 5   | 0.75   | 0.6591        | 0.5799        | 0.5298        | 0.4909        | 0.4387        | 0.3885         |
| 5.25                                      | 0.75   | 0.6801        | 0.5966        | 0.5441        | 0.5033        | 0.4492        | 0.3971         |
| 5.5                                       | 0.75   | 0.7009        | 0.6130        | 0.5581        | 0.5155        | 0.4591        | 0.4048         |
| 5.75                                      | 0.75   | 0.7239        | 0.6308        | 0.5726        | 0.5274        | 0.4680        | 0.4116         |
| 6   | 0.75   | 0.7439        | 0.6469        | 0.5862        | 0.5390        | 0.4769        | 0.4185         |
| 6.25                                      | 0.75   | 0.7616        | 0.6609        | 0.5982        | 0.5496        | 0.4858        | 0.4260         |
| 6.5                                       | 0.75   | 0.7750        | 0.6726        | 0.6092        | 0.5600        | 0.4953        | 0.4346         |
| 6.75                                      | 0.75   | 0.7877        | 0.6840        | 0.6199        | 0.5702        | 0.5046        | 0.4433         |
| 7   | 0.75   | 0.7993        | 0.6947        | 0.6302        | 0.5802        | 0.5142        | 0.4526         |
| 7.25                                      | 0.75   | 0.8085        | 0.7037        | 0.6392        | 0.5891        | 0.5230        | 0.4616         |
| 7.5                                       | 0.75   | 0.8169        | 0.7125        | 0.6480        | 0.5979        | 0.5317        | 0.4704         |
| 7.75                                      | 0.75   | 0.8252        | 0.7210        | 0.6565        | 0.6065        | 0.5402        | 0.4789         |
| 8   | 0.75   | 0.8348        | 0.7296        | 0.6650        | 0.6150        | 0.5486        | 0.4871         |
| 8.5                                       | 0.75   | 0.8545        | 0.7468        | 0.6809        | 0.6298        | 0.5625        | 0.5001         |
| 9   | 0.75   | 0.8761        | 0.7651        | 0.6970        | 0.6442        | 0.5751        | 0.5116         |
| 9.5                                       | 0.75   | 0.9016        | 0.7869        | 0.7164        | 0.6617        | 0.5910        | 0.5262         |
| 10  | 0.75   | 0.9267        | 0.8081        | 0.7353        | 0.6788        | 0.6069        | 0.5411         |
| 10.5                                      | 0.7545 | 0.9553        | 0.8325        | 0.7572        | 0.6989        | 0.6256        | 0.5586         |
| 11  | 0.7588 | 0.9839        | 0.8567        | 0.7790        | 0.7187        | 0.6433        | 0.5745         |
| 11.5                                      | 0.7629 | 1.0138        | 0.8814        | 0.8007        | 0.7381        | 0.6604        | 0.5897         |
| 12  | 0.7669 | 1.0419        | 0.9050        | 0.8218        | 0.7572        | 0.6773        | 0.6048         |
| 12.5                                      | 0.7708 | 1.0675        | 0.9274        | 0.8421        | 0.7759        | 0.6943        | 0.6203         |
| 13  | 0.7745 | 1.0917        | 0.9479        | 0.8609        | 0.7935        | 0.7108        | 0.6357         |
| 13.5                                      | 0.7781 | 1.1125        | 0.9668        | 0.8789        | 0.8108        | 0.7269        | 0.6510         |
| 14  | 0.7815 | 1.1325        | 0.9850        | 0.8965        | 0.8278        | 0.7431        | 0.6663         |
| 14.5                                      | 0.7849 | 1.1504        | 1.0023        | 0.9134        | 0.8445        | 0.7585        | 0.6805         |
| 15  | 0.7882 | 1.1722        | 1.0217        | 0.9312        | 0.8610        | 0.7730        | 0.6934         |
| 16  | 0.7944 | 1.2032        | 1.0492        | 0.9572        | 0.8858        | 0.7965        | 0.7156         |
| 17  | 0.8003 | 1.2314        | 1.0752        | 0.9820        | 0.9097        | 0.8190        | 0.7367         |
| 18  | 0.8060 | 1.2595        | 1.1009        | 1.0063        | 0.9329        | 0.8413        | 0.7582         |
| 20  | 0.8256 | 1.3331        | 1.1657        | 1.0657        | 0.9882        | 0.8916        | 0.8039         |

Table A-2 (2 of 3)

| HRHF Vertical Target Response Spectra (g) |        |               |               |               |               |               |                |
|---|--------|---------------|---------------|---------------|---------------|---------------|----------------|
| Frequency<br>(Hz)                         | V/H    | 2%<br>Damping | 3%<br>Damping | 4%<br>Damping | 5%<br>Damping | 7%<br>Damping | 10%<br>Damping |
| 22  | 0.8493 | 1.3906        | 1.2175        | 1.1139        | 1.0335        | 0.9327        | 0.8415         |
| 25  | 0.8800 | 1.4685        | 1.2874        | 1.1789        | 1.0948        | 0.9897        | 0.8942         |
| 28  | 0.9149 | 1.5174        | 1.3309        | 1.2190        | 1.1322        | 1.0234        | 0.9246         |
| 30  | 0.9368 | 1.5496        | 1.3591        | 1.2445        | 1.1556        | 1.0444        | 0.9436         |
| 31  | 0.9474 | 1.5596        | 1.3680        | 1.2524        | 1.1628        | 1.0509        | 0.9495         |
| 34  | 0.9818 | 1.5904        | 1.3954        | 1.2787        | 1.1881        | 1.0757        | 0.9738         |
| 35  | 0.9929 | 1.6004        | 1.4046        | 1.2873        | 1.1963        | 1.0834        | 0.9810         |
| 37  | 1.0147 | 1.6091        | 1.4127        | 1.2952        | 1.2040        | 1.0909        | 0.9882         |
| 40  | 1.0503 | 1.6279        | 1.4301        | 1.3118        | 1.2199        | 1.1060        | 1.0027         |
| 43  | 1.0831 | 1.6199        | 1.4261        | 1.3099        | 1.2198        | 1.1080        | 1.0067         |
| 45  | 1.1024 | 1.6122        | 1.4212        | 1.3066        | 1.2177        | 1.1075        | 1.0075         |
| 46  | 1.1118 | 1.6001        | 1.4118        | 1.2990        | 1.2114        | 1.1028        | 1.0042         |
| 49  | 1.1231 | 1.5433        | 1.3656        | 1.2591        | 1.1765        | 1.0737        | 0.9807         |
| 50  | 1.1245 | 1.5226        | 1.3484        | 1.2441        | 1.1632        | 1.0625        | 0.9713         |
| 52  | 1.1272 | 1.4599        | 1.2968        | 1.1994        | 1.1238        | 1.0296        | 0.9440         |
| 55  | 1.1311 | 1.3748        | 1.2265        | 1.1382        | 1.0698        | 0.9843        | 0.9064         |
| 58  | 1.1348 | 1.2942        | 1.1612        | 1.0822        | 1.0210        | 0.9442        | 0.8742         |
| 60  | 1.1371 | 1.2453        | 1.1214        | 1.0480        | 0.9910        | 0.9196        | 0.8544         |
| 61  | 1.1383 | 1.2145        | 1.0958        | 1.0255        | 0.9710        | 0.9026        | 0.8401         |
| 64  | 1.1374 | 1.1251        | 1.0209        | 0.9594        | 0.9116        | 0.8518        | 0.7969         |
| 65  | 1.1357 | 1.0964        | 0.9966        | 0.9378        | 0.8922        | 0.8350        | 0.7825         |
| 67  | 1.1323 | 1.0401        | 0.9497        | 0.8965        | 0.8552        | 0.8036        | 0.7562         |
| 70  | 1.1275 | 0.9639        | 0.8858        | 0.8401        | 0.8046        | 0.7603        | 0.7196         |
| 73  | 1.1229 | 0.8905        | 0.8240        | 0.7853        | 0.7553        | 0.7178        | 0.6835         |
| 75  | 1.1200 | 0.8462        | 0.7865        | 0.7520        | 0.7251        | 0.6918        | 0.6612         |
| 76  | 1.1138 | 0.8214        | 0.7654        | 0.7329        | 0.7077        | 0.6763        | 0.6476         |
| 79  | 1.0959 | 0.7531        | 0.7069        | 0.6802        | 0.6594        | 0.6334        | 0.6095         |
| 80  | 1.0901 | 0.7321        | 0.6889        | 0.6638        | 0.6444        | 0.6199        | 0.5976         |

# **APPENDIX B**

## **COMPARISON OF INCOHERENT-MOTION SSI ANALYSIS RESULTS USING 7 AND 12 MODES**

Page intentionally blank



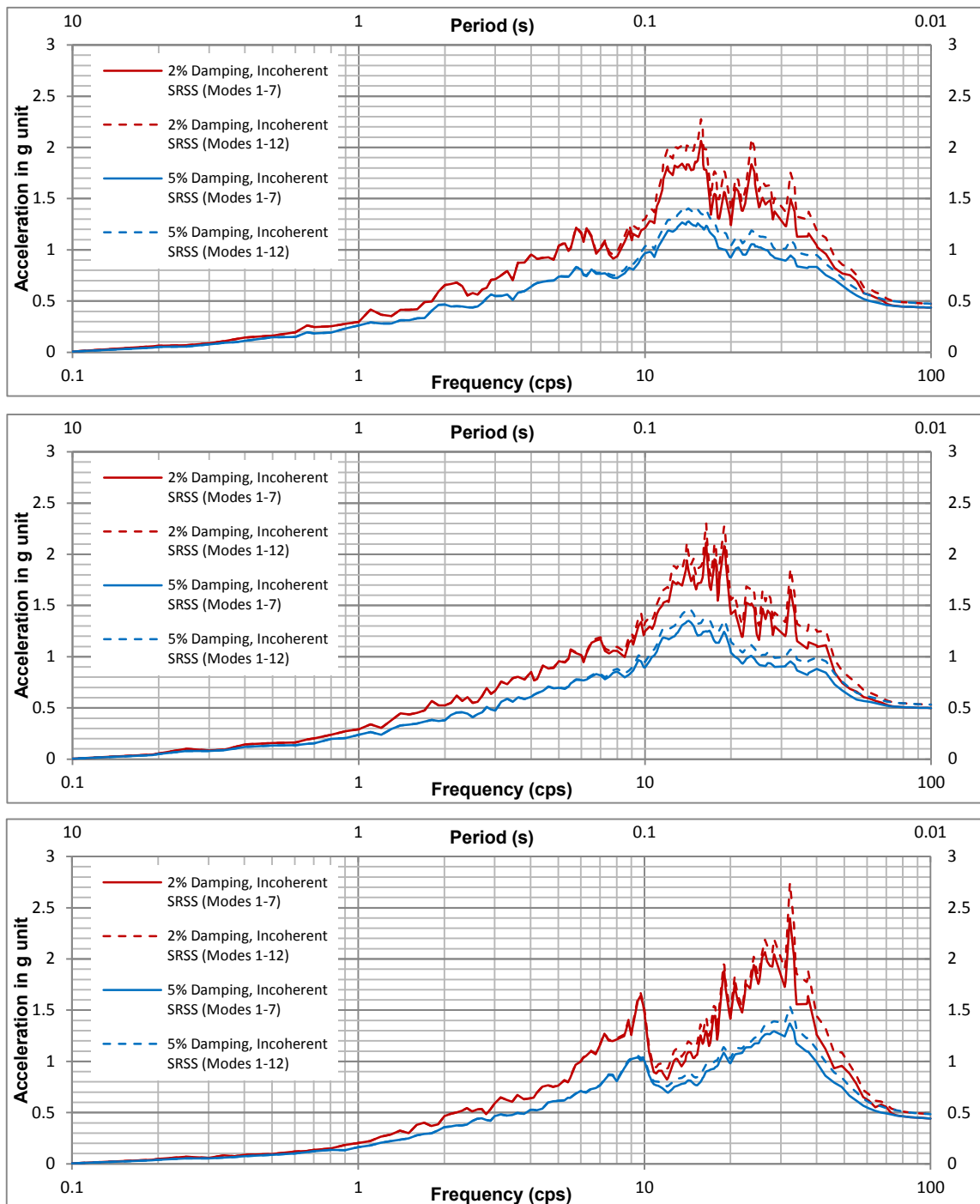


**Figure B-1 Comparison of Incoherent Results Using the 7 Modes and 12 Modes, Cracked Concrete Condition - Containment Structure at El. 78'-0"**

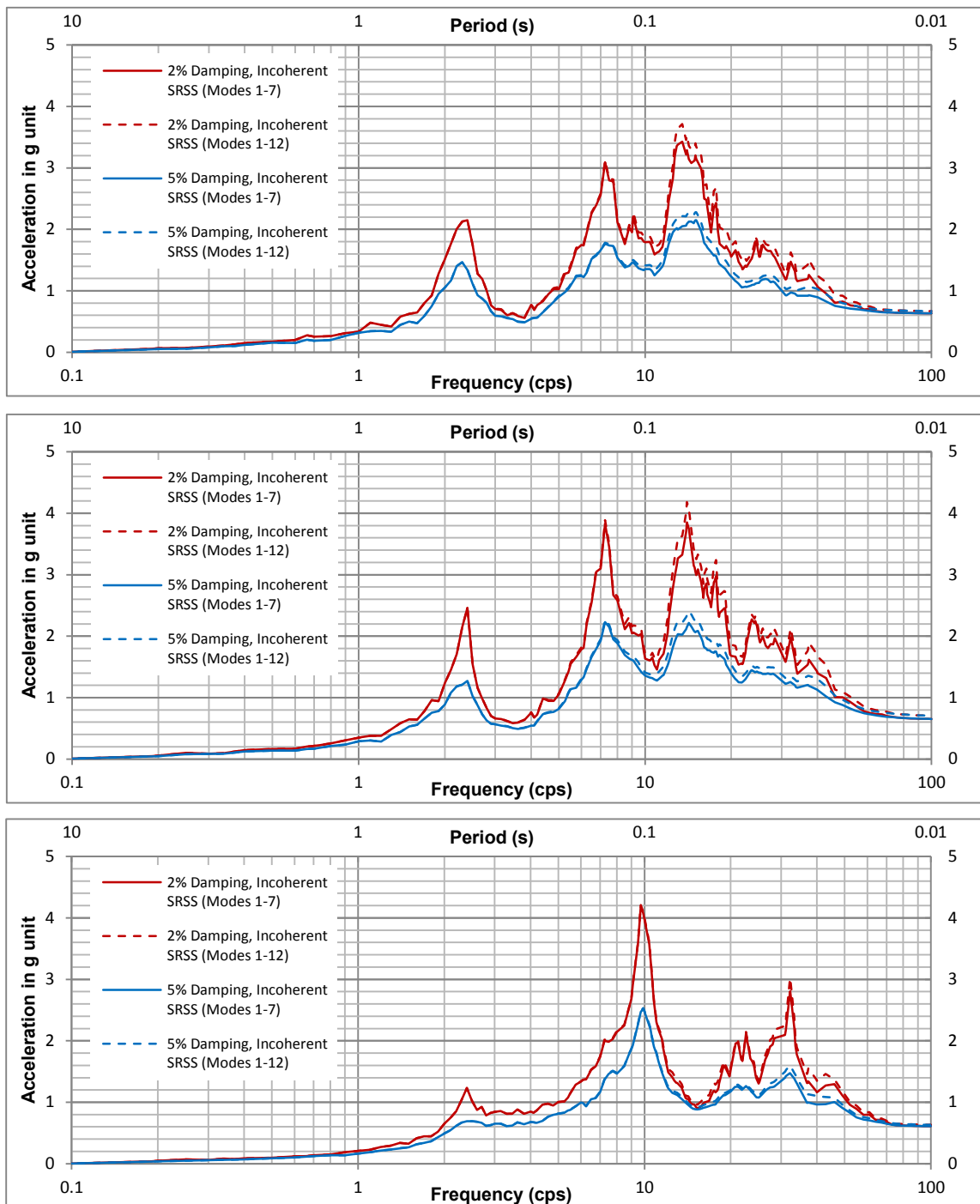


**Figure B-2 Comparison of Incoherent Results Using the 7 Modes and 12 Modes, Cracked Concrete Condition - Containment Structure at El. 160'-0"**

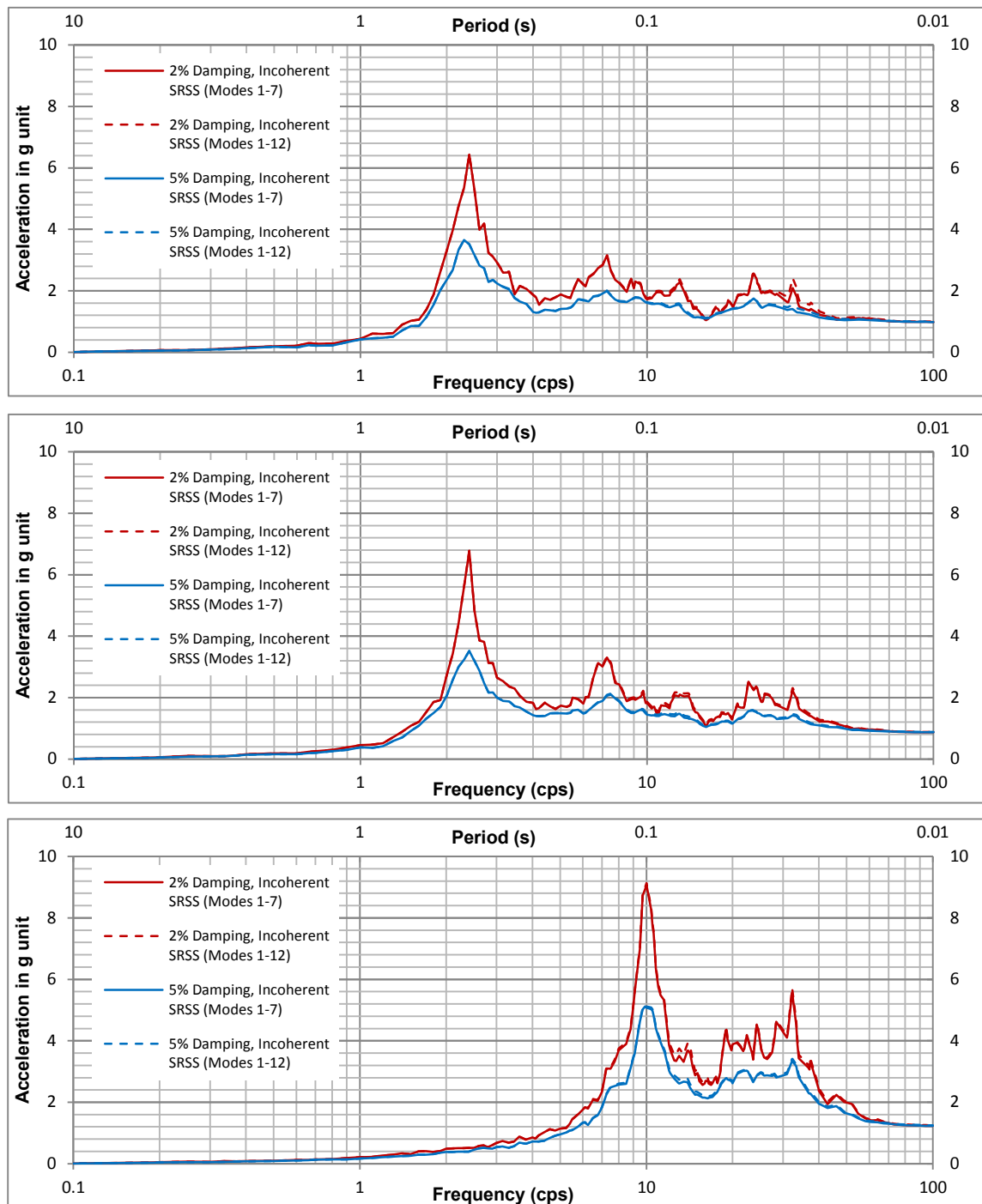


**Figure B-3 Comparison of Incoherent Results Using the 7 Modes and 12 Modes, Cracked Concrete Condition - Containment Structure at El. 332'-0"**

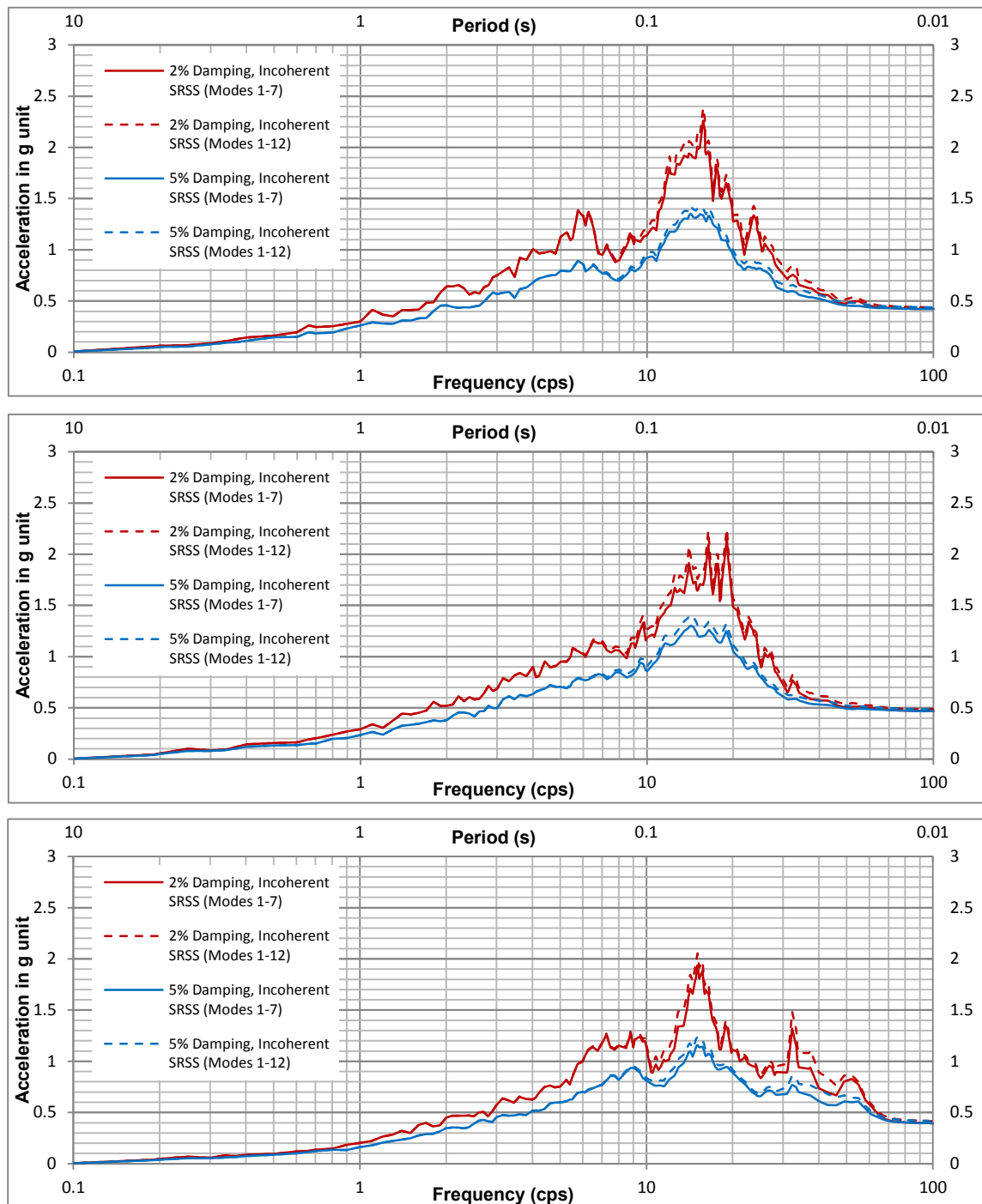


**Figure B-4 Comparison of Incoherent Results Using the 7 Modes and 12 Modes, Cracked Concrete Condition – Primary Shield Wall at El. 78'-0"**

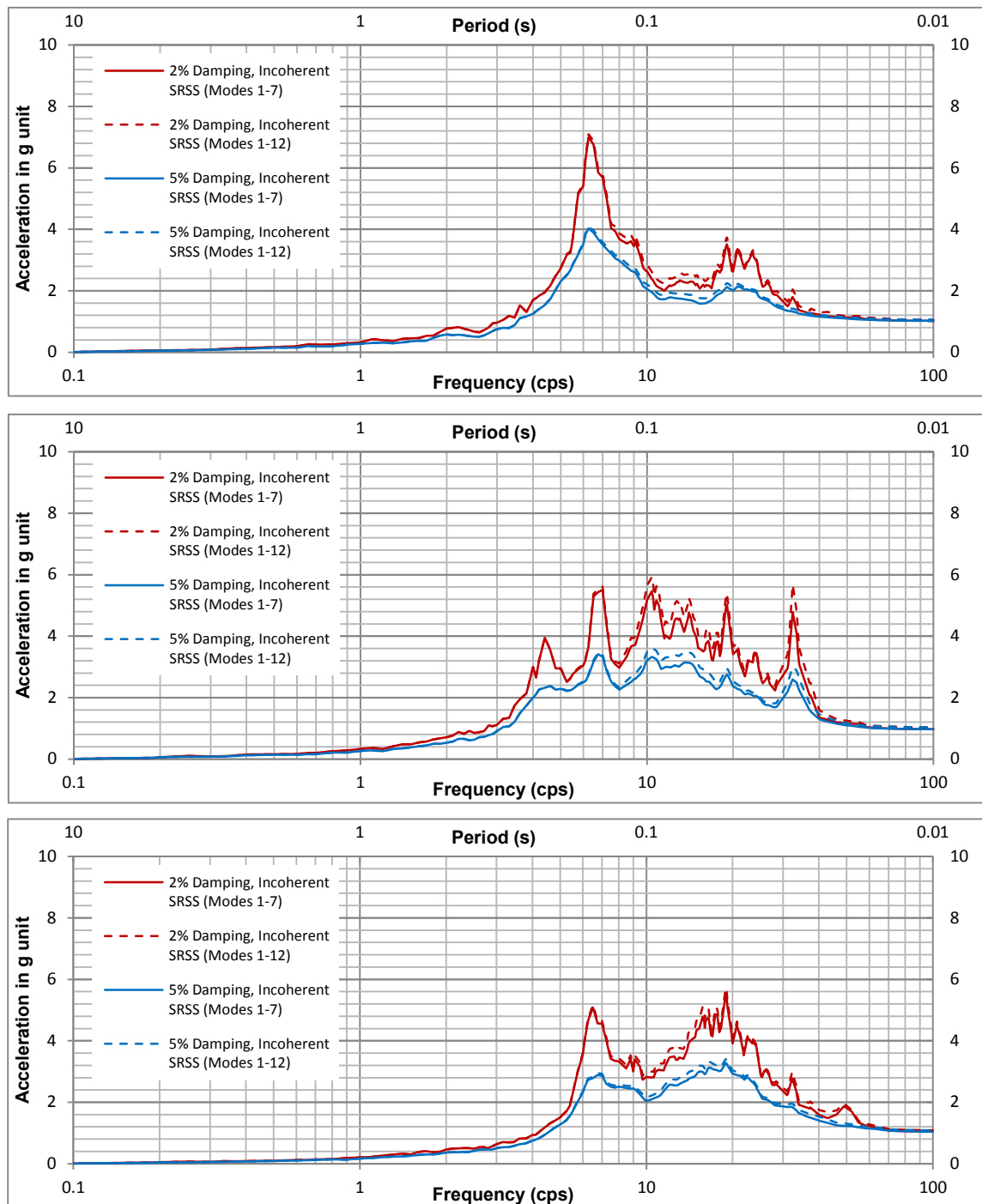


**Figure B-5 Comparison of Incoherent Results Using the 7 Modes and 12 Modes, Cracked Concrete Condition – Primary Shield Wall at El. 156'-0"**

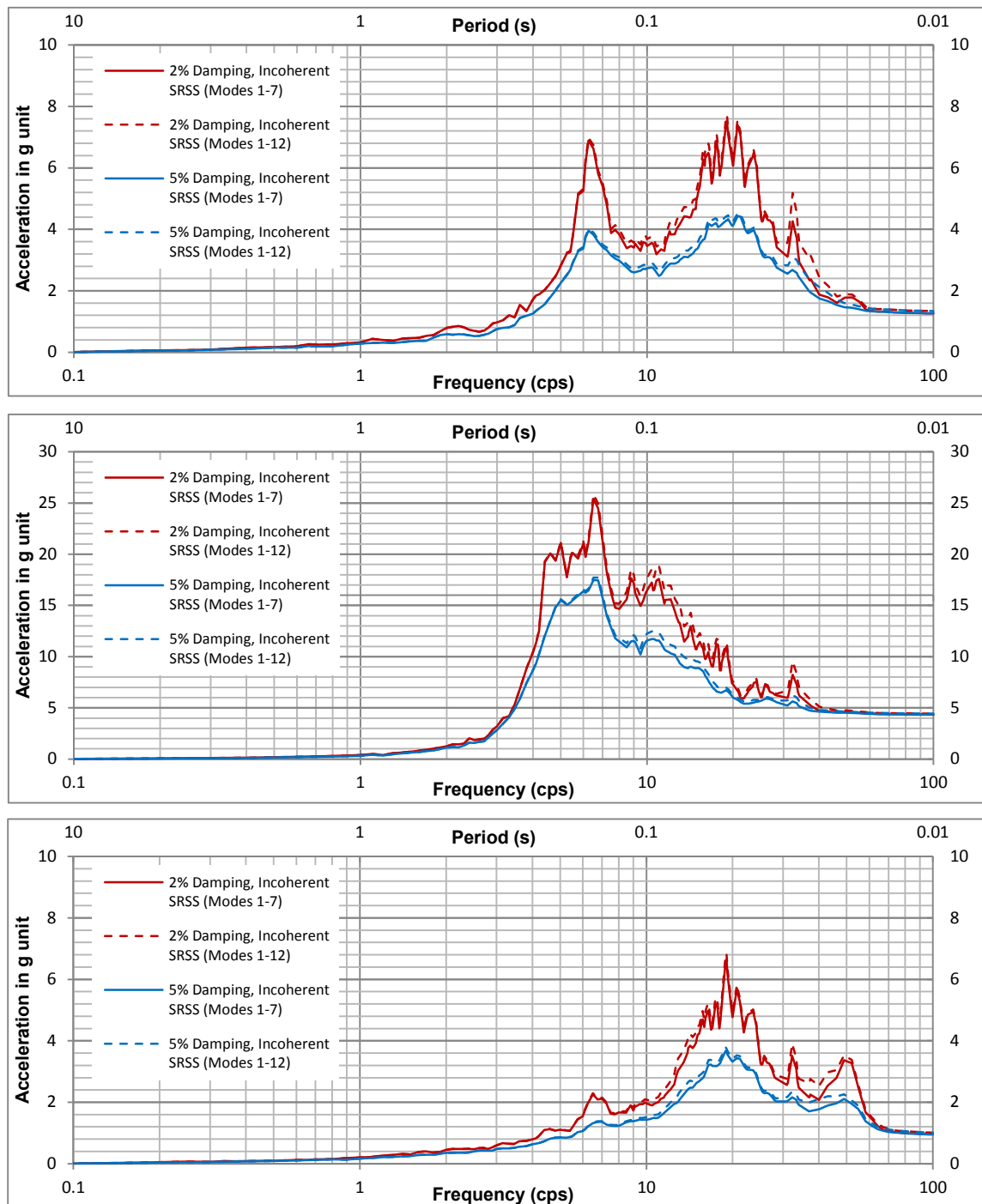


**Figure B-6 Comparison of Incoherent Results Using the 7 Modes and 12 Modes, Cracked Concrete Condition – Primary Shield Wall at El. 191'-0"**

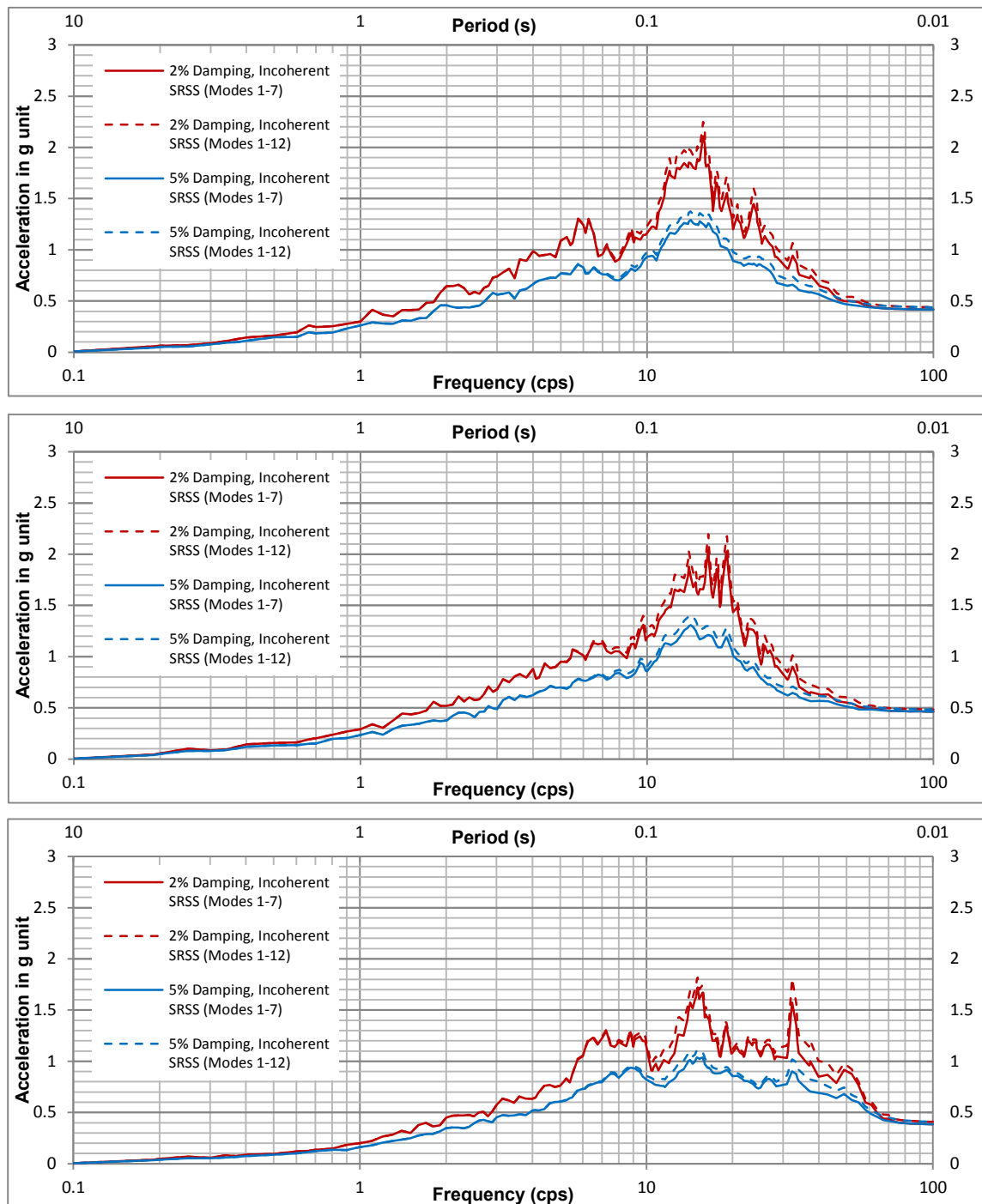


**Figure B-7 Comparison of Incoherent Results Using the 7 Modes and 12 Modes, Cracked Concrete Condition – Secondary Shield Wall at El. 78'-0"**

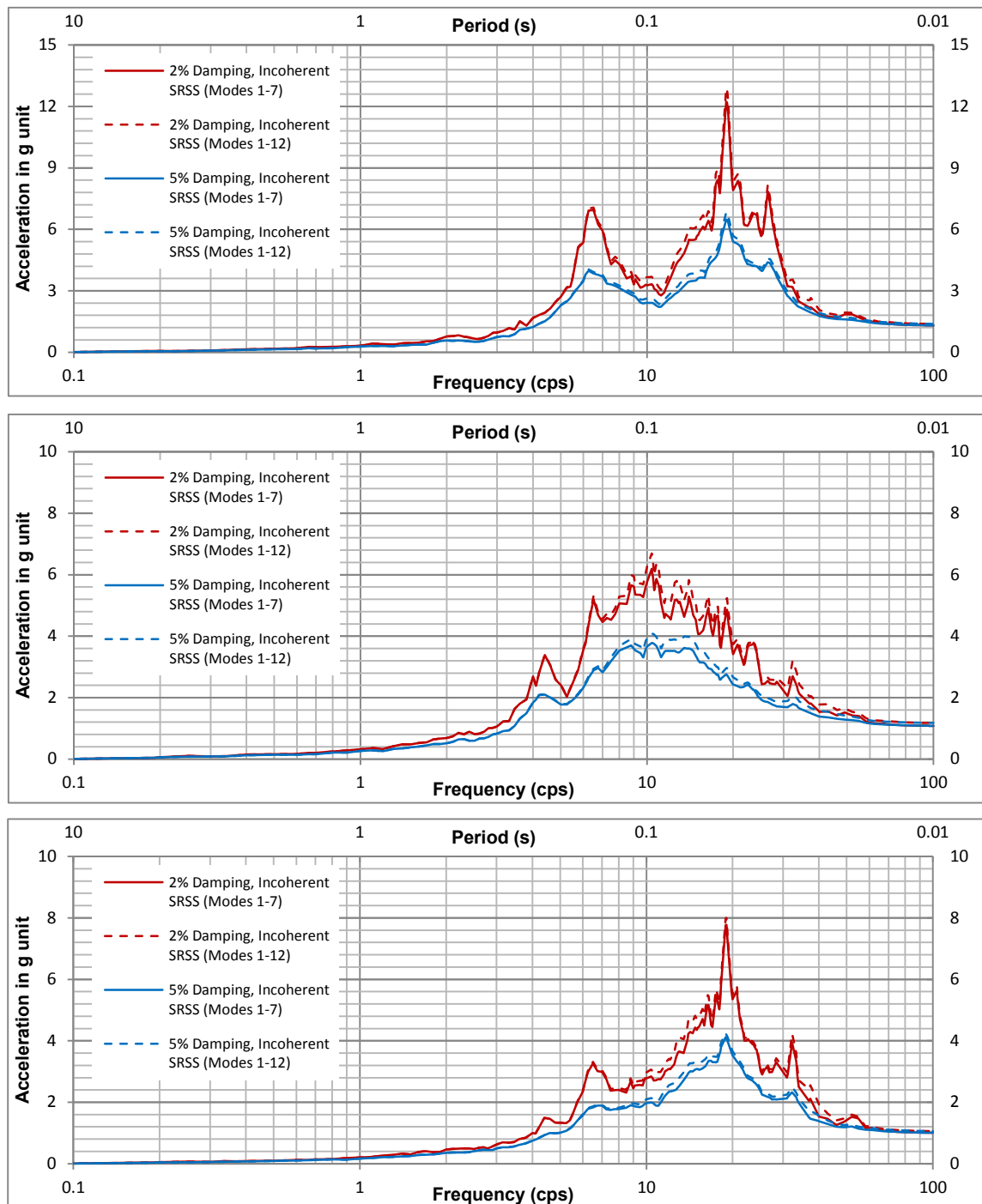


**Figure B-8 Comparison of Incoherent Results Using the 7 Modes and 12 Modes, Cracked Concrete Condition – Secondary Shield Wall at El. 156'-0"**



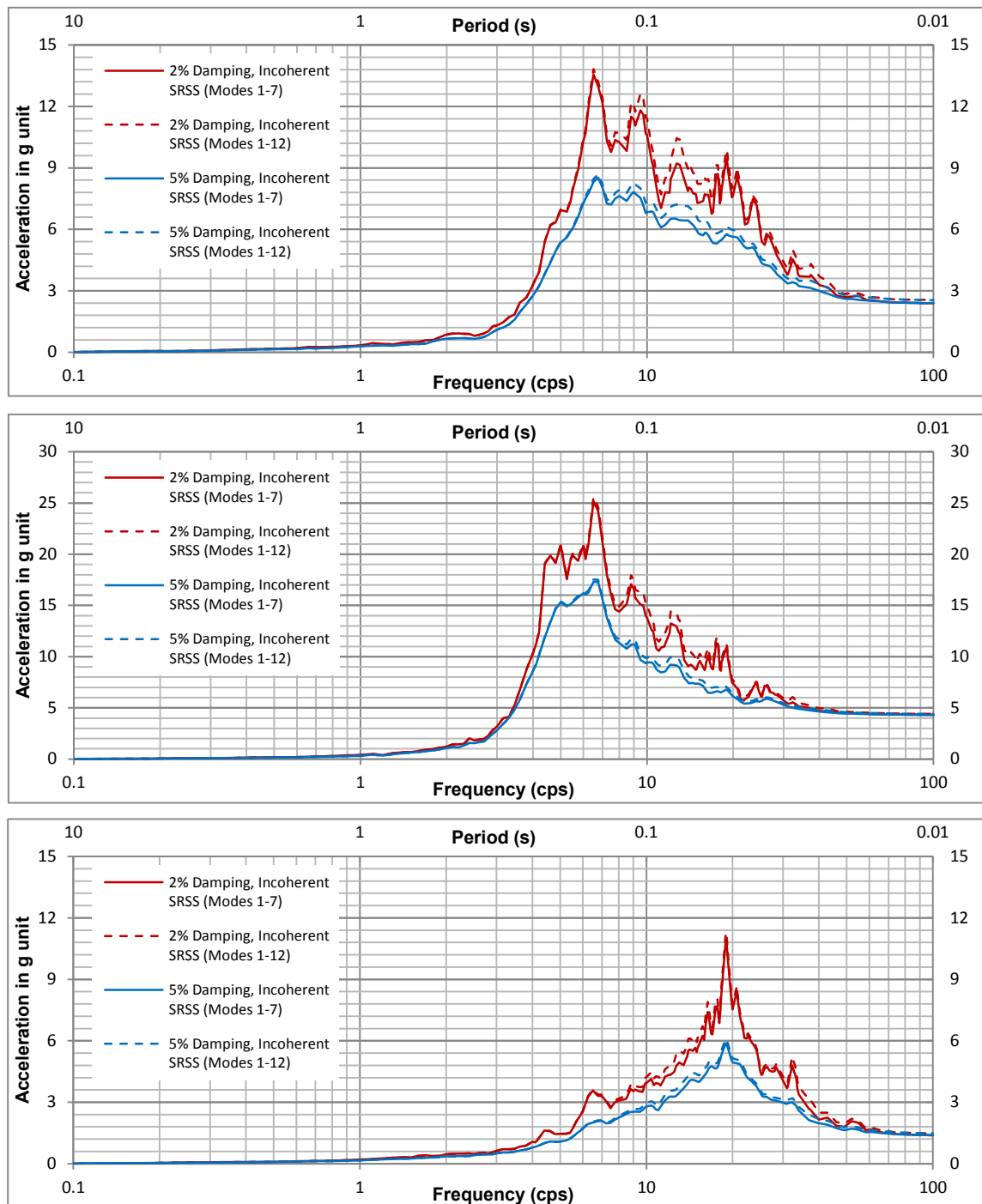


**Figure B-9 Comparison of Incoherent Results Using the 7 Modes and 12 Modes, Cracked Concrete Condition – Secondary Shield Wall at El. 191'-0"**

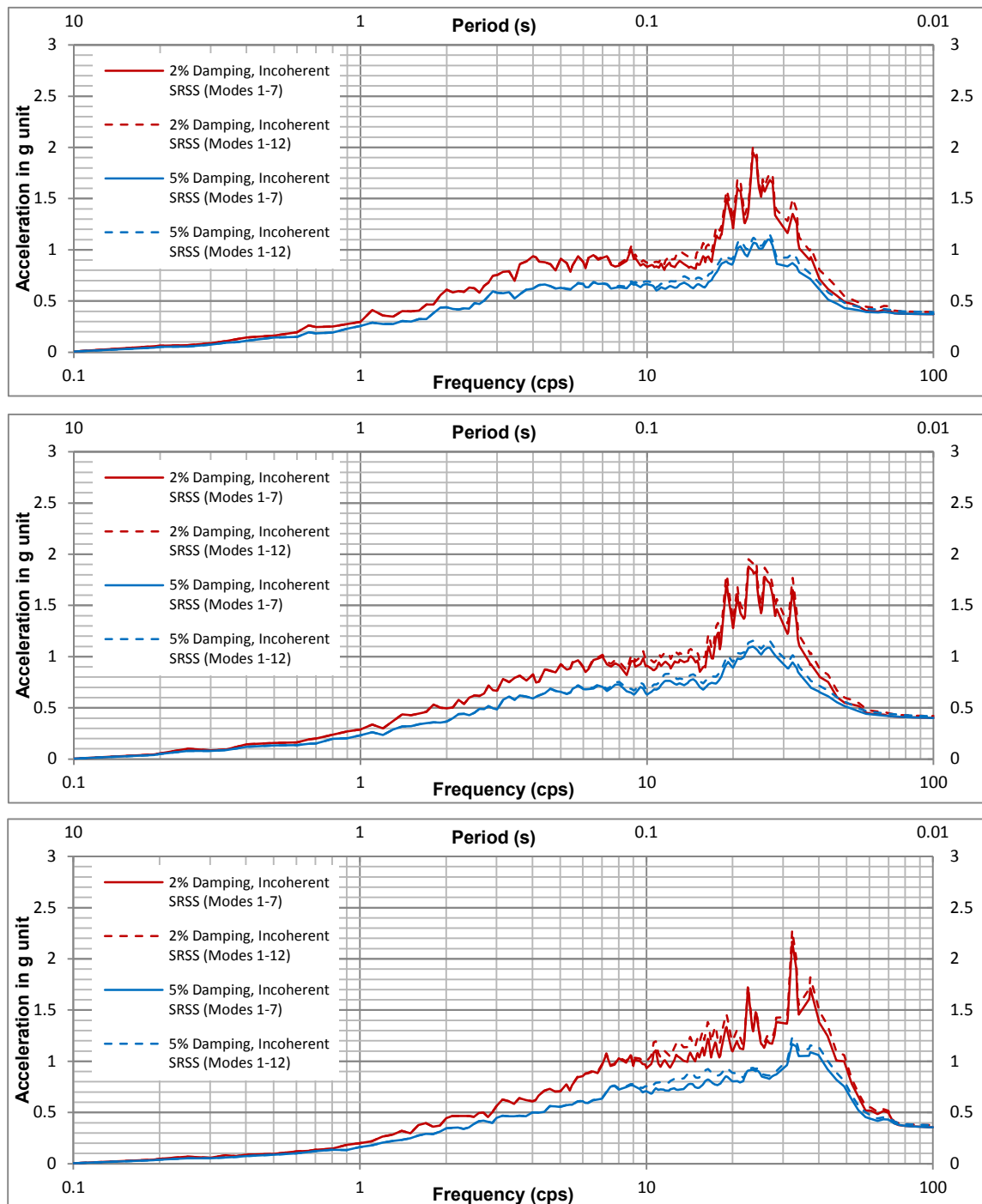


**Figure B-10 Comparison of Incoherent Results Using the 7 Modes and 12 Modes, Cracked Concrete Condition – Auxiliary Building Shearwall at El. 55'-0"**

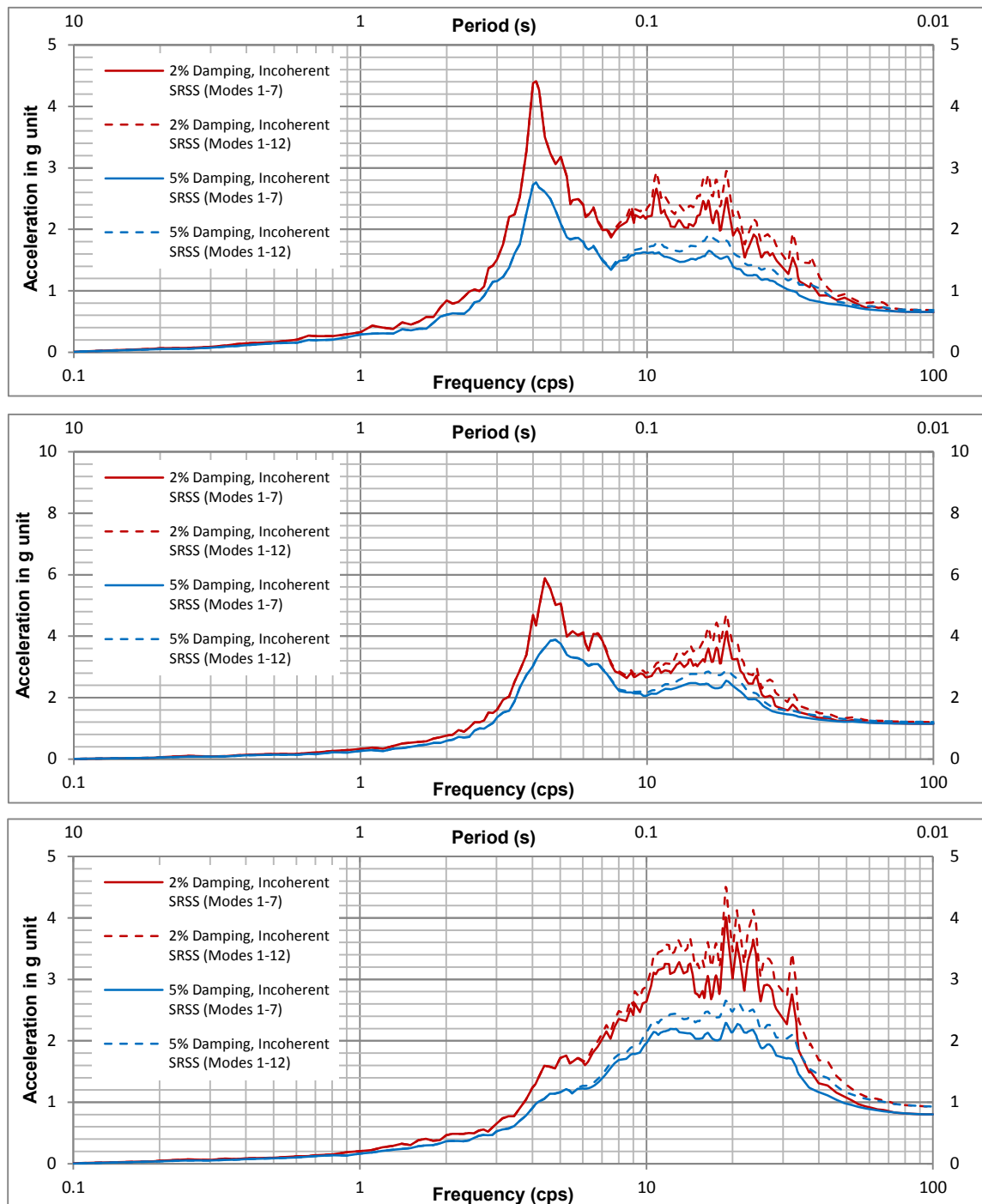


**Figure B-11 Comparison of Incoherent Results Using the 7 Modes and 12 Modes, Cracked Concrete Condition – Auxiliary Building Shearwall at El. 156'-0"**

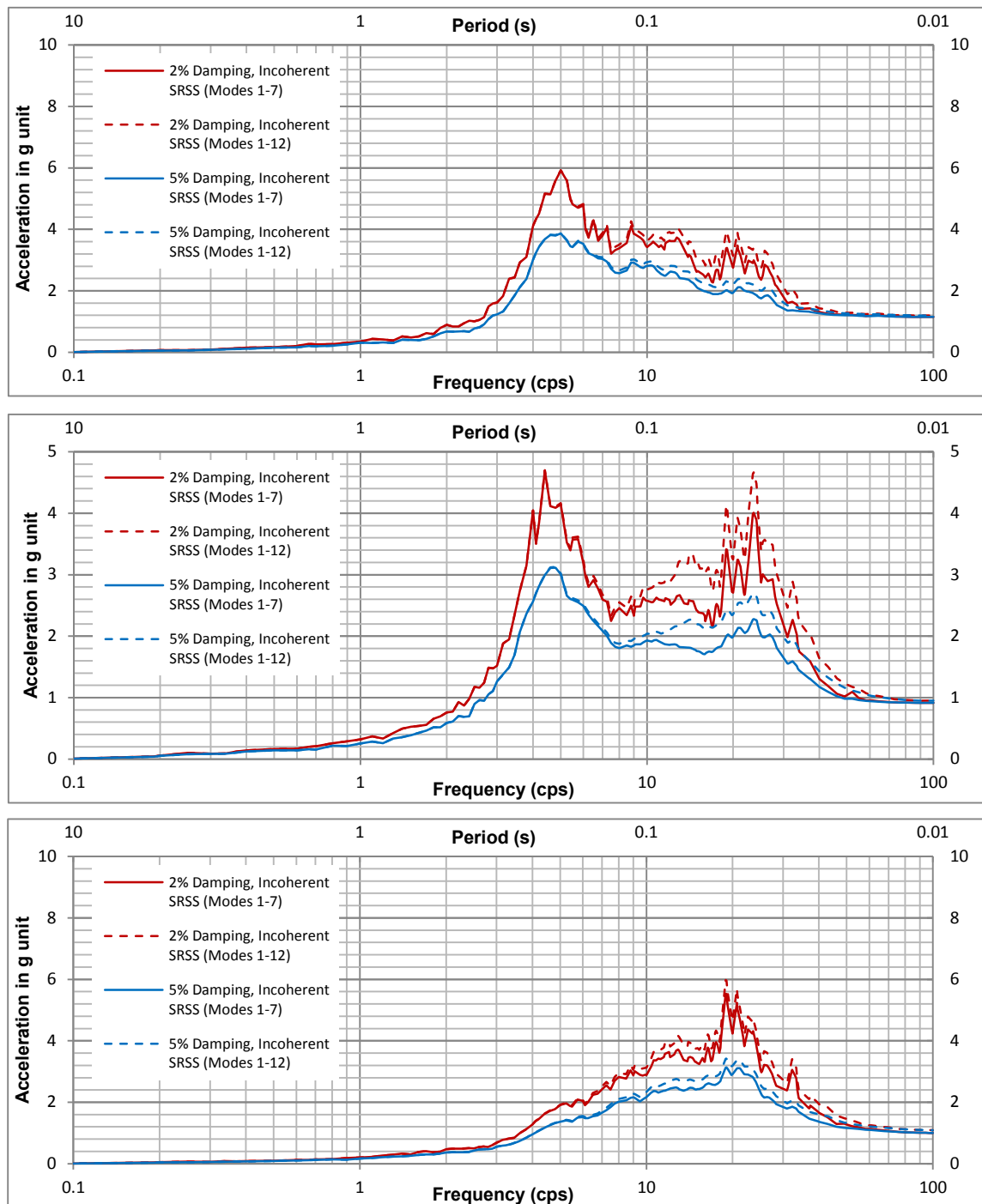


**Figure B-12 Comparison of Incoherent Results Using the 7 Modes and 12 Modes, Cracked Concrete Condition – Auxiliary Building Shearwall at El. 213'-6"**

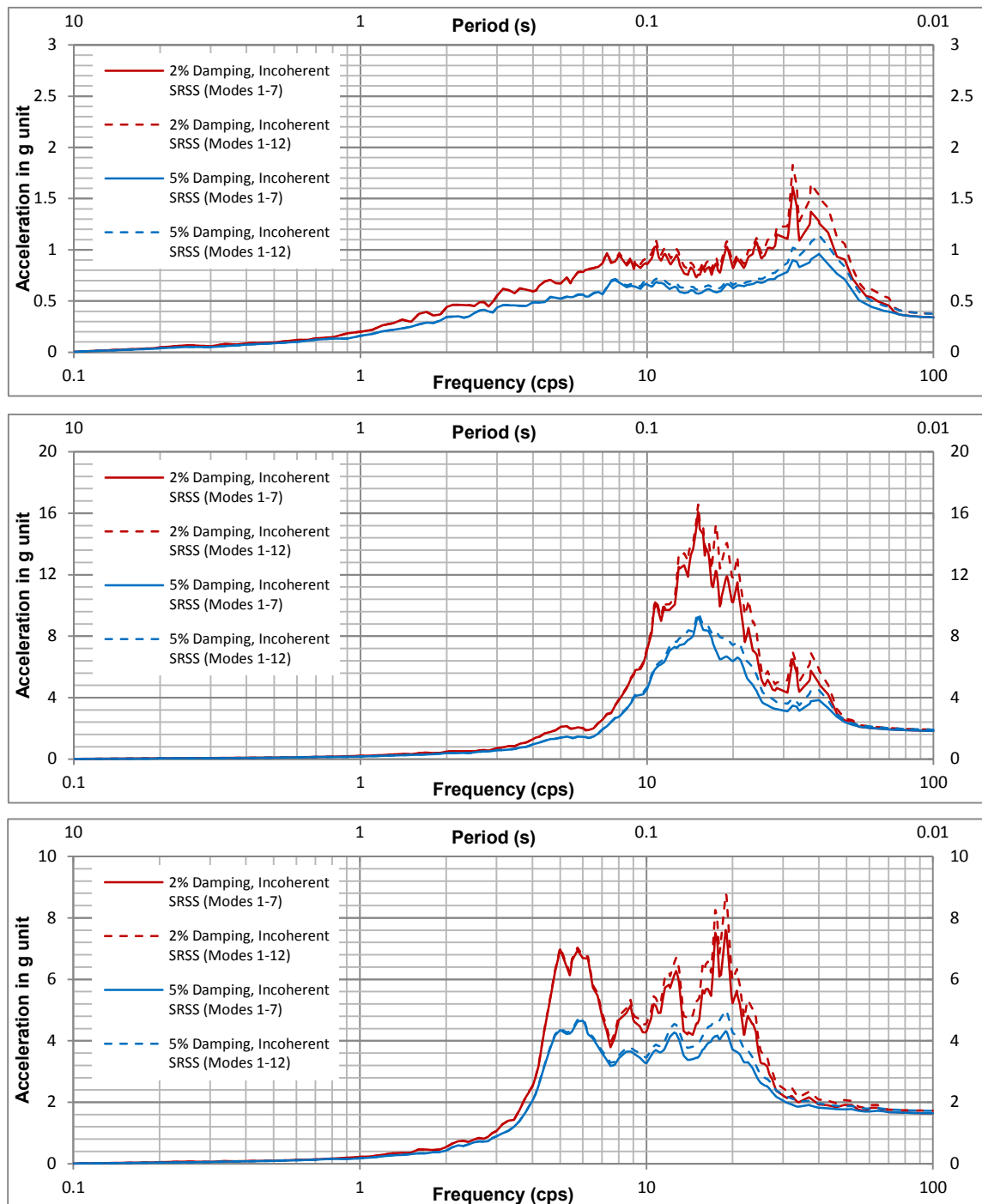


**Figure B-13 Comparison of Incoherent Results Using the 7 Modes and 12 Modes, Cracked Concrete Condition – Auxiliary Building Slabs at El. 55'-0", 156'-0" and 213'-6"**

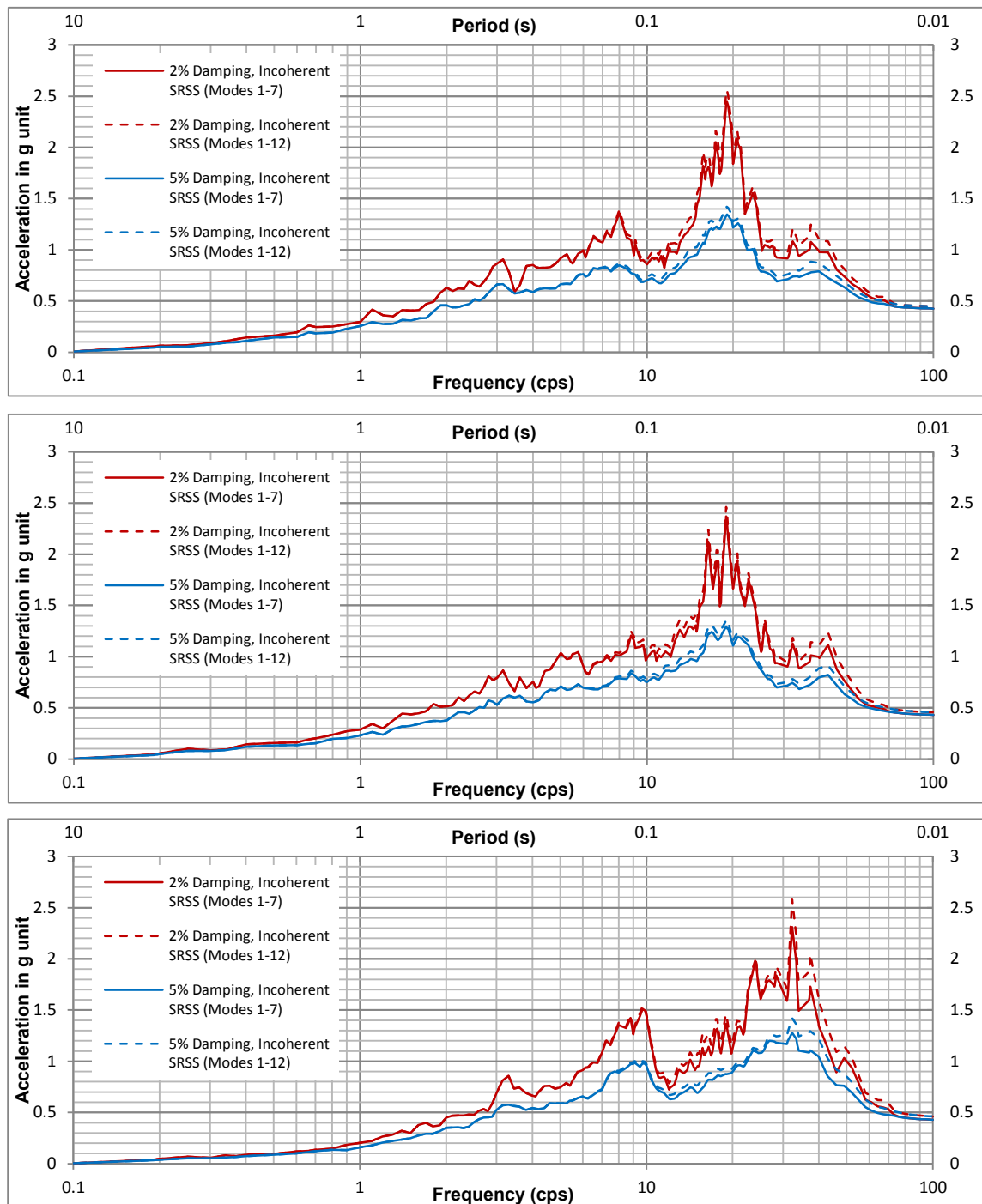


**Figure B-14 Comparison of Incoherent Results Using the 7 Modes and 12 Modes, Uncracked Concrete Condition - Containment Structure at El. 78'-0"**

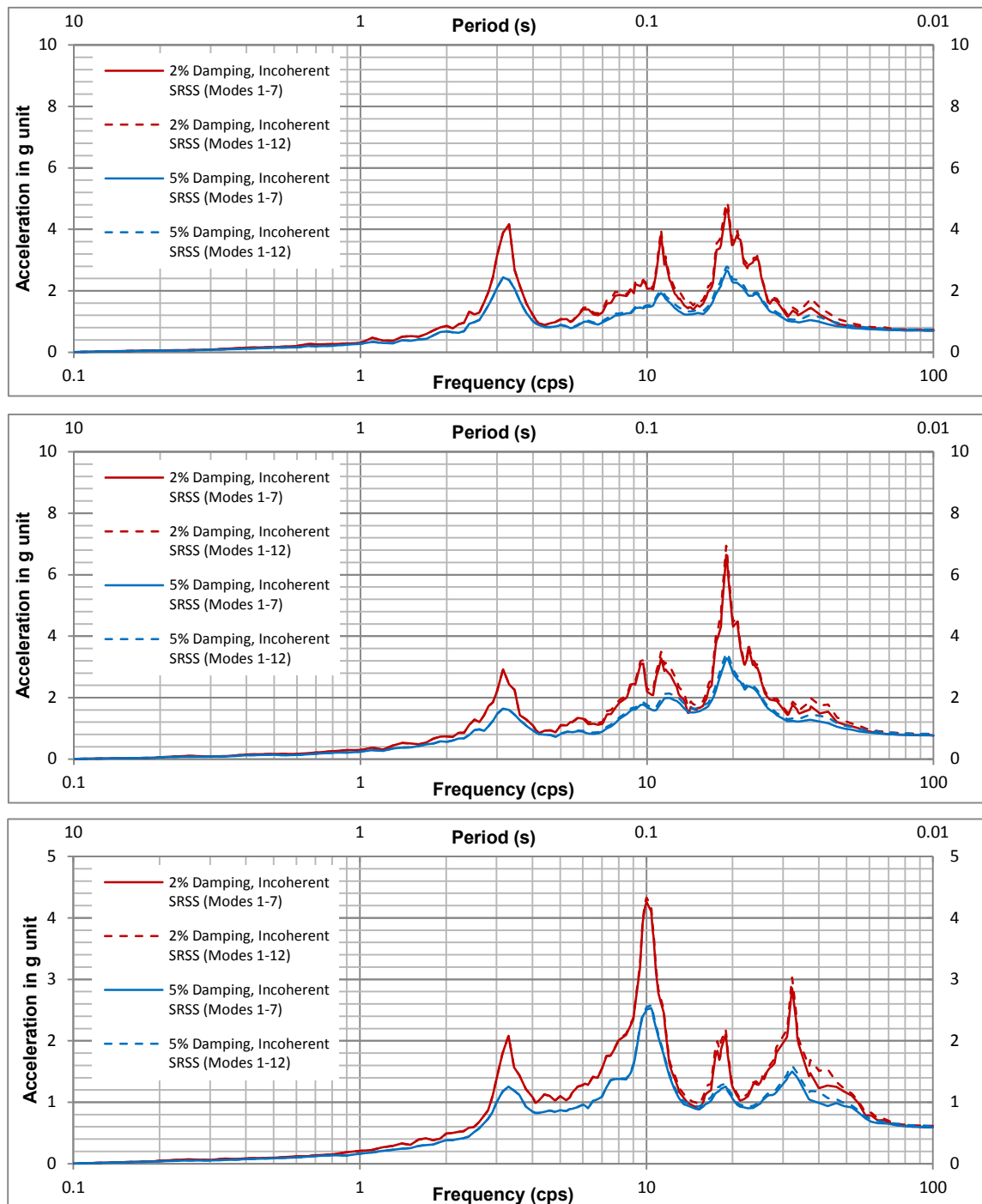


**Figure B-15 Comparison of Incoherent Results Using the 7 Modes and 12 Modes, Uncracked Concrete Condition - Containment Structure at El. 160'-0"**

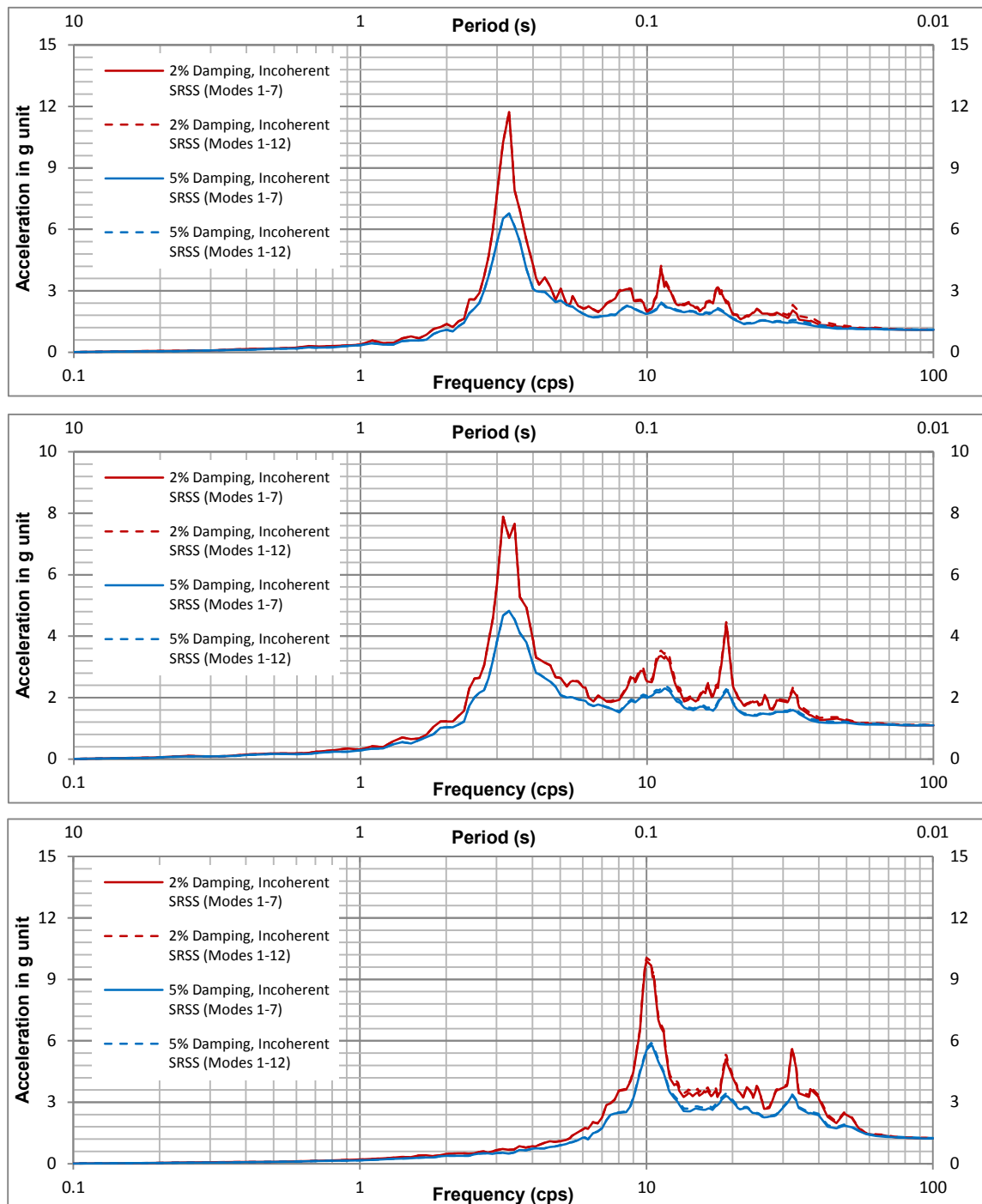


**Figure B-16 Comparison of Incoherent Results Using the 7 Modes and 12 Modes, Uncracked Concrete Condition - Containment Structure at El. 332'-0"**



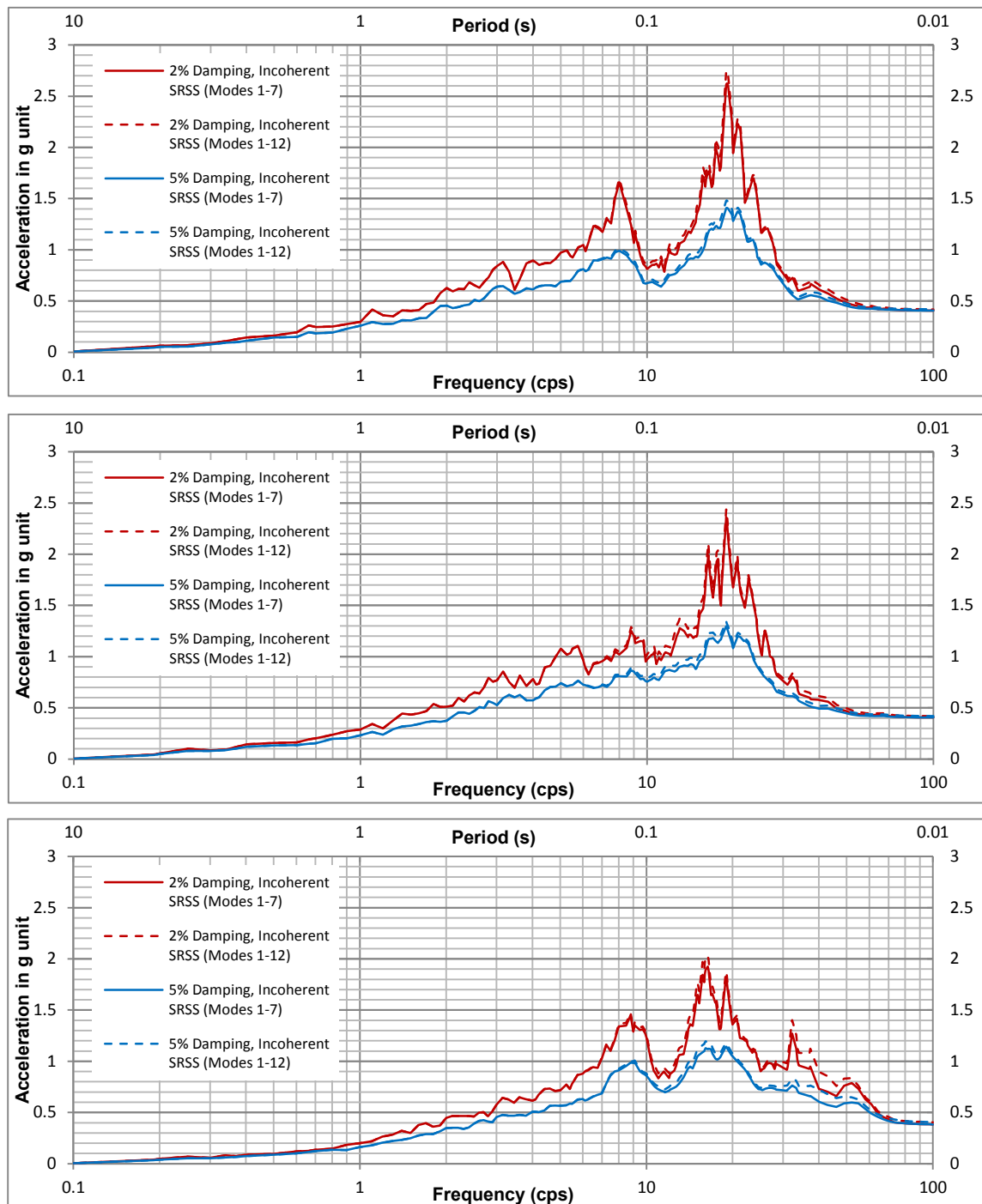


**Figure B-17 Comparison of Incoherent Results Using the 7 Modes and 12 Modes, Uncracked Concrete Condition – Primary Shield Wall at El. 78'-0"**

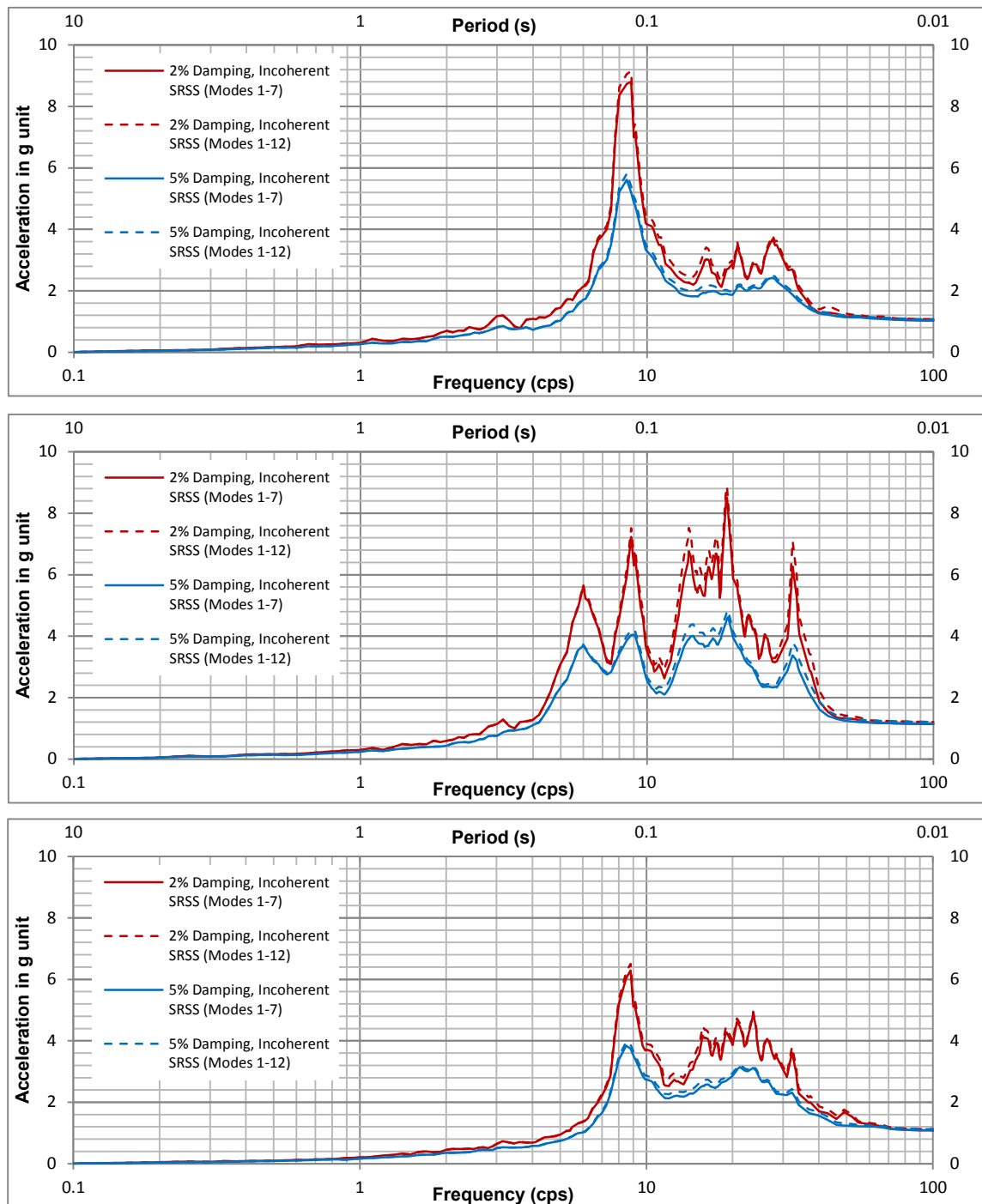


**Figure B-18 Comparison of Incoherent Results Using the 7 Modes and 12 Modes, Uncracked Concrete Condition – Primary Shield Wall at El. 156'-0"**

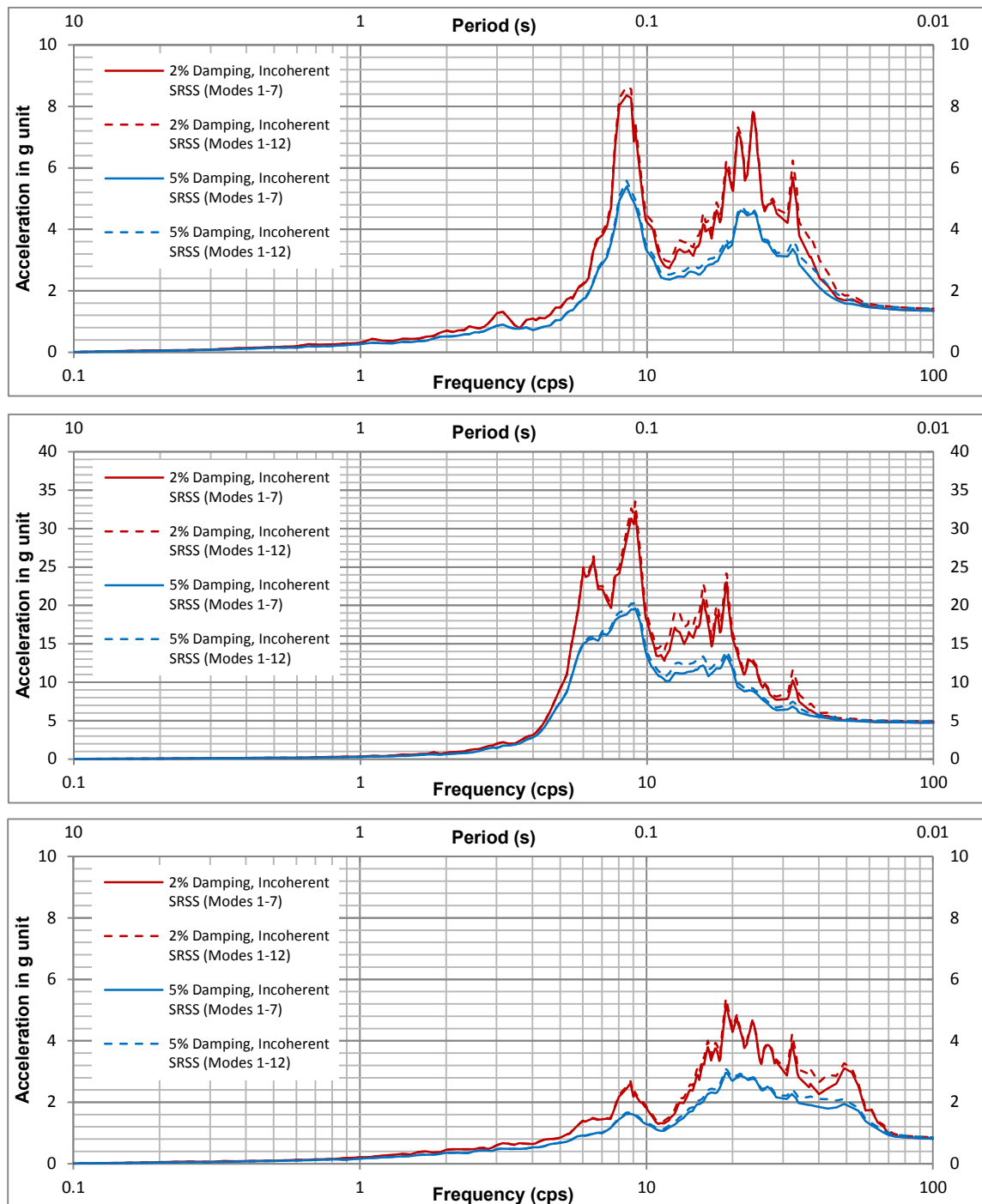


**Figure B-19 Comparison of Incoherent Results Using the 7 Modes and 12 Modes, Uncracked Concrete Condition – Primary Shield Wall at El. 191'-0"**

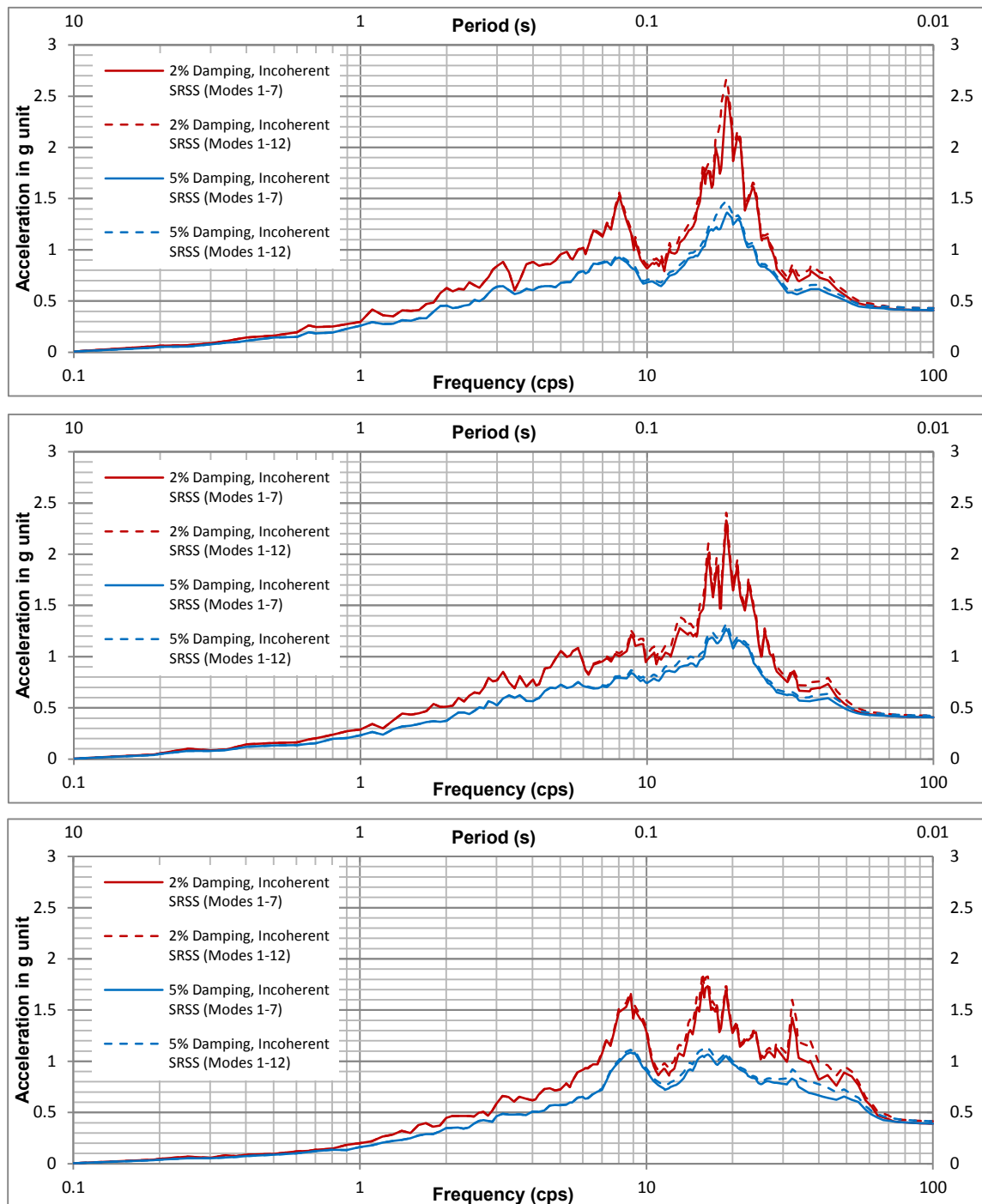


**Figure B-20 Comparison of Incoherent Results Using the 7 Modes and 12 Modes, Uncracked Concrete Condition – Secondary Shield Wall at El. 78'-0"**

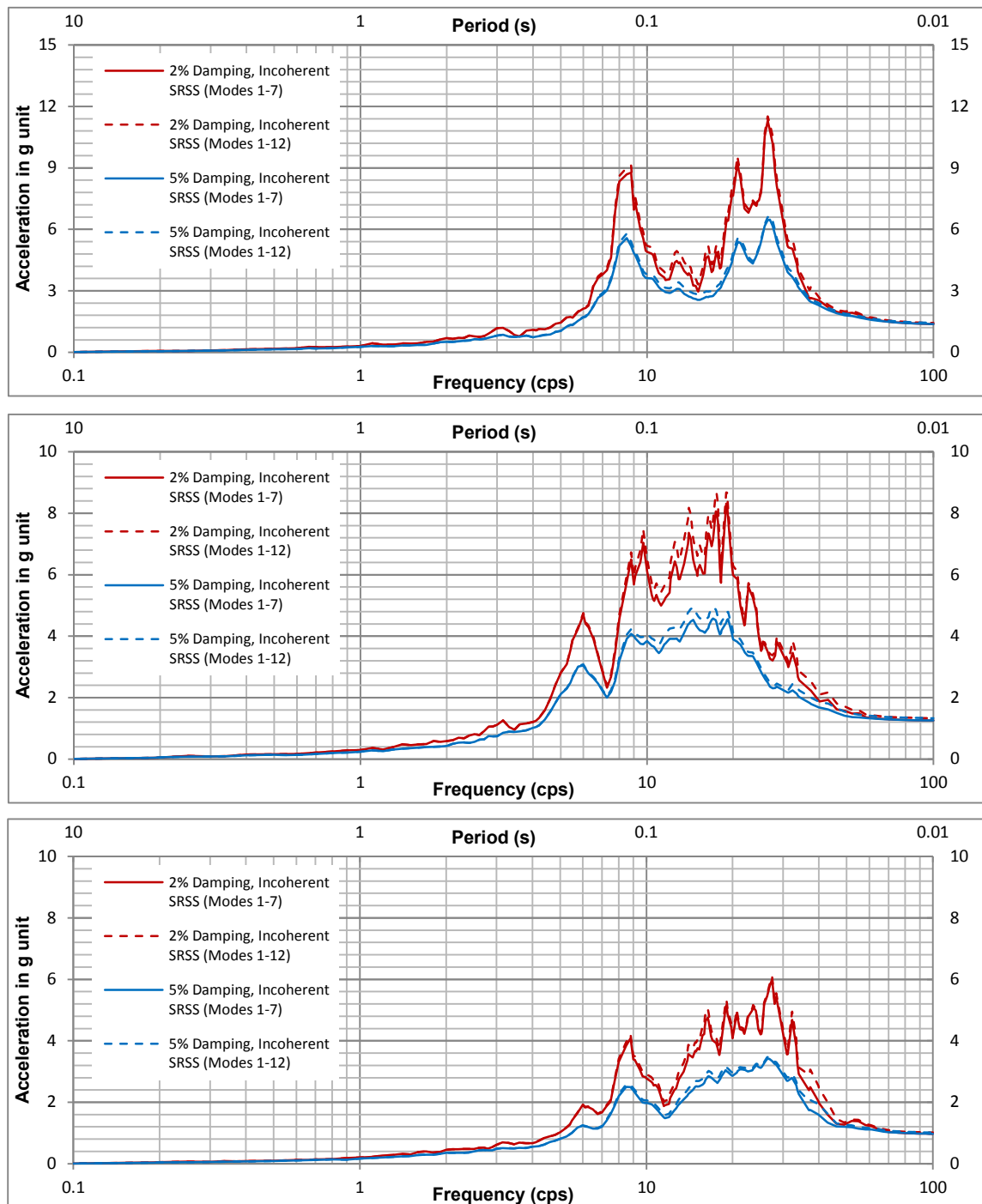


**Figure B-21 Comparison of Incoherent Results Using the 7 Modes and 12 Modes, Uncracked Concrete Condition – Secondary Shield Wall at El. 156'-0"**

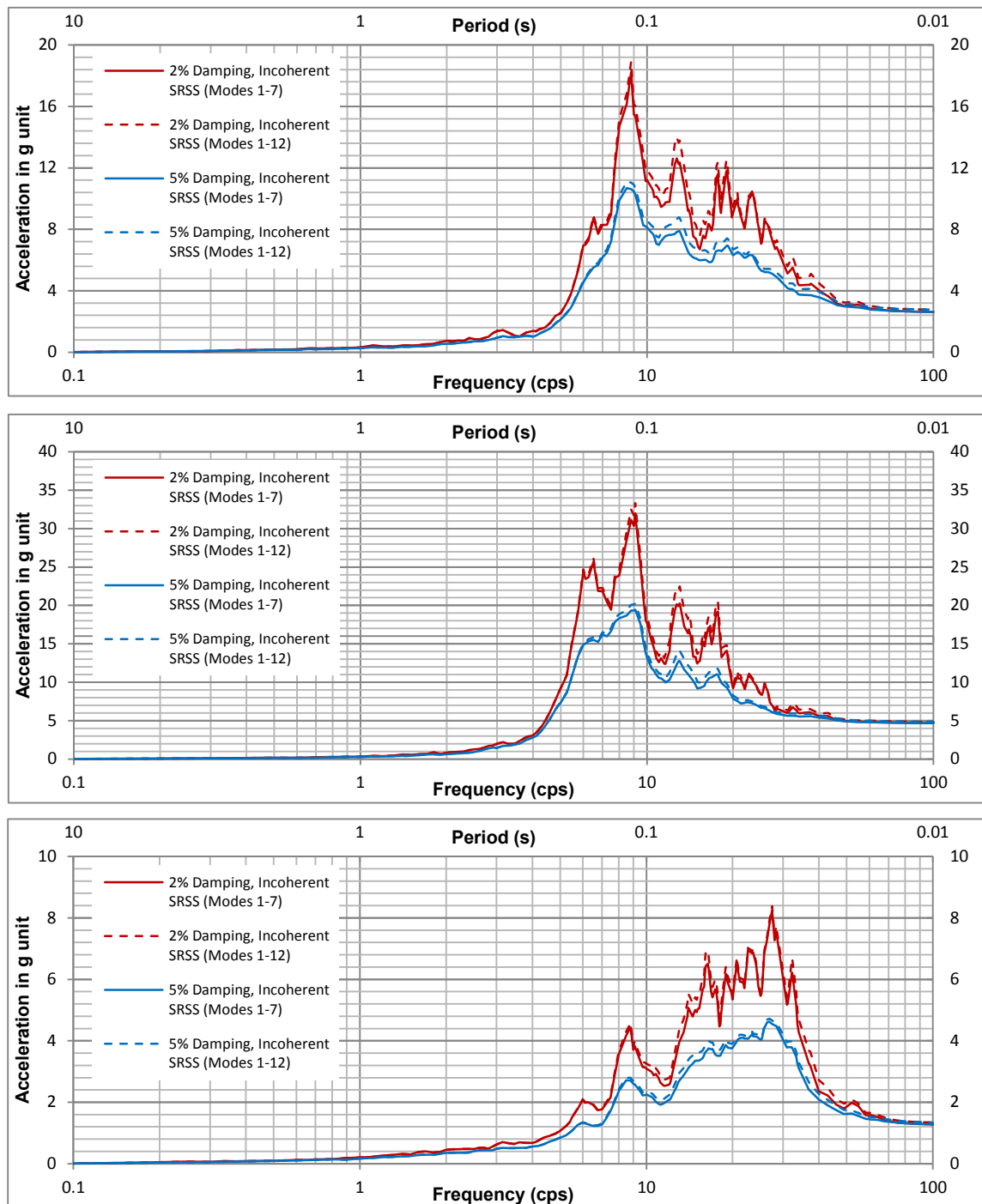


**Figure B-22 Comparison of Incoherent Results Using the 7 Modes and 12 Modes, Uncracked Concrete Condition – Secondary Shield Wall at El. 191'-0"**

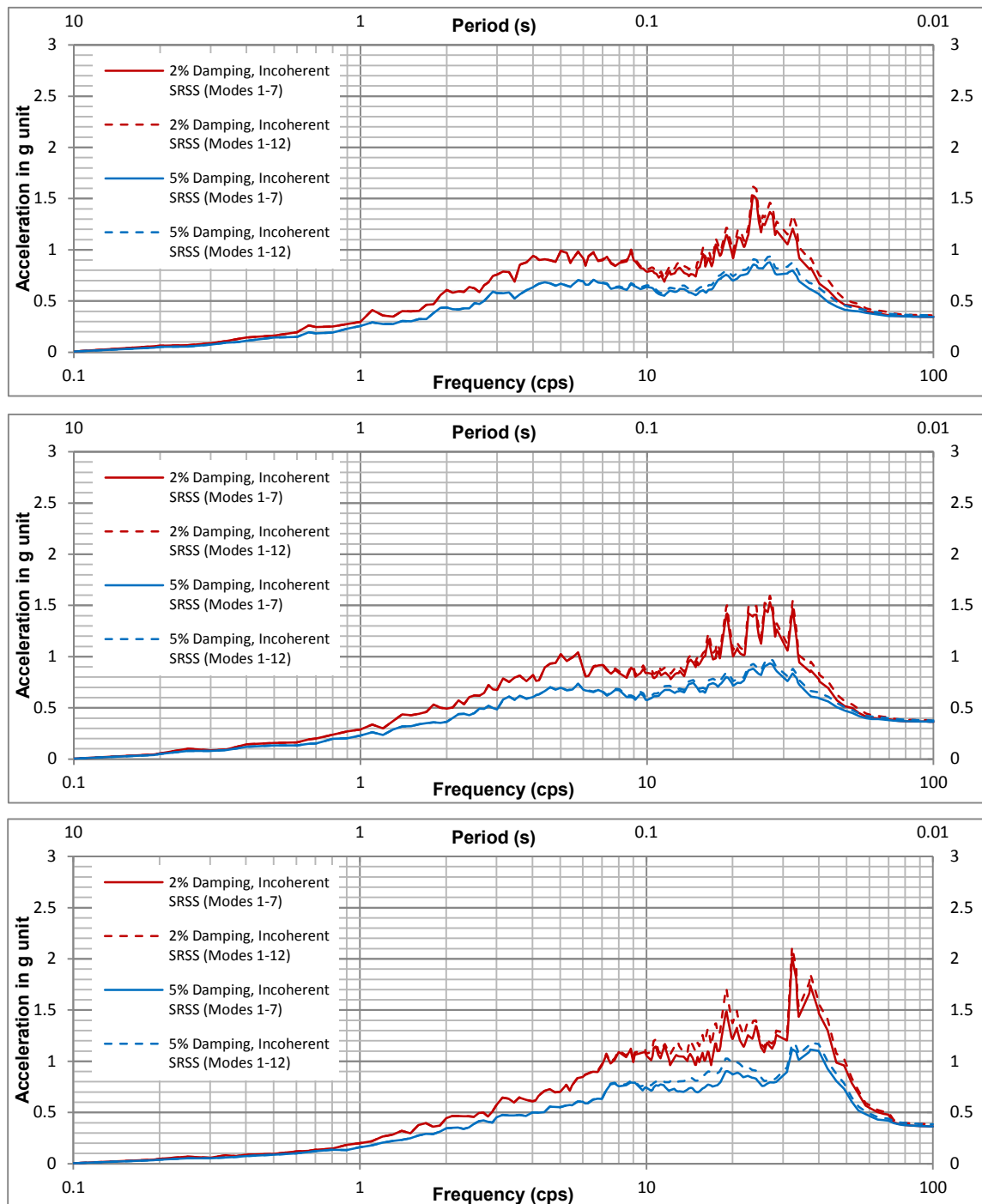


**Figure B-23 Comparison of Incoherent Results Using the 7 Modes and 12 Modes, Uncracked Concrete Condition – Auxiliary Building Shearwall at El. 55'-0"**

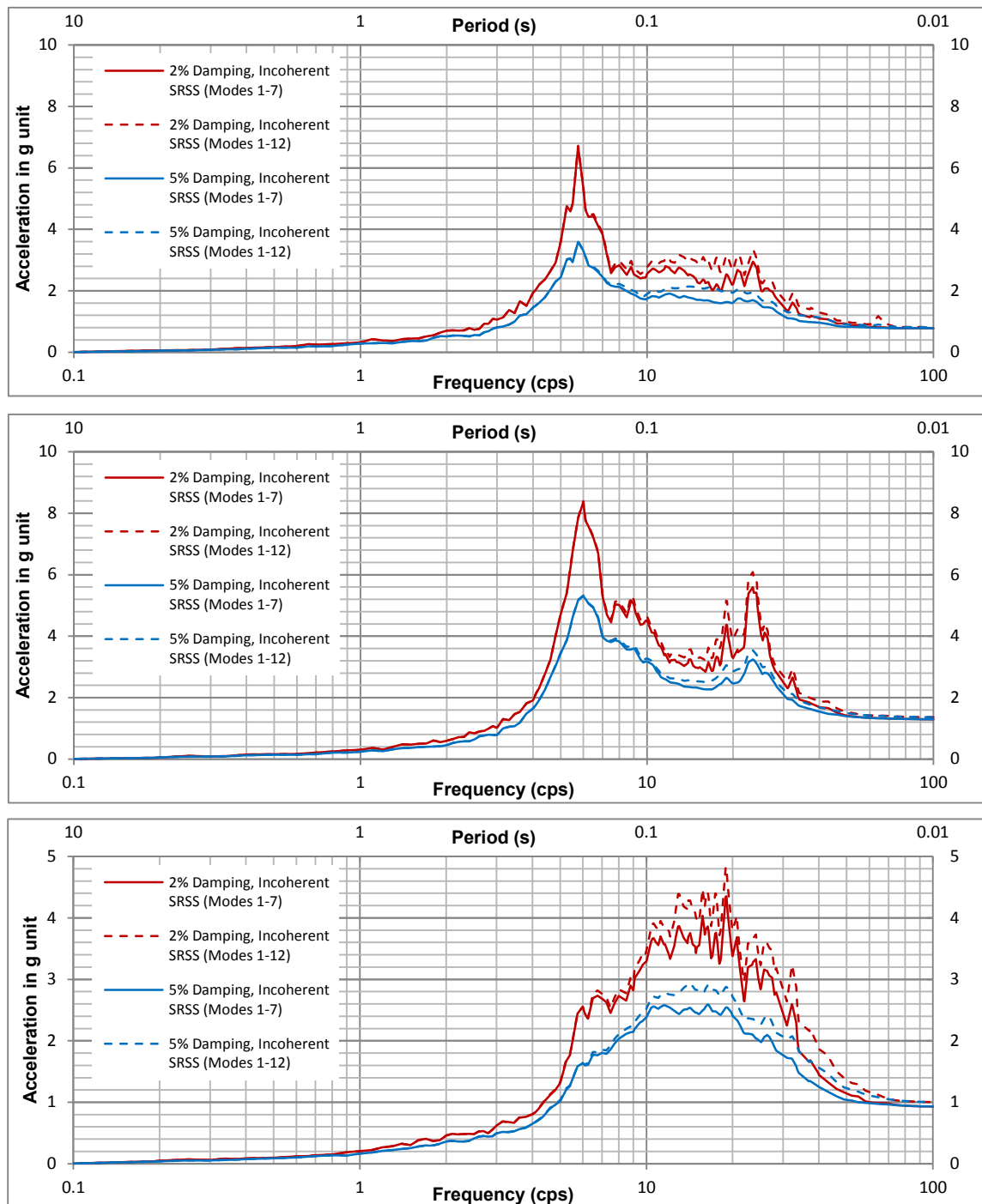


**Figure B-24 Comparison of Incoherent Results Using the 7 Modes and 12 Modes, Uncracked Concrete Condition – Auxiliary Building Shearwall at El. 156'-0"**



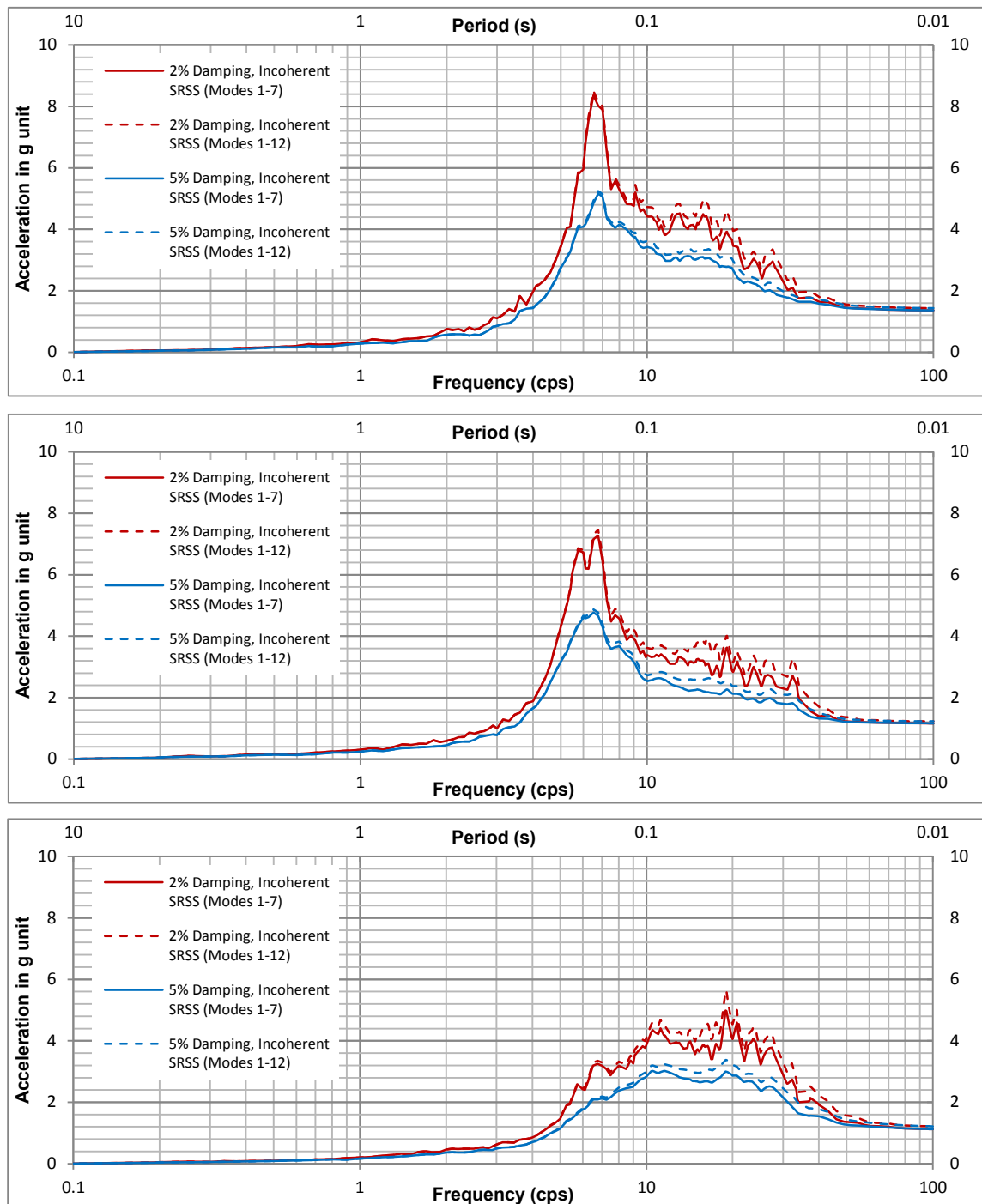


**Figure B-25 Comparison of Incoherent Results Using the 7 Modes and 12 Modes, Uncracked Concrete Condition – Auxiliary Building Shearwall at El. 213'-6"**

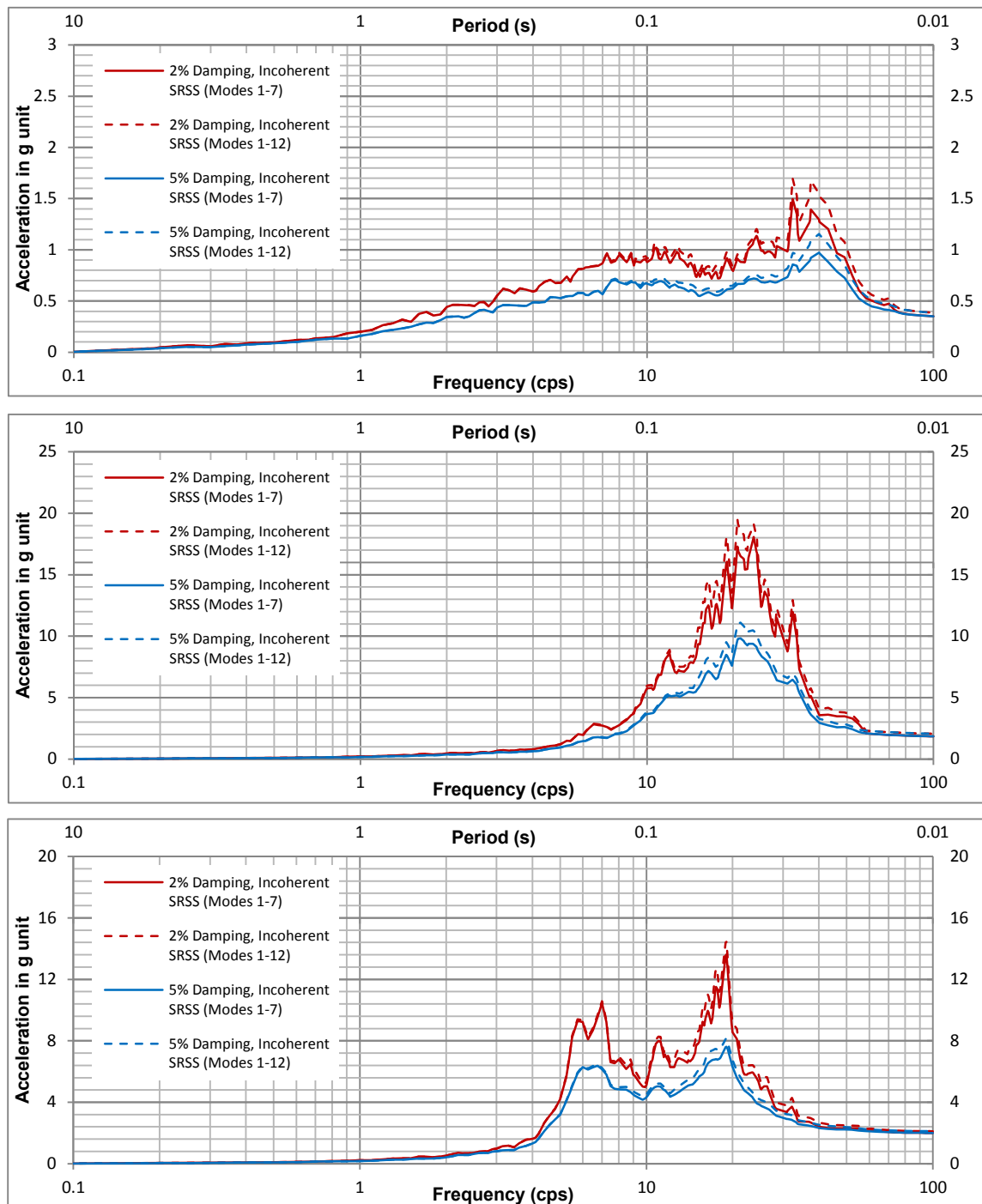


**Figure B-26 Comparison of Incoherent Results Using the 7 Modes and 12 Modes, Uncracked Concrete Condition – Auxiliary Building Slabs at El. 55'-0", 156'-0" and 213'-6"**

# **APPENDIX C**

## **INVESTIGATION OF SPATIAL COHERENCY**

### **MODE EXPANSION CONVERGENCE**

Page intentionally blank

## **C.1 INTRODUCTION**

In order to provide justification for implementing ISRS reduction levels in excess of those provided in SRP Section 3.7.2.II.4 and for the selection of the appropriate number of modes to be used in the SSI analysis to capture the incoherent-motion structural response, an investigation of spatial mode expansion convergence is performed in this Appendix. Based on the result of the investigation, it is concluded that the 16-mode-combined incoherent-motion responses are adequate for the APR1400 standard design for HRHF input motion. This Appendix also describes the evaluation of the seismic demand on the NI structures based on the 16-mode-combined response.

## C.2 IN-STRUCTURE RESPONSE SPECTRA (ISRS) REDUCTION LIMITS

The magnitude of ISRS amplitude reductions due to incoherence of hard-rock high-frequency (HRHF) seismic input motion shown in this report is justifiable since the ISRS results obtained from incoherence SSI analyses that include additional coherency modes (13 to 16) as described in the C.3 below demonstrate that the converged solution has ISRS amplitude reductions still exceeding the reduction limits set forth in SRP Section 3.7.2.II.4.

To further confirm that the cumulated effect of principal coherency modes higher than the 16 modes is insignificant and, thus, can be neglected, a supplementary study has been performed. For this supplemental study, a simplified basemat model extracted from the full SSI FE model of APR1400 NI for the S09 hard-rock soil profile case is created. The basemat foundation in this model is modeled with solid elements with the element shape and mesh being exactly the same as the NI full model, as shown in Figure C-1. The concrete material property is assigned to the entire basemat (elements in blue in Figure C-1). The elements surrounding the basemat (elements in red in Figure C-1) are assigned the backfill properties between El. 45' to 55'. Additional rigid beams are installed in the locations of the major shear walls to properly simulate the stiffening effect of the walls to the foundation basemat stiffness, as shown in Figure C-2.

Incoherence SSI analyses for the vertical direction motion input, which is considered most sensitive to the incoherent-motion SSI response, are performed using the ACS SASSI V3.0 (Reference 1) for principal coherency modes up to 50 modes. The frequency points selected for these analyses are the same as those documented in Section 5. The amplitudes of vertical Acceleration Response Spectra (ARS) obtained for the vertical response motions, with different number of cumulated spatial coherency modes, are compared with each other at the locations of the corners, the center of the basemat, and selected locations between walls. The selected different numbers of spatial coherency modes cumulated are as follows: 1-7 modes, 1-16 modes, and 1-50 modes. The locations for the selected shear wall and floor slab nodes are shown in Figure C-3 and Figure C-4, respectively. The comparisons shown in Figure C-5 through Figure C-33 are intended to demonstrate that the additional thirty plus coherency modes beyond the first 16 modes have an insignificant effect on the basemat vertical response due to the HRHF incoherent vertical input motion considered in the study.

Based on the results shown in Figure C-5 through Figure C-33, the accumulative effect of spatial coherency modes higher than 16 on the ISRS for the vertical response motions of the basemat are concluded to be insignificant and the 16-mode-combined results are concluded to have achieved a converged solution.

### C.3 SSI ANALYSIS FOR ADDITIONAL COHERENCY MODES 13 THROUGH 16

To provide the technical justification for the selection of the appropriate number of principal coherency modes to be used in the SSI analysis to capture the incoherent-motion structural response, incoherence SSI analyses using the same methodology as documented in Section 2 are performed for the additional coherency modes 13 through 16. This additional set of analyses is in addition to the 7 and 12 total numbers of modes that have been considered in the previous analyses.

From these additional analyses, the incoherent-motion SSI responses of the structures are obtained for the combination of modes 1 through 16 using the square-root-of-the-sum-of-squares (SRSS) combination rule. The adequacy of using 16 modes to capture the APR1400 NI HRHF incoherent-motion effect satisfying the response convergence acceptance criteria is confirmed from the comparisons of responses developed from the study in CC-1 and CC-2 outlined as follows:

- CC-1. Compare the 12-modes-combined and 16-modes-combined, 5%-damped in structure response spectra (ISRS) at selected key locations. The convergence acceptance criterion is set as the differences of responses from the two sets of analysis results being within 5%.
- CC-2. Compare the amplitudes of vertical response acceleration transfer function (ATF) due to the vertical input at the key locations as defined in item a) at the foundation level mode by mode from modes 12 to 16, based on the consideration that the vertical response due to vertical incoherent motion input at the foundation level is most sensitive to the addition of higher coherency modes.

These are further explained below.

The incoherent-motion SSI analysis models and the coherency functions used in the study for CC-1 described above are identical to those used in this report. Both uncracked and cracked concrete stiffness conditions are considered. All other conditions such as the input site properties and input ground motion for HRHF are the same as those documented in this report.

For this study, the INCOH program module, as used in this report, is developed and used to perform the modal decomposition for coherency matrices based on the NRC approved Abrahamson 2007 hard-rock spatial coherency functions. The SASSI seismic input motion load vector for each principal coherency modes considered in the analysis is developed following the methodology described in EPRI Technical Report No. TR-106231 (Reference 2). The resulting seismic load vectors for all the coherency modes considered in the analysis so developed are then incorporated into ACS SASSI. The responses of the SSI system to the modal seismic load vectors developed are then obtained using the ACS SASSI module ANALYS. The modal responses for all the coherency modes considered so computed are then combined using the SRSS combination rule. These combined responses are considered as the system response to the incoherent ground motions. The INCOH program module used in these analyses is validated and verified by comparing the results computed using the procedures described above with the corresponding results documented in this report.

For the incoherent-motion SSI analyses carried out for the additional coherency modes 13 through 16, SSI response transfer functions are calculated at 86 frequencies ranging from 0 to 71 Hz. These frequencies are consistent with the frequencies used for the analyses documented in Section 5. To provide results for comparison purposes, the coherent-motion SSI analysis using the same model is also performed for the same frequency points as those considered for in the incoherent-motion SSI analysis.

The same analysis procedure as that documented in this report is employed to develop the ISRS at selected locations considering ground motion incoherency. This procedure is summarized as follows:

- Step 1 Perform SSI analyses for the principal coherency modes to be considered and three directional seismic excitations.
- Step 2 For each principal coherency mode and each selected node, obtain the directional

responses in terms of ARS.

- Step 3 Combine the co-directional nodal response ARS using the SRSS rule.
- Step 4 Repeat Steps 2 and 3 for other principal coherency modes considered in the analysis.
- Step 5 Combine the modal responses obtained in Step 4 for all modes considered using the SRSS rule.
- Step 6 Repeat Steps 2 to Steps 5 for other nodes in the group and envelop the ISRS for the responses in the same group and then broaden the resulting enveloped ISRS to obtain the design ISRS for the group.

In the study of convergence of response in CC-2 described above, the vertical response ATF at representative nodes of the foundation basemat due to vertical input at the foundation level is computed to show the relatively low amplitude of higher modes 13 through 16 as compared to the SRSS-combined response amplitude obtained using modes 1 through 12. Figure C-35 through Figure C-48 show the ATF for the nodes shown in Figure C-34.

In each plot in these figures, the black data line named "Mode 1-12" is computed using a function of the MOTION module of ACS SASSI to combine the modal transfer function results using the rule of SRSS (ATF-SRSS) rule. The results show that the vertical response amplitude of the higher modes 13 through 16 is small as compared to the amplitude of the SRSS-combined response from modes 1 through 12.

However, for the 1-F slab locations, the results generally do not show a decaying pattern from mode to mode. As indicated in Figure C-49 (node 9501), mode 15 has the highest amplitude of the 4 additional higher modes considered, namely, modes 13 through 16. This is also apparent in other locations throughout the NI model. Figure C-50 and Figure C-51 show as examples the ATF results for nodes 12875 (2-F Wall, Uncracked) and 18165 (3-F Wall, Cracked), respectively. These results show that there is no clear decaying response pattern from mode to mode up to mode 16 for these locations, as the ATF amplitudes of some modes from 2 through 16 are of the same magnitude or greater than that of mode 1.

As shown in the ATF comparison in Figure C-35 to Figure C-51, the SRSS-combined ATFs for the first 12 modes are generally smooth and the amplitudes of the combined ATF are much greater than the amplitudes of the individual modes from 13 to mode 16. As indicated from these figures, the interpolated ATF curves for mode 16 are not as smooth as expected and exhibit suspicious spikes and dips in some frequency ranges, while the interpolated ATF curves for other individual modes presented in the figures are generally smooth. The suspicious spikes and dips are suspected to be due to the transfer function interpolation scheme used. While the suspicious spikes in the ATF always result in a conservative acceleration response spectrum, the suspicious dips in the interpolated ATF for mode 16 have insignificant effects on the multiple-mode SRSS-combined ISRS of interest due to their relatively lower amplitudes at their frequencies as compared to the amplitudes at other frequencies. The sensitivity of such response anomalies is further investigated as described below.

#### Investigation of Response Sensitivity due to Interpolation Scheme

The interpolation scheme used in the ATF comparison figures for all the modes considered is a five-point interpolation scheme based on complex response of a 2-DOF oscillator (ACS SASSI interpolation Option 0). If the responses of the two adjacent frequency steps analyzed have abrupt phase change (e.g. phase difference is greater than 90 degrees), it is likely that the Option 0 interpolation scheme will produce a dip or peak between the two calculated frequencies. For coherent analysis, if the frequencies analyzed are adequately spaced, the interpolation will capture correctly the dips and peaks of the responses. However, for the incoherence analysis using modal decomposition of the coherency matrix, it is possible that for two reasonably close enough frequencies, the interpolation Option 0 may predict a suspicious peak or dip in between. For a particular frequency considered in incoherence analysis, the phase angle of complex ATF could be flipped 180 degrees and still satisfy the SASSI SSI dynamic system equations, because the eigenvector of the coherency matrix or resulting SASSI seismic load vector could be in the opposite



direction. Therefore, the complex ATF phase difference between two adjacent frequencies analyzed is possible to be greater than 90 degrees and a suspicious peak or dip may be predicted in between by using interpolation scheme Option 0 for incoherence analysis even with the use of reasonably spaced analysis frequencies.

Figure C-37 and Figure C-39 show typical unsmooth ATF curves of mode 16 that result from the use of interpolation scheme Option 0. From the curves, nine frequencies, 15.00, 16.31, 16.85, 17.50, 18.55, 18.80, 18.99, 20.99, and 21.50 Hz, are determined approximately as the frequencies of potential suspicious interpolated ATF peaks and dips. Incoherence analysis for mode 16 and the nine frequencies mentioned above are performed for the uncracked case HRHF NI model to evaluate the adequacy of the 86 selected frequencies used in the analysis. Figure C-52 and Figure C-53 shown below compare the mode-16 ATFs of the uncracked HRHF NI model for the four cases for nodes 9501 and 9579, respectively. The four cases considered are described as follows: The black and red dots are the ATF magnitudes obtained from incoherent analyses using the original 86 frequencies (Case 1) and the original 86 frequencies plus the additional nine frequencies, i.e., a total of 95 frequencies (Case 2), respectively; the solid black line represents the interpolated ATF using Option 0 from the 86-frequency ATF directly obtained from the INCOH+ACS SASSI analysis. The 86-frequency ATFs are evaluated for the phase angle difference and the phase angles are then adjusted to limit the difference within 90 degrees for the adjacent frequencies. The blue dashed curve presents the interpolated curve obtained using interpolation Option 0 with the phase-adjusted 86-frequency ATFs (Case 3). These figures indicate that, while the black curve (Case 1), which has no phase adjustments, shows unexpected spikes and dips at the frequencies that are approximate to the added nine frequencies, the blue curve (Case 4), which has phase adjustments, is smooth and contains no suspicious peaks or dips. Furthermore, the red dots (Case 2) that result from the use of 95 frequencies, agree very well with the blue curve (Case 4) that results from the use of 86 phase-adjusted-frequencies obtained using Option 0 interpolation scheme. This indicates that the phase adjustments made (Case 3) correctly captures the dynamic responses at the nine additional frequencies (Case 4).

The comparisons shown in Figure C-52 and Figure C-53 demonstrate as typical examples that, while the 86 frequencies selected for the incoherence analysis for mode 16 may contain some irregular peaks and dips, the 86 frequencies select are adequate, as compared to the response obtained using more closely spaced frequencies, to capture the incoherent-motion SSI response within the frequency range of interest are adequate.

ACS SASSI provides interpolation scheme Option 6 as an alternative to Option 0 intended to produce smoother interpolated ATF curves. Option 6 uses a complex bi-cubic spline function to eliminate the suspicious spikes and dips assuming that the frequencies analyzed are adequate. Figure C-54 and Figure C-55 compare the mode 16 interpolated ATF using Options 0 and 6. The black curve and black and red dots represent the same quantities as described previously for the Figure C-52 and Figure C-53. The green dashed line shows the interpolated ATF using the Option 6 from the 86-frequency ATF output of INCOH+ACS SASSI without limiting the phase angle difference. Figure C-54 and Figure C-55 demonstrate that Option 6 produces smoother interpolated ATFs and predicted ATFs at the nine additional frequencies are in good agreement with the calculated ATFs for the added 9 frequencies.

Figure C-56 and Figure C-57 present comparison of the mode 16 vertical ARS due to vertical input resulting from the interpolation of the analysis results using 86 frequencies for the nodes 9501 and 9579, respectively, which are selected as typical examples. The black solid lines and the green dashed lines are obtained from the interpolation of the 86-frequency ATF results without limiting the phase angle difference using Options 0 and 6, respectively. The red dashed lines show the response spectra obtained from Option 0 interpolation of the 86-frequency ATF results but limiting the phase differences within 90 degrees. The comparisons shown in these figures show minor differences between the three curves. Figure C-58 demonstrates that the minor difference shown in Figure C-56 and Figure C-57 has an insignificant and, thus, negligible impact on the SRSS-combined design basis ISRS. Figure C-58 presents the enveloped and frequency-broadened vertical ISRS obtained from the SRSS-combined ISRS for mode 1 through mode 16 for the AB 1-F slab. The ISRS shown in this figure represent the enveloped and broadened ISRS for the group of responses at nodes 9501, 9579, and other nodes. In this figure, the black line

represents the ISRS obtained from using Option 0 interpolation of the computed 86-frequency ATFs and the red dashed line is the mode-1-to-16 SRSS-combined ISRS obtained using the same interpolation Option 0 for the same set of 86 frequencies but with the mode 16 ATF phase angles limited to the difference of 90 degrees. As shown this figure, there is practically no difference between the two lines. This demonstrates that the enveloped and broadened ISRS obtained using mode 1 through mode 16 is not sensitive to the different interpolation scheme options used for this group of nodes.

#### Convergence of 16-Mode-Combined Incoherent-Motion SSI Responses

The study performed for convergence criterion CC-2 as described previously demonstrates that the enveloped and broadened ISRS obtained using coherency mode 1 through mode 16 has achieved convergence of solution. Thus, the incoherent-motion SSI responses obtained using mode 1 through mode 16 are concluded to be adequate to capture the incoherent-motion SSI response.

In-structure response spectra (ISRS) are developed using the procedure described in CC-1 above in Step 1 through Step 6 to demonstrate the convergence of SSI analysis results considering 12 principal coherency modes based on comparing the 12-mode-combined responses to the 16-mode-combined responses (convergence criterion CC-1). The designated structure locations and their nodal points used in these response comparisons are the same as those documented in Technical Report APR1400-E-S-NR-14003. The ISRS for all locations are calculated for 5% damping ratio.

Figure C-59 through Figure C-218 show the ISRS comparison of results of NI between the responses of three levels, the 7-mode-combined, 12-mode-combined, and 16-mode-combined, and the coherent-input-motion SSI analysis results. Based on the ISRS comparisons (Figure C-59 through Figure C-218), the results satisfy the convergence criteria for most of the locations in the NI except for few locations, which are considered the outliers.

Therefore, the results of the studies for CC-1 and CC-2 as presented previously demonstrate that the 16-mode-combined incoherent-motion SSI response has achieved convergence response in general and, thus, is adequate to capture the incoherent-motion SSI effect. Thus, for the APR1400 standard design for the HRHF input motion, the 16-mode-combined incoherent-motion SSI response is used to substituted the current 7-mode-combined response. The responses at a few outlier structure locations that do not show clear convergent response using 16 modes are further investigated below.

#### Investigation of Sensitivity of Responses at the Outlier AB Below-Grade Exterior Shear Wall Responses due to Different Backfill Modeling Approaches

North-South (NS) direction ISRS developed at the five locations (each location consisting of a node group and being associated with uncracked and cracked concrete stiffness cases) associated with the AB below-grade shear walls, designated as 1-M and 2-F for uncracked, 1-M, 2-F and 3-F for cracked concrete stiffness cases were identified to be outlier locations that exhibit noticeable response deviations that do not satisfy the specified modal-response combination convergence criterion, for the responses of three levels of modal response combination, namely, the 7-mode-combined, 12-mode-combined, and 16-mode-combined. The comparisons of the ISRS generated at these three levels for the five aforementioned outlier locations are shown in Figure C-150, Figure C-151, and Figure C-169 through Figure C-171.

In addition to the observed noticeable differences between the responses for the three levels of modal response combination, Figure C-151, Figure C-170, and Figure C-171 show suspicious coherency-mode-combined responses indicated by the observation that the NS direction response to corresponding coherent ground motion over the full range of frequency. It is noted that for those five outlier locations/cases, the multiple-mode-combined, incoherent-motion-response ISRS for the EW and vertical directions show reasonable comparisons with the corresponding coherent-motion-response ISRS and their 16-mode-combined incoherent-motion-response ISRS show converged response and, thus, these incoherent-motion-response ISRS are adequate for capturing the incoherent ground motion SSI response effects.

For the APR1400 standard design, the seismic response for a designated structural location is represented by the envelope of the responses of a group of representative nodes (node group) at that location. For the aforementioned AB below-grade shear wall locations identified as the outlier locations, the node groups consist of selected representative nodes at interior and perimeter (exterior) basement (below-grade) shear walls.

A review of the multiple-coherency-modes-combined ISRS at the five locations (node groups) indicates that the ISRS for these five locations are generally controlled by the responses at the nodes representing the exterior walls, as shown typically in Figure C-219. Figure C-219 presents the two sets of ISRS for the AB shear wall group 2-F and uncracked concrete stiffness case, one for the entire set of nodes in the node group (black line) and one for the subgroup with the exterior wall nodes excluded (red line). This figure shows that the black lines (exterior-wall nodes included) dominate the ISRS amplitude and envelop the red lines (exterior-wall nodes excluded), indicating that the responses associated with the exterior-wall nodes dominate the response at the location of AB shear wall group 2-F.

The APR1400 design basis model for the HRHF SSI analysis, referred to herein as the original model, simulates the near-field backfill using solid elements, which are modeled as replacement of the free-field soil. The nodes of the AB below-grade exterior shear wall elements are connected to the nodes of the backfill solid elements at the interface of the basement structure and the backfill by rigid spring elements. The backfill elements share the same nodes with the excavated soil elements at the same locations. These backfill element nodes are therefore also interaction nodes in the SSI analysis. A second approach to backfill modeling in SASSI is to model the backfill soil as “structural elements,” which are connected to nodes that are different from the excavated-soil nodes (interaction nodes). The backfill structural elements share the nodes with the excavated soil elements only at the interface of the backfill structural elements and the free-field soils.

The first backfill modeling approach described above is considered an approximate modeling approach to the second backfill modeling approach, which is more consistent with the actual intent of the SASSI substructuring formulation. It should, however, be noted that the first backfill modeling approach adopted by the APR1400 design-basis SSI model produces a correct solution for the extreme case in which the backfill soil is exactly identical to the free-field soil. Whereas, the second backfill modeling approach, which is considered more consistent with the SASSI substructuring formulation, will produce an approximate solution since for this extreme case the structural elements of the backfill do not model the excavated soil elements exactly since they do not share exactly the same nodes.

To investigate the degree of approximation of the first approximate backfill modeling approach described above, the original HRHF SSI models for the uncracked (UC), cracked horizontal (CH), and cracked vertical (CV) models were modified by removing the rigid spring elements between the basement structure and the backfill, merging the exterior shear wall element nodes and backfill element nodes at the interfaces, and decoupling the interaction nodes and the backfill element nodes except at the exterior boundary nodes of the backfill. Incoherent-motion SSI analyses using the same methodology and the same set of analysis frequencies as the original analyses using the original design-basis models were performed on the modified UC, CH, and CV models with coherency modes 1 to 16. Analysis results obtained from the modified UC, CH, and CV models are also used to study convergence of the 16-mode-combined response at the identified outlier structure locations. The comparisons of the results obtained from the original models and corresponding results obtained from the modified models are made. These comparison results are described below.

Figure C-220 to Figure C-224 compare the ISRS results from the original models and modified models at the five identified response locations (node groups). The ISRS are the 16-mode-combined response for both the uncracked (UC) and cracked models. The ISRS curves for original models and modified models are denoted in these figures by “Orig.” (black line) and “OS” (red line), respectively. The comparisons shown in these figures present noticeable differences in all-three-direction ISRS results obtained from the two sets of models. However, for the responses in the NS direction, the ISRS of the modified models are generally enveloped by the corresponding ISRS of the original models. For the uncracked cases as shown in Figure C-220 and Figure C-221, the EW-direction, 16-mode-combined, ISRS from the original

and modified models are comparable although the responses from the original models do not always envelop the responses from the modified models.

For the AB below-grade shear wall locations, ISRS are developed separately for the subgroups that contain only the representative nodes at the interior walls of each shear wall node group. Comparisons of the ISRS developed for the AB interior shear wall node subgroups from the original models and modified models are presented in Figure C-225 through Figure C-229. Figure C-230 through Figure C-247 compare the ISRS at selected critical locations in the RCB. As shown by the comparisons in these figures, the two sets of model yield similar and comparable responses for the AB interior shear wall locations and the selected critical RCB locations.

For the uncracked modified model, Figure C-248 through Figure C-259 compare the 7-mode-combined, 12-mode-combined, and 16-mode-combined ISRS at the three levels at selected AB shear wall and representative RCB critical locations. For the cracked modified model, Figure C-260 through Figure C-271 compare the 7-mode-combined, 12-mode-combined, 14-mode-combined, and 16-mode-combined ISRS at the three levels at selected AB shear wall and representative RCB critical locations. The comparisons in these figures demonstrate convergence of the 16-mode-combined responses. Compared to the suspicious behavior as shown for the original models for the AB shear wall NS direction responses in Figure C-150, Figure C-151, and Figure C-169 through Figure C-171, the modified models yield more reasonable and expected mode-combined responses at the selected locations.

Based on the response results obtained from the analysis performed with the modified model as presented, it demonstrates with quantitative results that

The modeling approach for the backfill used in the original APR1400 HRHF SSI models (original models) approximates the intended SASSI substructuring formulation, whereas the modeling approach for the backfill of the modified models are considered more consistent with the original intent of the SASSI substructuring formulation. The response of the nodes adjacent to the nodes of the AB below-grade exterior shear walls that are connected to the backfill elements are affected by the different backfill modeling approaches. The original models and the modified models yield similar and comparable responses at the locations away from the interface of the structure and the backfill because their responses are not affected by the backfill modeling approaches. Further, the abnormal behavior for the NS direction response obtained from the original models at the AB below-grade shear walls in contact with the backfill is not observed in the modified models.

Based on the mode-combined ISRS from the modified uncracked and cracked models, the 16-mode-combined EW, NS, and vertical responses of the modified models are observed to have achieved the converged responses. For the five identified outlier locations/cases, namely, the NS responses of the AB shear wall node-groups 1-M and 2-F for the uncracked, and 1-M, 2-F, and 3-F for cracked concrete stiffness cases, the analyses using the original models generally produce conservative results as compared to the corresponding results obtained from the modified models.

### Summary

Based on the results of the response sensitivity investigation due to the different backfill modeling approach adopted in the original models versus that adopted in the modified models that have demonstrated convergence of the 16-mode-combined response obtained from the modified models, the non-convergence of the 16-mode-combined responses at the five identified outlier locations as observed from the original model results are concluded to be adequate for the APR1400 standard design.

For these outlier AB below-grade shear wall locations/cases, namely, 1-M and 2-F for uncracked, and 1-M, 2-F, and 3-F for cracked, the envelope of 16-mode-combined ISRS obtained from the original models and modified models is conservatively used in the APR1400 standard design.

For the RCB locations, the 16-mode-combined responses from both original models and modified models show converged responses, and the two different backfill modeling approaches have insignificant effects on these responses. As such, the 16-mode-combined incoherent-motion ISRS developed from the

original model for the RCB locations are adequate and, therefore, can be used for the APR1400 standard design.

#### C.4 SEISMIC RESPONSE DEMAND BASED ON 16 MODE-COMBINED RESPONSE

To re-evaluate the seismic demand on the NI structures based on the 16-mode-combined response, the results of seismic load analysis using the 16-mode-combined response of each structure are calculated and compared with the results obtained from the CSDRS seismic analysis response and the 7-mode-combined HRHF incoherent-motion seismic response results.

The seismic design forces of the containment structure (CS) and CIS are computed through the response spectrum analysis using the ISRS computed at the top of the basemat at EL. 78'.

For the CS, the ISRS curves from the CSDRS, 7-mode-combined, and 16-mode-combined HRHF response spectra computed at EL. 78' are compared in Figure C-272. As shown in Figure C-272, the ISRS obtained from the HRHF response spectra are higher than the corresponding ISRS obtained from the CSDRS in the higher frequency range above approximately 10 Hz. The comparisons show an increase of spectral amplitude for the HRHF ISRS as the number of coherency modes increases up to 16 modes. However, the comparisons also show that the main spectral amplitude peaks in the CSDRS ISRS are shifted to the higher frequency range. Since the governing natural frequencies of the CS lie below about 10 Hz (the dominant horizontal and vertical natural frequencies for the uncracked concrete model are 3.5 Hz and 10.6 Hz, respectively), the peak shift in the HRHF ISRS curves to the higher frequency range will not influence the overall seismic load analysis results for the CS.

To evaluate the effect of 16-mode-combined response on the CIS, the response spectrum analysis using the 16-mode-combined basemat ISRS is performed. The stresses of rebar calculated from the seismic forces and moments in the CIS, especially for the PSW and SSW, obtained from the response spectrum analysis are summarized in Table C-1. Although the rebar stresses at some locations exceed the allowable stress of 54 ksi by 1~8%, their magnitudes are still below the yield stress of the rebar. Hence, the current rebar arrangement can still be maintained while still maintaining the rebar stress demands to within the elastic range of the material even subjected to seismic load increase due to the increased 16-mode-combined incoherent-motion seismic response. The response spectrum analysis, which is used to obtain the seismic demands for the design of the CIS, produces conservative seismic demands relative to the seismic demands obtained from the time history analysis. In addition, the ISRS enveloping the two sets of ISRS for the uncracked and cracked concrete stiffness conditions are conservatively used in the response spectrum analysis. Based on the level of conservatism in the seismic demands obtained from the response spectrum analysis over the seismic demands obtained from the time history analysis, and comparing such level of conservatism with the level of increased rebar stresses based on the response spectrum analysis with HRHF input over the allowable rebar stresses, the rebar stresses based on seismic demands from the time history analysis (i.e., SASSI analysis) with HRHF input are not expected to exceed the allowable stress.

For the AB, equivalent accelerations of the AB derived from the seismic response story forces are calculated for the 16-mode-combined response. The comparisons of the equivalent accelerations so derived from the CSDRS, 7-mode-combined, and 16 mode-combined HRHF response for the AB are presented in Table C-2. As shown by the comparison in Table C-2, equivalent accelerations calculated from the 16-mode-combined HRHF response are not much greater than the corresponding accelerations calculated from the 7-mode-combined HRHF response. Most of the acceleration values calculated from the 7-mode and 16-mode-combined HRHF response are enveloped by the corresponding values calculated from the CSDRS response, except the vertical acceleration values of Fuel Handling Area 1 (El. 213'-6" to 226'-6") and Fuel Handling Area 3 (El. 195'-0" to 213'-0"). These exceptional local acceleration values in the global z-direction can be accommodated by the current design of the shear walls. Based on the revised results developed following the approach described above, the equivalent accelerations calculated for the AB with consideration of the envelope of the 16-mode-combined response from the original model and modified models for the five identified locations/cases of the AB below-grade shear wall are expected not to exceed the equivalent accelerations calculated from CSDRS seismic input.

Thus, based on the results of re-evaluation of the seismic response force demands due to the converged, 16-coherency-mode-combined incoherent-motion seismic responses, the current design of the CS, CIS,

and AB is concluded to have adequate design margin to accommodate the increased, 16-mode-combined incoherent-motion seismic response demands.

**C.5 REFERENCES**

1. ACS SASSI NQA Version 3.0 R2 Including Options A and FS, "An Advanced Computational Software for 3D Dynamic Analysis Including Soil-Structure Interaction," User Manuals Revision 3, Ghiocel Predictive Technologies, Inc., March 31, 2015.
2. W. S. Tseng and K. Lihanand, "Soil-Structure Interaction Analysis Incorporating Spatial Incoherence of Ground Motions," Electric Power Research Institute, Palo Alto, CA, Report No. TR-102631, October, 1997.



**Table C-1 Rebar Stresses Calculated from 16 Mode-combined Response of RCB Internal Structure**

| Structure | Location   | Calculated Stress (ksi) |       | Yield Stress (ksi) |
|-----------|------------|-------------------------|-------|--------------------|
|           |            |                         |       |                    |
| PSW       | North Wall |                         | 55.99 | 51.52              |
|           | East Wall  |                         | 49.40 | 58.36              |
|           | South Wall |                         | 53.41 | 52.72              |
| SSW       | SSW        |                         | 51.49 | 51.68              |
|           | RFP        | South/North             | 55.80 | 55.35              |
|           |            | West                    | 53.16 | 52.56              |
|           | SG         | Circular                | 48.07 | 54.76              |
|           |            | Straight                | 49.34 | 52.96              |
|           | PZR        |                         | 48.82 | 45.57              |

**Table C-2 Comparison of Equivalent Accelerations for Auxiliary Building**

| Location  | Elevation (ft) |         | CSDRS      |            |            | HRHF Response Spectra |            |            |            |            |            |
|-----------|----------------|---------|------------|------------|------------|-----------------------|------------|------------|------------|------------|------------|
|           |                |         |            |            |            | Modes 1~7             |            |            | Modes 1~16 |            |            |
|           | Bottom         | Top     | Acc. X (g) | Acc. Y (g) | Acc. Z (g) | Acc. X (g)            | Acc. Y (g) | Acc. Z (g) | Acc. X (g) | Acc. Y (g) | Acc. Z (g) |
| AB-FHA: 1 | 213'-6"        | 226'-6" | 1.39       | 1.84       | 0.75       | 1.04                  | 1.50       | 0.73       | 1.13       | 1.63       | 0.77       |
| AB-FHA: 2 | 213'-0"        | 213'-6" | 1.60       | 1.05       | 0.61       | 1.02                  | 0.83       | 0.44       | 1.07       | 0.88       | 0.44       |
| AB-FHA: 3 | 195'-0"        | 213'-0" | 1.33       | 1.27       | 0.34       | 0.86                  | 0.96       | 0.47       | 0.89       | 1.01       | 0.47       |
| AB-MCR: 1 | 195'-0"        | 213'-0" | 1.48       | 1.12       | 0.77       | 1.34                  | 0.90       | 0.61       | 1.40       | 0.92       | 0.62       |
| AB: 1     | 174'-0"        | 195'-0" | 1.00       | 1.07       | 0.49       | 0.58                  | 0.69       | 0.39       | 0.58       | 0.68       | 0.38       |
| AB: 2     | 156'-0"        | 174'-0" | 0.71       | 0.96       | 0.51       | 0.54                  | 0.69       | 0.42       | 0.54       | 0.69       | 0.42       |
| AB: 3     | 137'-6"        | 156'-0" | 0.60       | 0.77       | 0.50       | 0.45                  | 0.46       | 0.41       | 0.45       | 0.45       | 0.38       |
| AB: 4     | 120'-0"        | 137'-6" | 0.62       | 0.71       | 0.45       | 0.39                  | 0.50       | 0.41       | 0.40       | 0.51       | 0.41       |
| AB: 5     | 98'-6"         | 120'-0" | 0.51       | 0.64       | 0.42       | 0.33                  | 0.45       | 0.33       | 0.33       | 0.45       | 0.29       |
| AB: 6     | 77'-0"         | 98'-6"  | 0.33       | 0.47       | 0.34       | 0.25                  | 0.33       | 0.30       | 0.25       | 0.33       | 0.28       |
| AB: 7     | 67'-0"         | 77'-0"  | 0.27       | 0.31       | 0.31       | 0.23                  | 0.27       | 0.27       | 0.20       | 0.27       | 0.27       |
| AB: 8     | 55'-0"         | 67'-0"  | 0.26       | 0.26       | 0.31       | 0.23                  | 0.23       | 0.24       | 0.18       | 0.23       | 0.24       |

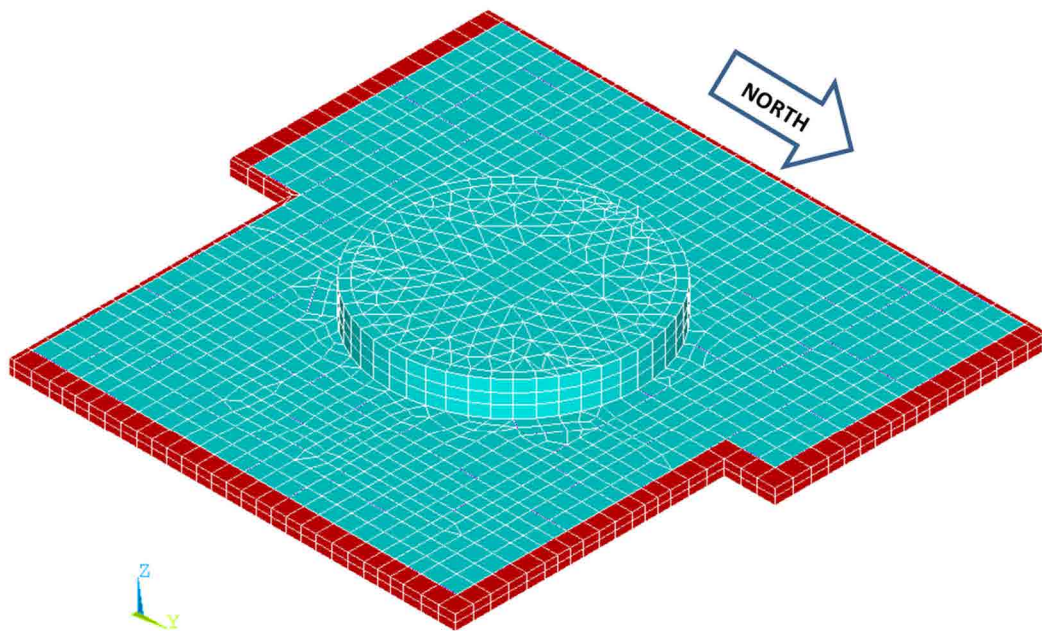


**Figure C-1 Simplified Basemat Model for APR1400 NI**

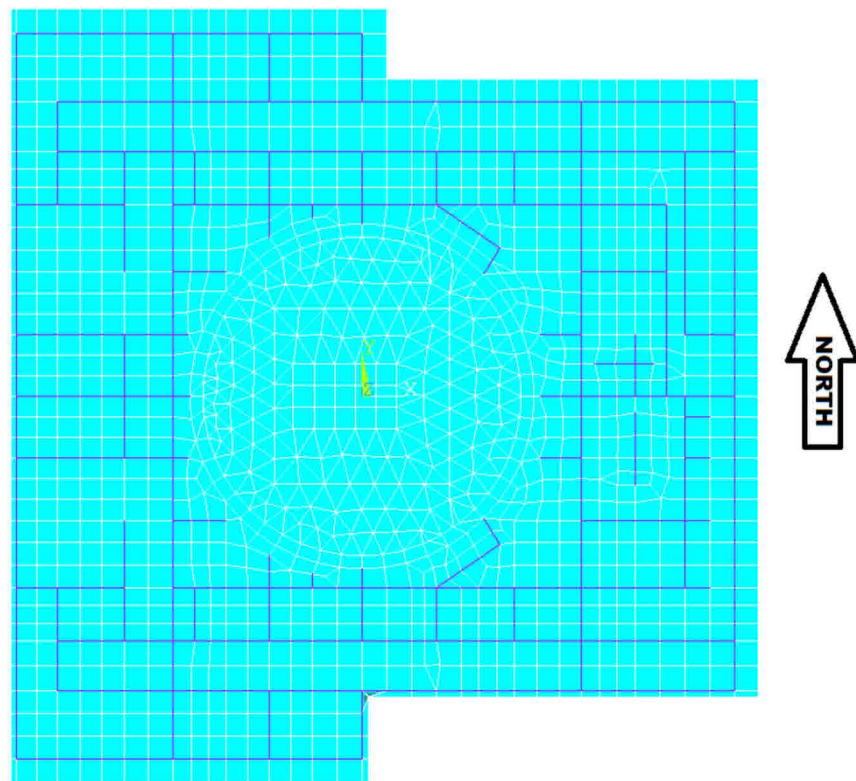


**Figure C-2 Rigid Beam Locations in Simplified Basemat Model**

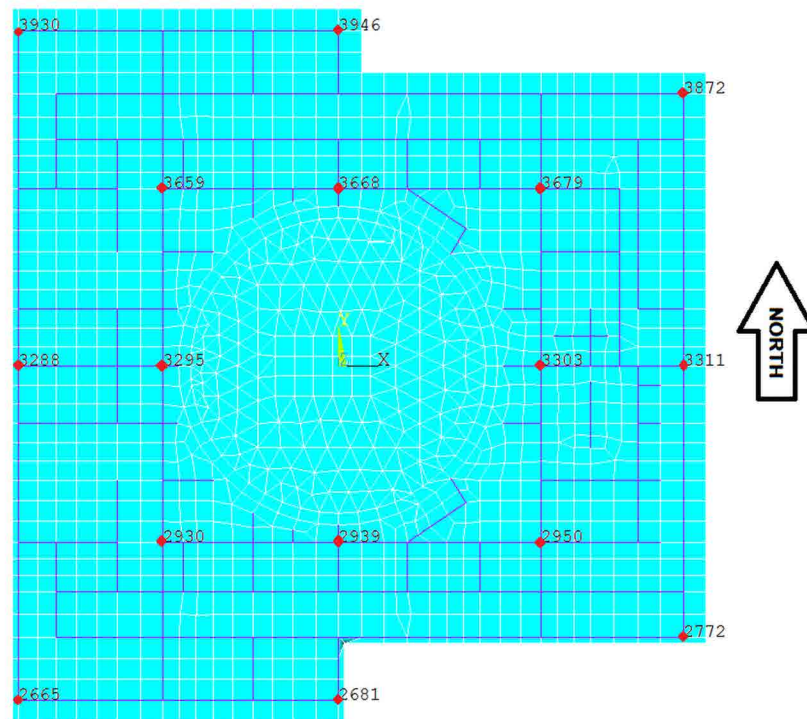


Figure C-3 Locations for Selected Shear Wall Nodes at Basemat

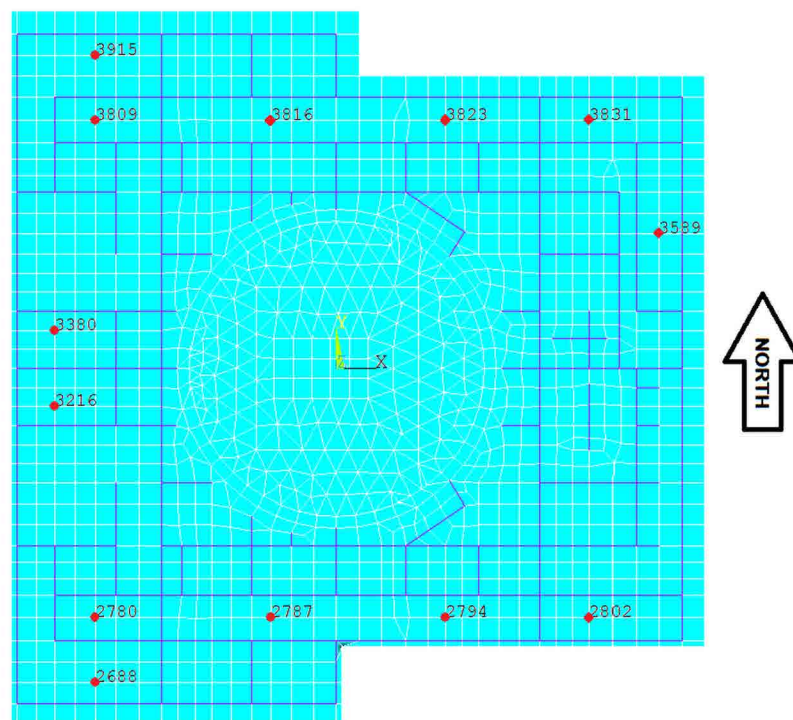


Figure C-4 Locations for Selected Slab Nodes at Basemat

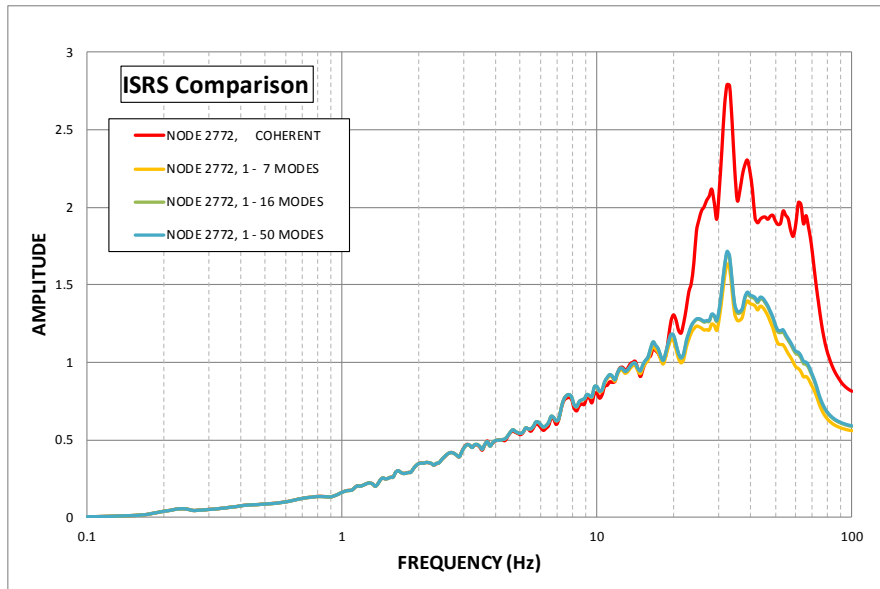


Figure C-5 ARS – Shear Wall Node 2772 – Response in Vert. Direction

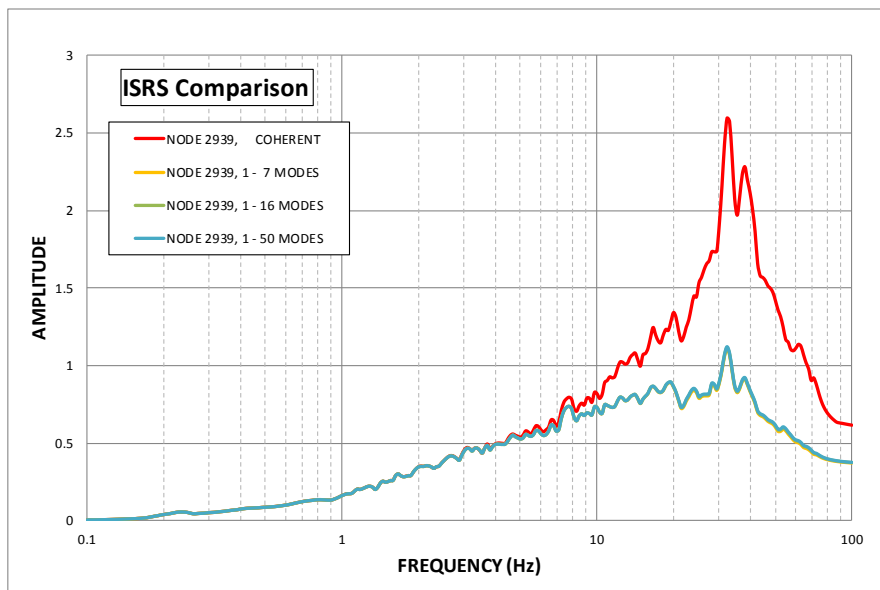


Figure C-6 ARS – Shear Wall Node 2939 – Response in Vert. Direction

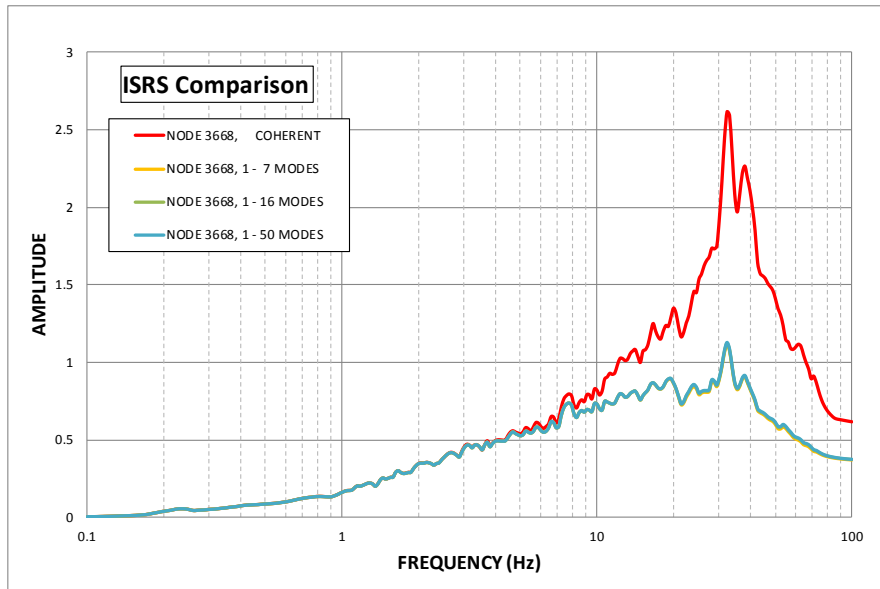


Figure C-7 ARS – Shear Wall Node 3668 – Response in Vert. Direction

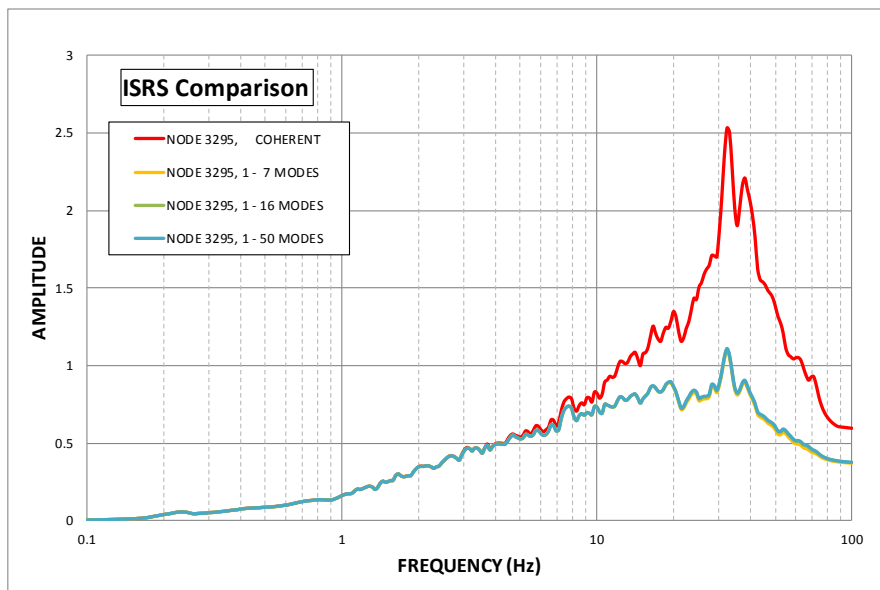


Figure C-8 ARS – Shear Wall Node 3295 – Response in Vert. Direction

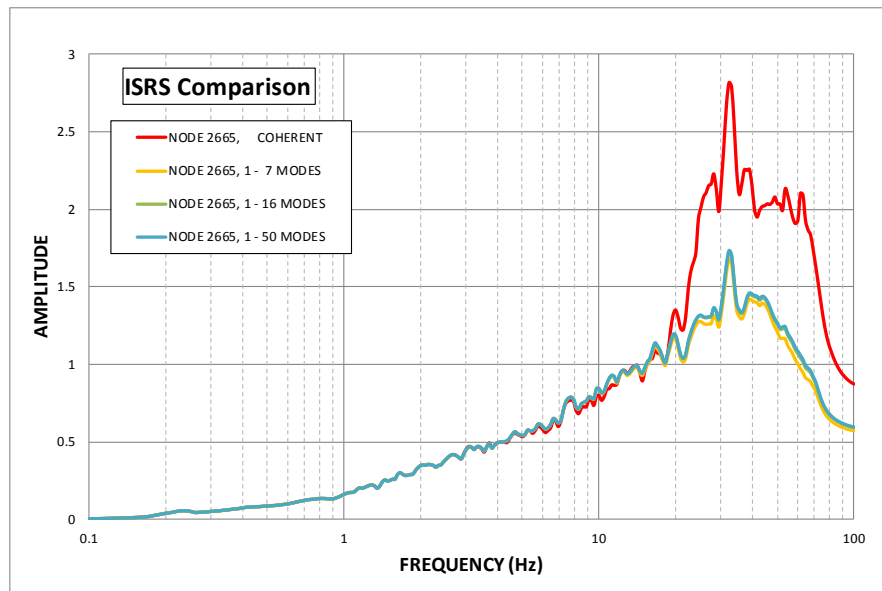


Figure C-9 ARS – Shear Wall Node 2665 – Response in Vert. Direction

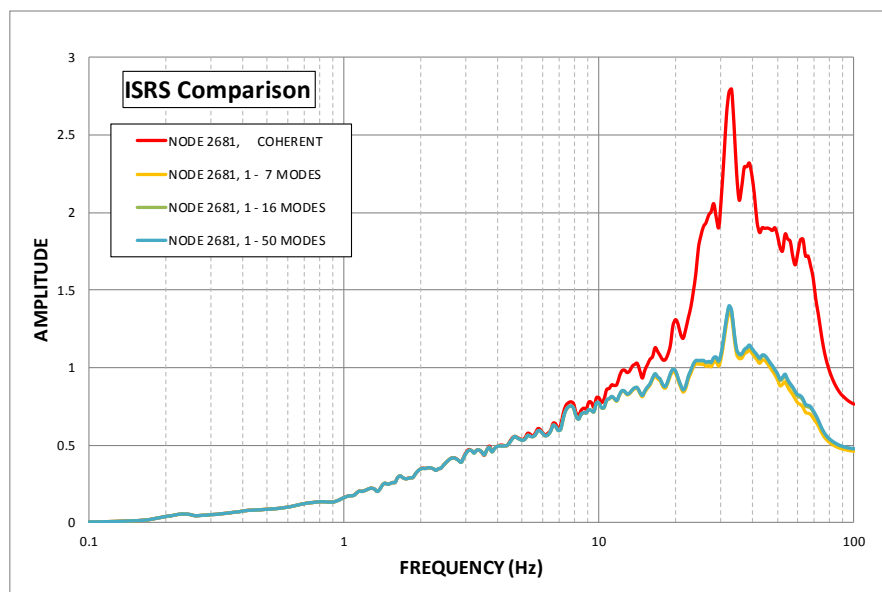


Figure C-10 ARS – Shear Wall Node 2681 – Response in Vert. Direction

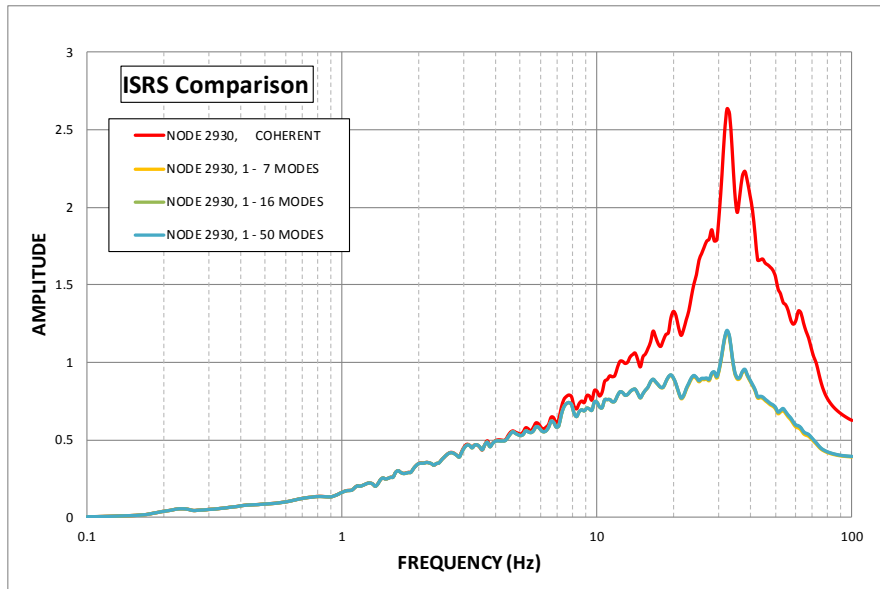


Figure C-11 ARS – Shear Wall Node 2930 – Response in Vert. Direction

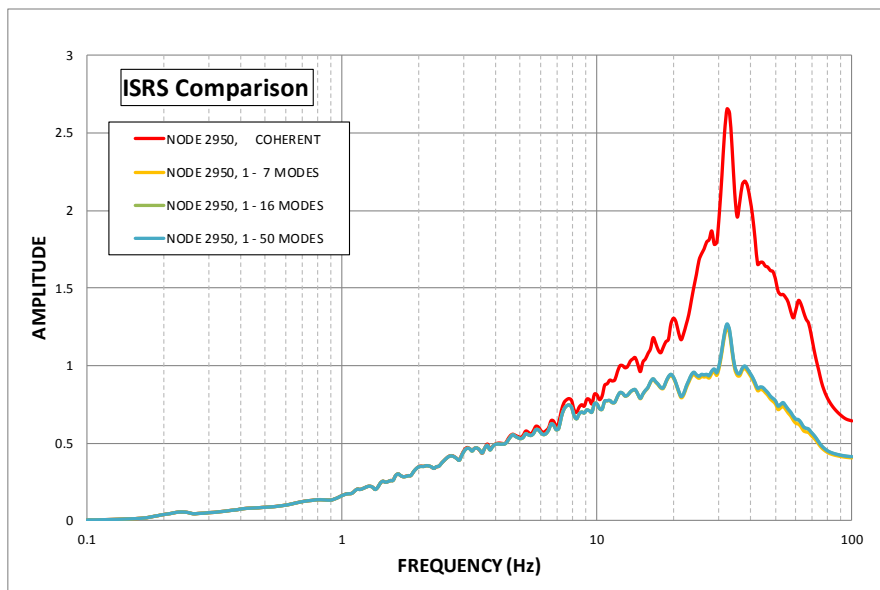


Figure C-12 ARS – Shear Wall Node 2950 – Response in Vert. Direction

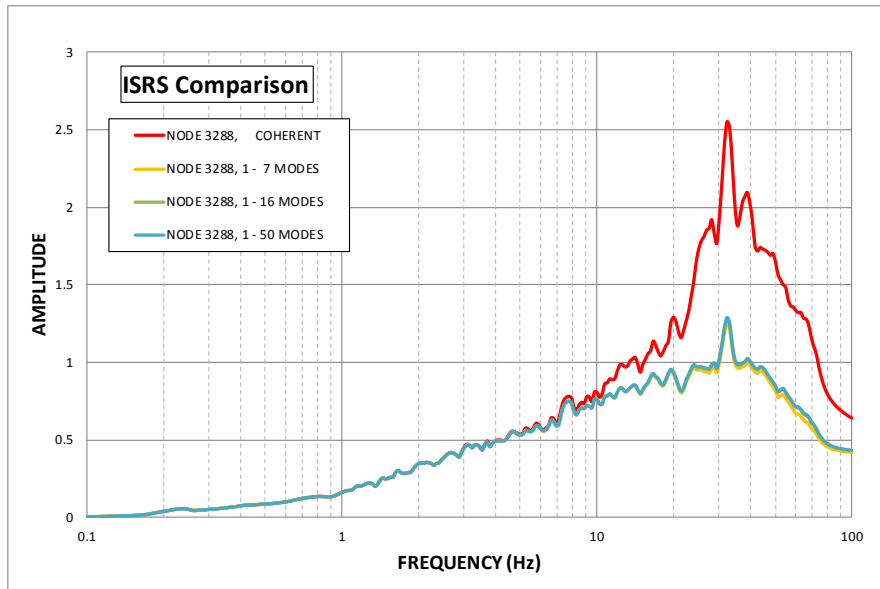


Figure C-13 ARS – Shear Wall Node 3288 – Response in Vert. Direction

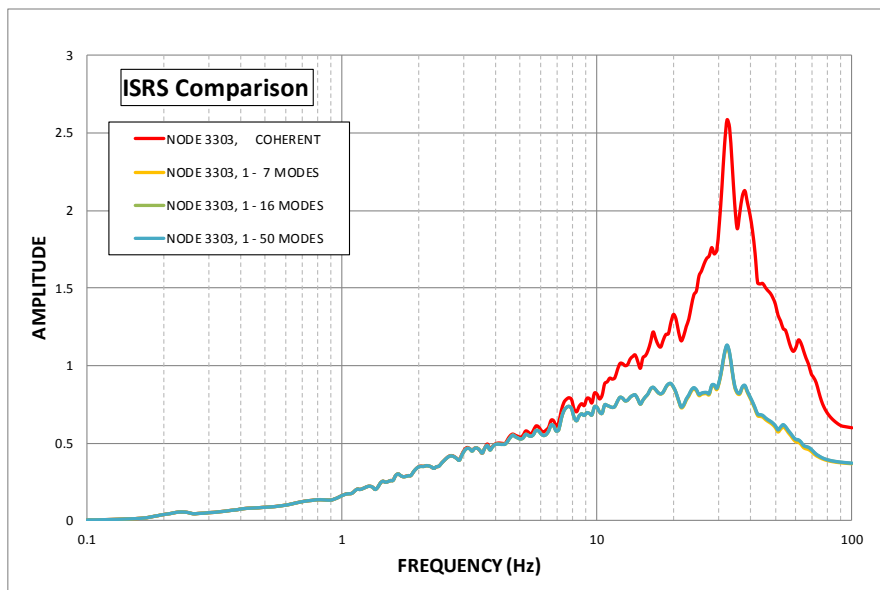


Figure C-14 ARS – Shear Wall Node 3303 – Response in Vert. Direction



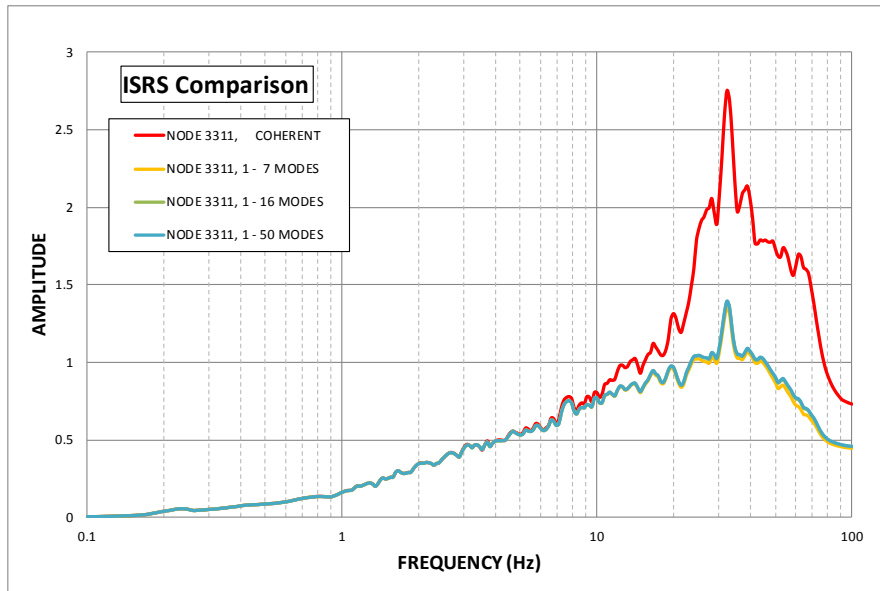


Figure C-15 ARS – Shear Wall Node 3311 – Response in Vert. Direction

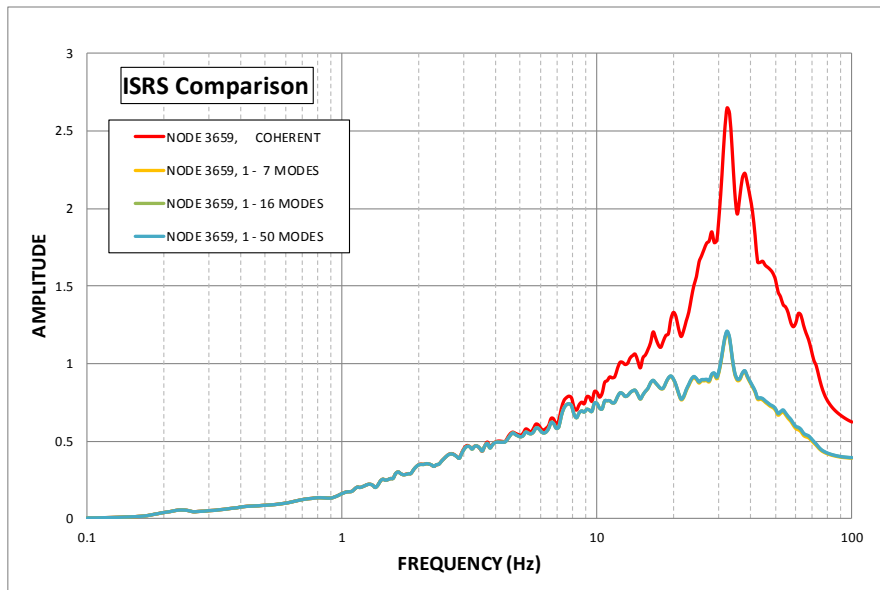


Figure C-16 ARS – Shear Wall Node 3659 – Response in Vert. Direction

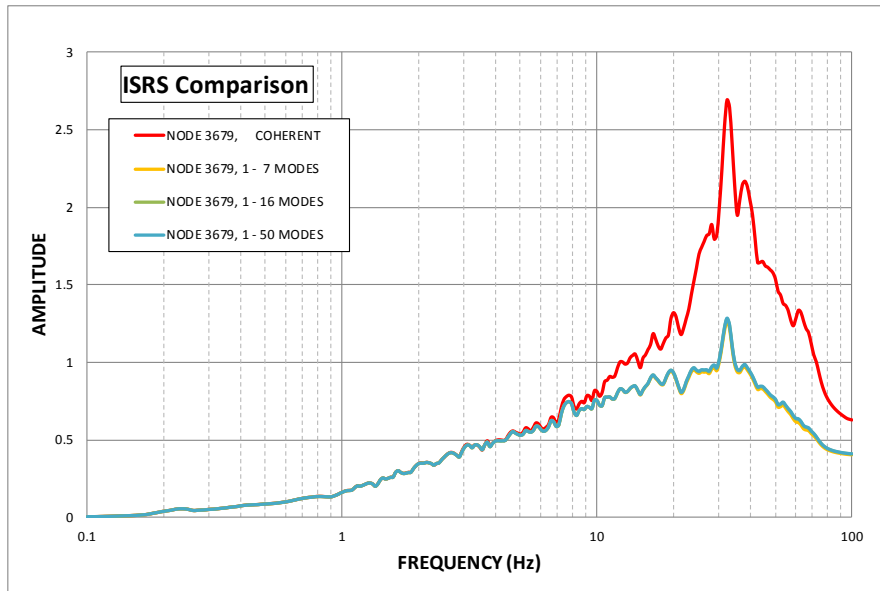


Figure C-17 ARS – Shear Wall Node 3679 – Response in Vert. Direction

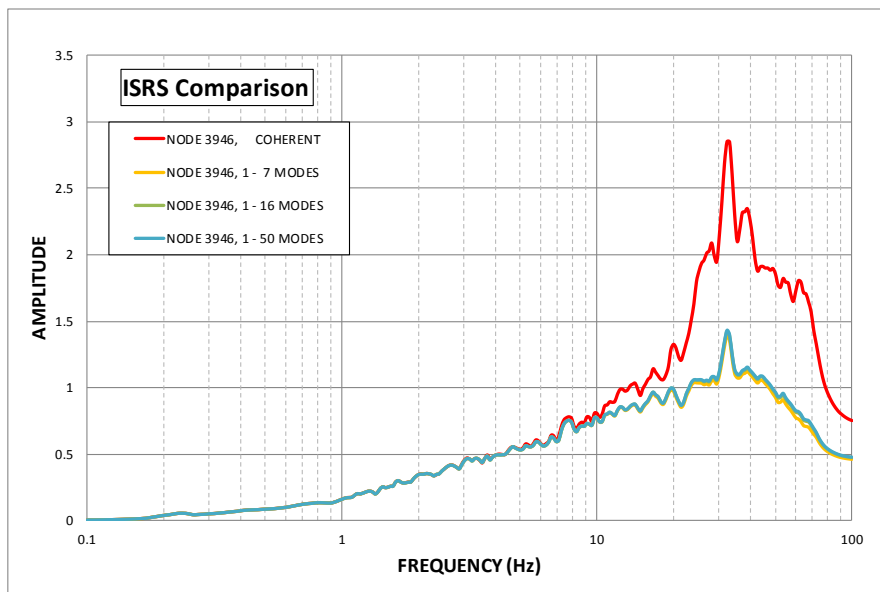


Figure C-18 ARS – Shear Wall Node 3946 – Response in Vert. Direction

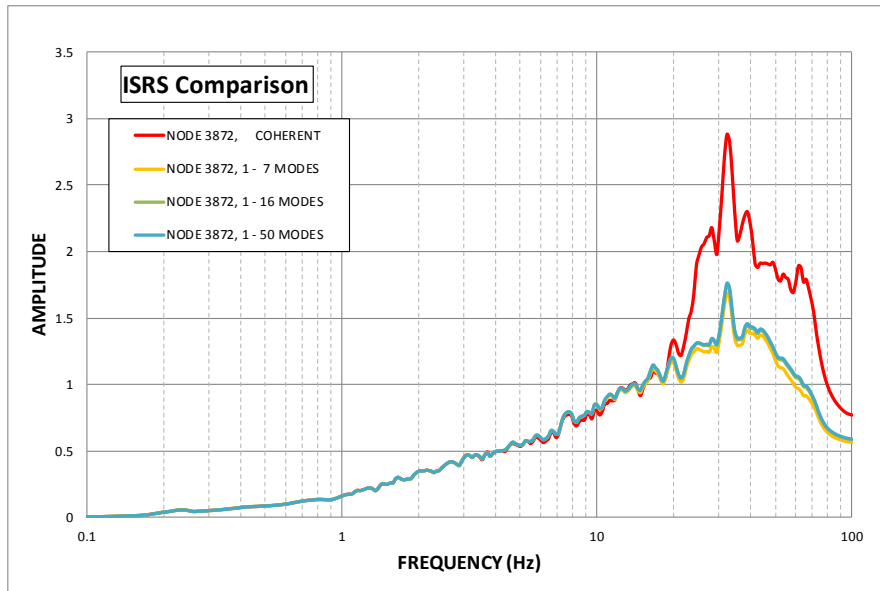


Figure C-19 ARS – Shear Wall Node 3872 – Response in Vert. Direction

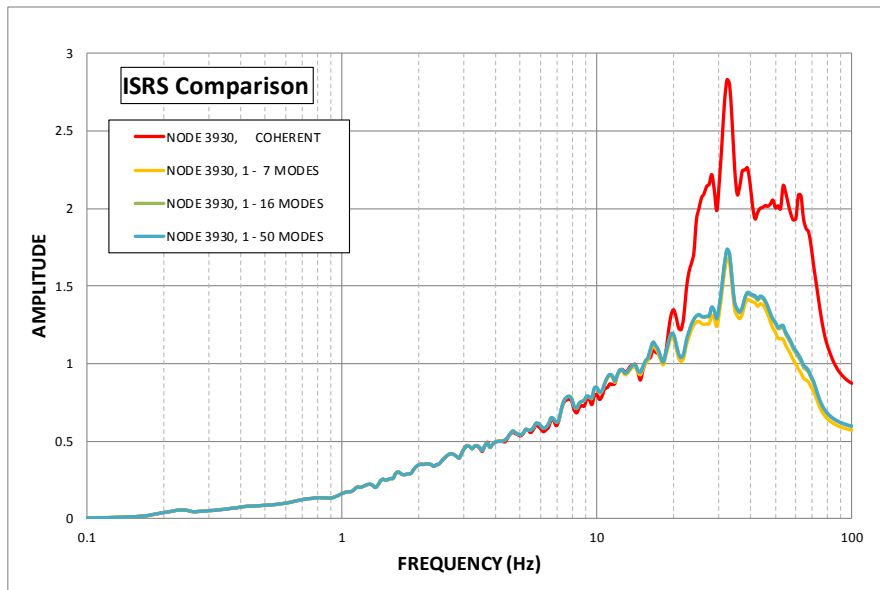


Figure C-20 ARS – Shear Wall Node 3930 – Response in Vert. Direction

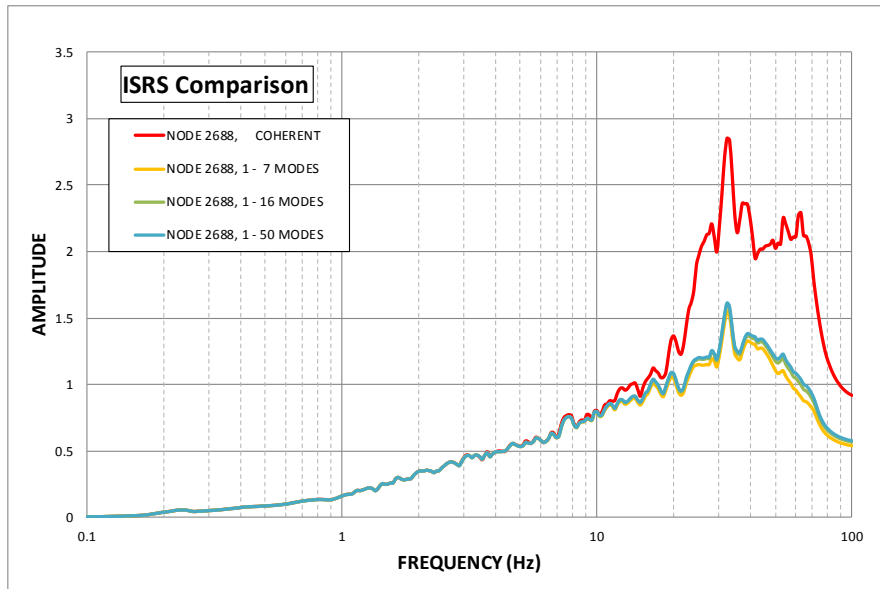


Figure C-21 ARS – Floor Slab Node 2688 – Response in Vert. Direction

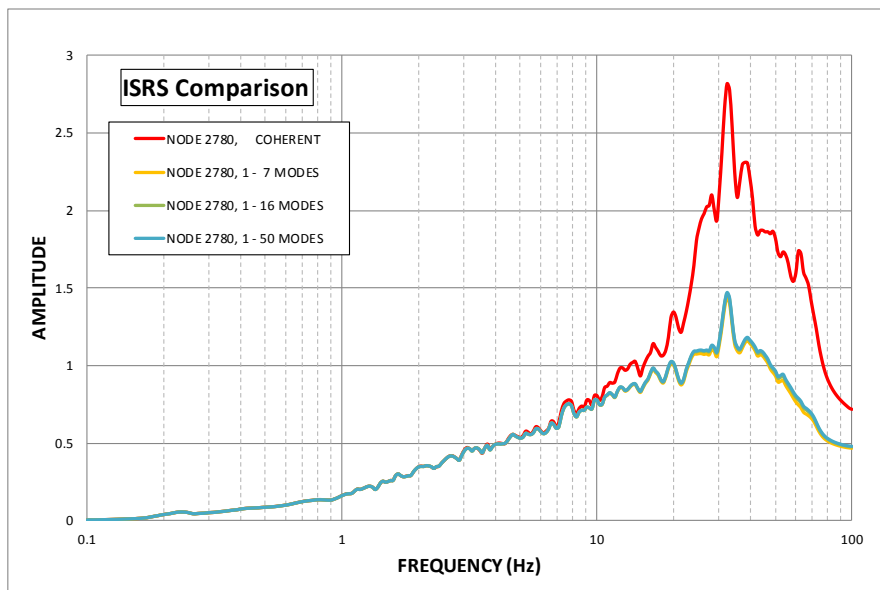


Figure C-22 ARS – Floor Slab Node 2780 – Response in Vert. Direction

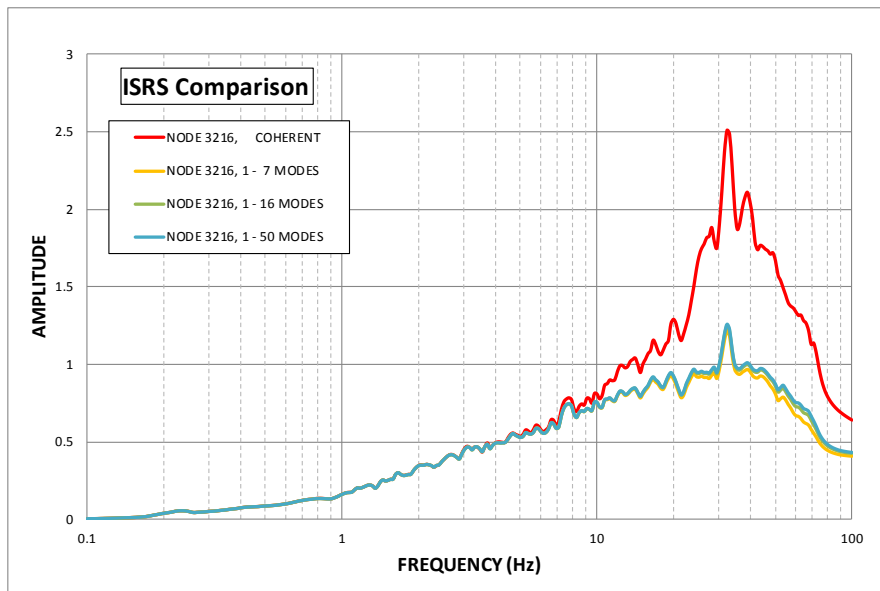


Figure C-23 ARS – Floor Slab Node 3216 – Response in Vert. Direction

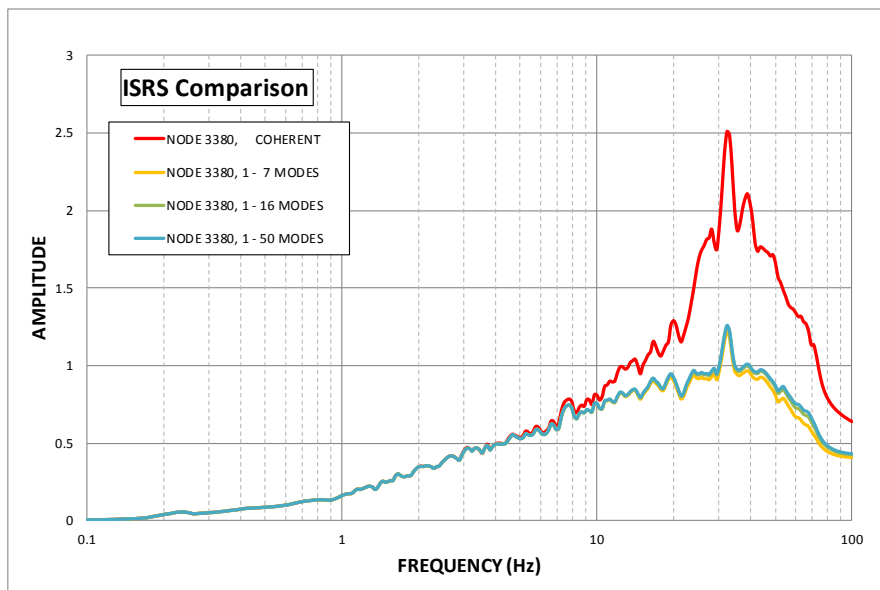


Figure C-24 ARS – Floor Slab Node 3380 – Response in Vert. Direction

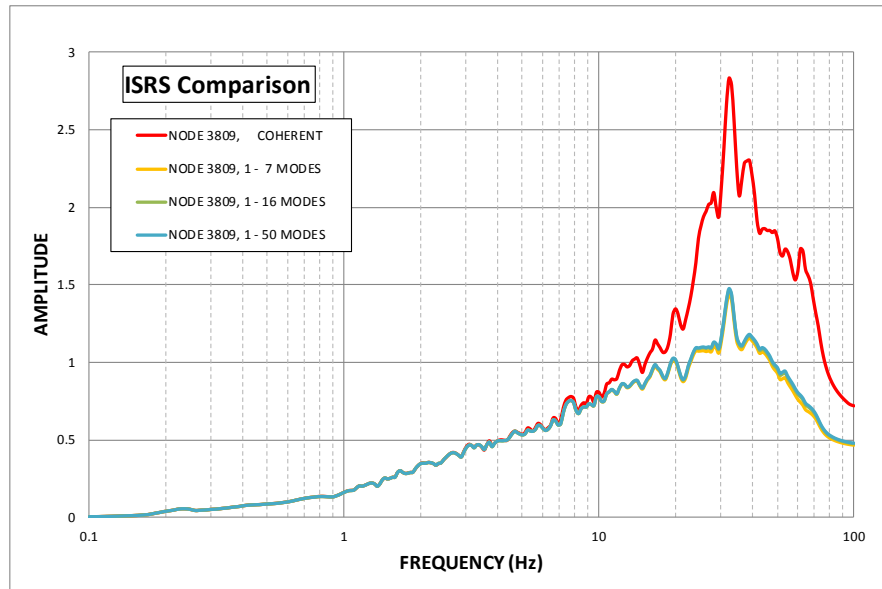


Figure C-25 ARS – Floor Slab Node 3809 – Response in Vert. Direction

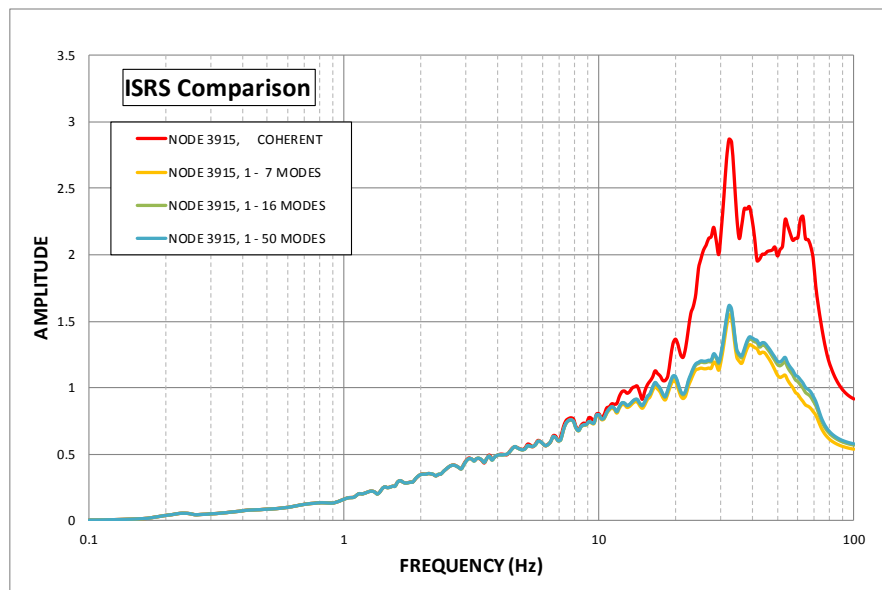


Figure C-26 ARS – Floor Slab Node 3915 – Response in Vert. Direction

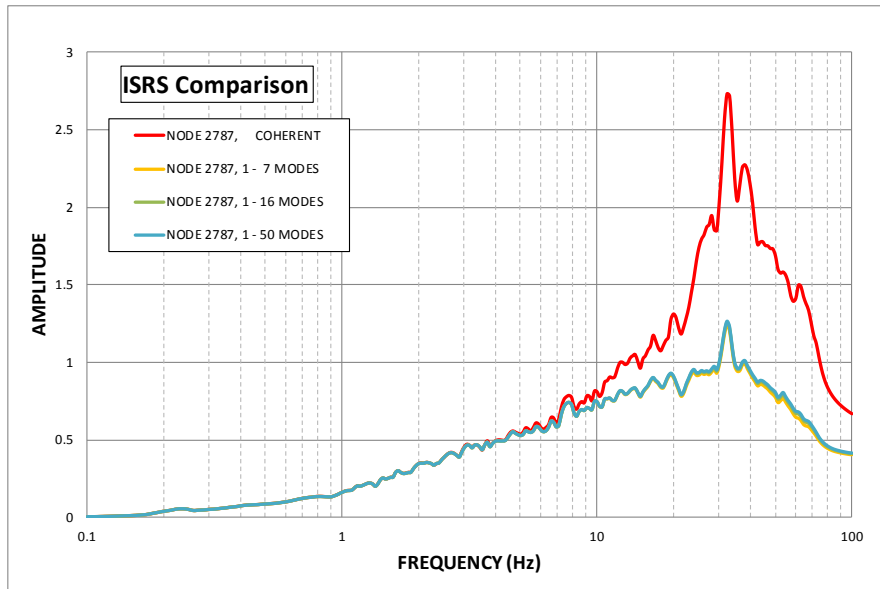


Figure C-27 ARS – Floor Slab Node 2787 – Response in Vert. Direction

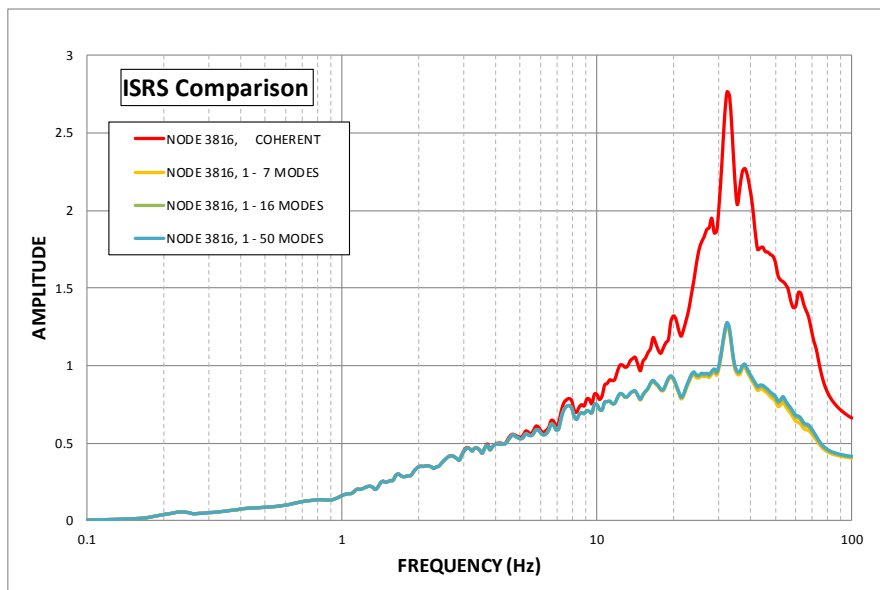
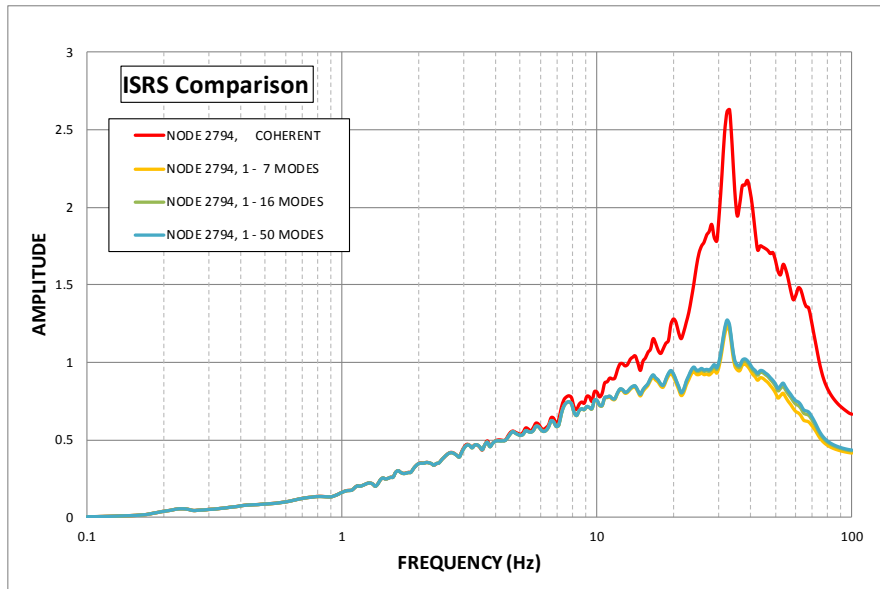
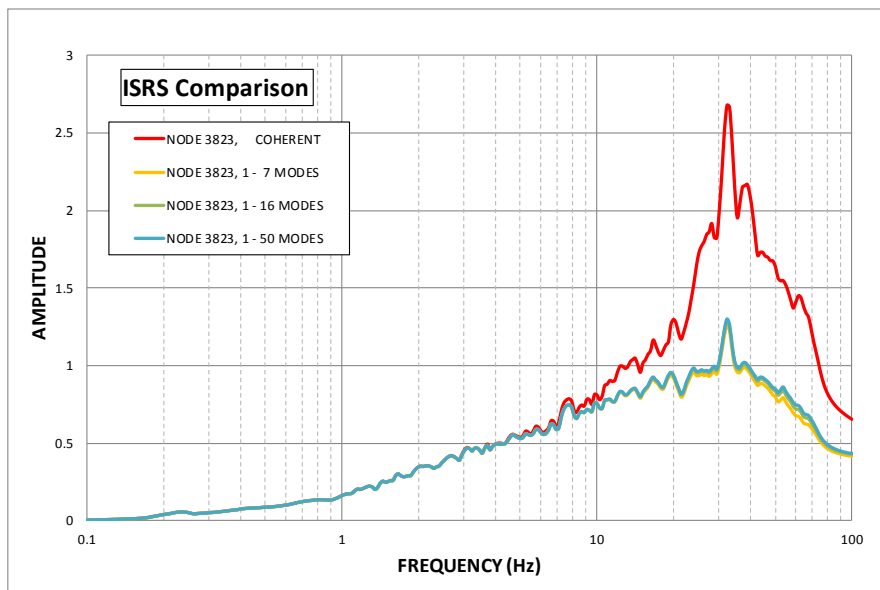


Figure C-28 ARS – Floor Slab Node 3816 – Response in Vert. Direction



**Figure C-29 ARS – Floor Slab Node 2794 – Response in Vert. Direction**



**Figure C-30 ARS – Floor Slab Node 3823 – Response in Vert. Direction**



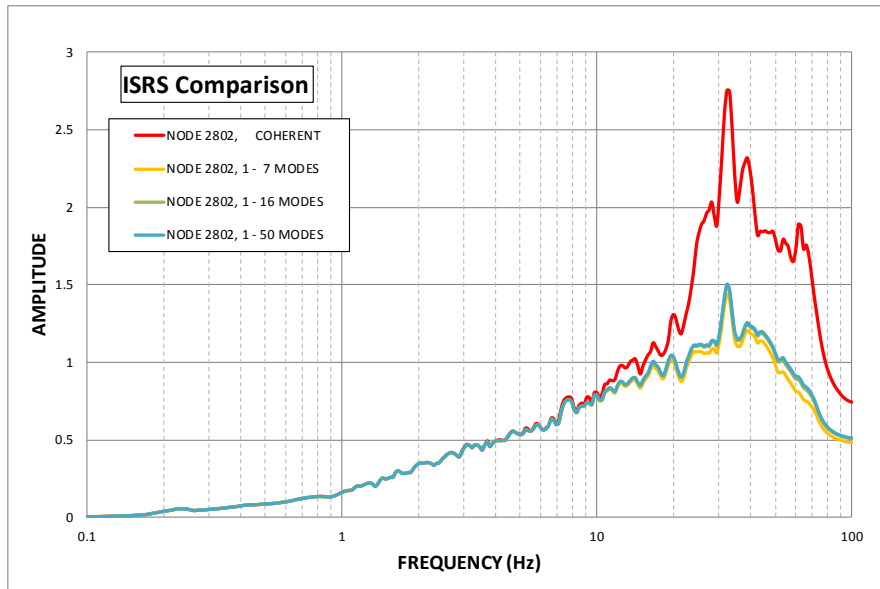


Figure C-31 ARS – Floor Slab Node 2802 – Response in Vert. Direction

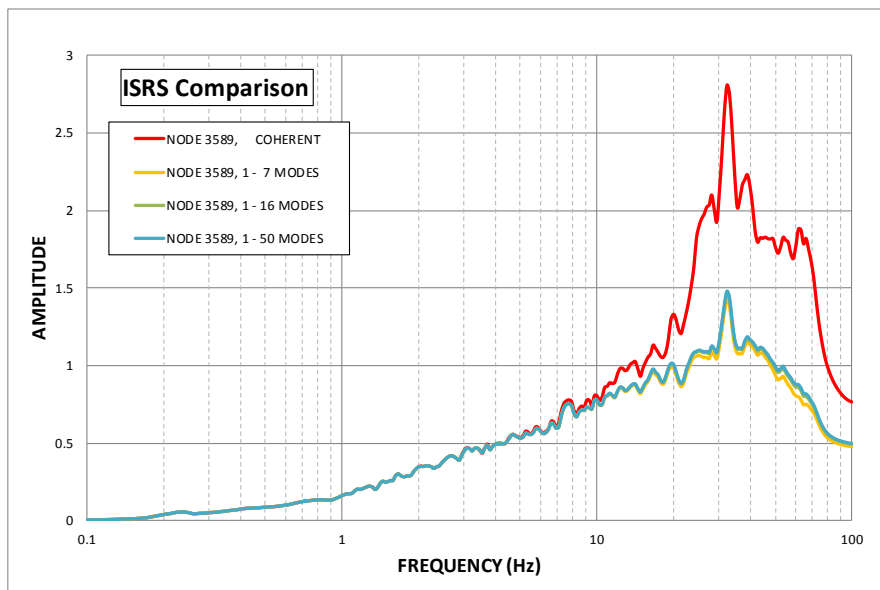


Figure C-32 ARS – Floor Slab Node 3589 – Response in Vert. Direction

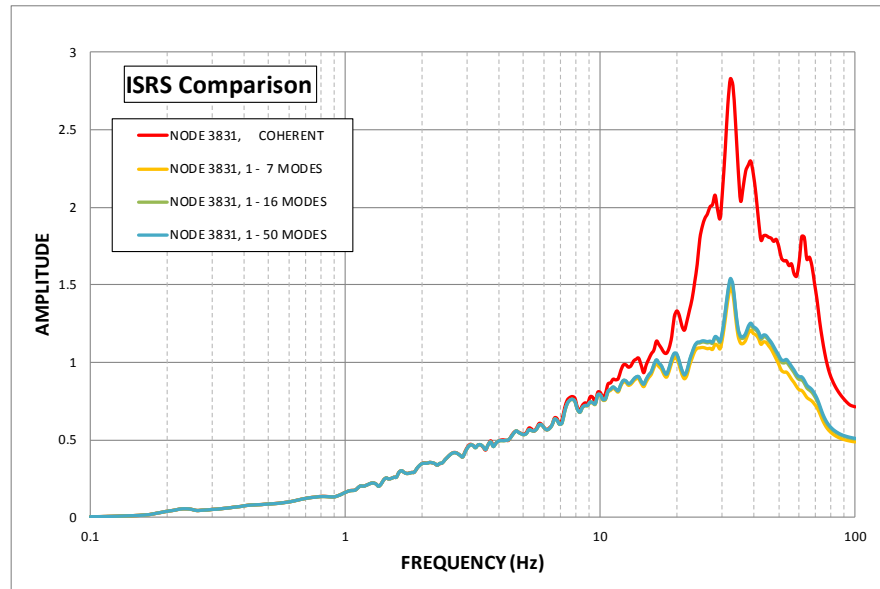


Figure C-33 ARS – Floor Slab Node 3831 – Response in Vert. Direction

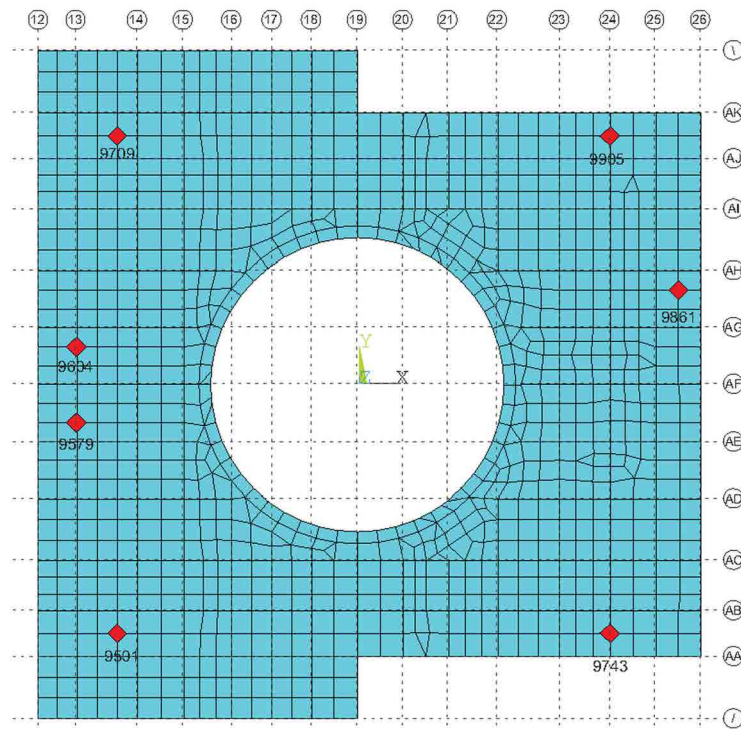


Figure C-34 Selected Nodes for AB Floor Slab at El. 55' (1-F)

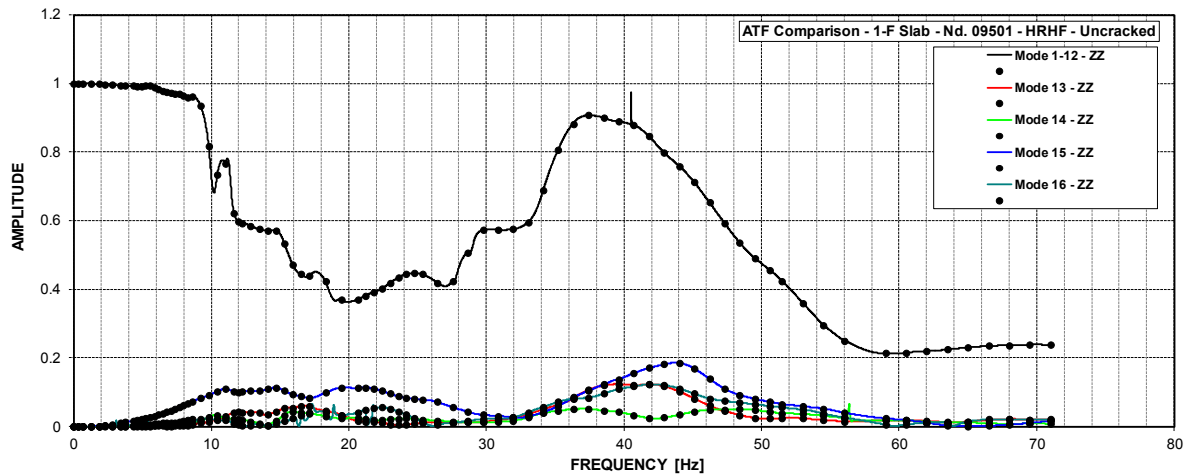


Figure C-35 ATF – AB Slabs (1-F) at El. 55' – Node 9501 – Z Resp. due to Z Input – Uncracked

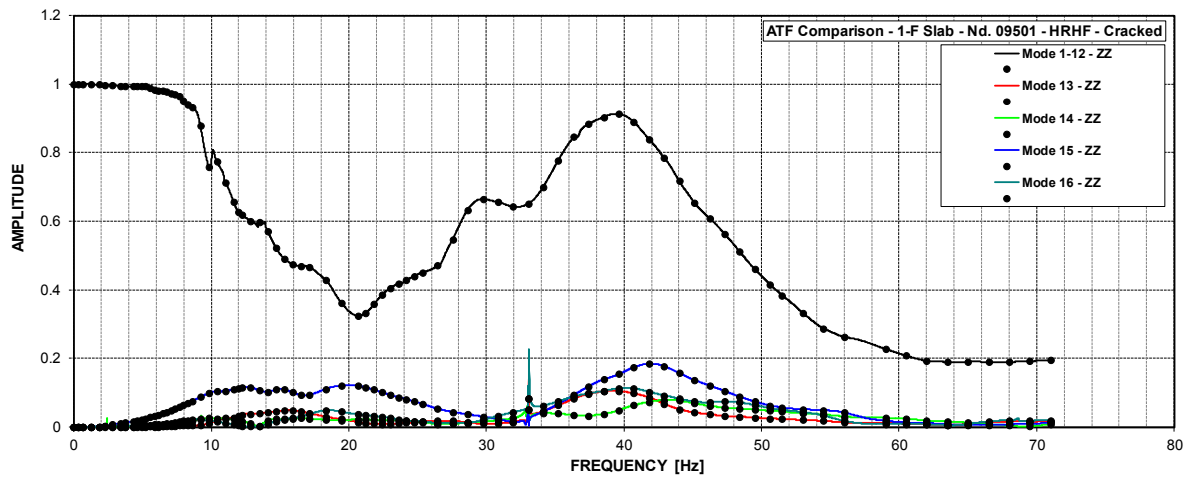


Figure C-36 ATF – AB Slabs (1-F) at El. 55' – Node 9501 – Z Resp. due to Z Input - Cracked

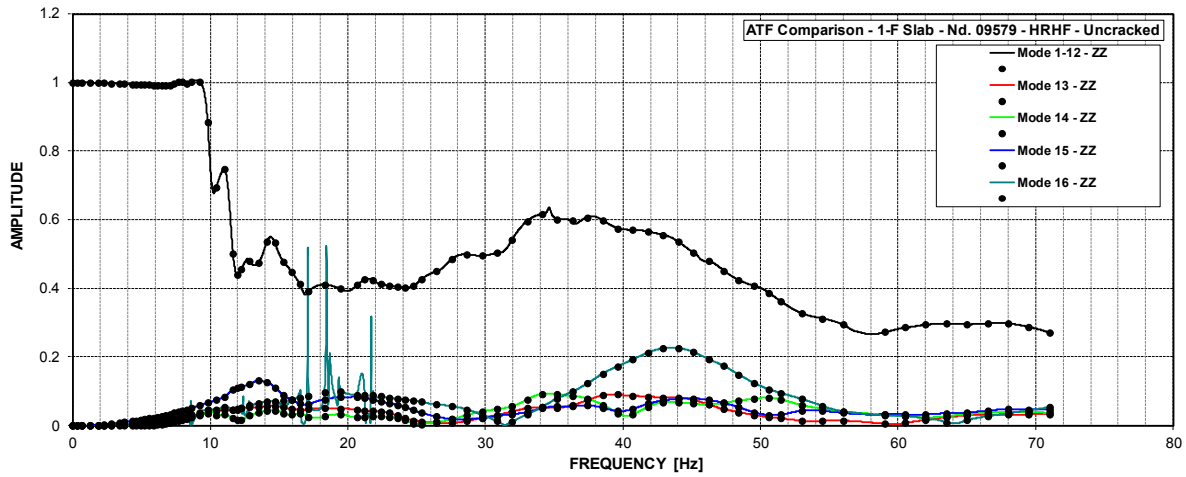


Figure C-37 ATF – AB Slabs (1-F) at El. 55' – Node 9579 – Z Resp. due to Z Input - Uncracked

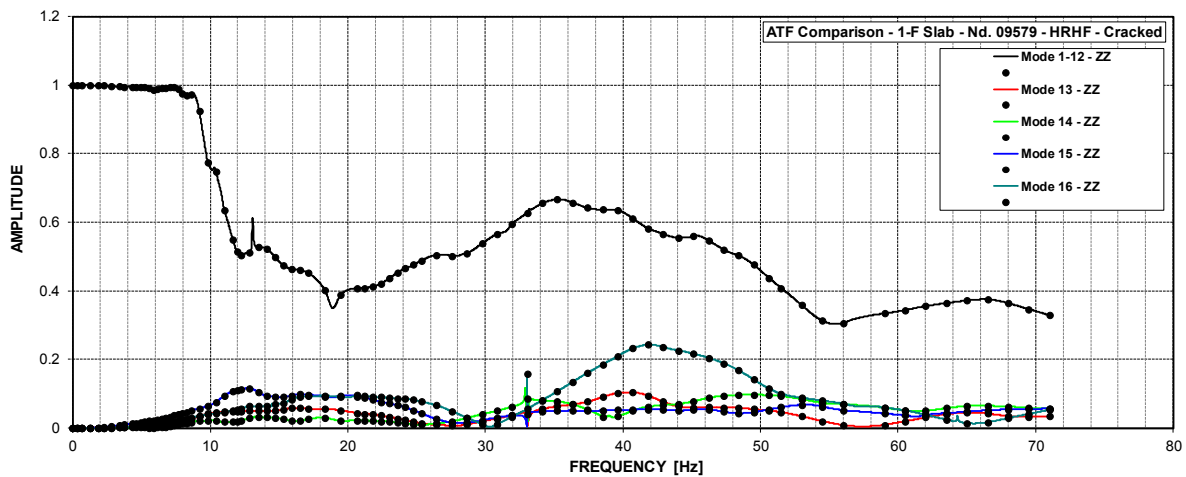


Figure C-38 ATF – AB Slabs (1-F) at El. 55' – Node 9579 – Z Resp. due to Z Input - Cracked

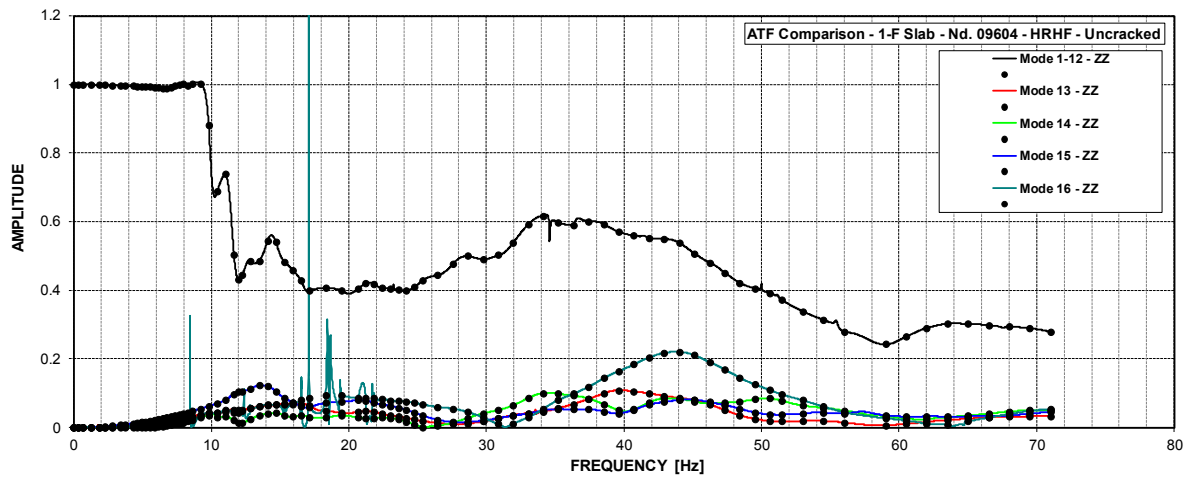


Figure C-39 ATF – AB Slabs (1-F) at El. 55' – Node 9604 – Z Resp. due to Z Input - Uncracked

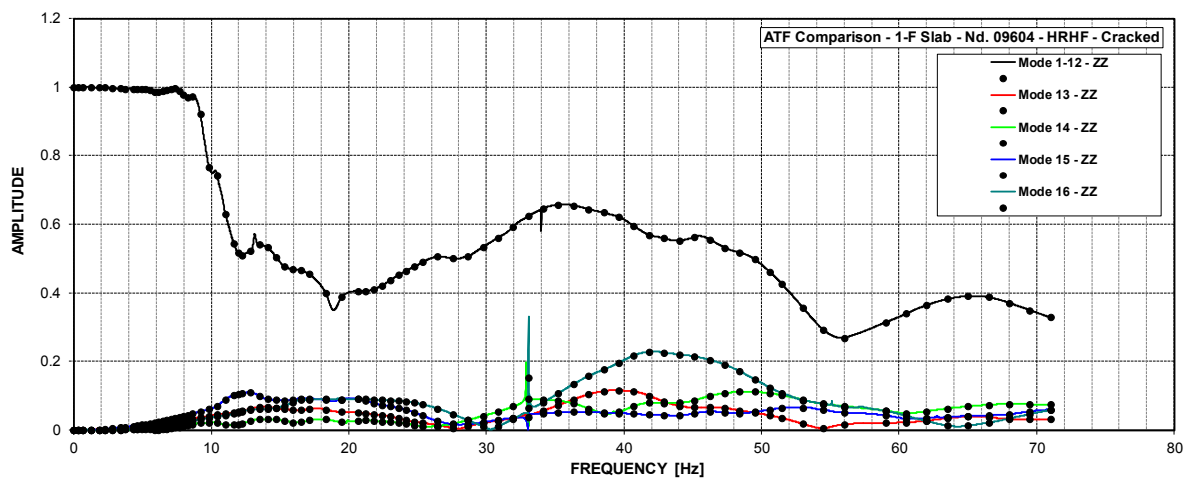


Figure C-40 ATF – AB Slabs (1-F) at El. 55' – Node 9604 – Z Resp. due to Z Input - Cracked

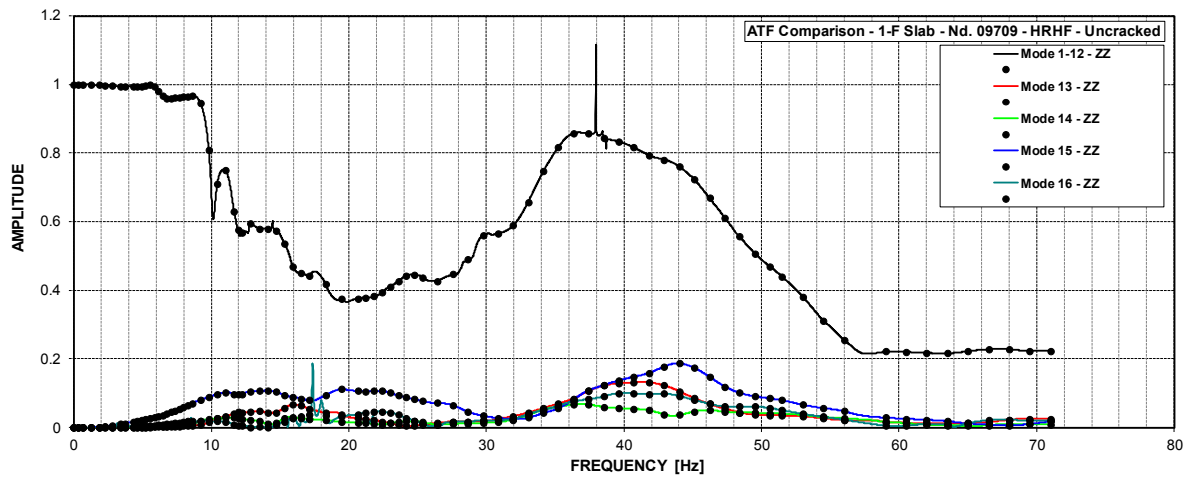


Figure C-41 ATF – AB Slabs (1-F) at El. 55' – Node 9709 – Z Resp. due to Z Input - Uncracked

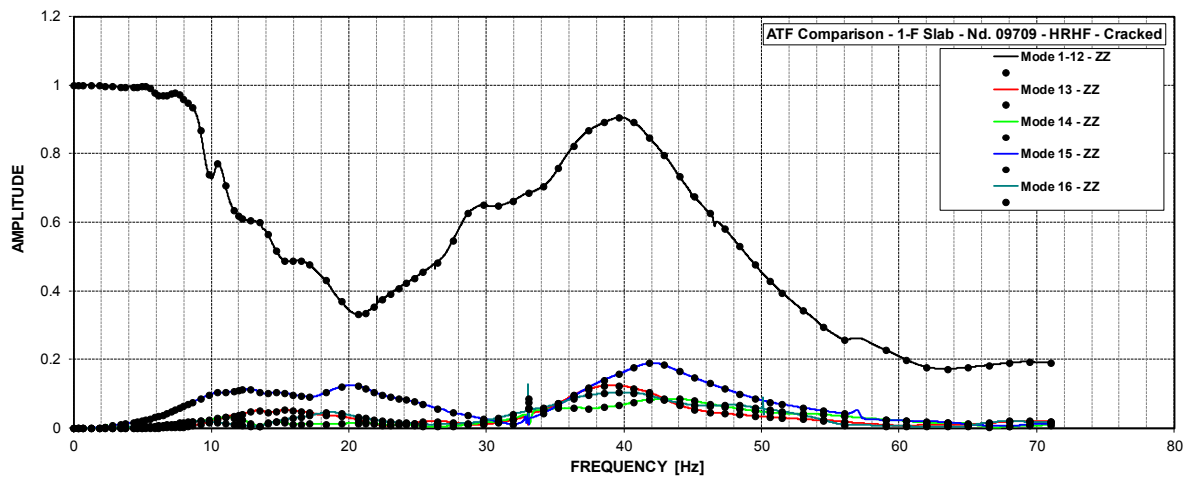


Figure C-42 ATF – AB Slabs (1-F) at El. 55' – Node 9709 – Z Resp. due to Z Input - Cracked

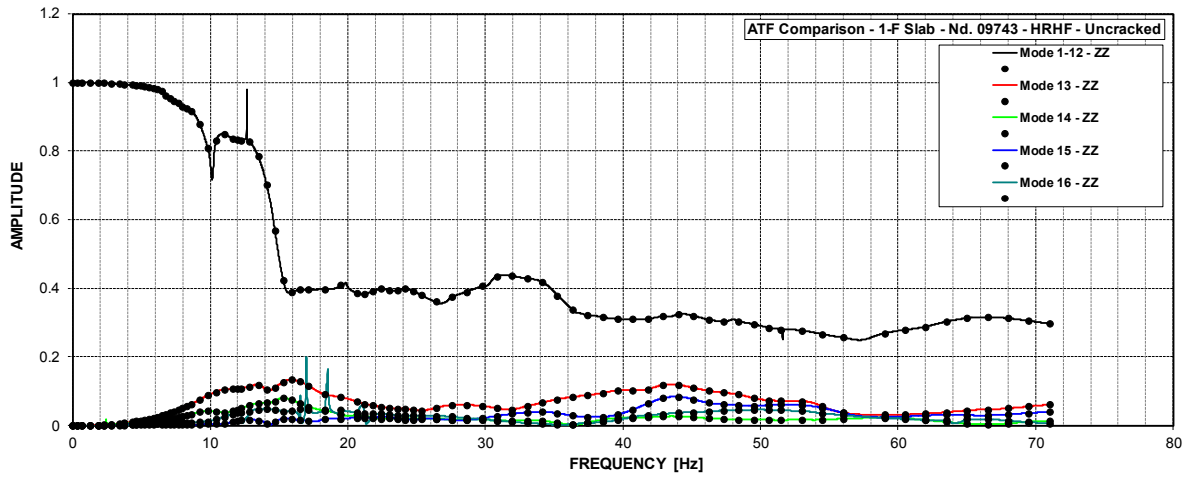


Figure C-43 ATF – AB Slabs (1-F) at El. 55' – Node 9743 – Z Resp. due to Z Input - Uncracked

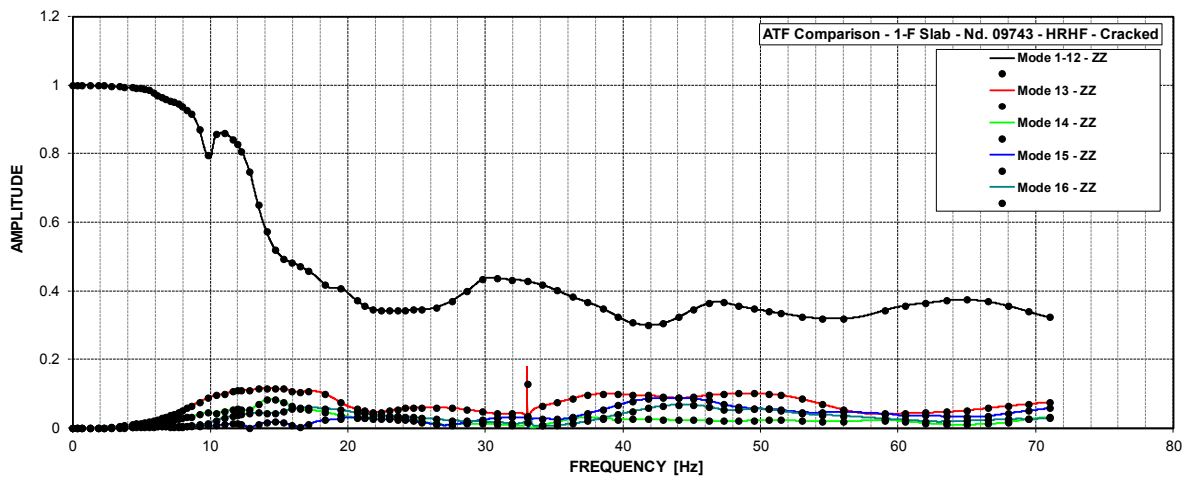


Figure C-44 ATF – AB Slabs (1-F) at El. 55' – Node 9743 – Z Resp. due to Z Input - Cracked



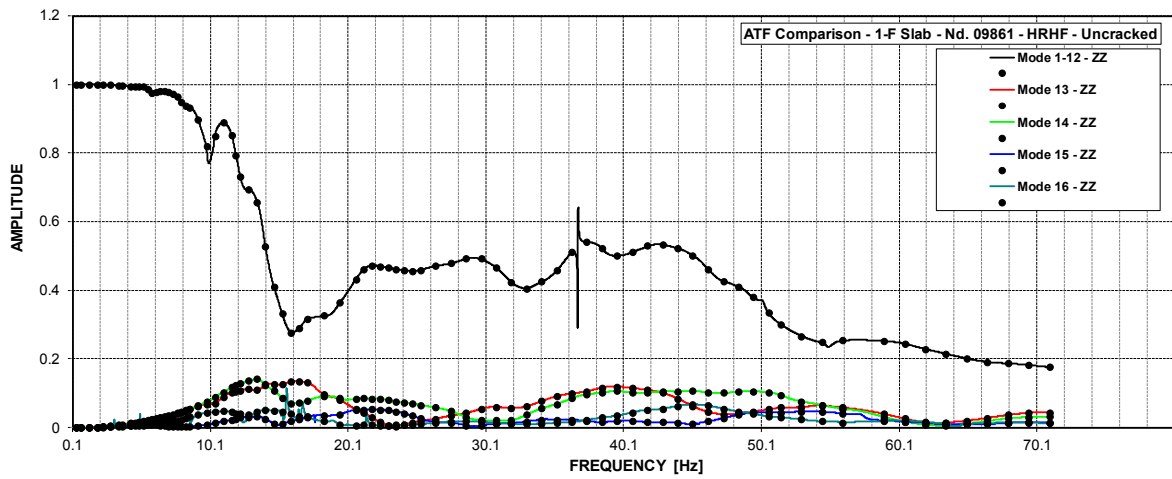


Figure C-45 ATF – AB Slabs (1-F) at El. 55' – Node 9861 – Z Resp. due to Z Input - Uncracked

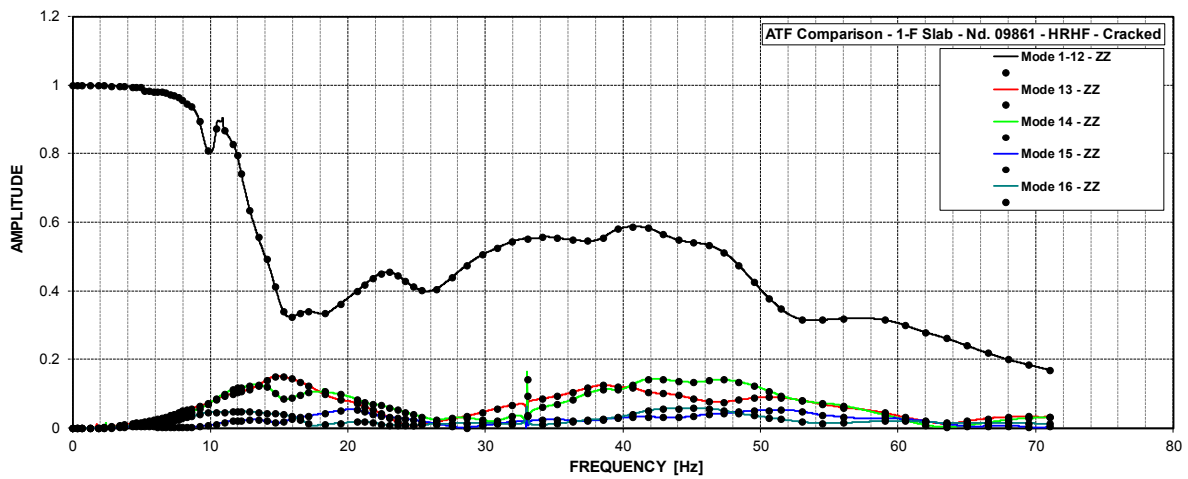


Figure C-46 ATF – AB Slabs (1-F) at El. 55' – Node 9861 – Z Resp. due to Z Input - Cracked

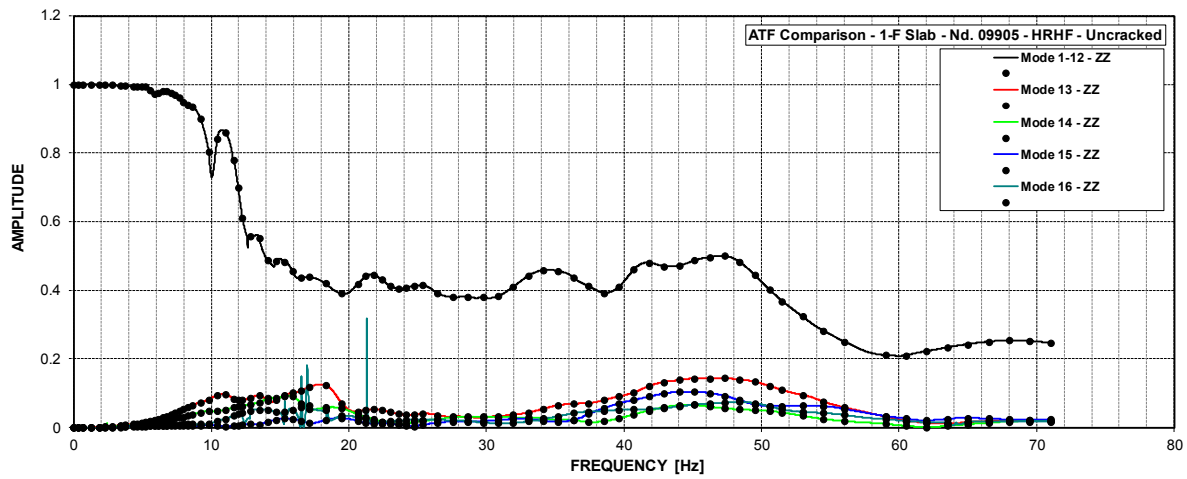


Figure C-47 ATF – AB Slabs (1-F) at El. 55' – Node 9905 – Z Resp. due to Z Input - Uncracked

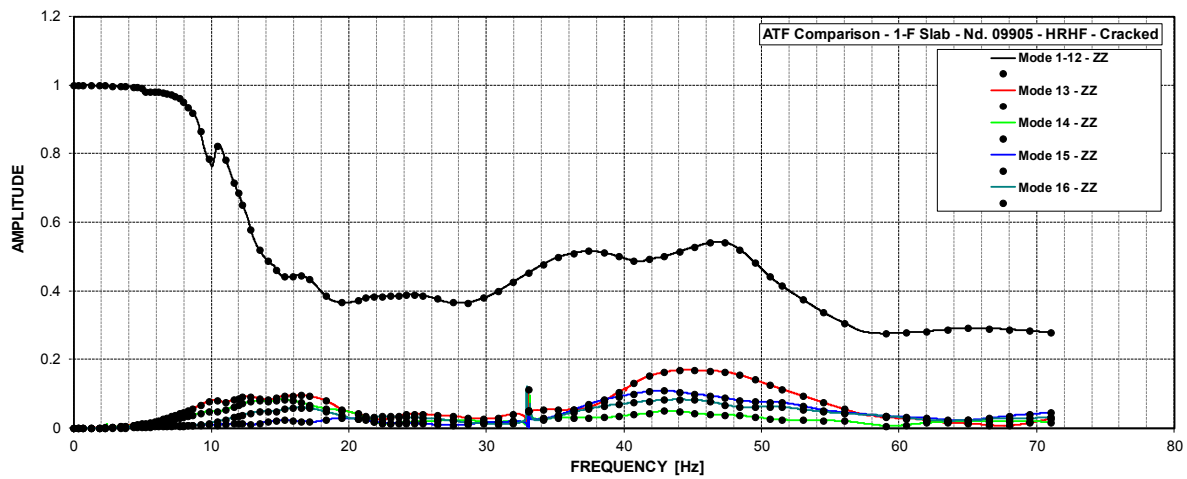


Figure C-48 ATF – AB Slabs (1-F) at El. 55' – Node 9905 – Z Resp. due to Z Input – Cracked

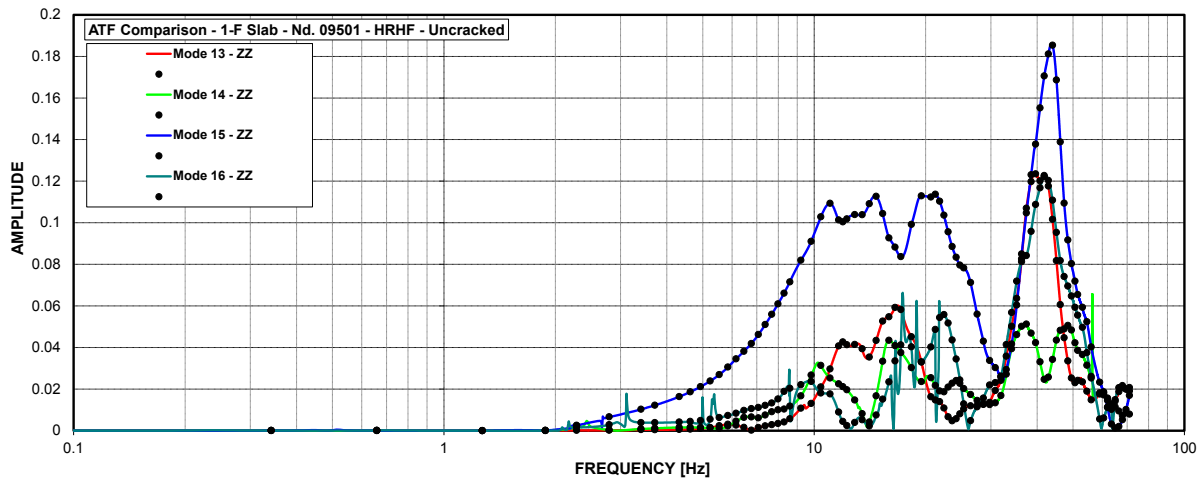


Figure C-49 ATF – AB Slabs (1-F) at El. 55' – Node 9501 – Z Resp. due to Z Input – Uncracked – Modes 13 through 16

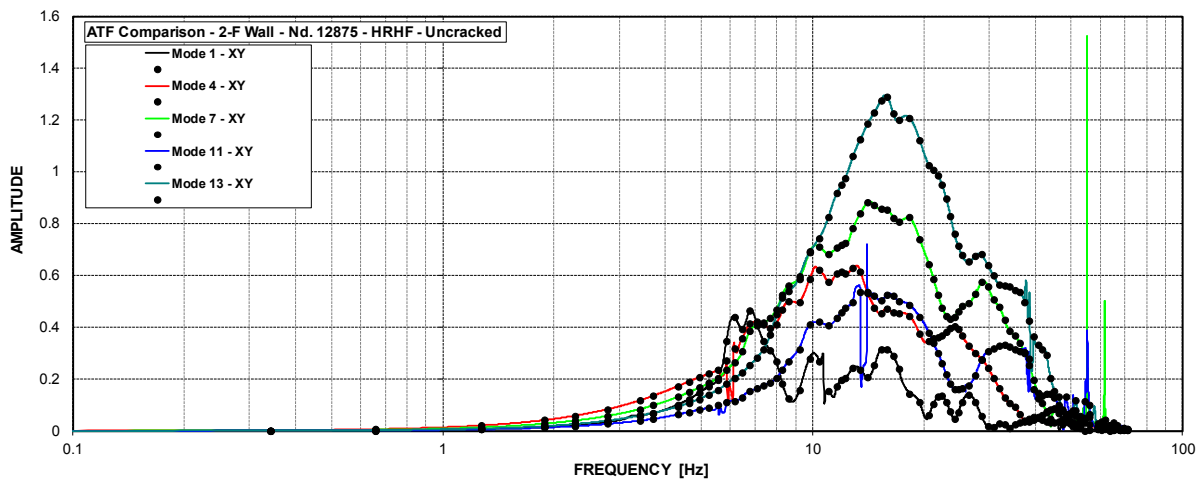


Figure C-50 ATF – AB Walls (2-F) at El. 78' – Node 12875 – Y Resp. due to X Input – Uncracked – Modes 1, 4, 7, 11, 13

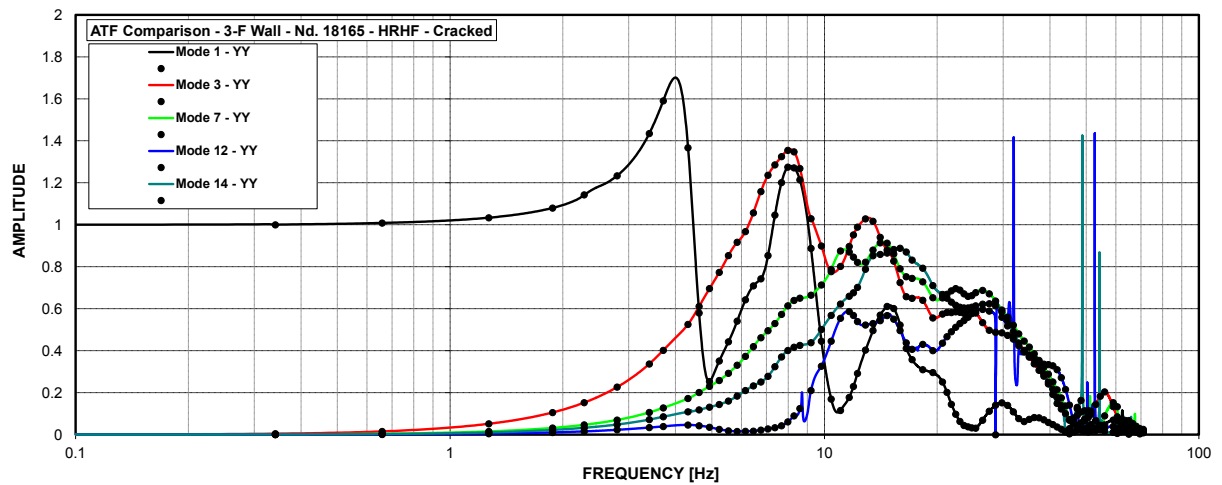


Figure C-51 ATF – AB Walls (3-F) at El. 100' – Node 18165 – Y Resp. due to Y Input – Cracked – Modes 1, 3, 7, 12, 14

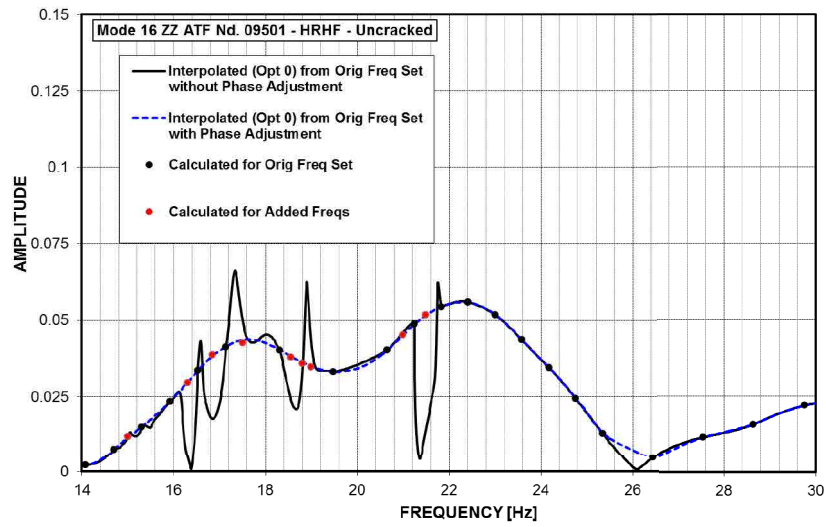


Figure C-52 Node 9501 ATF Comparison Option 0 Phase Adjusted vs No Phase Adjustment

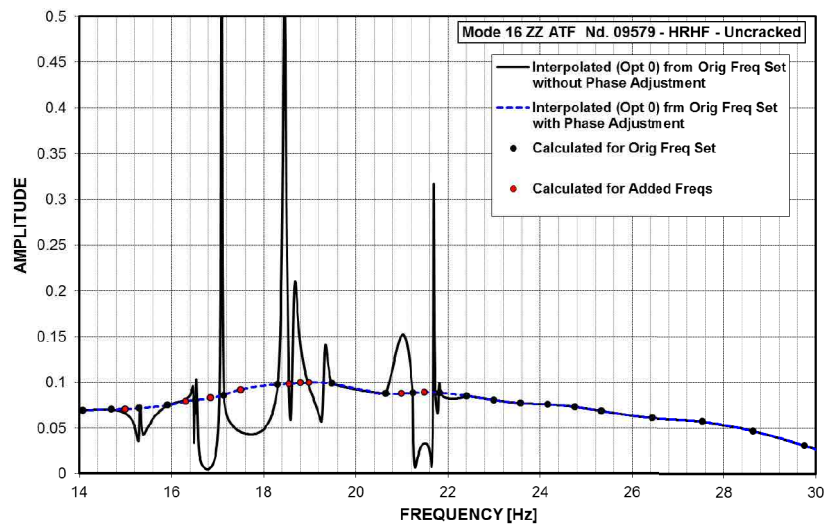


Figure C-53 Node 9579 ATF Comparison Option 0 Phase Adjusted vs No Phase Adjustment

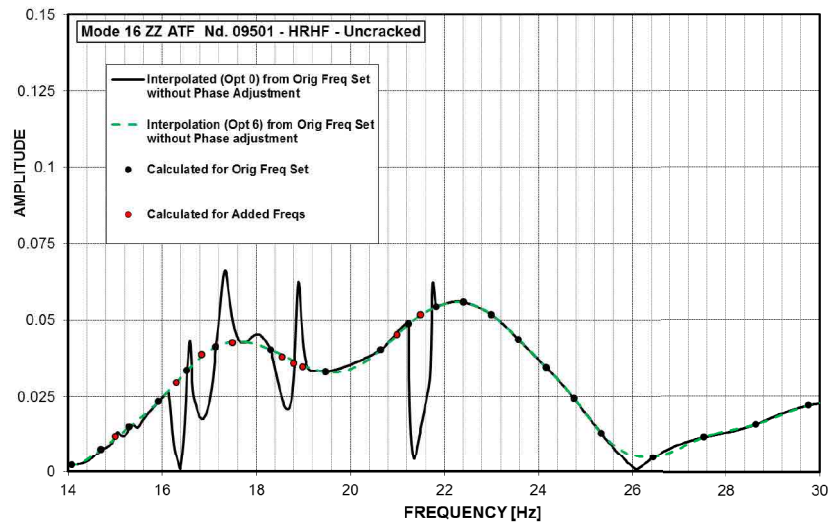


Figure C-54 Node 9501 ATF Comparison No Phase Adjustment Option 0 vs Option 6

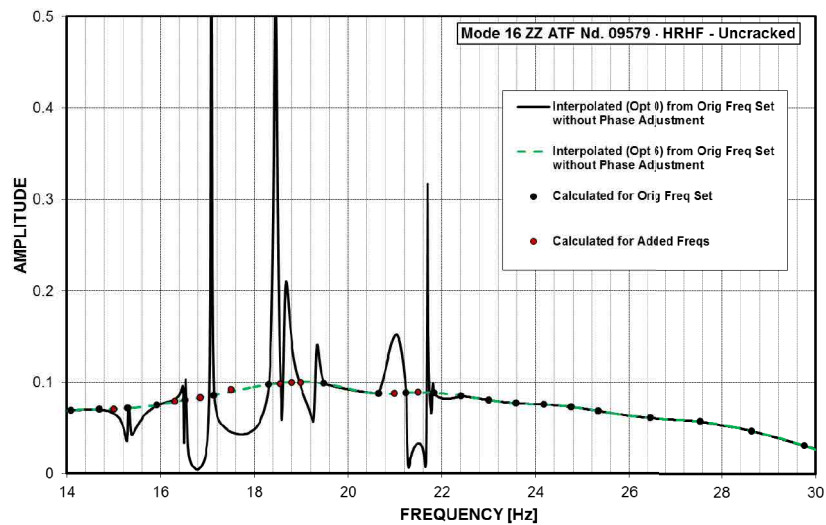
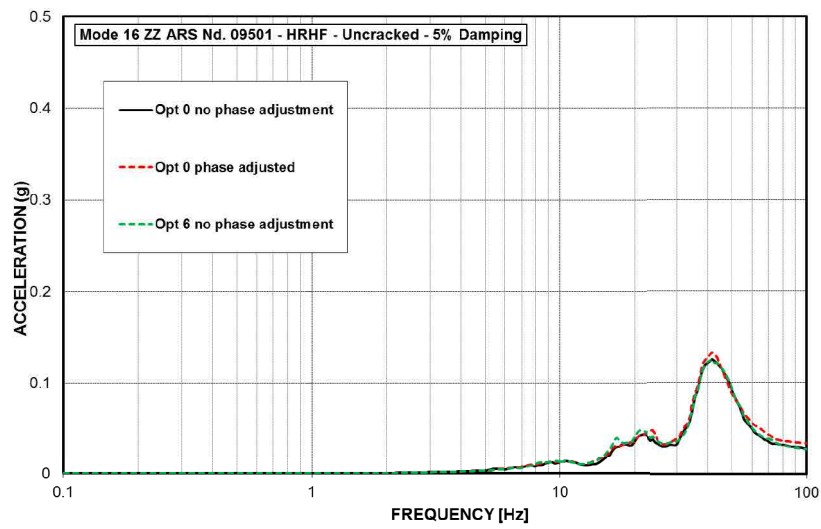
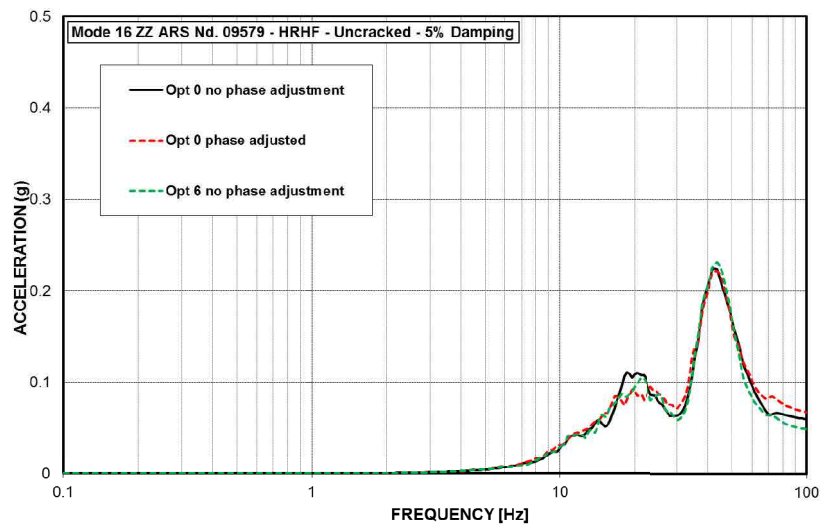
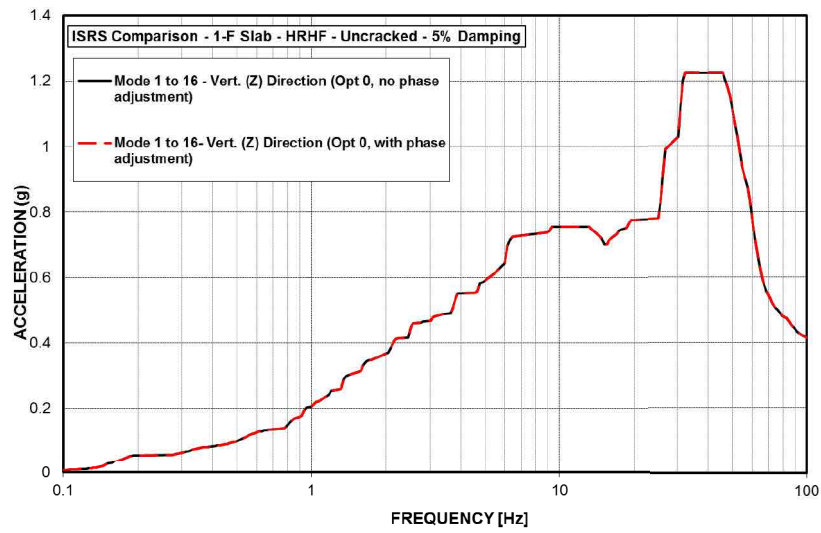


Figure C-55 Node 9579 ATF Comparison No Phase Adjustment Option 0 vs Option 6

**Figure C-56 Node 9501 Vertical ARS Comparison****Figure C-57 Node 9579 Vertical ARS Comparison**



**Figure C-58 ISRS – AB Floor Slabs (1-F) at El. 55' - Uncracked – Vertical Response**



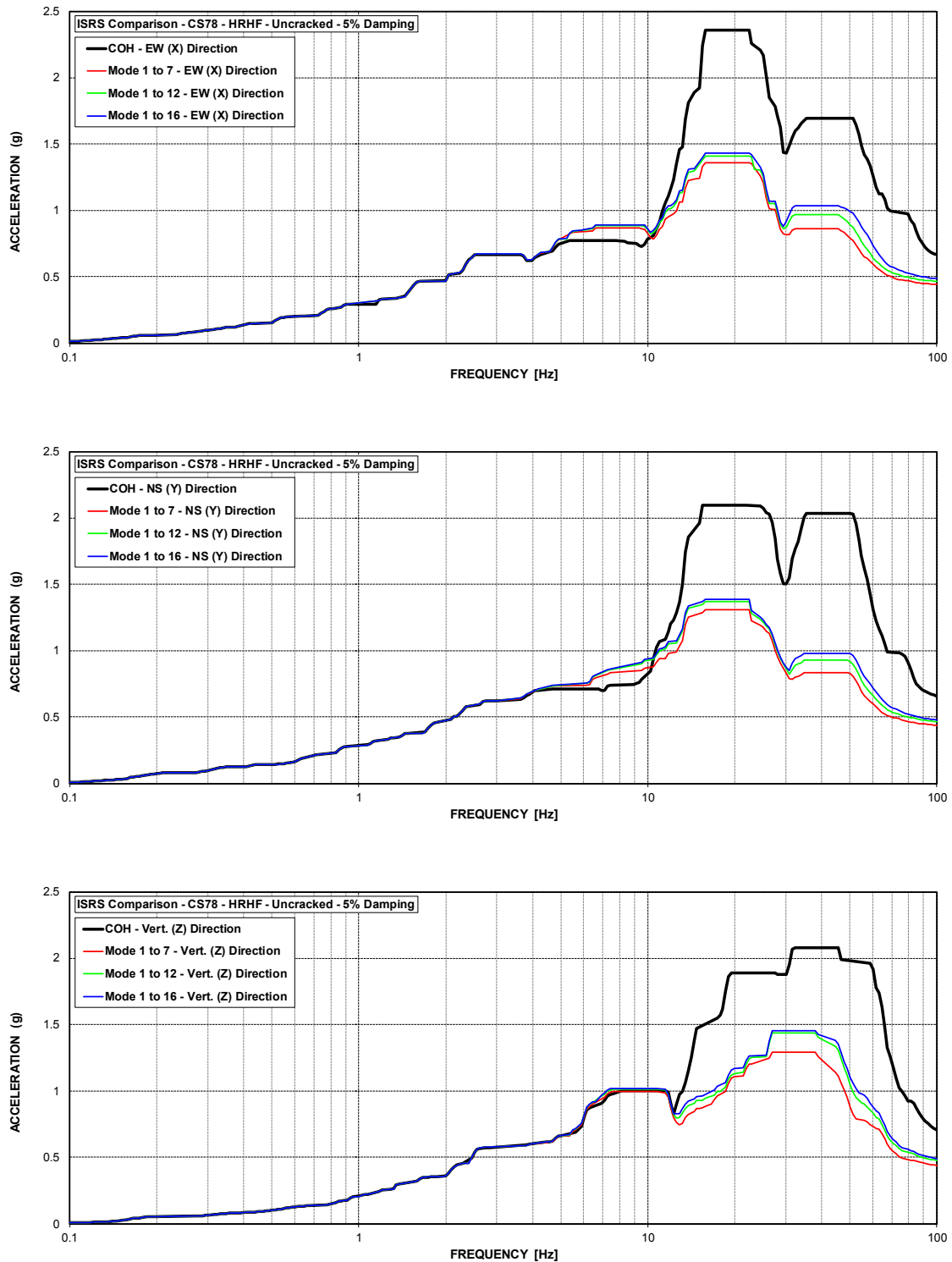


Figure C-59 ISRS – Containment Structure (CS78) at El. 78' – HRHF – Uncracked

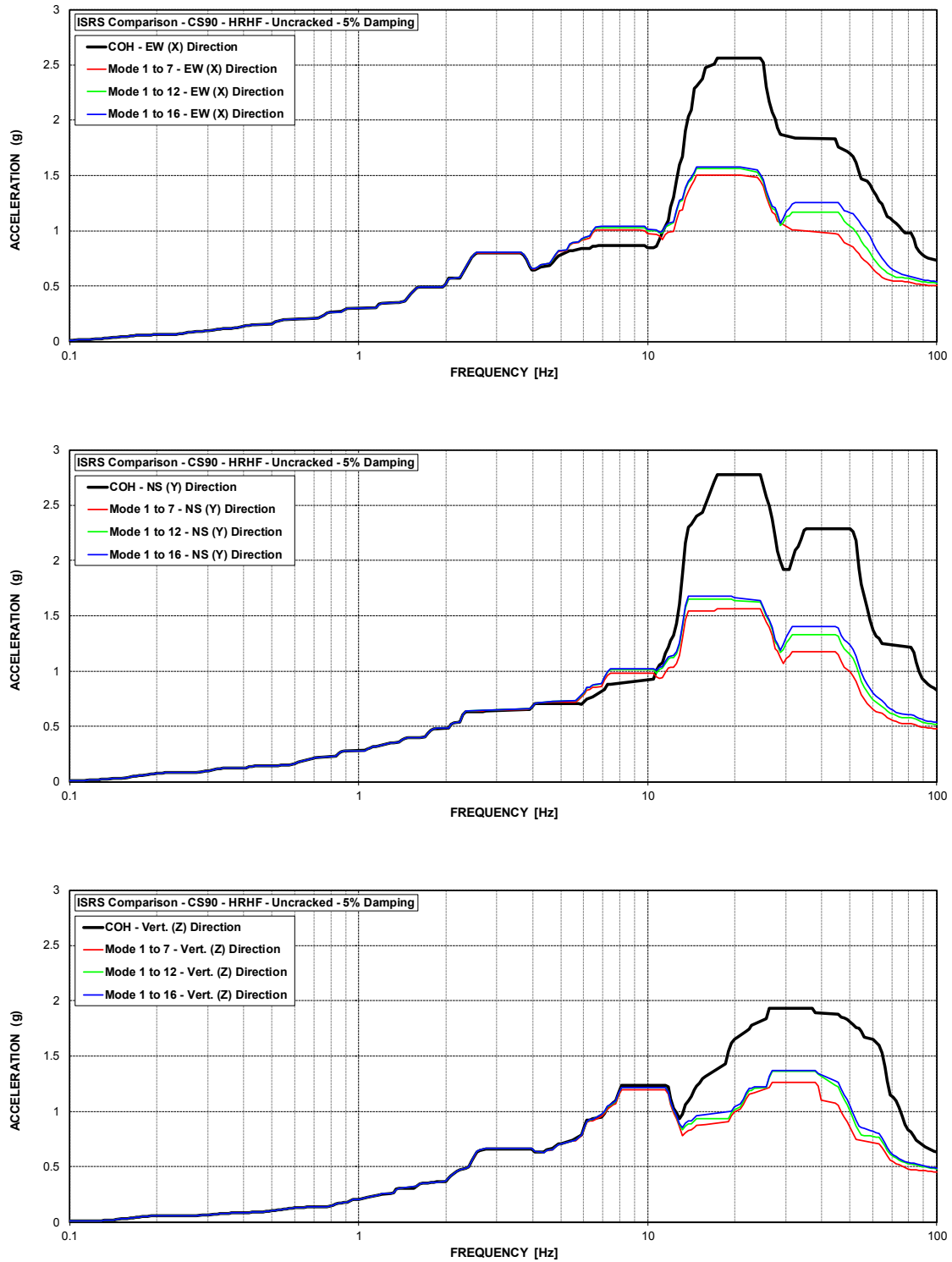


Figure C-60 ISRS – Containment Structure (CS90) at El. 89.75' – HRHF – Uncracked

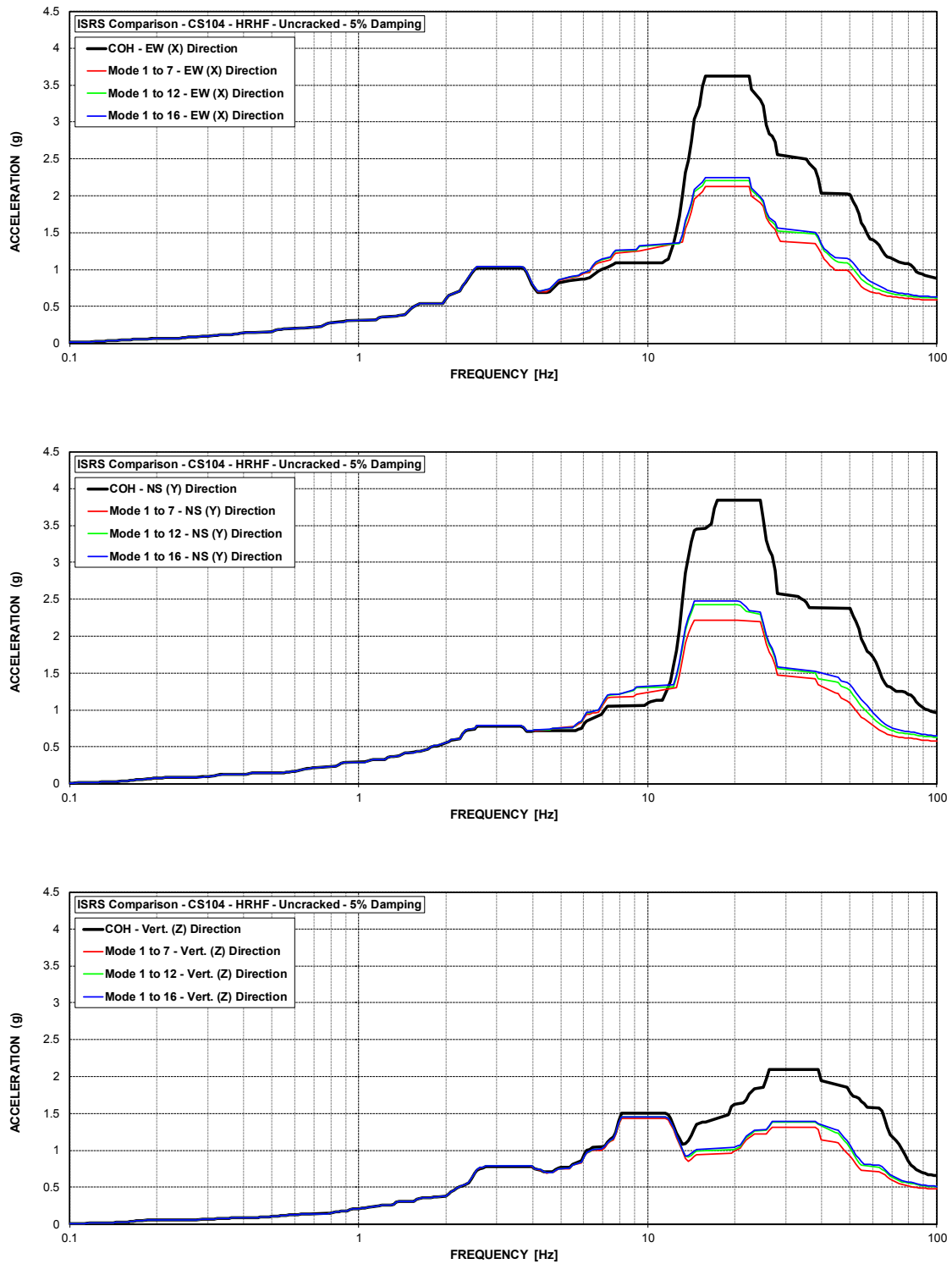


Figure C-61 ISRS – Containment Structure (CS104) at El. 103.75' – HRHF – Uncracked

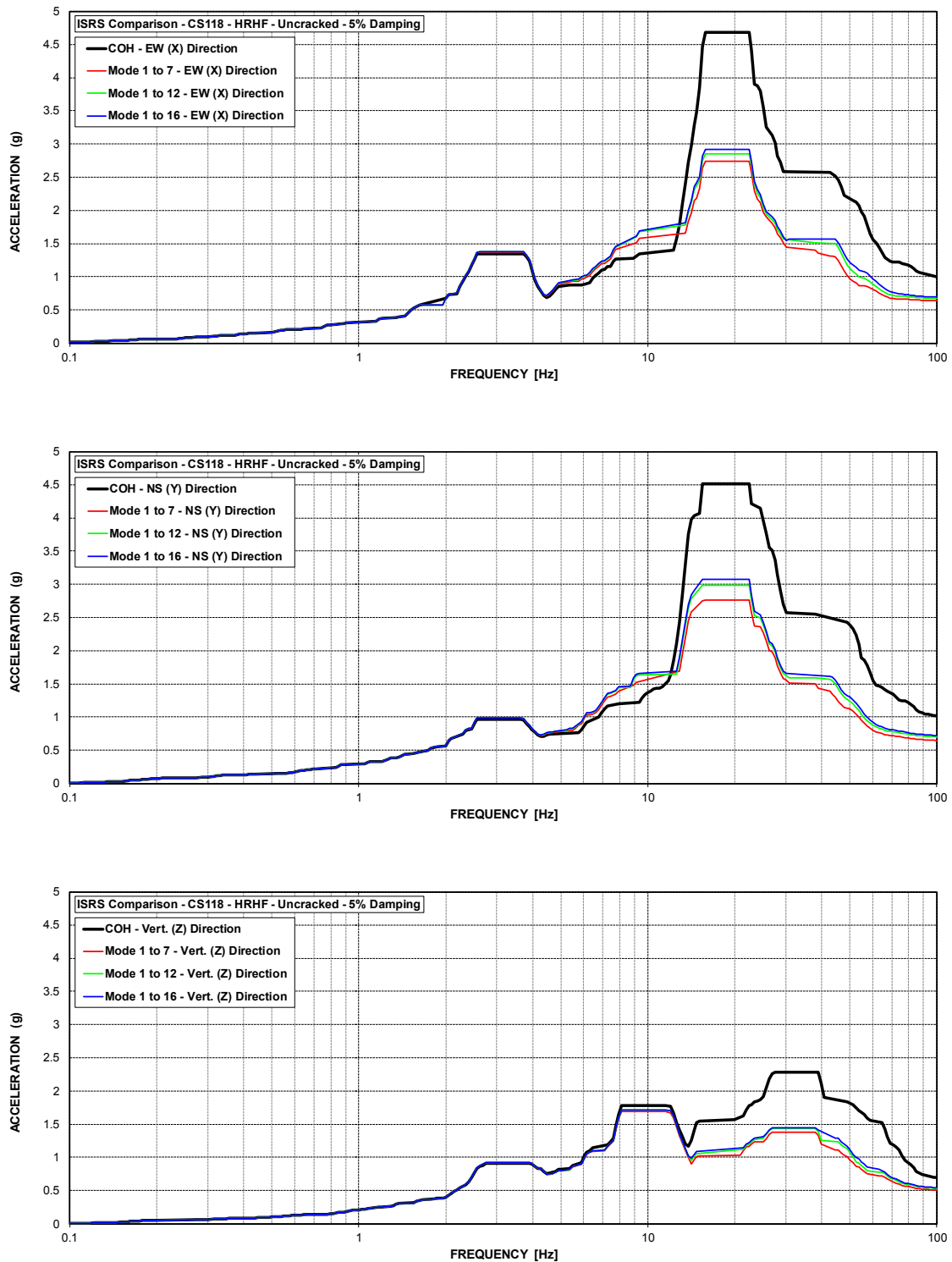


Figure C-62 ISRS – Containment Structure (CS118) at El. 117.75' – HRHF – Uncracked

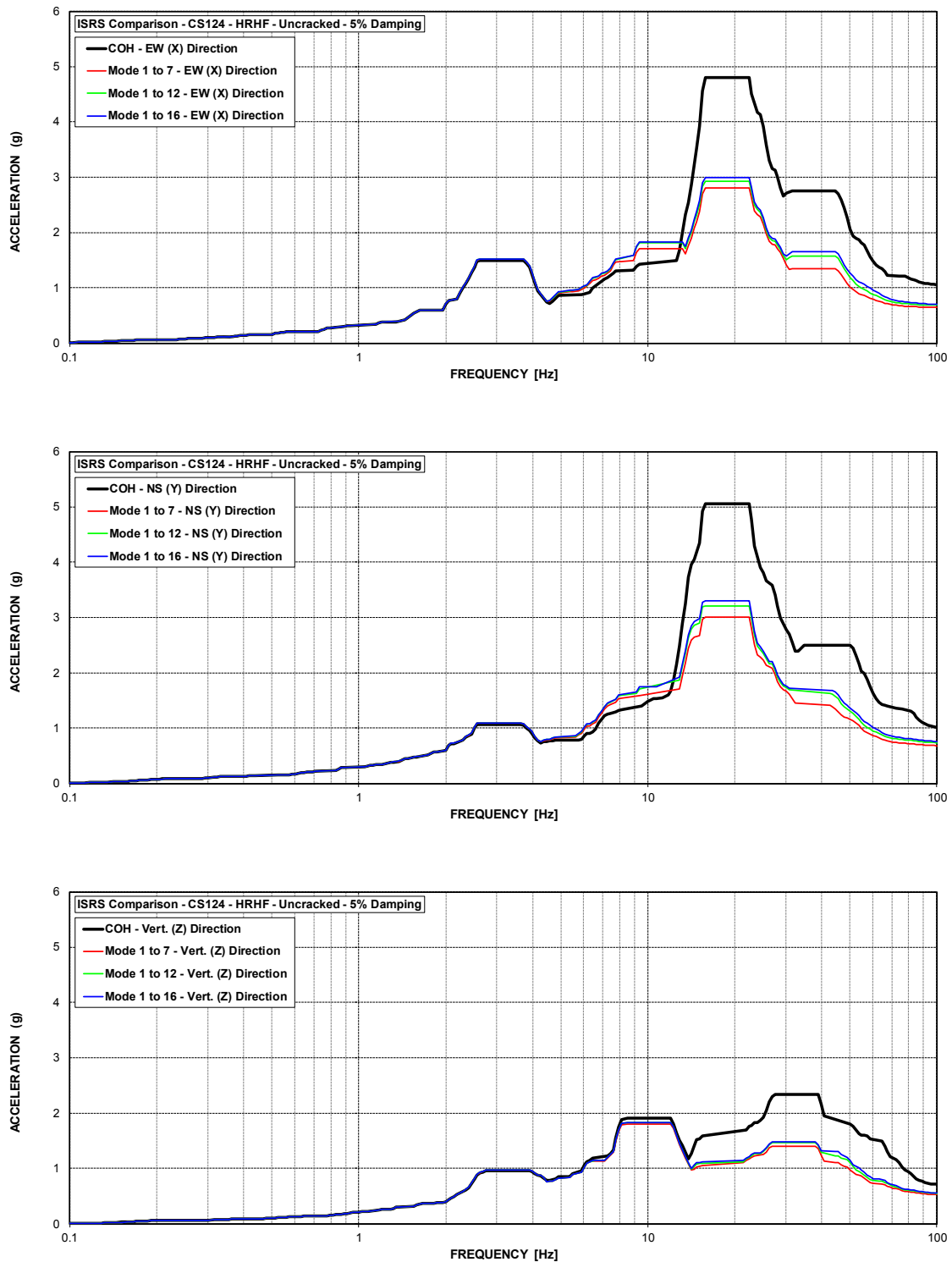


Figure C-63 ISRS – Containment Structure (CS124) at El. 123.62' – HRHF – Uncracked

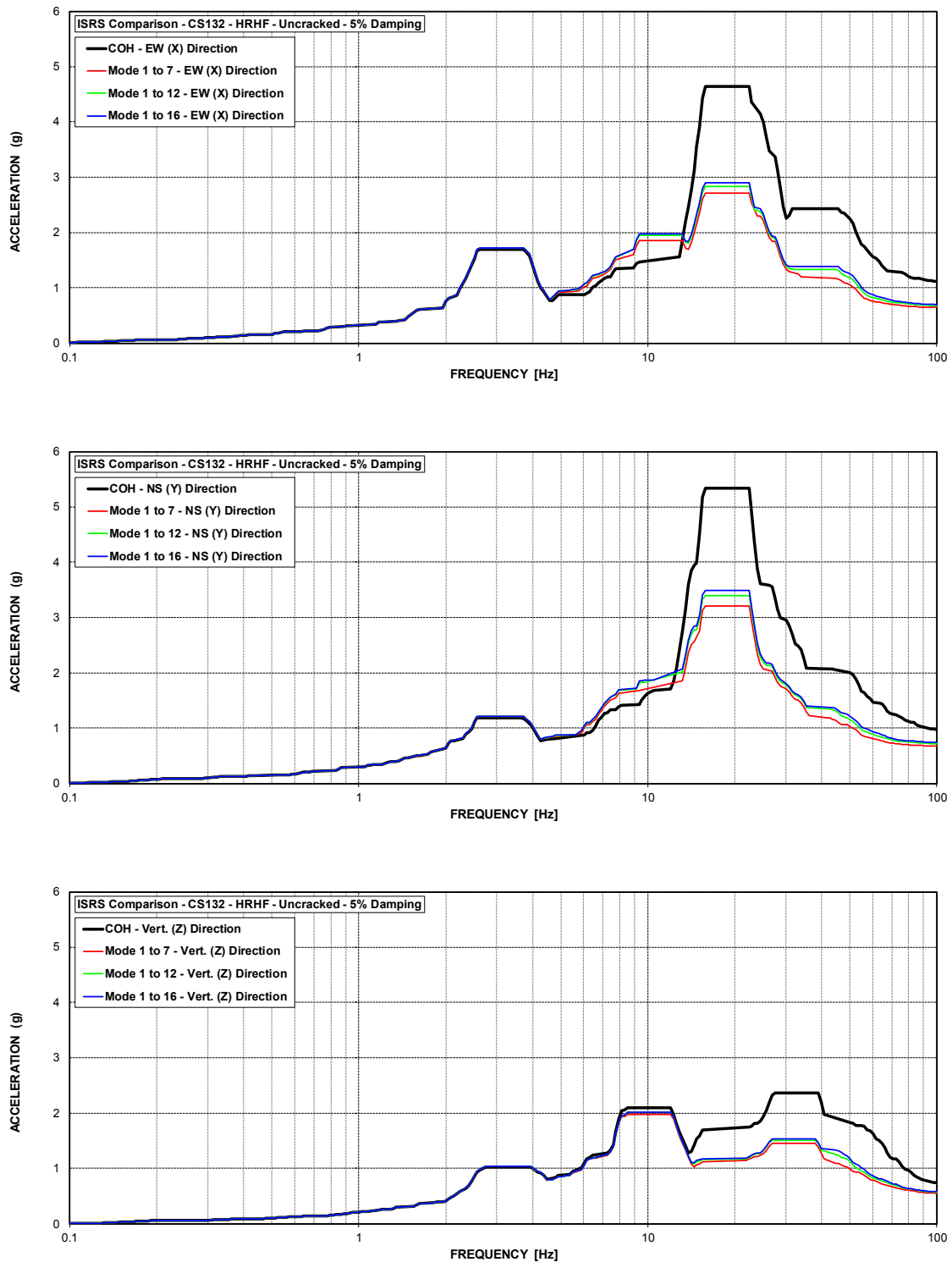


Figure C-64 ISRS – Containment Structure (CS132) at El. 131.56' – HRHF – Uncracked

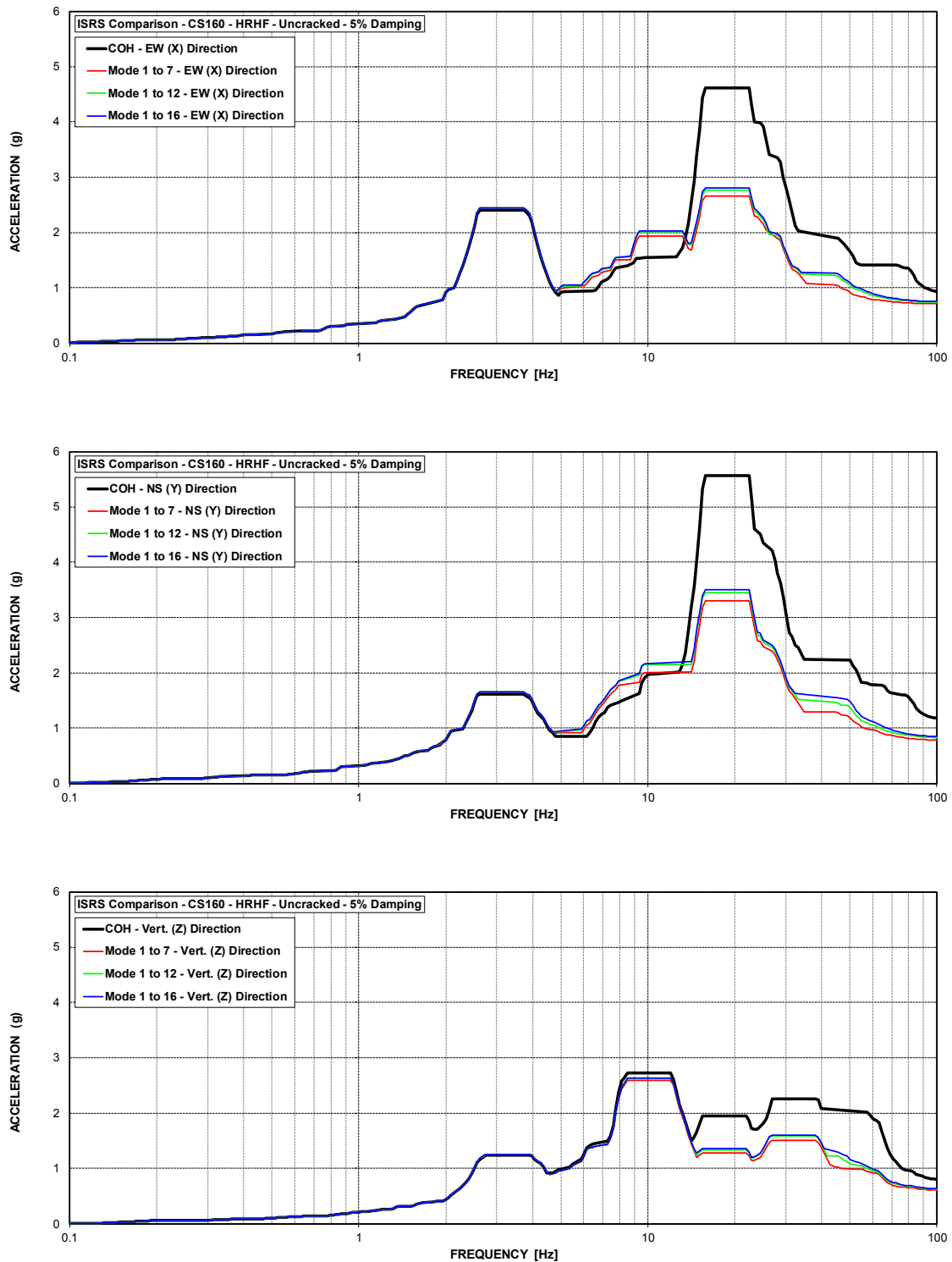


Figure C-65 ISRS – Containment Structure (CS160) at El. 159.75' – HRHF – Uncracked

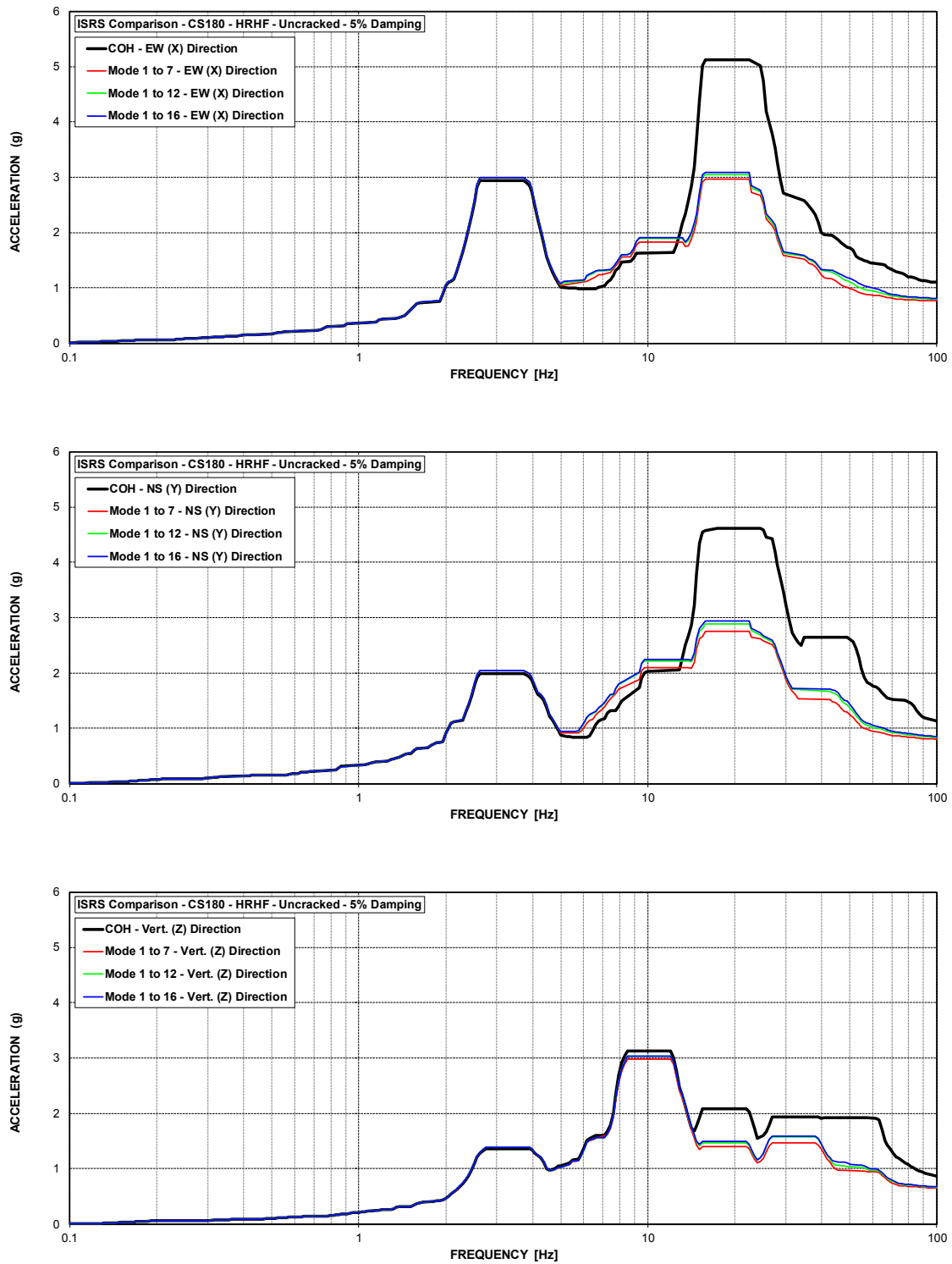


Figure C-66 ISRS – Containment Structure (CS180) at El. 180' – HRHF – Uncracked



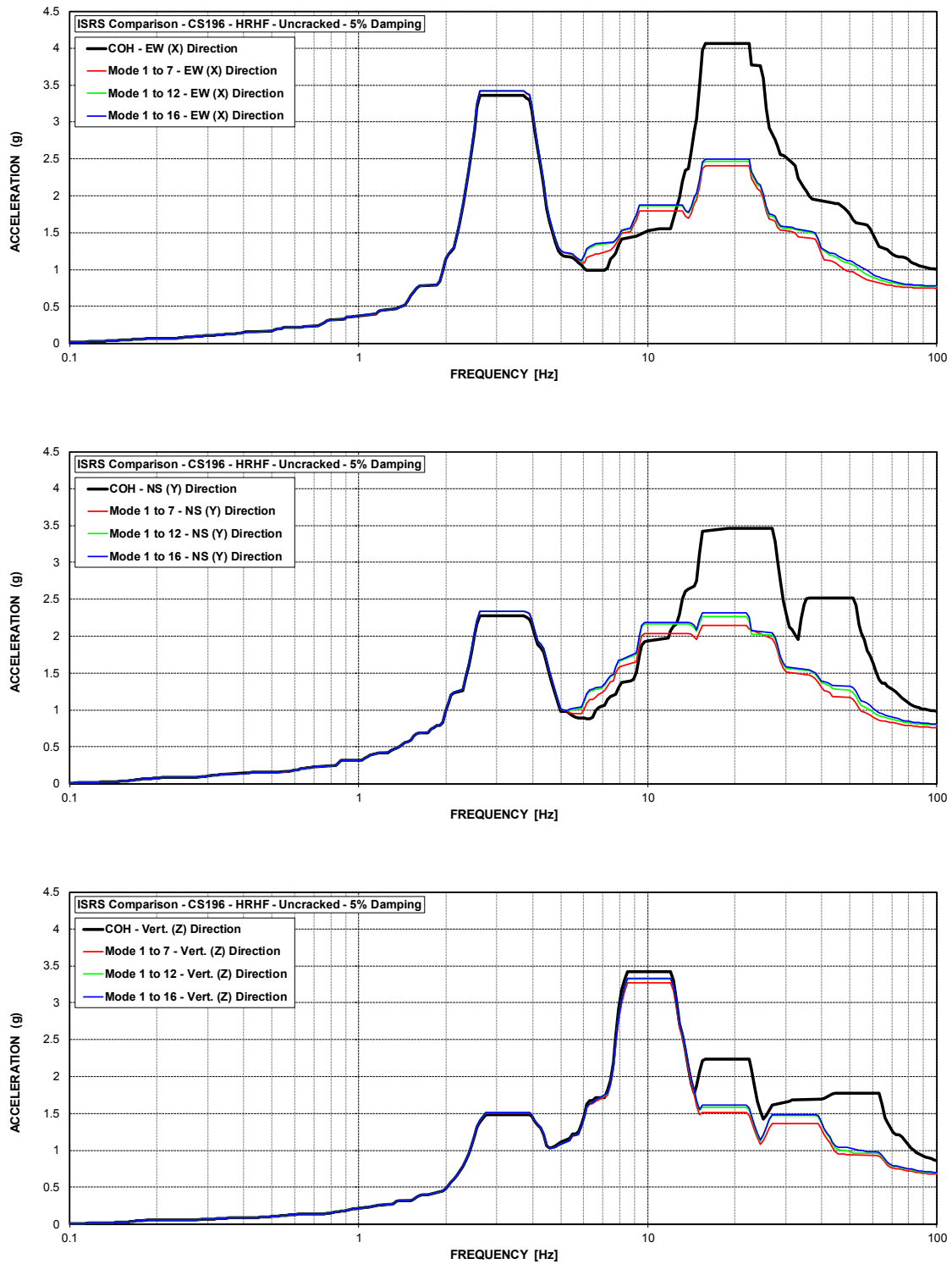


Figure C-67 ISRS – Containment Structure (CS196) at El. 195.5' – HRHF – Uncracked

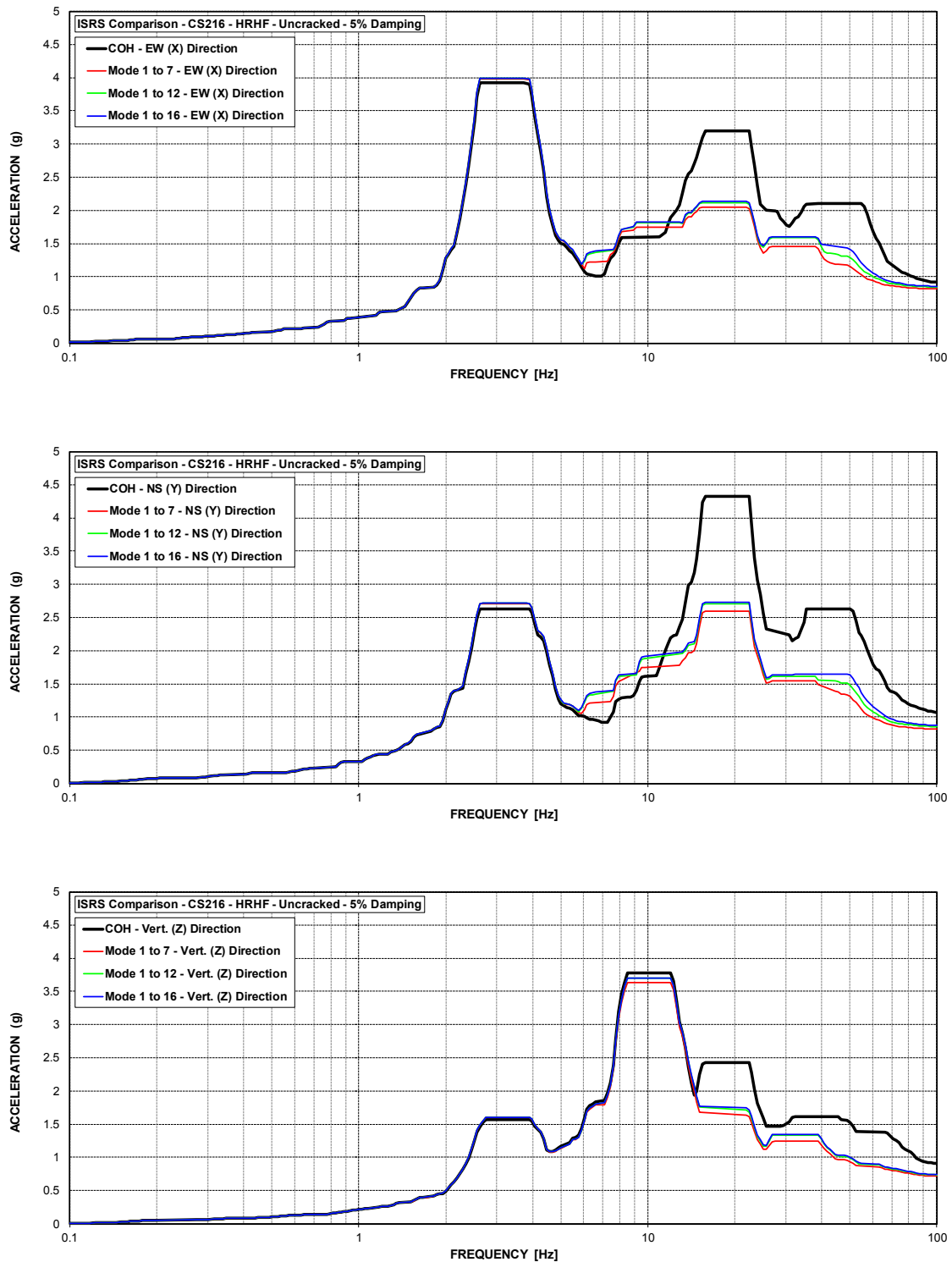


Figure C-68 ISRS – Containment Structure (CS216) at El. 215.96' – HRHF – Uncracked

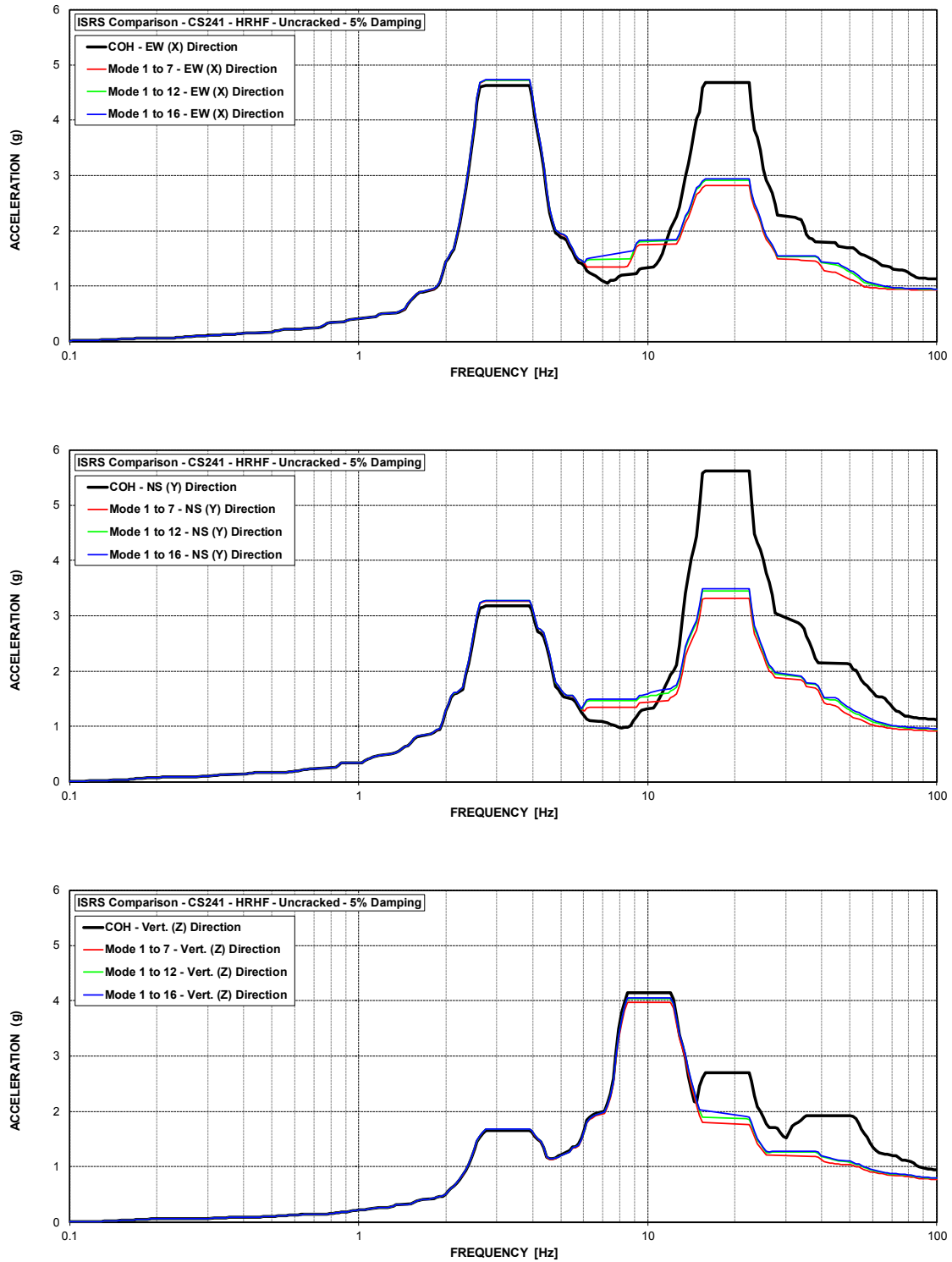


Figure C-69 ISRS – Containment Structure (CS241) at El. 241' – HRHF – Uncracked

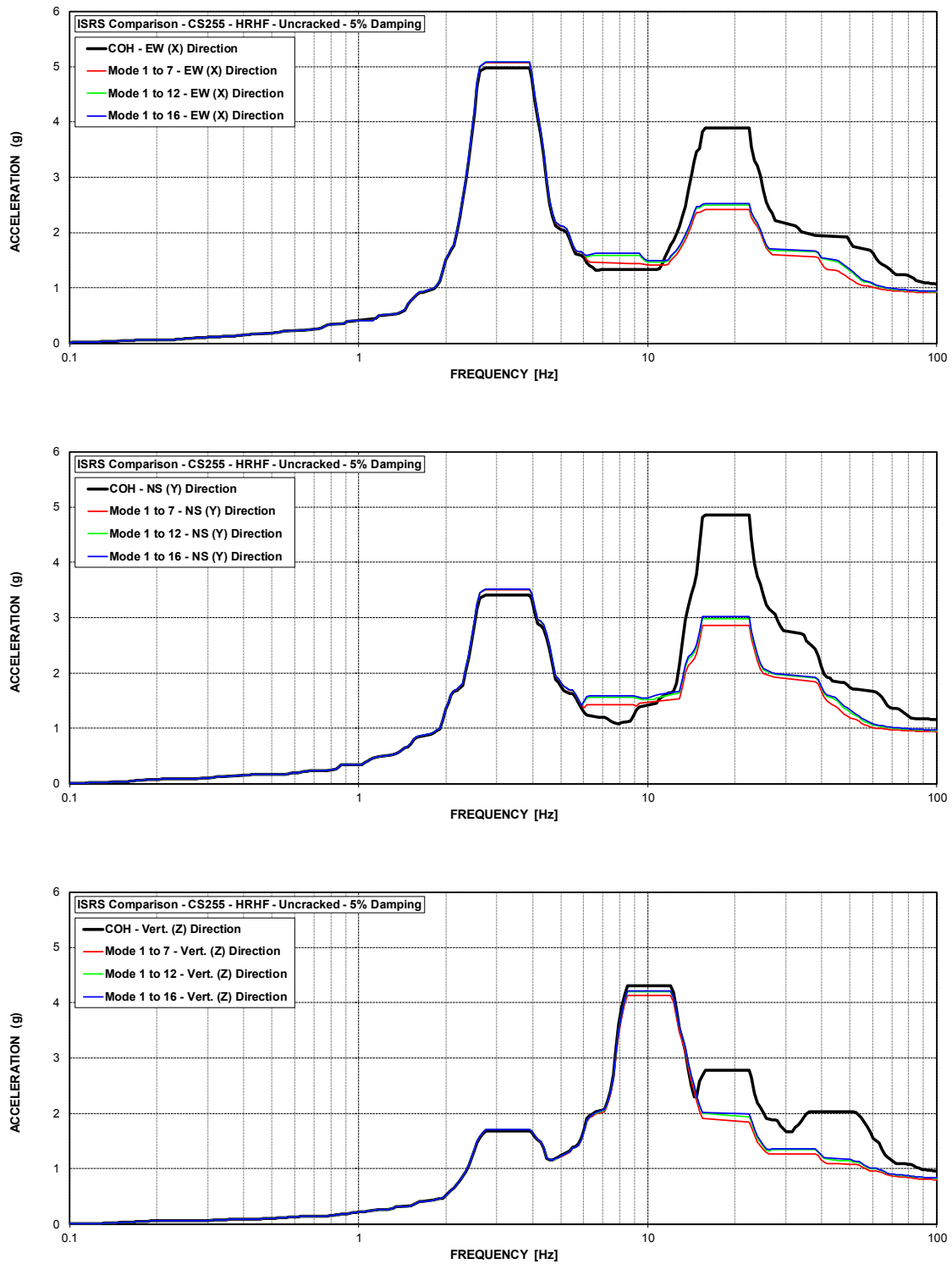


Figure C-70 ISRS – Containment Structure (CS255) at El. 254.5' – HRHF – Uncracked

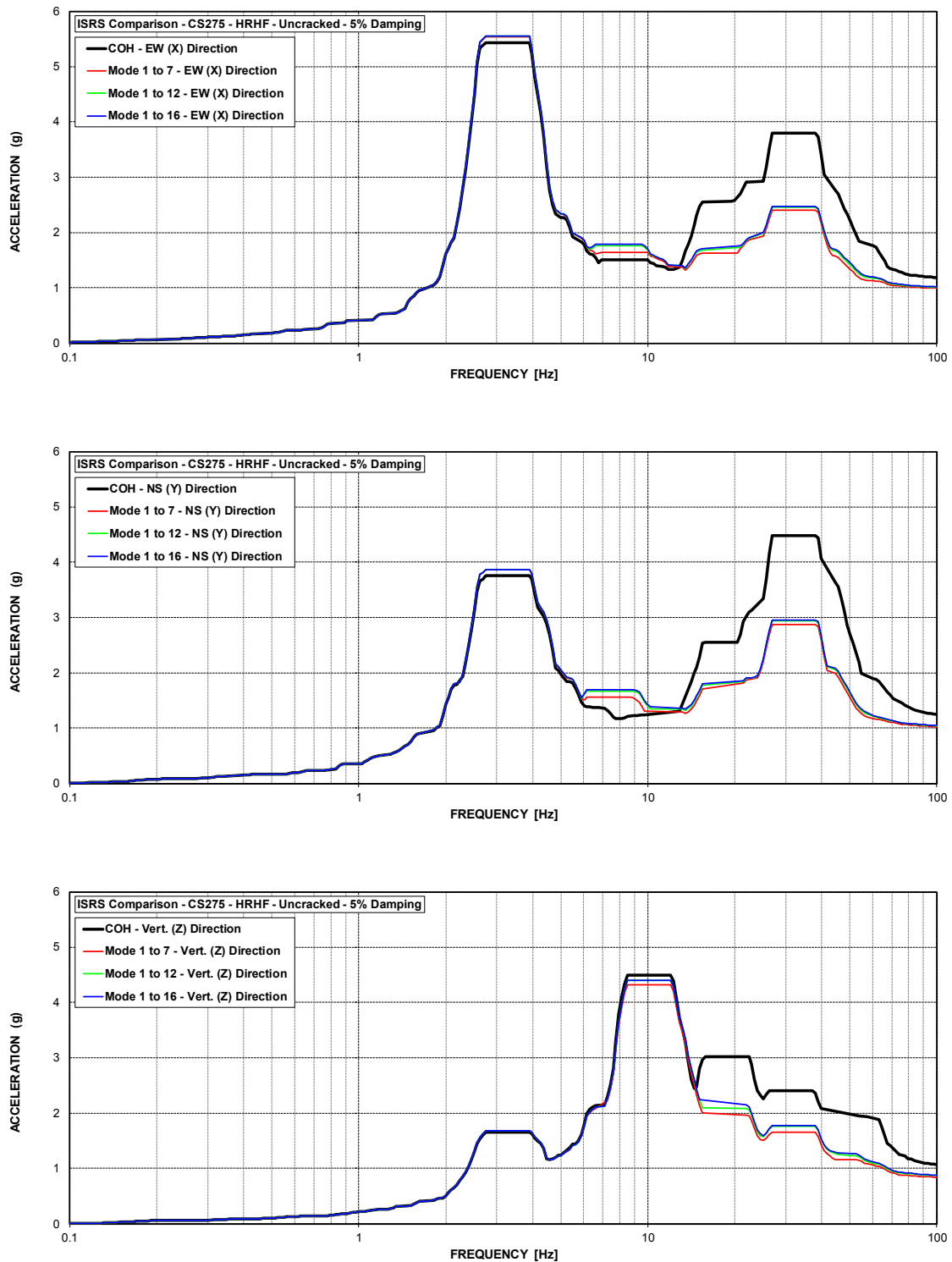


Figure C-71 ISRS – Containment Structure (CS275) at El. 274.49' – HRHF – Uncracked

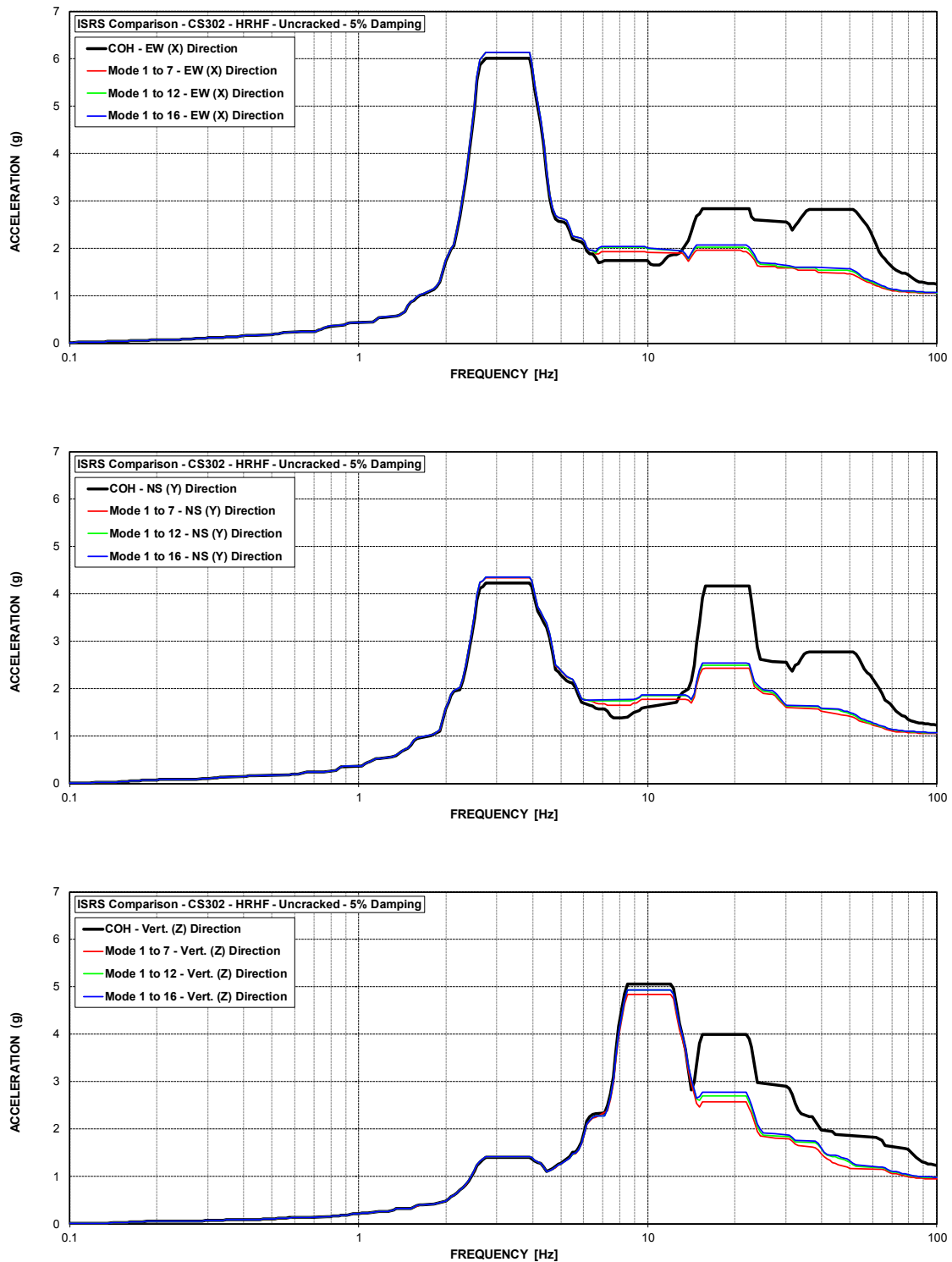


Figure C-72 ISRS – Containment Structure (CS302) at El. 301.53' – HRHF – Uncracked

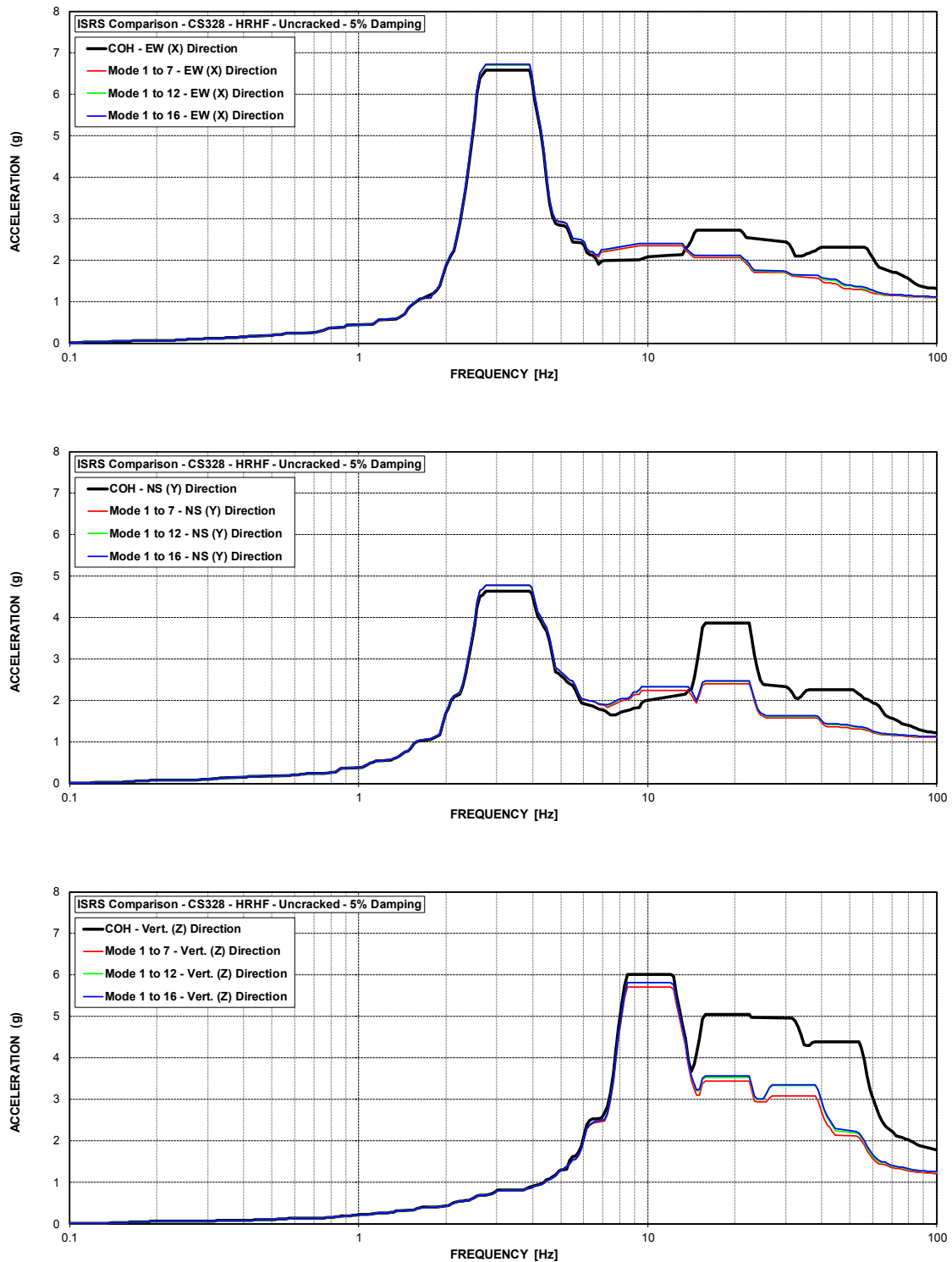


Figure C-73 ISRS – Containment Structure (CS328) at El. 328.42' – HRHF – Uncracked

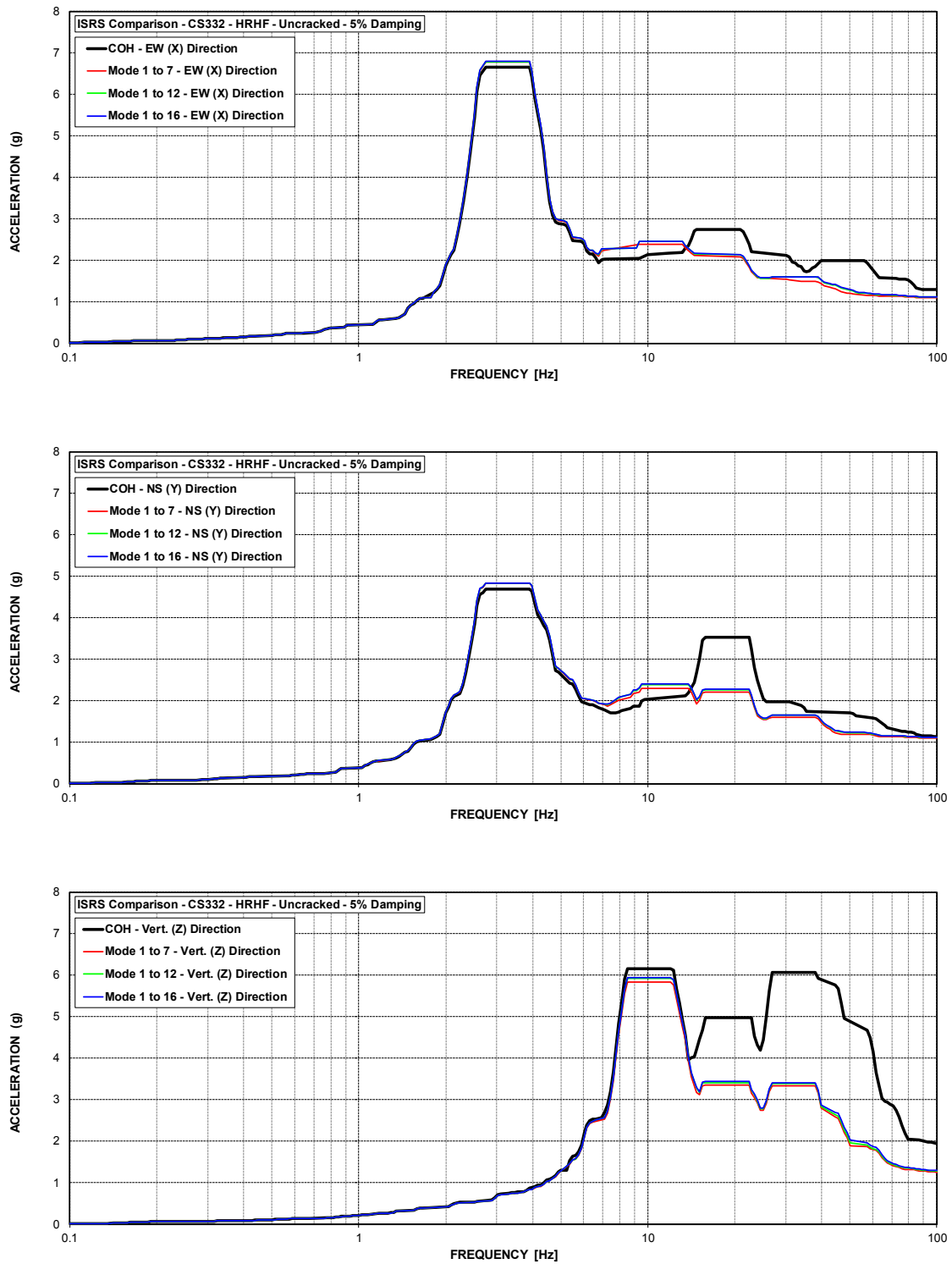


Figure C-74 ISRS – Containment Structure (CS332) at El. 331.75' – HRHF – Uncracked



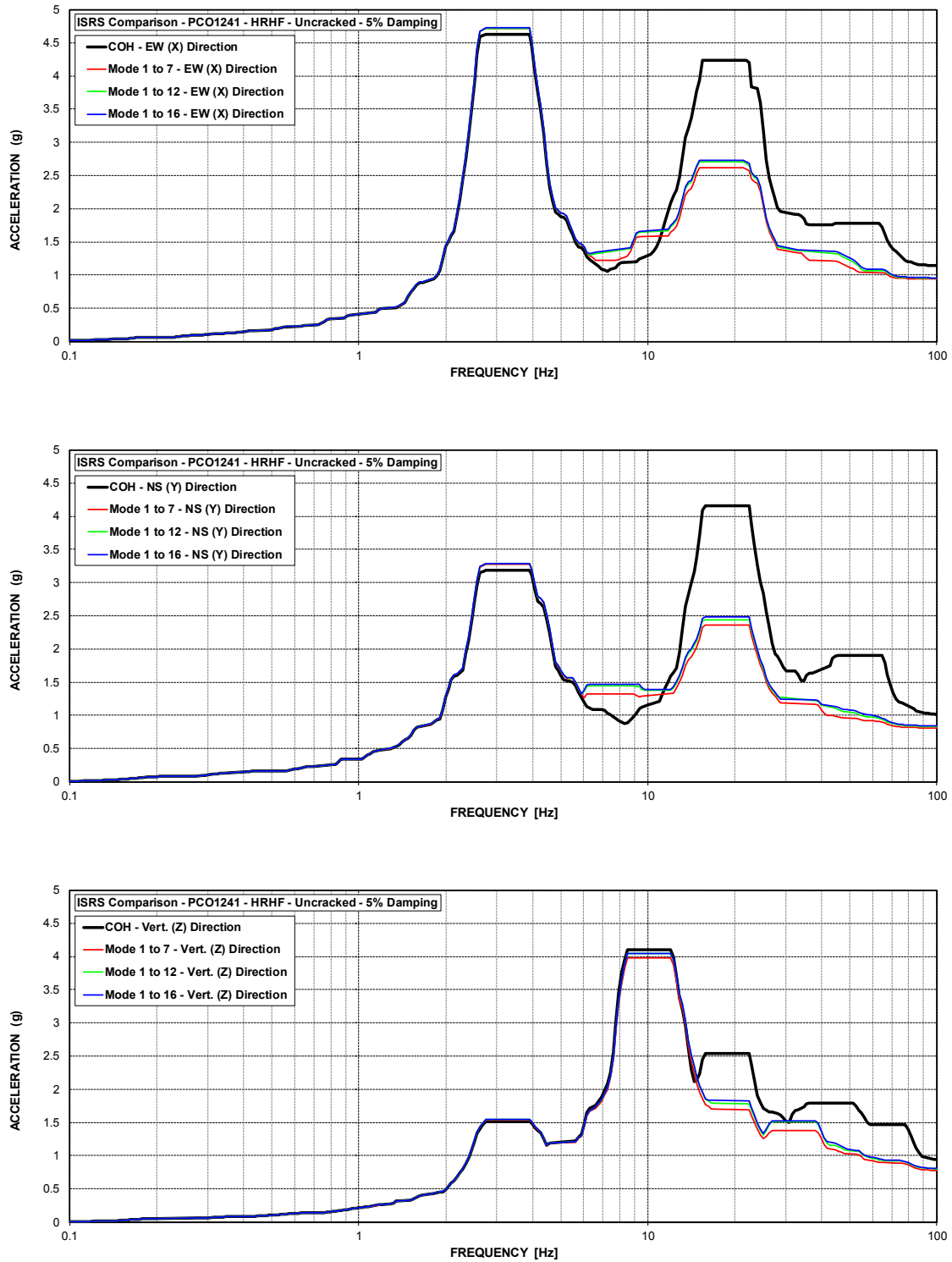


Figure C-75 ISRS – Polar Crane (PCO1241) at El. 241' – HRHF – Uncracked

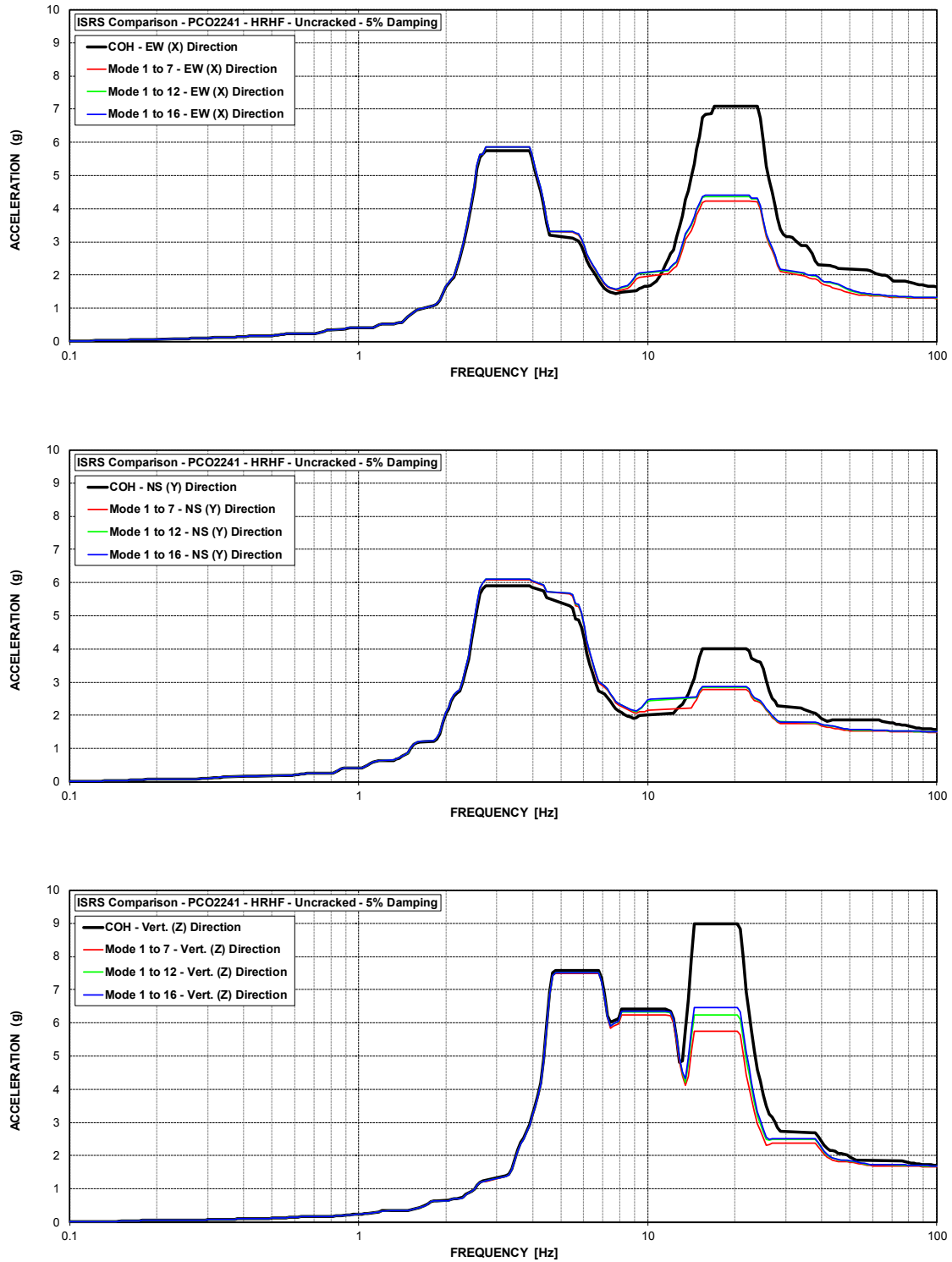


Figure C-76 ISRS – Polar Crane (PCO2241) at El. 241' – HRHF – Uncracked

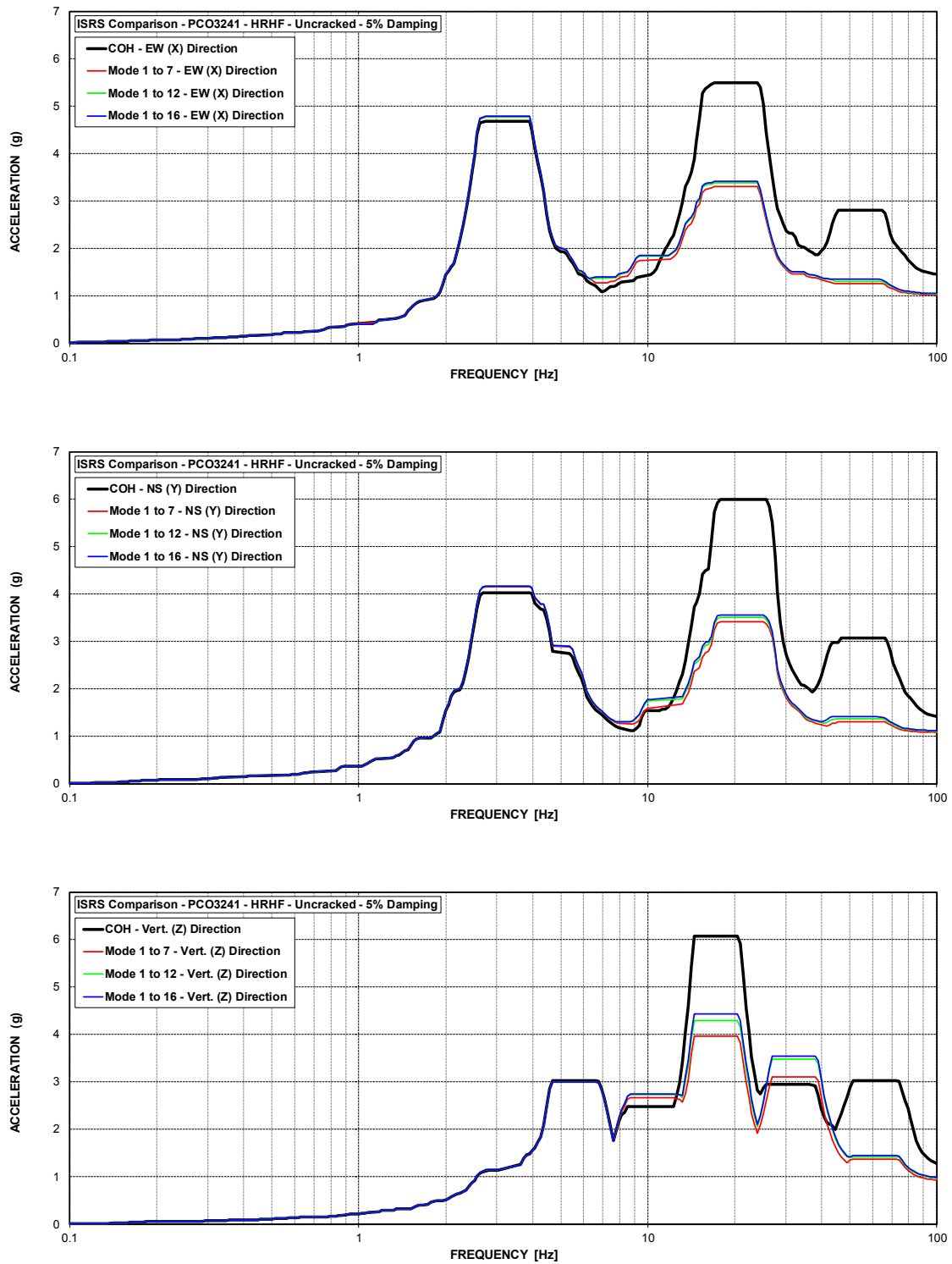


Figure C-77 ISRS – Polar Crane (PCO3241) at El. 241' – HRHF – Uncracked

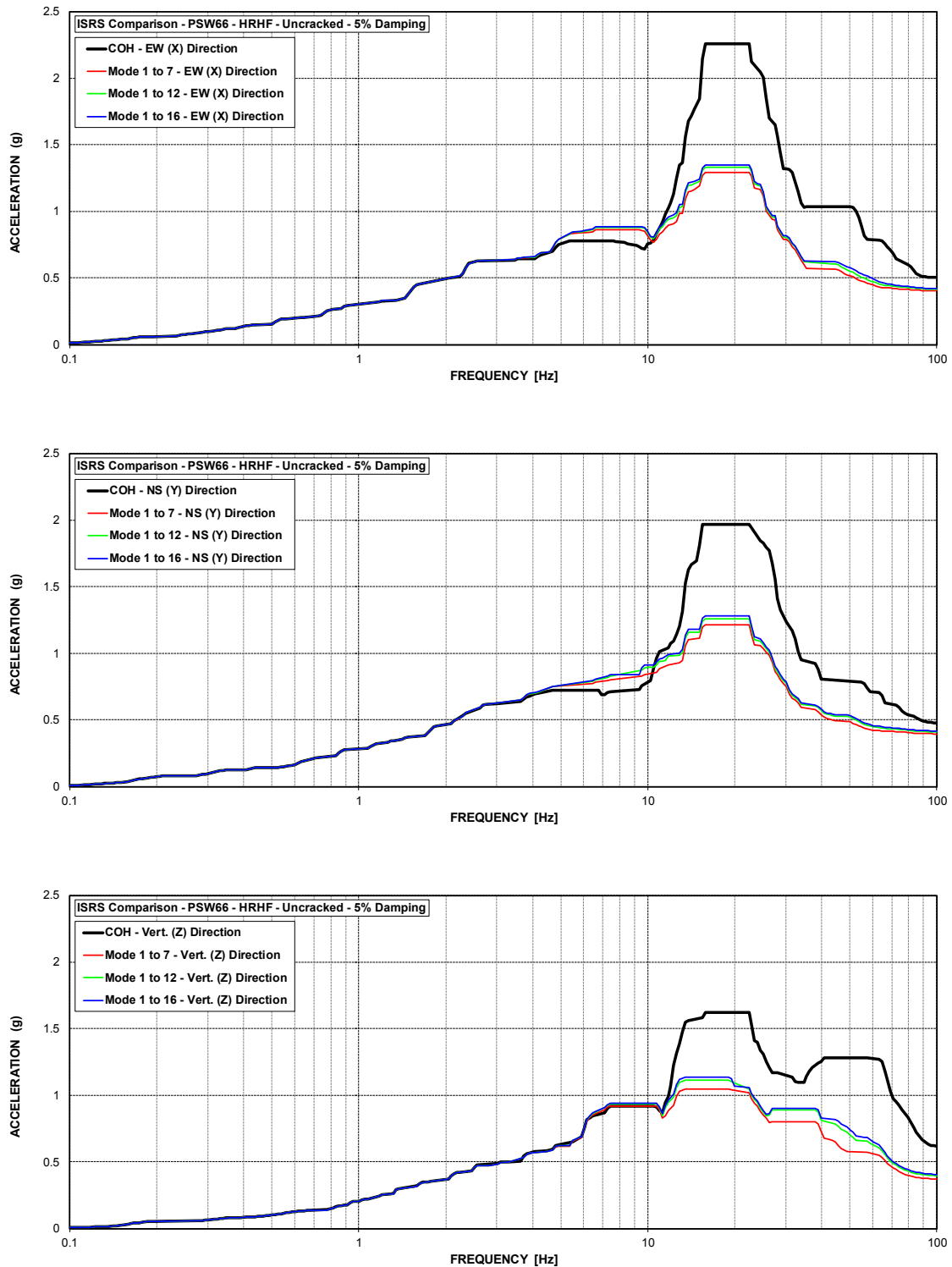


Figure C-78 ISRS – Primary Shield Wall (PSW66) at El. 66' – HRHF – Uncracked

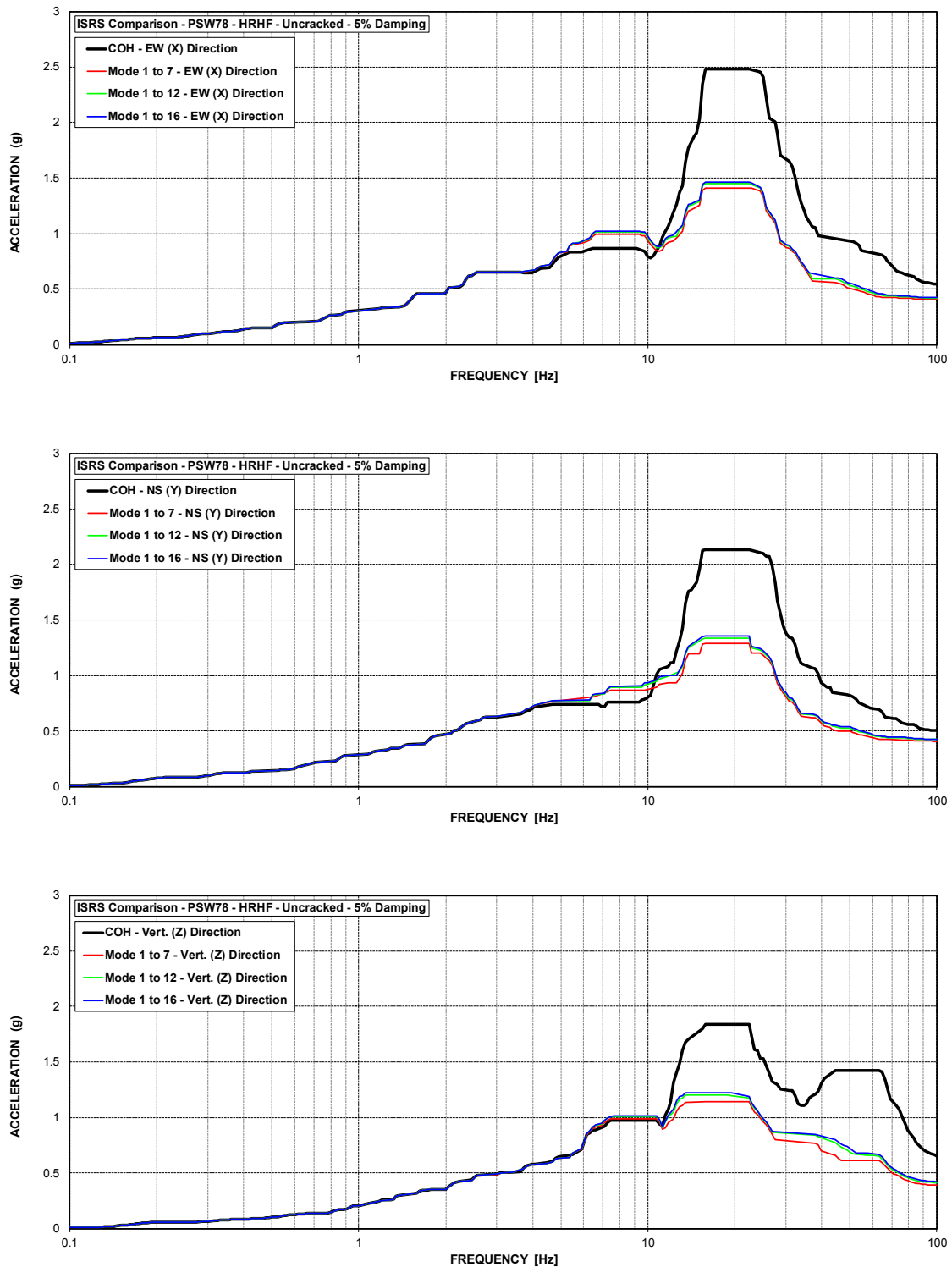


Figure C-79 ISRS – Primary Shield Wall (PSW78) at El. 78' – HRHF – Uncracked

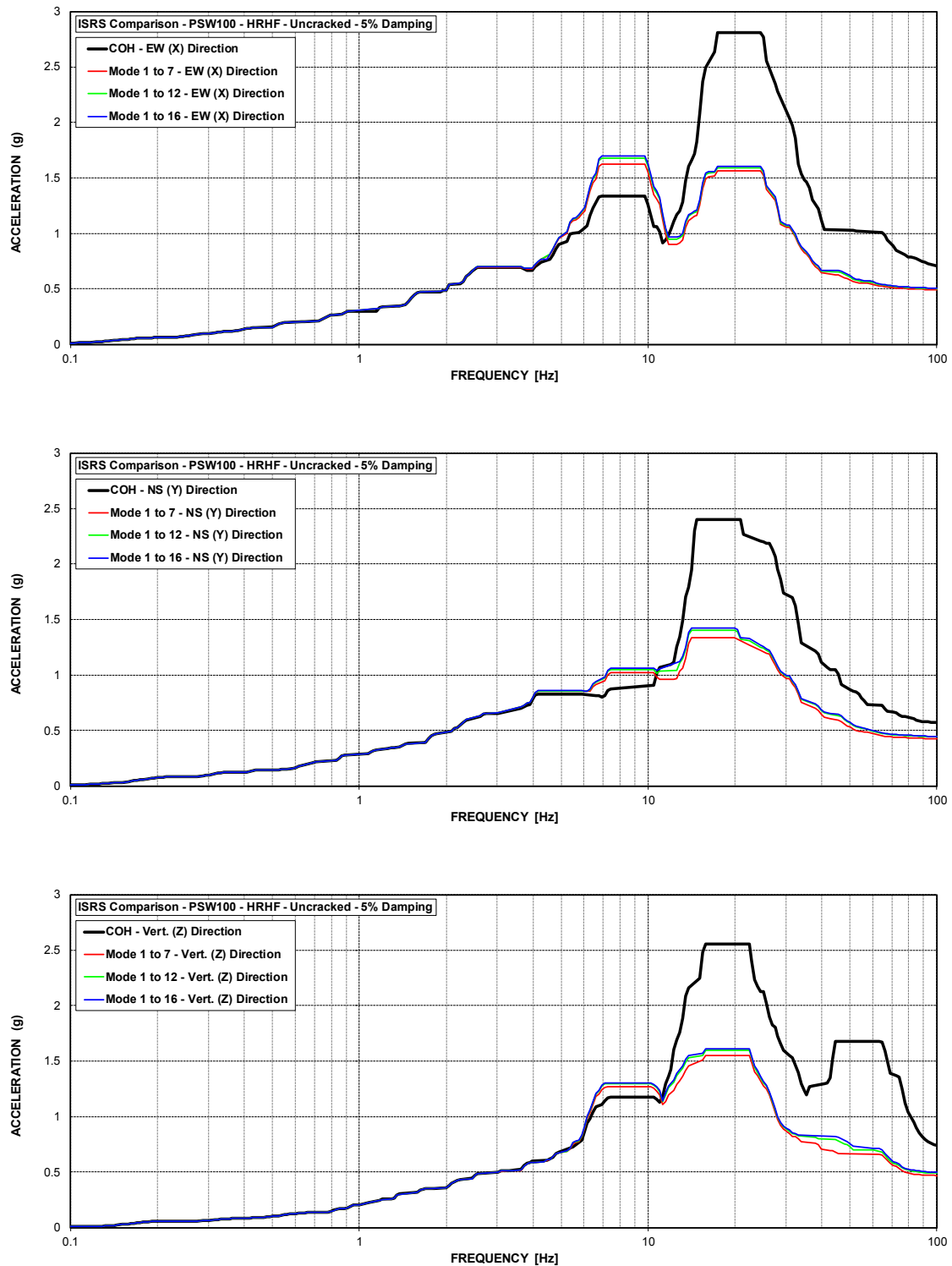


Figure C-80 ISRS – Primary Shield Wall (PSW100) at El. 100' – HRHF – Uncracked

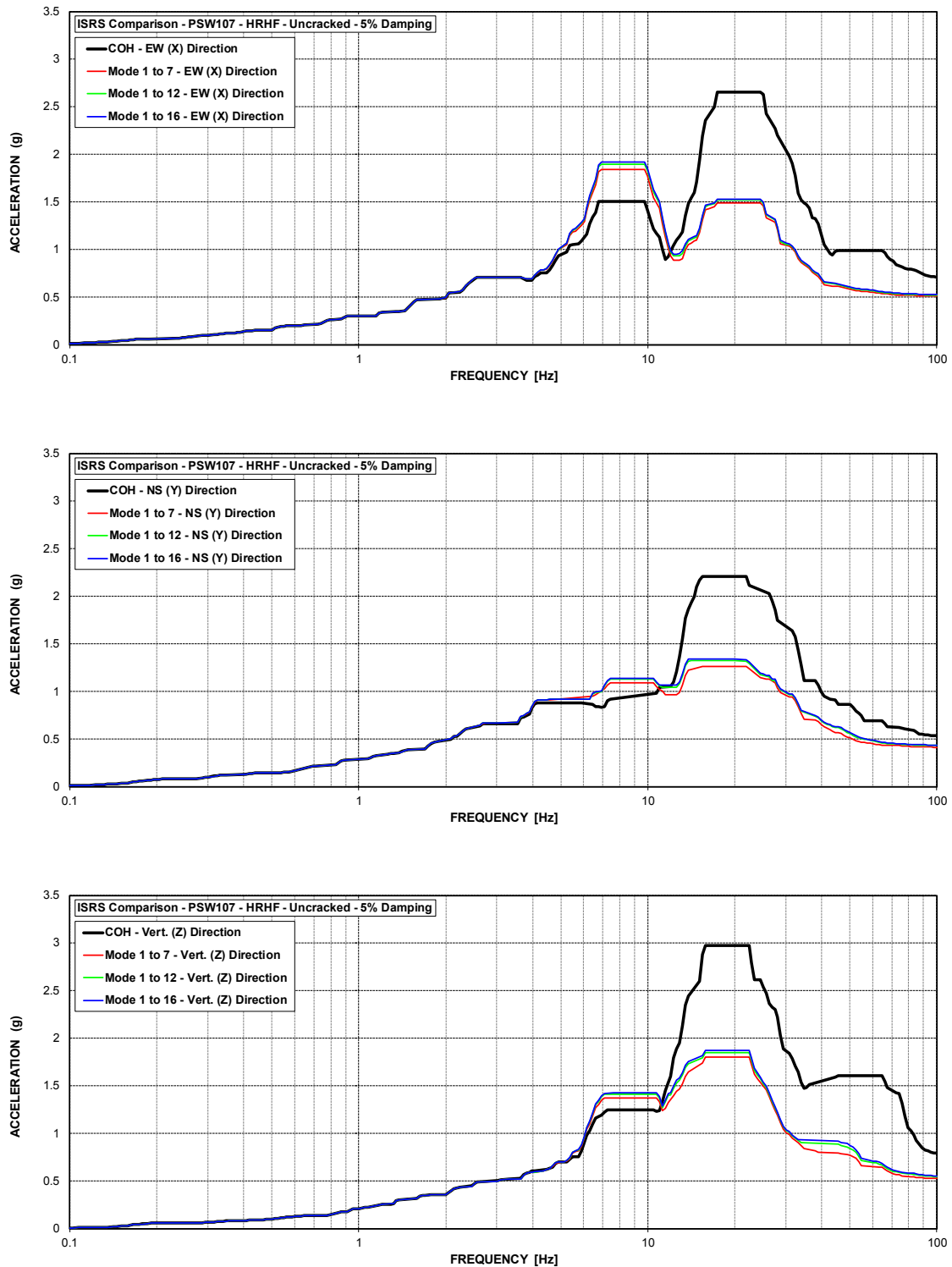


Figure C-81 ISRS – Primary Shield Wall (PSW107) at El. 106.5' – HRHF – Uncracked

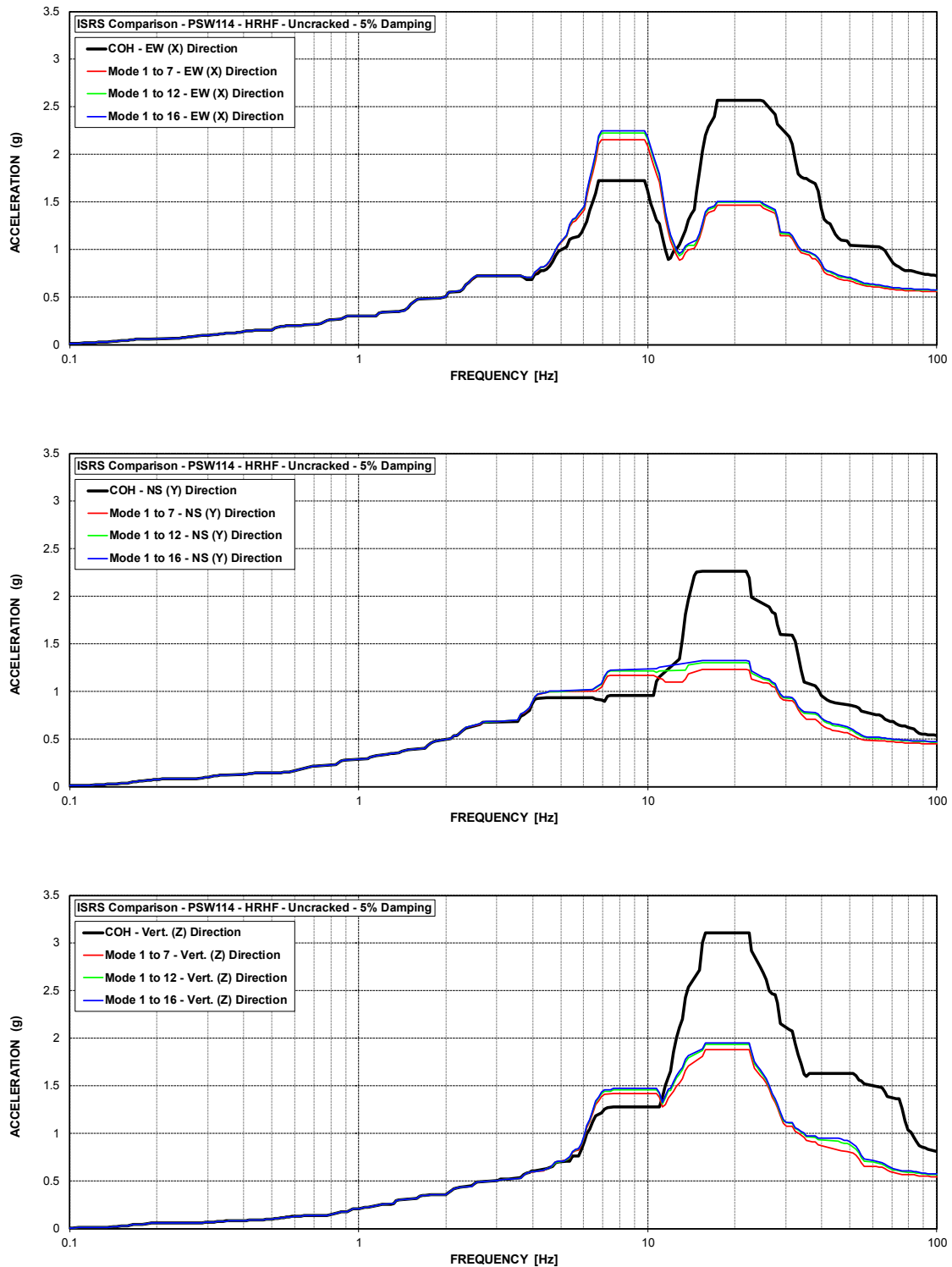


Figure C-82 ISRS – Primary Shield Wall (PSW114) at El. 114' – HRHF – Uncracked



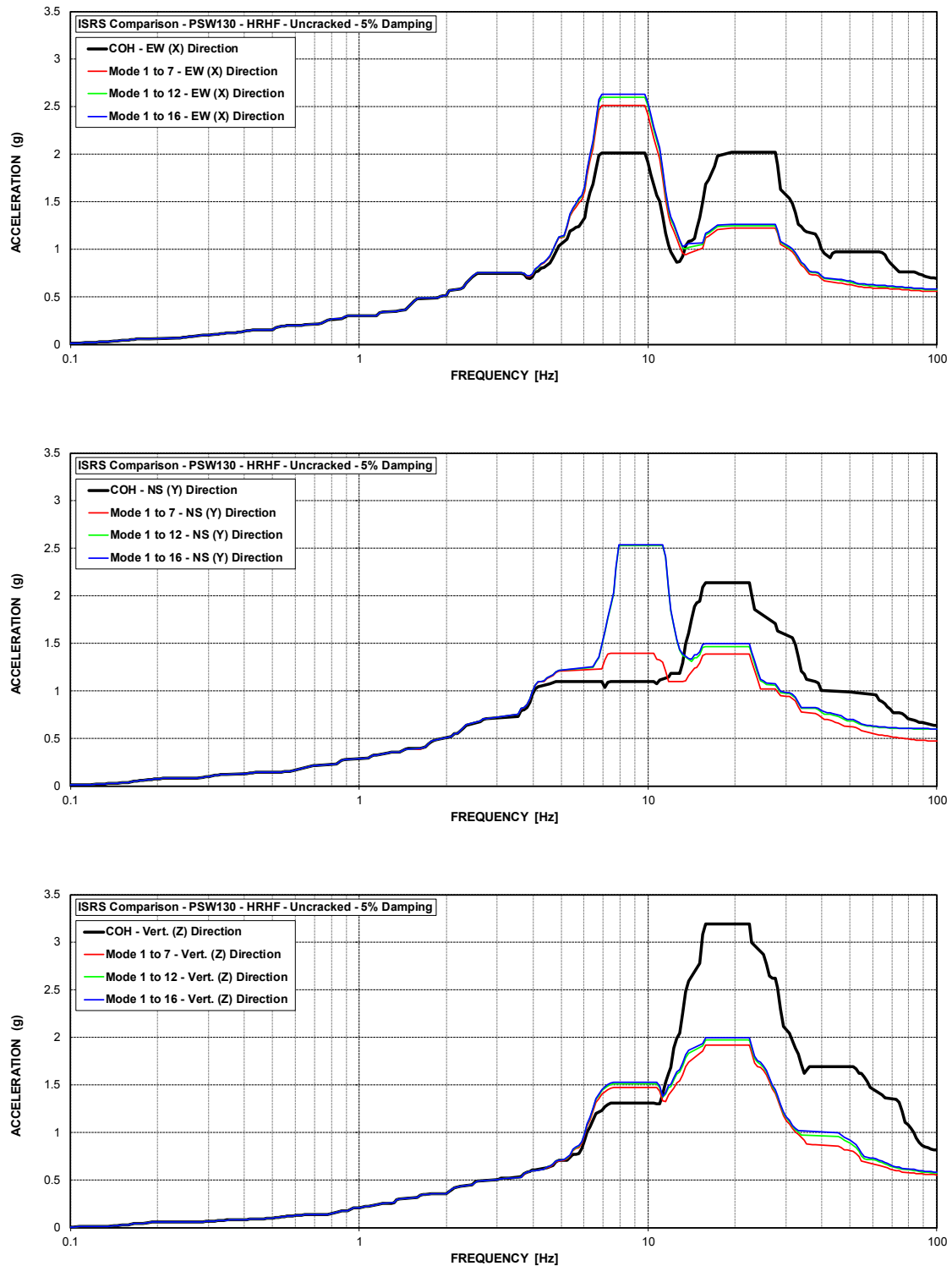


Figure C-83 ISRS – Primary Shield Wall (PSW130) at El. 130' – HRHF – Uncracked

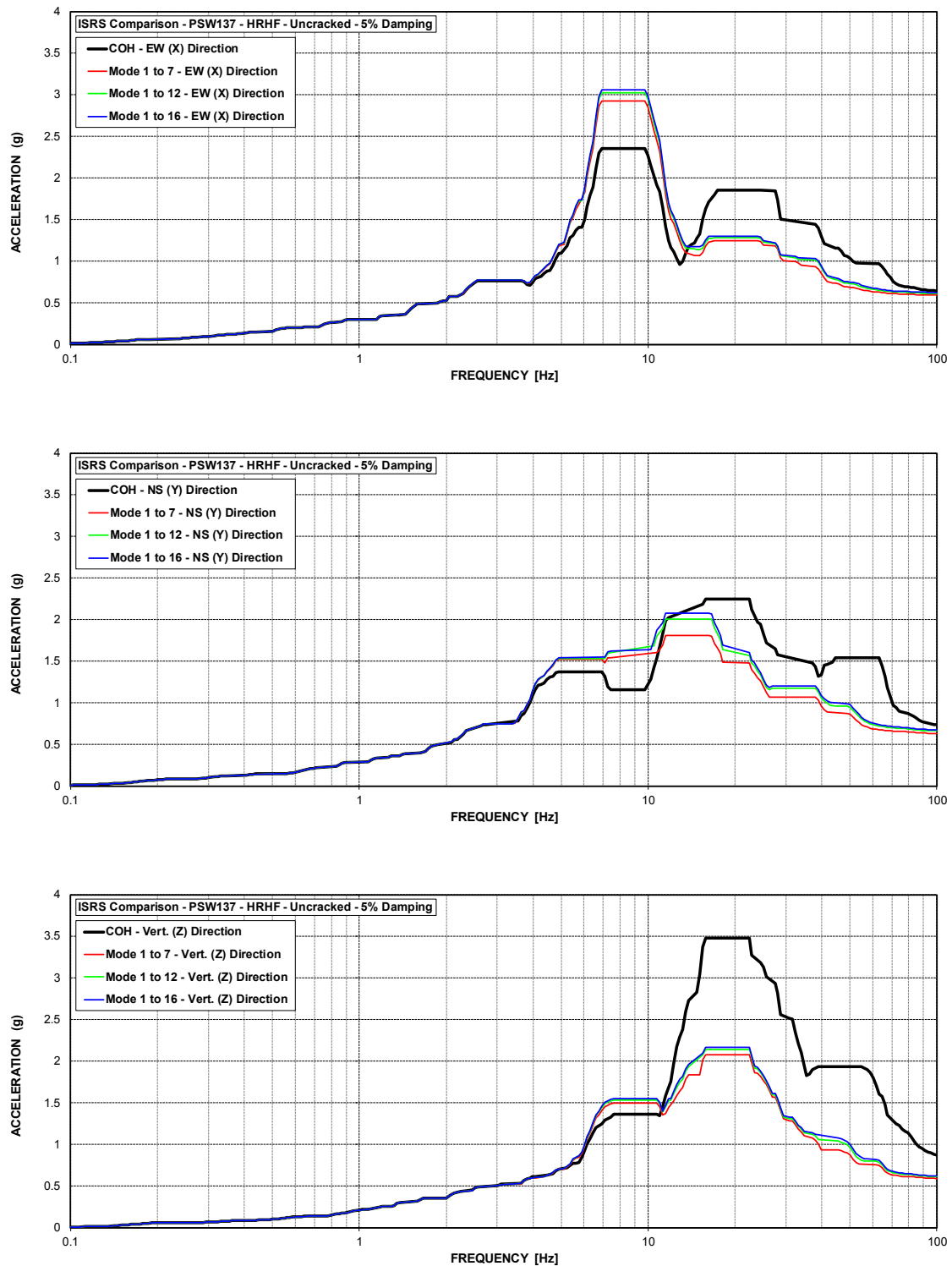


Figure C-84 ISRS – Primary Shield Wall (PSW137) at El. 136.5 – HRHF – Uncracked

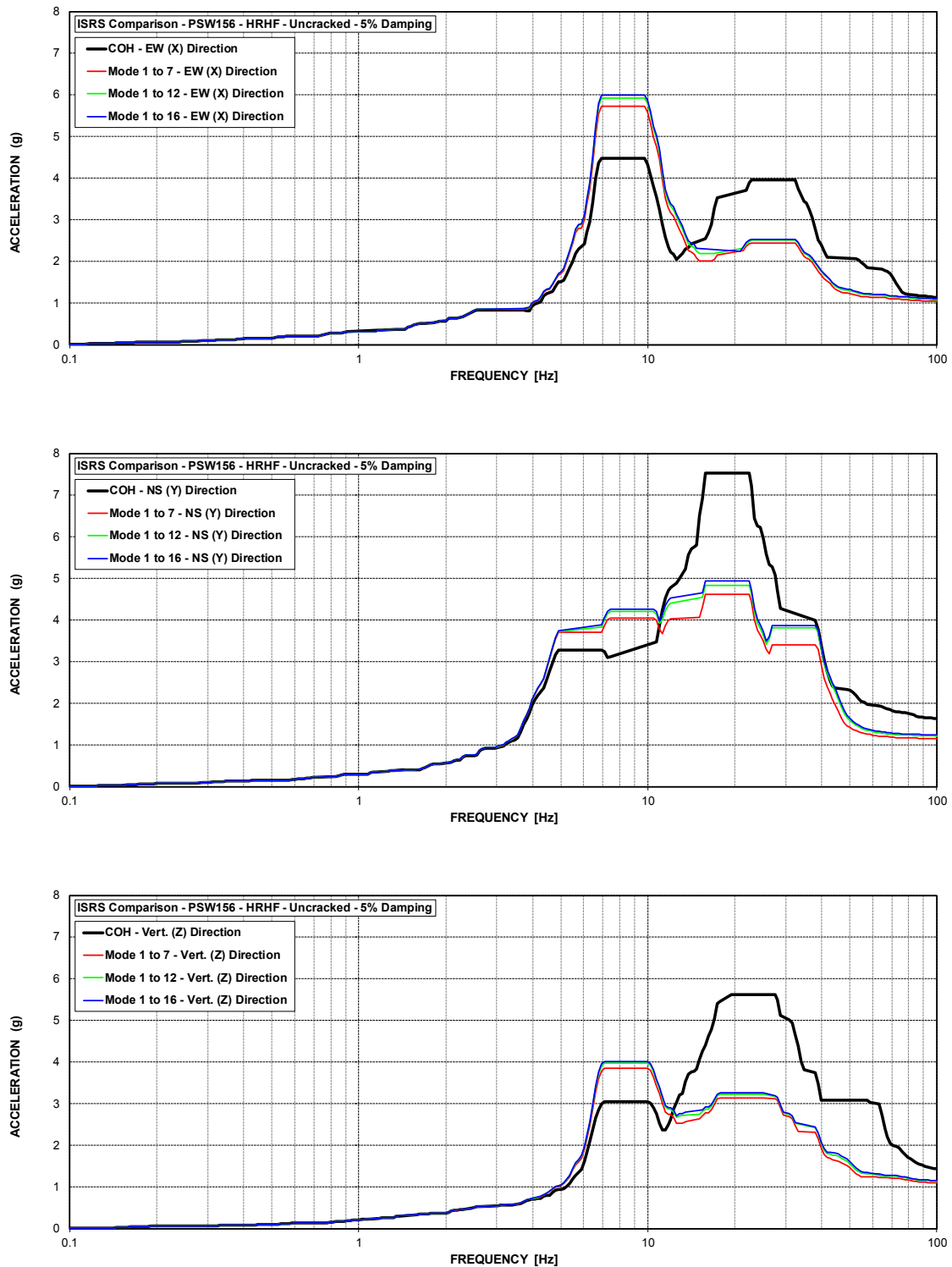


Figure C-85 ISRS – Primary Shield Wall (PSW156) at El. 156' – HRHF – Uncracked

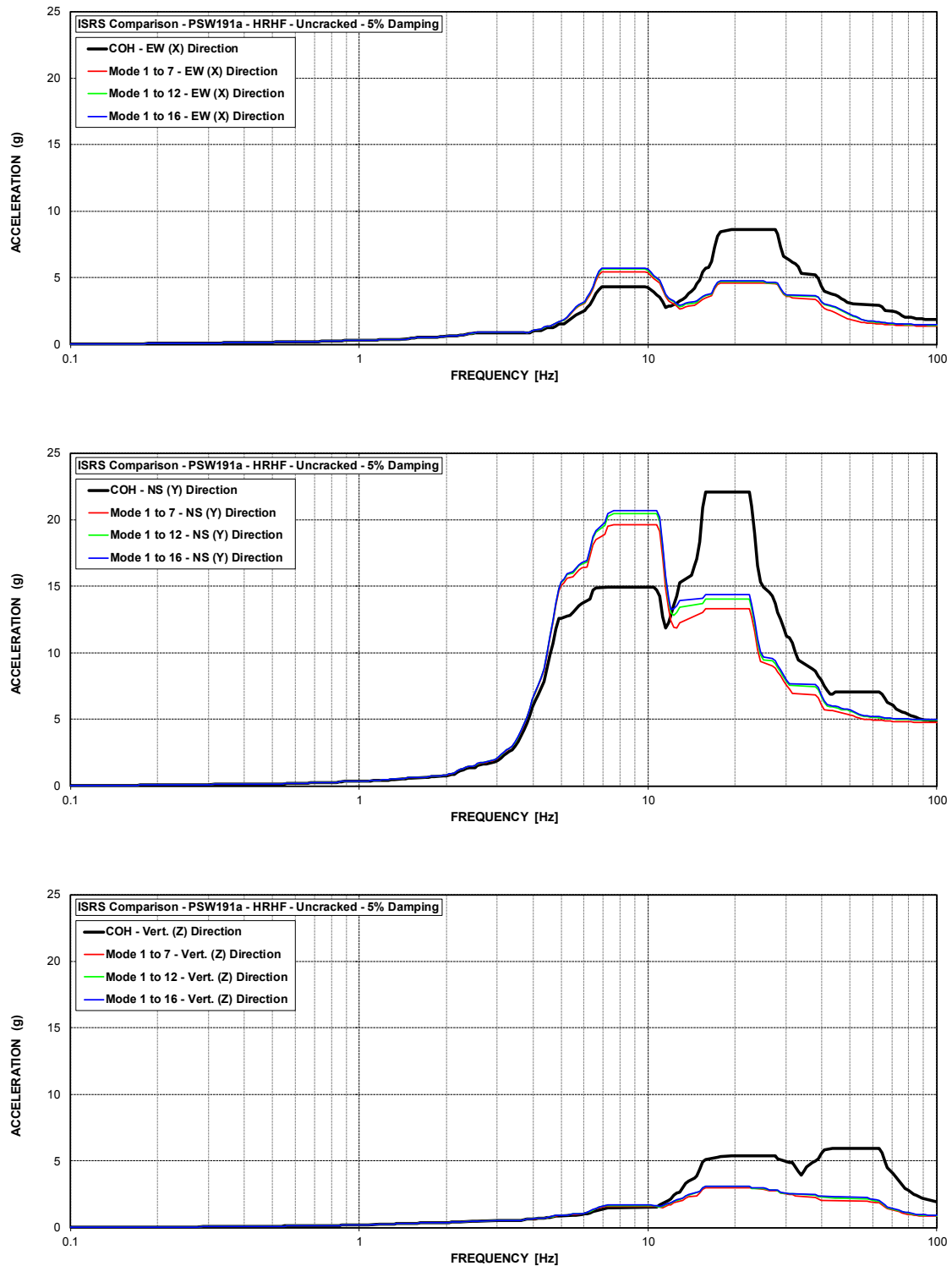


Figure C-86 ISRS – Primary Shield Wall (PSW191a) at El. 191' – HRHF – Uncracked

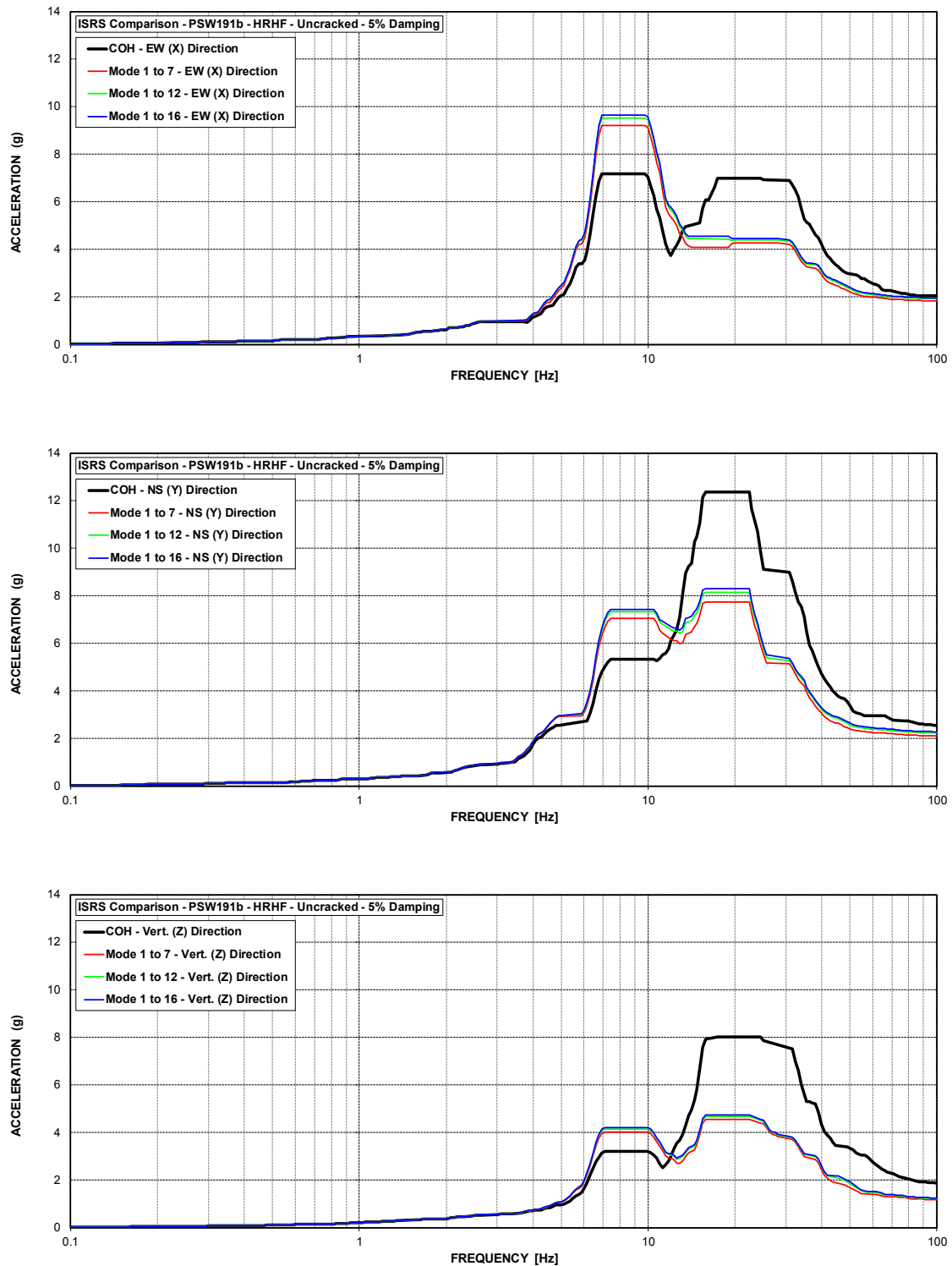


Figure C-87 ISRS – Primary Shield Wall (PSW191b) at El. 191' – HRHF – Uncracked

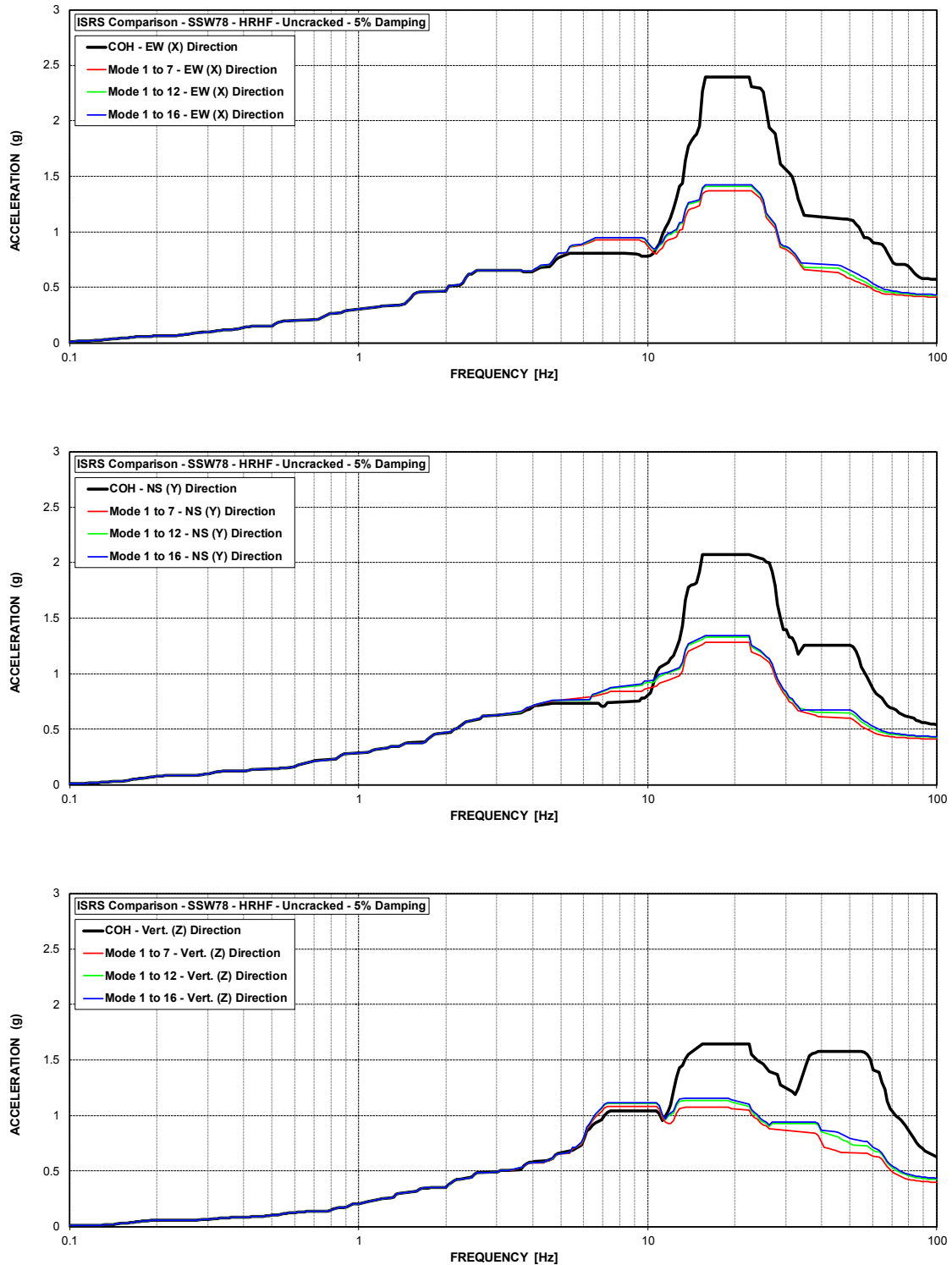


Figure C-88 ISRS – Secondary Shield Wall (SSW78) at El. 78' – HRHF – Uncracked

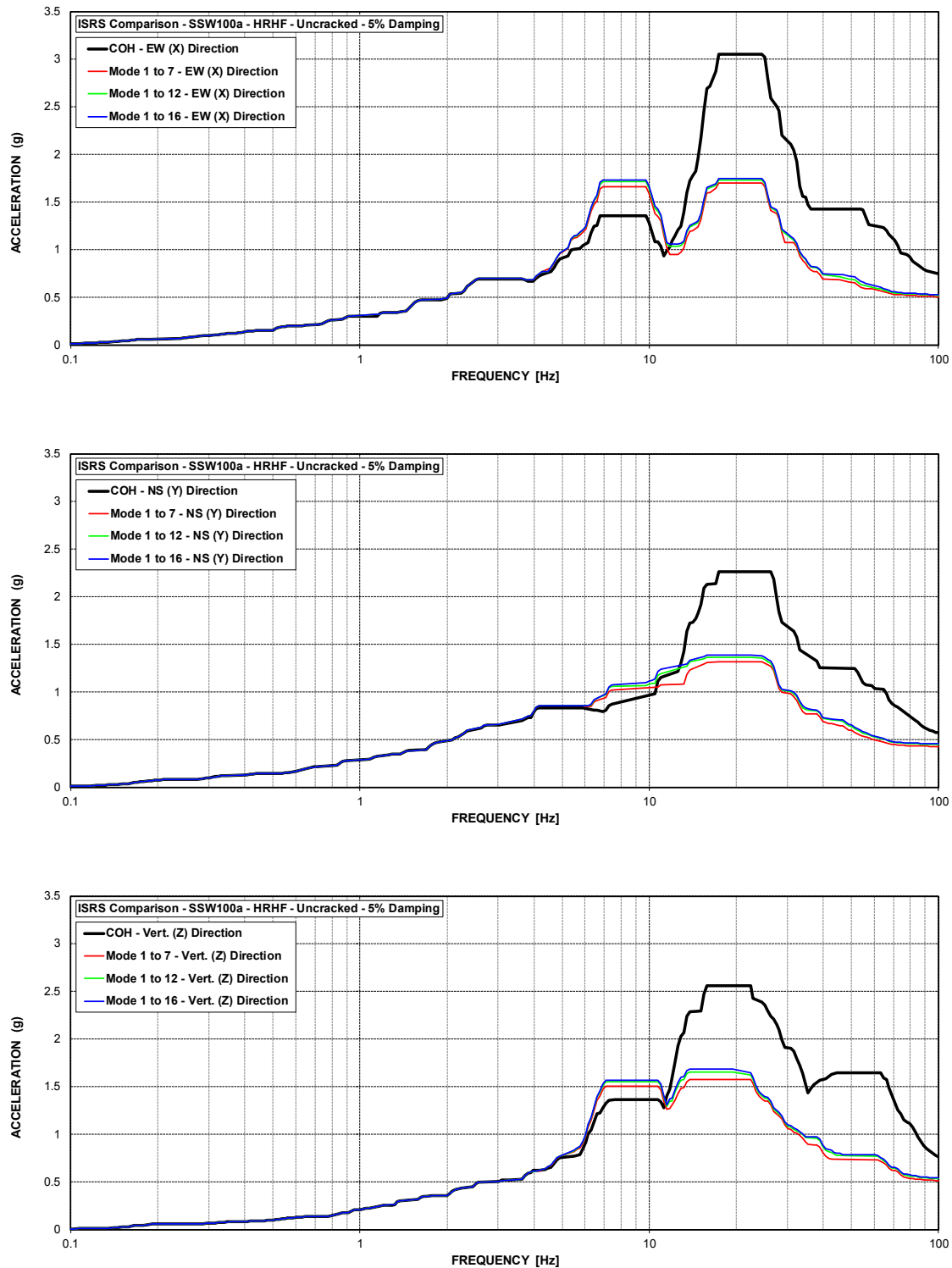


Figure C-89 ISRS – Secondary Shield Wall (SSW100a) at El. 100' – HRHF – Uncracked

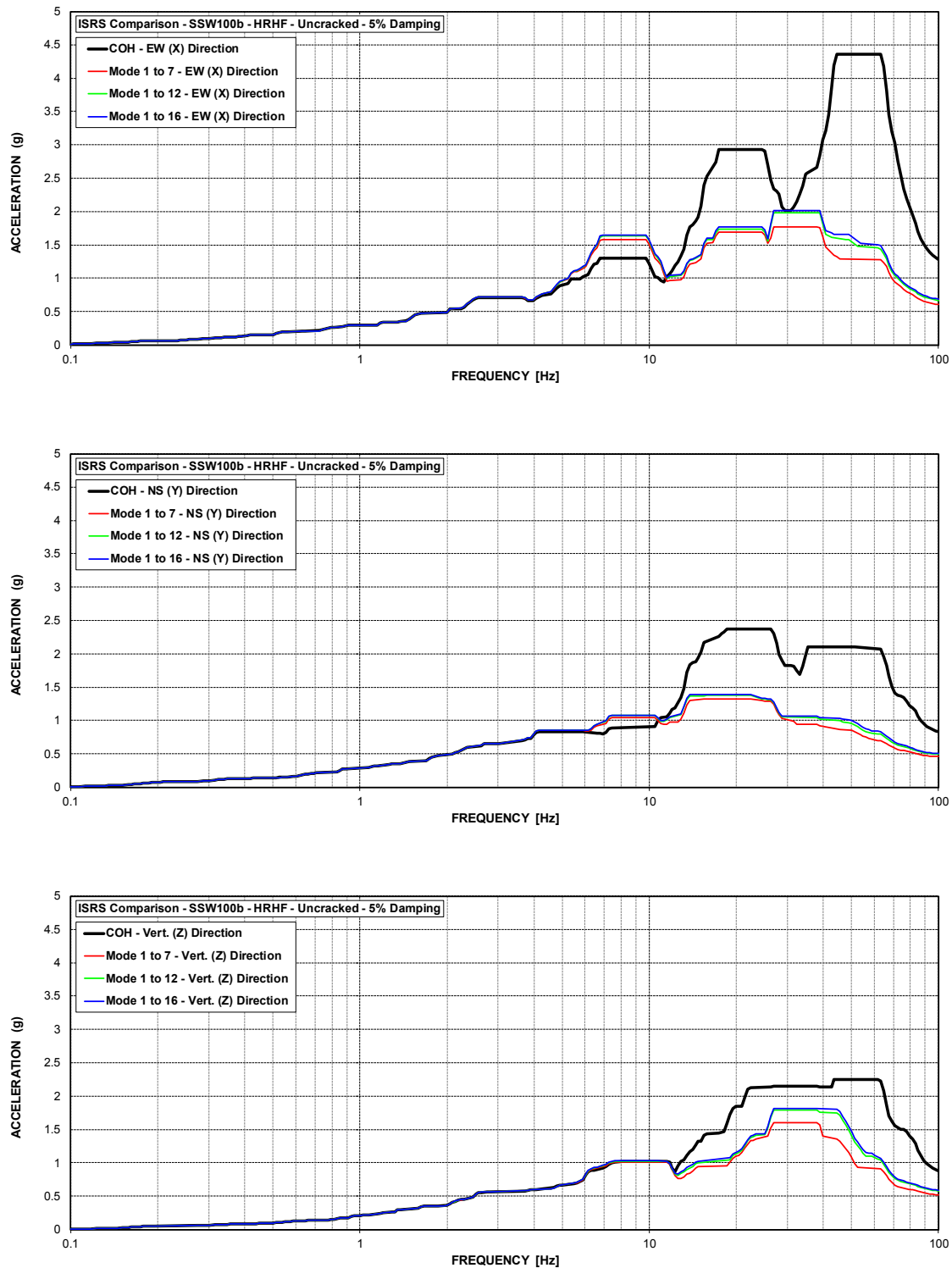


Figure C-90 ISRS – Secondary Shield Wall (SSW100b) at El. 100' – HRHF – Uncracked



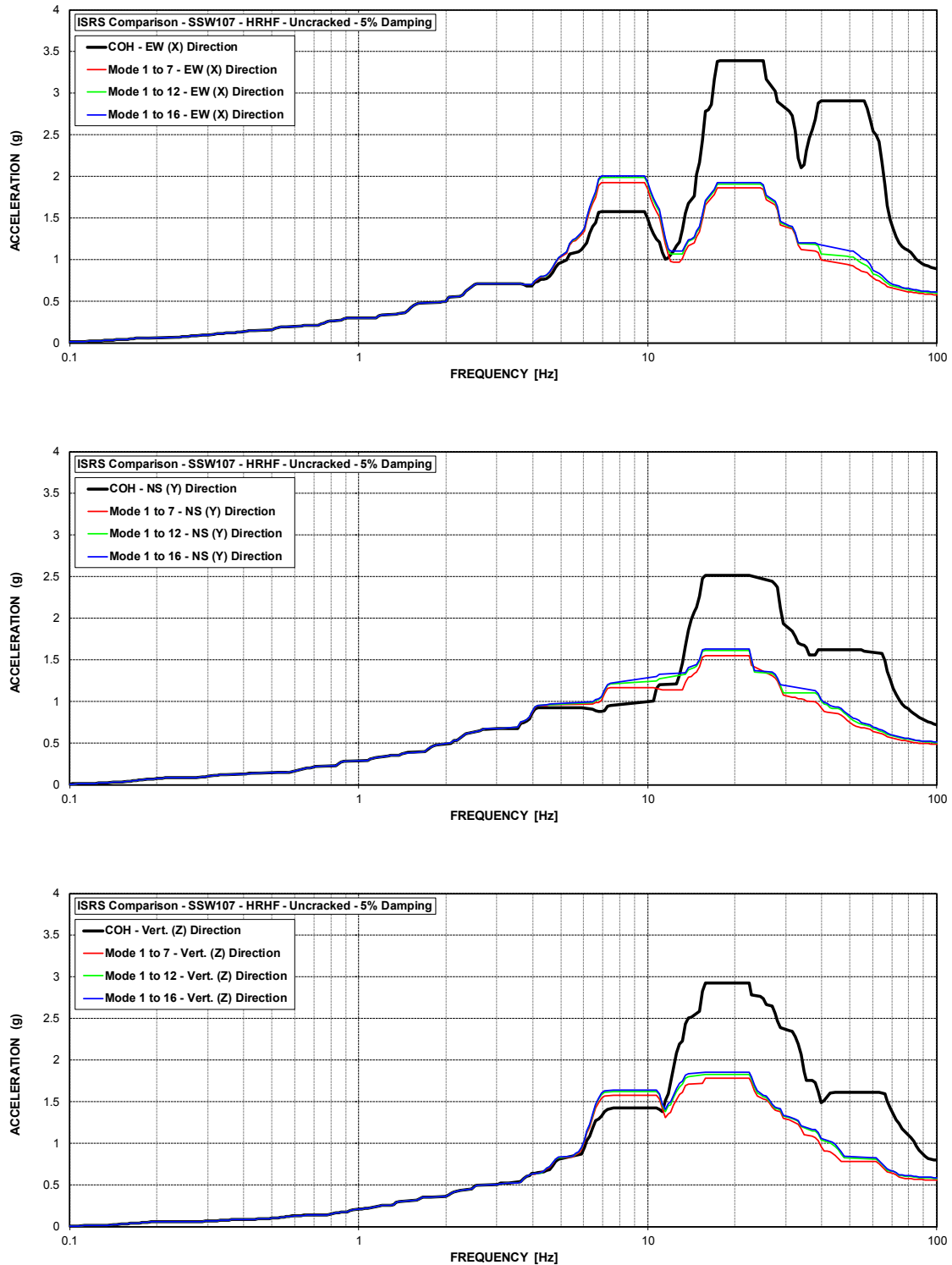


Figure C-91 ISRS – Secondary Shield Wall (SSW107) at El. 106.5' – HRHF – Uncracked

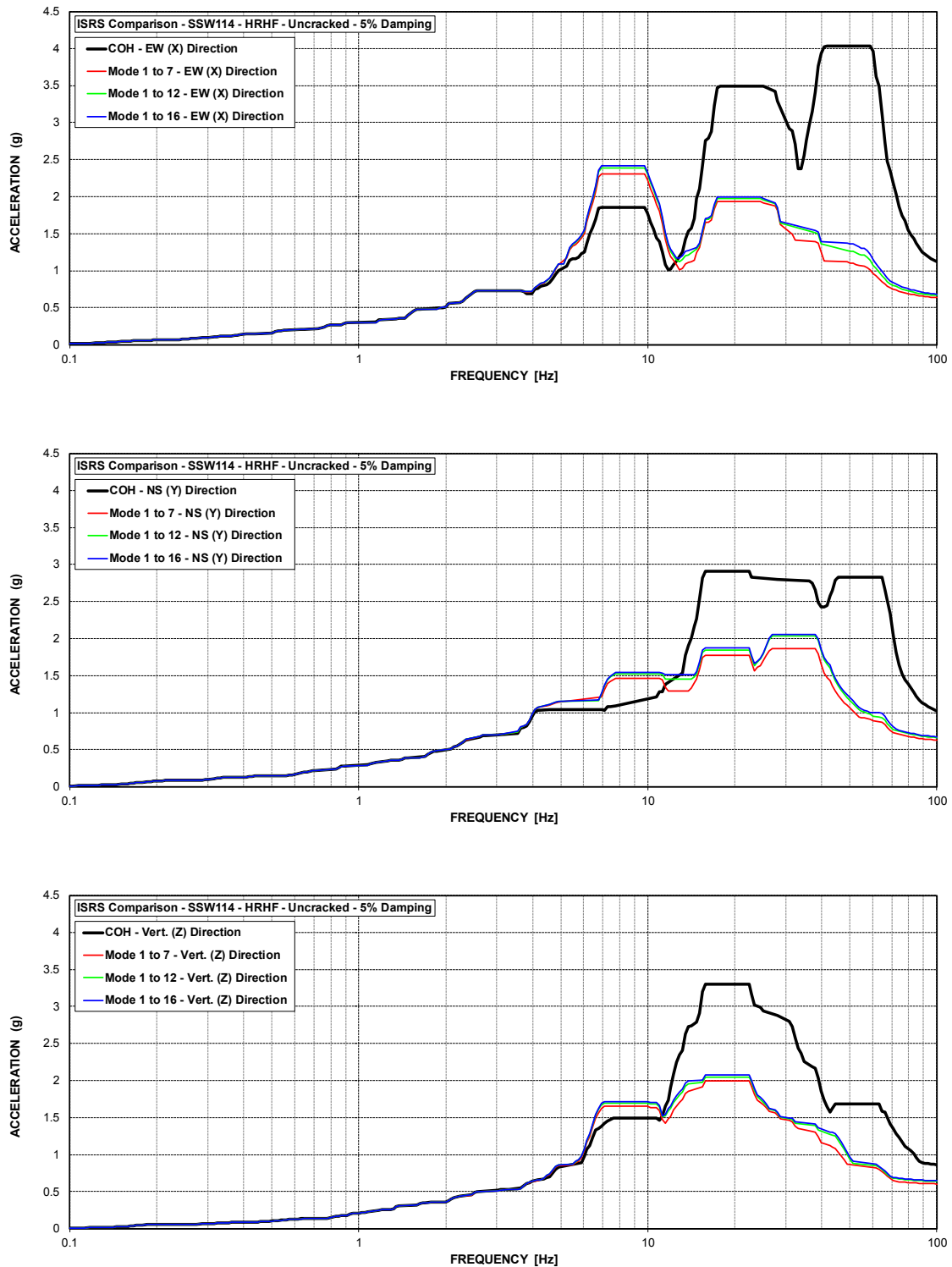


Figure C-92 ISRS – Secondary Shield Wall (SSW114) at El. 114' – HRHF – Uncracked

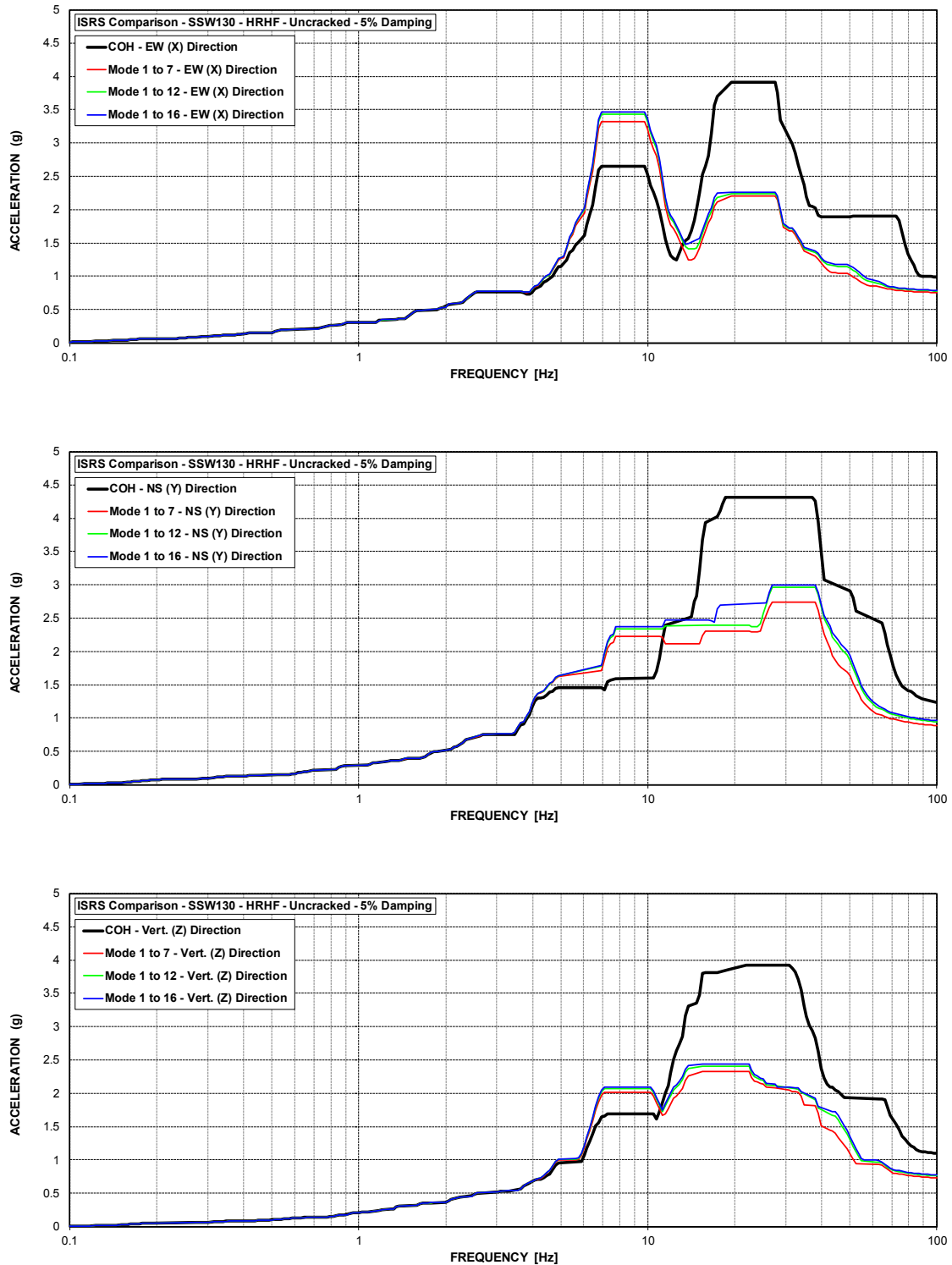


Figure C-93 ISRS – Secondary Shield Wall (SSW130) at El. 130' – HRHF – Uncracked

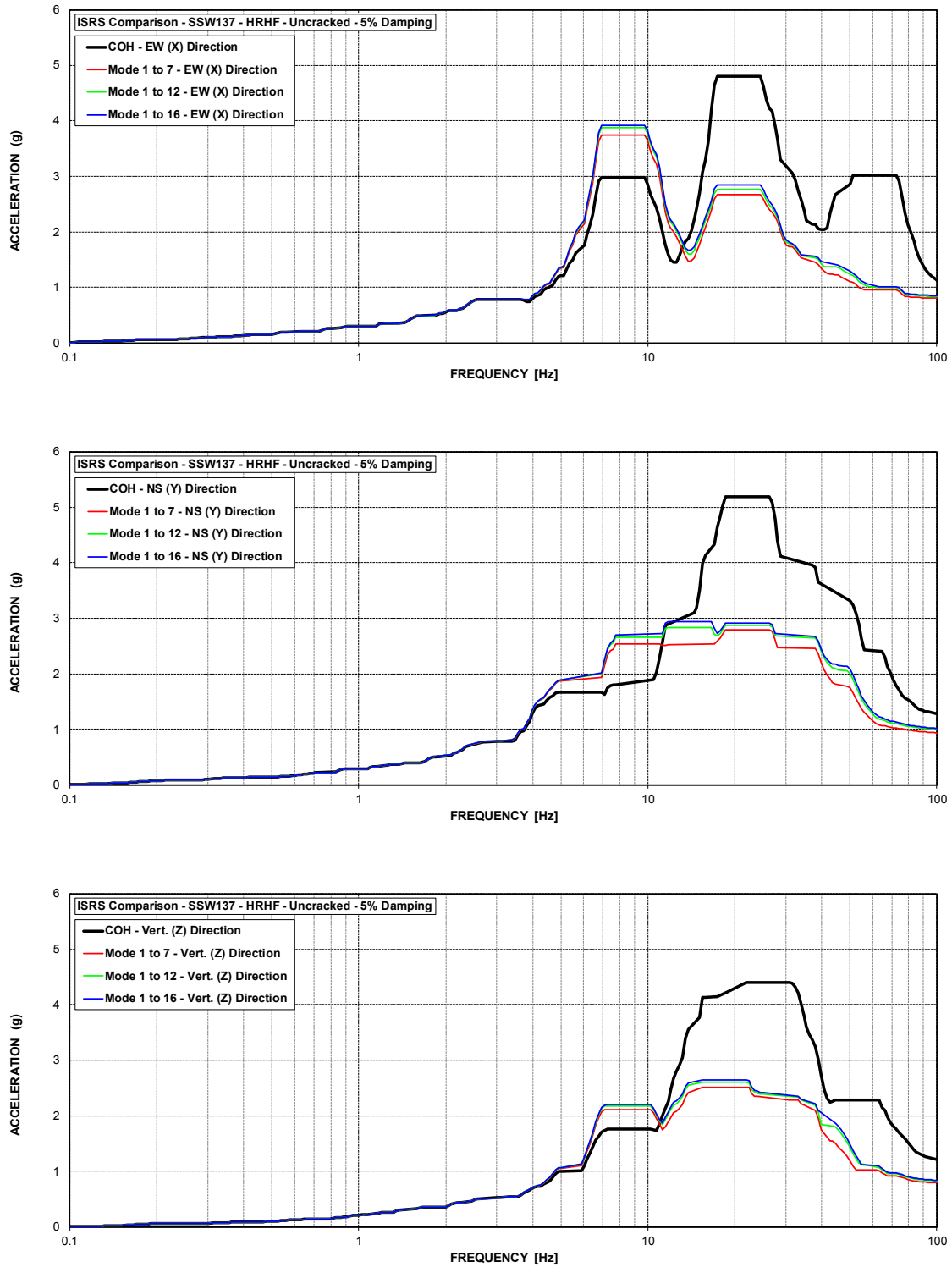


Figure C-94 ISRS – Secondary Shield Wall (SSW137) at El. 136.5' – HRHF – Uncracked

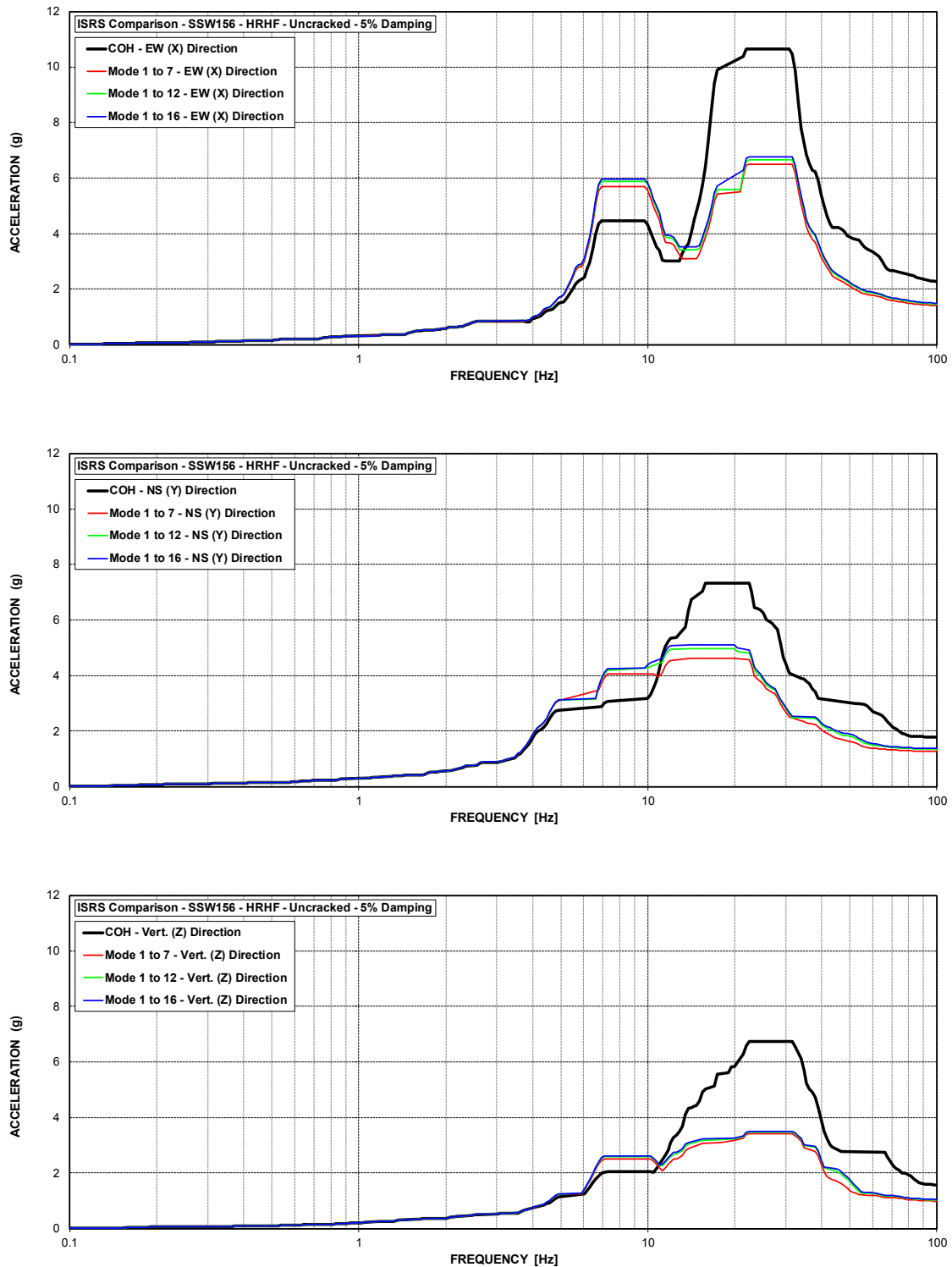


Figure C-95 ISRS – Secondary Shield Wall (SSW156) at El. 156' – HRHF – Uncracked

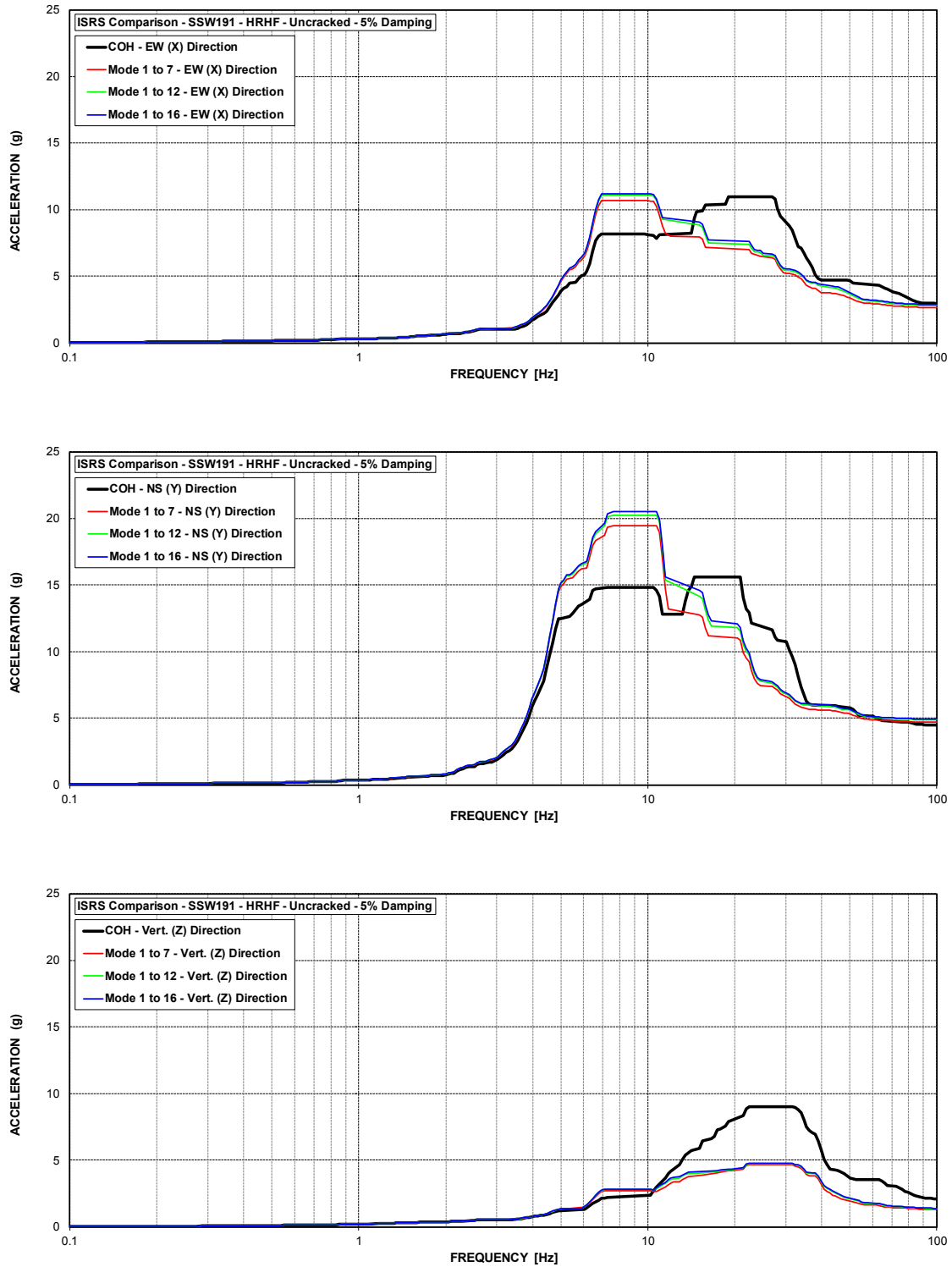


Figure C-96 ISRS – Secondary Shield Wall (SSW191) at El. 191' – HRHF – Uncracked

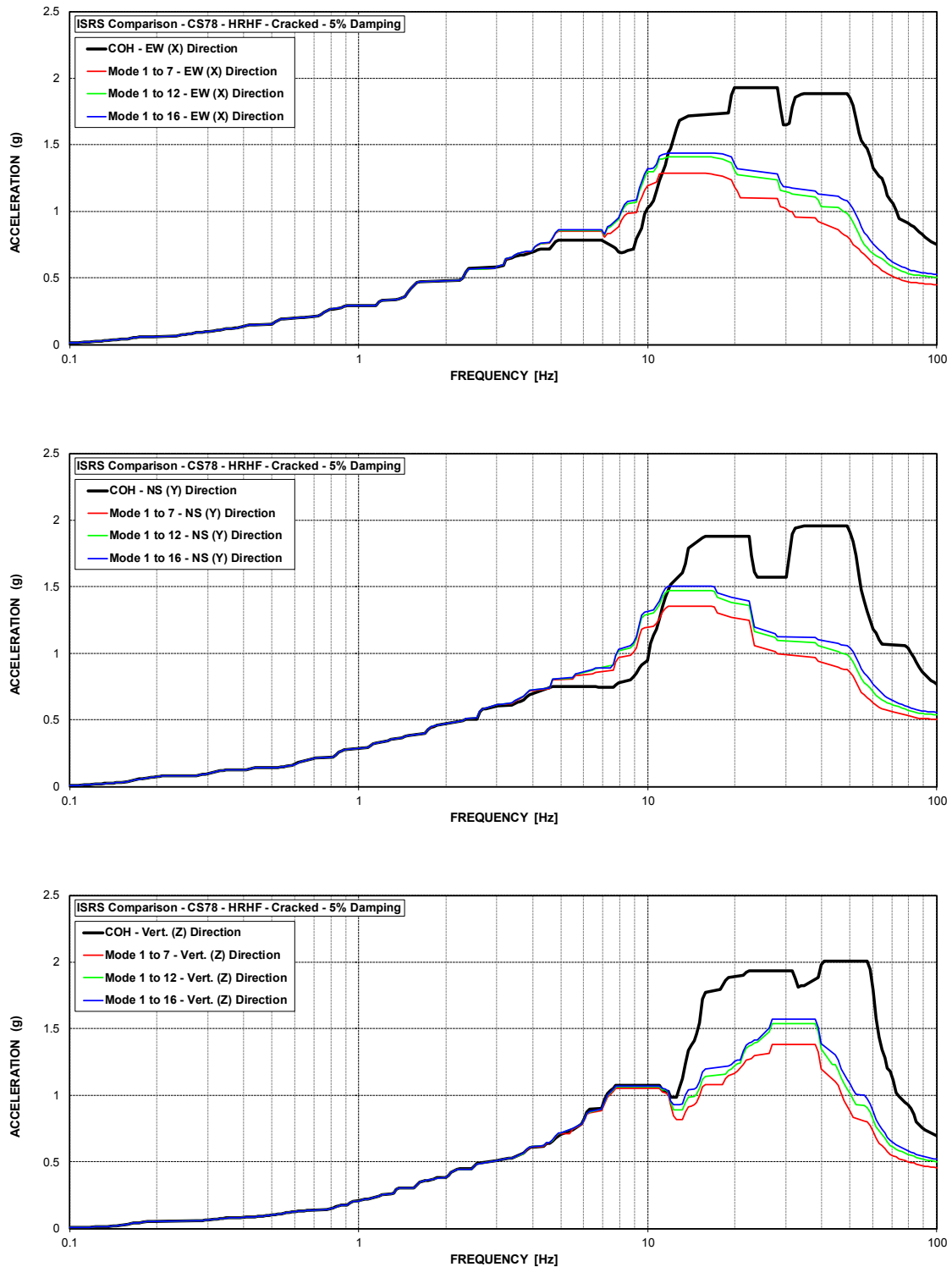


Figure C-97 ISRS – Containment Structure (CS78) at El. 78' – HRHF – Cracked

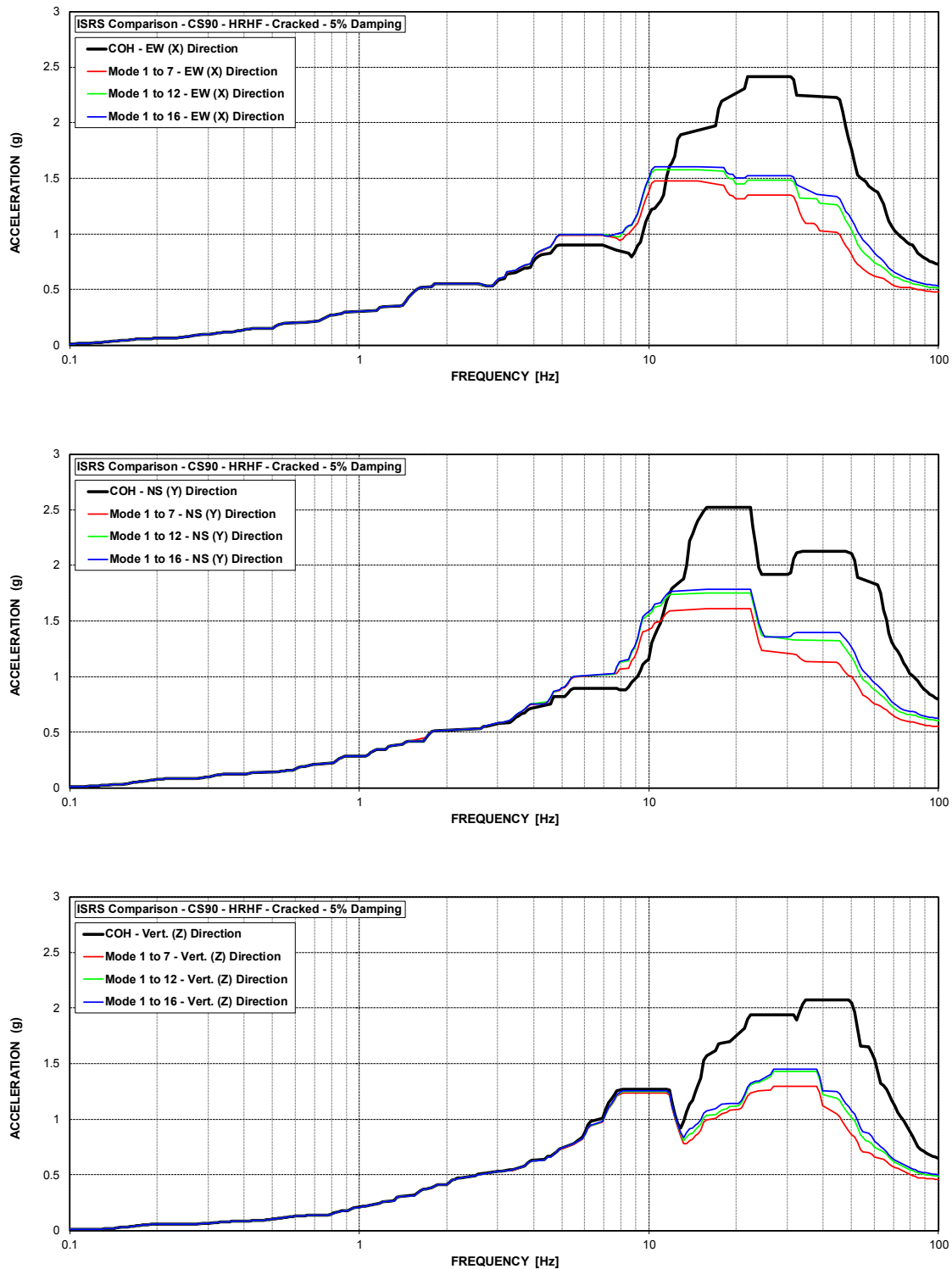


Figure C-98 ISRS – Containment Structure (CS90) at El. 89.75' – HRHF – Cracked



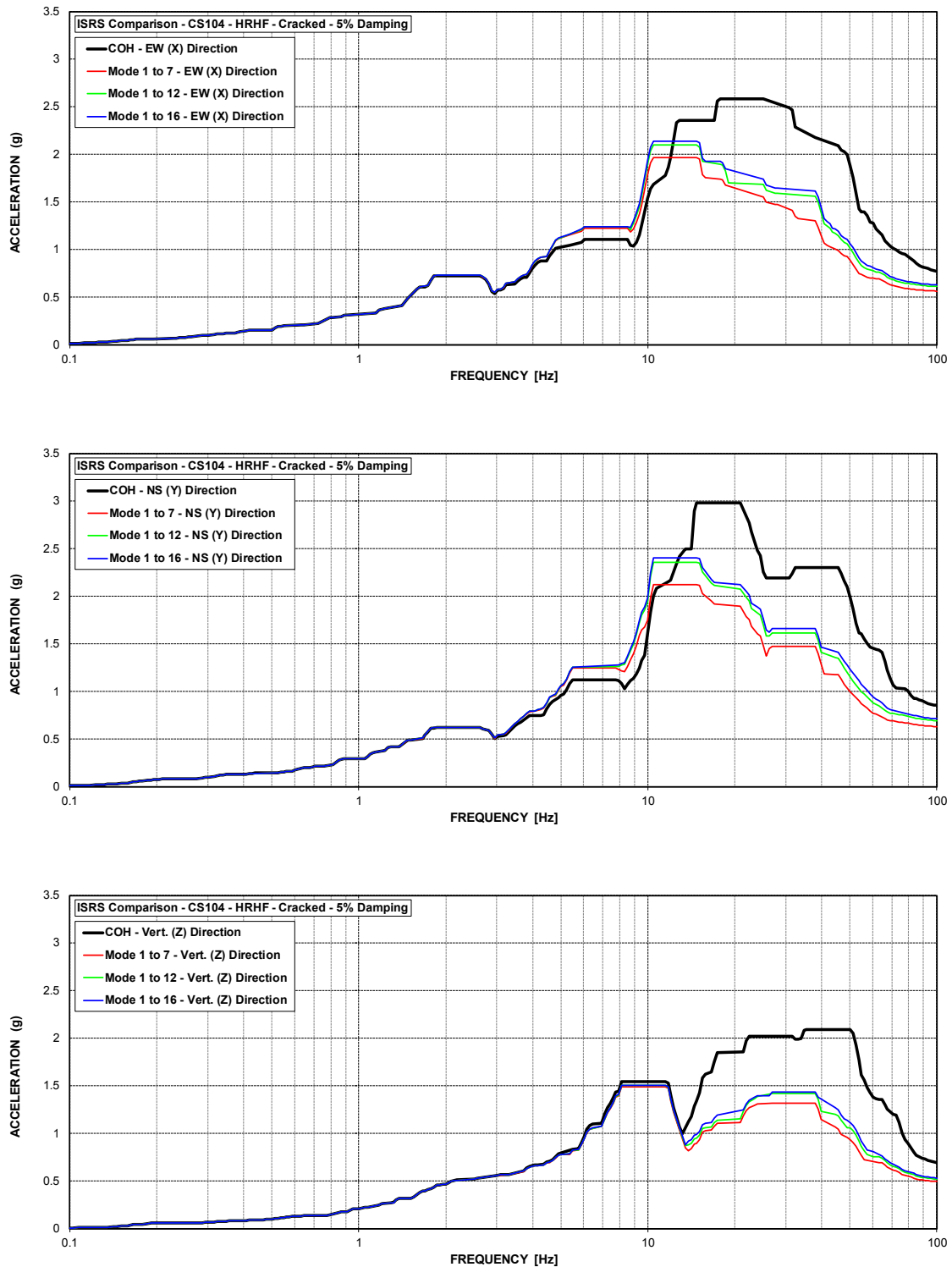


Figure C-99 ISRS – Containment Structure (CS104) at El. 103.75' – HRHF – Cracked

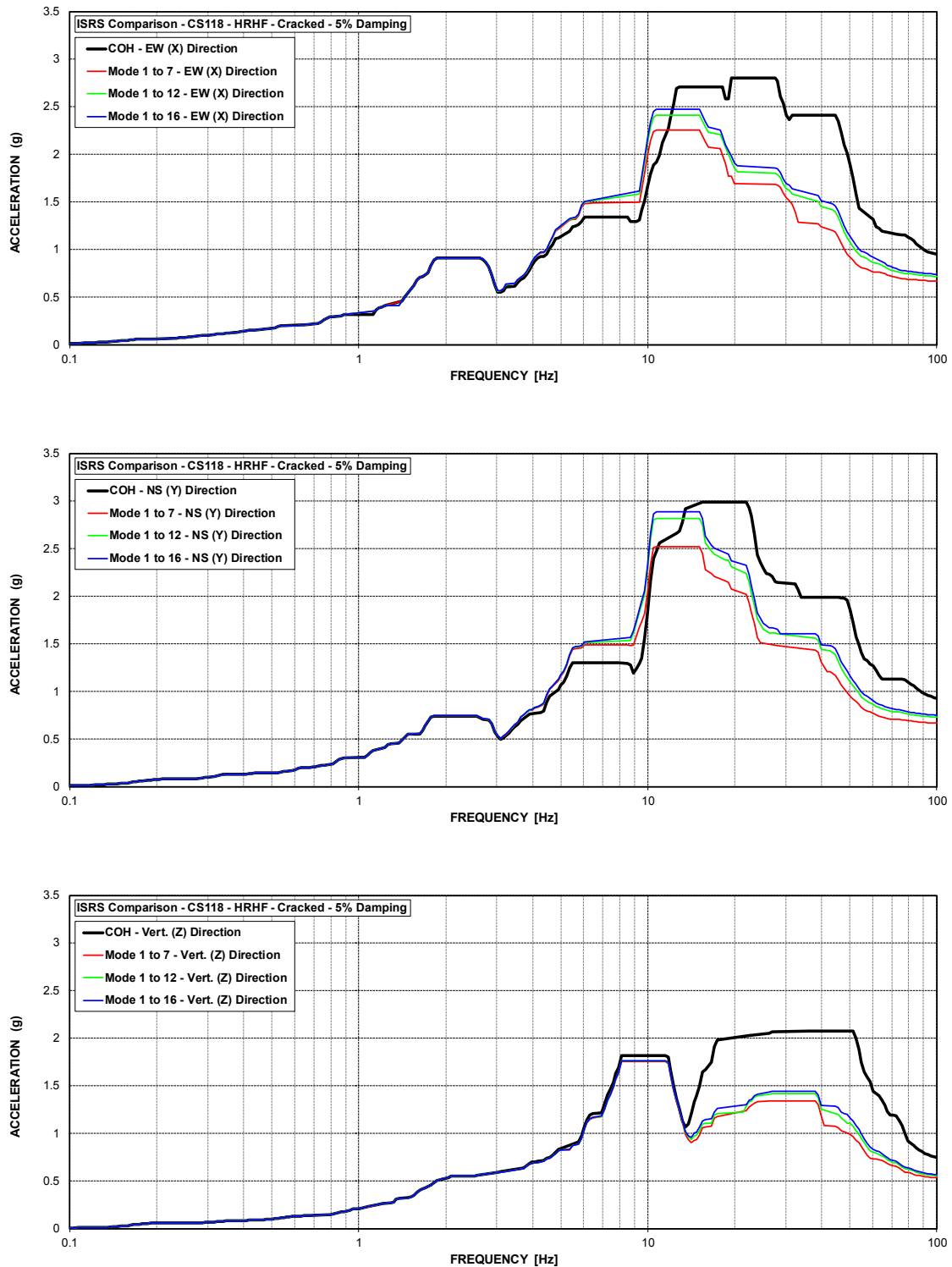


Figure C-100 ISRS – Containment Structure (CS118) at El. 117.75' – HRHF – Cracked

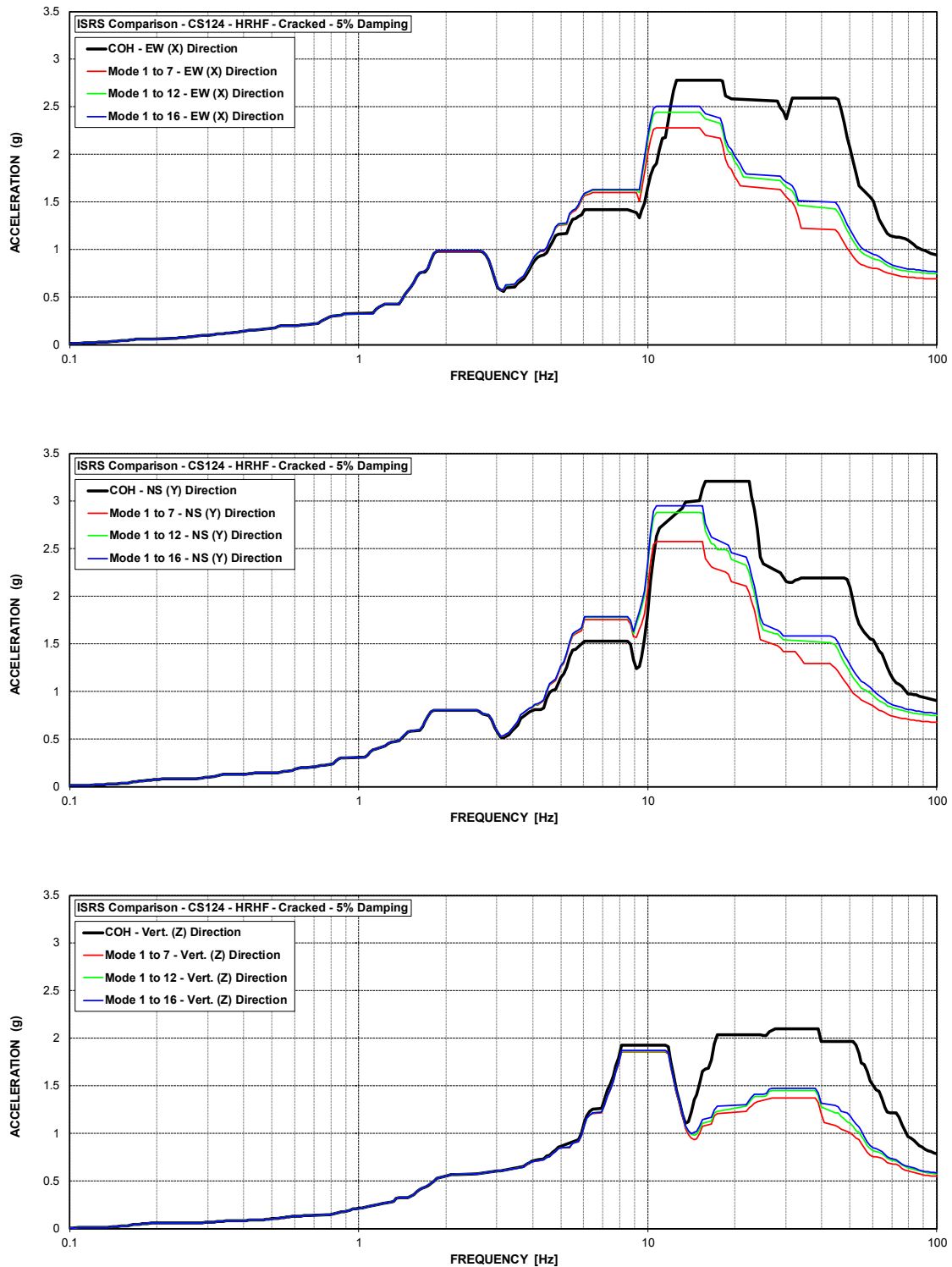


Figure C-101 ISRS – Containment Structure (CS124) at El. 123.62' – HRHF – Cracked

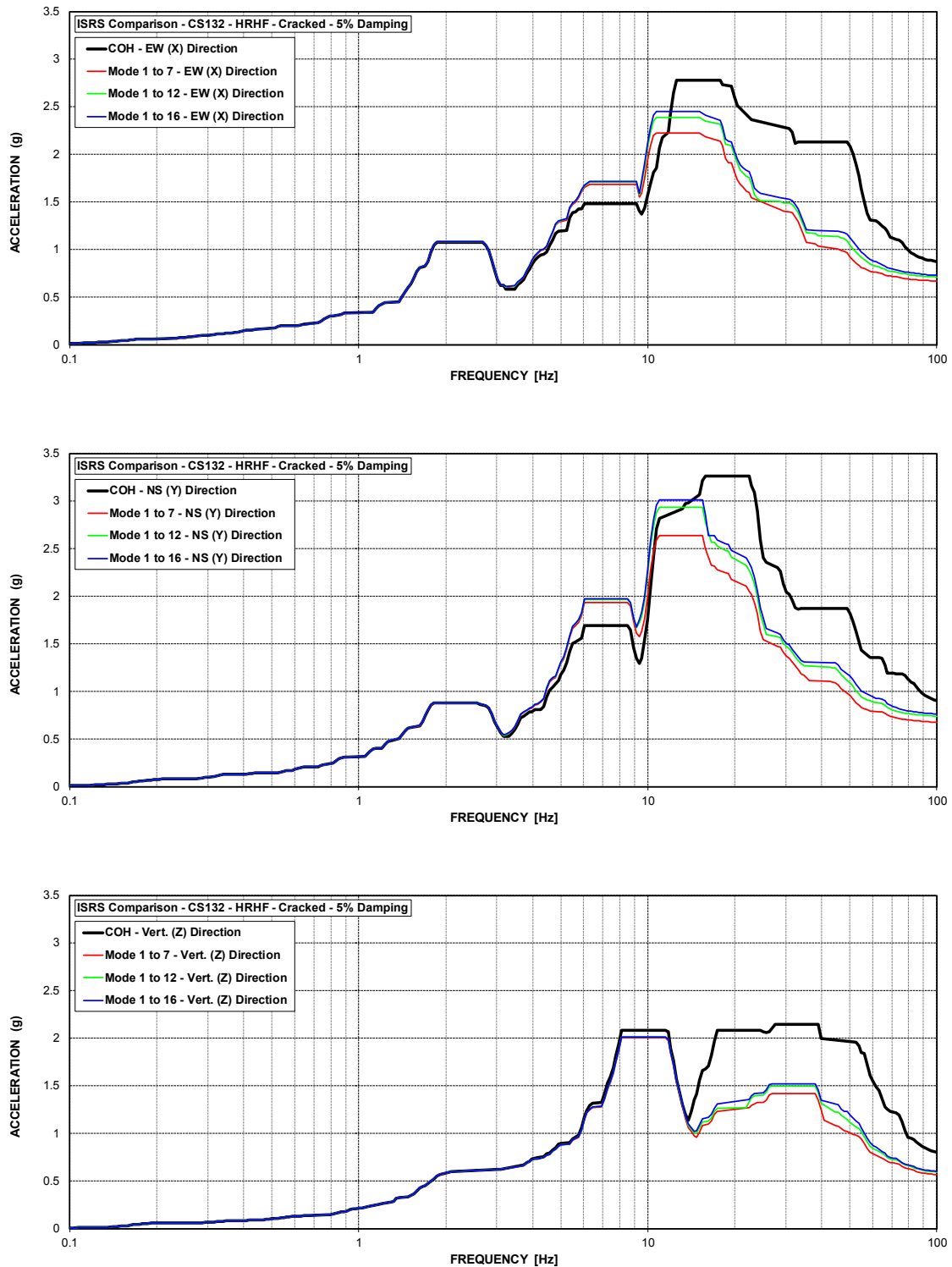


Figure C-102 ISRS – Containment Structure (CS132) at El. 131.56' – HRHF – Cracked

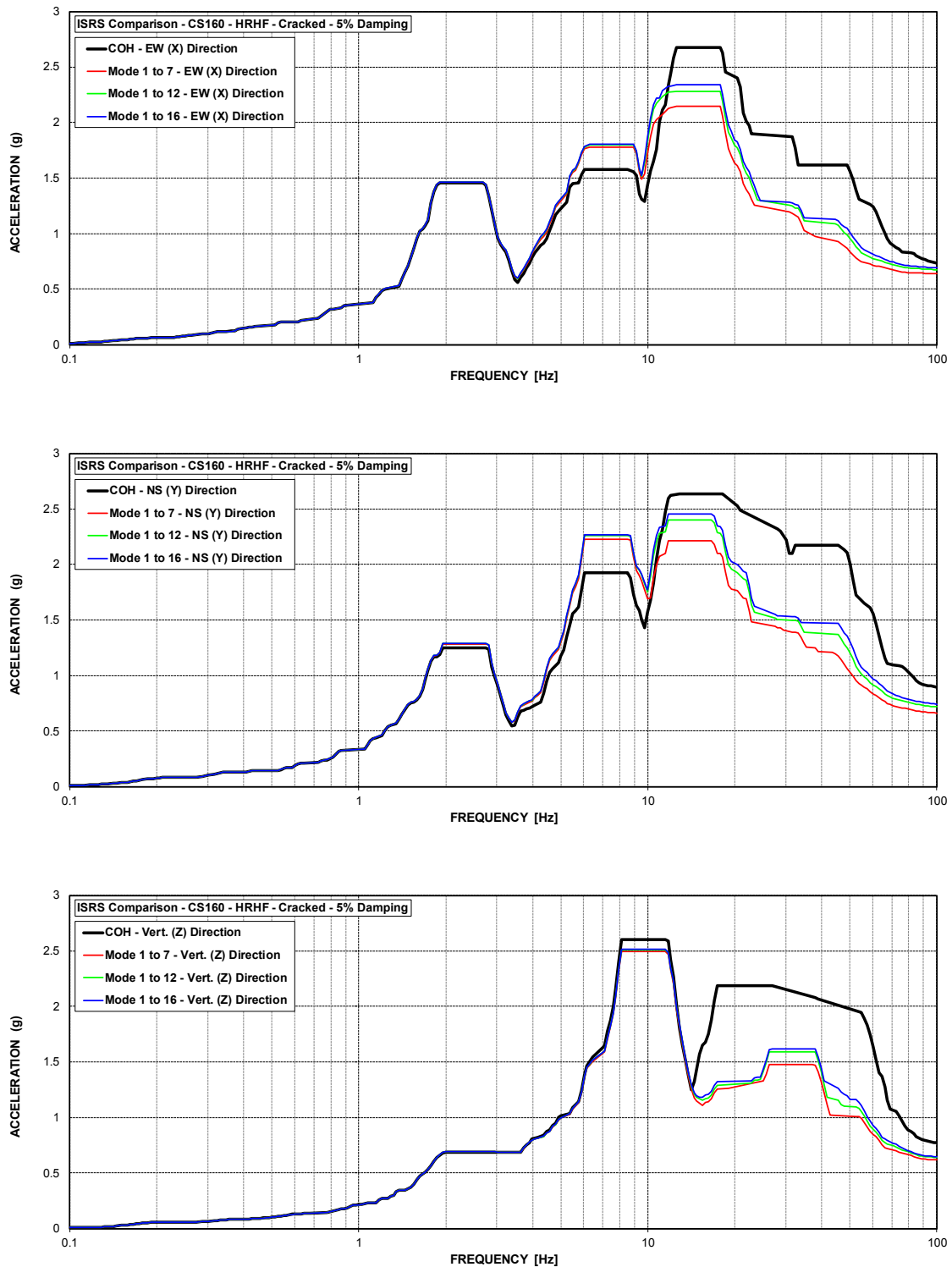


Figure C-103 ISRS – Containment Structure (CS160) at El. 159.75' – HRHF – Cracked

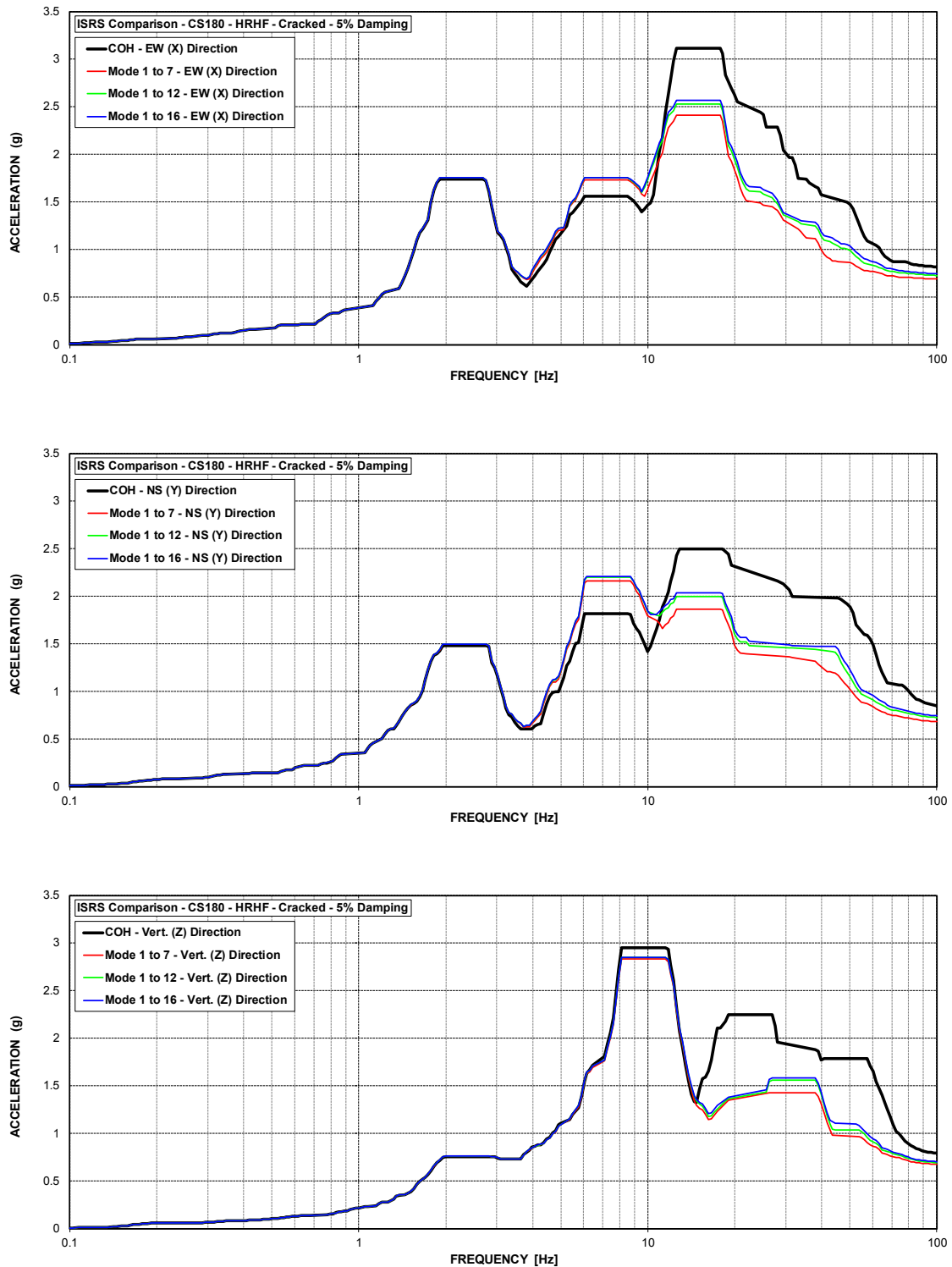


Figure C-104 ISRS – Containment Structure (CS180) at El. 180' – HRHF – Cracked

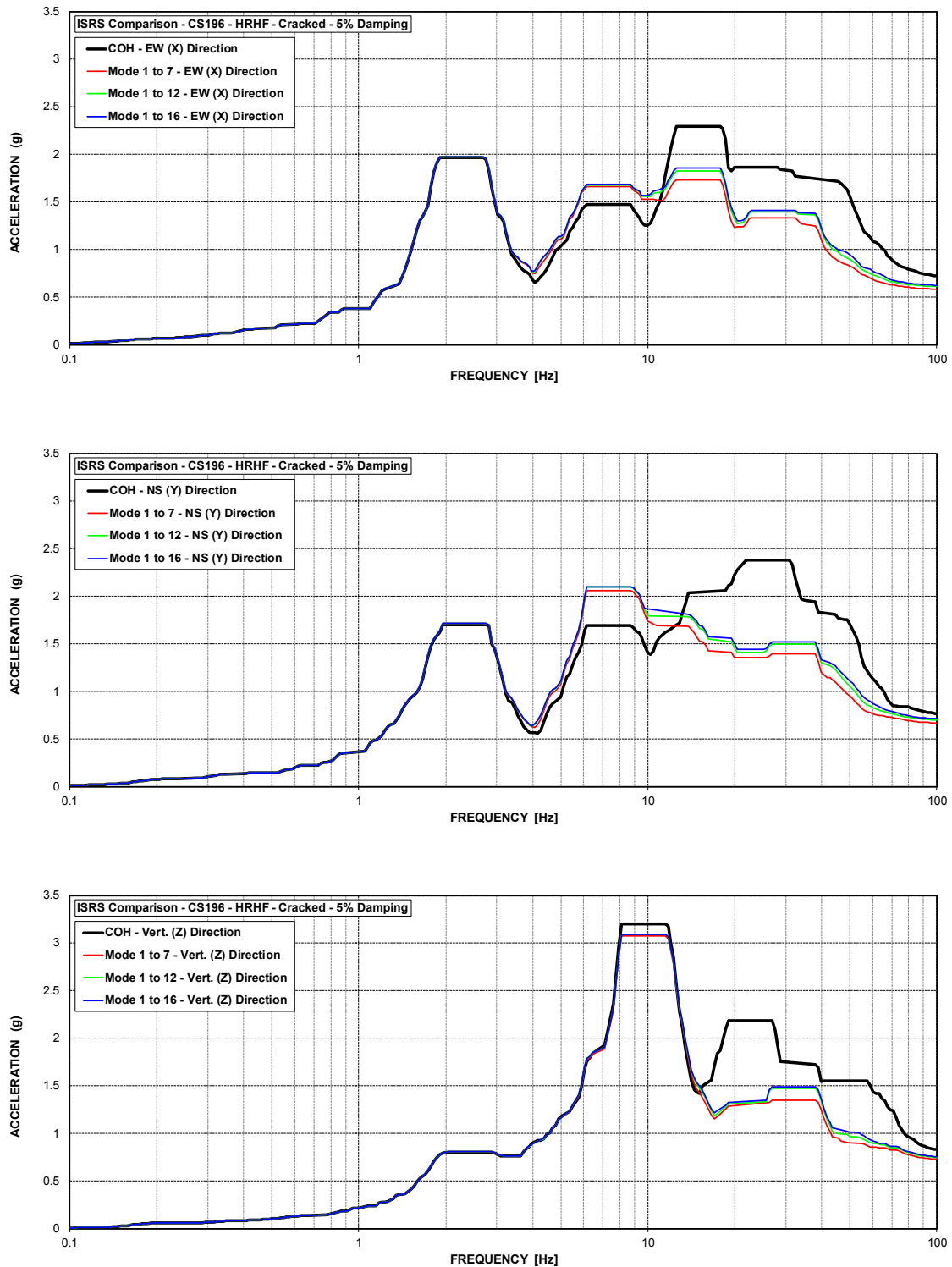


Figure C-105 ISRS – Containment Structure (CS196) at El. 195.5' – HRHF – Cracked

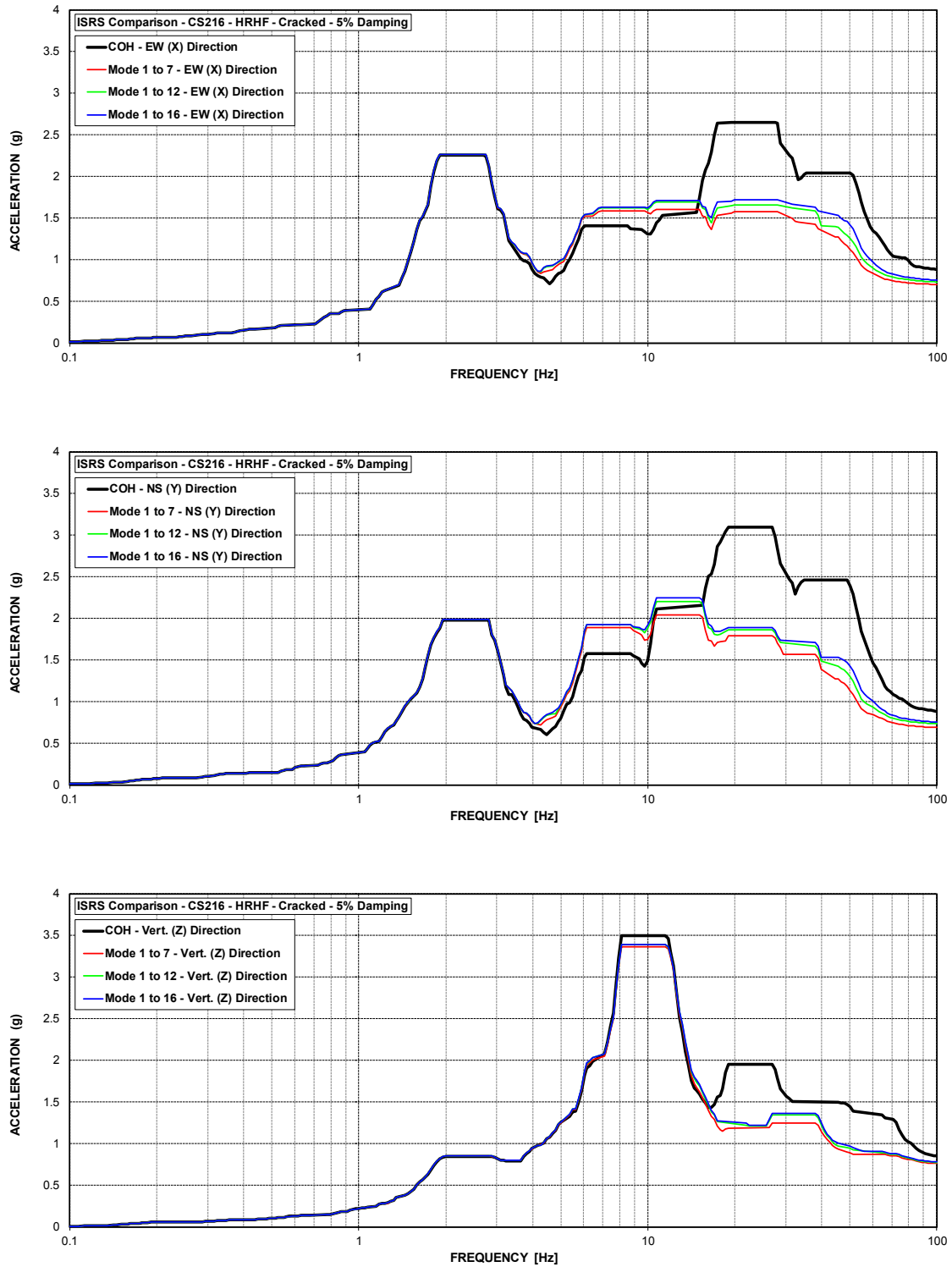


Figure C-106 ISRS – Containment Structure (CS216) at El. 215.96' – HRHF – Cracked



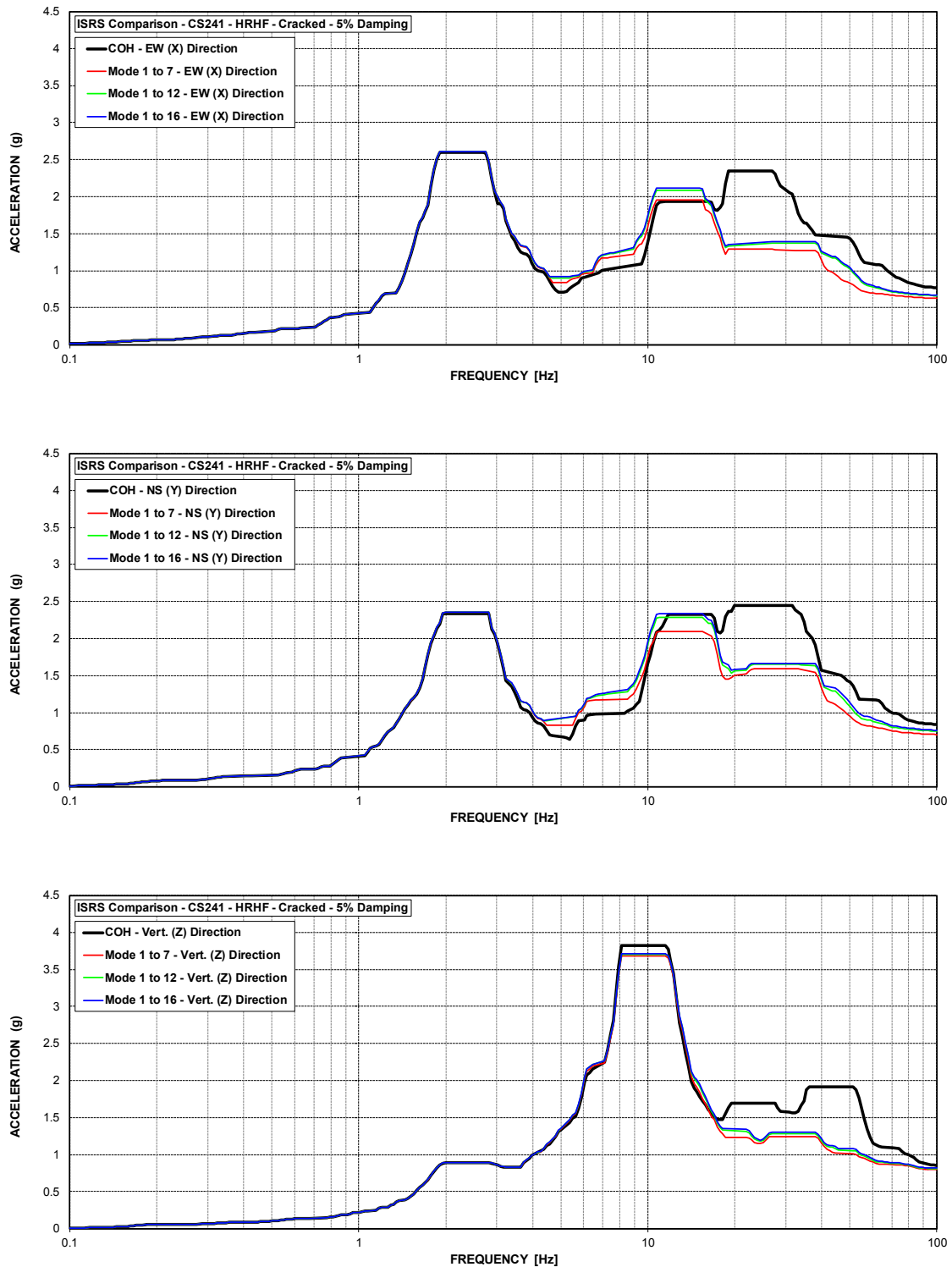


Figure C-107 ISRS – Containment Structure (CS241) at El. 241' – HRHF – Cracked

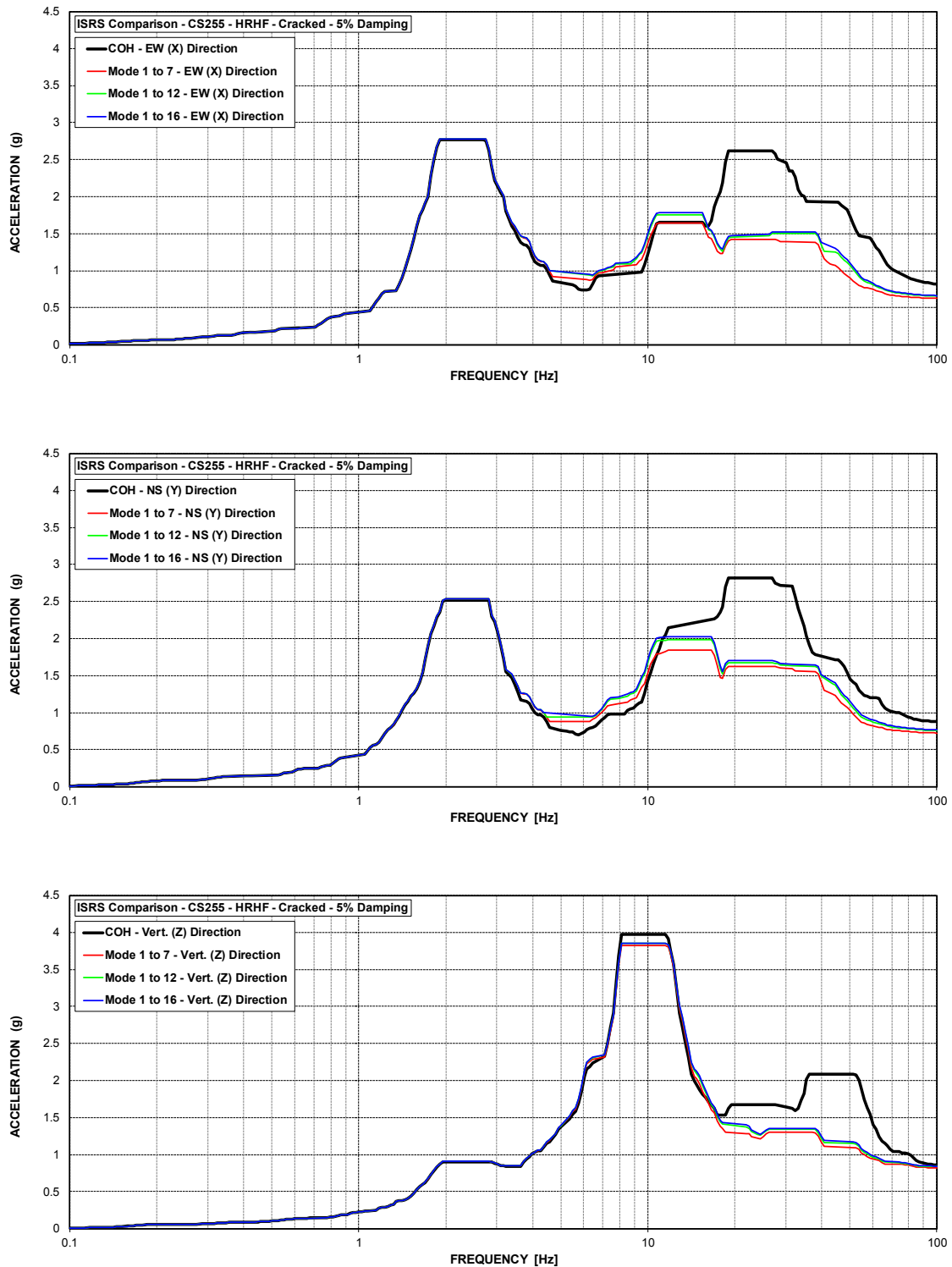


Figure C-108 ISRS – Containment Structure (CS255) at El. 254.5' – HRHF – Cracked

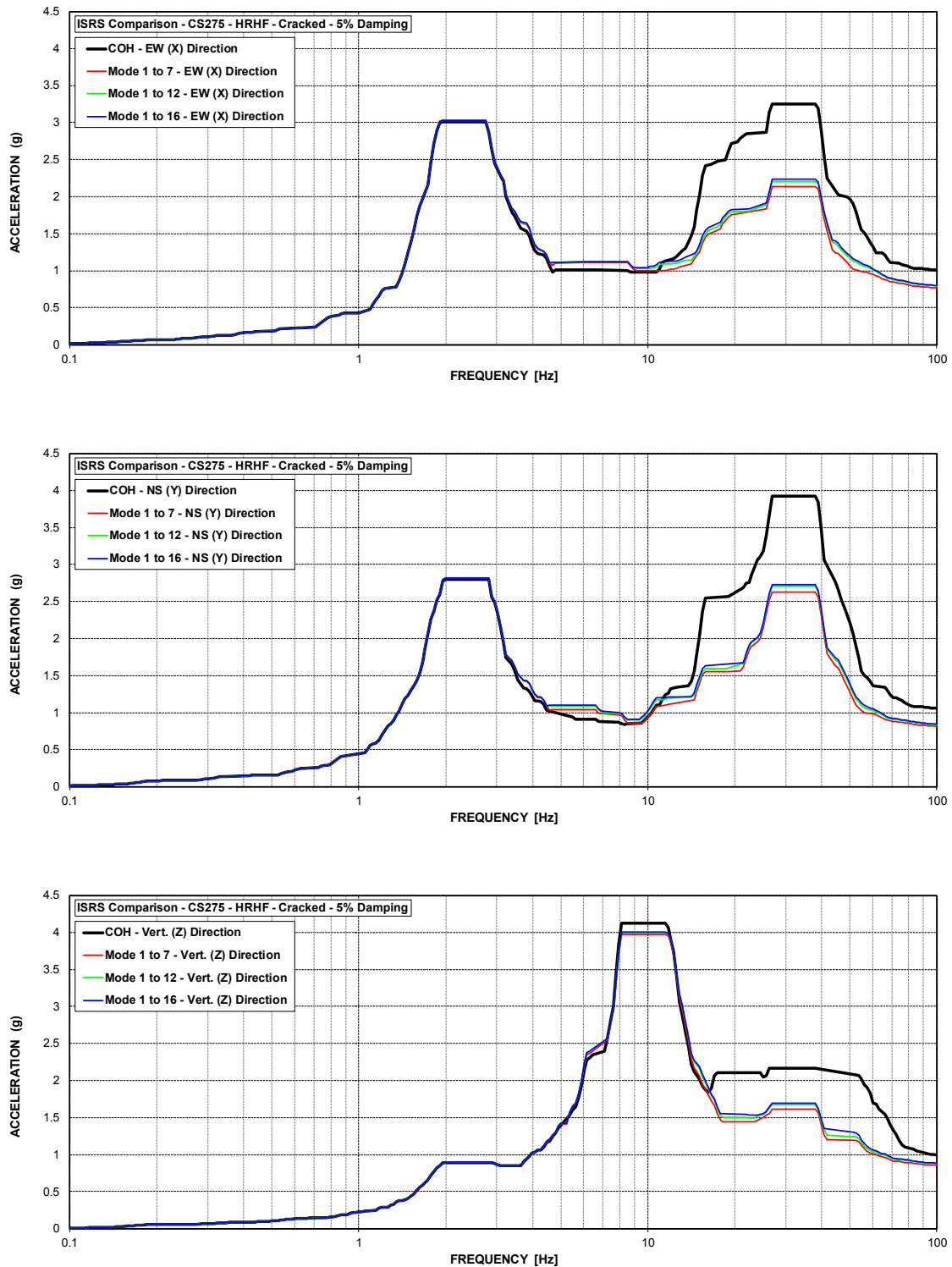


Figure C-109 ISRS – Containment Structure (CS275) at El. 274.49' – HRHF – Cracked

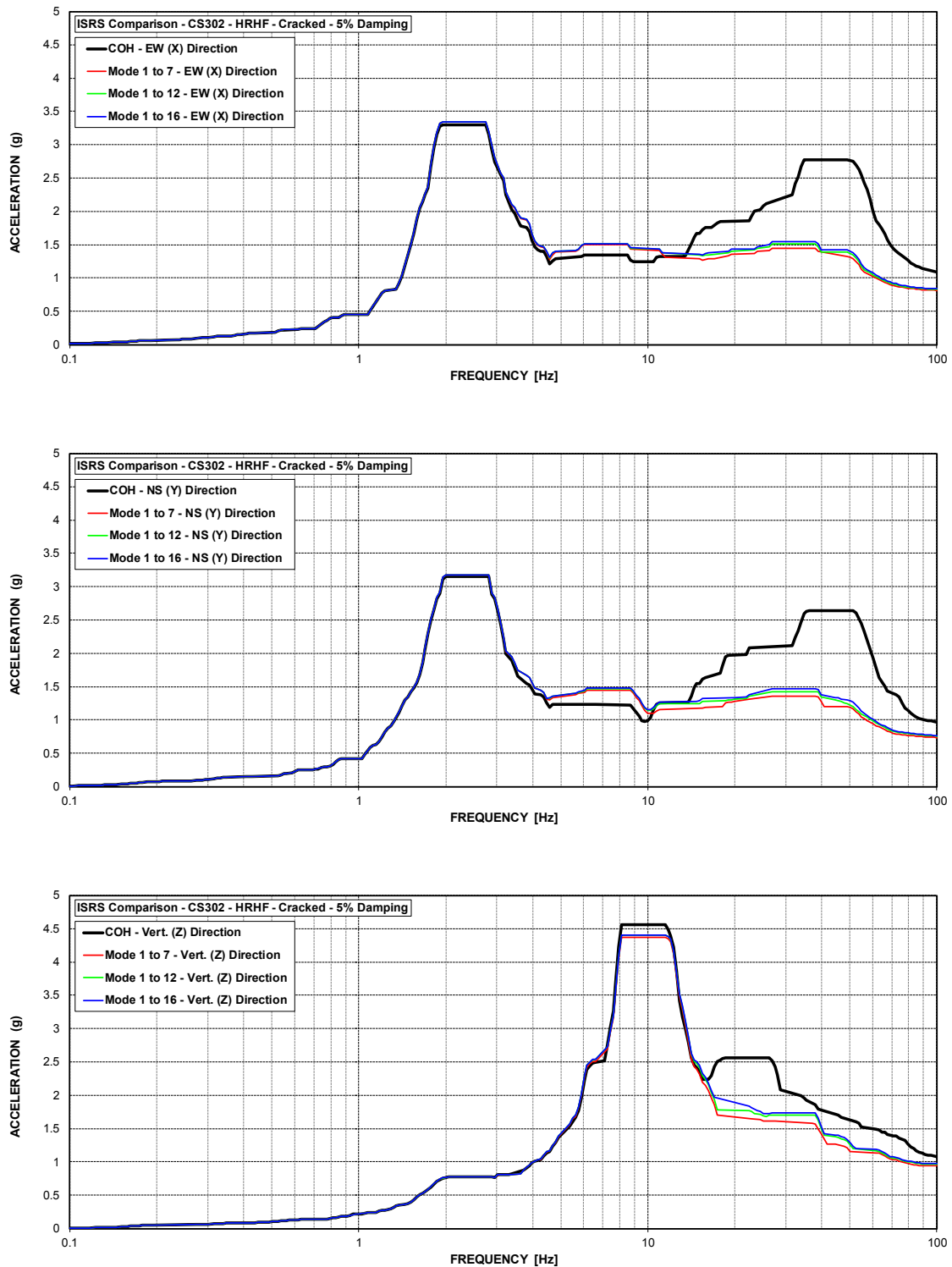


Figure C-110 ISRS – Containment Structure (CS302) at El. 301.53' – HRHF – Cracked

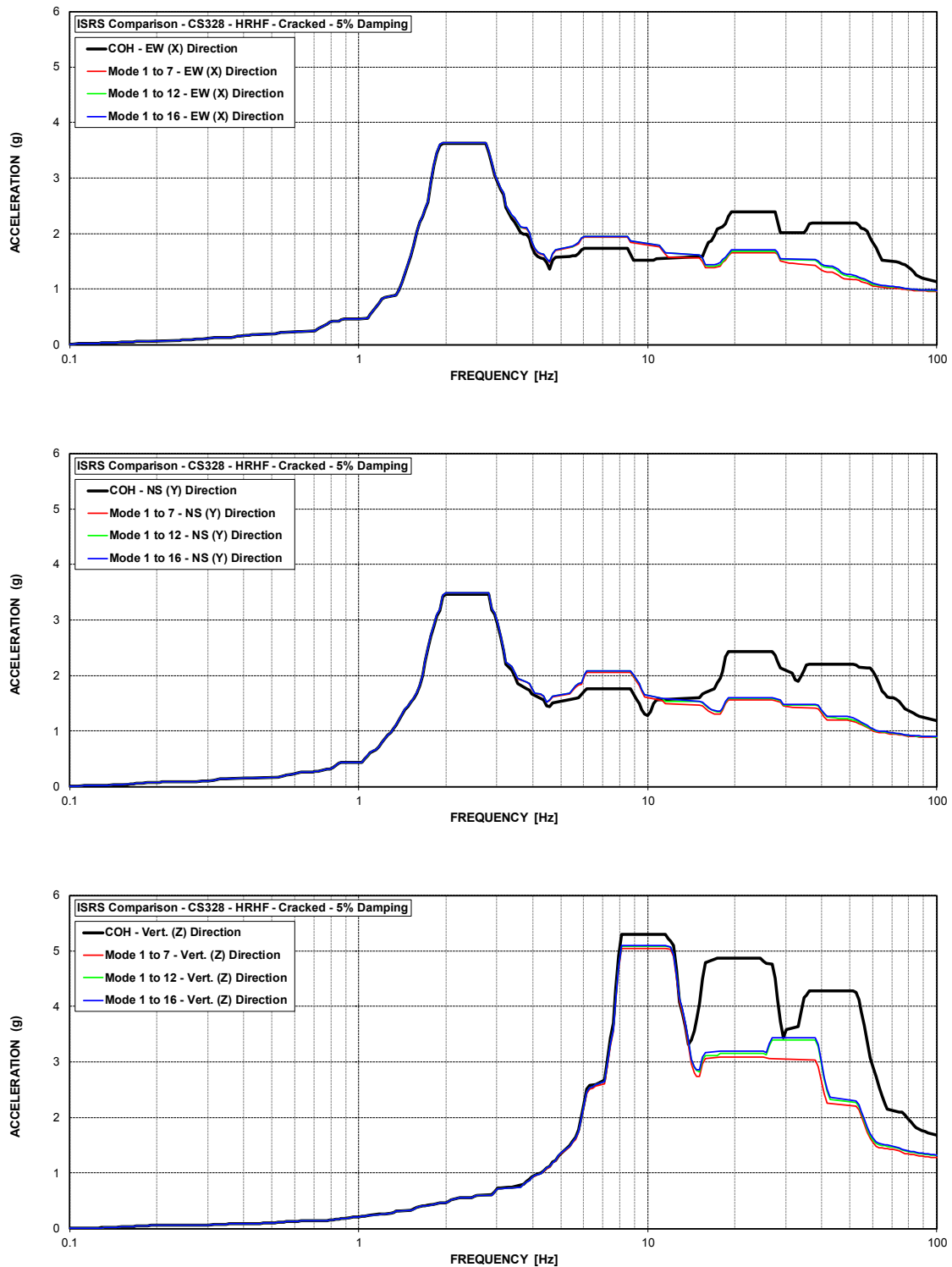


Figure C-111 ISRS – Containment Structure (CS328) at El. 328.42' – HRHF – Cracked

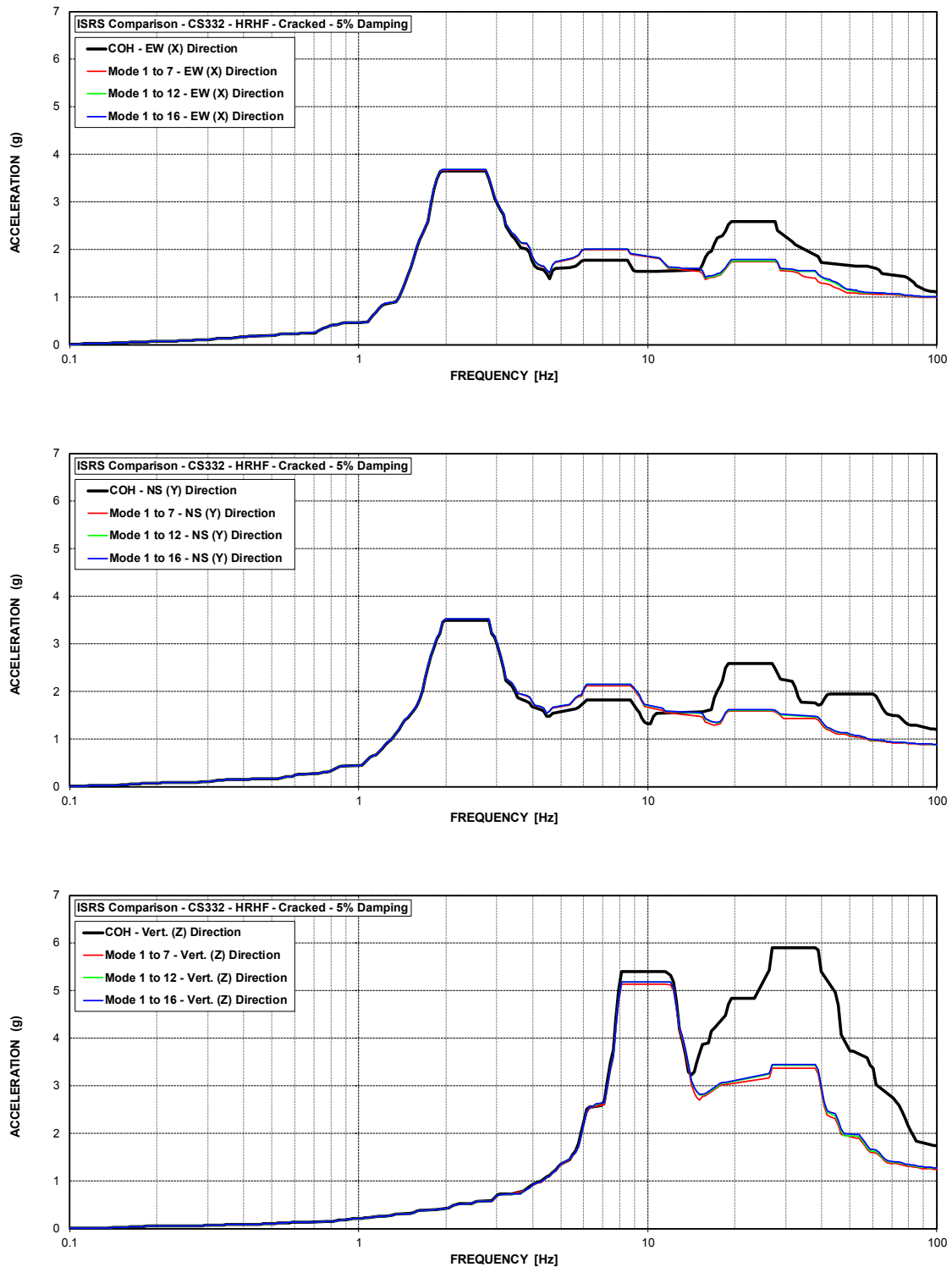


Figure C-112 ISRS – Containment Structure (CS332) at El. 331.75' – HRHF – Cracked

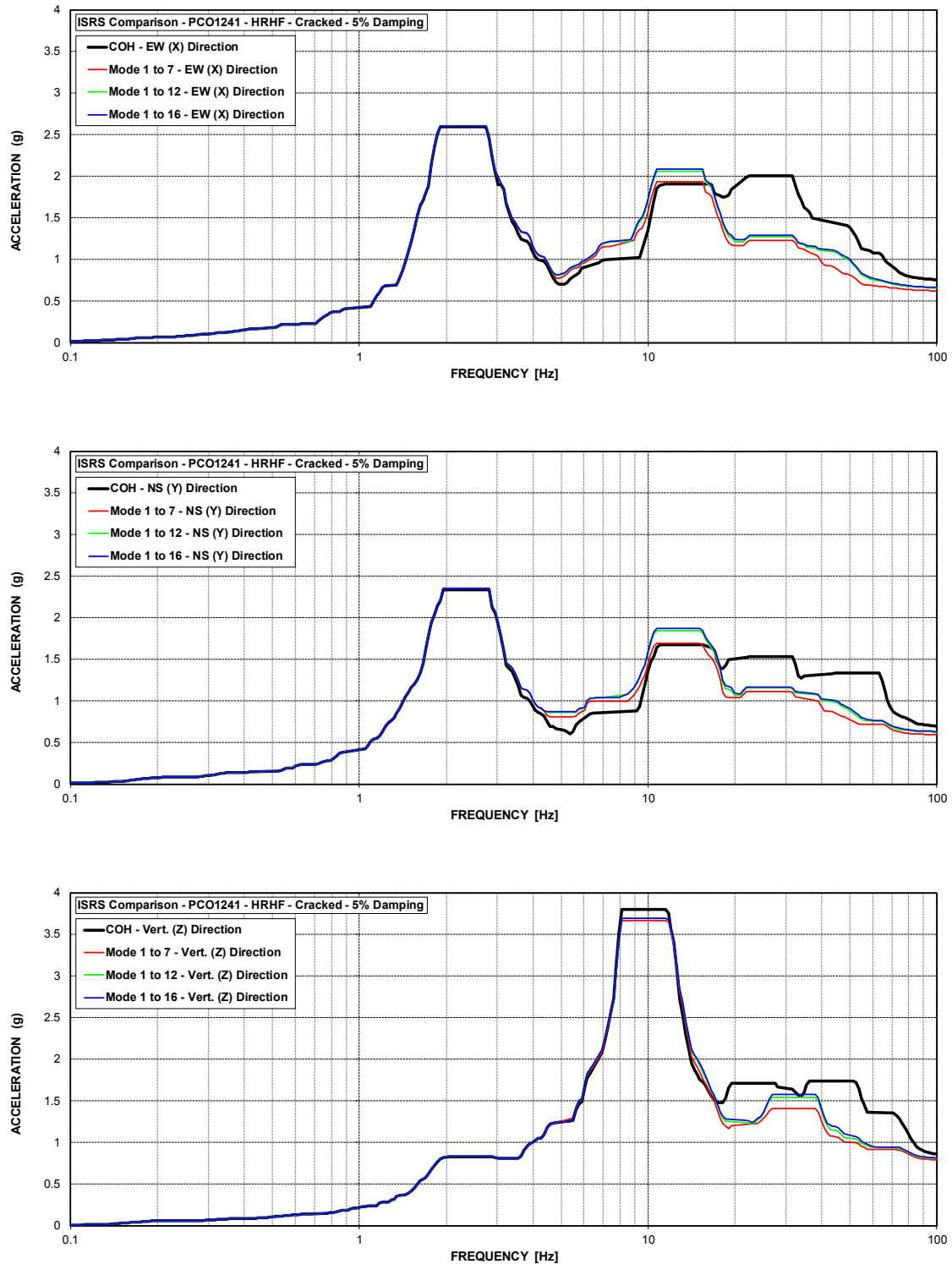


Figure C-113 ISRS – Polar Crane (PCO1241) at El. 241' – HRHF – Cracked

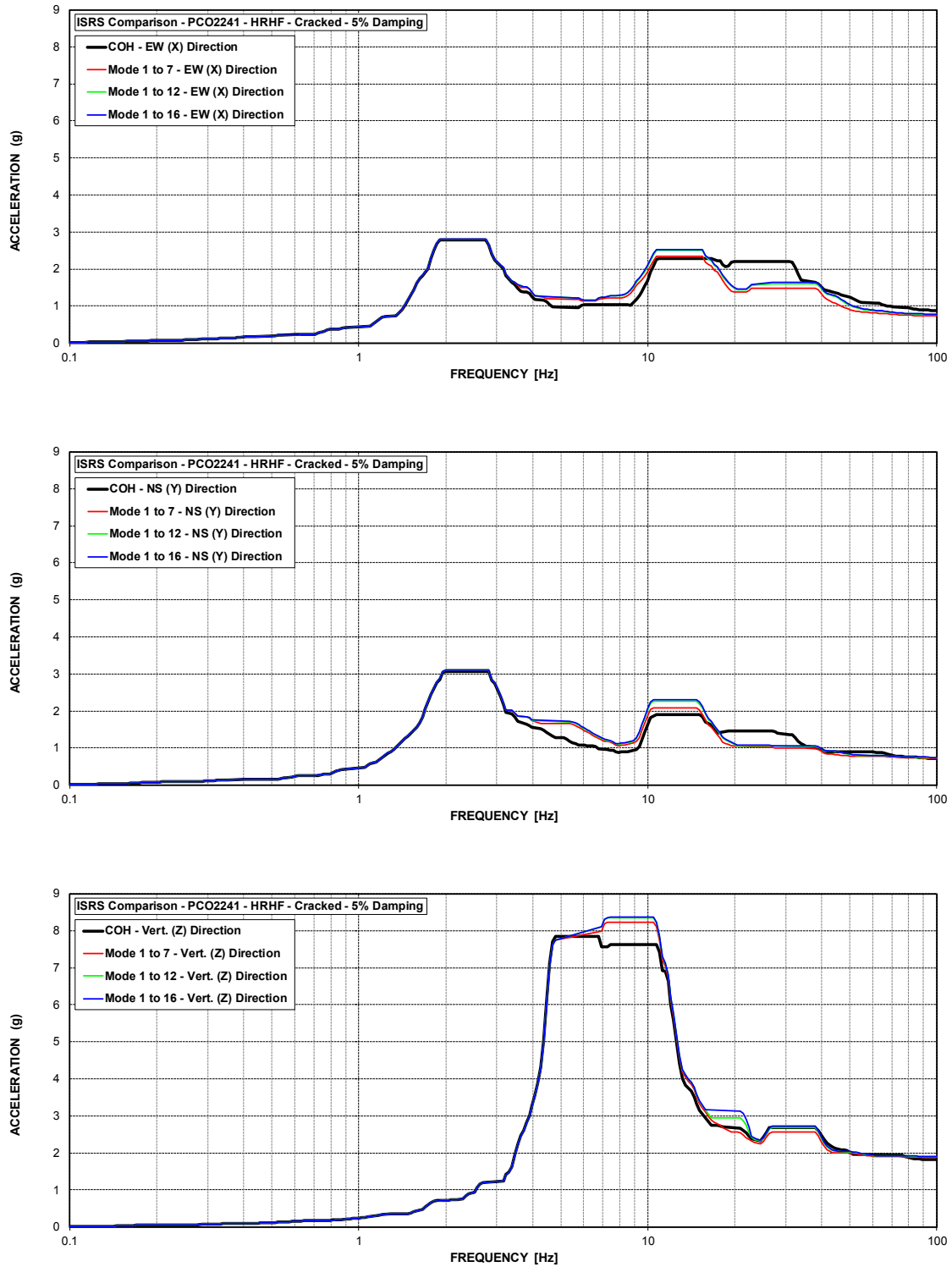


Figure C-114 ISRS – Polar Crane (PCO2241) at El. 241' – HRHF – Cracked



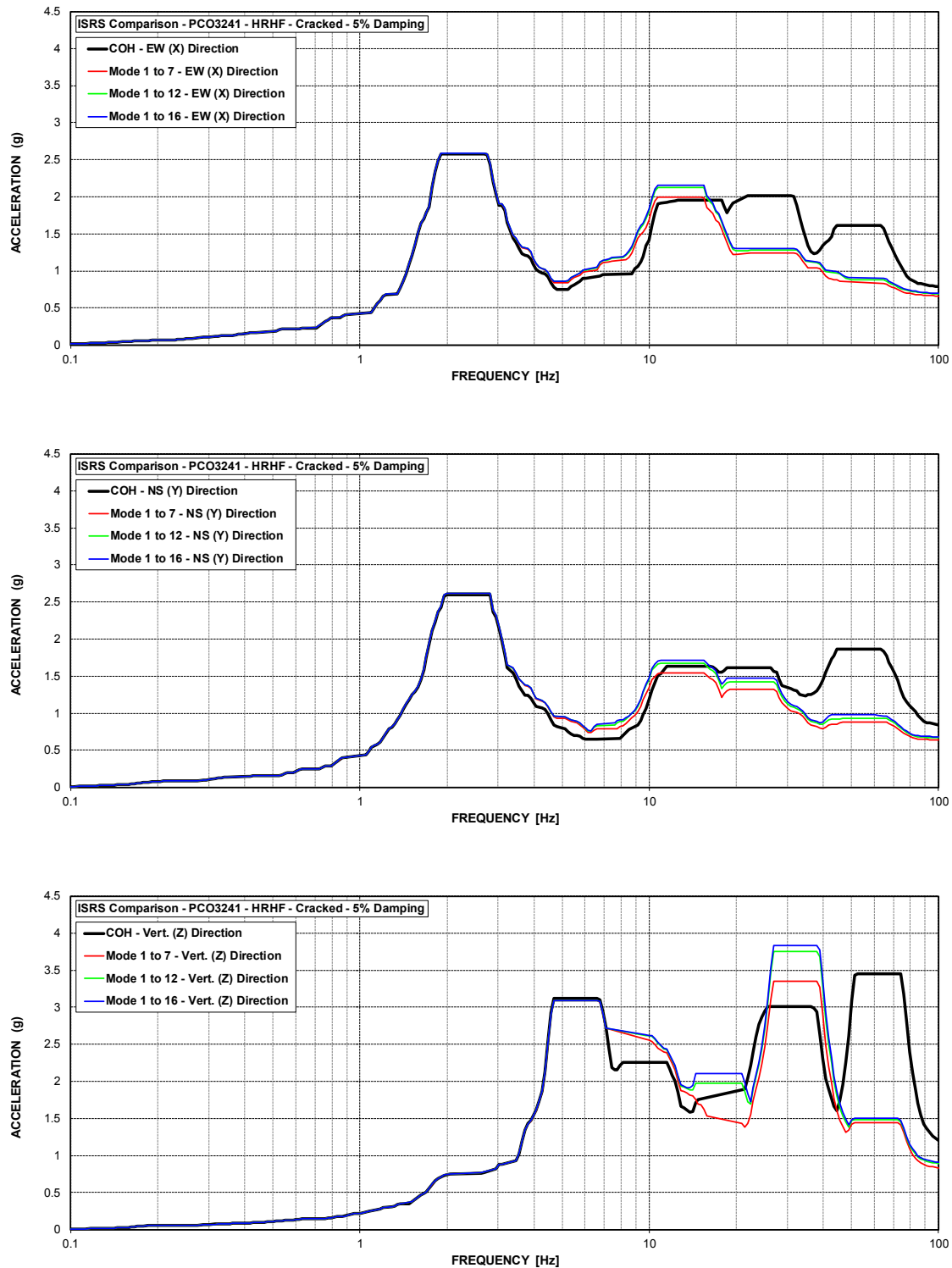


Figure C-115 ISRS – Polar Crane (PCO3241) at El. 241' – HRHF – Cracked

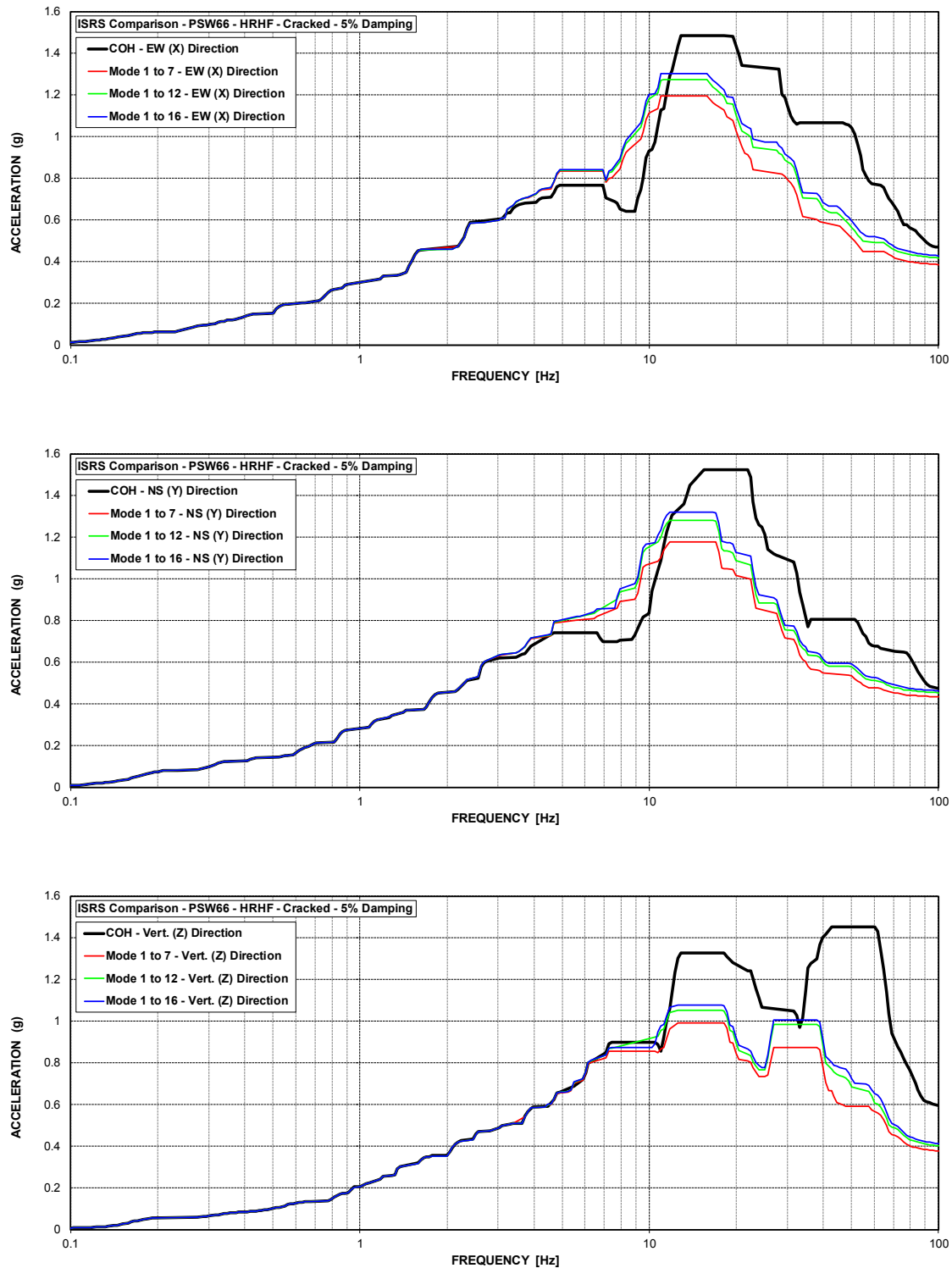


Figure C-116 ISRS – Primary Shield Wall (PSW66) at El. 66' – HRHF – Cracked

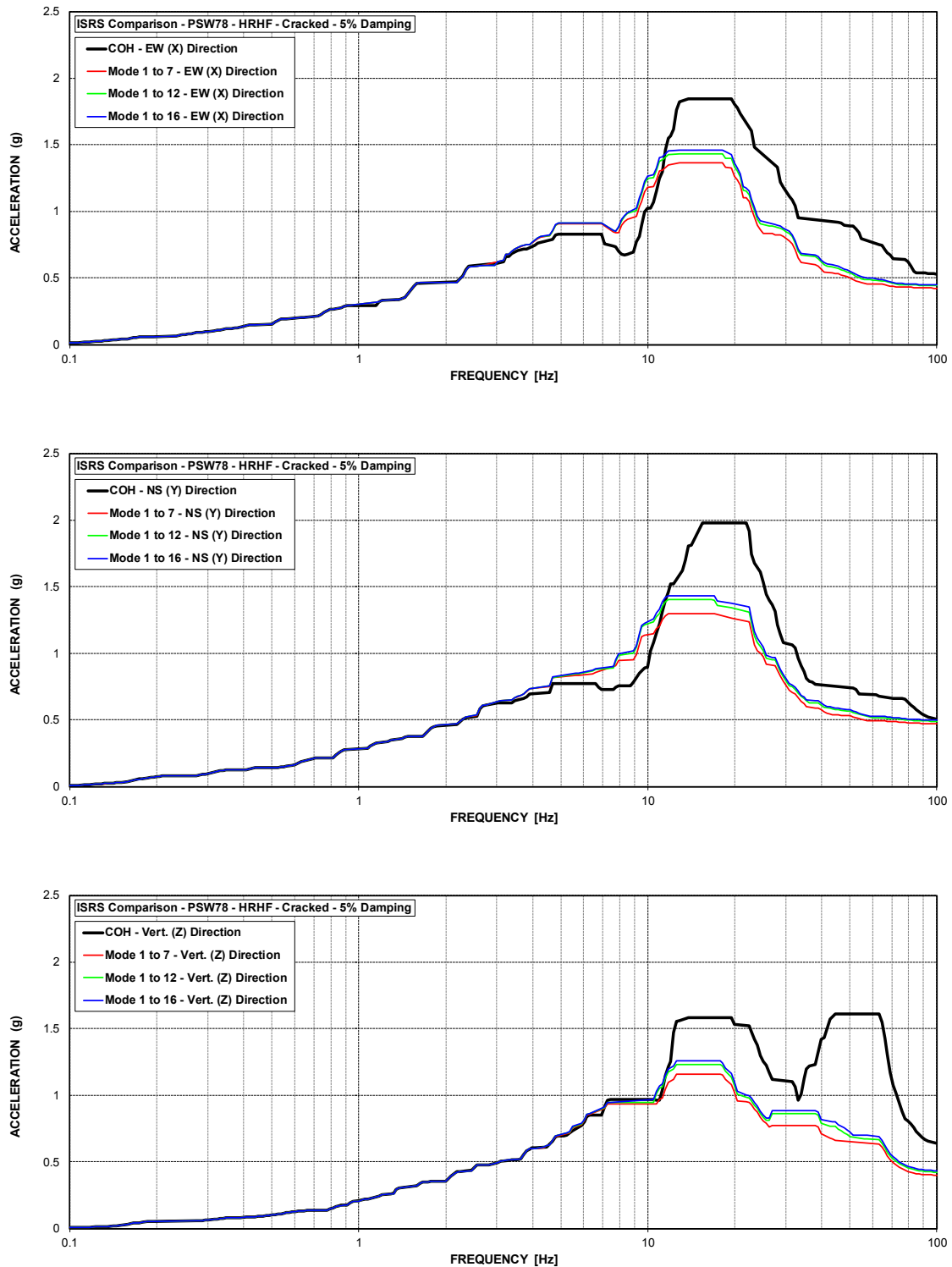


Figure C-117 ISRS – Primary Shield Wall (PSW78) at El. 78' – HRHF – Cracked

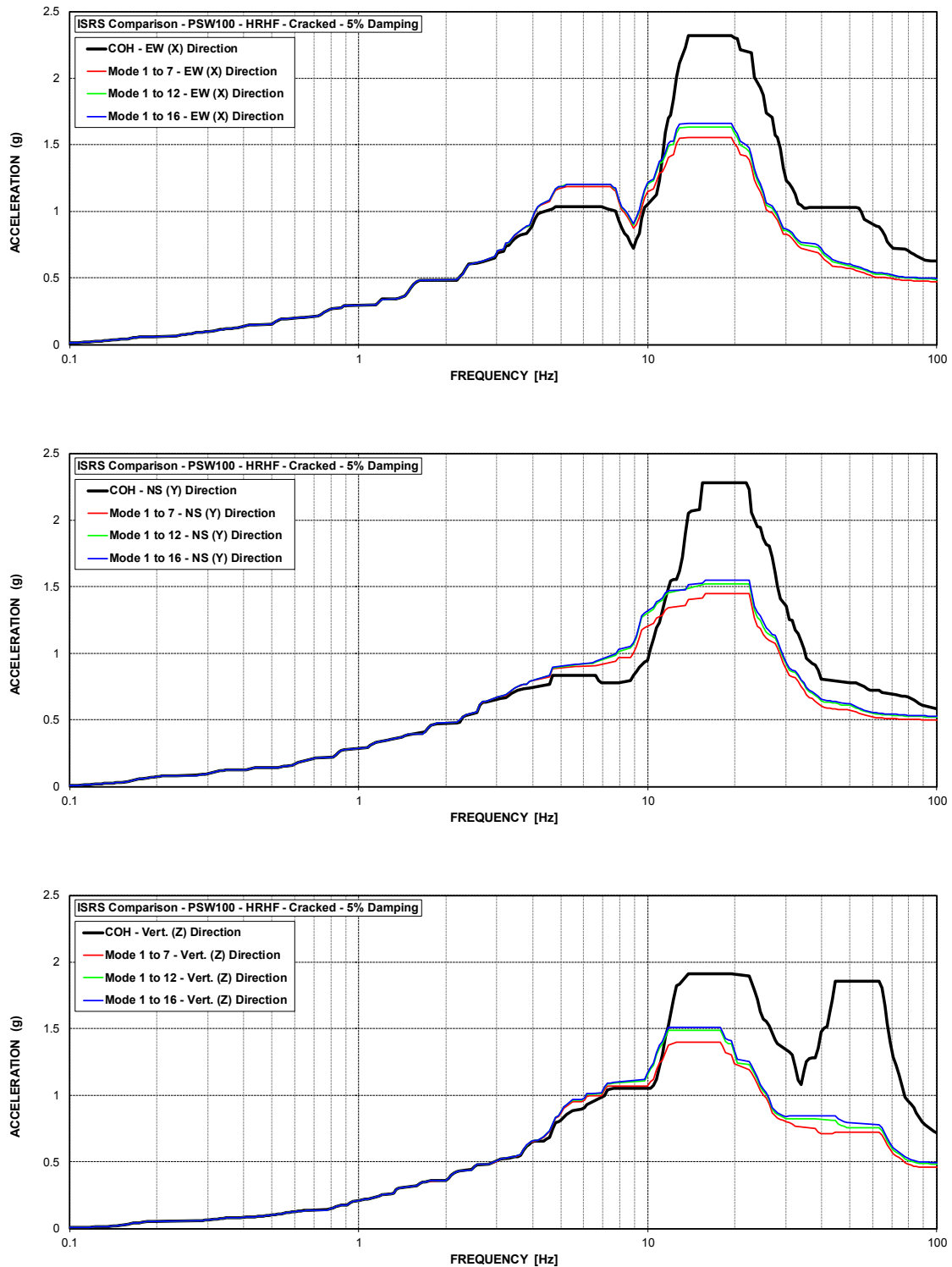


Figure C-118 ISRS – Primary Shield Wall (PSW100) at El. 100' – HRHF – Cracked

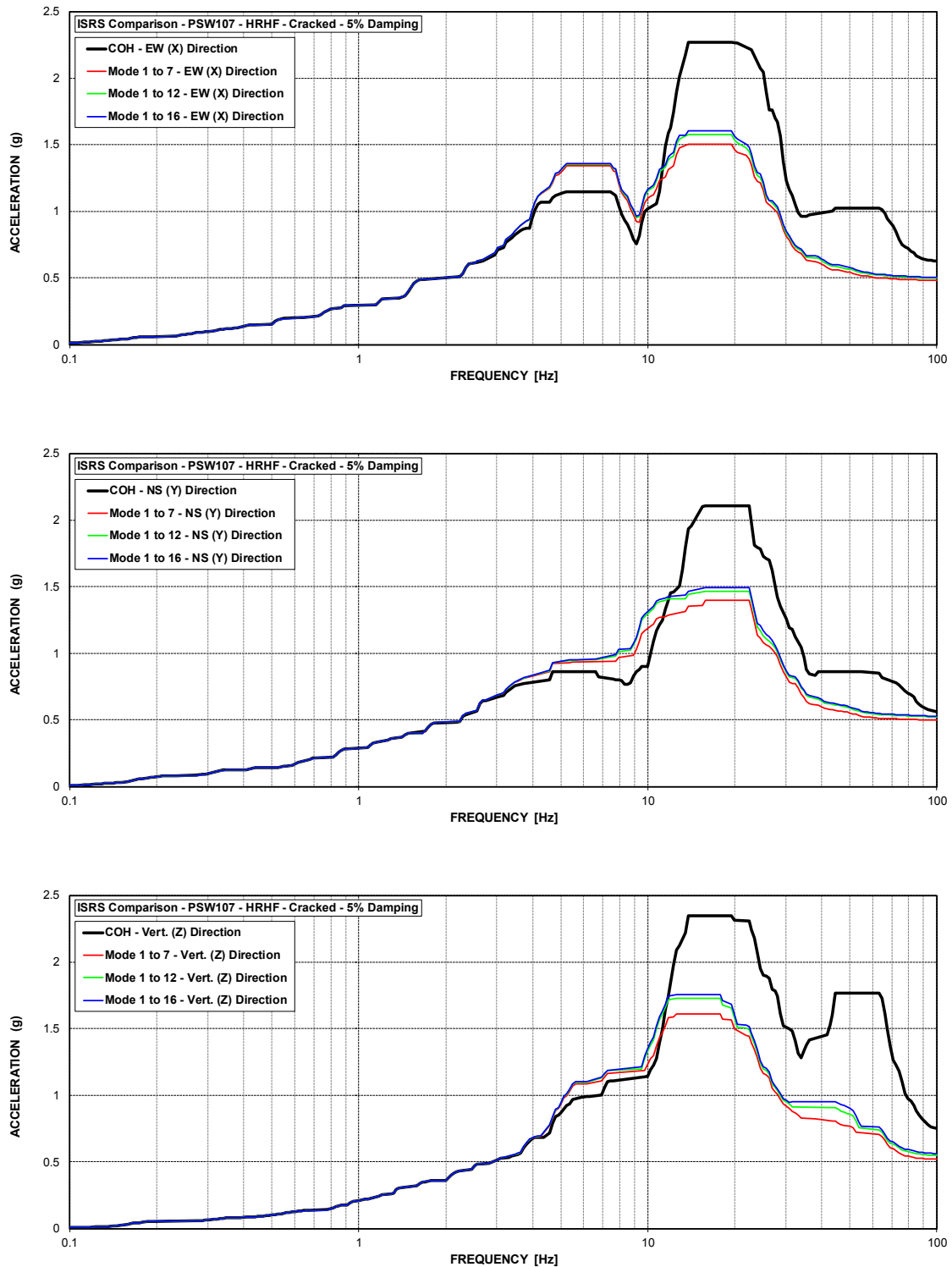


Figure C-119 ISRS – Primary Shield Wall (PSW107) at El. 106.5' – HRHF – Cracked

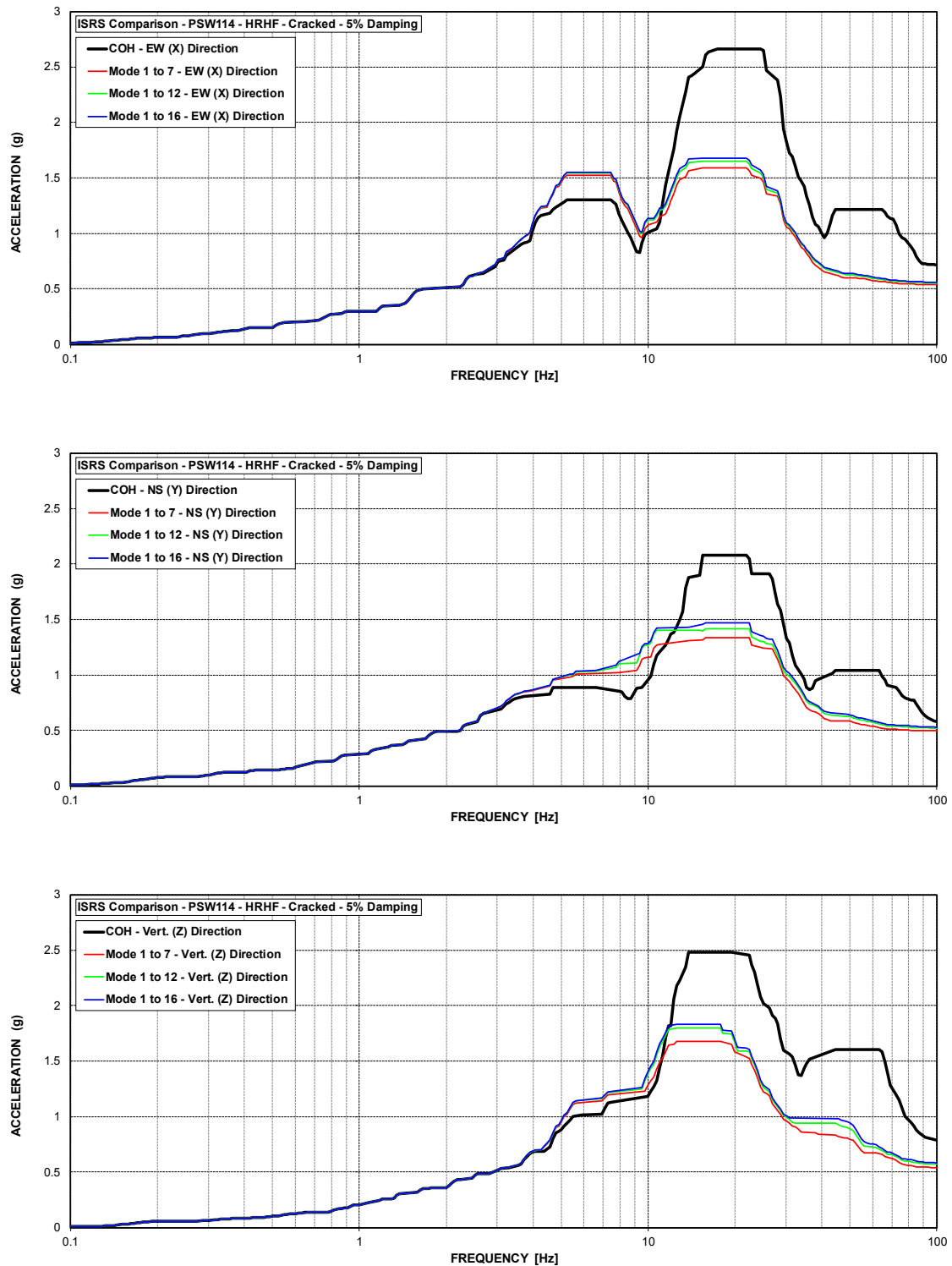


Figure C-120 ISRS – Primary Shield Wall (PSW114) at El. 114' – HRHF – Cracked

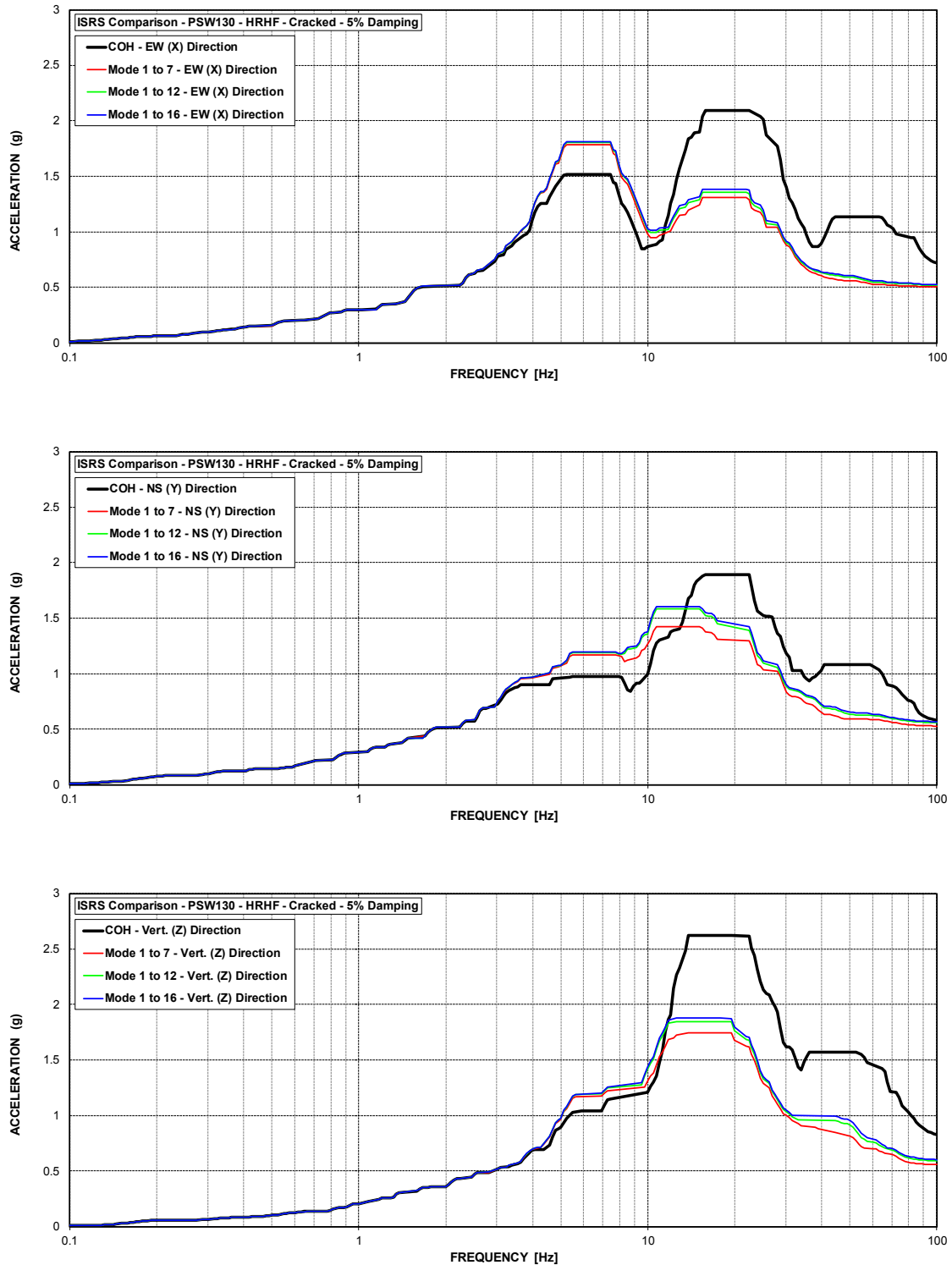


Figure C-121 ISRS – Primary Shield Wall (PSW130) at El. 130' – HRHF – Cracked

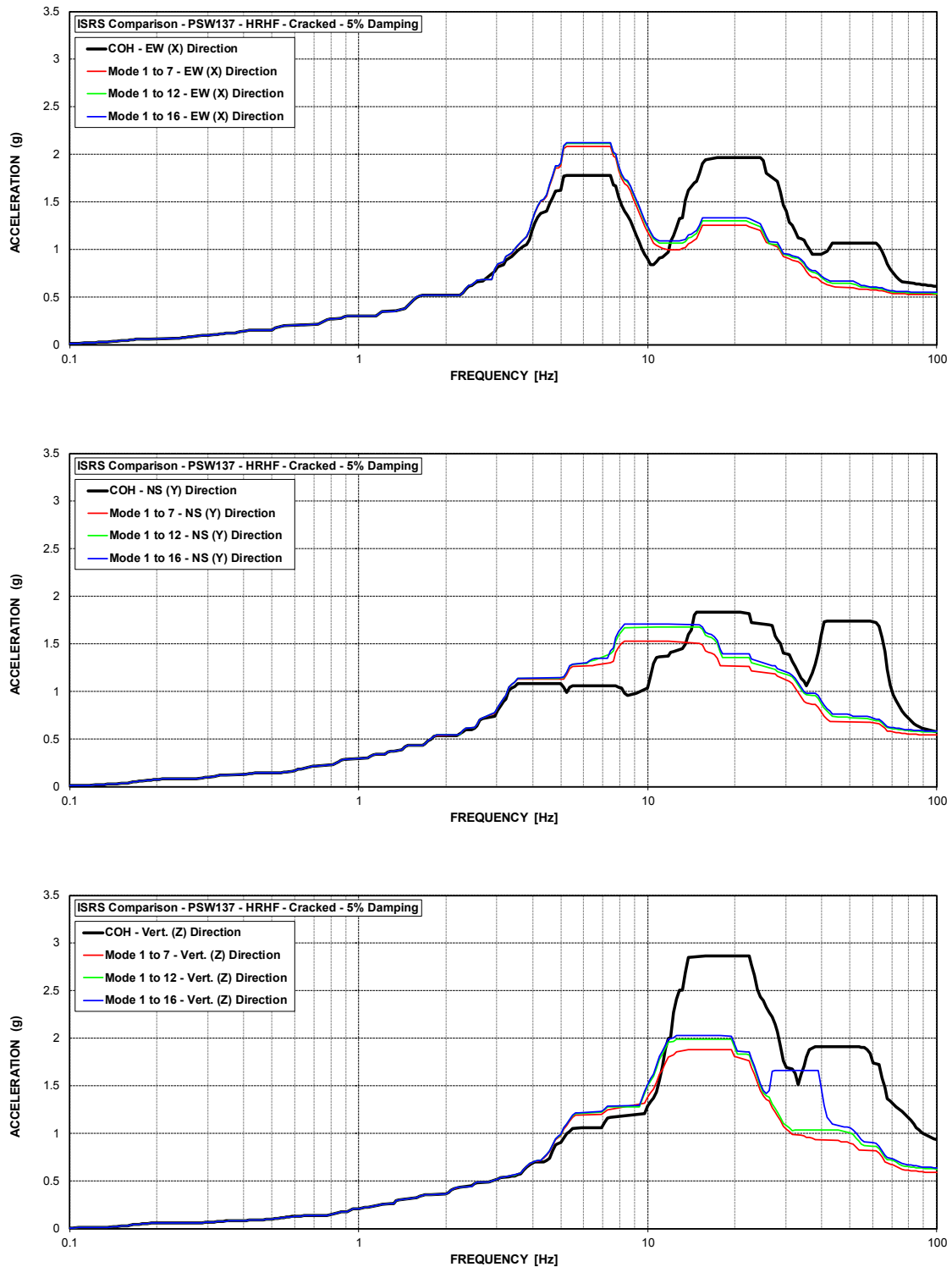


Figure C-122 ISRS – Primary Shield Wall (PSW137) at El. 136.5 – HRHF – Cracked



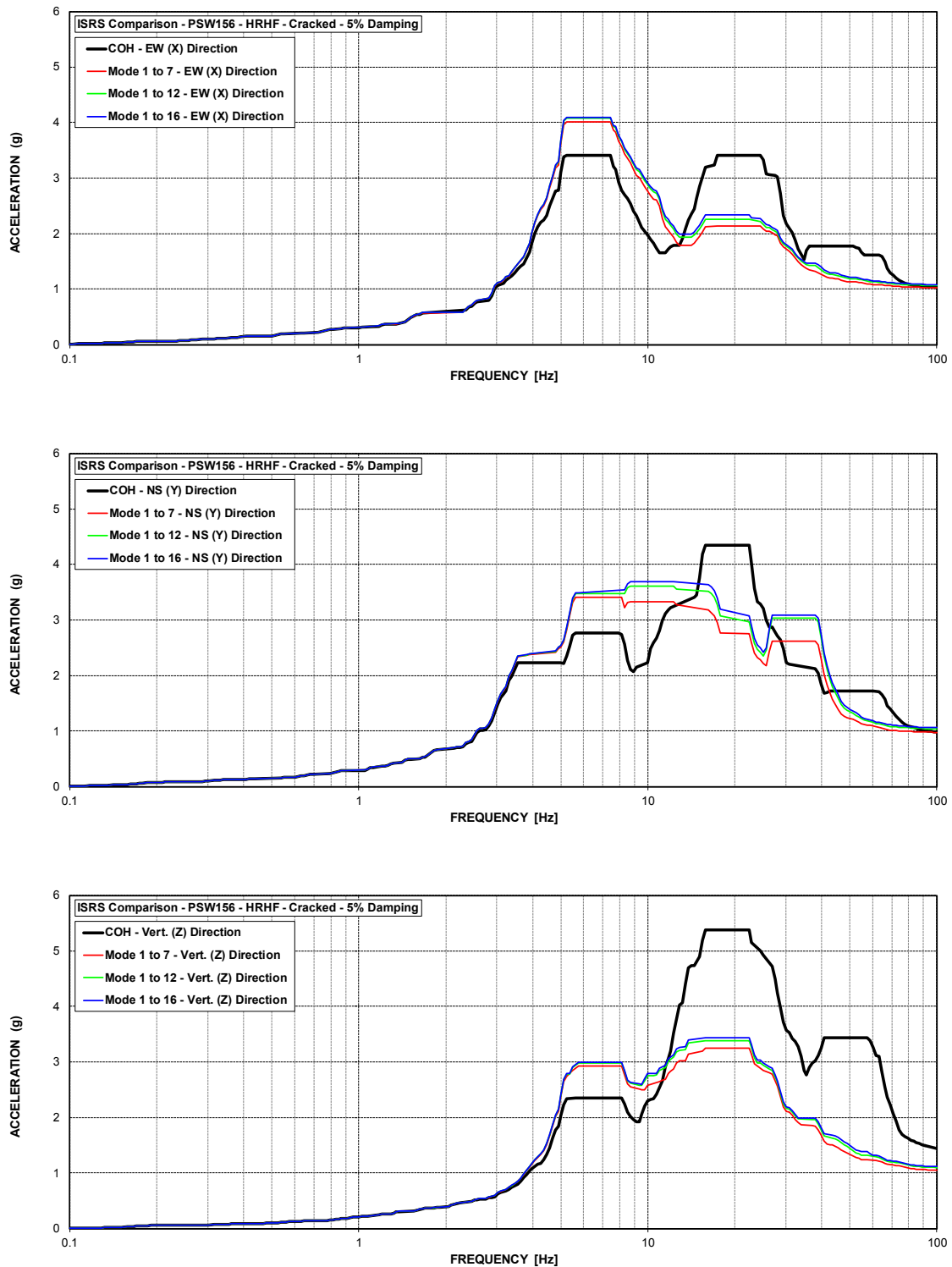


Figure C-123 ISRS – Primary Shield Wall (PSW156) at El. 156' – HRHF – Cracked

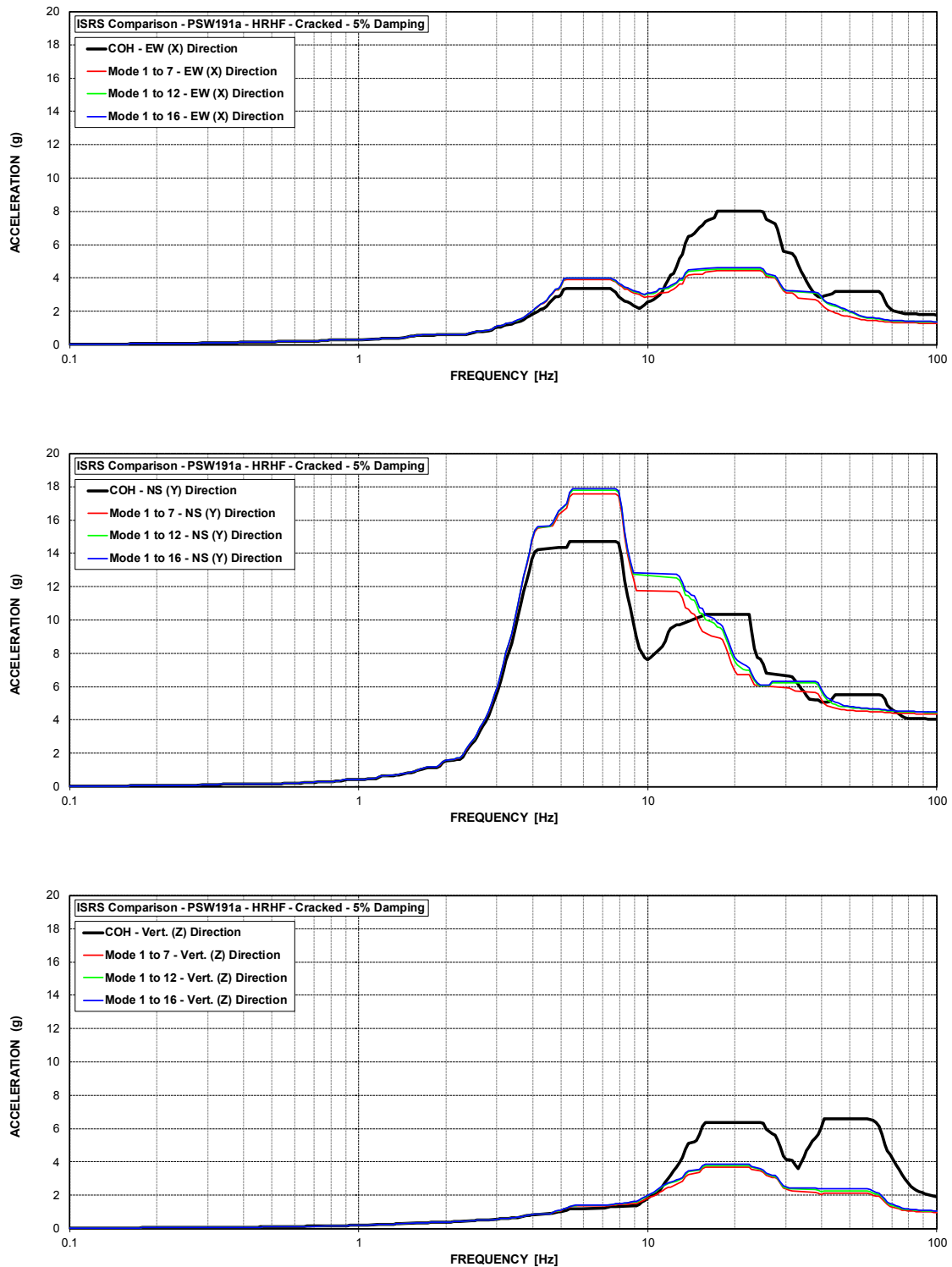
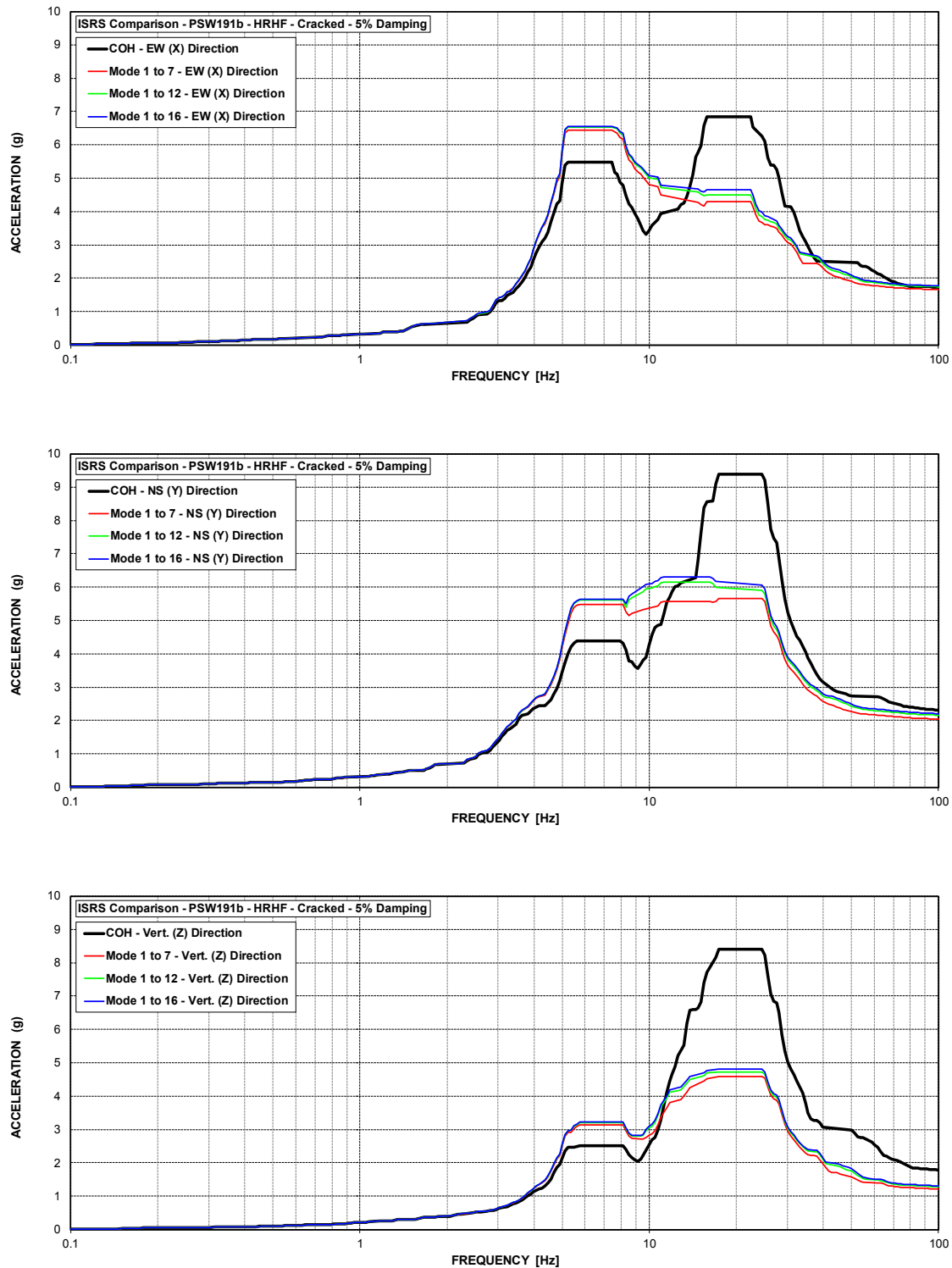


Figure C-124 ISRS – Primary Shield Wall (PSW191a) at El. 191' – HRHF – Cracked



**Figure C-125 ISRS – Primary Shield Wall (PSW191b) at El. 191' – HRHF – Cracked**

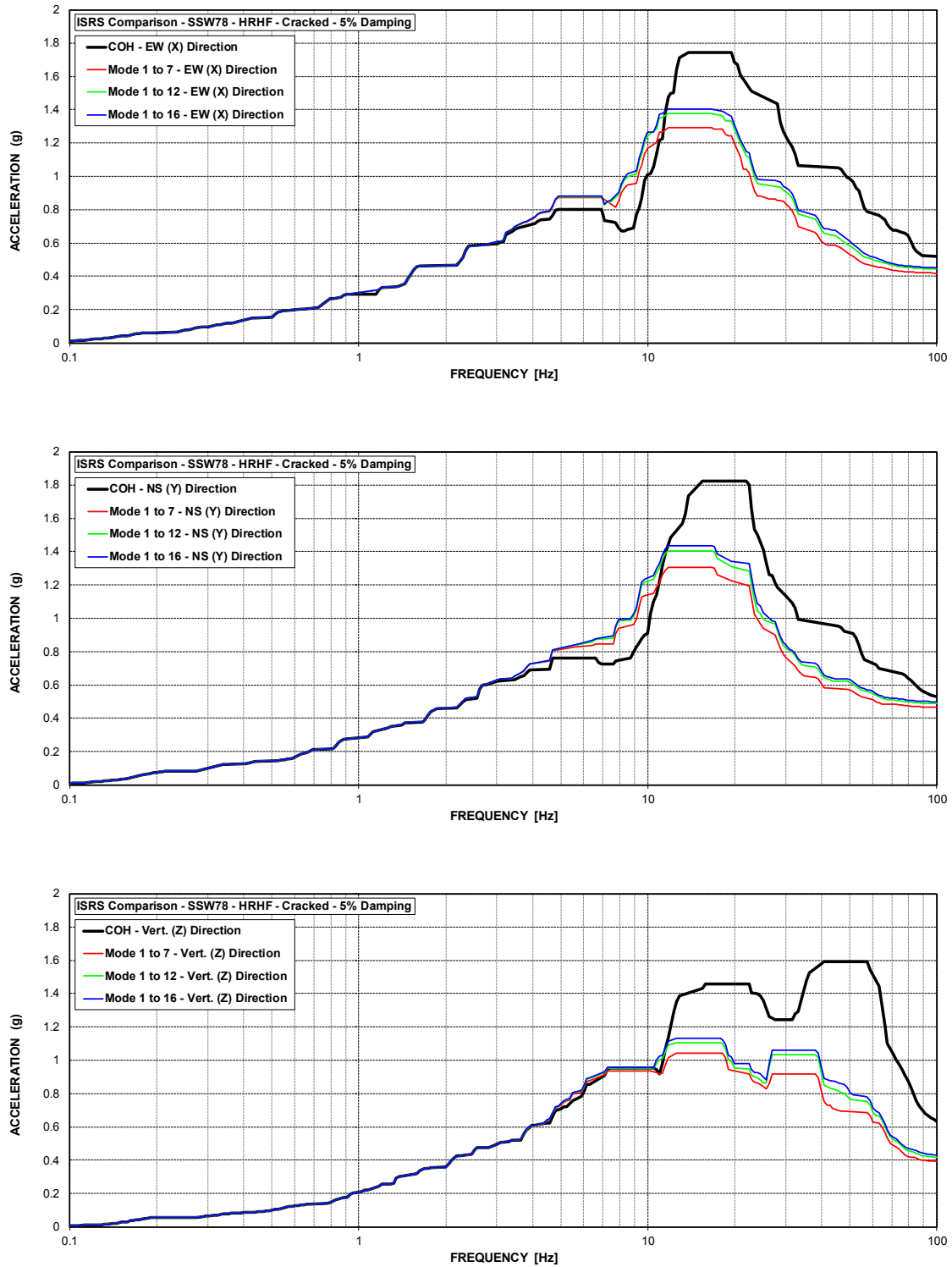


Figure C-126 ISRS – Secondary Shield Wall (SSW78) at El. 78' – HRHF – Cracked

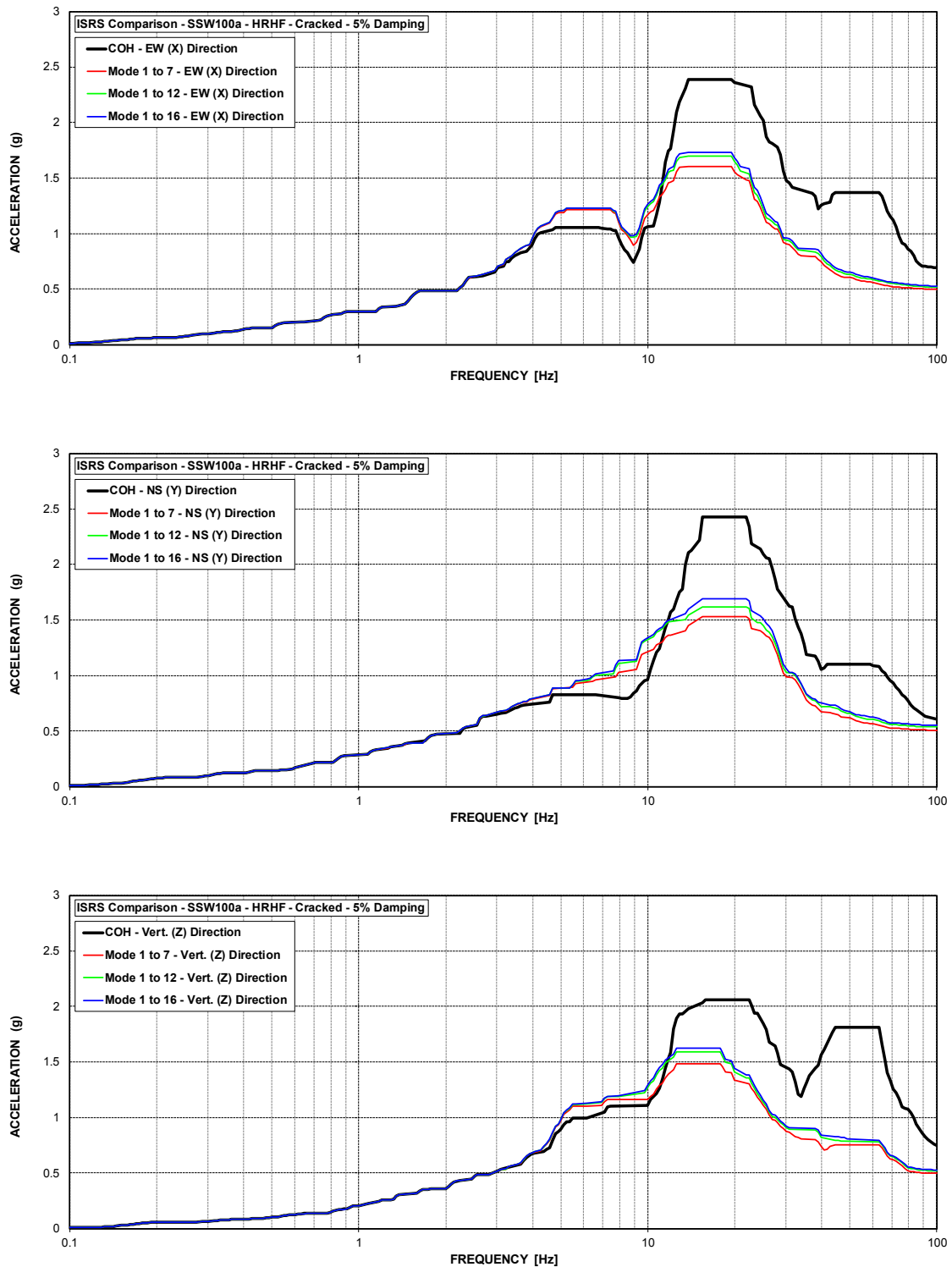


Figure C-127 ISRS – Secondary Shield Wall (SSW100a) at El. 100' – HRHF – Cracked

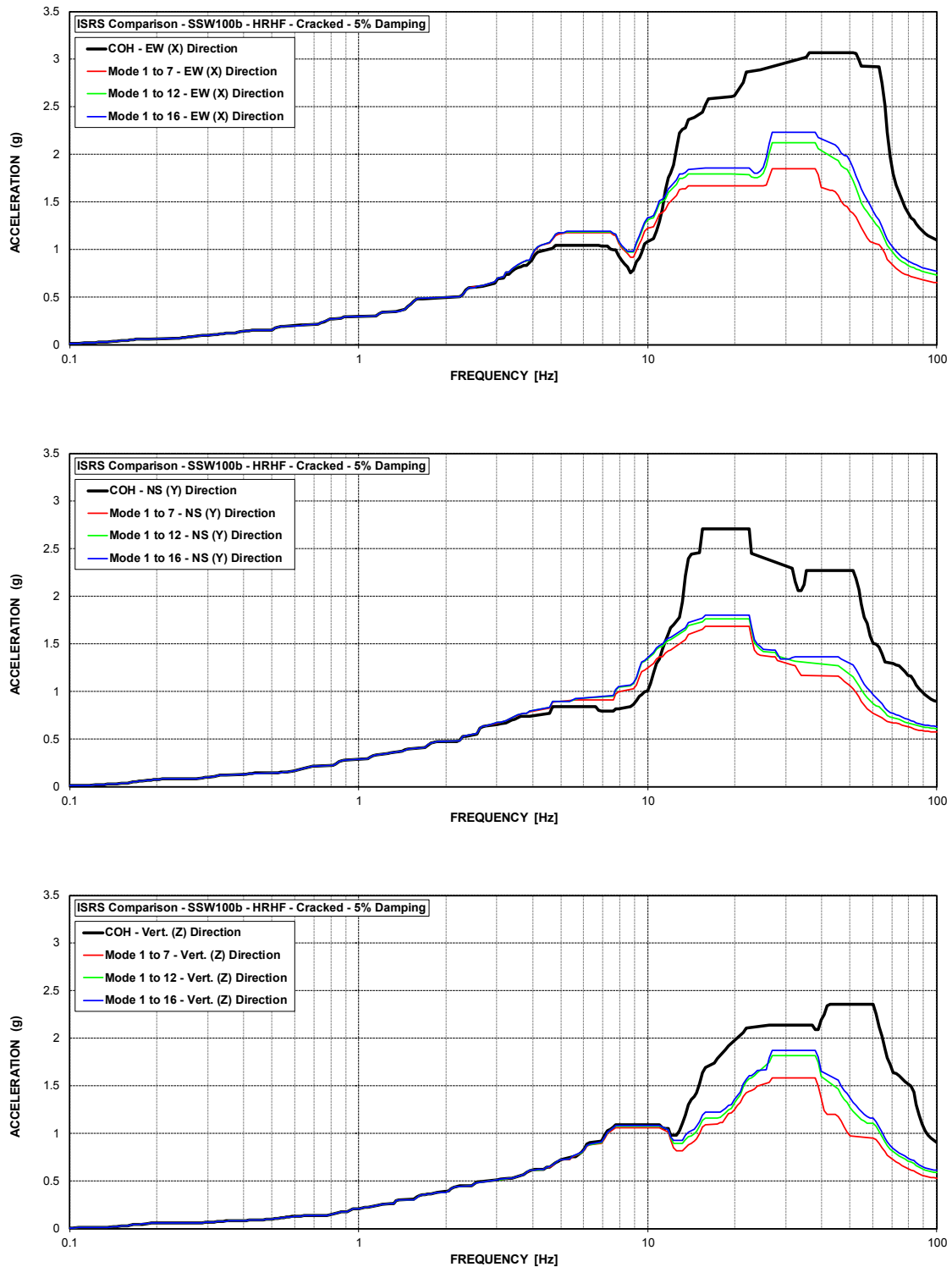


Figure C-128 ISRS – Secondary Shield Wall (SSW100b) at El. 100' – HRHF – Cracked

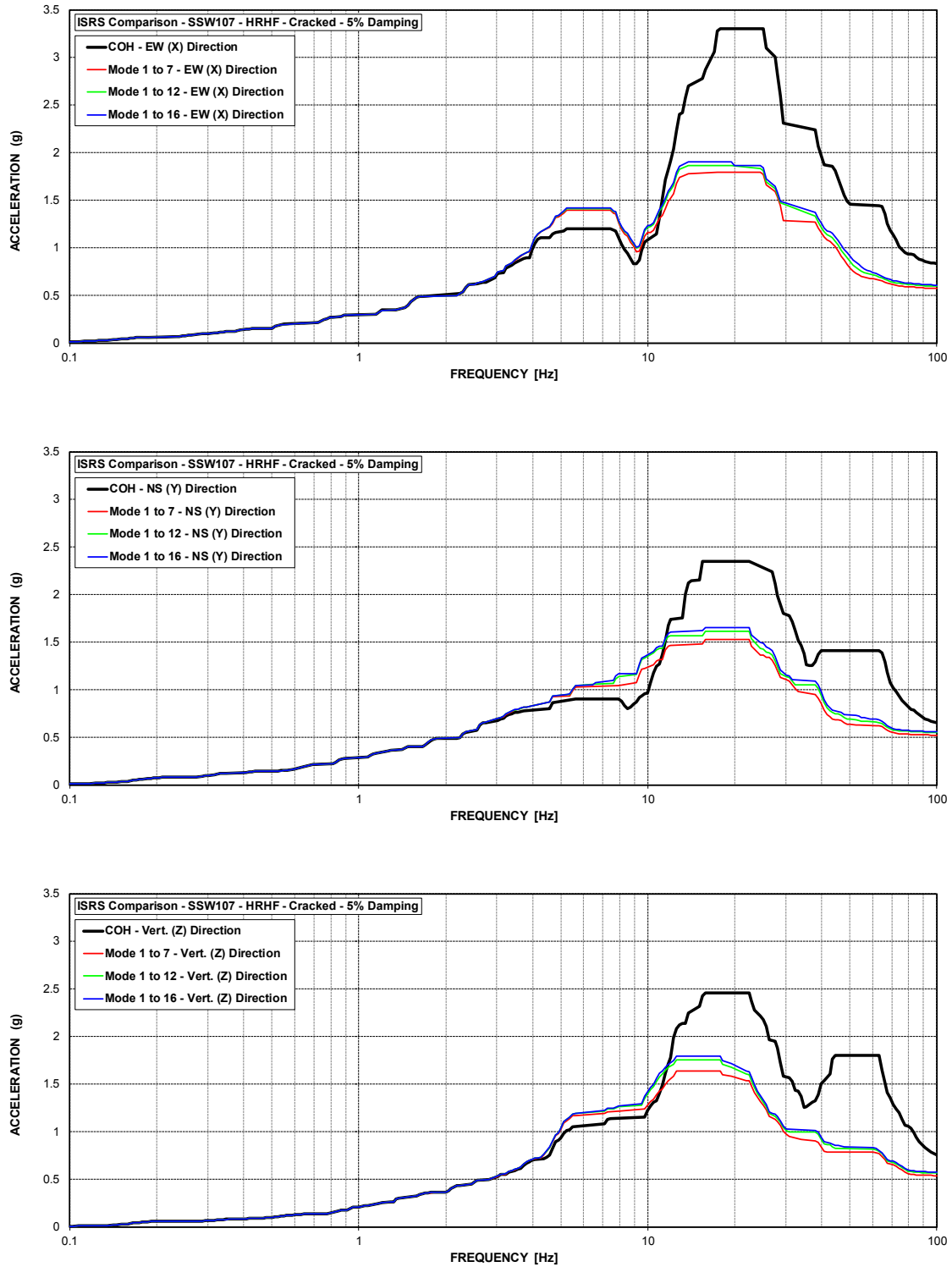


Figure C-129 ISRS – Secondary Shield Wall (SSW107) at El. 106.5' – HRHF – Cracked

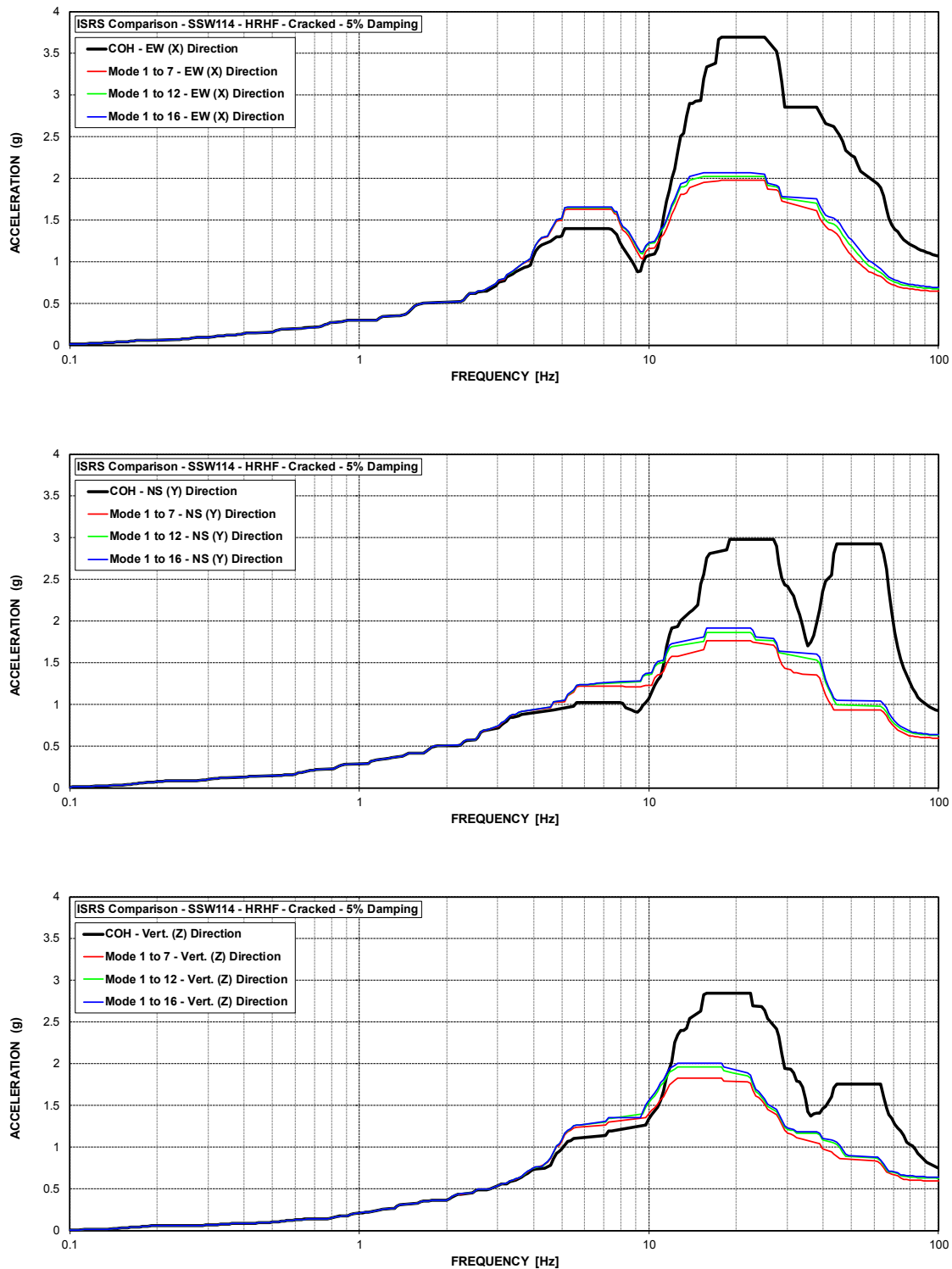


Figure C-130 ISRS – Secondary Shield Wall (SSW114) at El. 114' – HRHF – Cracked



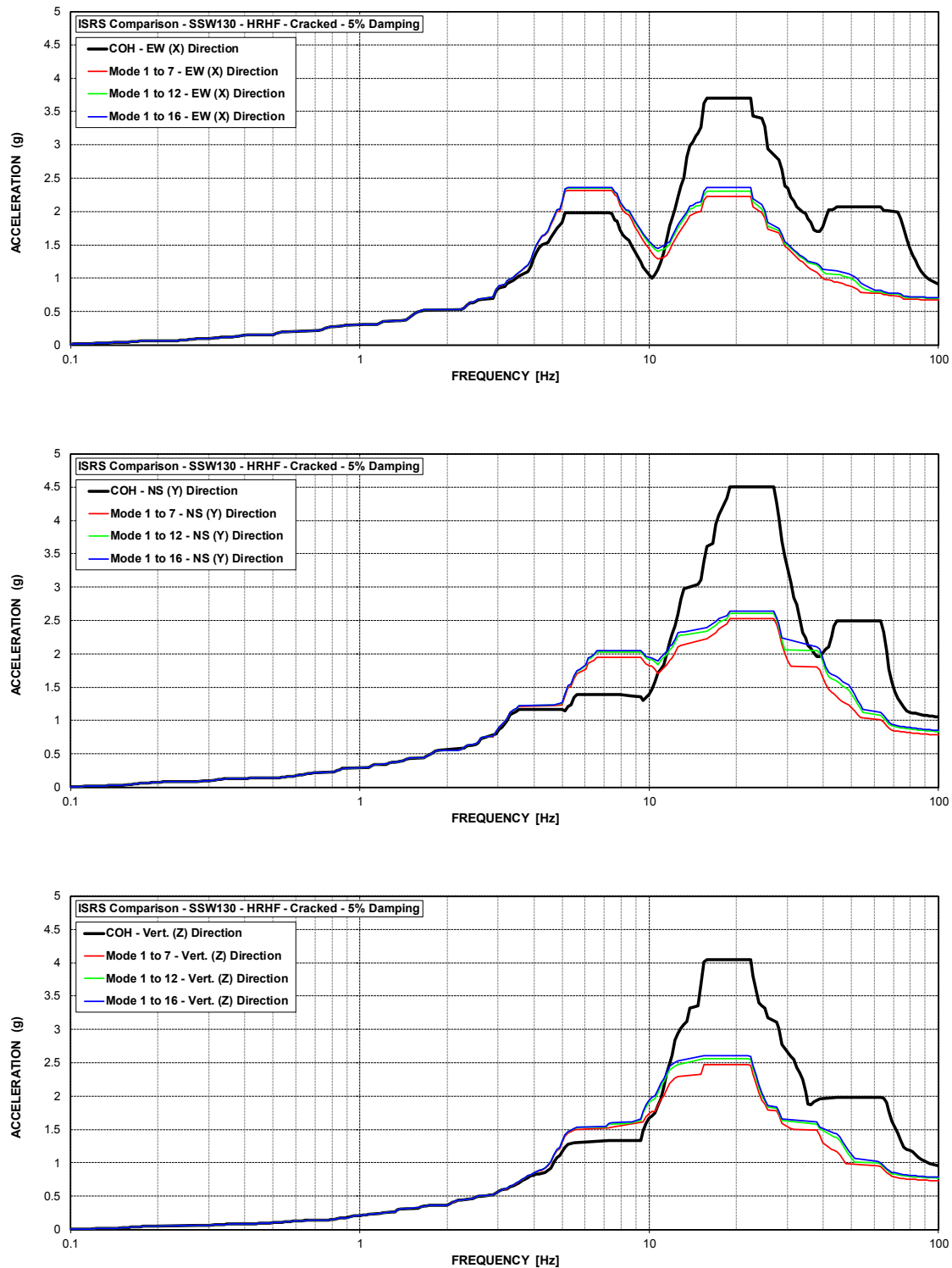


Figure C-131 ISRS – Secondary Shield Wall (SSW130) at El. 130' – HRHF – Cracked

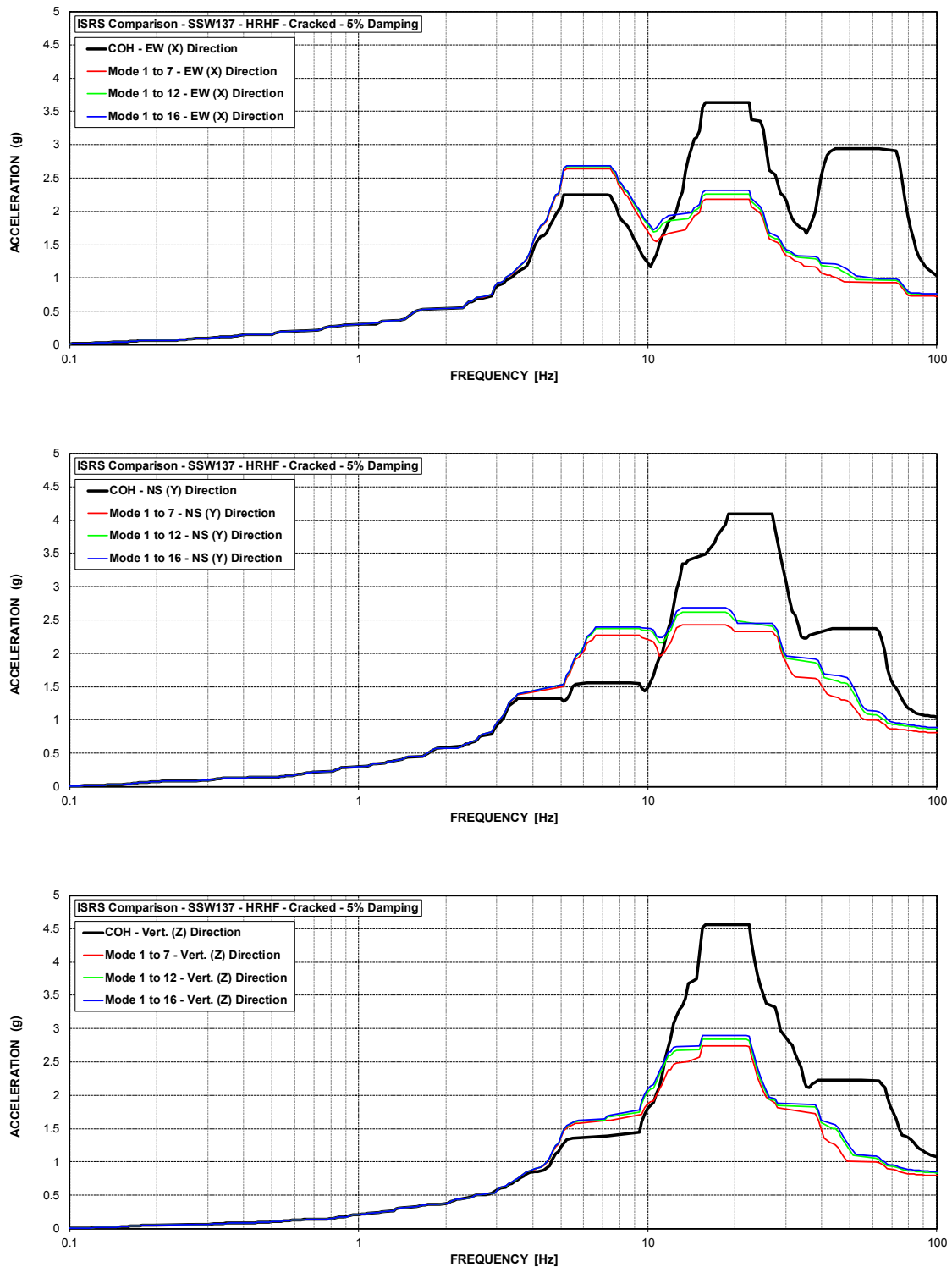


Figure C-132 ISRS – Secondary Shield Wall (SSW137) at El. 136.5' – HRHF – Cracked

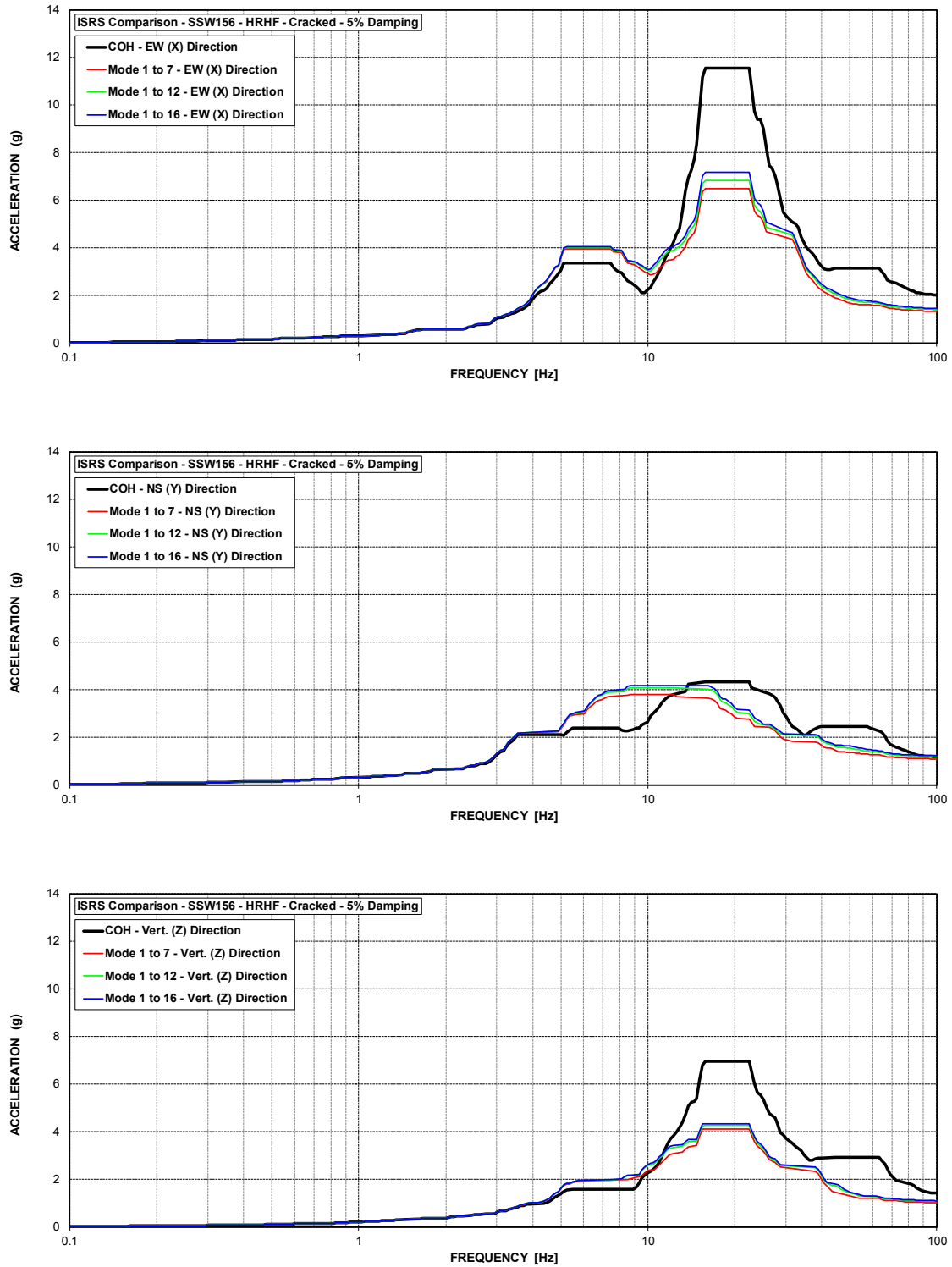


Figure C-133 ISRS – Secondary Shield Wall (SSW156) at El. 156' – HRHF – Cracked

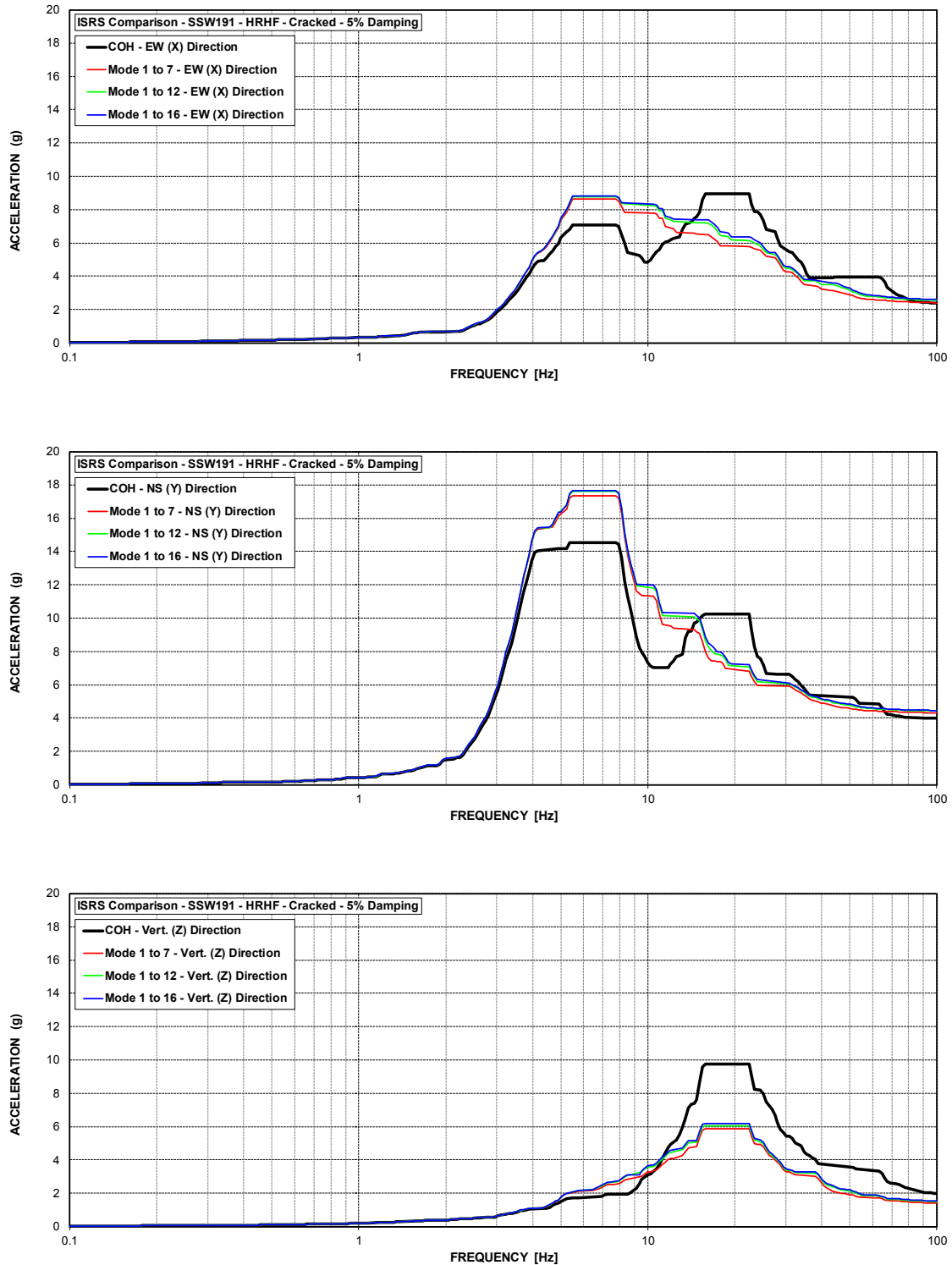


Figure C-134 ISRS – Secondary Shield Wall (SSW191) at El. 191' – HRHF – Cracked

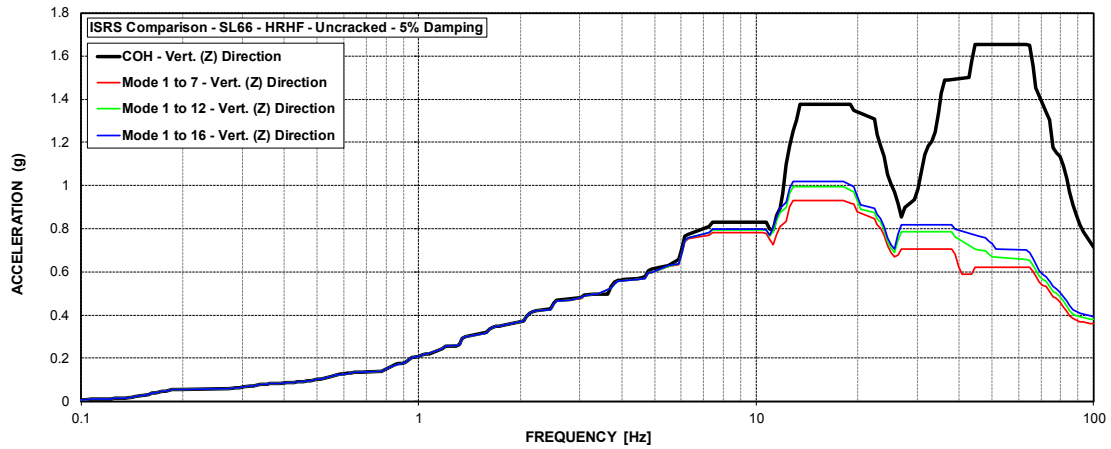


Figure C-135 ISRS – RCB Floor Slab (SL66) at El. 66' – HRHF – Uncracked

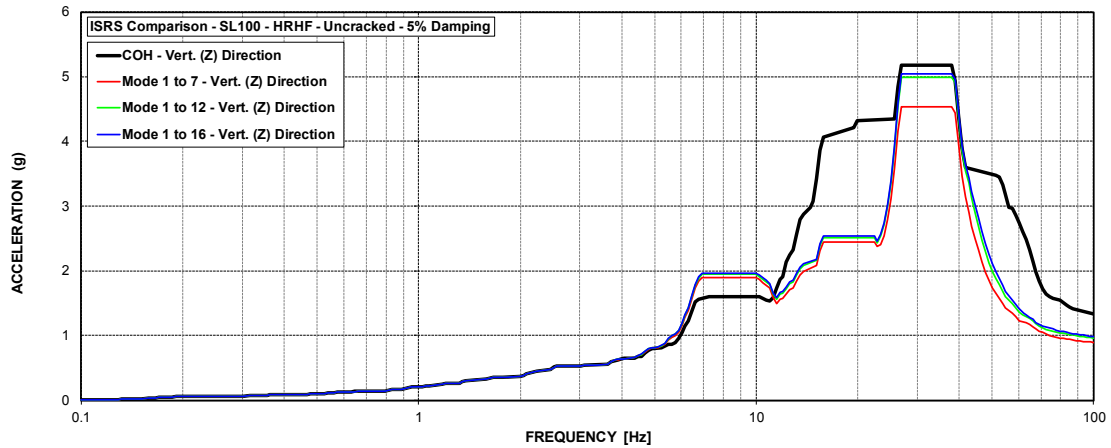


Figure C-136 ISRS – RCB Floor Slab (SL100) at El. 100' – HRHF – Uncracked

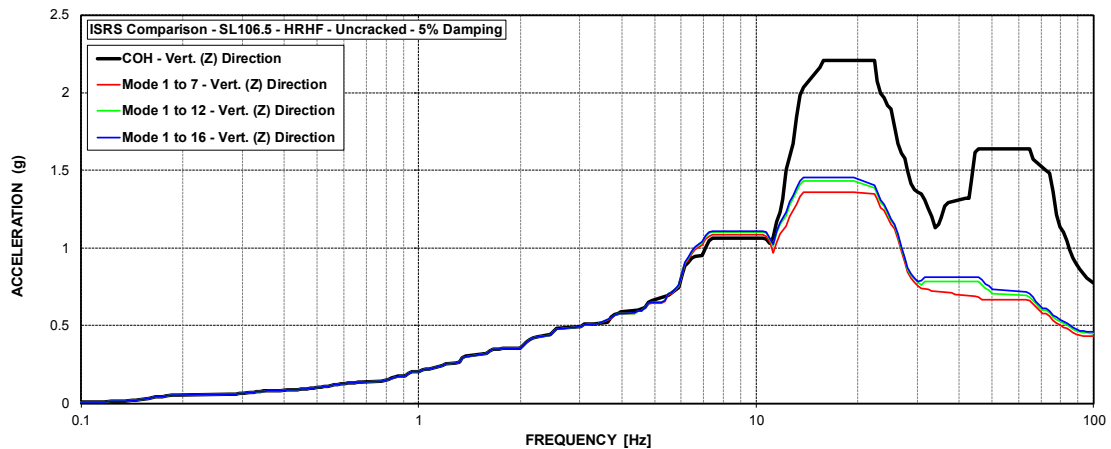


Figure C-137 ISRS – RCB Floor Slab (SL106.5) at El. 106.5' – HRHF – Uncracked

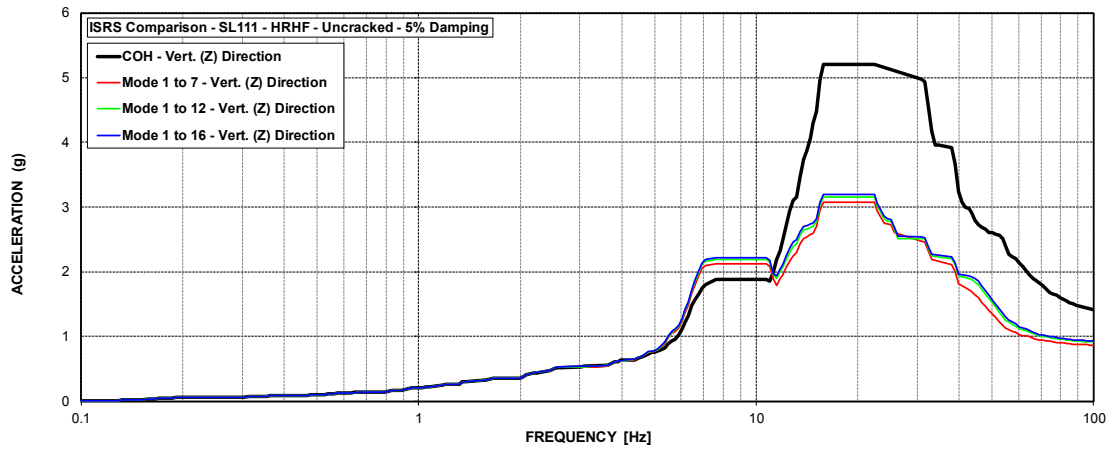


Figure C-138 ISRS – RCB Floor Slab (SL111) at El. 111' – HRHF – Uncracked

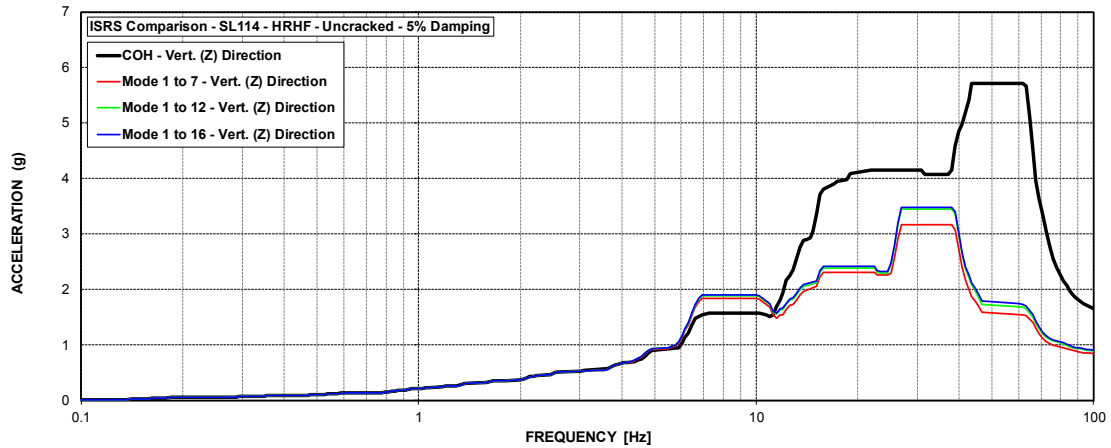


Figure C-139 ISRS – RCB Floor Slab (SL114) at El. 114' – HRHF – Uncracked

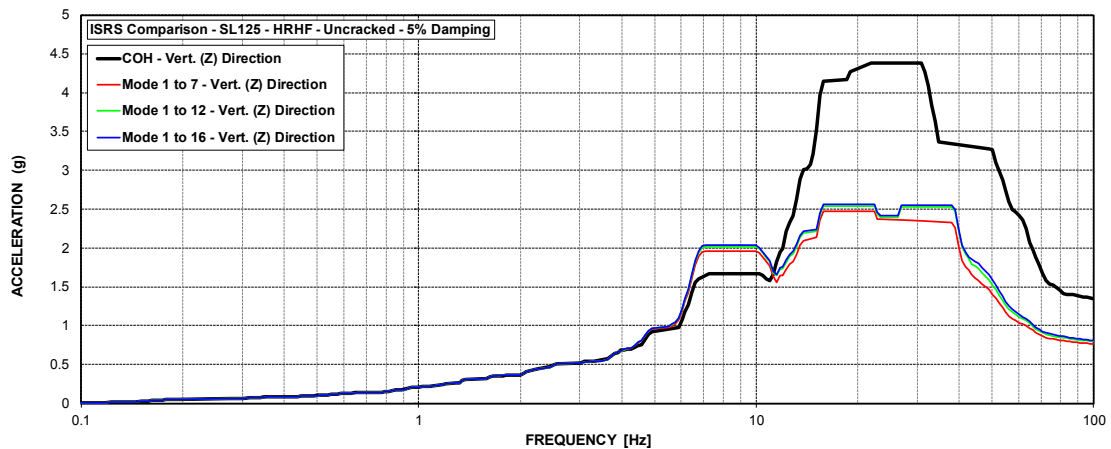


Figure C-140 ISRS – RCB Floor Slab (SL125) at El. 125' – HRHF – Uncracked

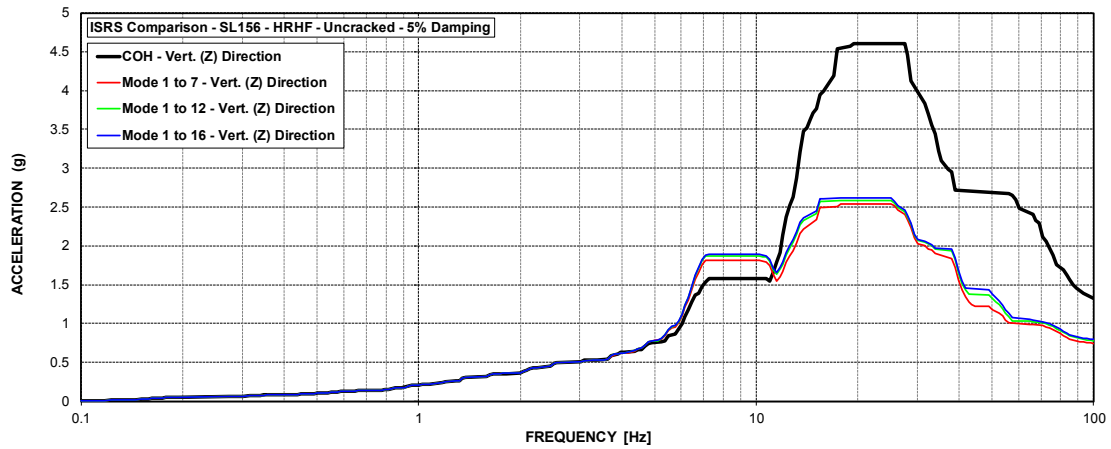


Figure C-141 ISRS – RCB Floor Slab (SL156) at El. 156' – HRHF – Uncracked

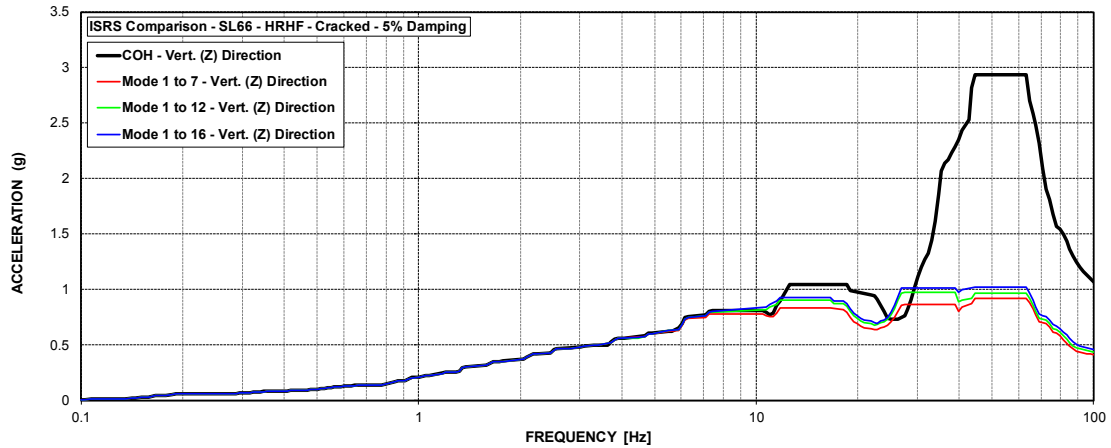


Figure C-142 ISRS – RCB Floor Slab (SL66) at El. 66' – HRHF – Cracked

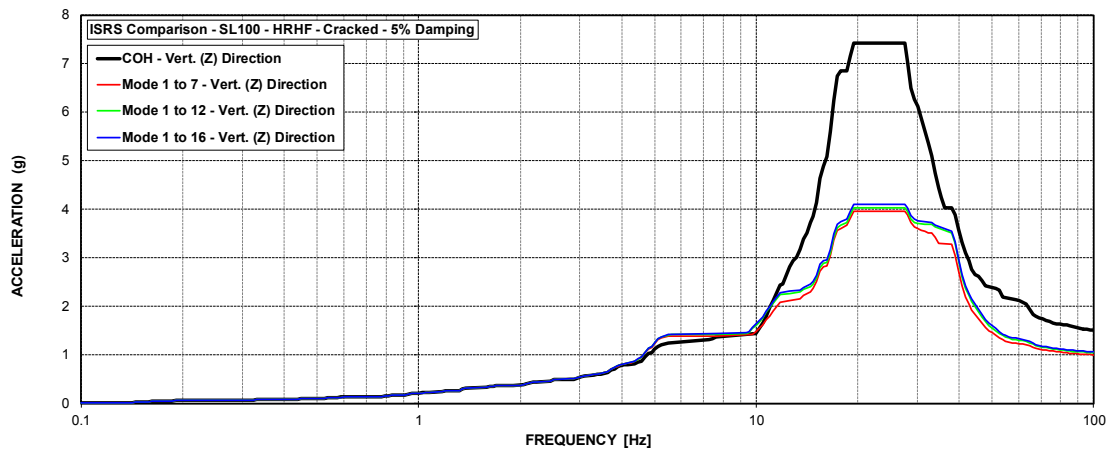


Figure C-143 ISRS – RCB Floor Slab (SL100) at El. 100' – HRHF – Cracked

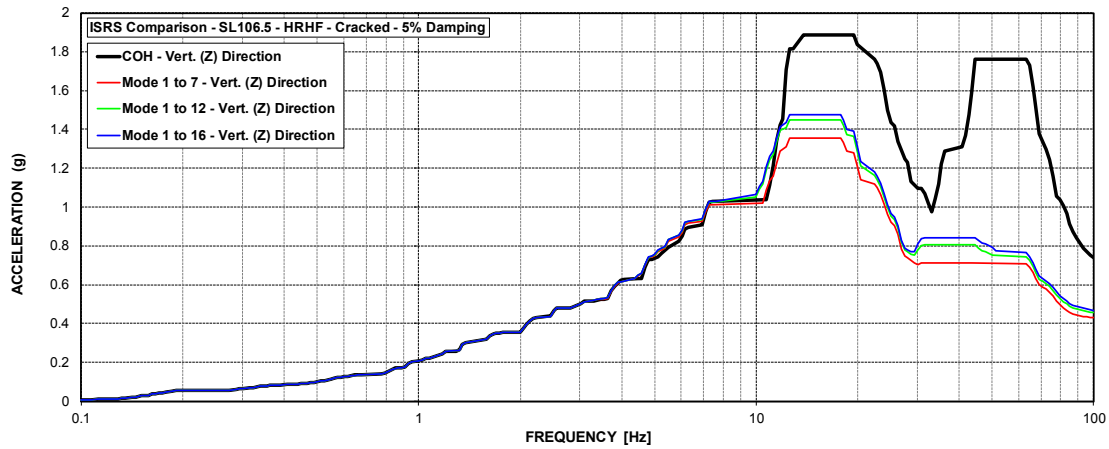


Figure C-144 ISRS – RCB Floor Slab (SL106.5) at El. 106.5' – HRHF – Cracked

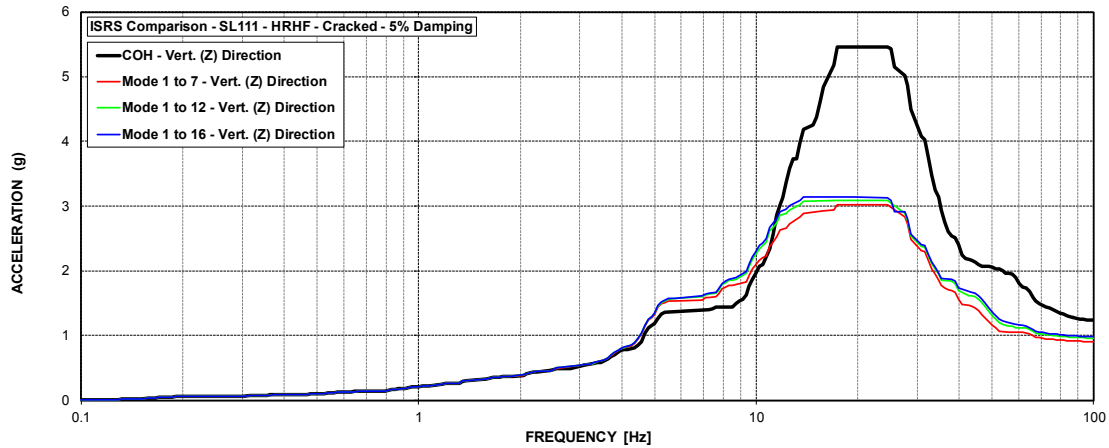


Figure C-145 ISRS – RCB Floor Slab (SL111) at El. 111' – HRHF – Cracked

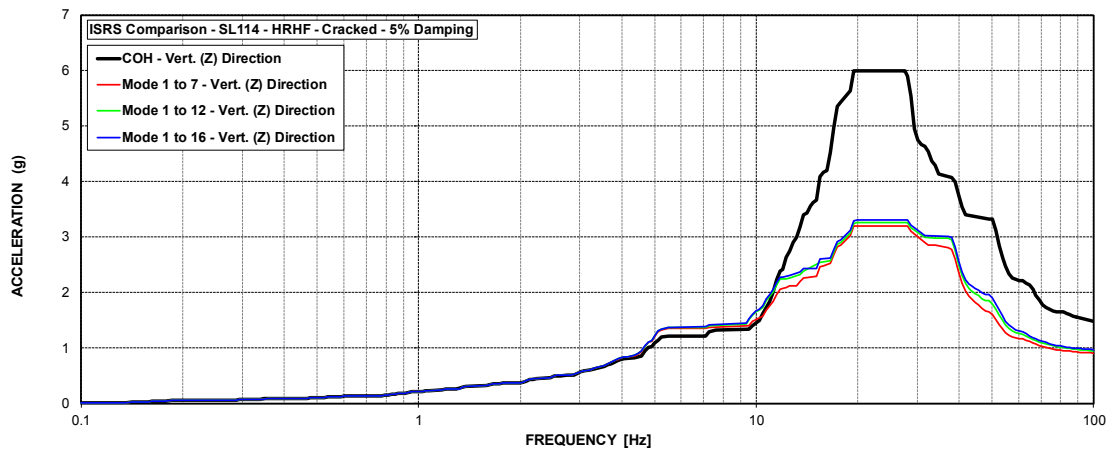


Figure C-146 ISRS – RCB Floor Slab (SL114) at El. 114' – HRHF – Cracked



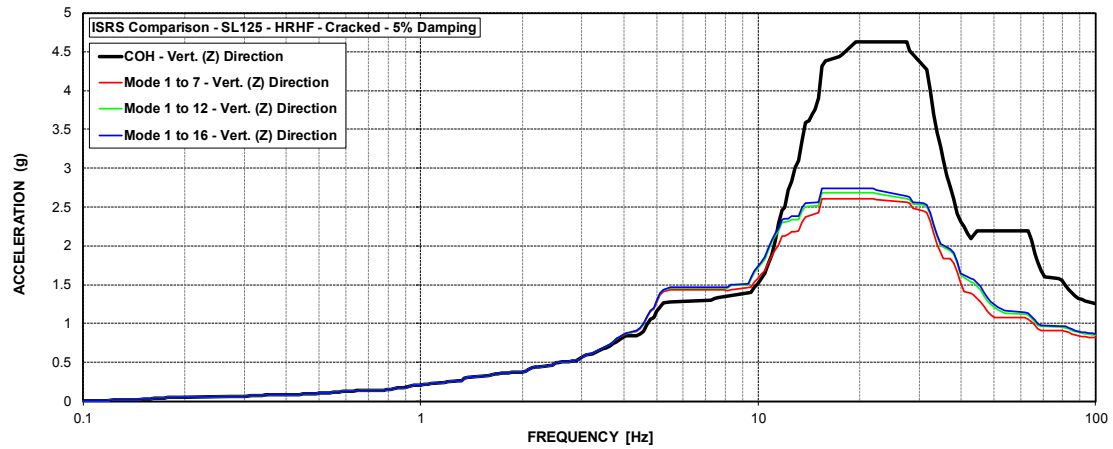


Figure C-147 ISRS – RCB Floor Slab (SL125) at El. 125' – HRHF – Cracked

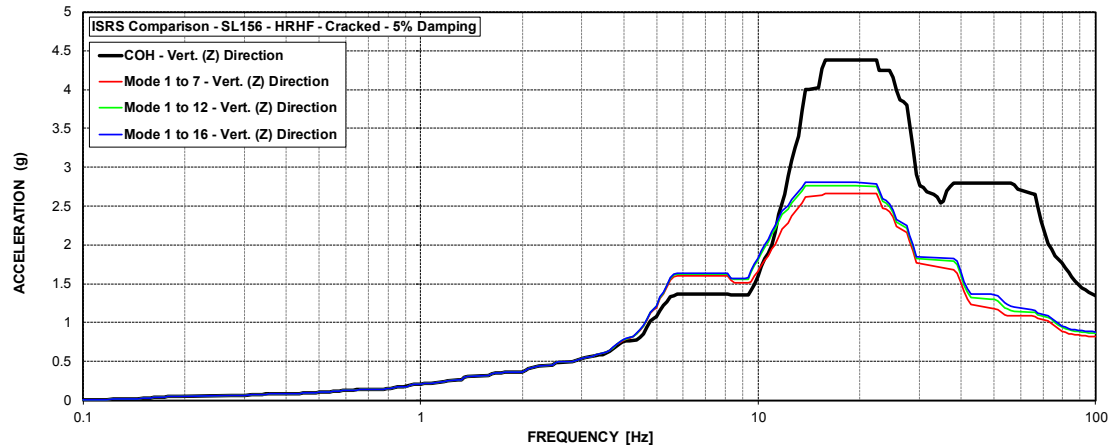


Figure C-148 ISRS – RCB Floor Slab (SL156) at El. 156' – HRHF – Cracked

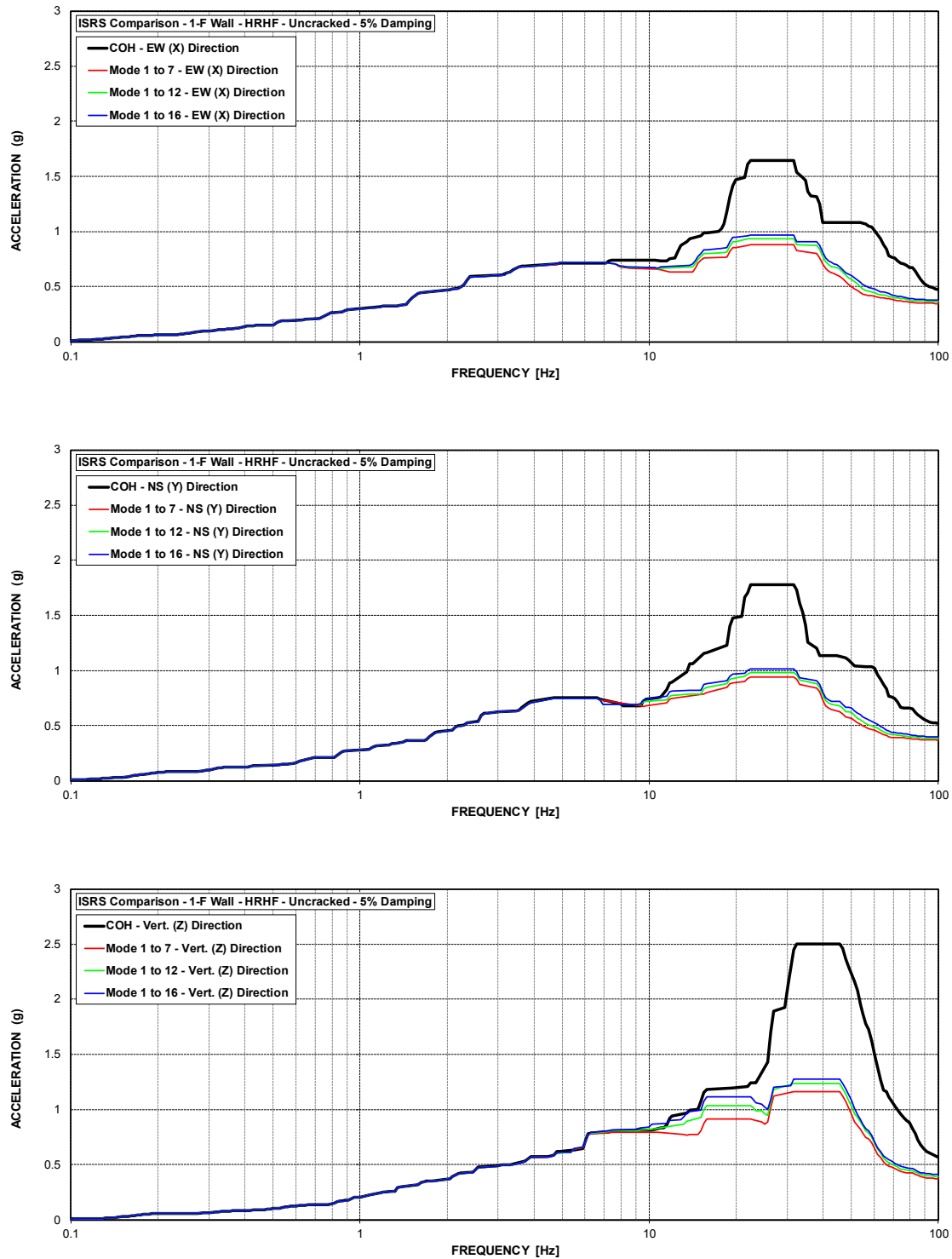


Figure C-149 ISRS – AB Shear Walls (1-F) at El. 55' – HRHF – Uncracked

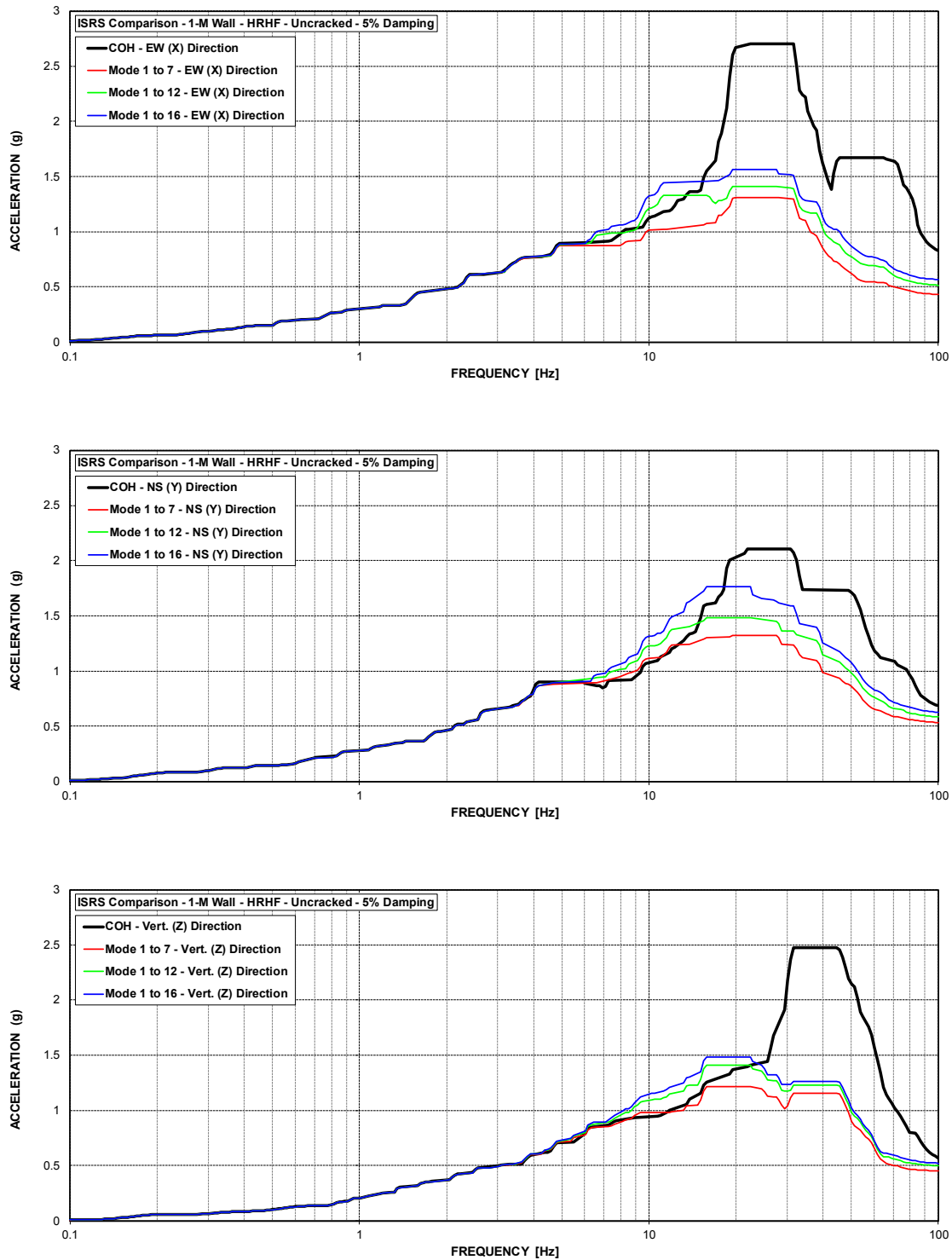


Figure C-150 ISRS – AB Shear Walls (1-M) at El. 68' – HRHF – Uncracked

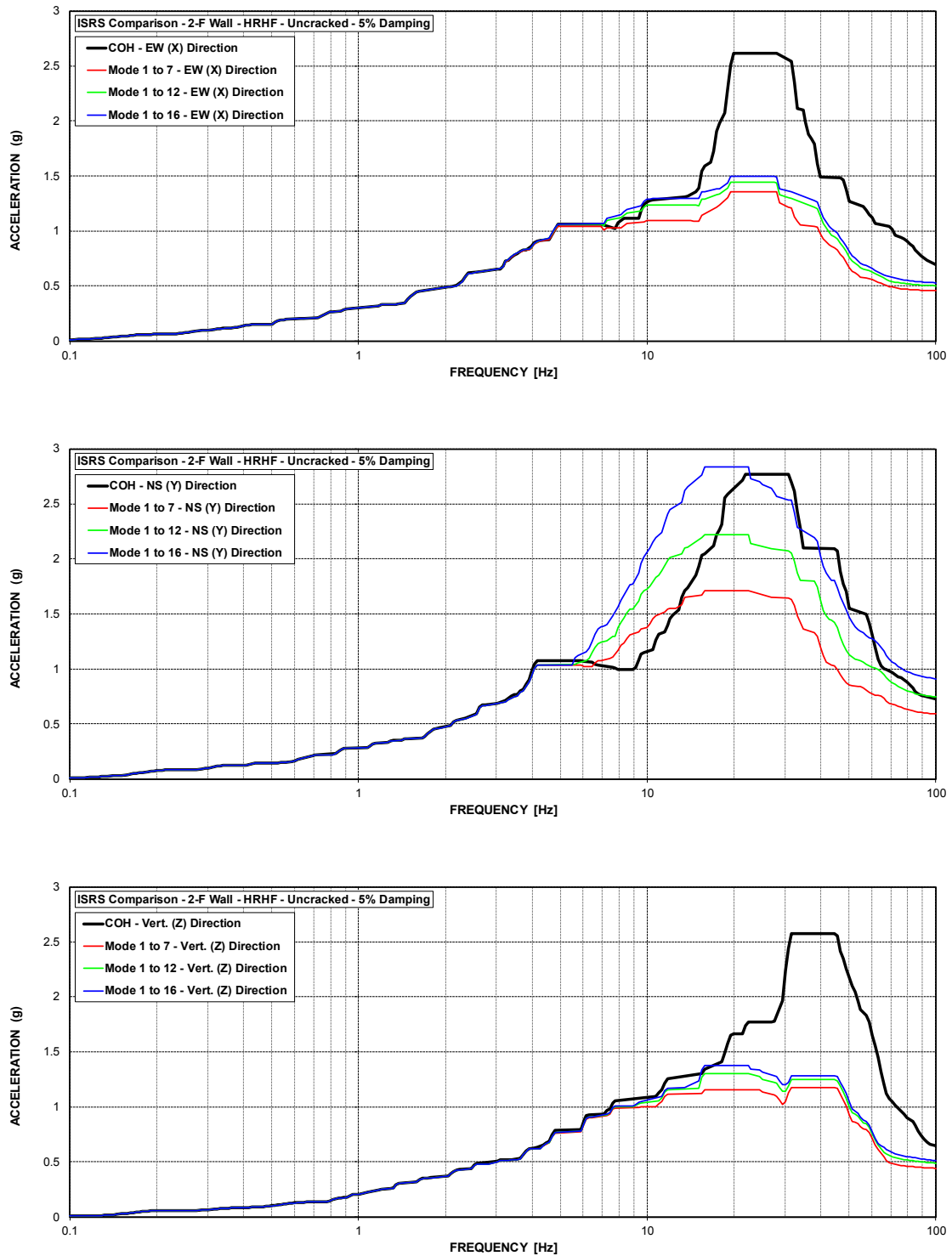


Figure C-151 ISRS – AB Shear Walls (2-F) at El. 78' – HRHF – Uncracked

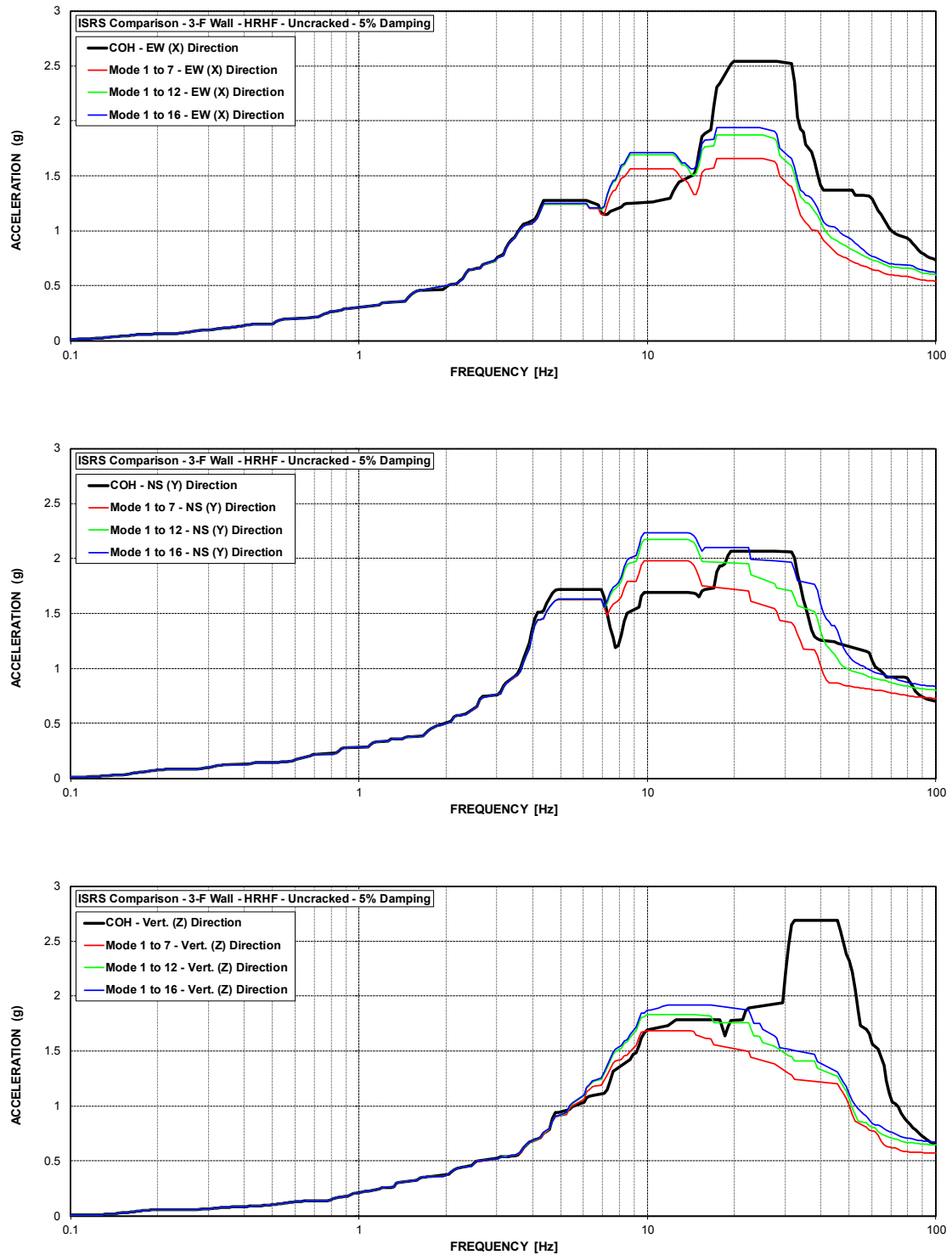


Figure C-152 ISRS – AB Shear Walls (3-F) at El. 100' – HRHF – Uncracked

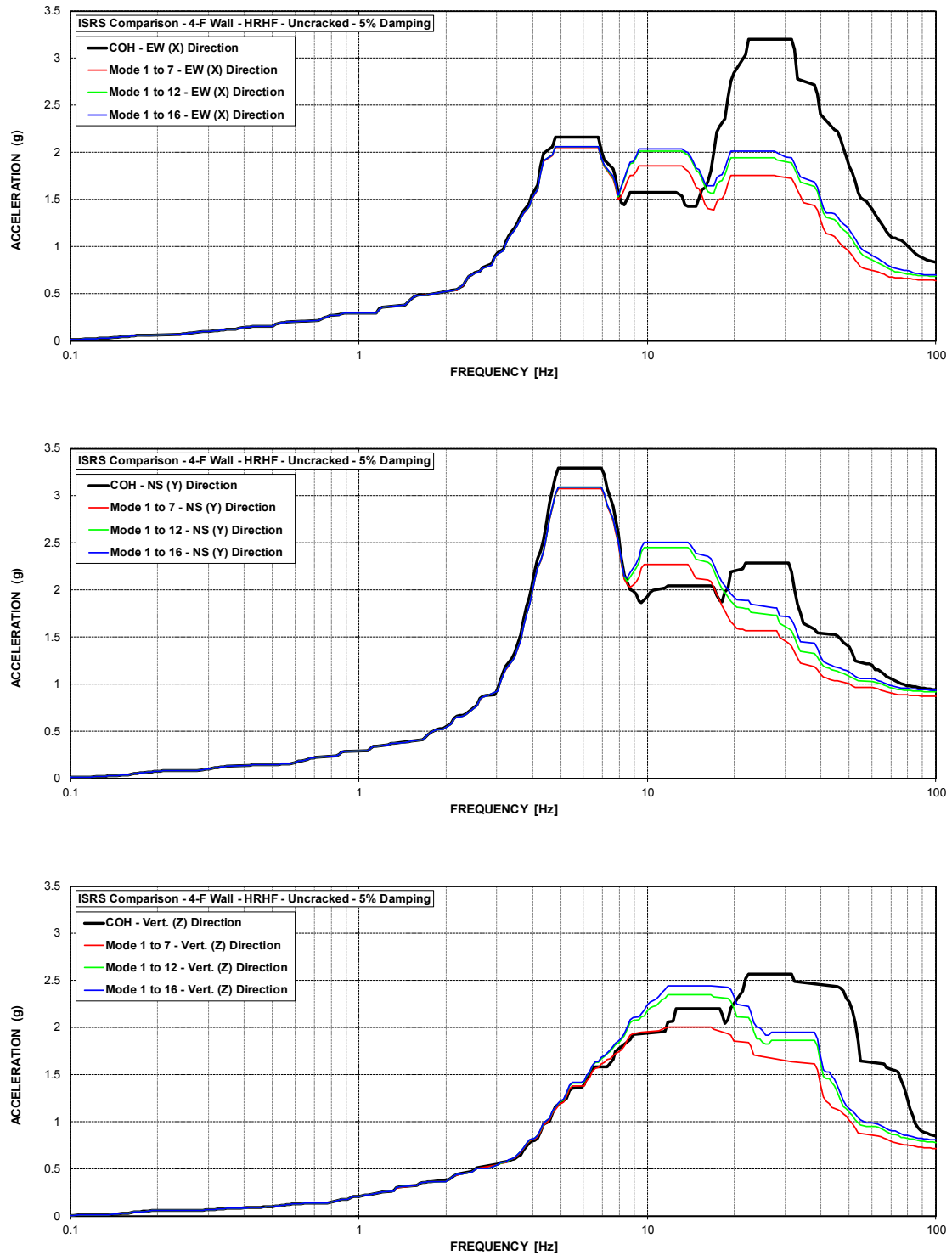


Figure C-153 ISRS – AB Shear Walls (4-F) at El. 120' – HRHF – Uncracked

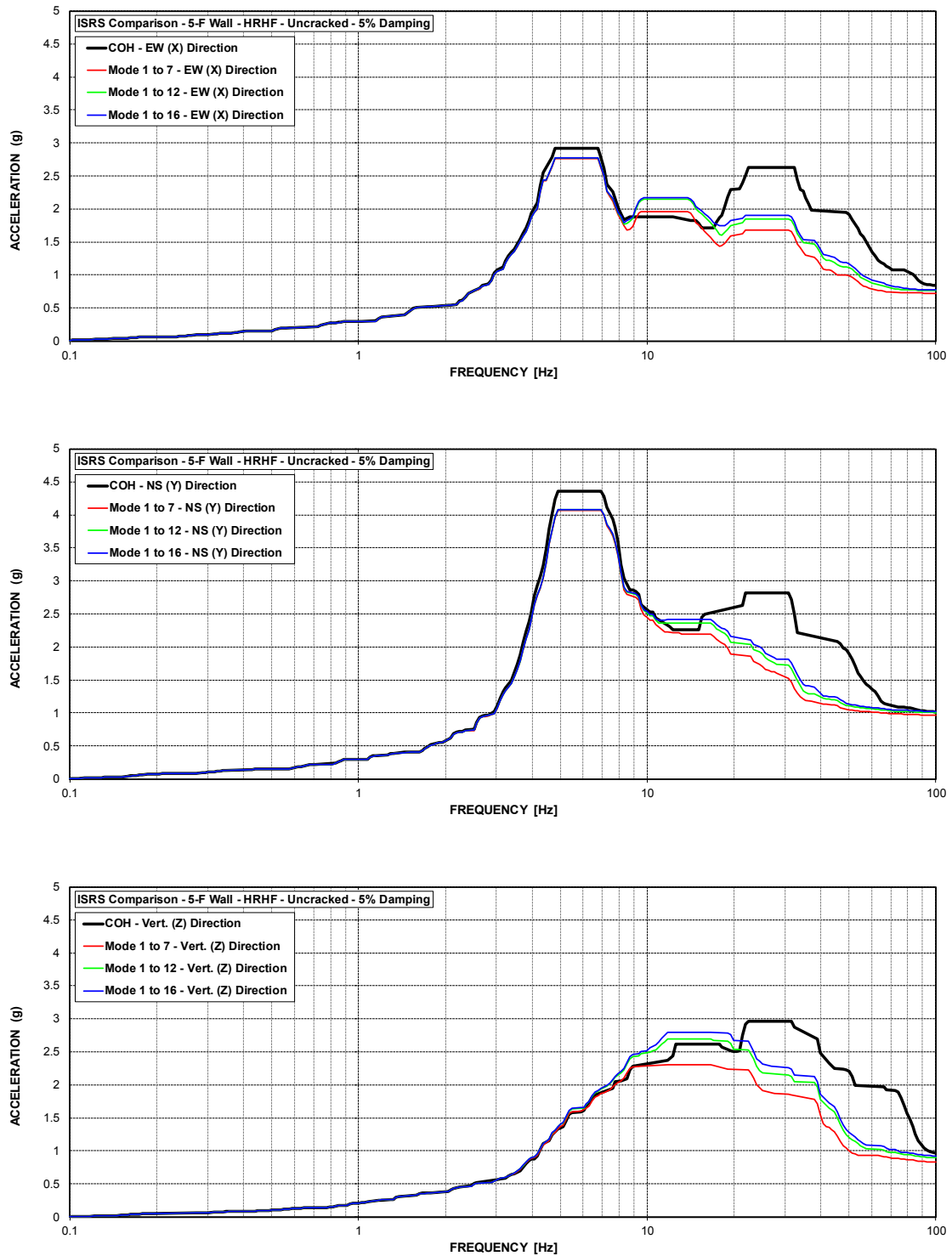


Figure C-154 ISRS – AB Shear Walls (5-F) at El. 137.5' – HRHF – Uncracked

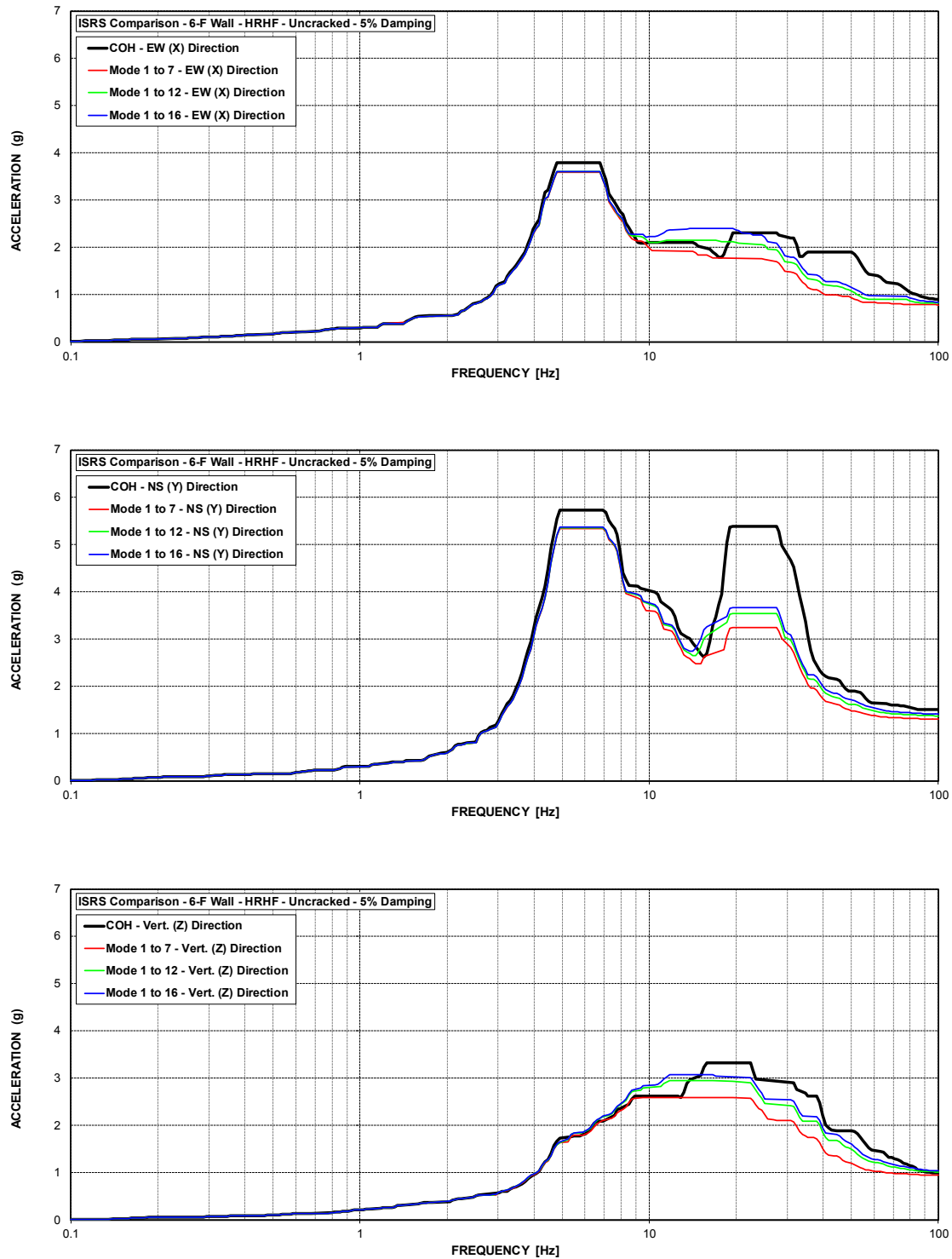


Figure C-155 ISRS – AB Shear Walls (6-F) at El. 156' – HRHF – Uncracked



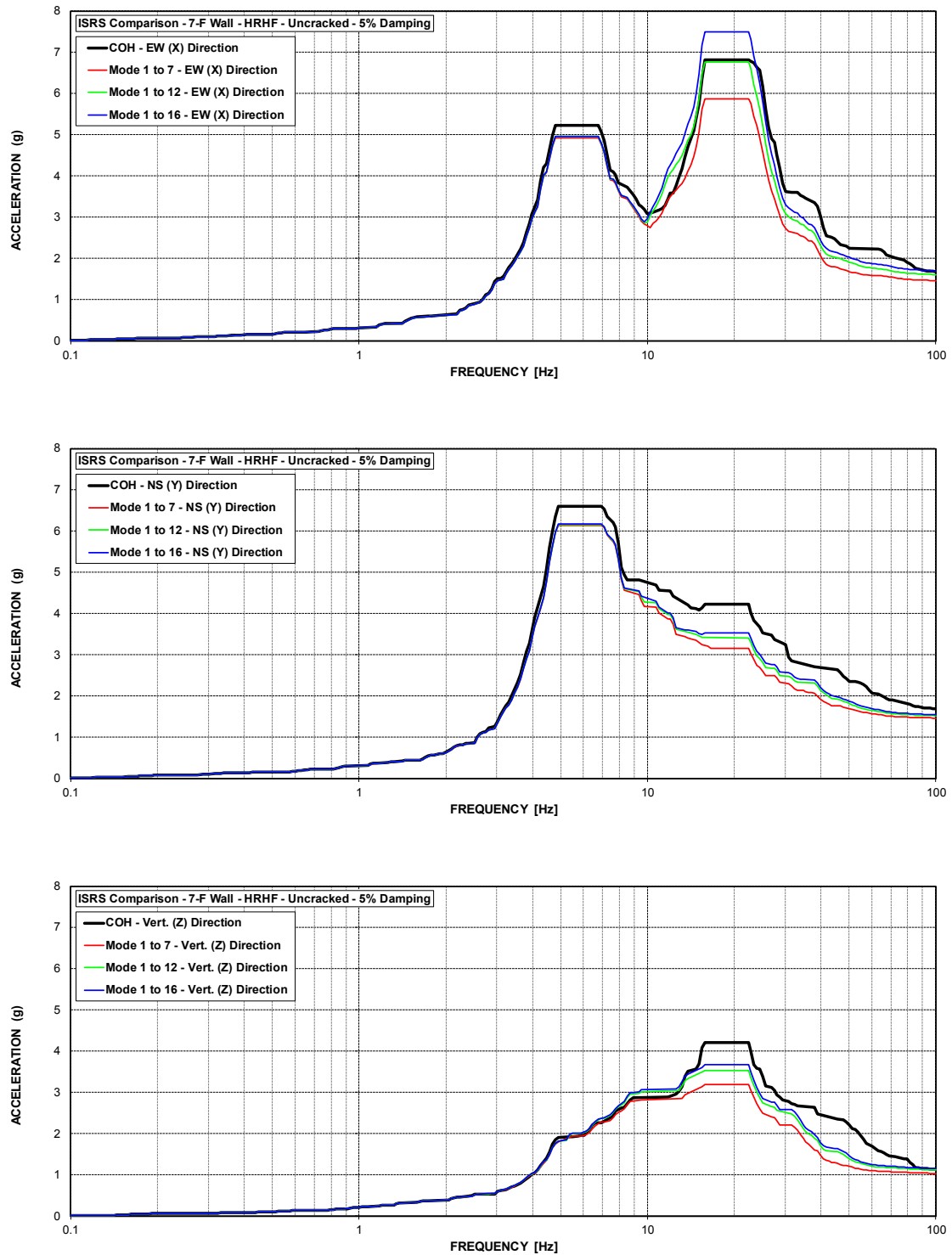


Figure C-156 ISRS – AB Shear Walls (7-F) at El. 174' – HRHF – Uncracked

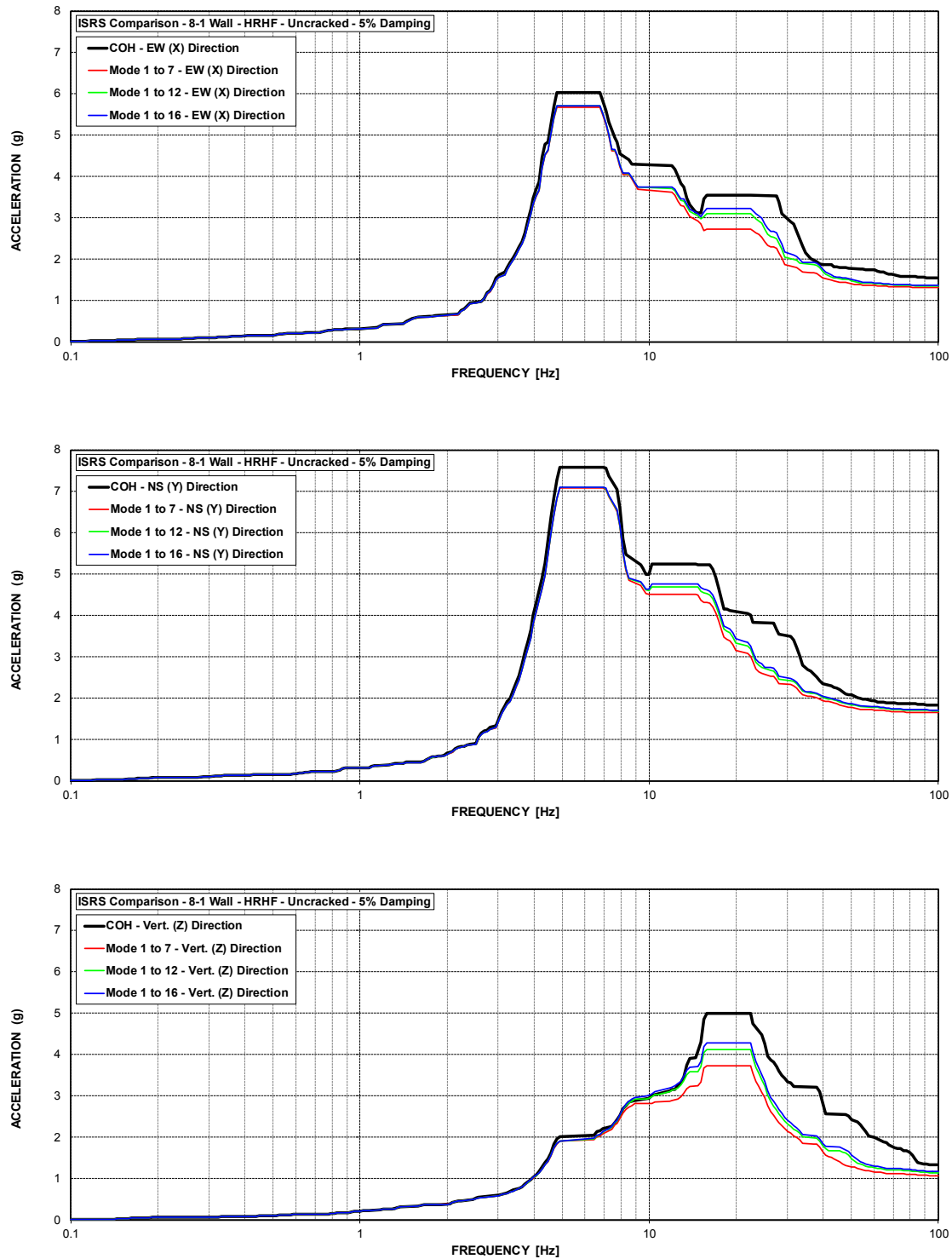


Figure C-157 ISRS – AB Shear Walls (8-1) at El. 195' – HRHF – Uncracked

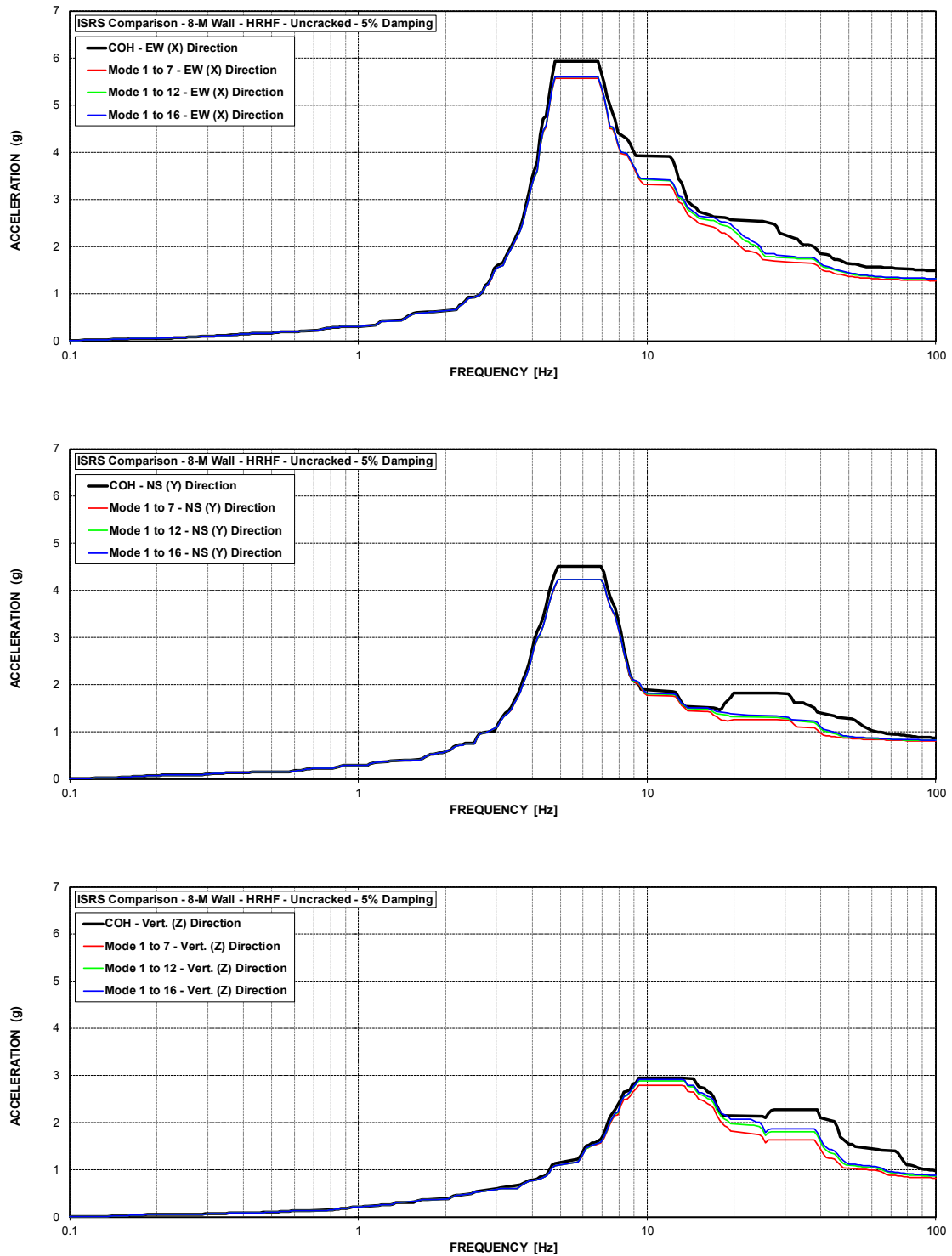


Figure C-158 ISRS – AB Shear Walls (8-M) at El. 195' – HRHF – Uncracked

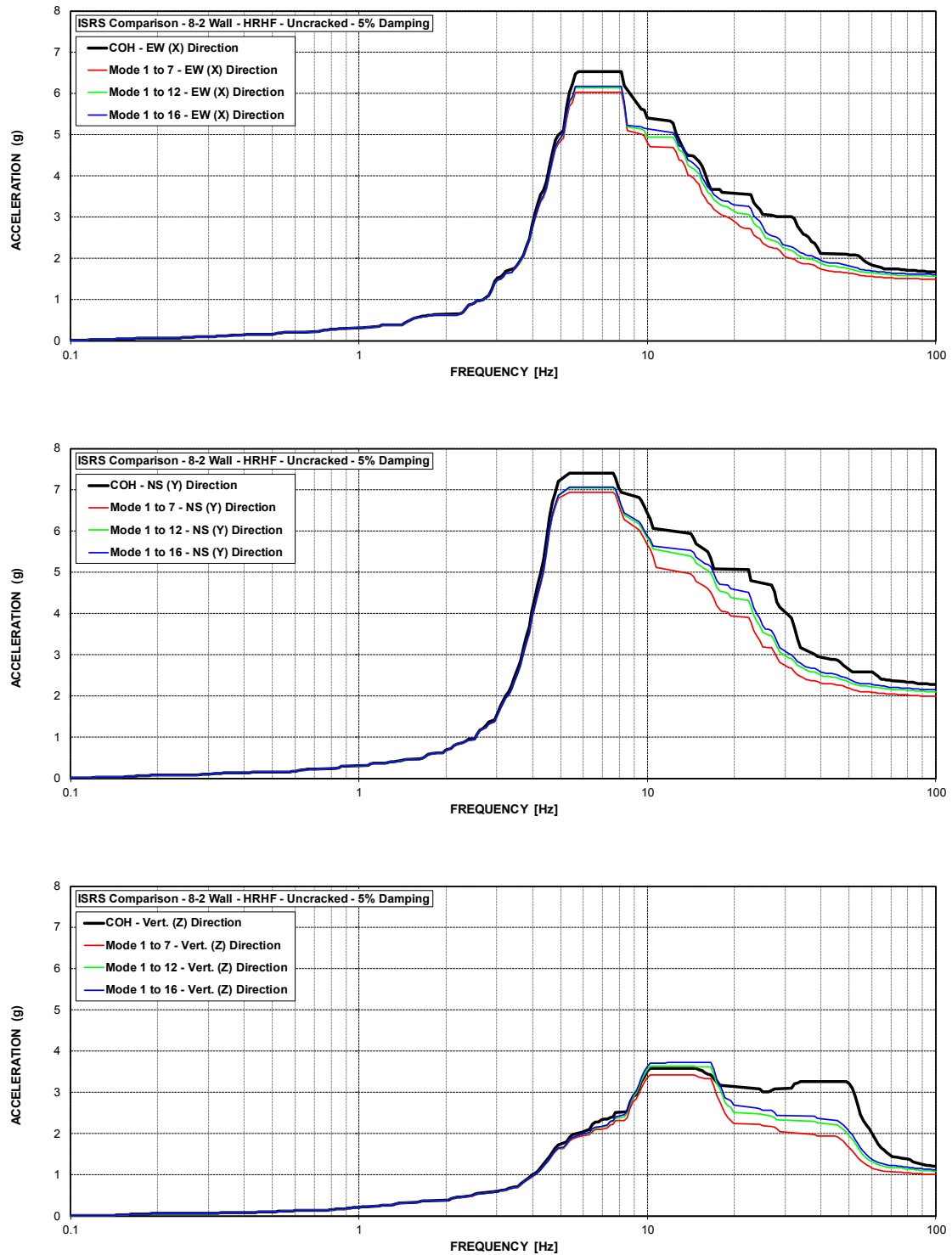


Figure C-159 ISRS – AB Shear Walls (8-2) at El. 216.75' – HRHF – Uncracked

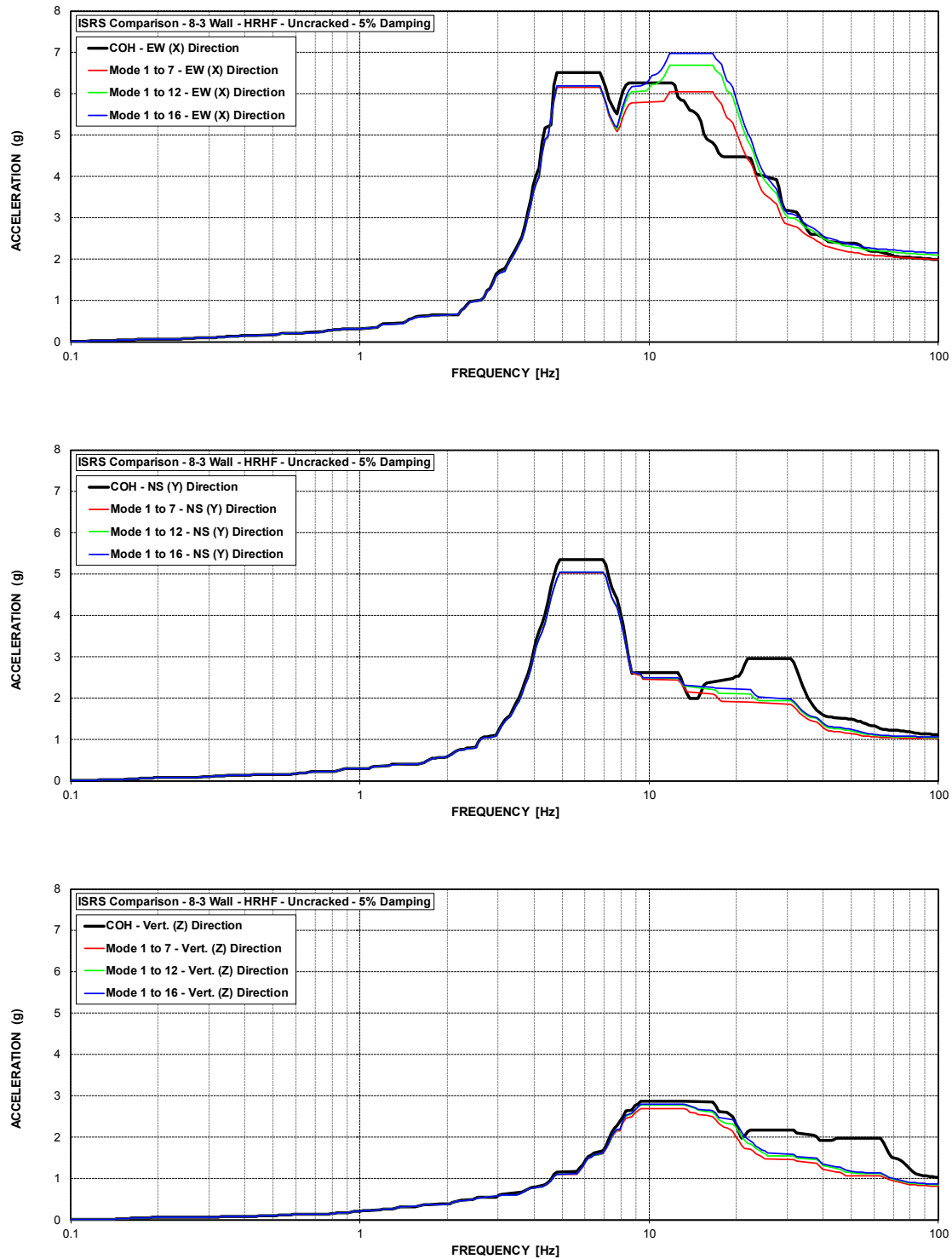


Figure C-160 ISRS – AB Shear Walls (8-3) at El. 213' – HRHF – Uncracked

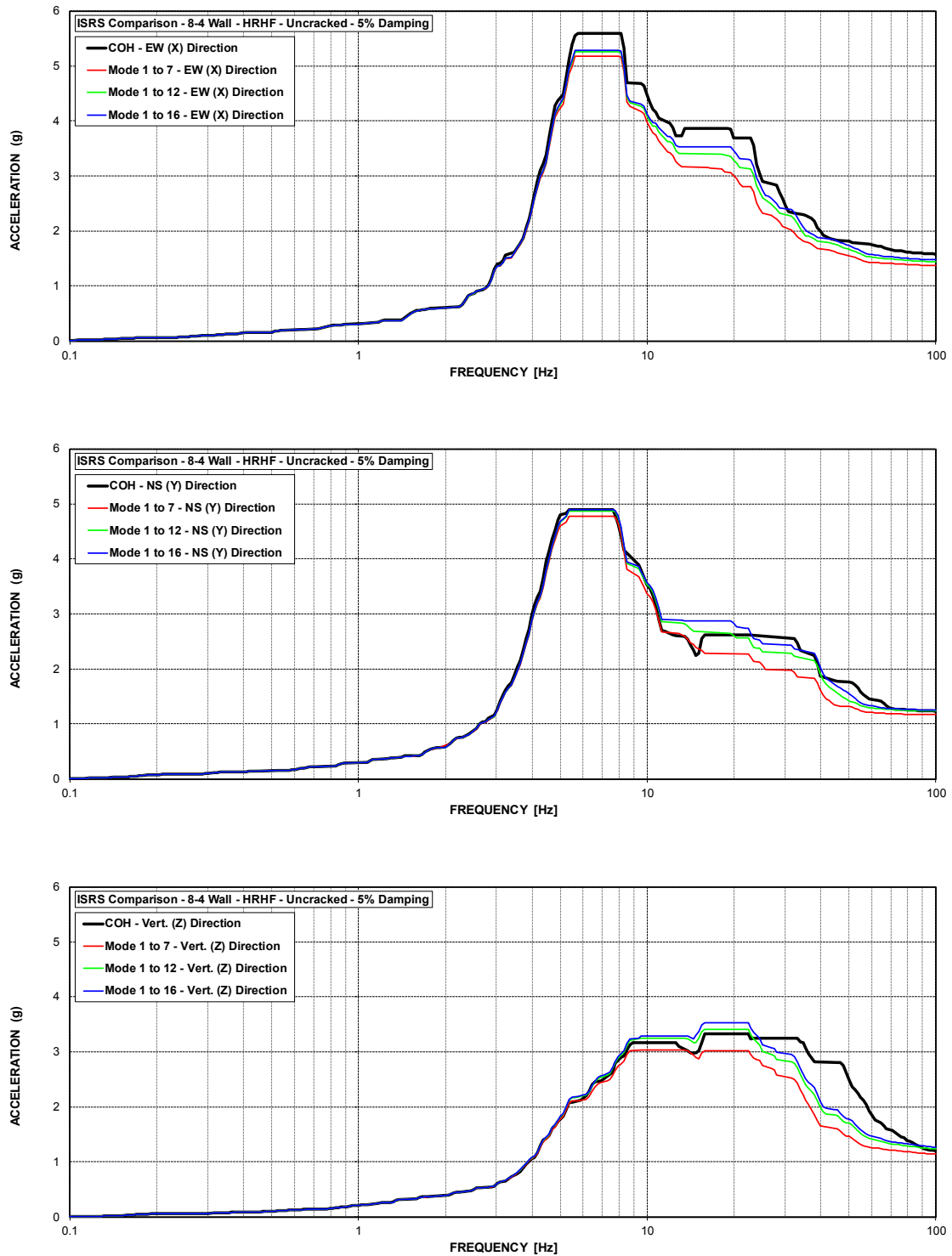


Figure C-161 ISRS – AB Shear Walls (8-4) at El. 213.5' – HRHF – Uncracked

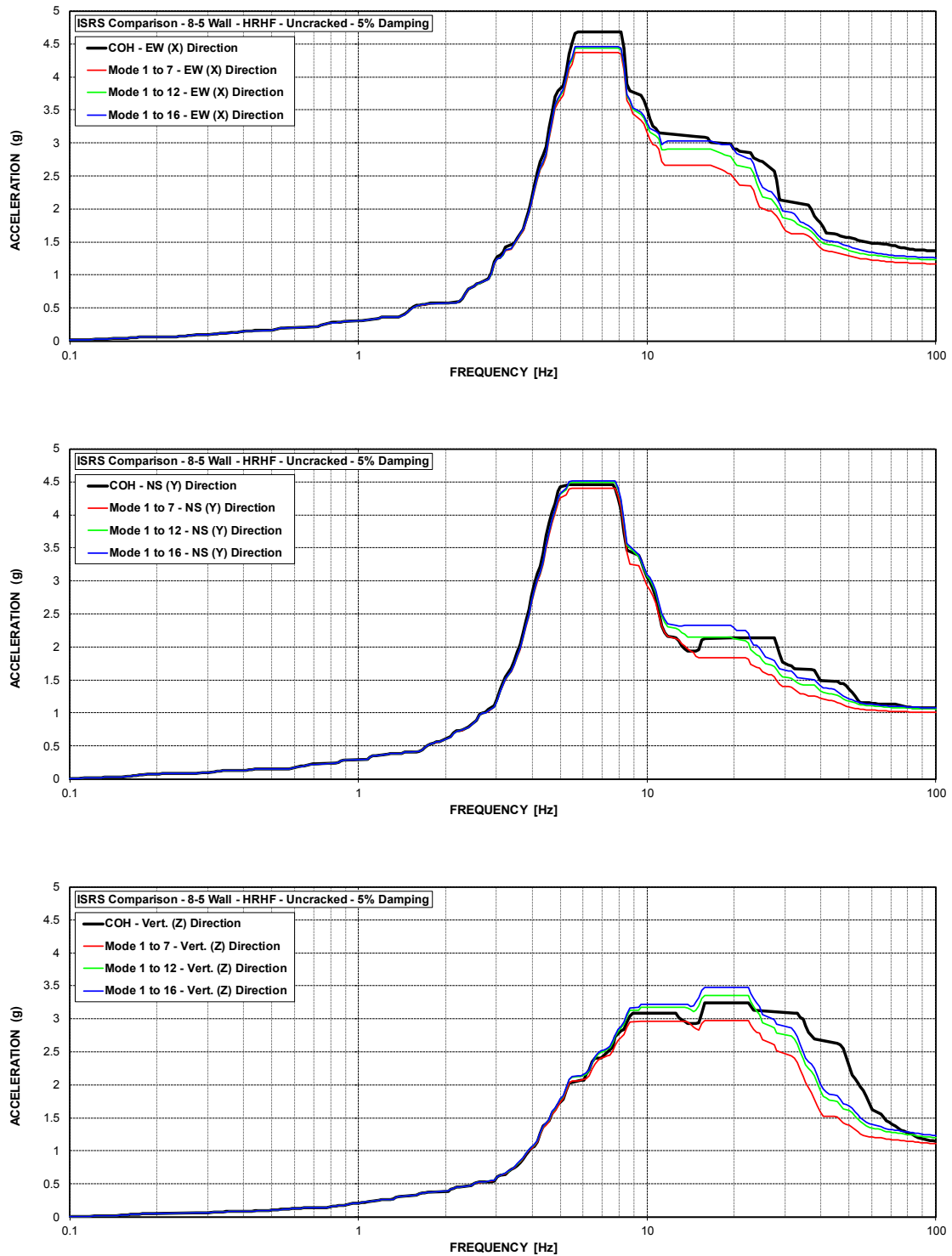


Figure C-162 ISRS – AB Shear Walls (8-5) at El. 195' – HRHF – Uncracked

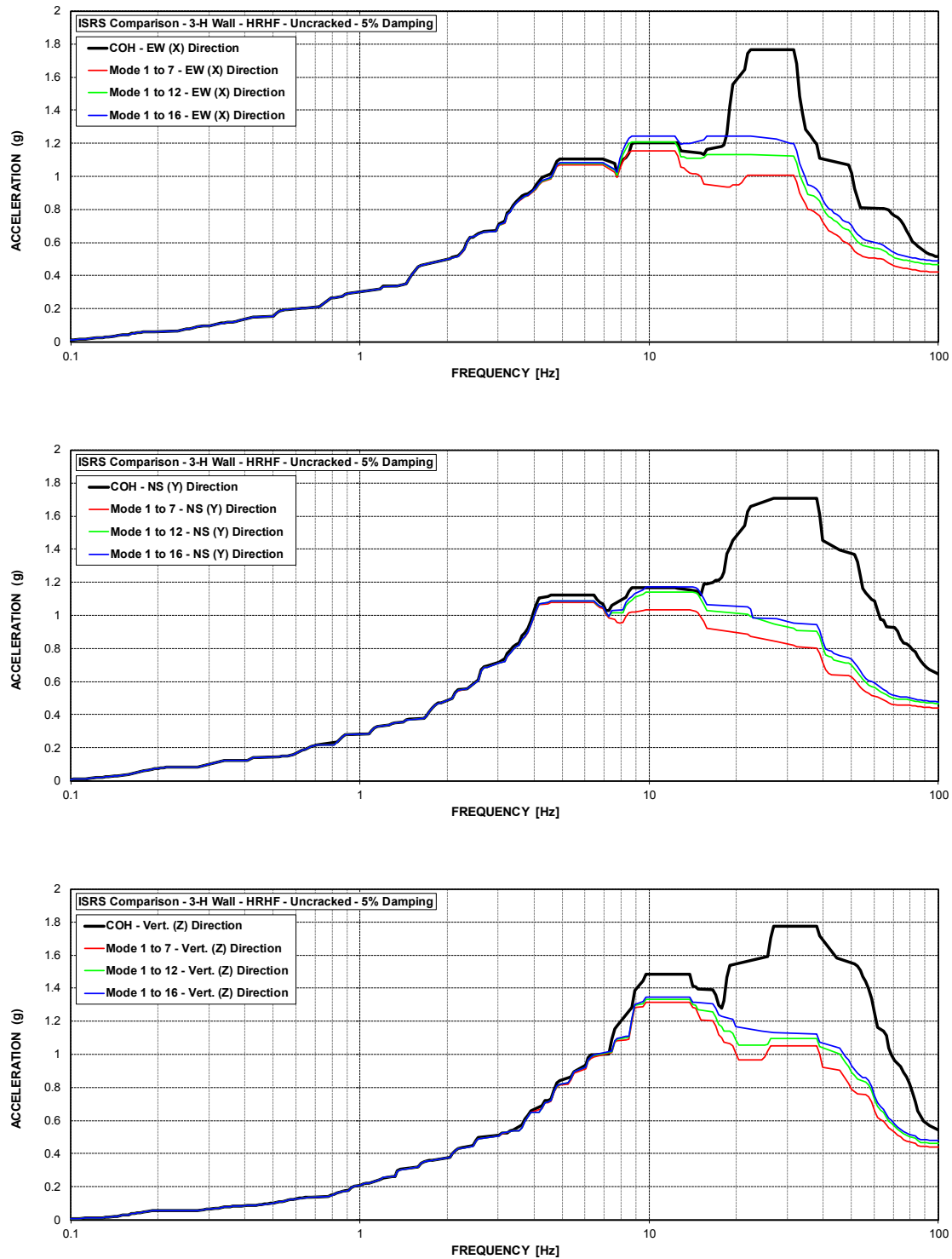


Figure C-163 ISRS – AB Shear Walls (3-H) at El. 100' – HRHF – Uncracked



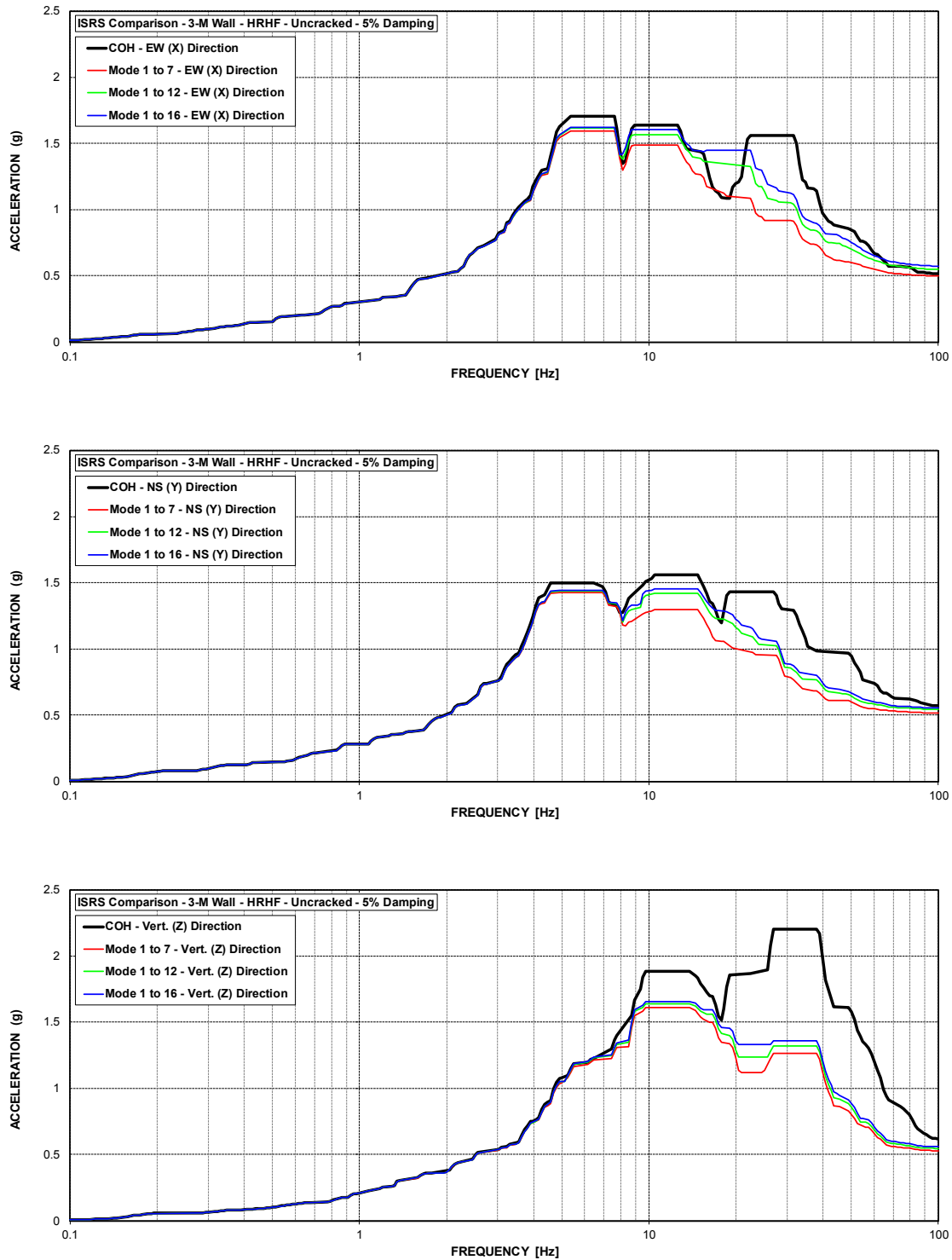


Figure C-164 ISRS – AB Shear Walls (3-M) at El. 114' – HRHF – Uncracked

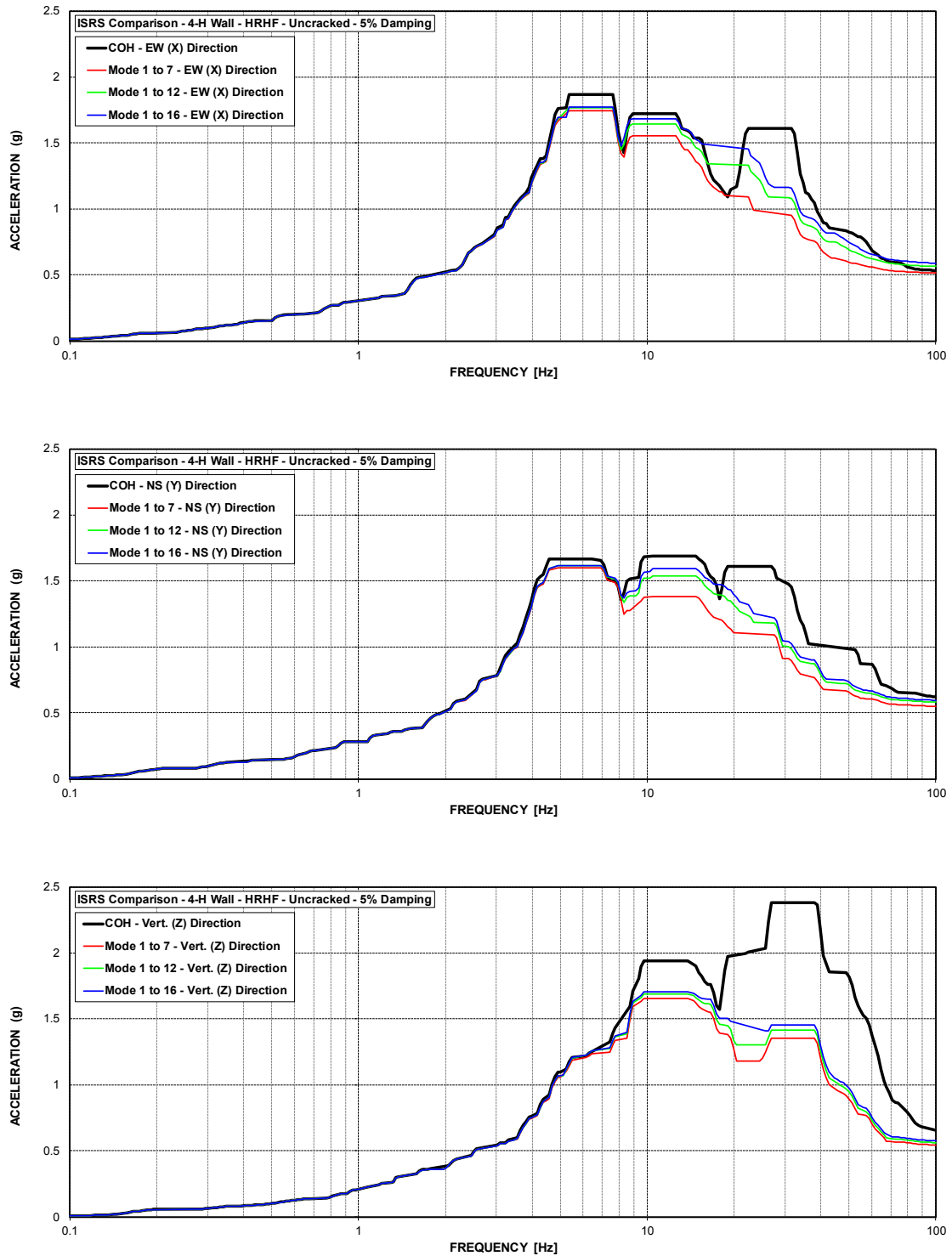


Figure C-165 ISRS – AB Shear Walls (4-H) at El. 120' – HRHF – Uncracked

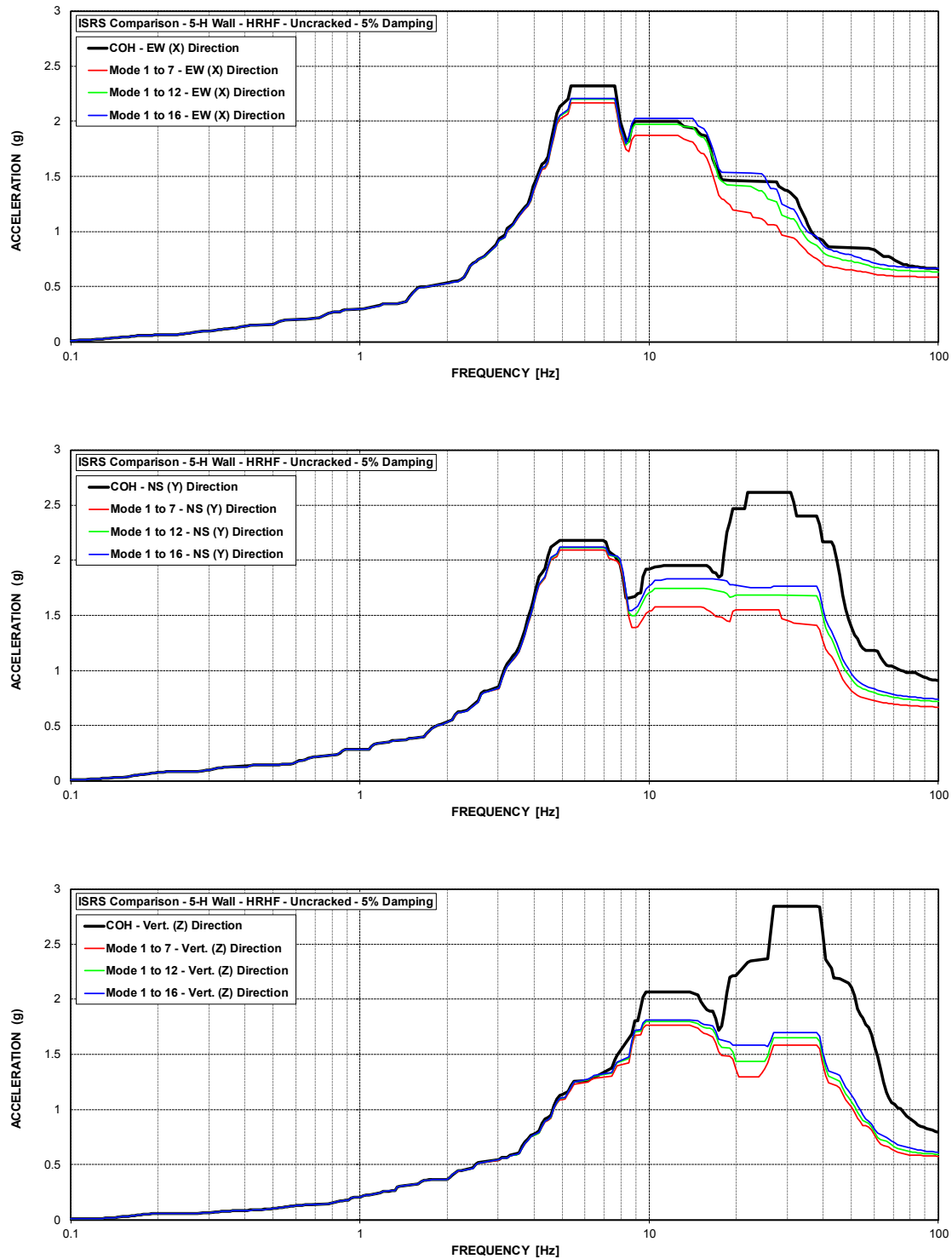


Figure C-166 ISRS – AB Shear Walls (5-H) at El. 137.5' – HRHF – Uncracked

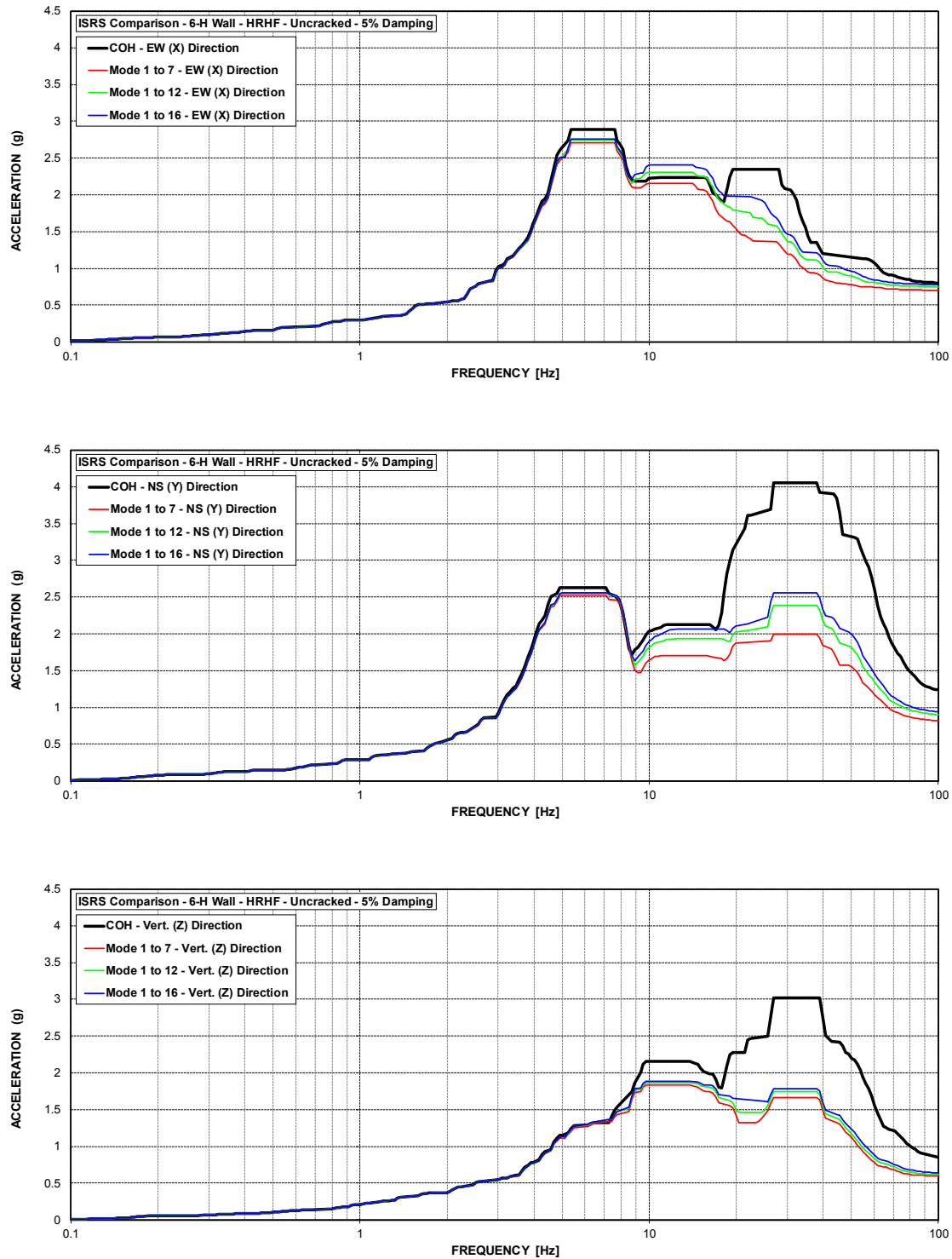


Figure C-167 ISRS – AB Shear Walls (6-H) at El. 156' – HRHF – Uncracked

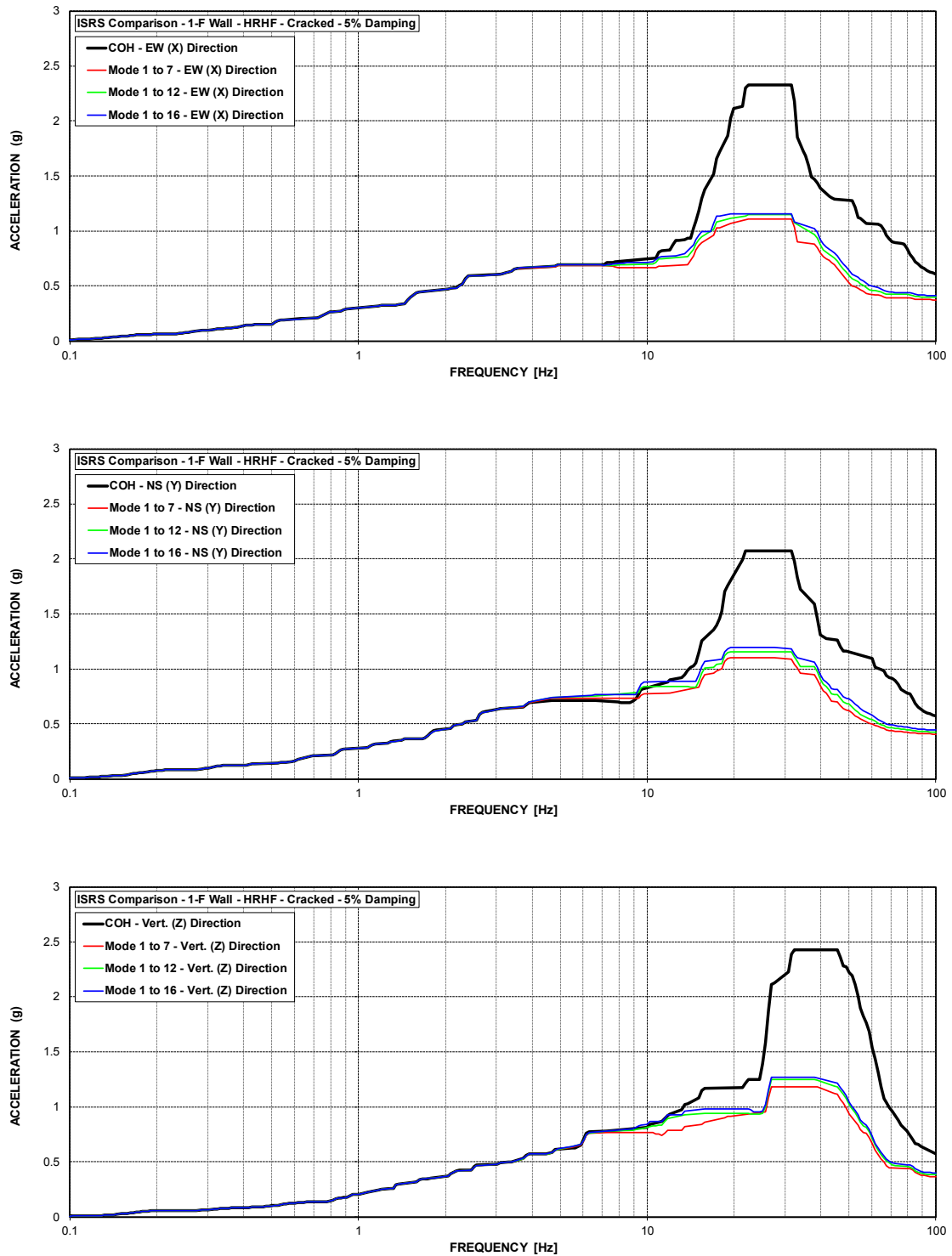


Figure C-168 ISRS – AB Shear Walls (1-F) at El. 55' – HRHF – Cracked

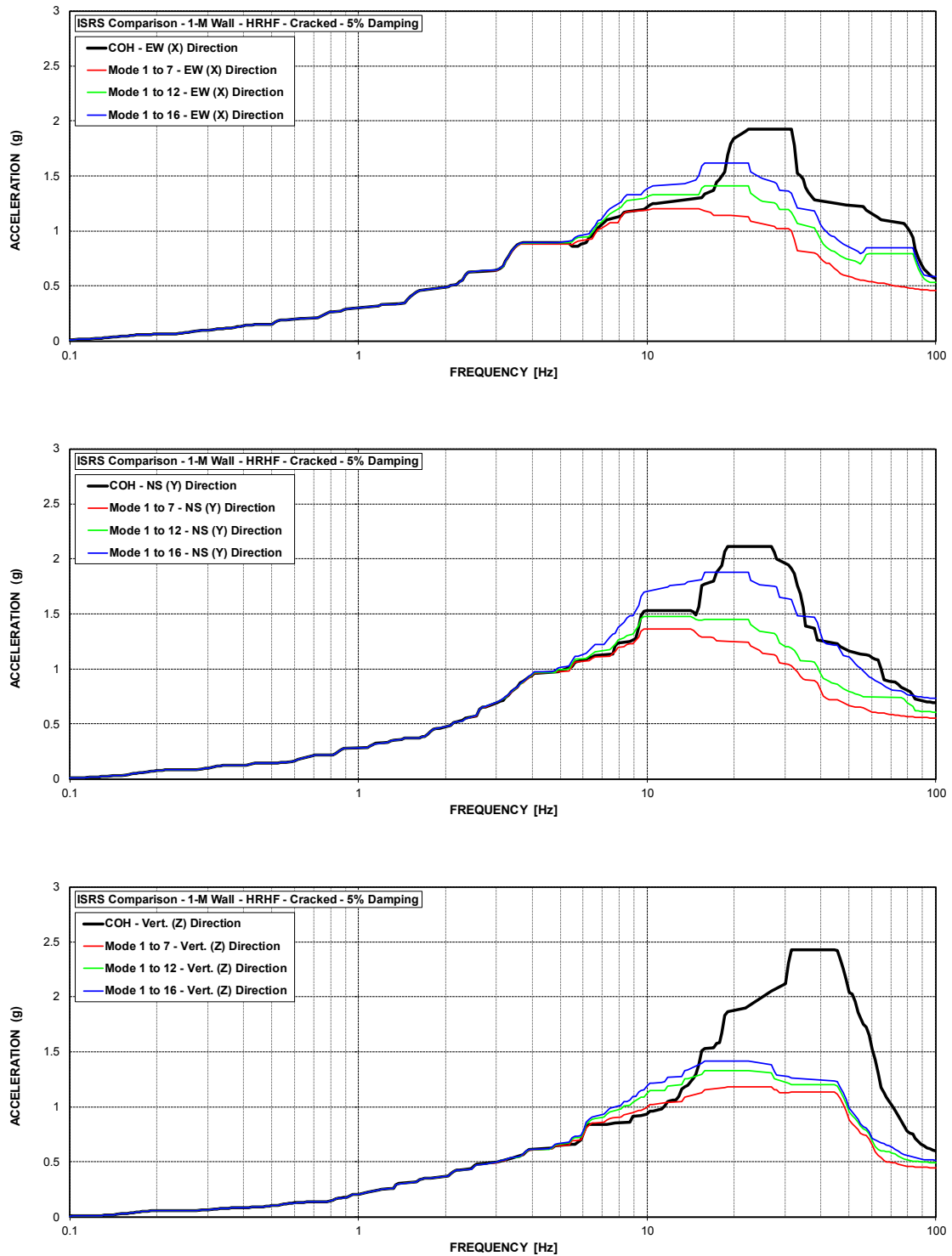


Figure C-169 ISRS – AB Shear Walls (1-M) at El. 68' – HRHF – Cracked

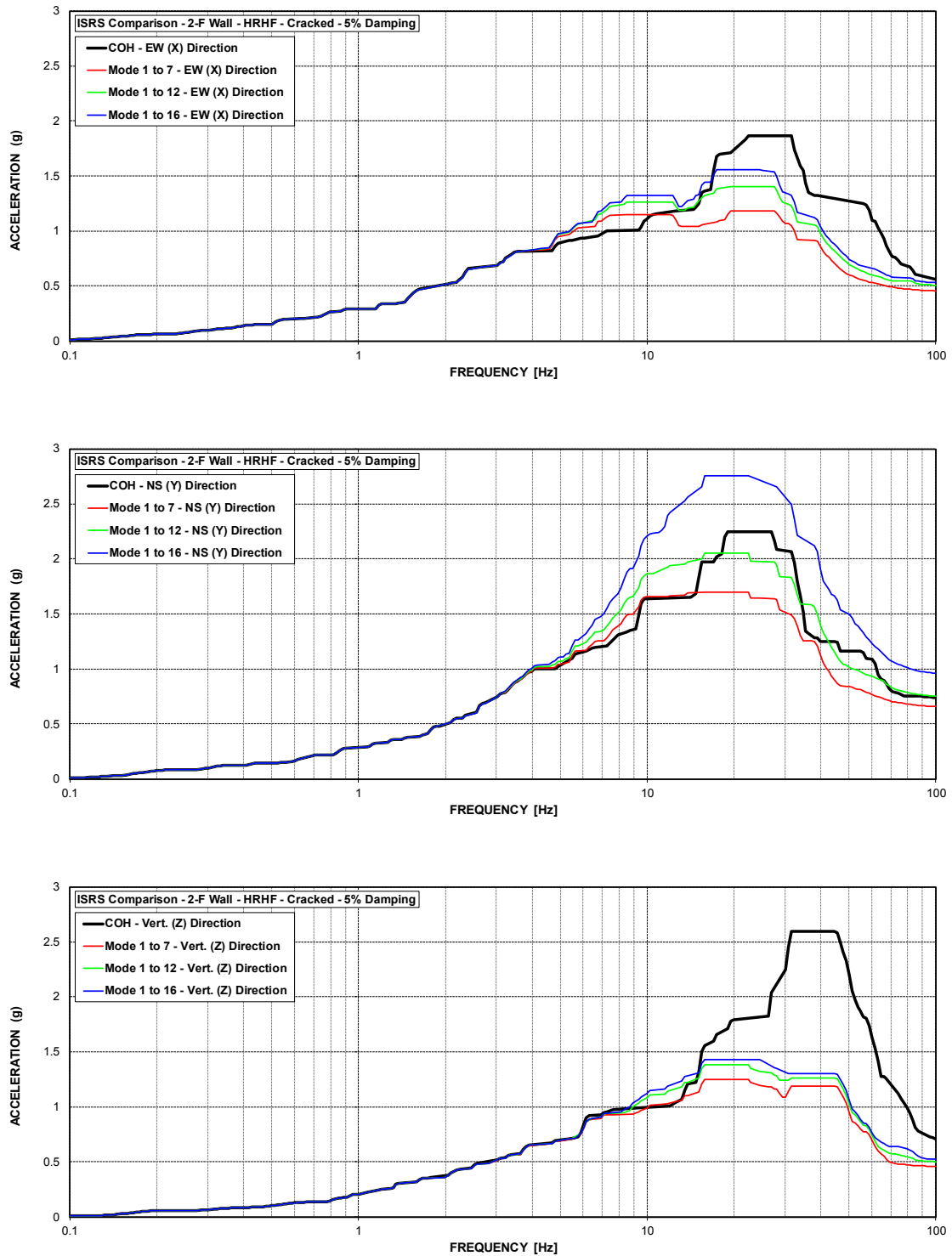


Figure C-170 ISRS – AB Shear Walls (2-F) at El. 78' – HRHF – Cracked

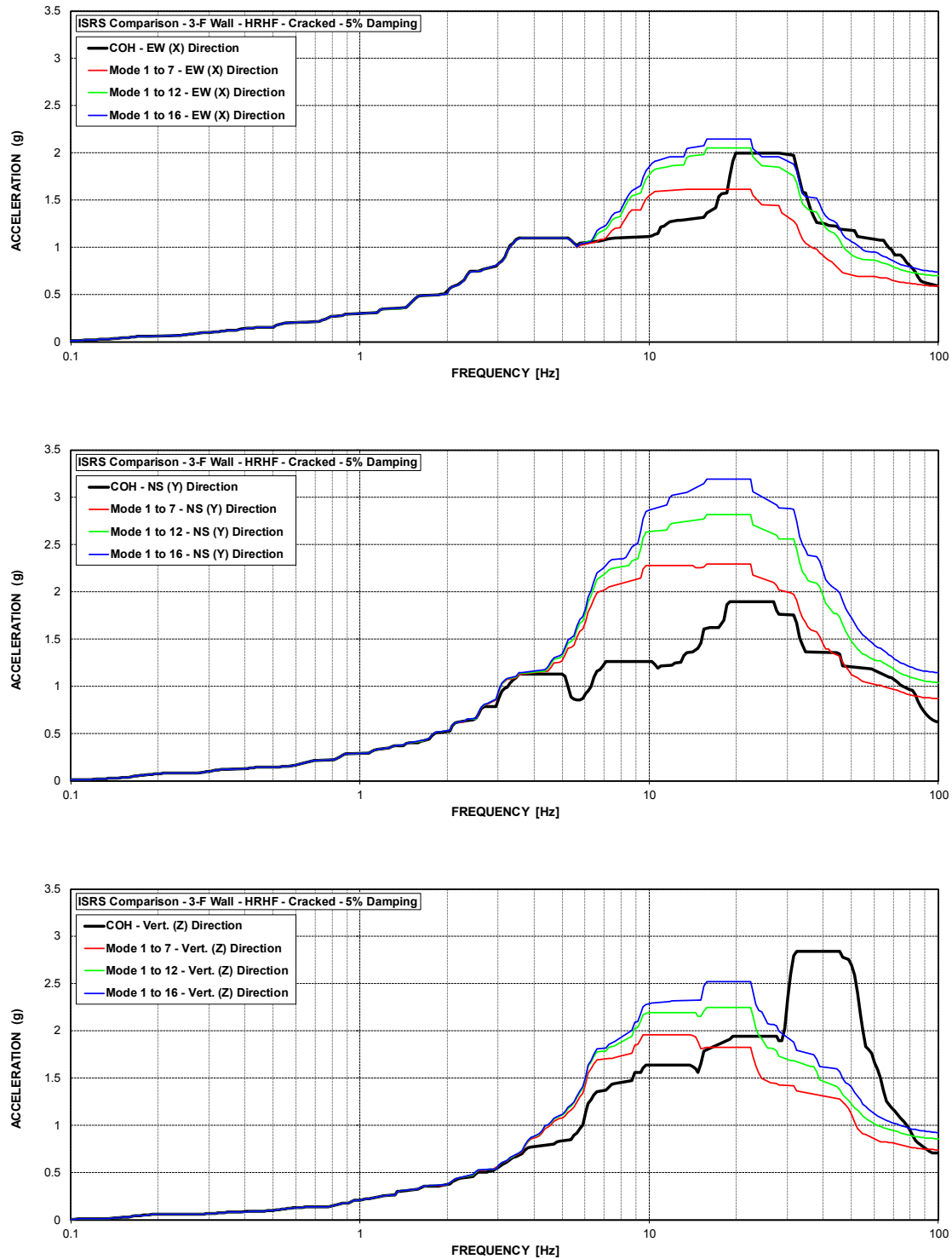


Figure C-171 ISRS – AB Shear Walls (3-F) at El. 100' – HRHF – Cracked



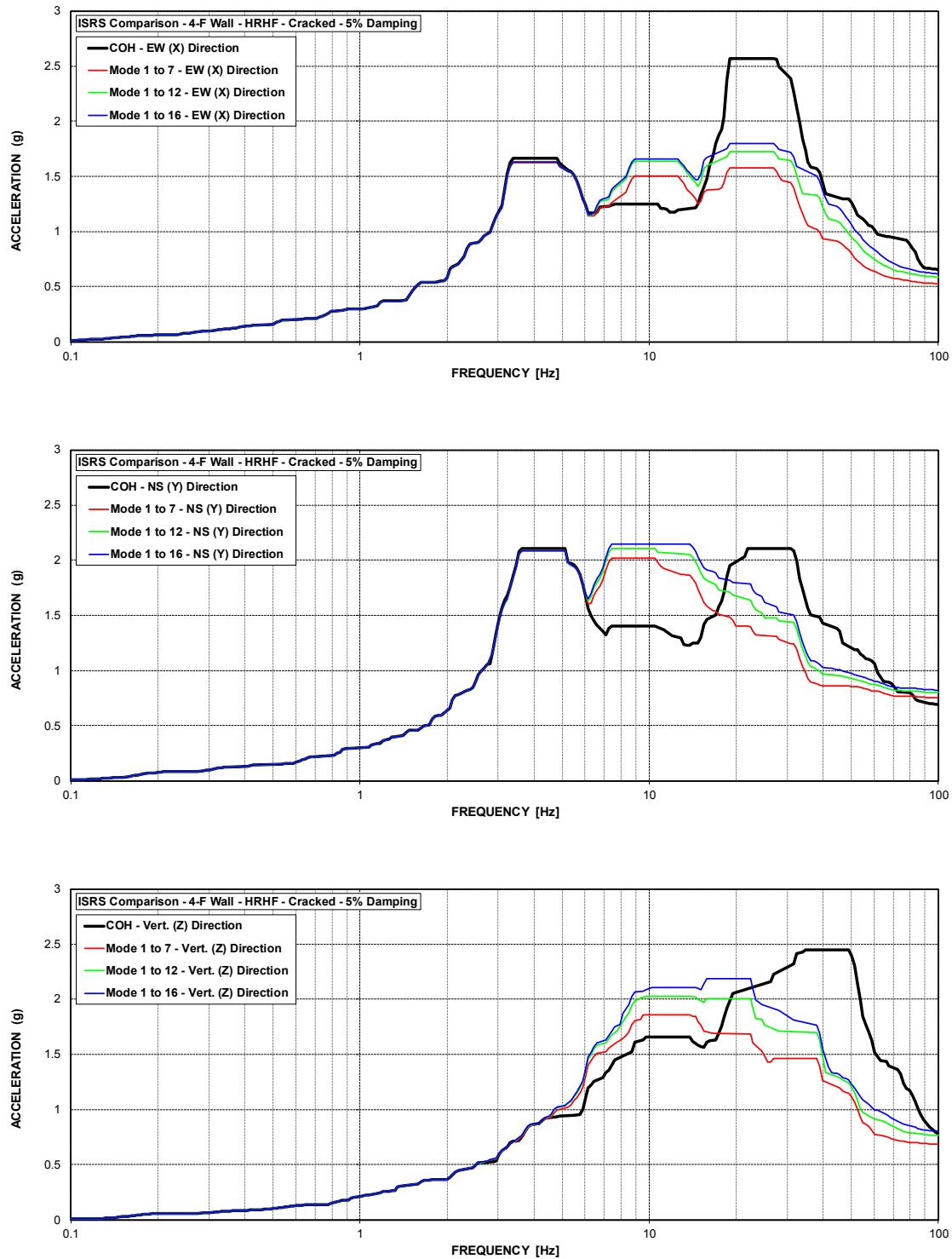


Figure C-172 ISRS – AB Shear Walls (4-F) at El. 120' – HRHF – Cracked

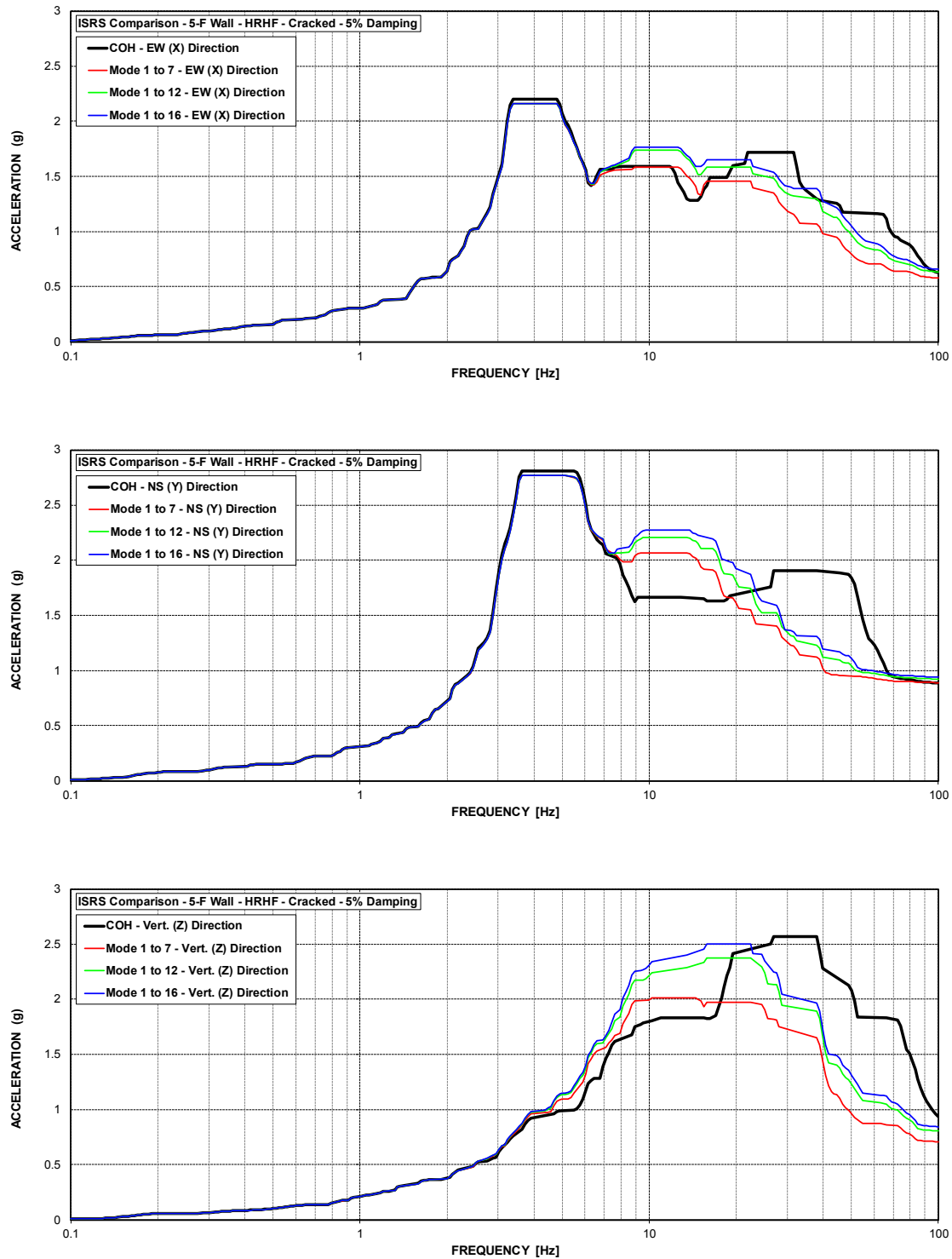


Figure C-173 ISRS – AB Shear Walls (5-F) at El. 137.5' – HRHF – Cracked

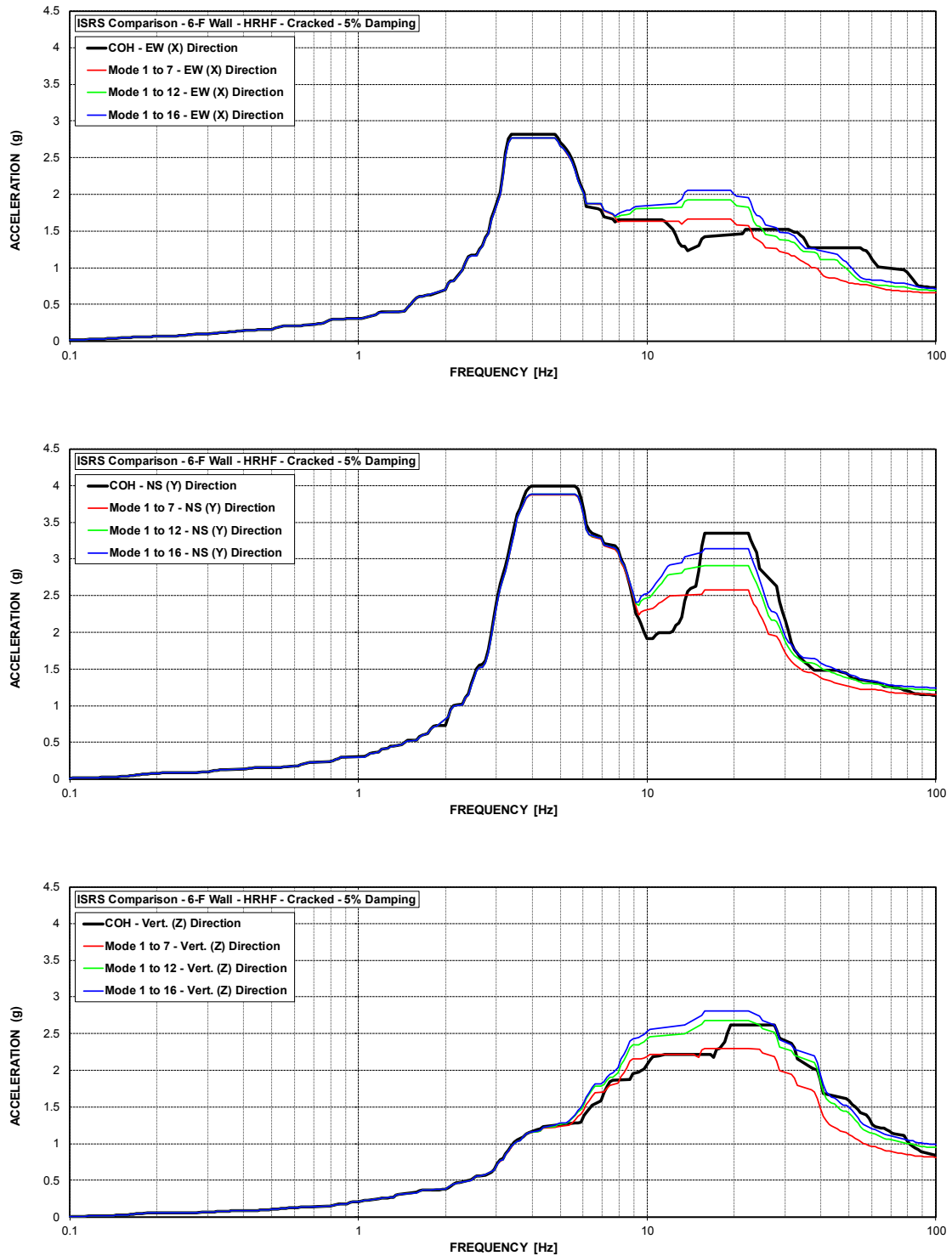


Figure C-174 ISRS – AB Shear Walls (6-F) at El. 156' – HRHF – Cracked

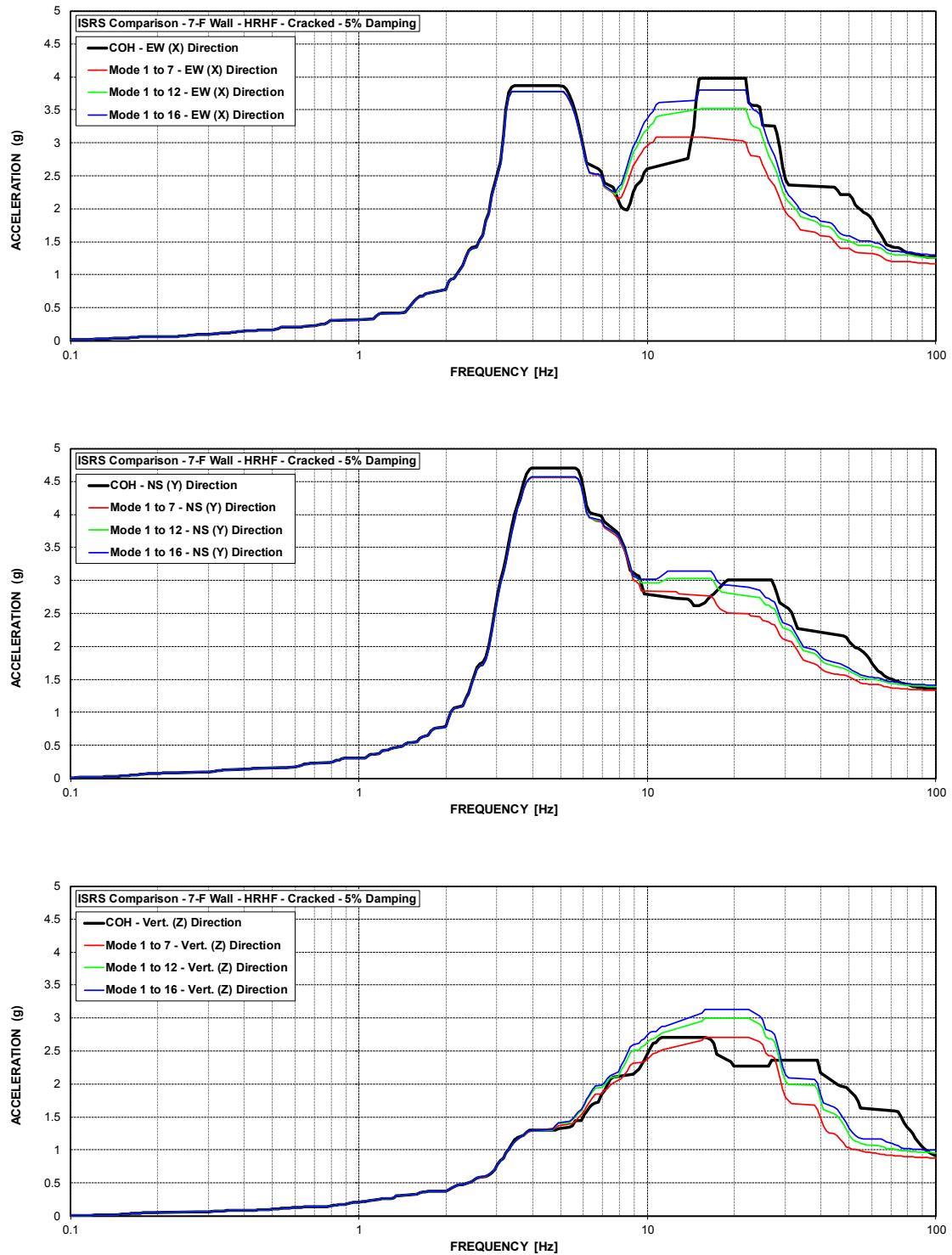


Figure C-175 ISRS – AB Shear Walls (7-F) at El. 174' – HRHF – Cracked

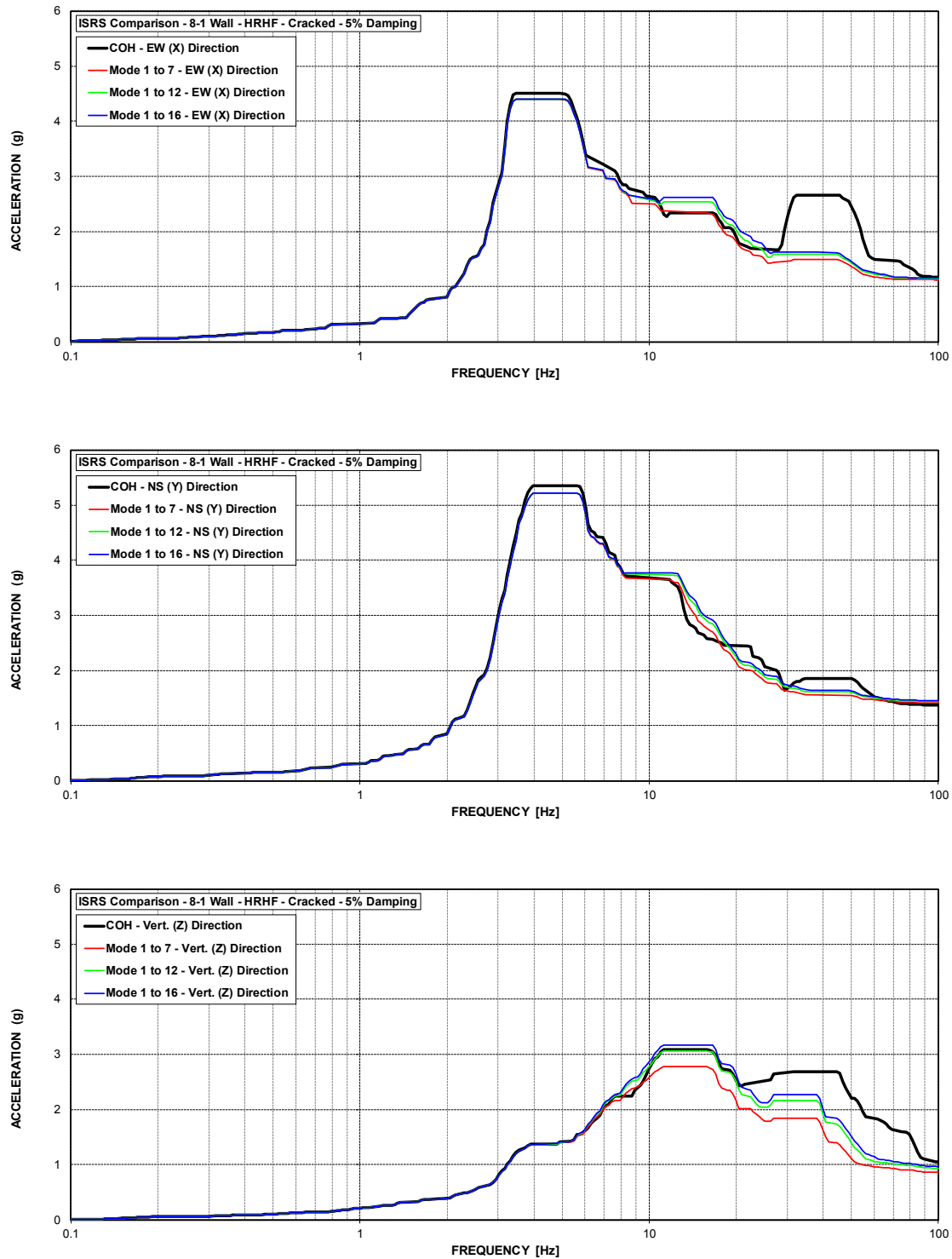


Figure C-176 ISRS – AB Shear Walls (8-1) at El. 195' – HRHF – Cracked

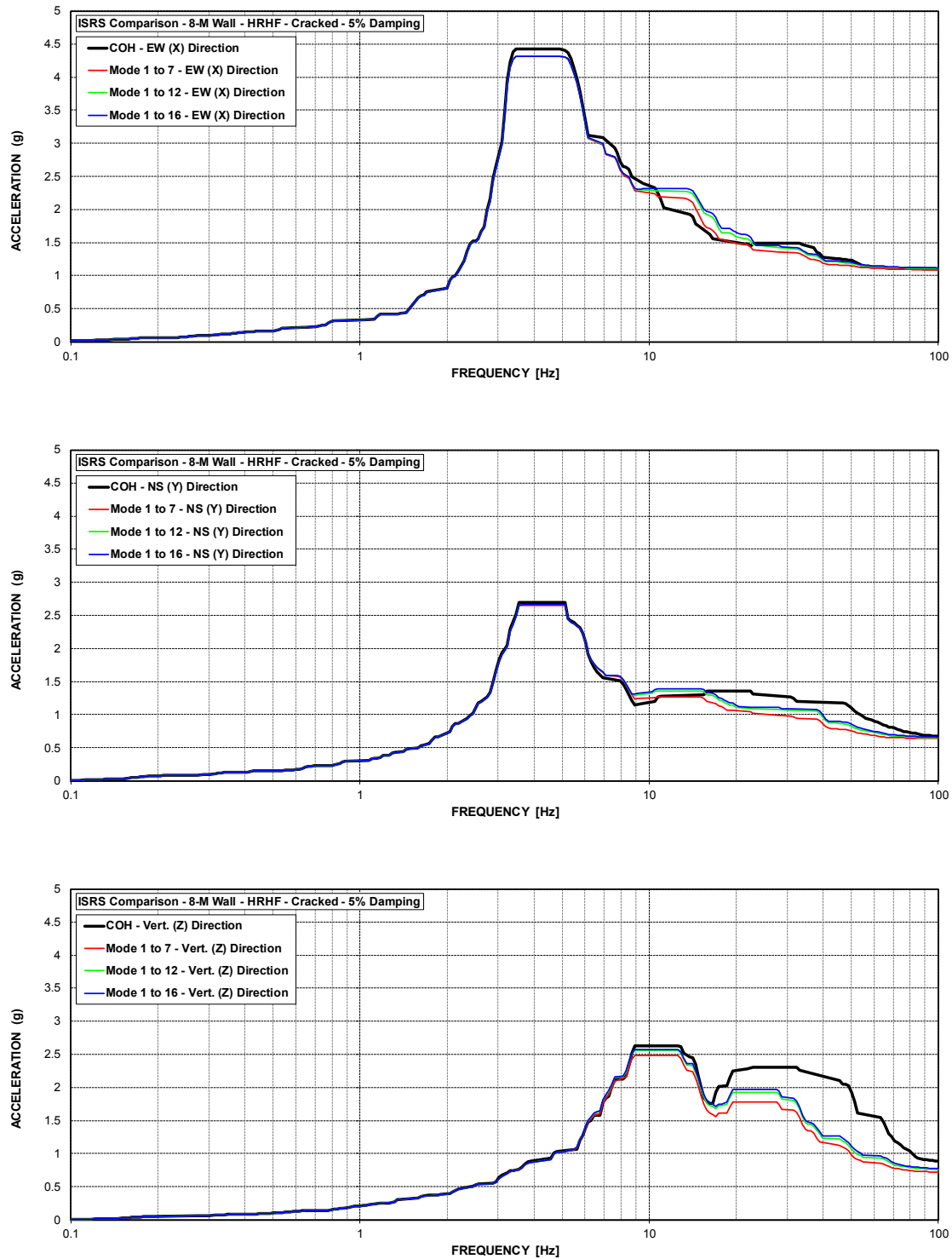


Figure C-177 ISRS – AB Shear Walls (8-M) at El. 195' – HRHF – Cracked

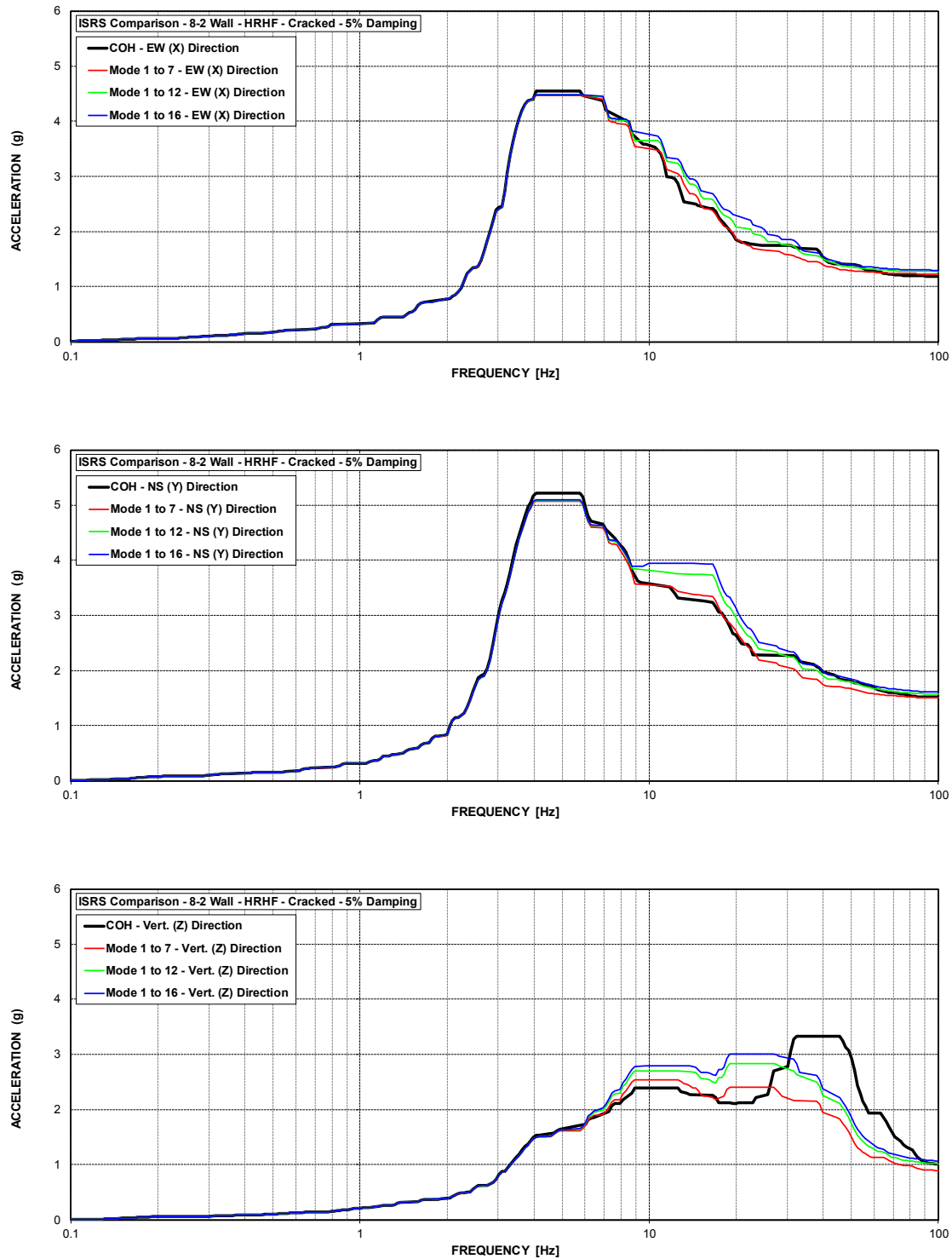


Figure C-178 ISRS – AB Shear Walls (8-2) at El. 216.75' – HRHF – Cracked

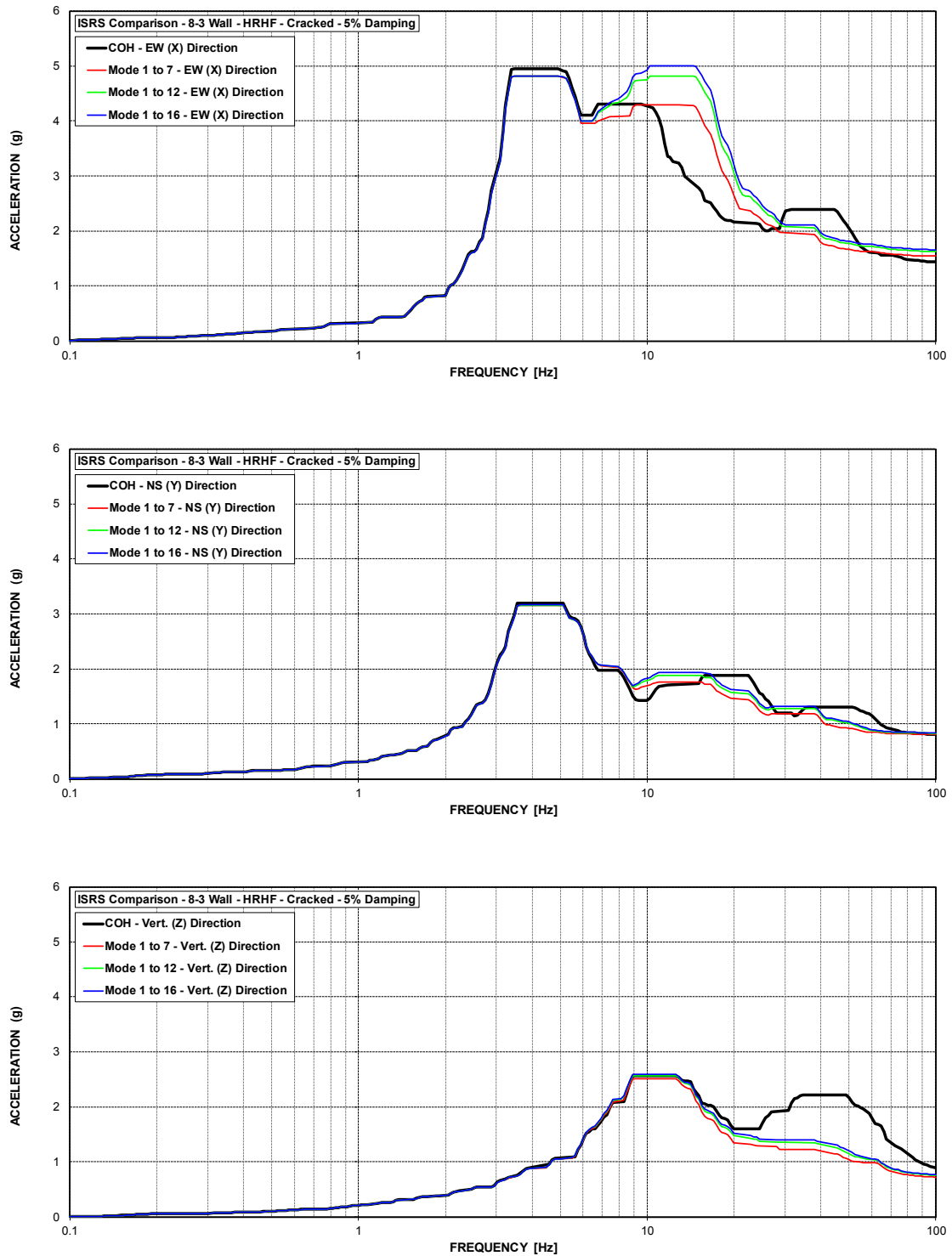


Figure C-179 ISRS – AB Shear Walls (8-3) at El. 213' – HRHF – Cracked



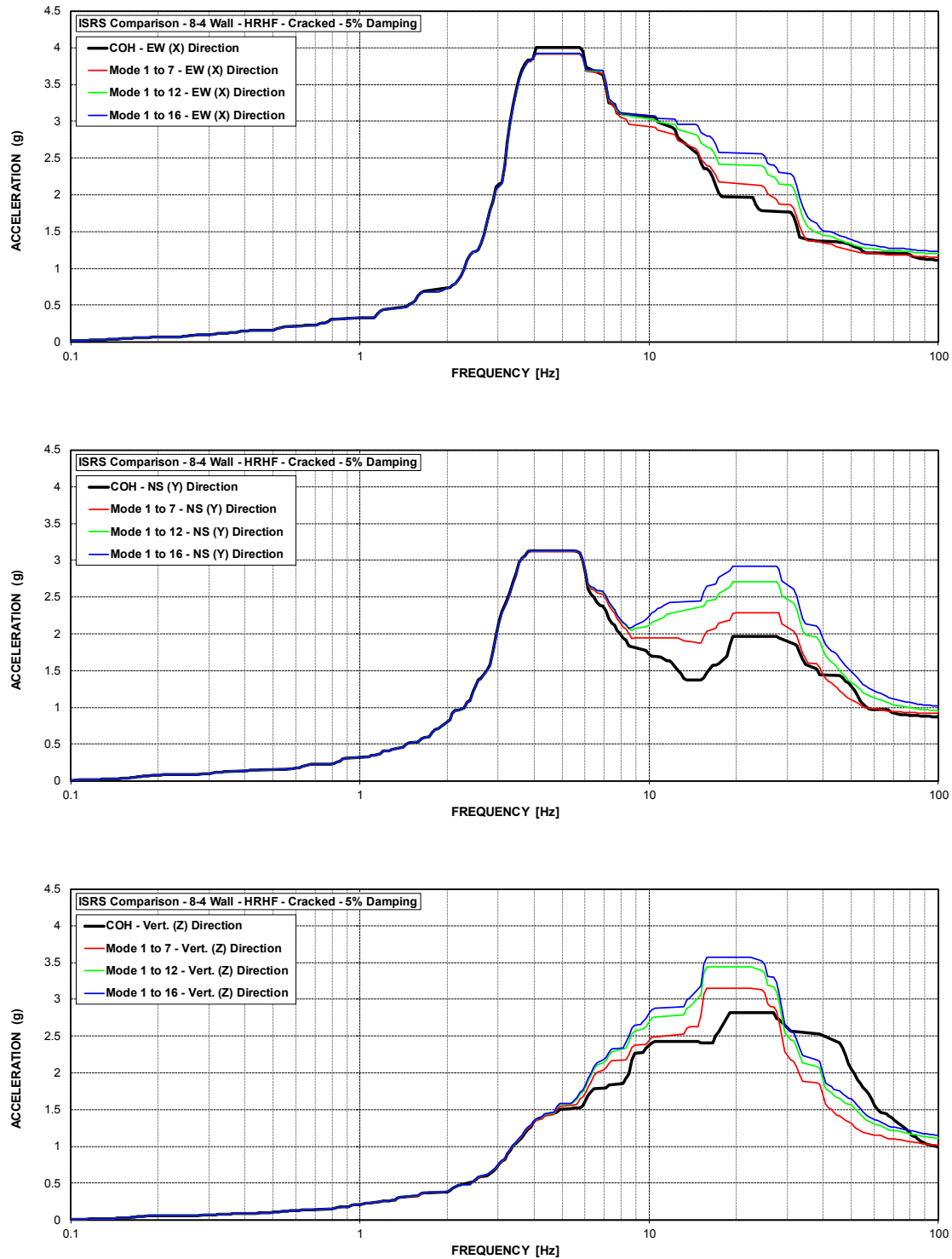


Figure C-180 ISRS – AB Shear Walls (8-4) at El. 213.5' – HRHF – Cracked

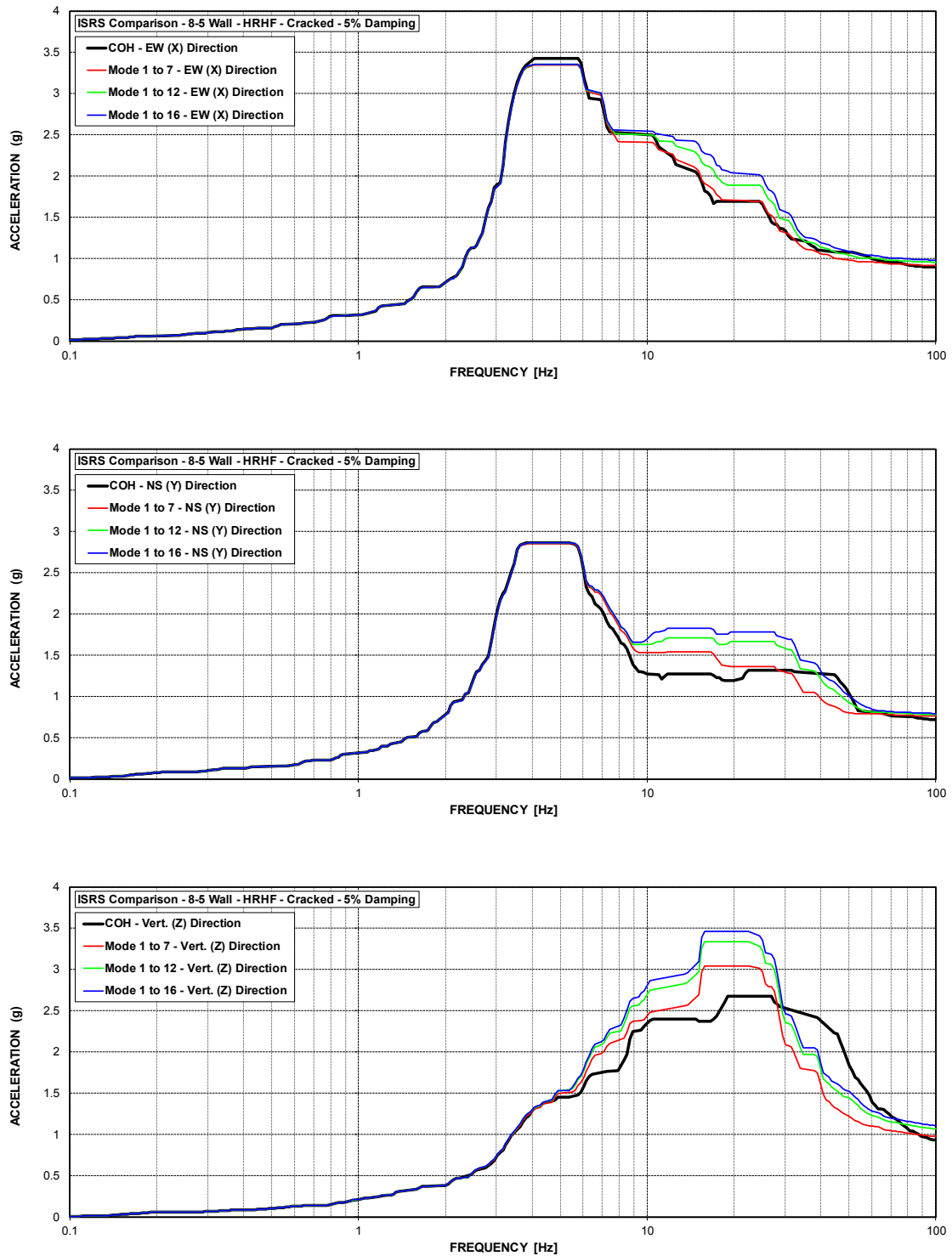


Figure C-181 ISRS – AB Shear Walls (8-5) at El. 195' – HRHF – Cracked

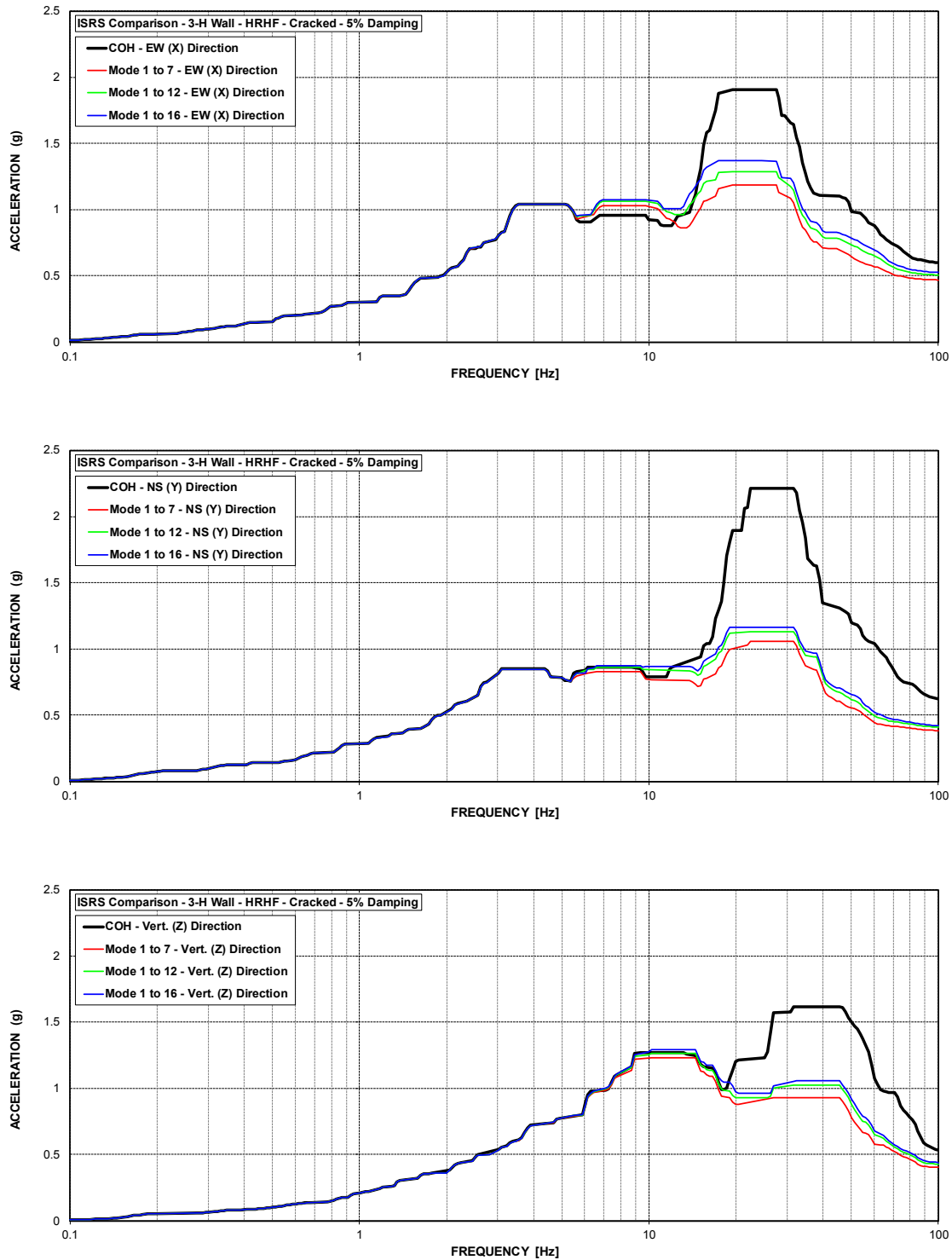


Figure C-182 ISRS – AB Shear Walls (3-H) at El. 100' – HRHF – Cracked

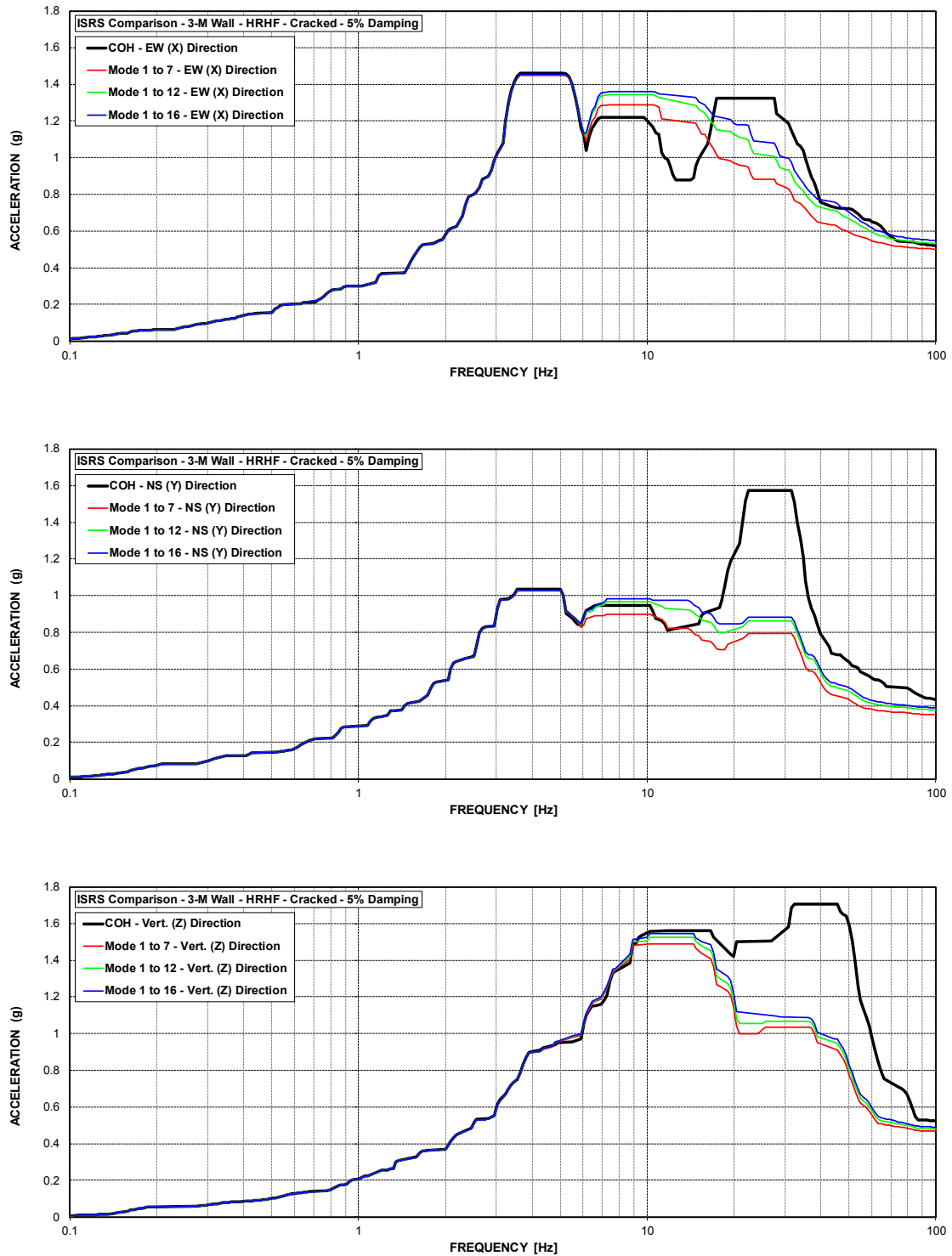


Figure C-183 ISRS – AB Shear Walls (3-M) at El. 114' – HRHF – Cracked

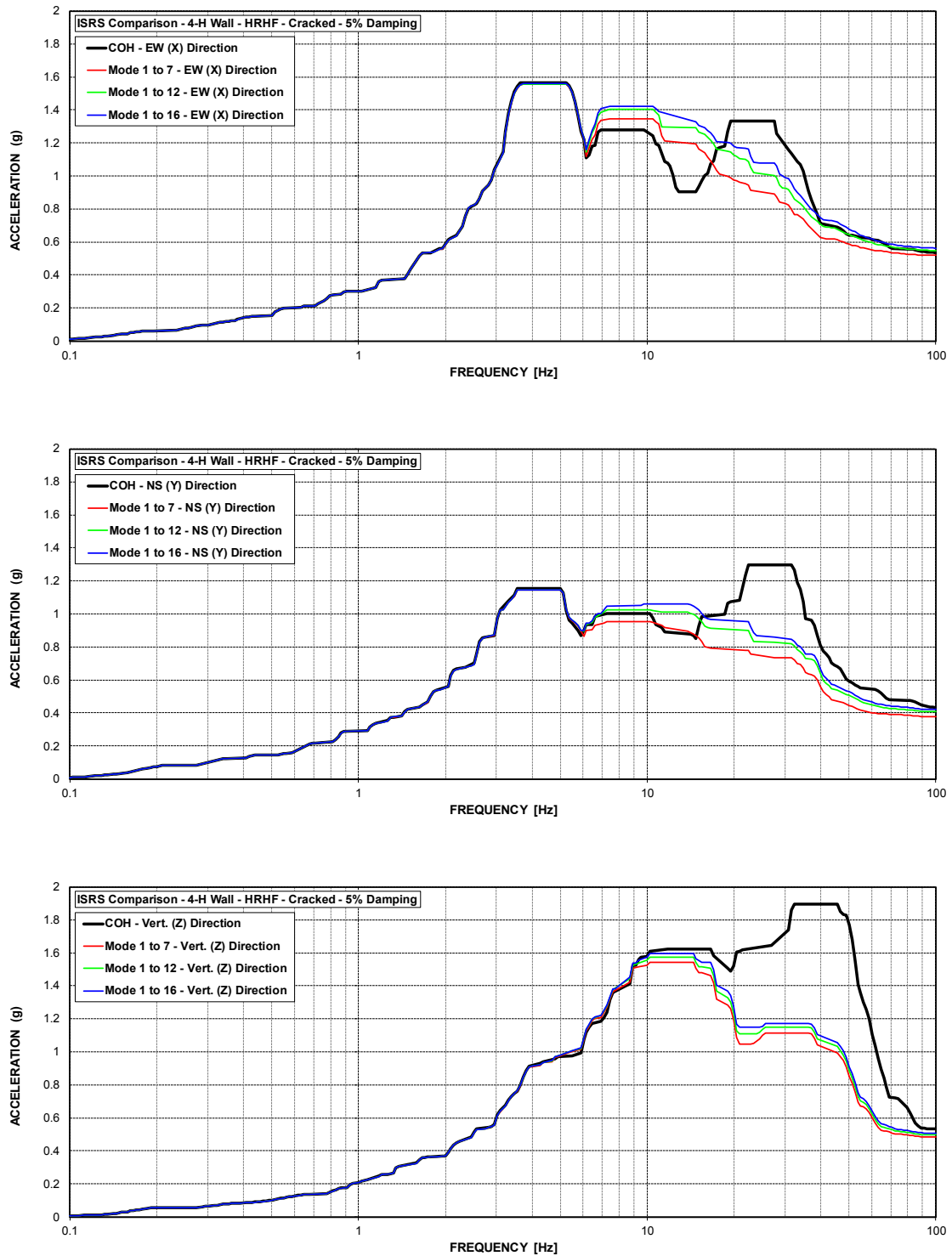


Figure C-184 ISRS – AB Shear Walls (4-H) at El. 120' – HRHF – Cracked

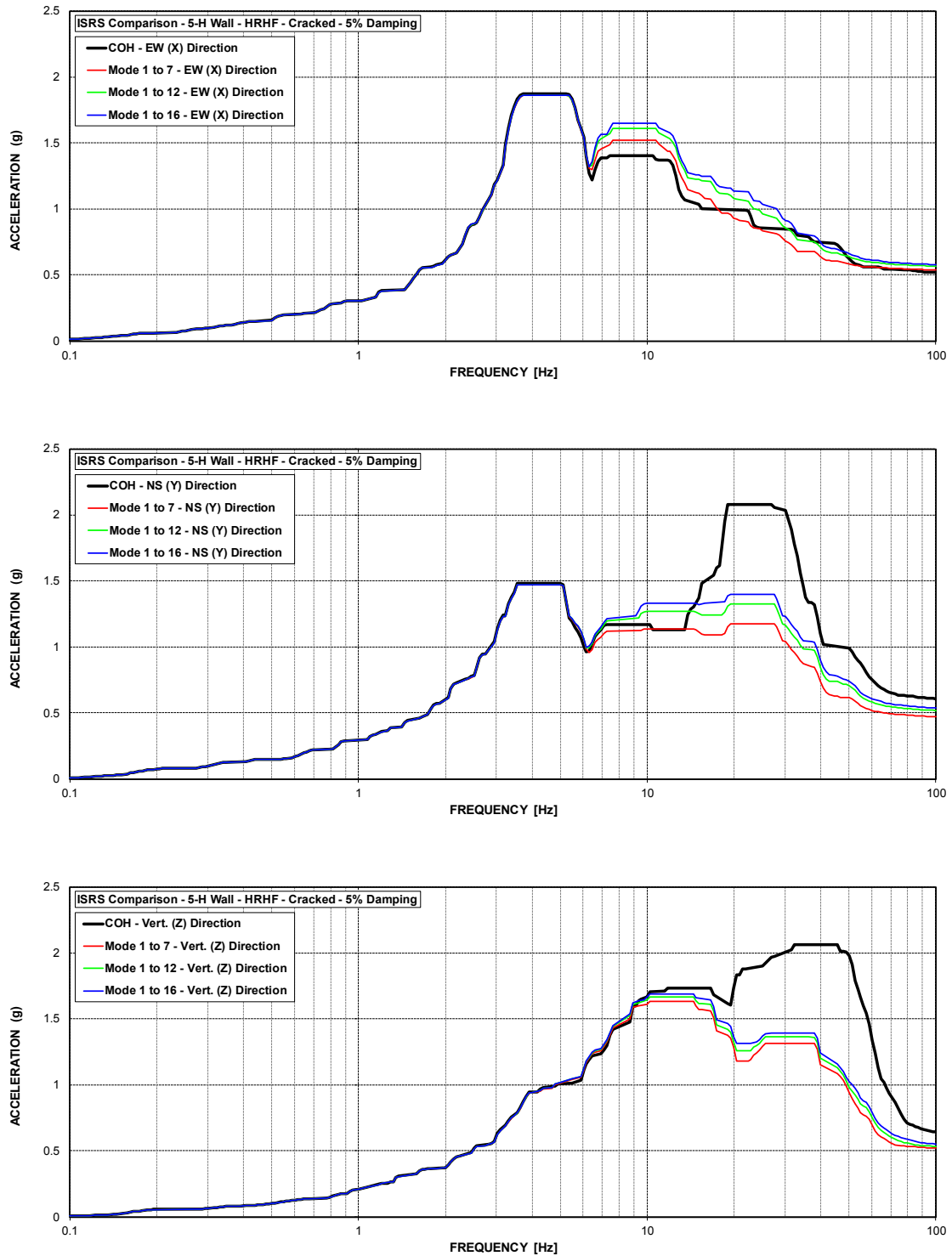


Figure C-185 ISRS – AB Shear Walls (5-H) at El. 137.5' – HRHF – Cracked

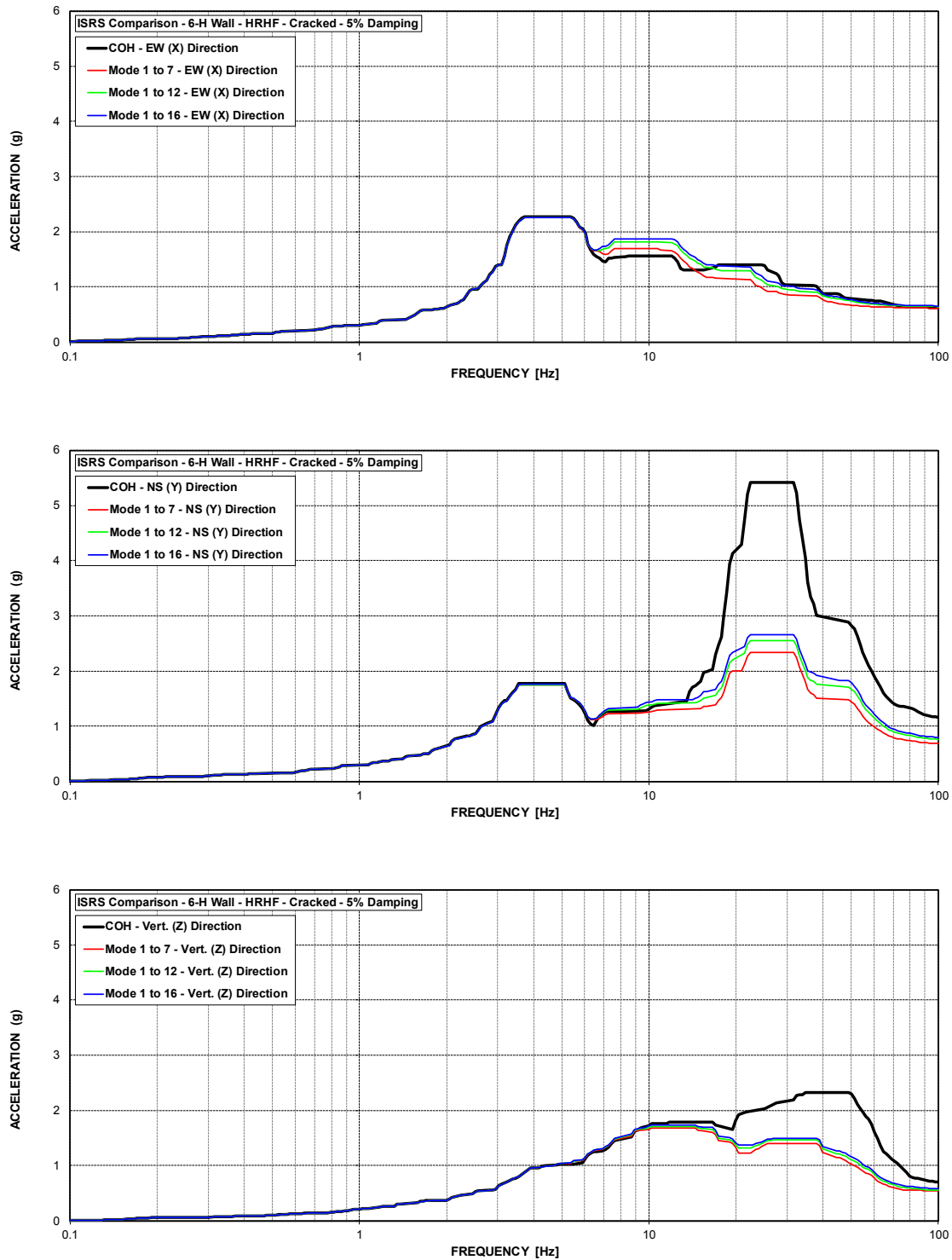


Figure C-186 ISRS – AB Shear Walls (6-H) at El. 156' – HRHF – Cracked

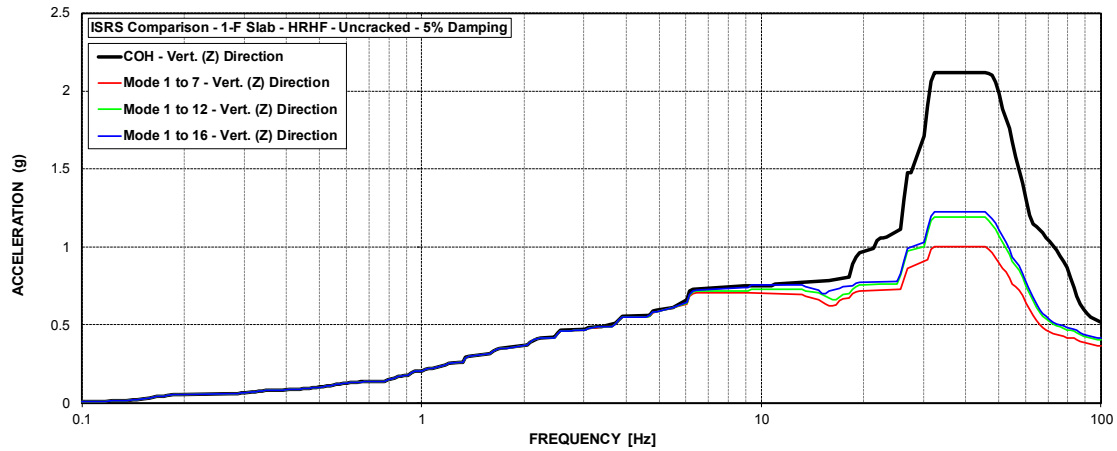


Figure C-187 ISRS – AB Floor Slabs (1-F) at El. 55' – HRHF – Uncracked

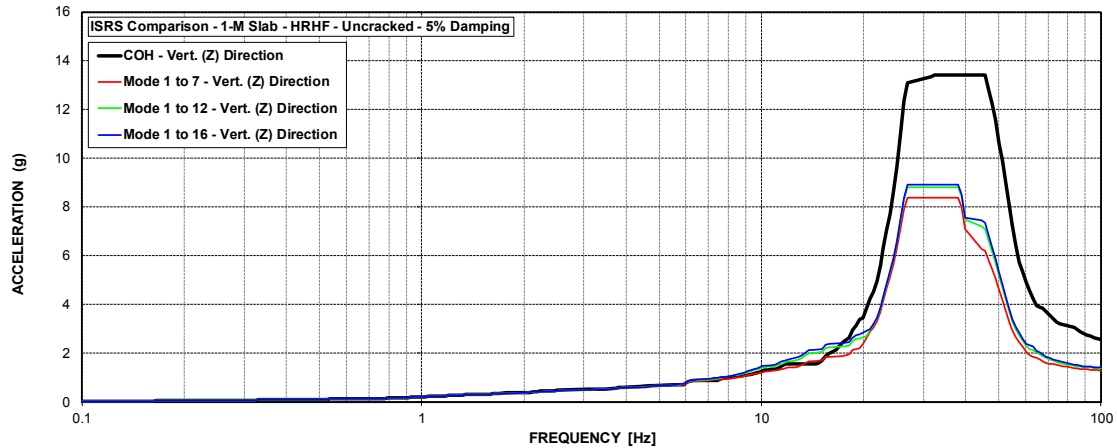


Figure C-188 ISRS – AB Floor Slabs (1-M) at El. 68' – HRHF – Uncracked

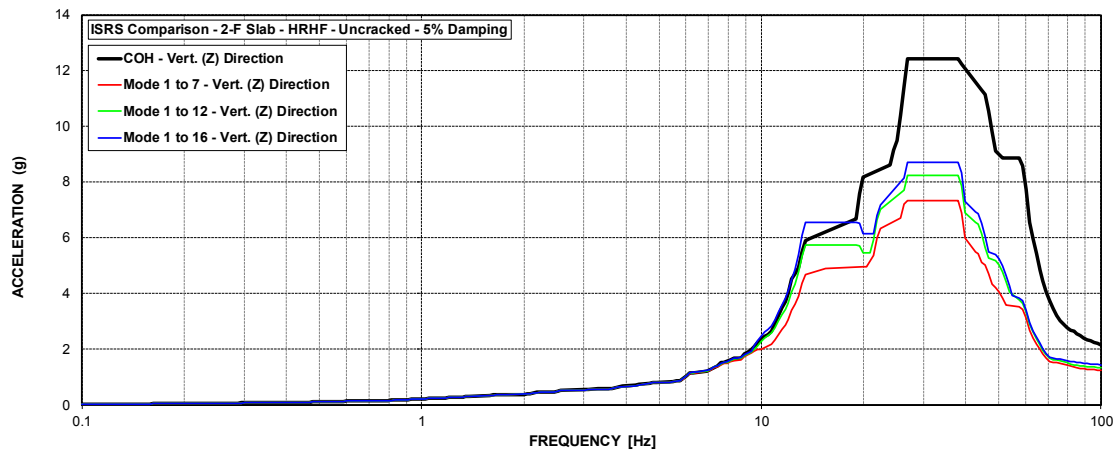


Figure C-189 ISRS – AB Floor Slabs (2-F) at El. 78' – HRHF – Uncracked



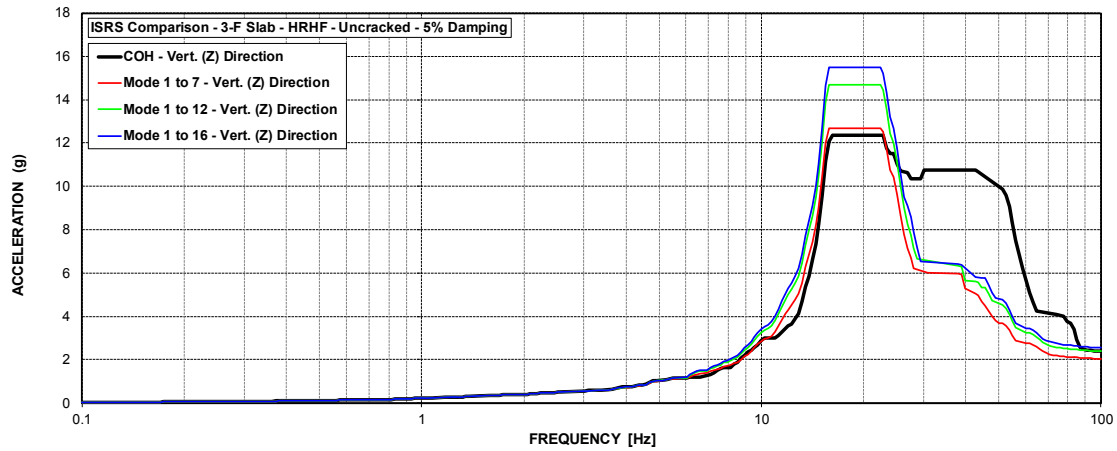


Figure C-190 ISRS – AB Floor Slabs (3-F) at El. 100' – HRHF – Uncracked

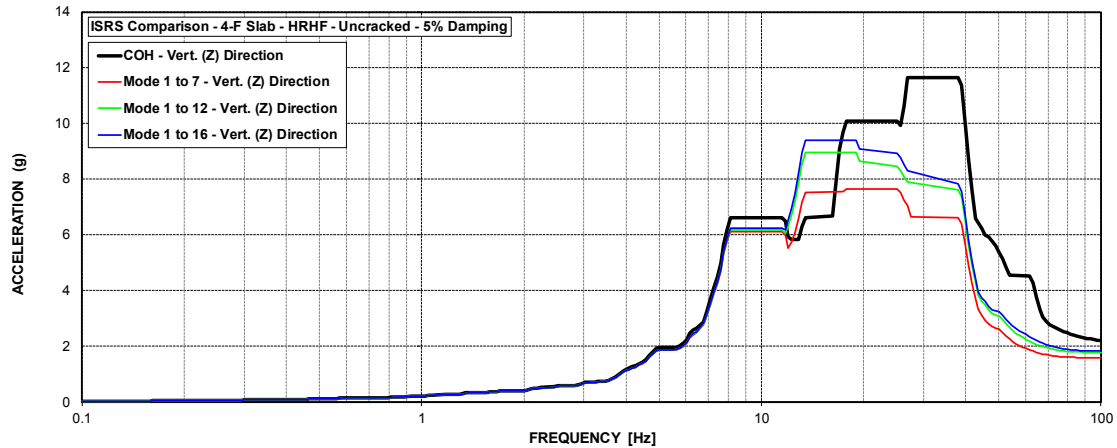


Figure C-191 ISRS – AB Floor Slabs (4-F) at El. 120' – HRHF – Uncracked

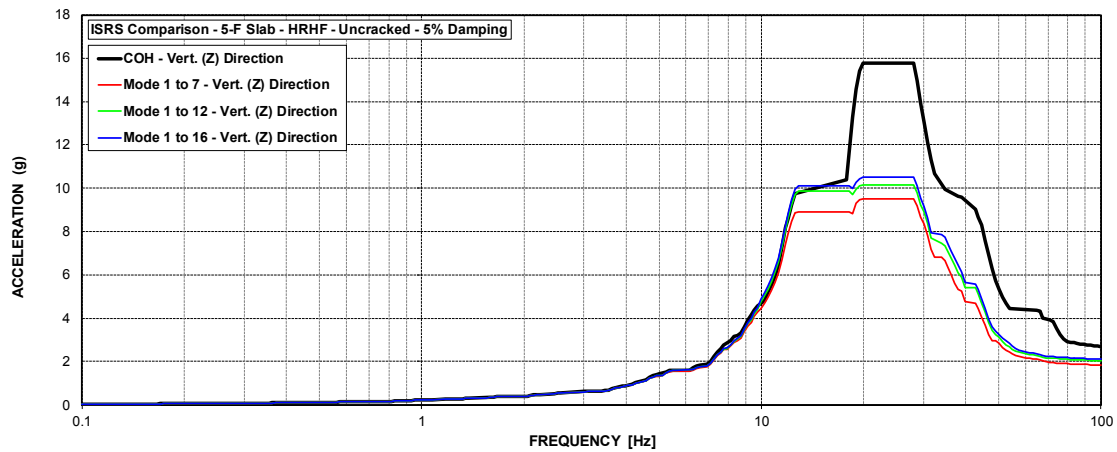
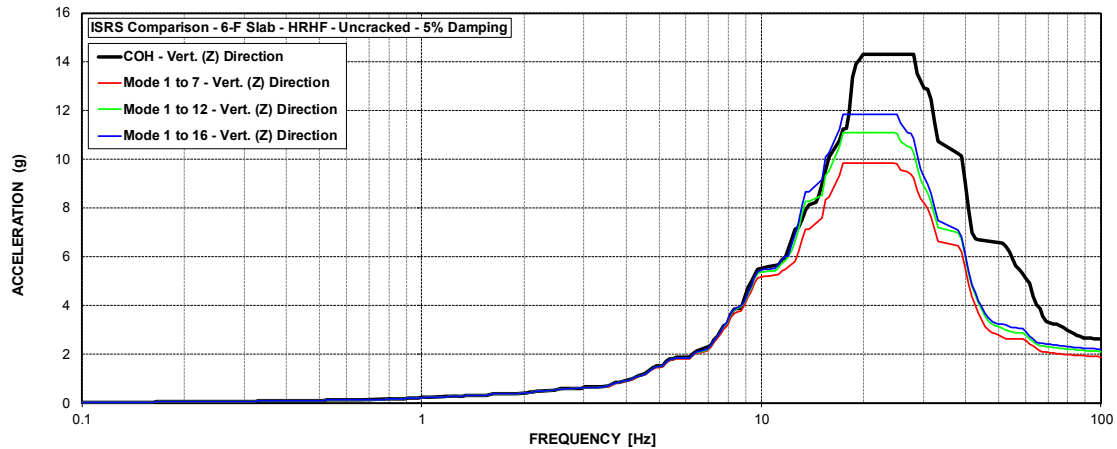
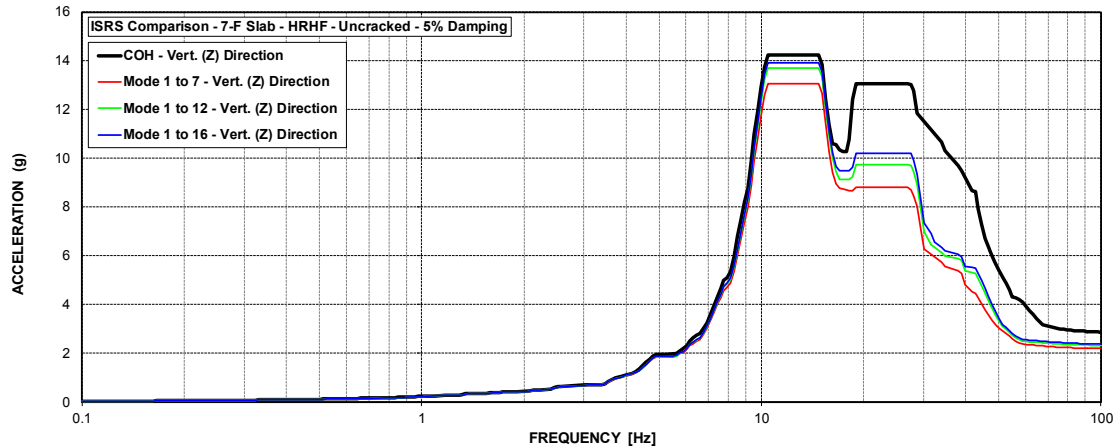
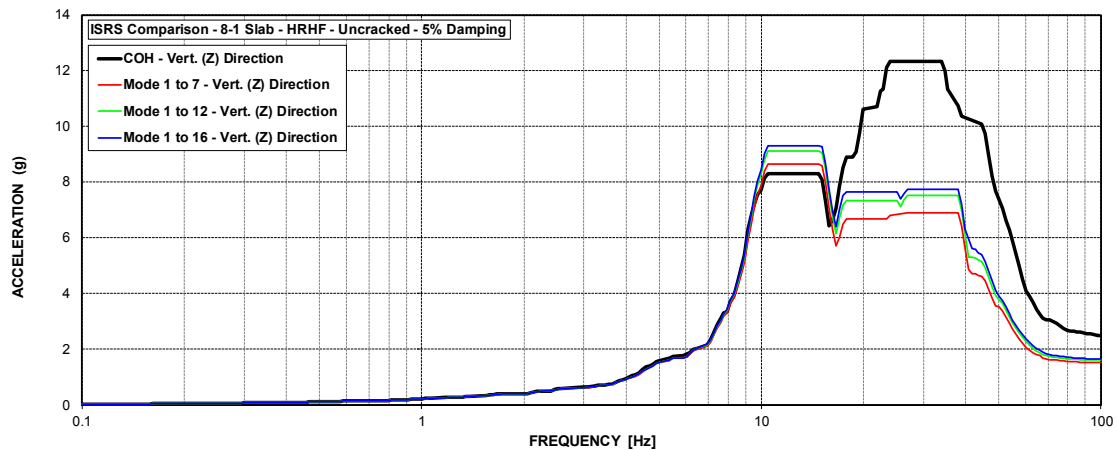


Figure C-192 ISRS – AB Floor Slabs (5-F) at El. 137.5' – HRHF – Uncracked

**Figure C-193 ISRS – AB Floor Slabs (6-F) at El. 156' – HRHF – Uncracked****Figure C-194 ISRS – AB Floor Slabs (7-F) at El. 174' – HRHF – Uncracked****Figure C-195 ISRS – AB Floor Slabs (8-1) at El. 195' – HRHF – Uncracked**

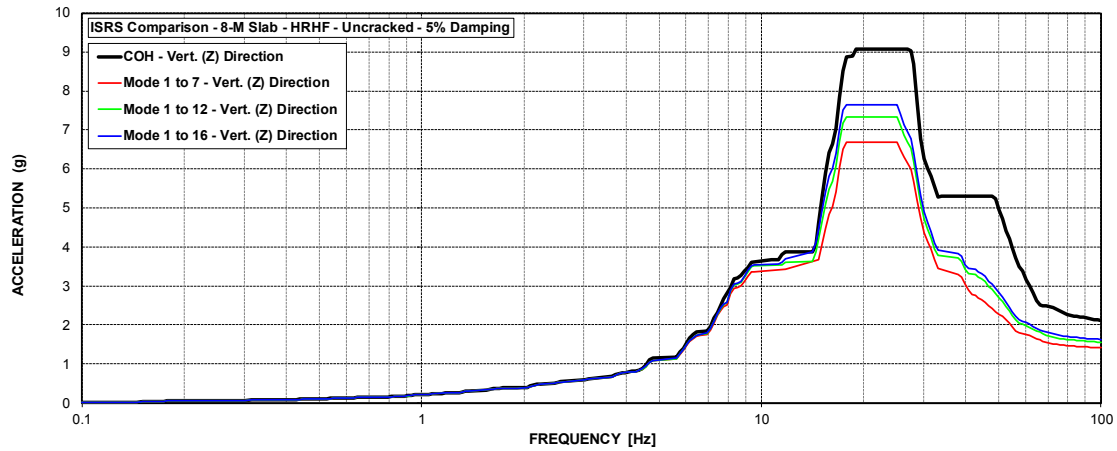


Figure C-196 ISRS – AB Floor Slabs (8-M) at El. 195' – HRHF – Uncracked

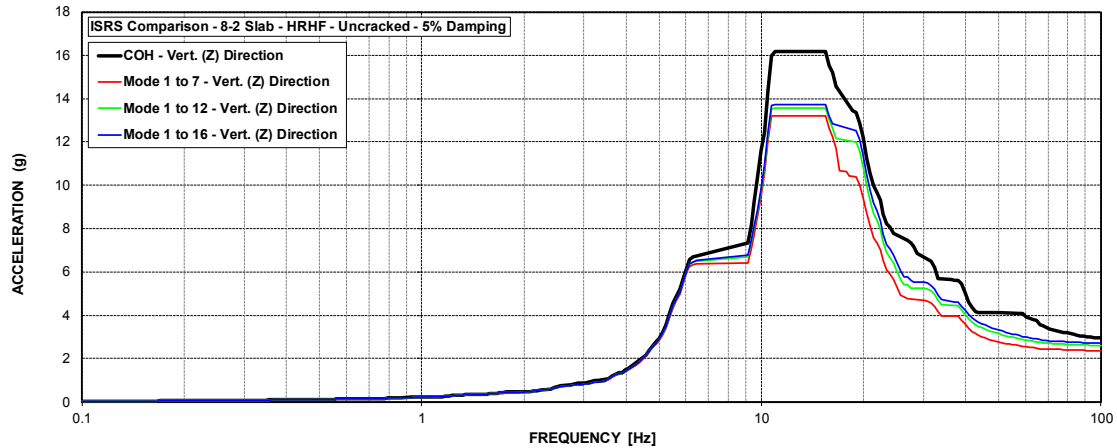


Figure C-197 ISRS – AB Floor Slabs (8-2) at El. 216.75' – HRHF – Uncracked

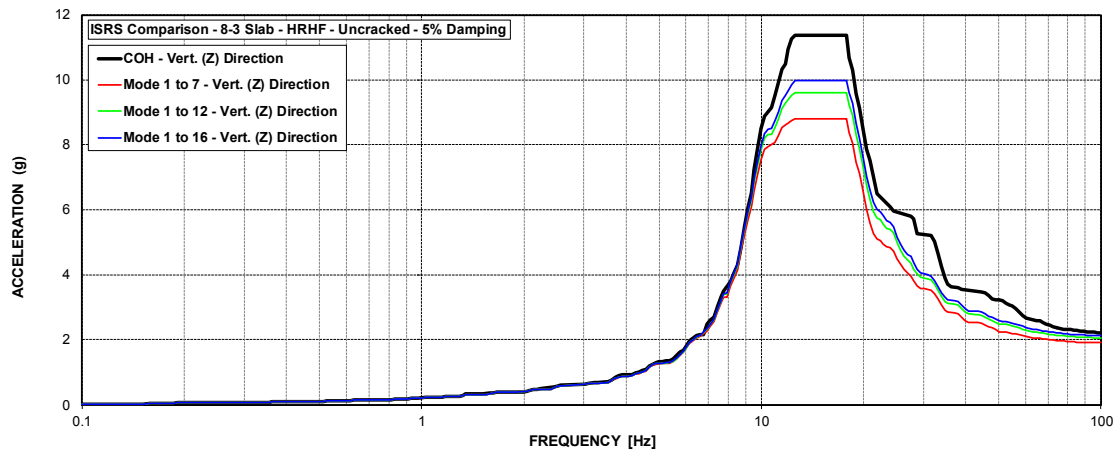


Figure C-198 ISRS – AB Floor Slabs (8-3) at El. 213' – HRHF – Uncracked

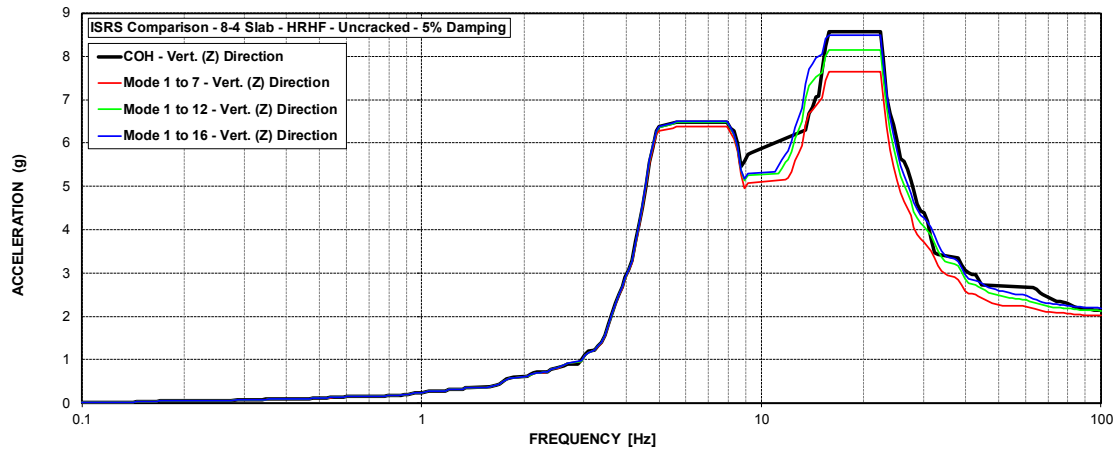


Figure C-199 ISRS – AB Floor Slabs (8-4) at El. 213.5' – HRHF – Uncracked

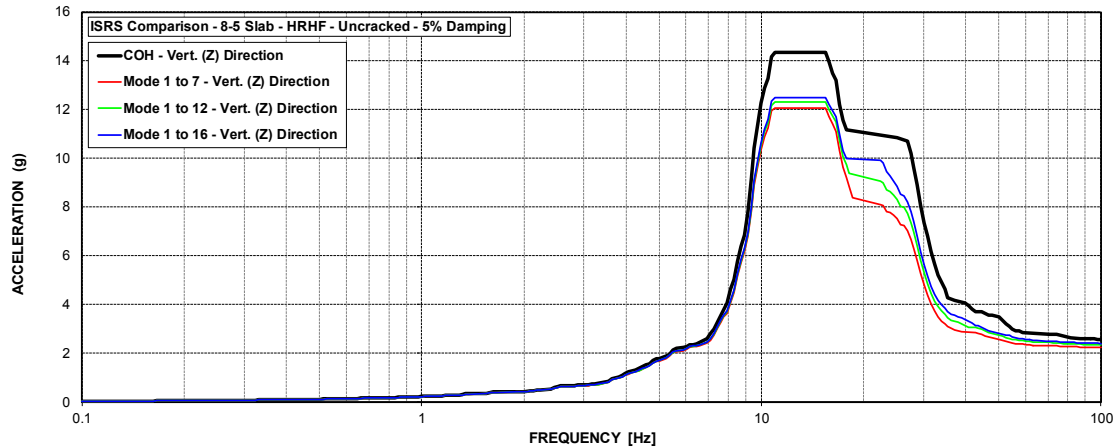


Figure C-200 ISRS – AB Floor Slabs (8-5) at El. 195' – HRHF – Uncracked

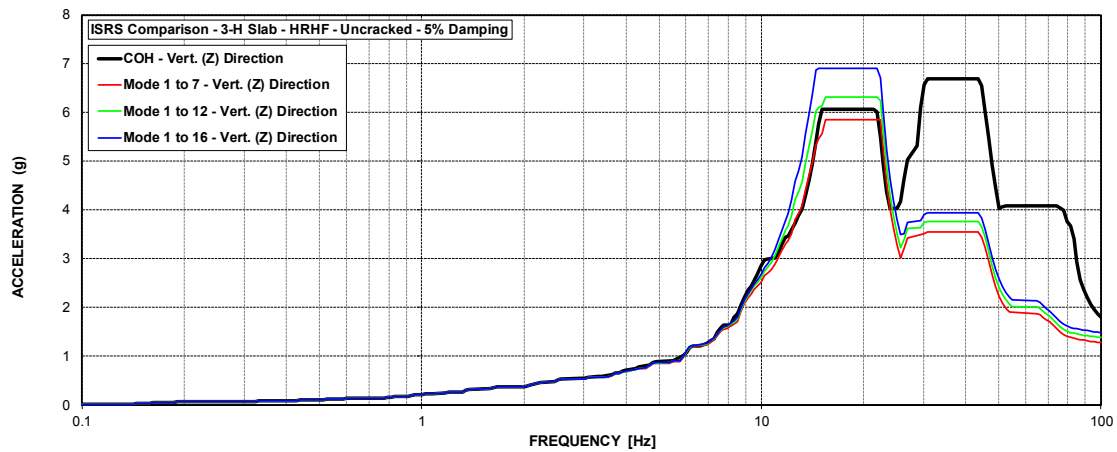


Figure C-201 ISRS – AB Floor Slabs (3-H) at El. 100' – HRHF – Uncracked

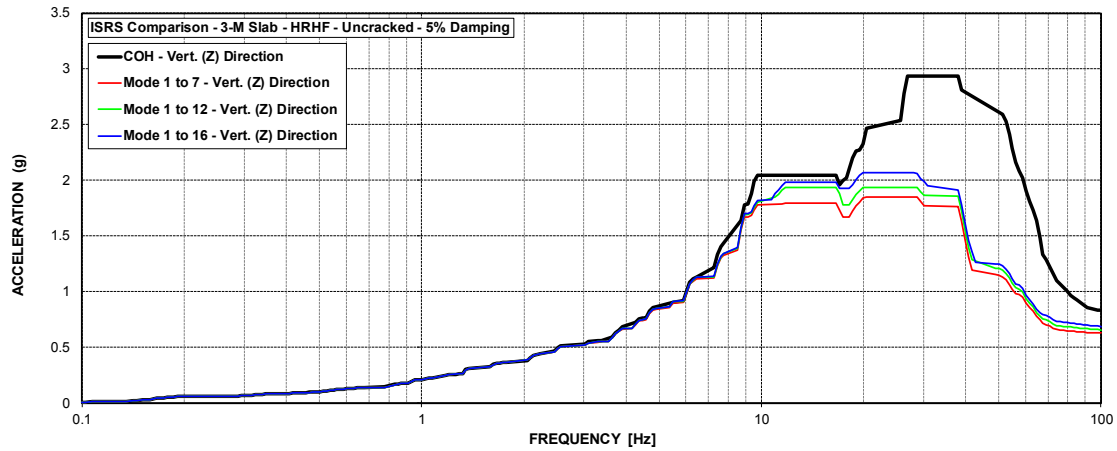


Figure C-202 ISRS – AB Floor Slabs (3-M) at El. 114' – HRHF – Uncracked

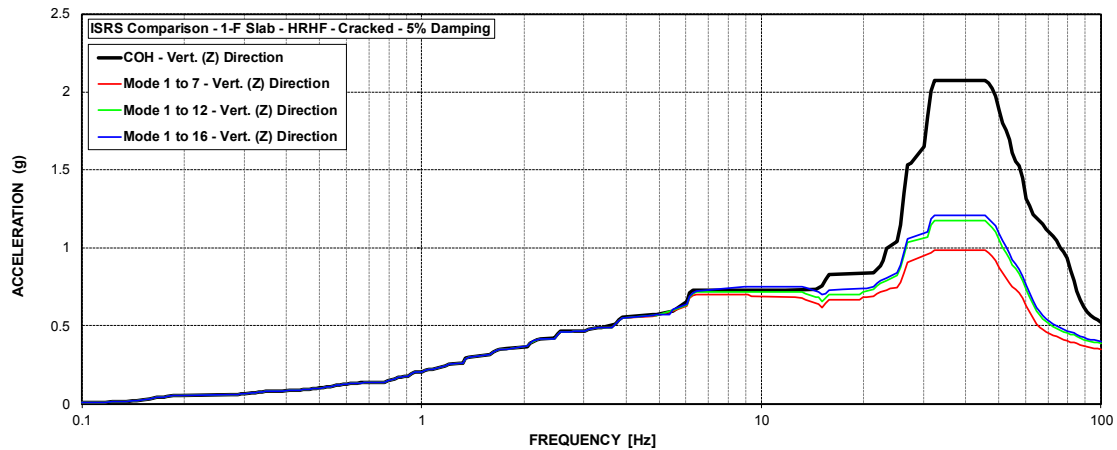


Figure C-203 ISRS – AB Floor Slabs (1-F) at El. 55' – HRHF – Cracked

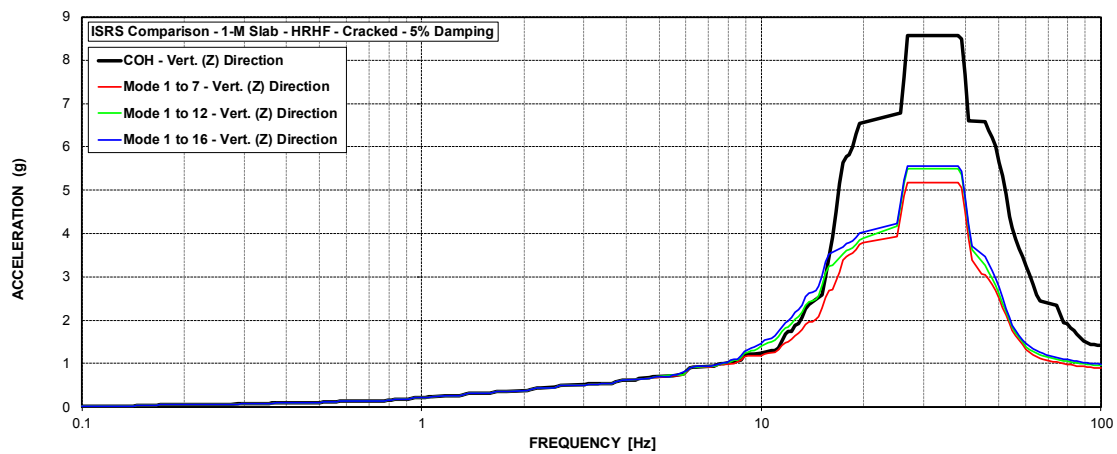


Figure C-204 ISRS – AB Floor Slabs (1-M) at El. 68' – HRHF – Cracked

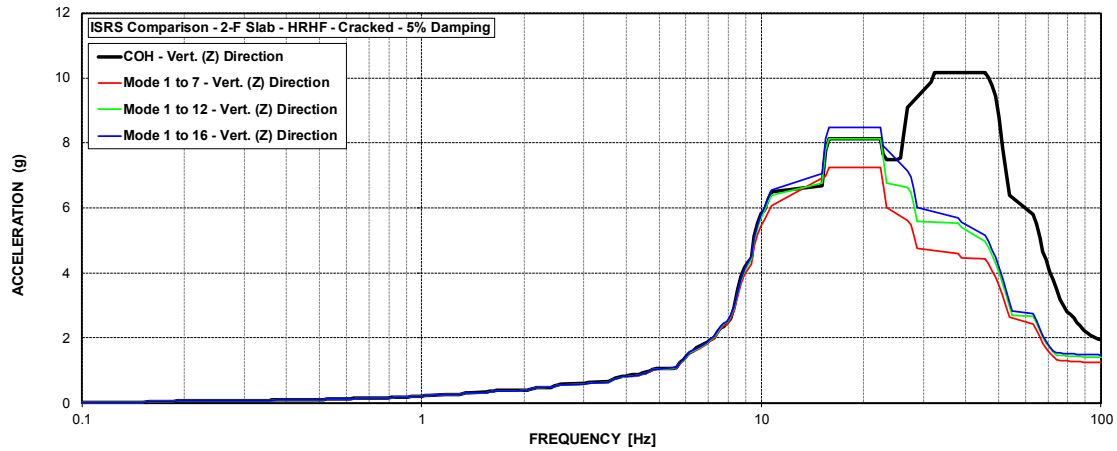


Figure C-205 ISRS – AB Floor Slabs (2-F) at El. 78' – HRHF – Cracked

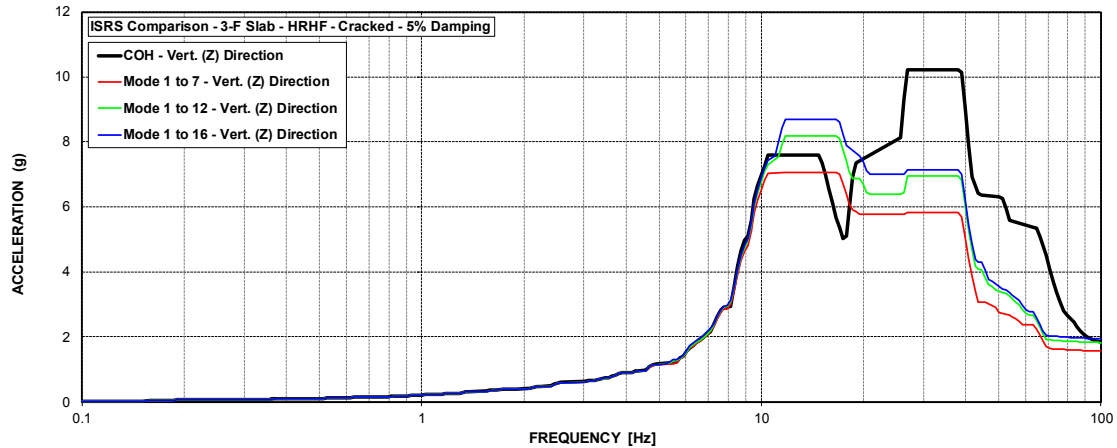


Figure C-206 ISRS – AB Floor Slabs (3-F) at El. 100' – HRHF – Cracked

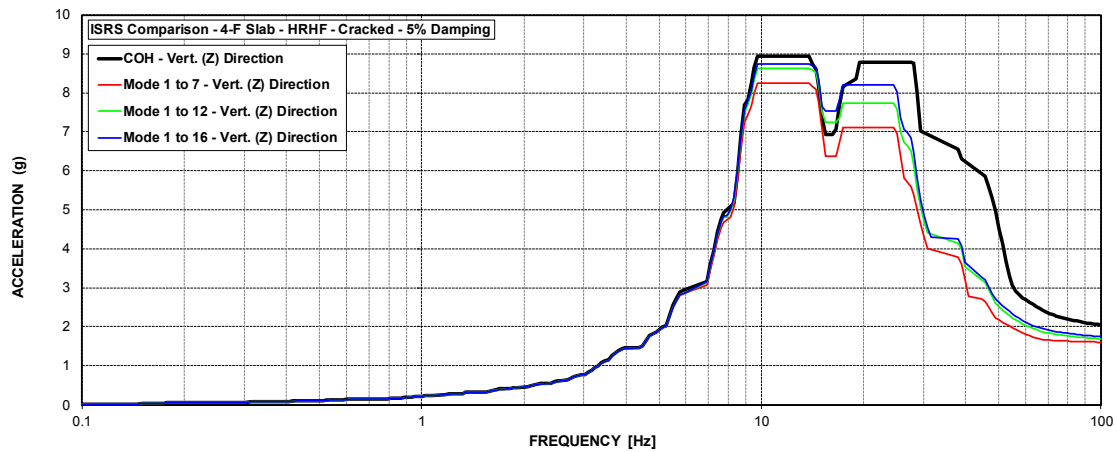


Figure C-207 ISRS – AB Floor Slabs (4-F) at El. 120' – HRHF – Cracked

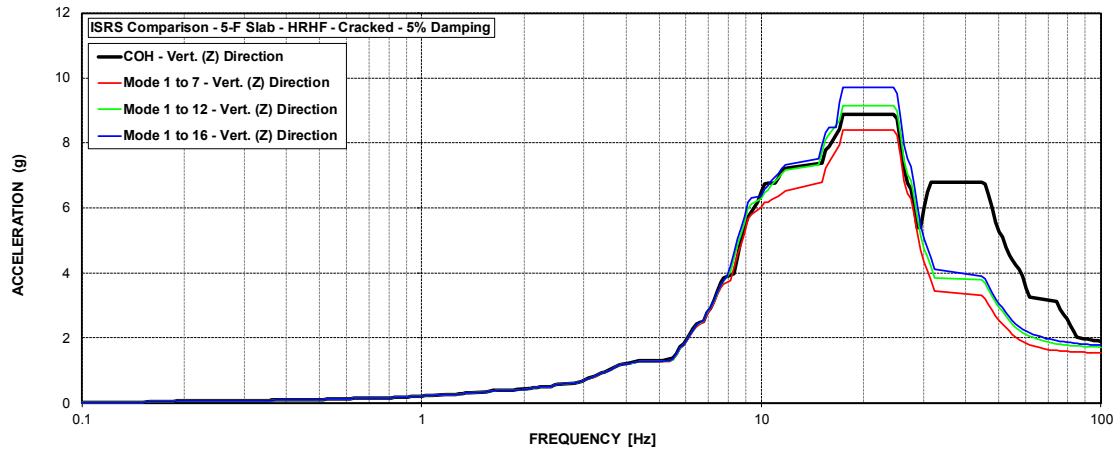


Figure C-208 ISRS – AB Floor Slabs (5-F) at El. 137.5' – HRHF – Cracked

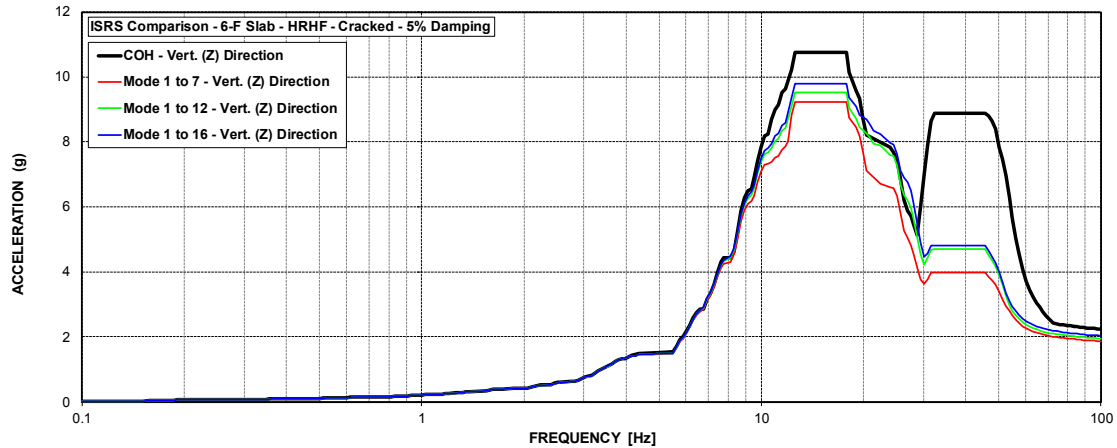


Figure C-209 ISRS – AB Floor Slabs (6-F) at El. 156' – HRHF – Cracked

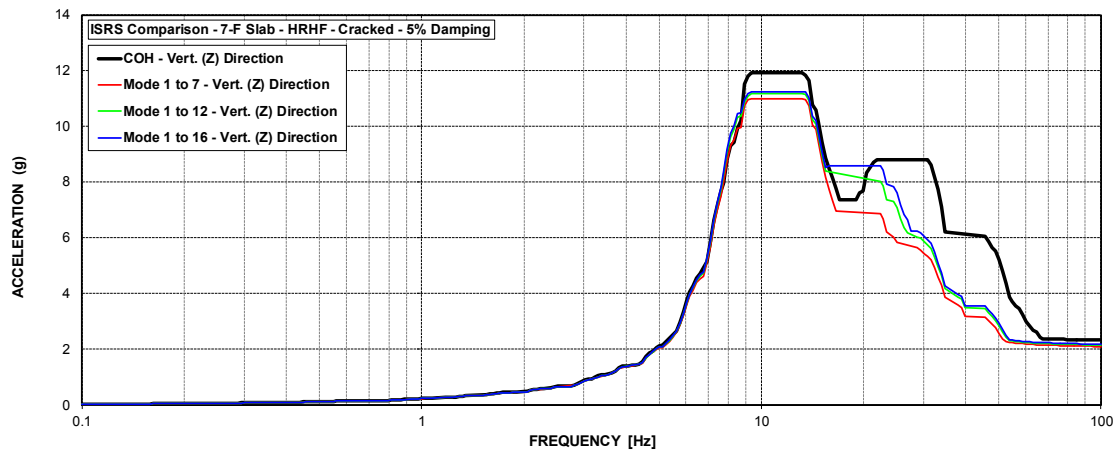


Figure C-210 ISRS – AB Floor Slabs (7-F) at El. 174' – HRHF – Cracked

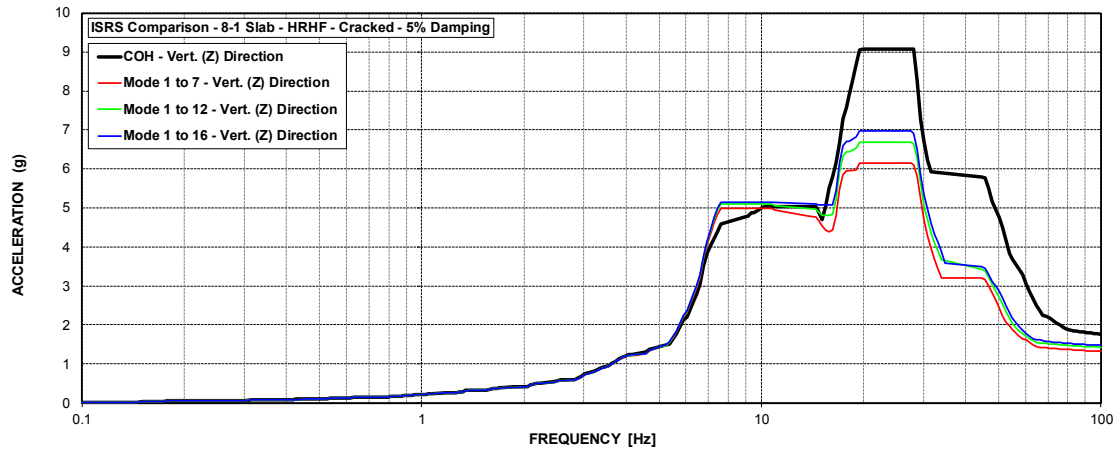


Figure C-211 ISRS – AB Floor Slabs (8-1) at El. 195' – HRHF – Cracked

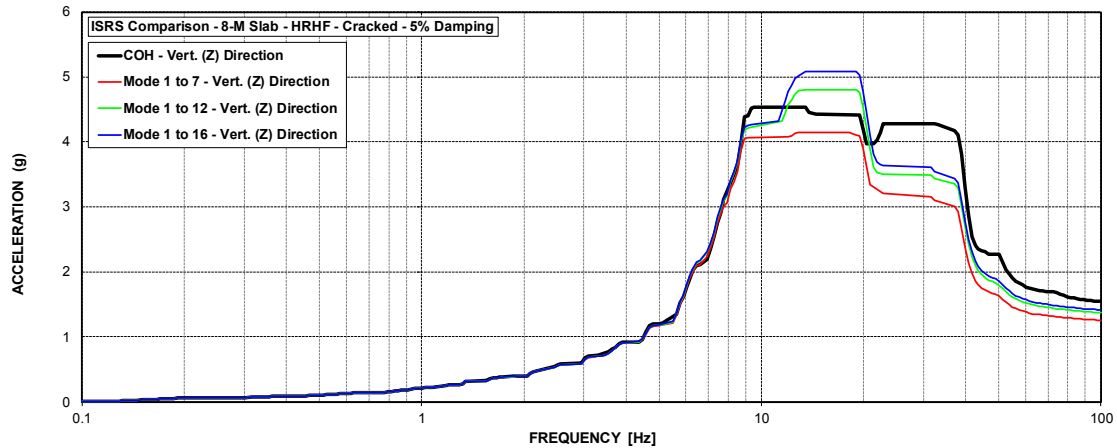


Figure C-212 ISRS – AB Floor Slabs (8-M) at El. 195' – HRHF – Cracked

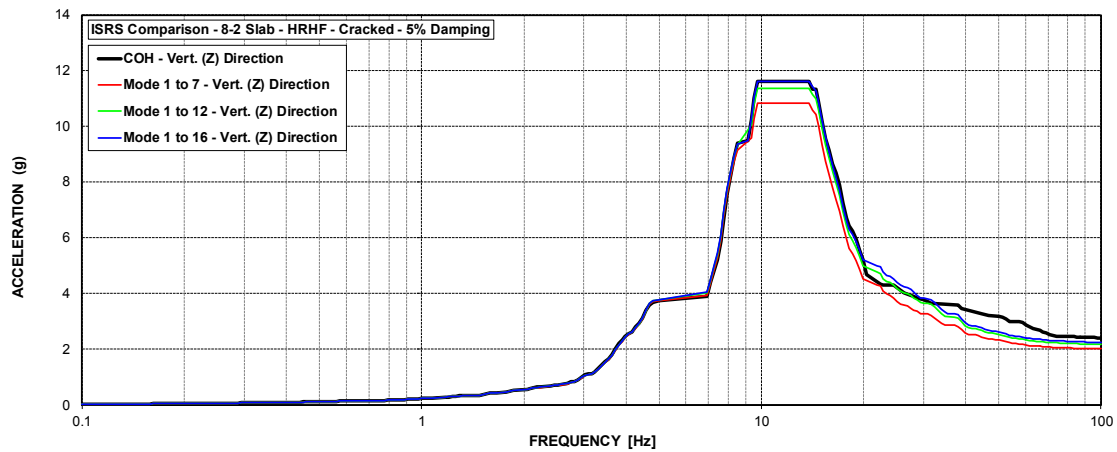


Figure C-213 ISRS – AB Floor Slabs (8-2) at El. 216.75' – HRHF – Cracked



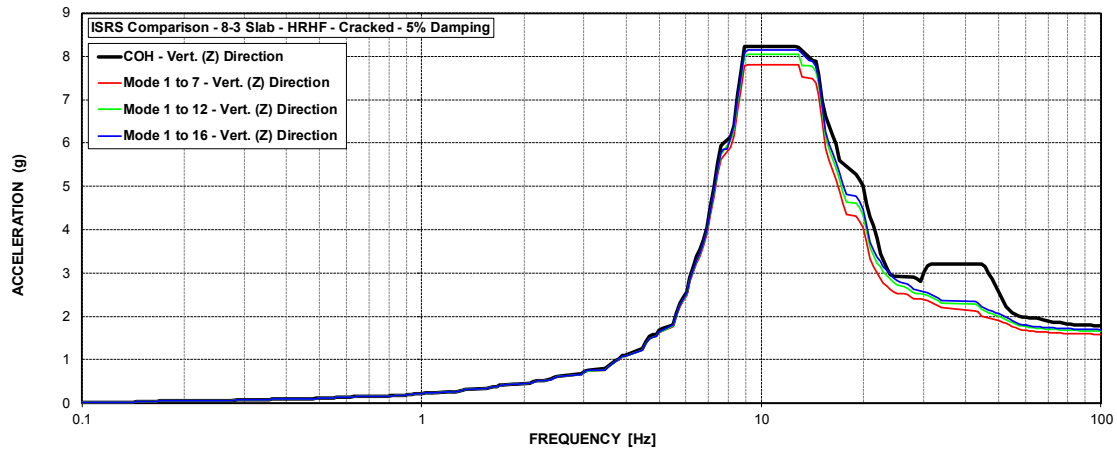


Figure C-214 ISRS – AB Floor Slabs (8-3) at El. 213' – HRHF – Cracked

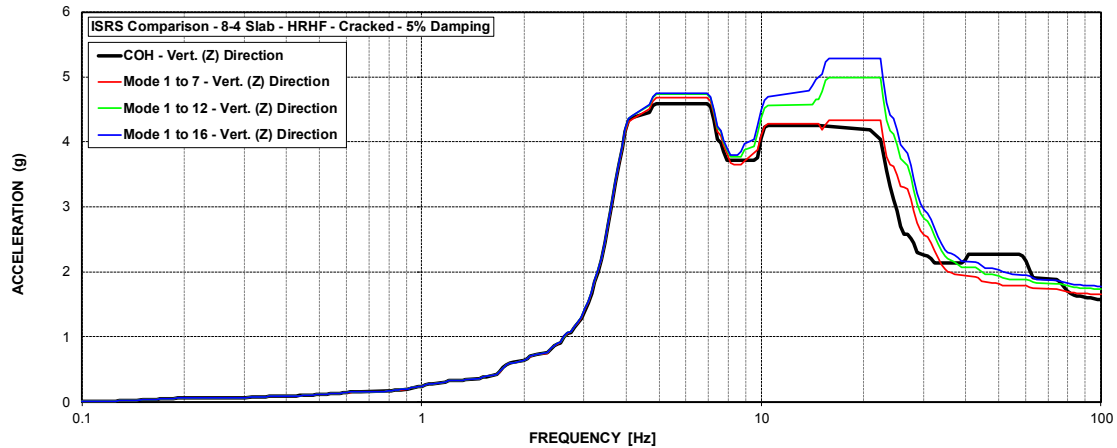


Figure C-215 ISRS – AB Floor Slabs (8-4) at El. 213.5' – HRHF – Cracked

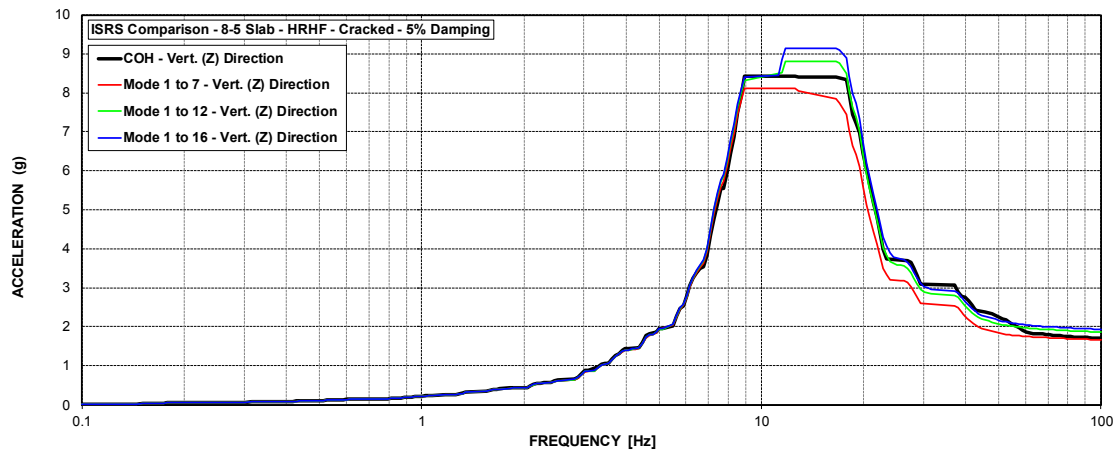


Figure C-216 ISRS – AB Floor Slabs (8-5) at El. 195' – HRHF – Cracked

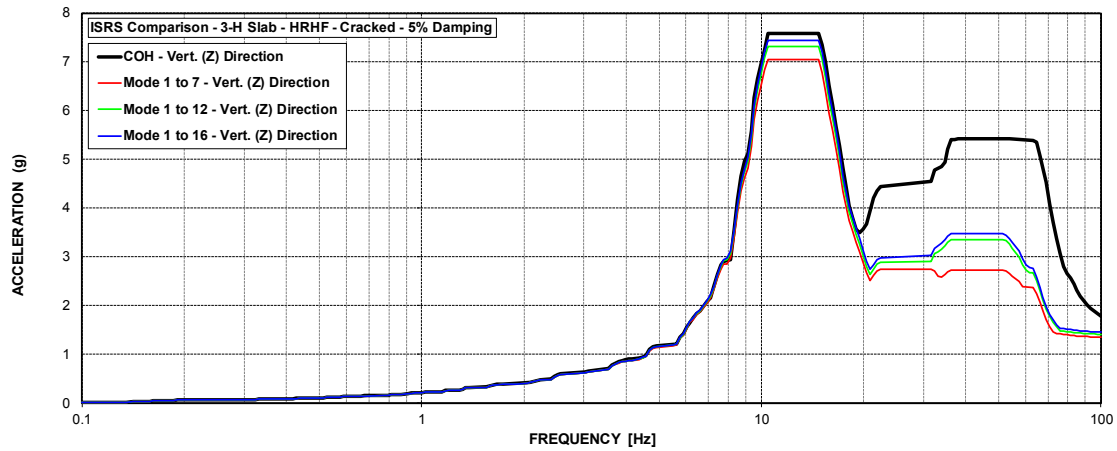


Figure C-217 ISRS – AB Floor Slabs (3-H) at El. 100' – HRHF – Cracked

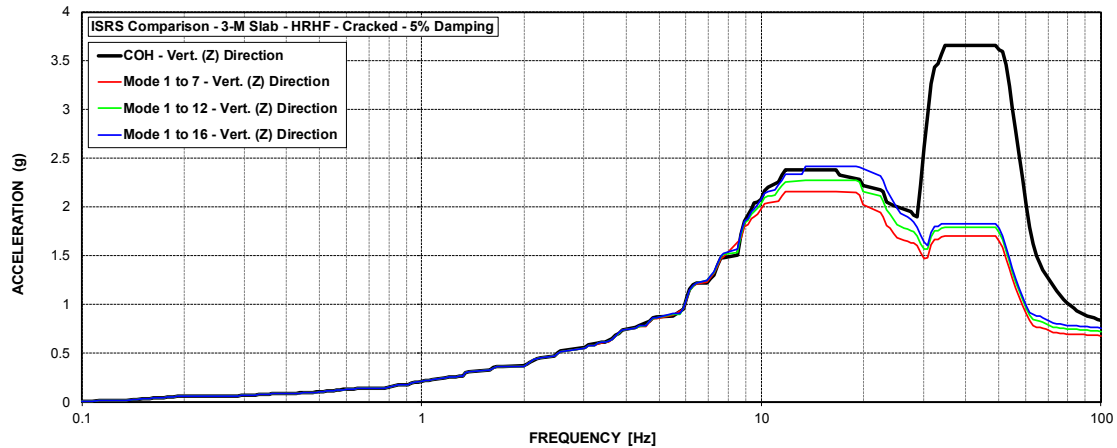


Figure C-218 ISRS – AB Floor Slabs (3-M) at El. 114' – HRHF – Cracked

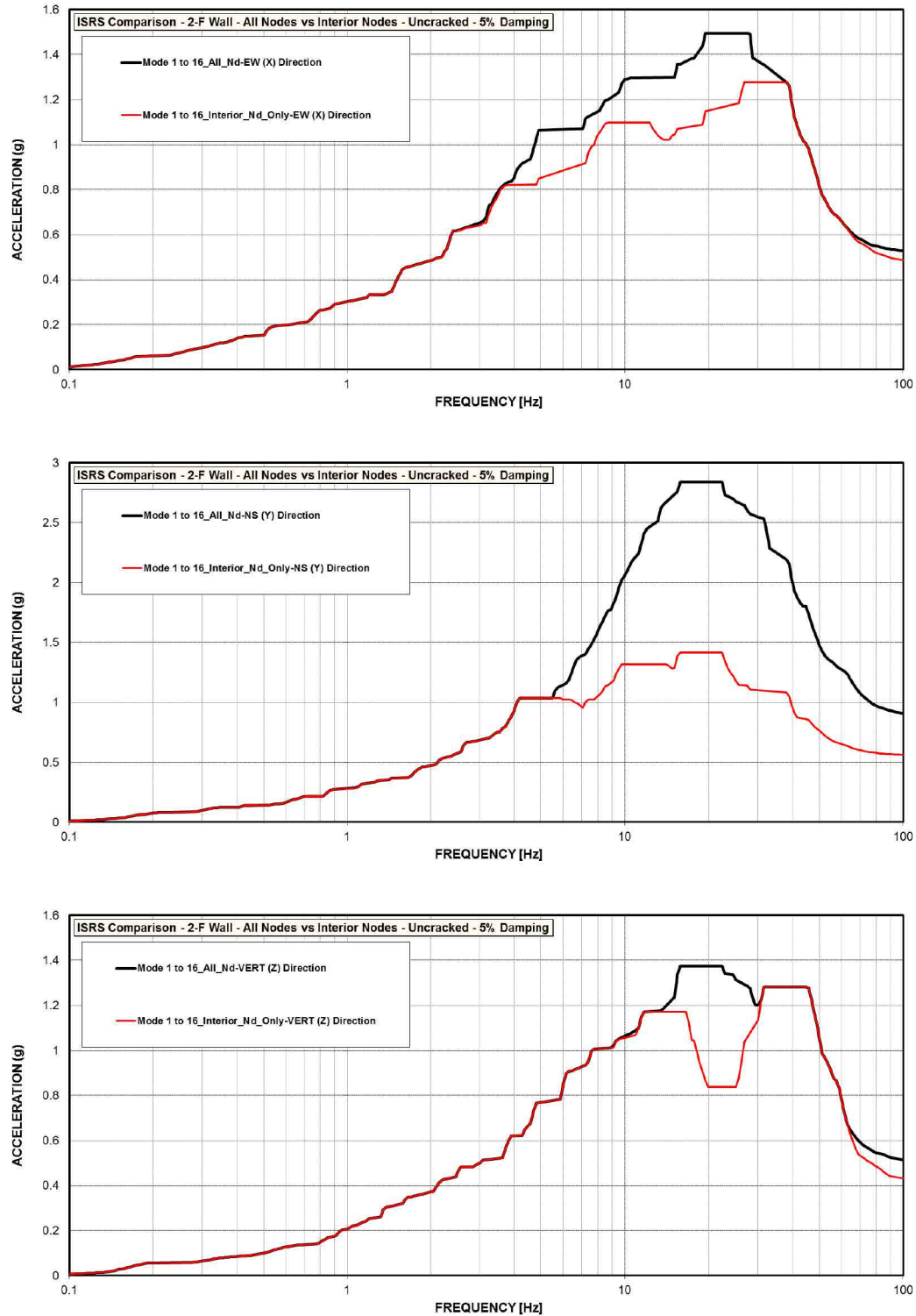


Figure C-219 Orig. Model ISRS AB Shear Walls (2-F and 2-F-Interior) at EL. 78' – HRHF – Uncracked

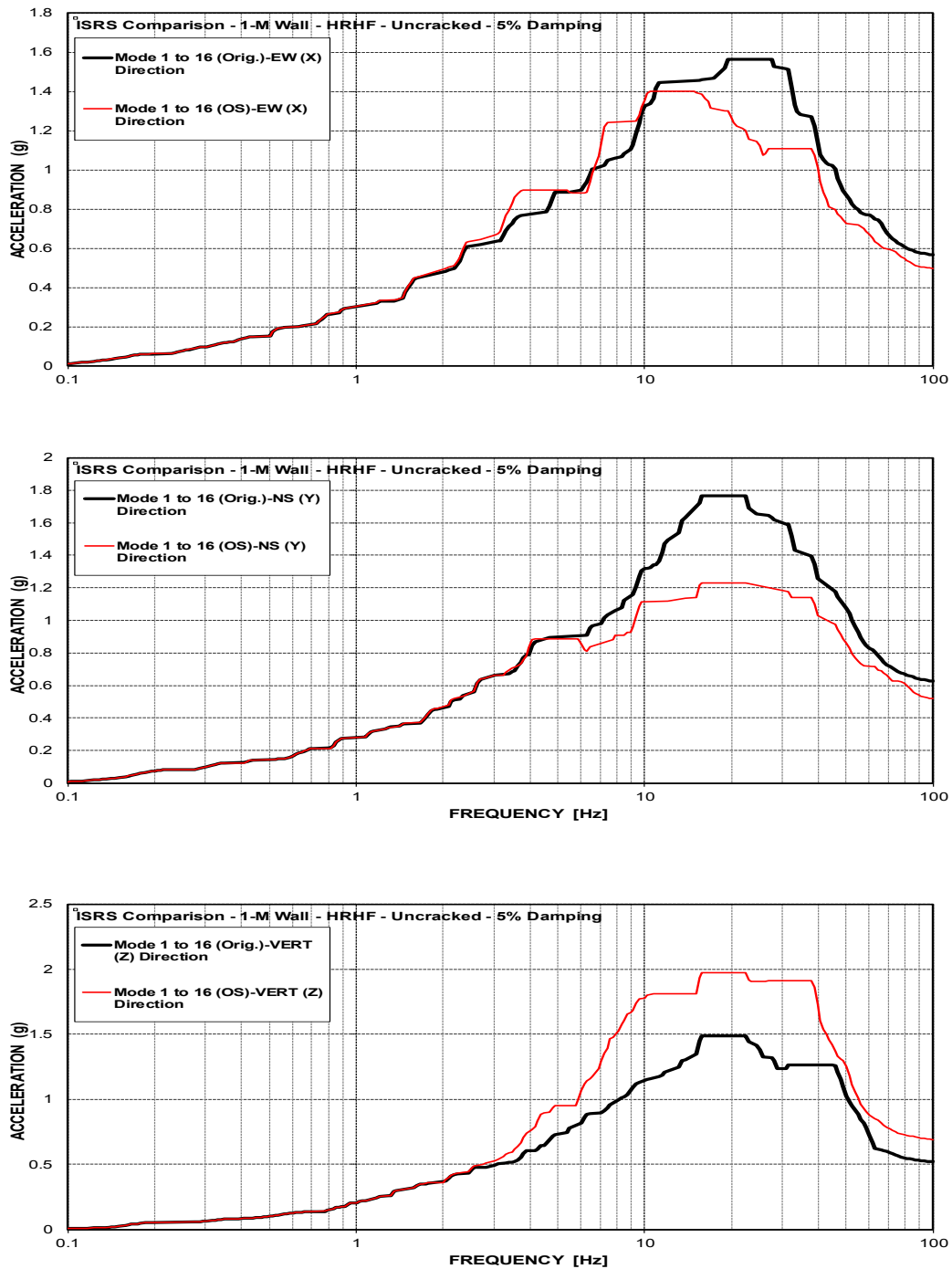


Figure C-220 ISRS Comparison-AB Shear Walls (1-M) at EL. 68' – HRHF – Uncracked

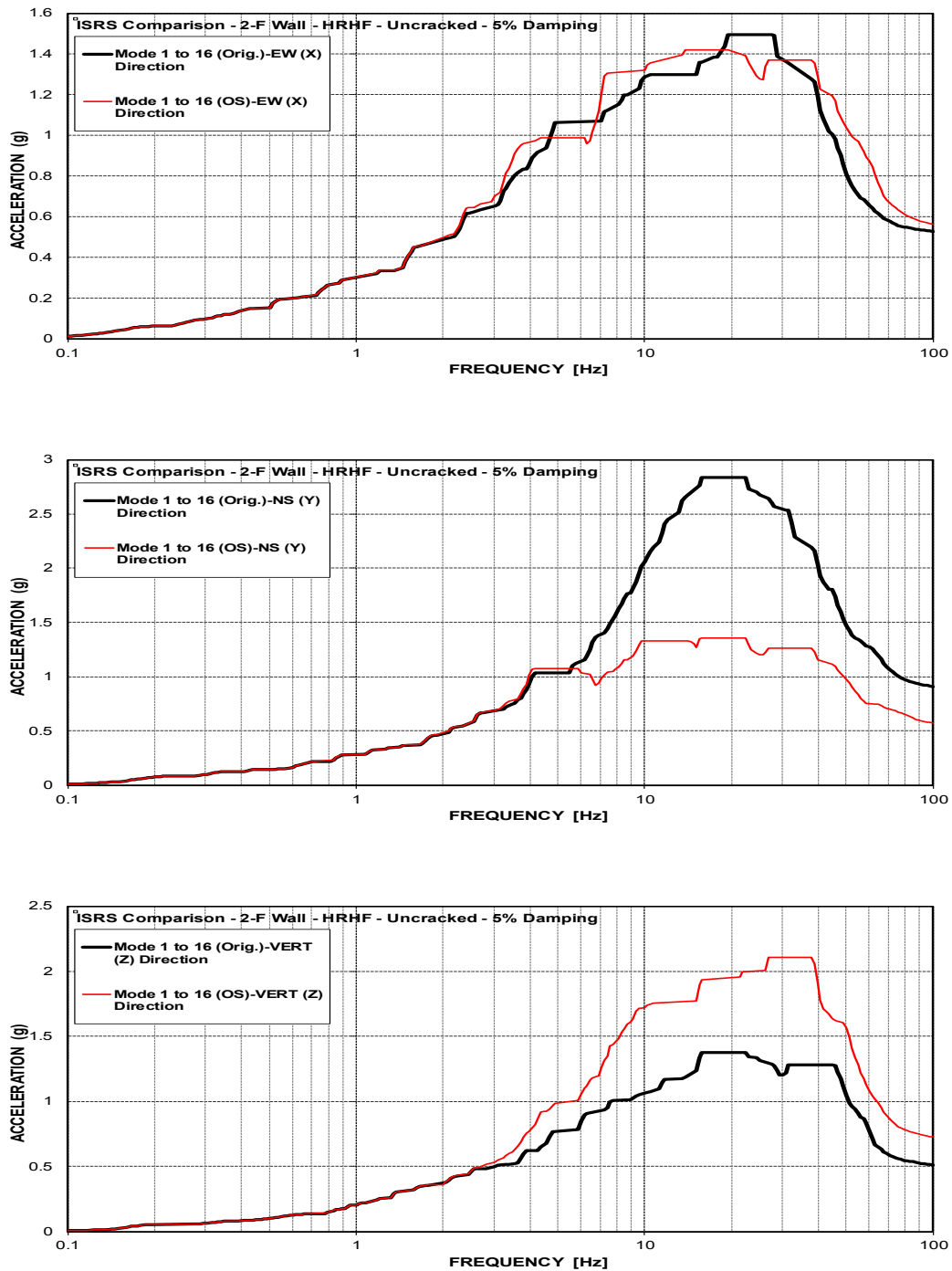


Figure C-221 ISRS Comparison -AB Shear Walls (2-F) at EL. 78' – HRHF – Uncracked

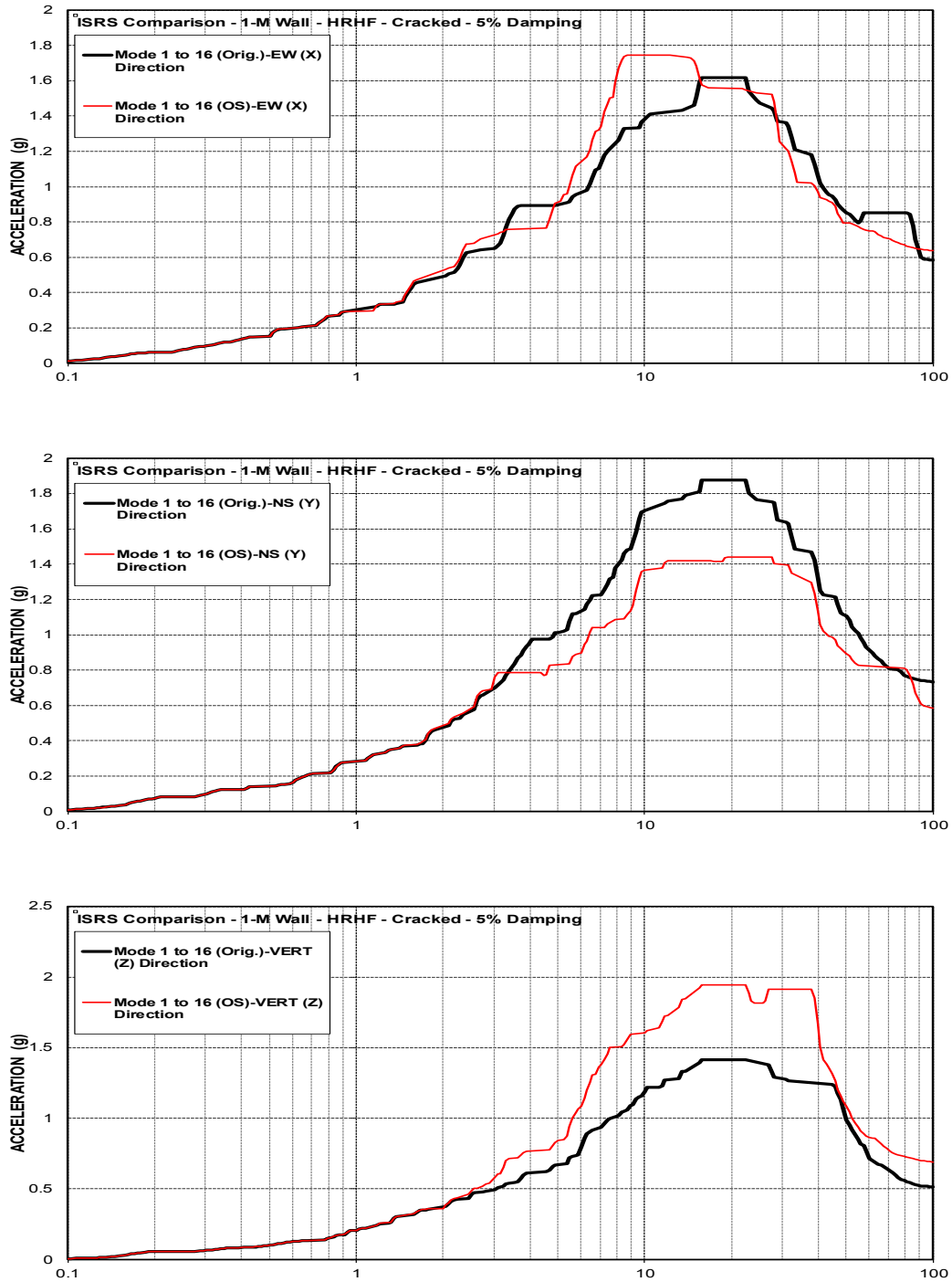


Figure C-222 ISRS Comparison -AB Shear Walls (1-M) at EL. 68' – HRHF – Cracked

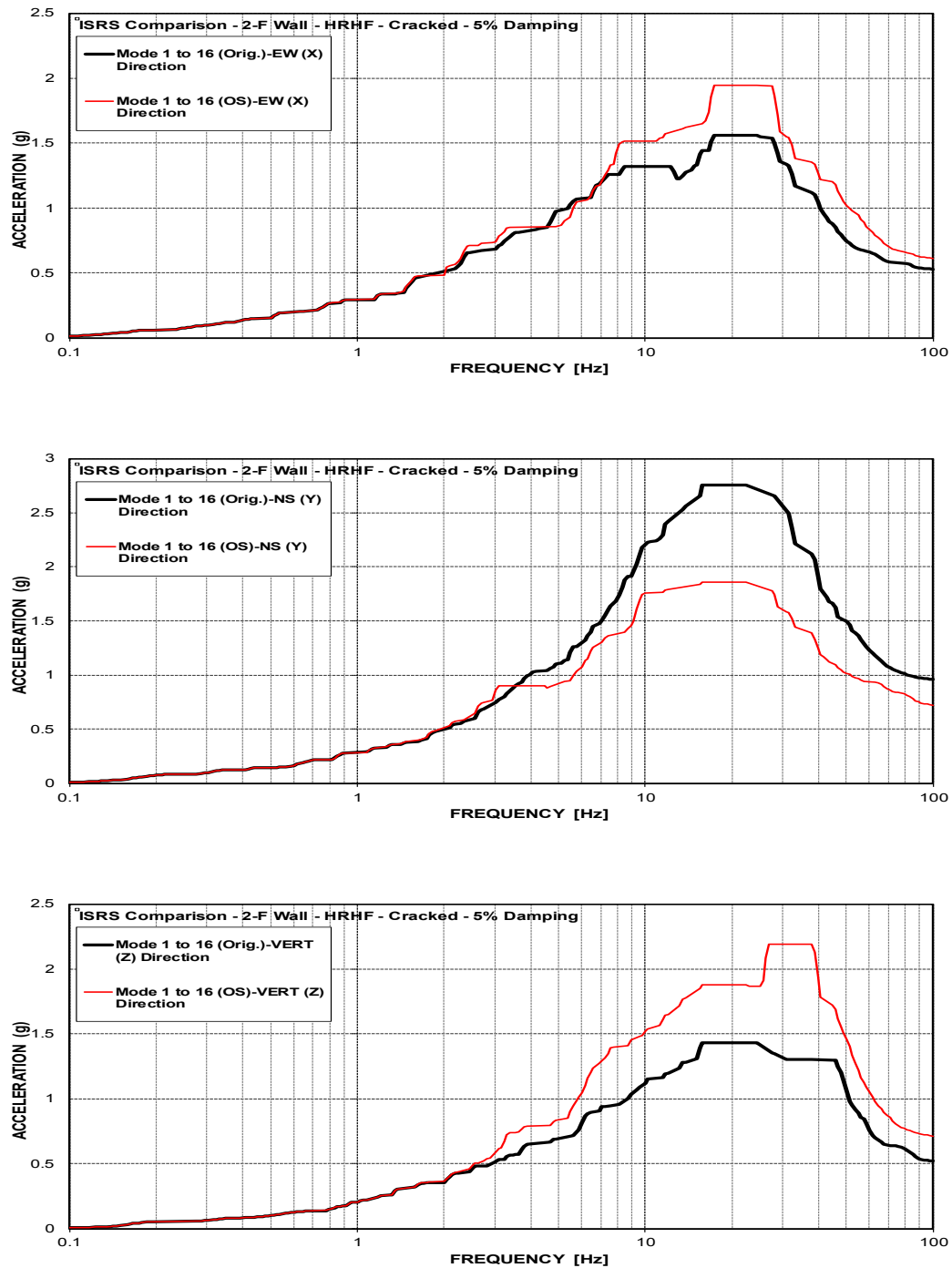


Figure C-223 ISRS Comparison -AB Shear Walls (2-F) at EL. 78' – HRHF – Cracked

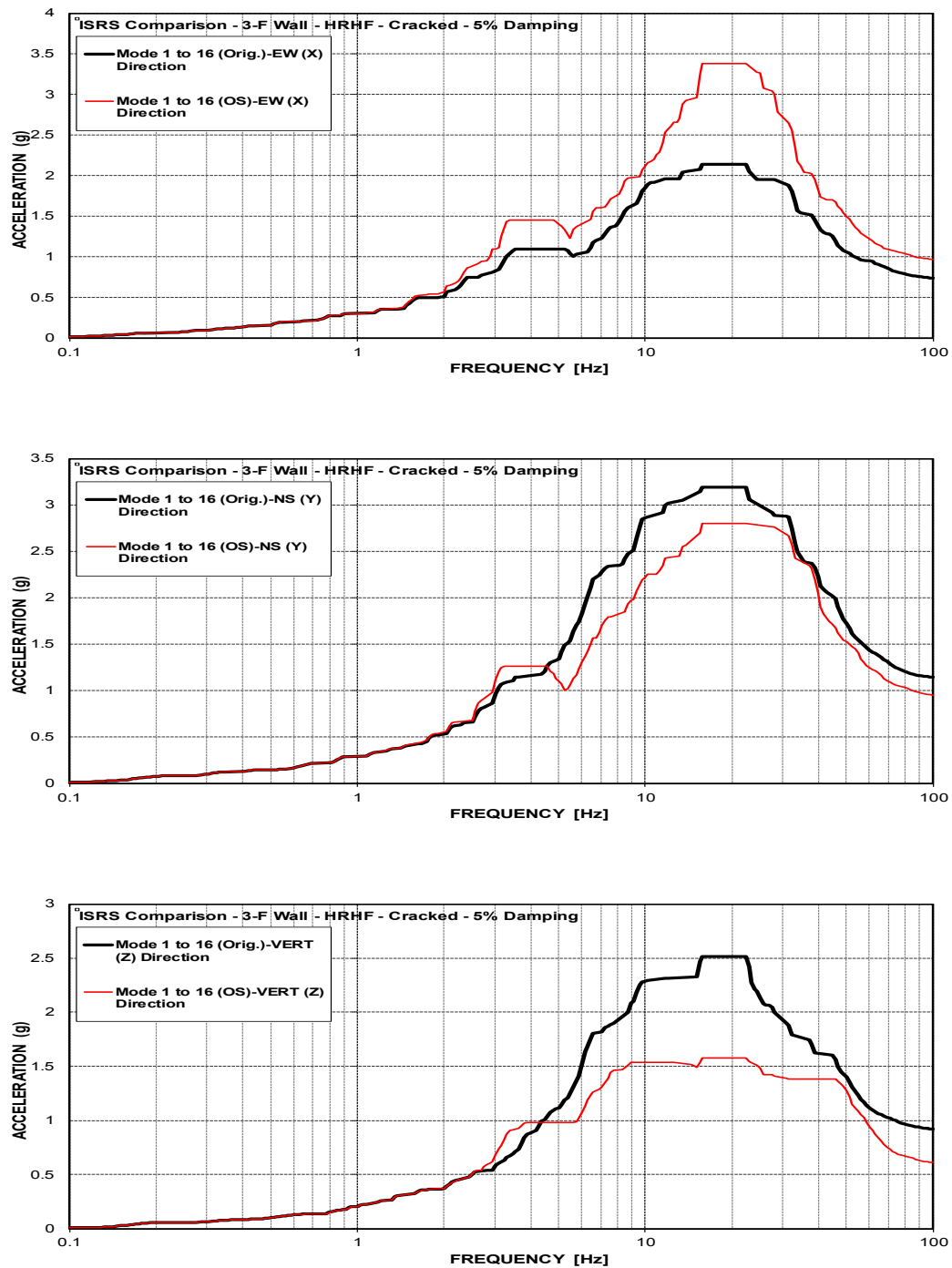


Figure C-224 ISRS Comparison -AB Shear Walls (3-F) at EL. 100' – HRHF – Cracked



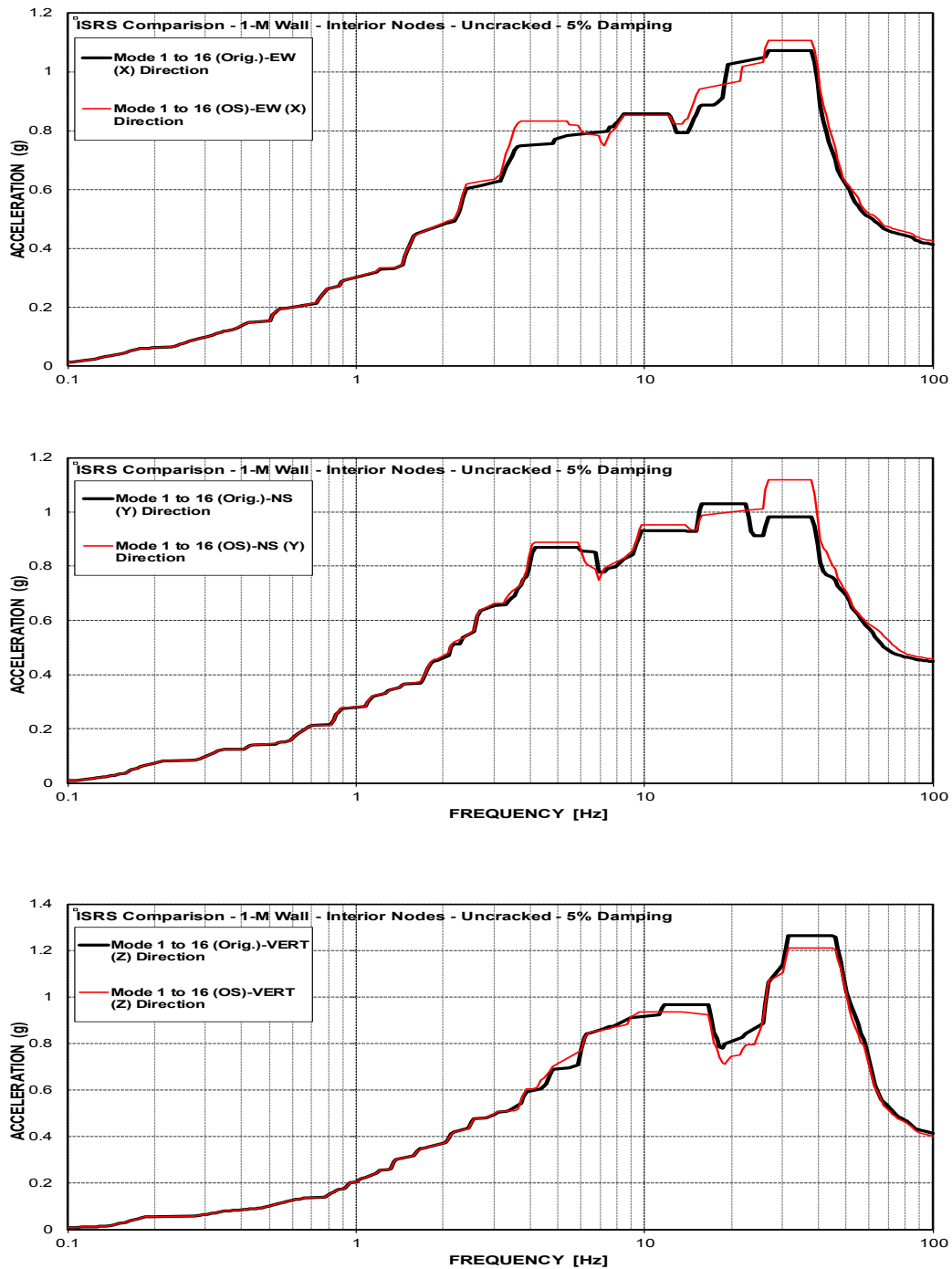


Figure C-225 ISRS Comparison-AB Shear Walls (1-M-Interior) at EL. 68' – HRHF – Uncracked

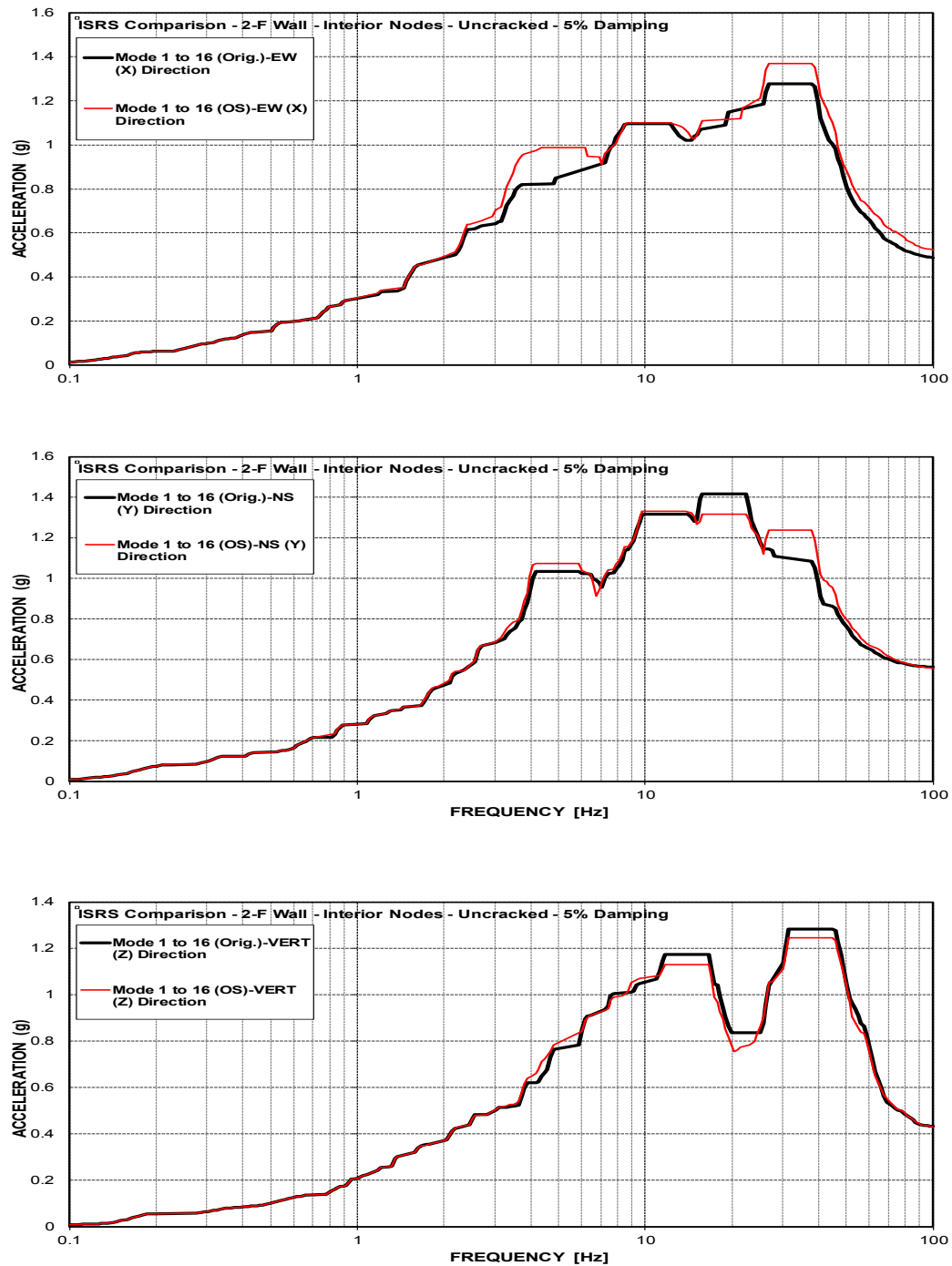


Figure C-226 ISRS Comparison -AB Shear Walls (2-F-Interior) at EL. 78' – HRHF – Uncracked

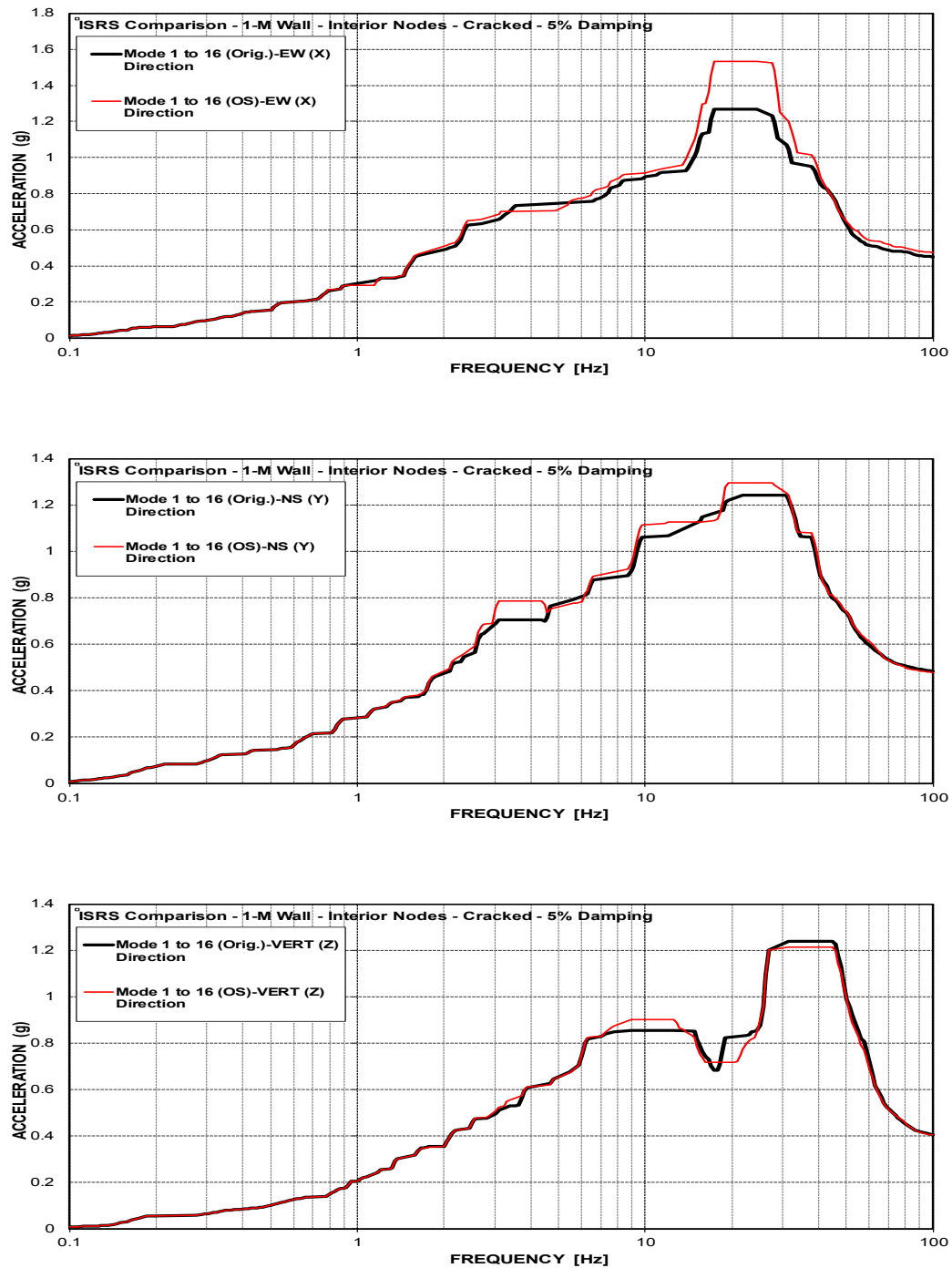


Figure C-227 ISRS Comparison -AB Shear Walls (1-M-Interior) at EL. 68' – HRHF – Cracked

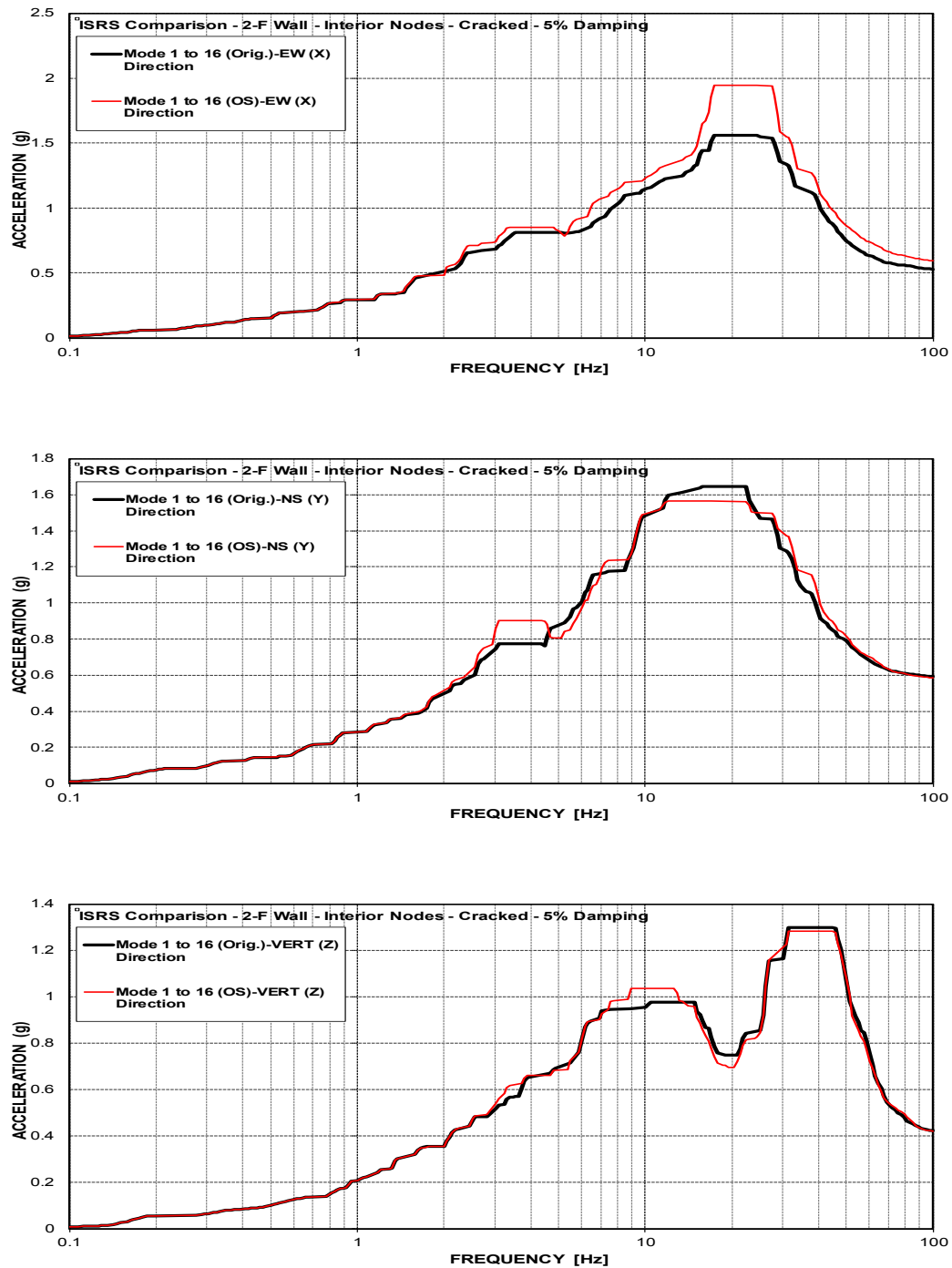


Figure C-228 ISRS Comparison -AB Shear Walls (2-F-Interior) at EL. 78' – HRHF – Cracked

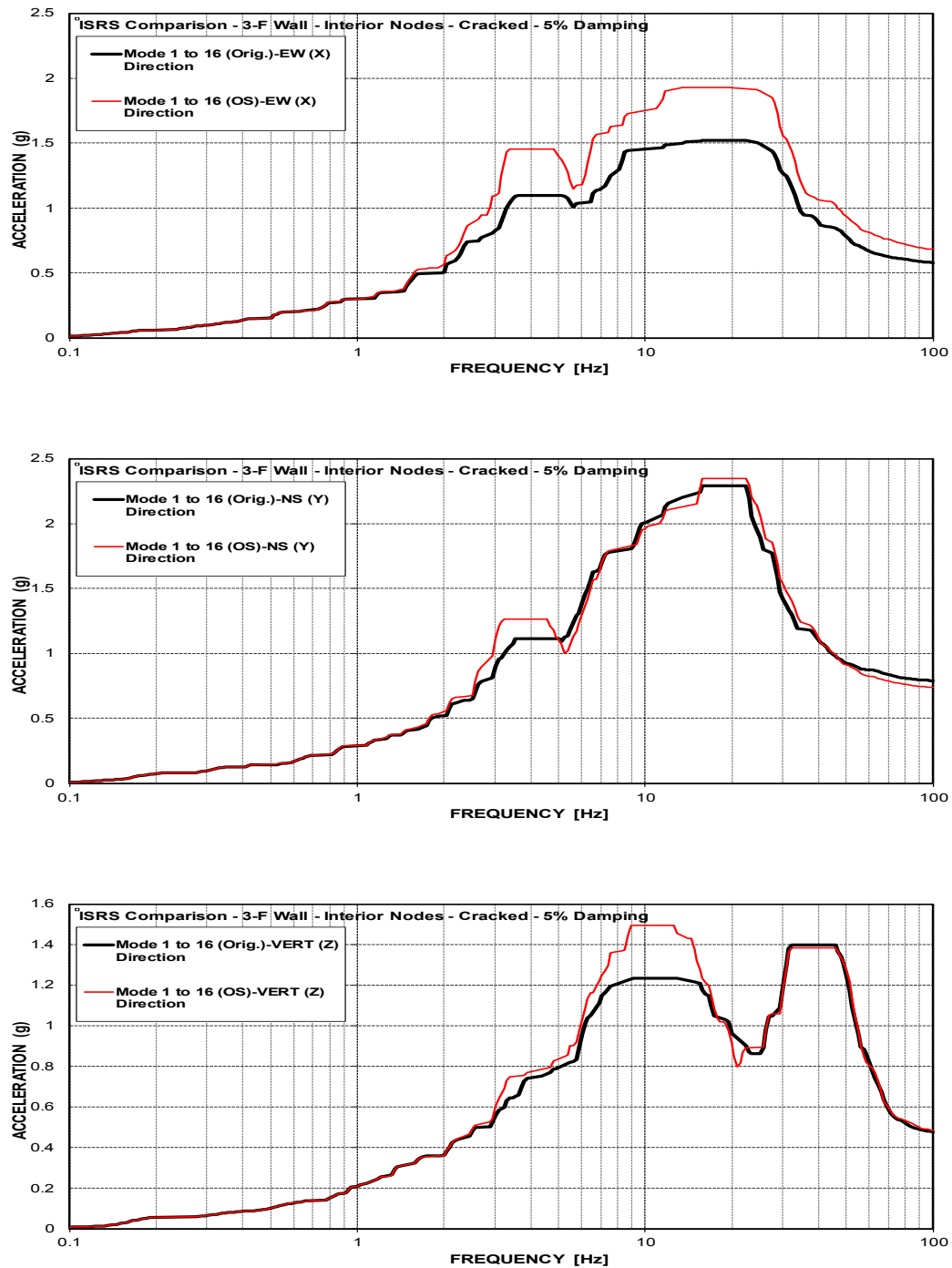


Figure C-229 ISRS Comparison -AB Shear Walls (3-F-Interior) at EL. 100' – HRHF – Cracked

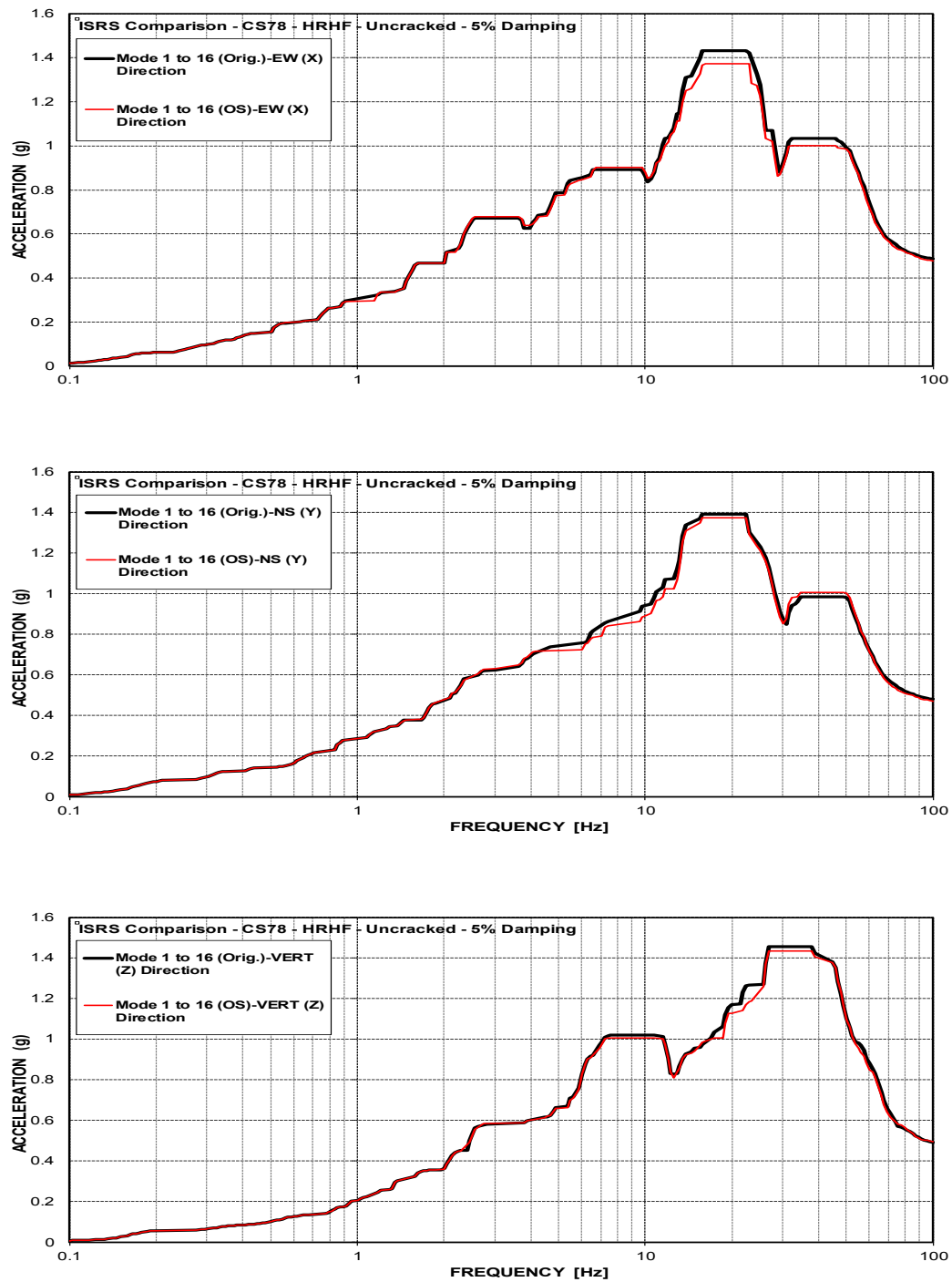


Figure C-230 ISRS Comparison-Containment Structure (CS78) at EL. 78' – HRHF – Uncracked

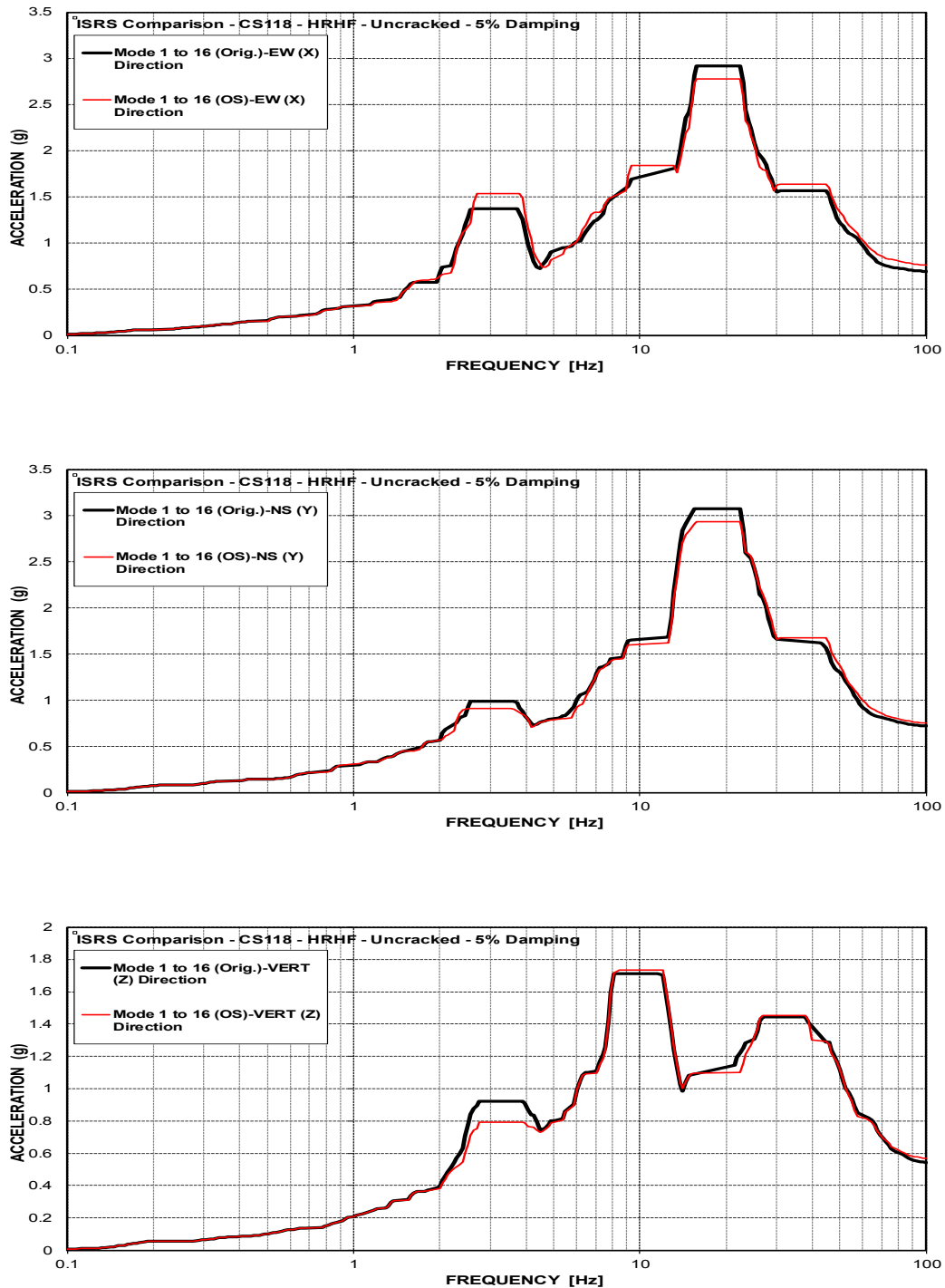


Figure C-231 ISRS Comparison-Containment Structure (CS118) at EL. 117.75' – HRHF – Uncracked

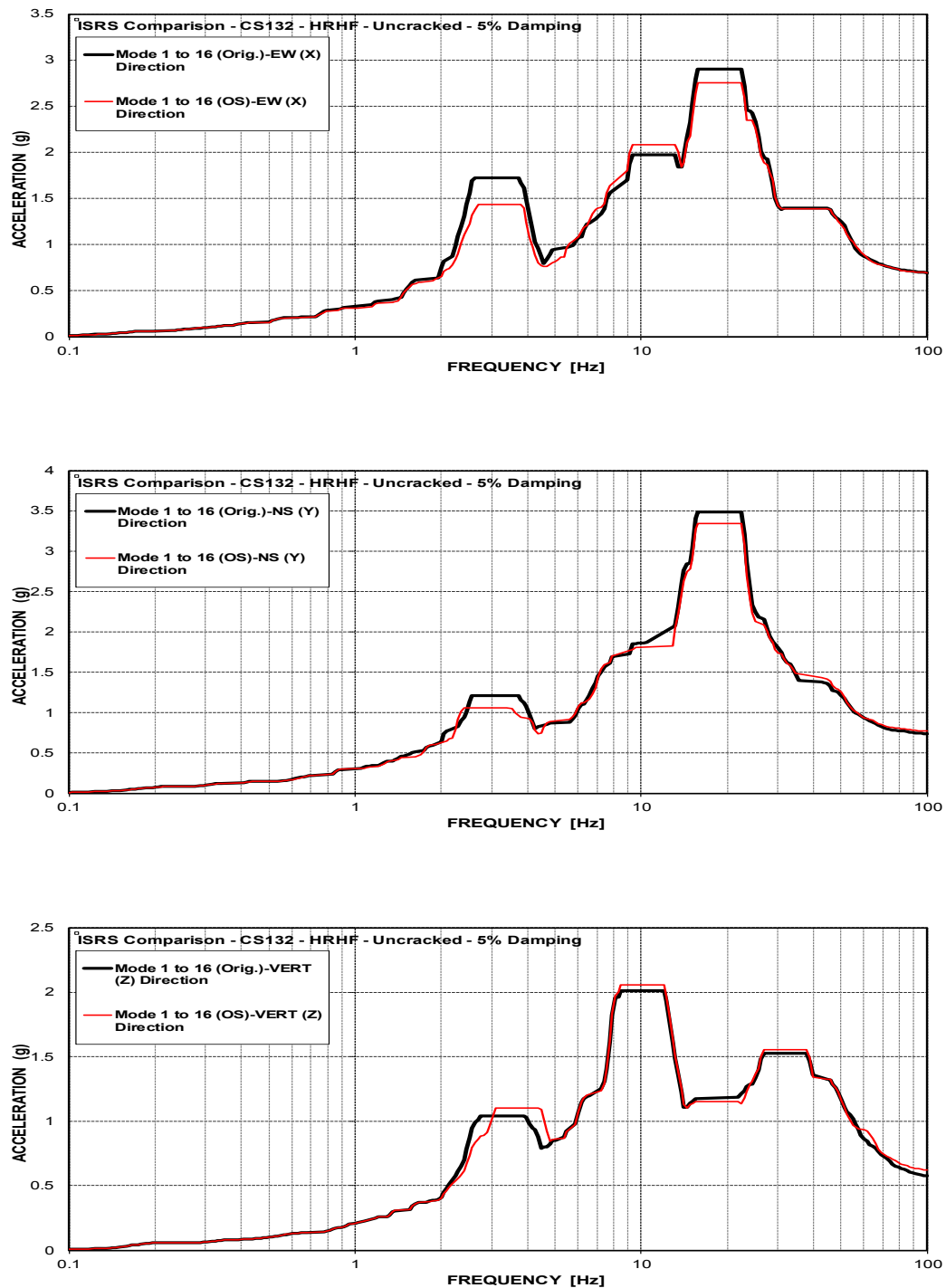


Figure C-232 ISRS Comparison-Containment Structure (CS132) at EL. 131.56' – HRHF – Uncracked



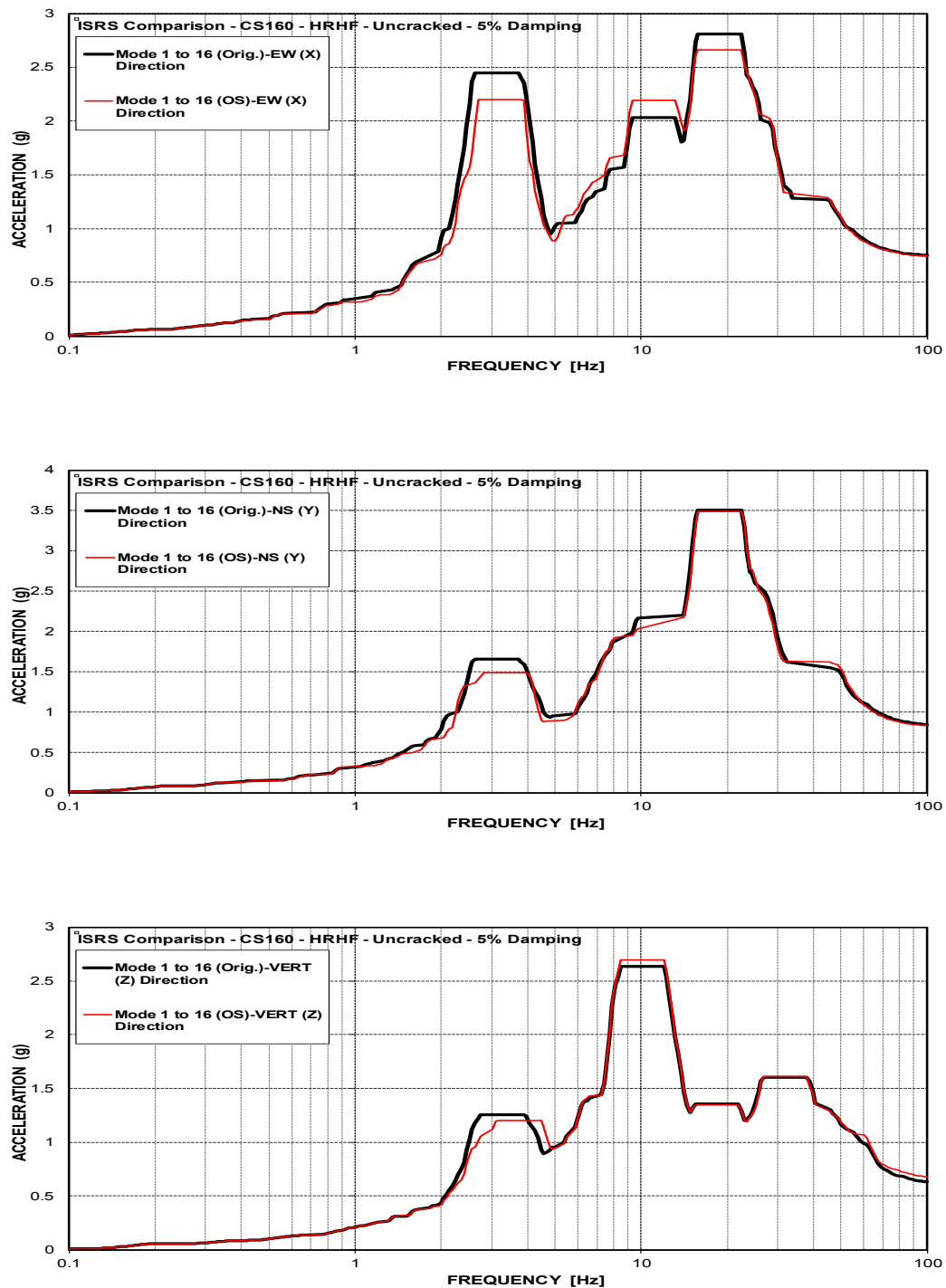


Figure C-233 ISRS Comparison-Containment Structure (CS160) at EL. 159.75' – HRHF – Uncracked

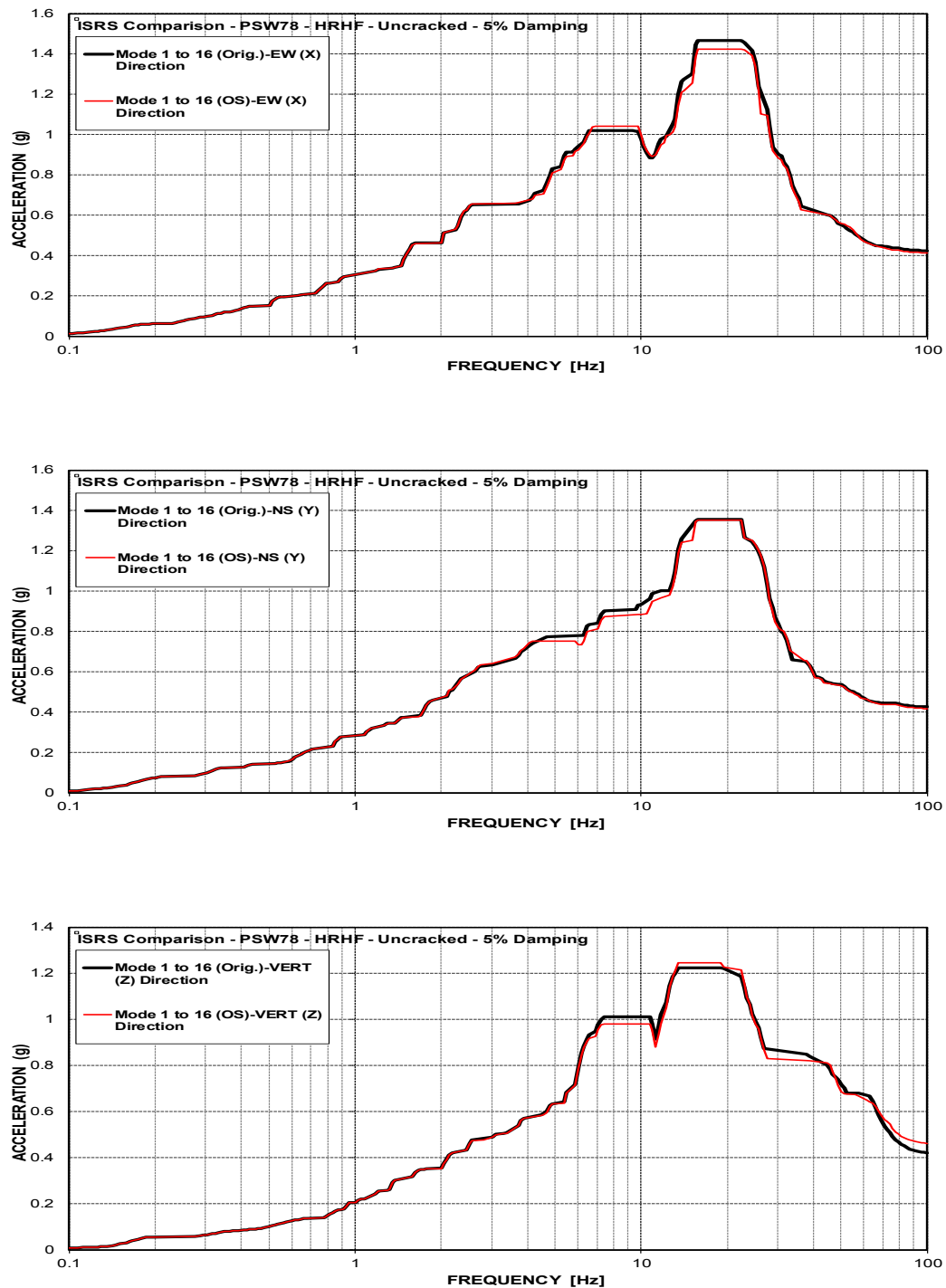


Figure C-234 ISRS Comparison-Primary Shield Wall (PSW78) at EL. 78' – HRHF – Uncracked

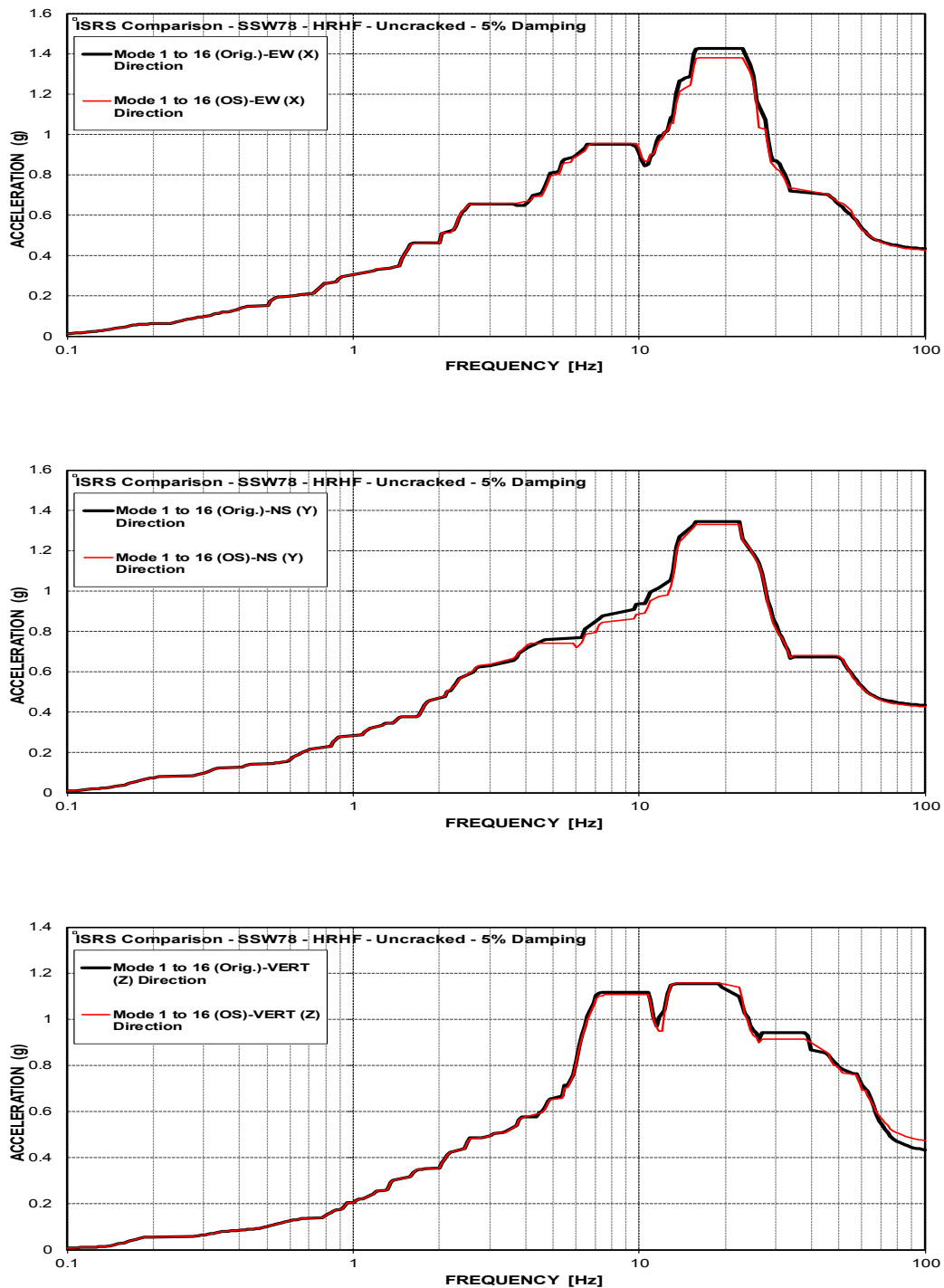


Figure C-235 ISRS Comparison-Secondary Shield Wall (SSW78) at EL. 78' – HRHF – Uncracked

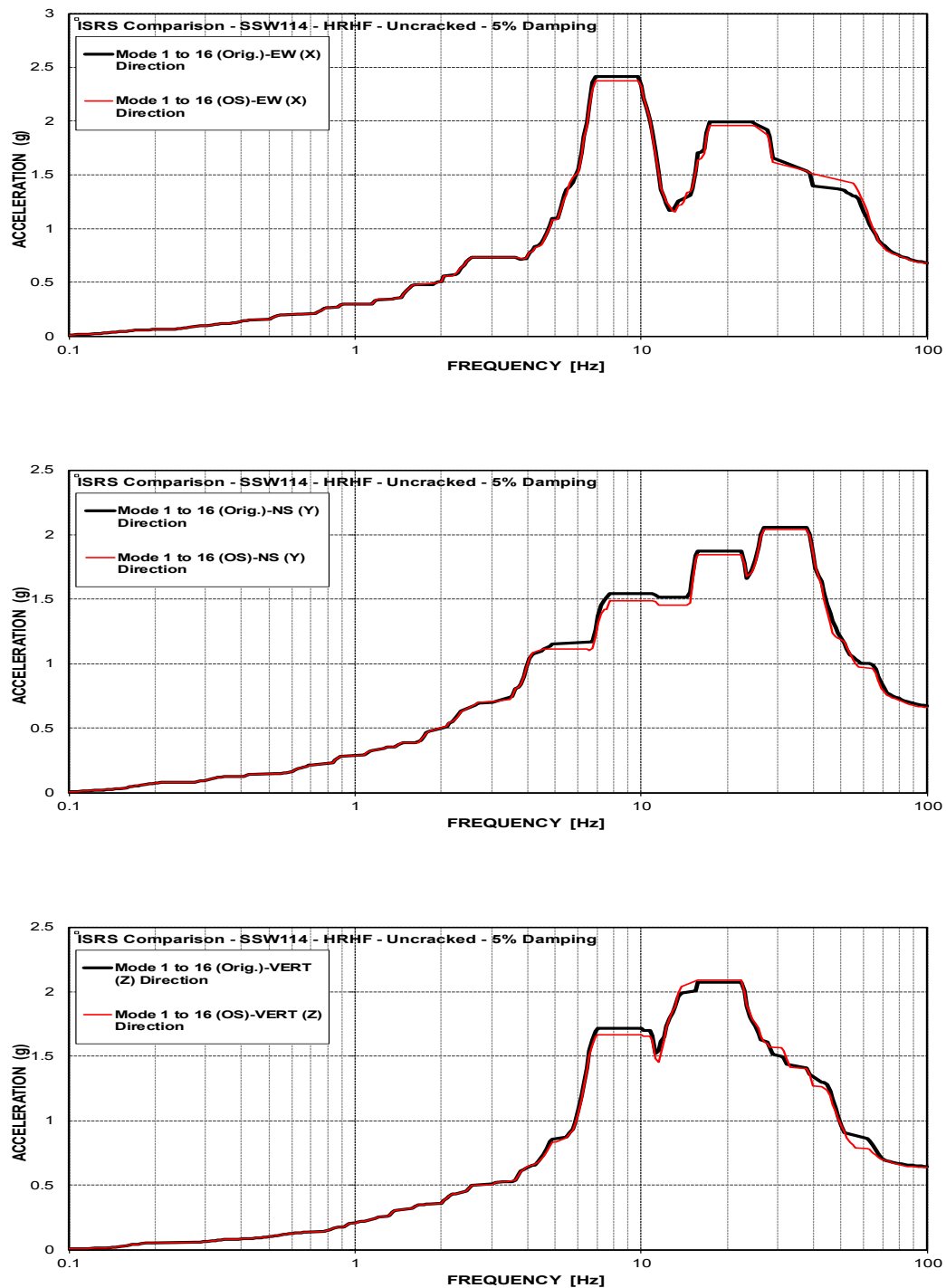


Figure C-236 ISRS Comparison-Secondary Shield Wall (SSW114) at EL. 114' – HRHF – Uncracked

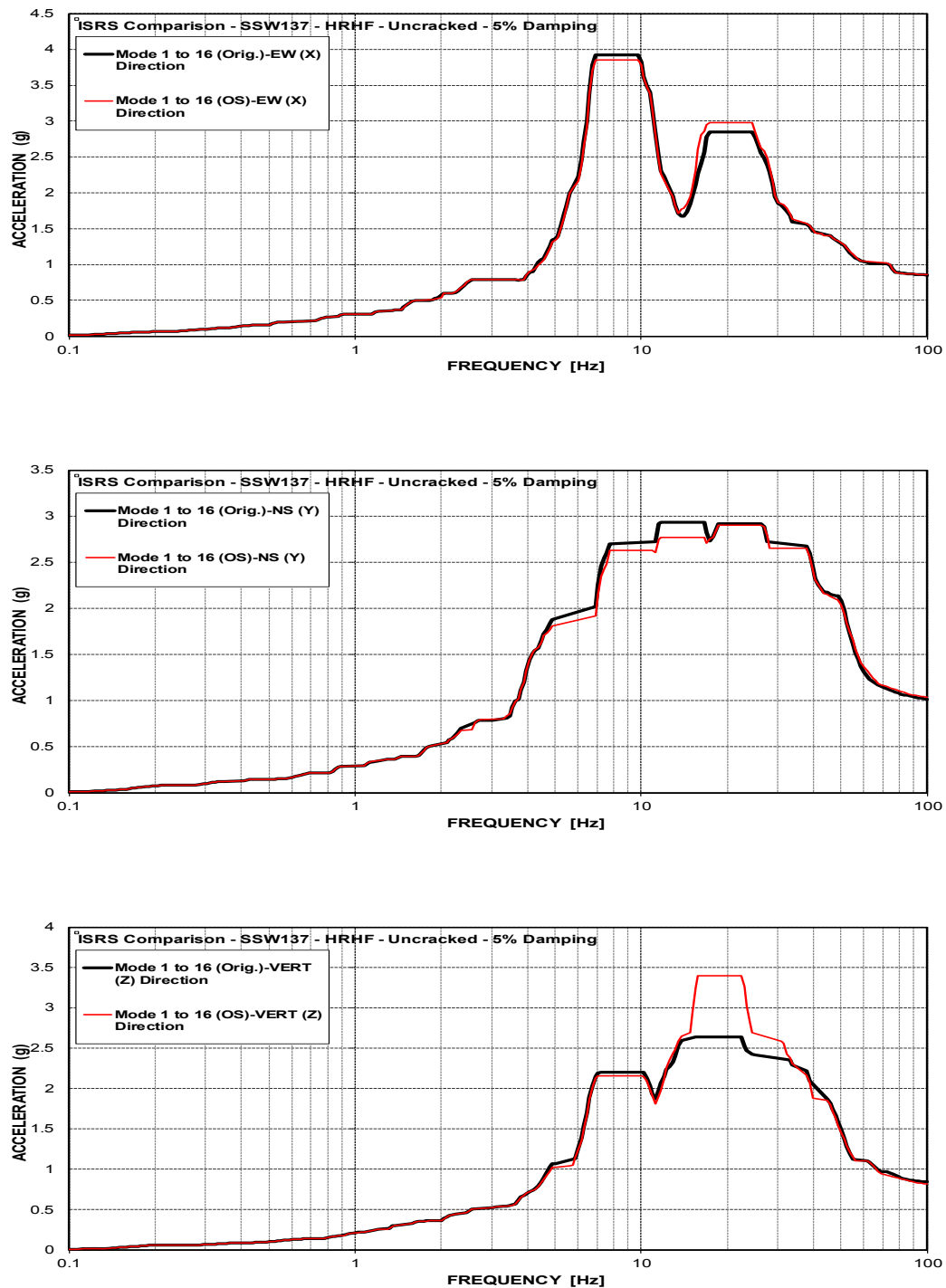


Figure C-237 ISRS Comparison-Secondary Shield Wall (SSW137) at EL. 137' – HRHF – Uncracked

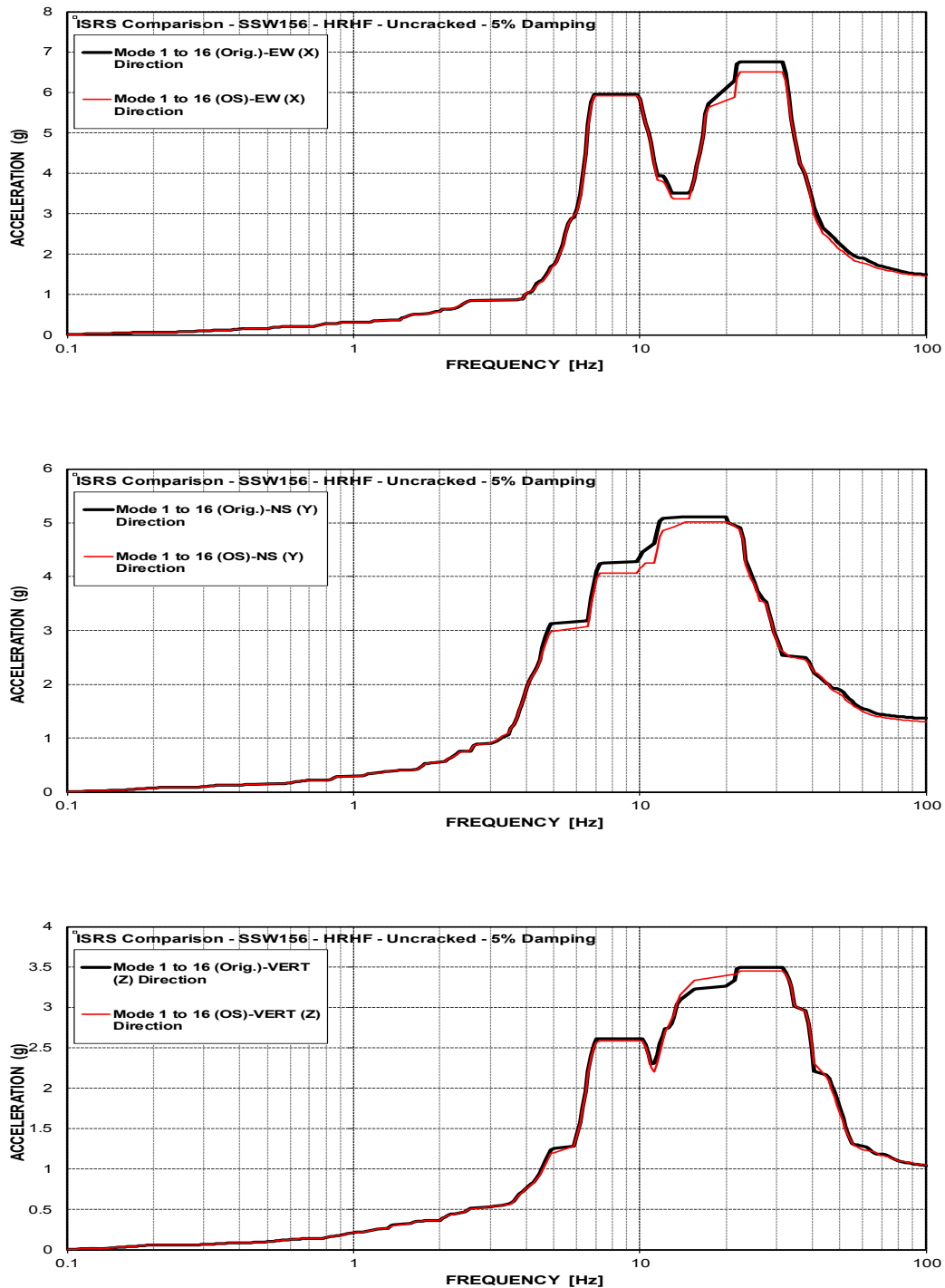


Figure C-238 ISRS Comparison-Secondary Shield Wall (SSW156) at EL. 156' – HRHF – Uncracked

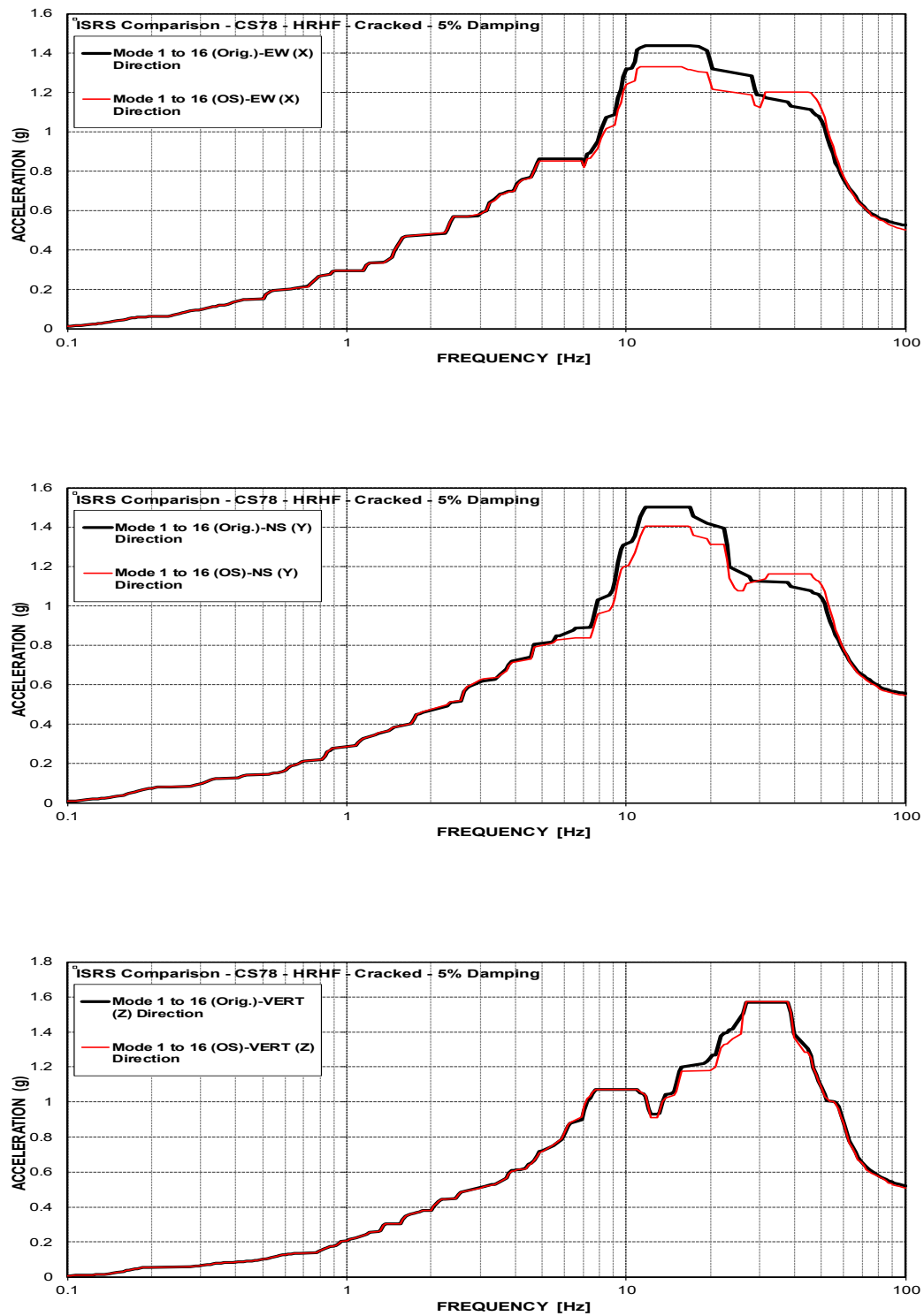


Figure C-239 ISRS Comparison-Containment Structure (CS78) at EL. 78' – HRHF – Cracked

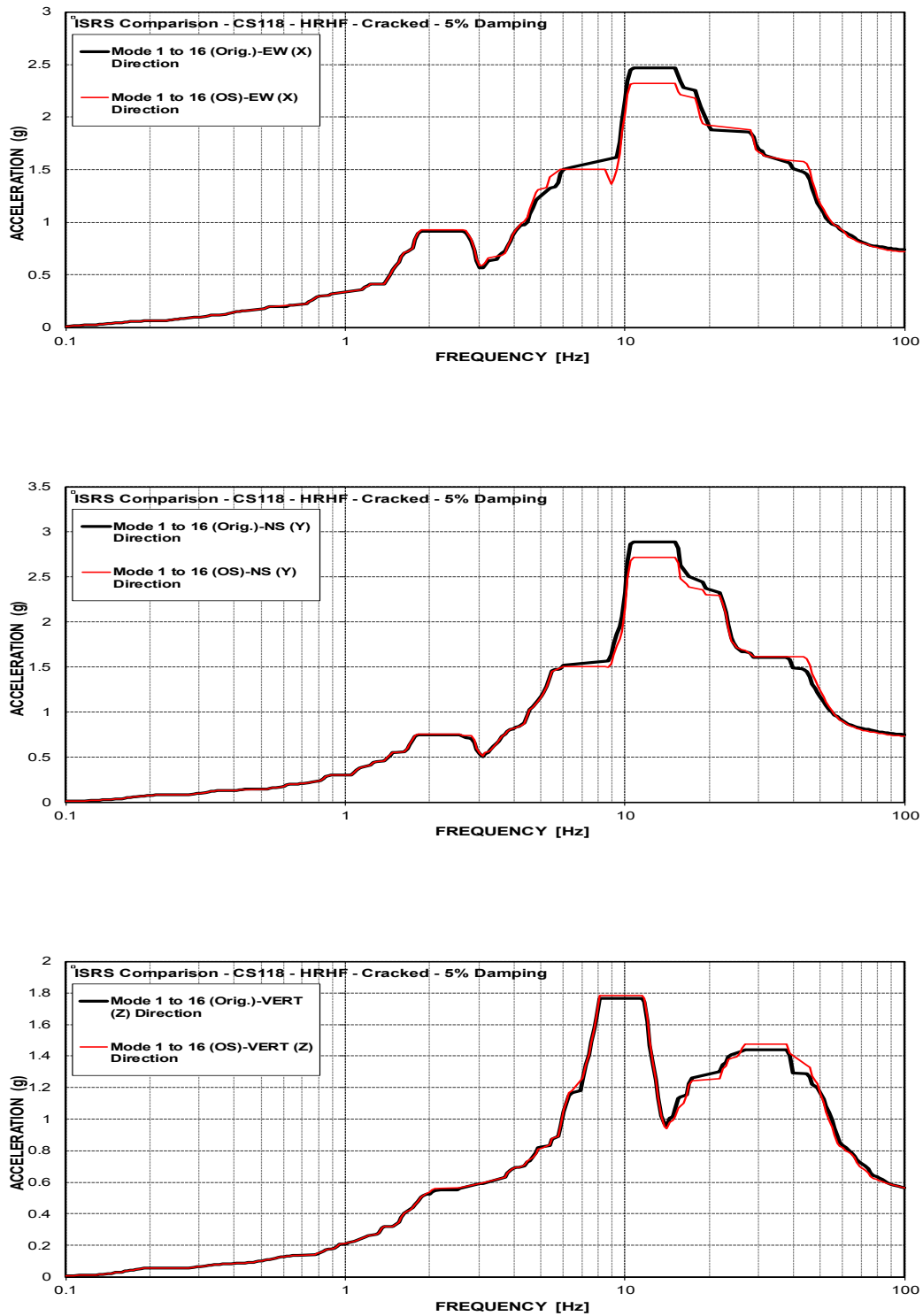


Figure C-240 ISRS Comparison-Containment Structure (CS118) at EL. 117.75' – HRHF – Cracked



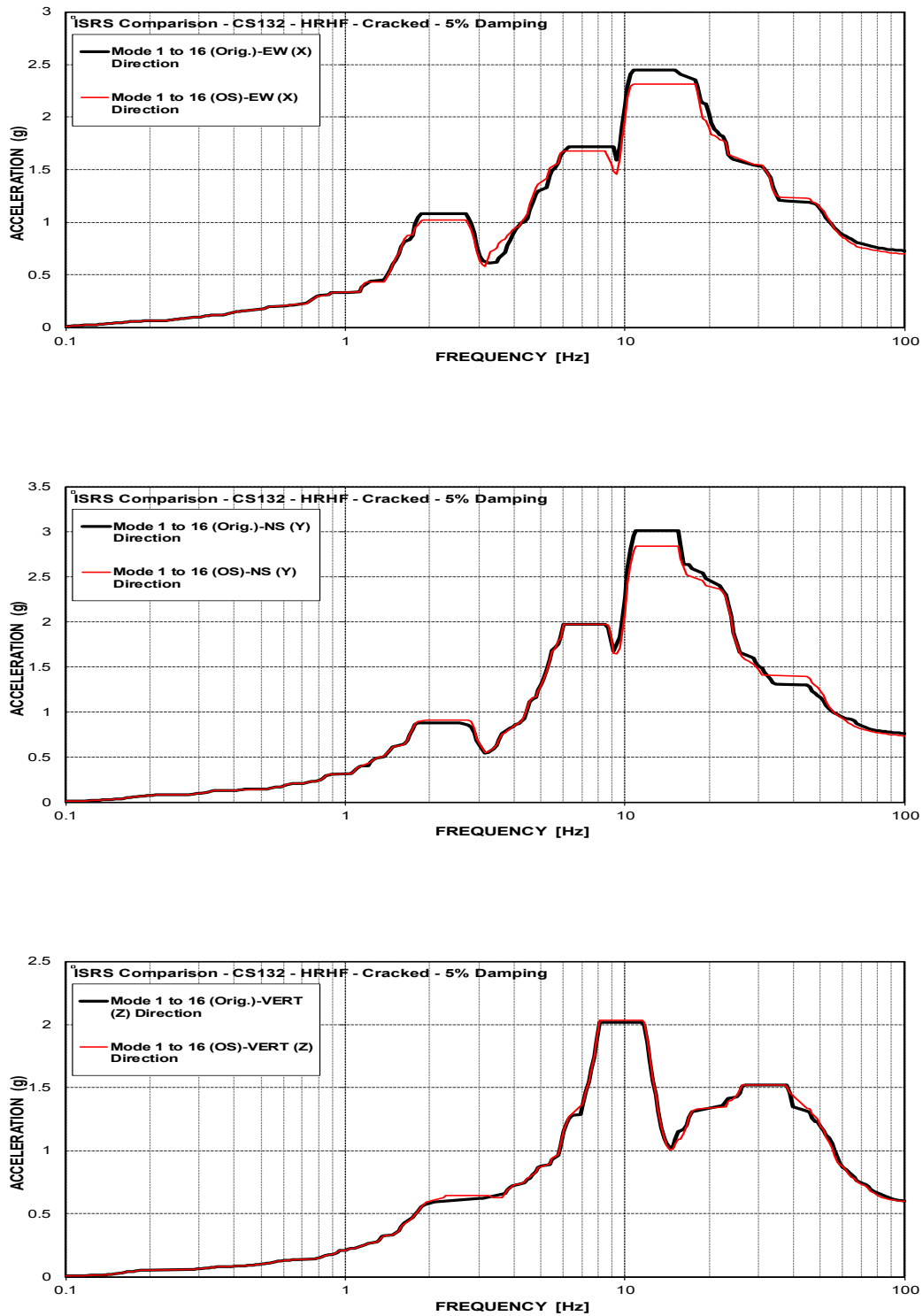


Figure C-241 ISRS Comparison-Containment Structure (CS132) at EL. 131.56' – HRHF – Cracked

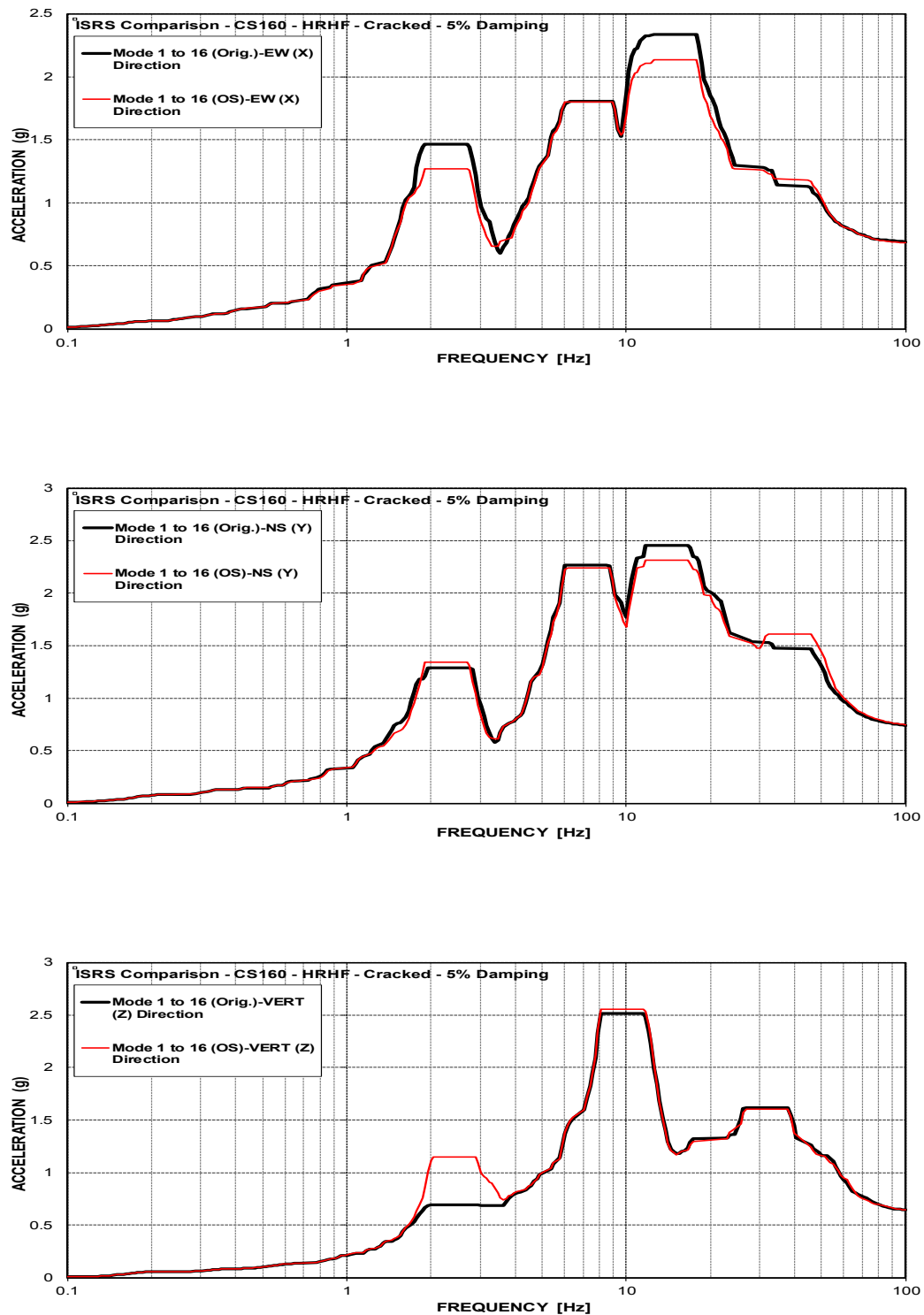


Figure C-242 ISRS Comparison-Containment Structure (CS160) at EL. 159.75' – HRHF – Cracked

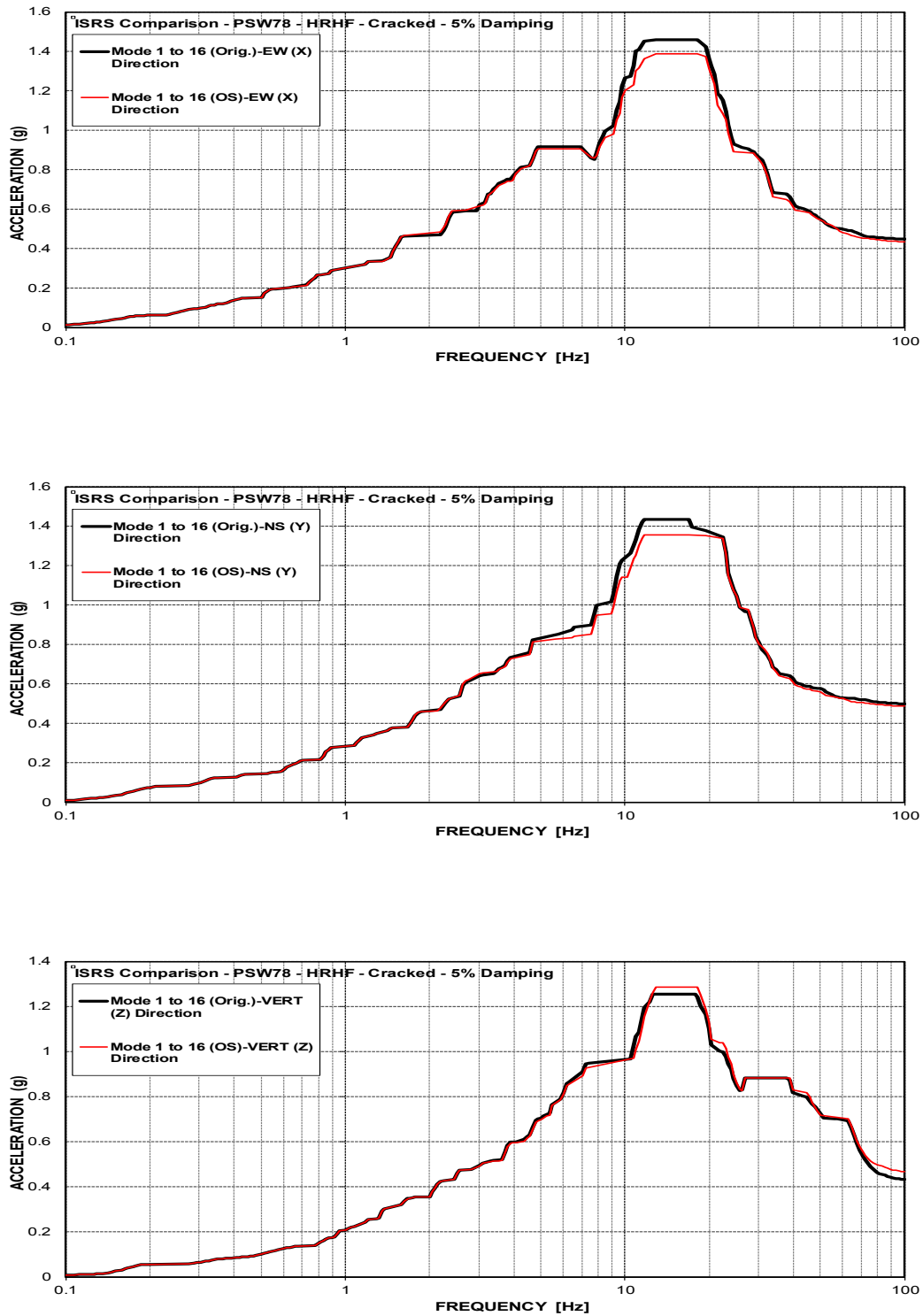


Figure C-243 ISRS Comparison-Primary Shield Wall (PSW78) at EL. 78' – HRHF – Cracked

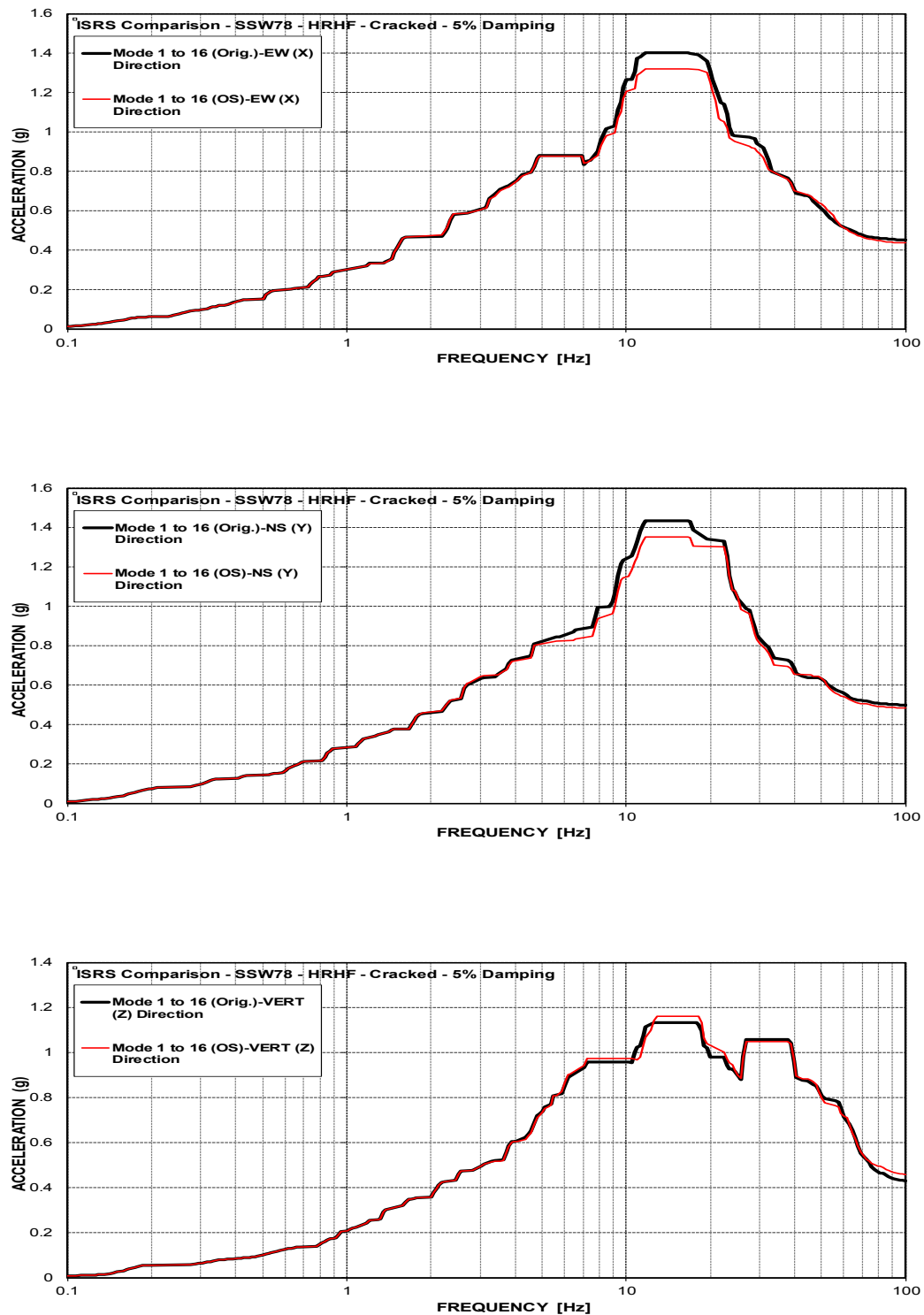


Figure C-244 ISRS Comparison-Secondary Shield Wall (SSW78) at EL. 78' – HRHF – Cracked

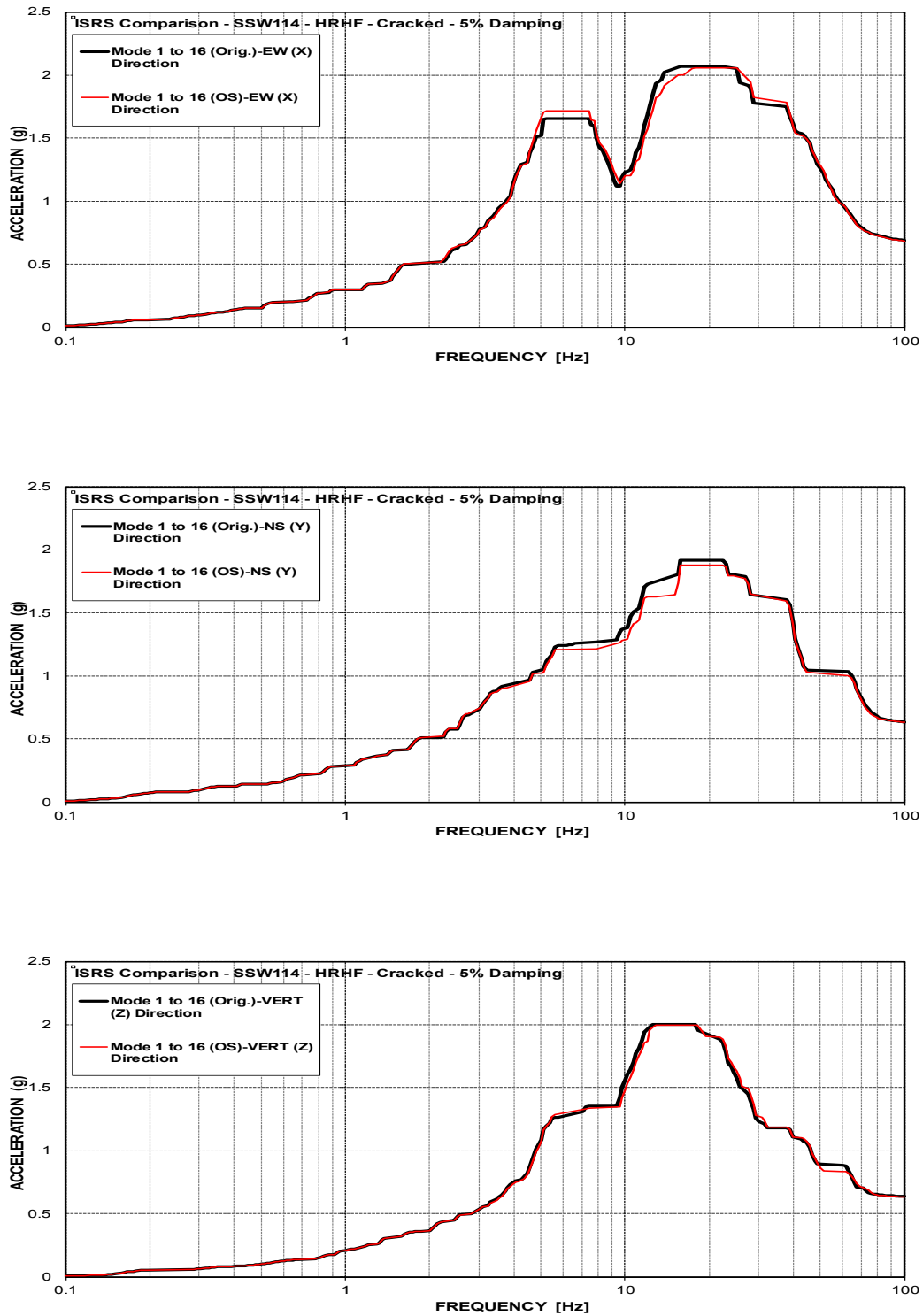


Figure C-245 ISRS Comparison-Secondary Shield Wall (SSW114) at EL. 114' – HRHF – Cracked

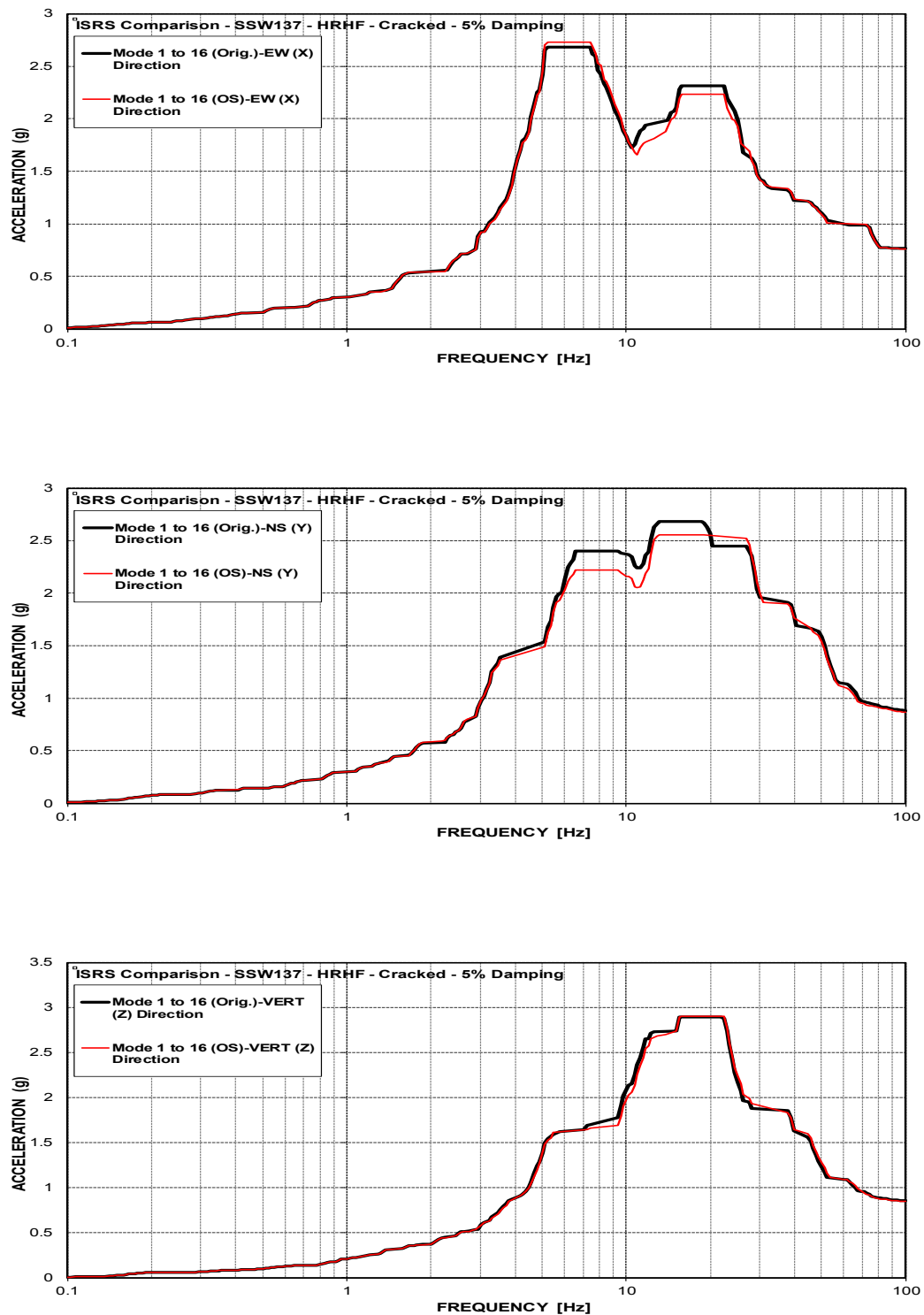


Figure C-246 ISRS Comparison-Secondary Shield Wall (SSW137) at EL. 137' – HRHF – Cracked

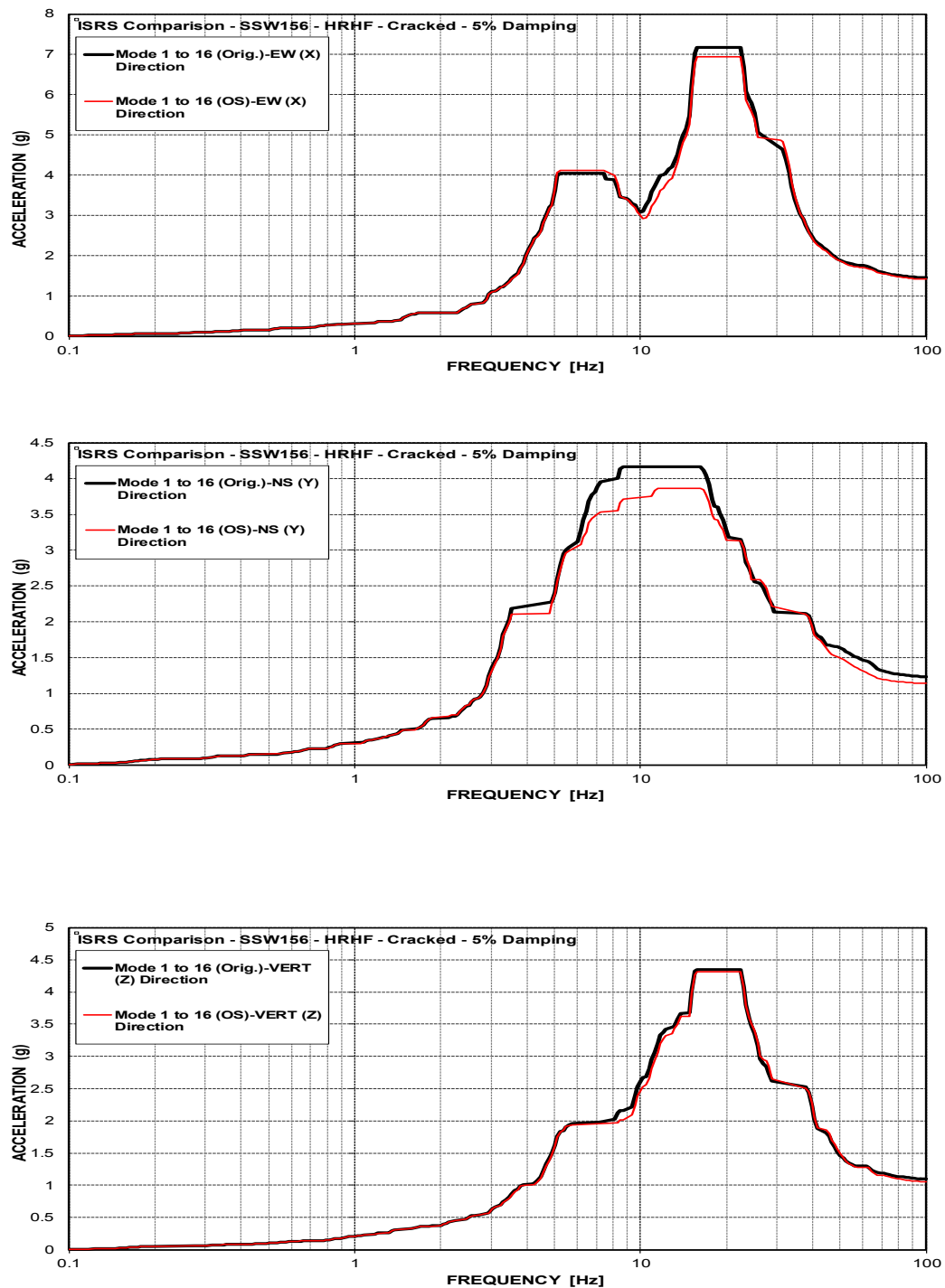


Figure C-247 ISRS Comparison-Secondary Shield Wall (SSW156) at EL. 156' – HRHF – Cracked

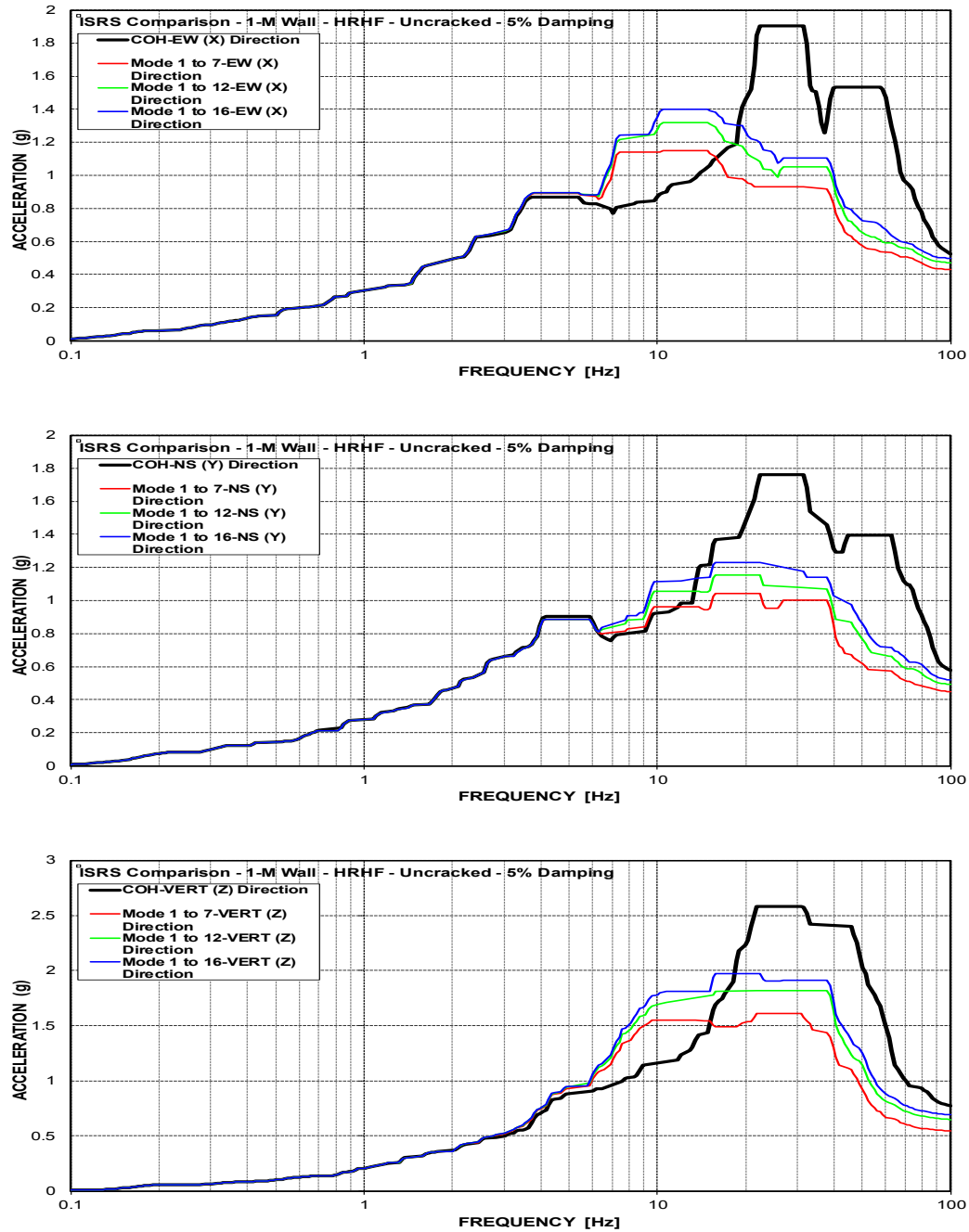


Figure C-248 Mod. Model ISRS– AB Shear Walls (1-M) at El. 68' – HRHF – Uncracked



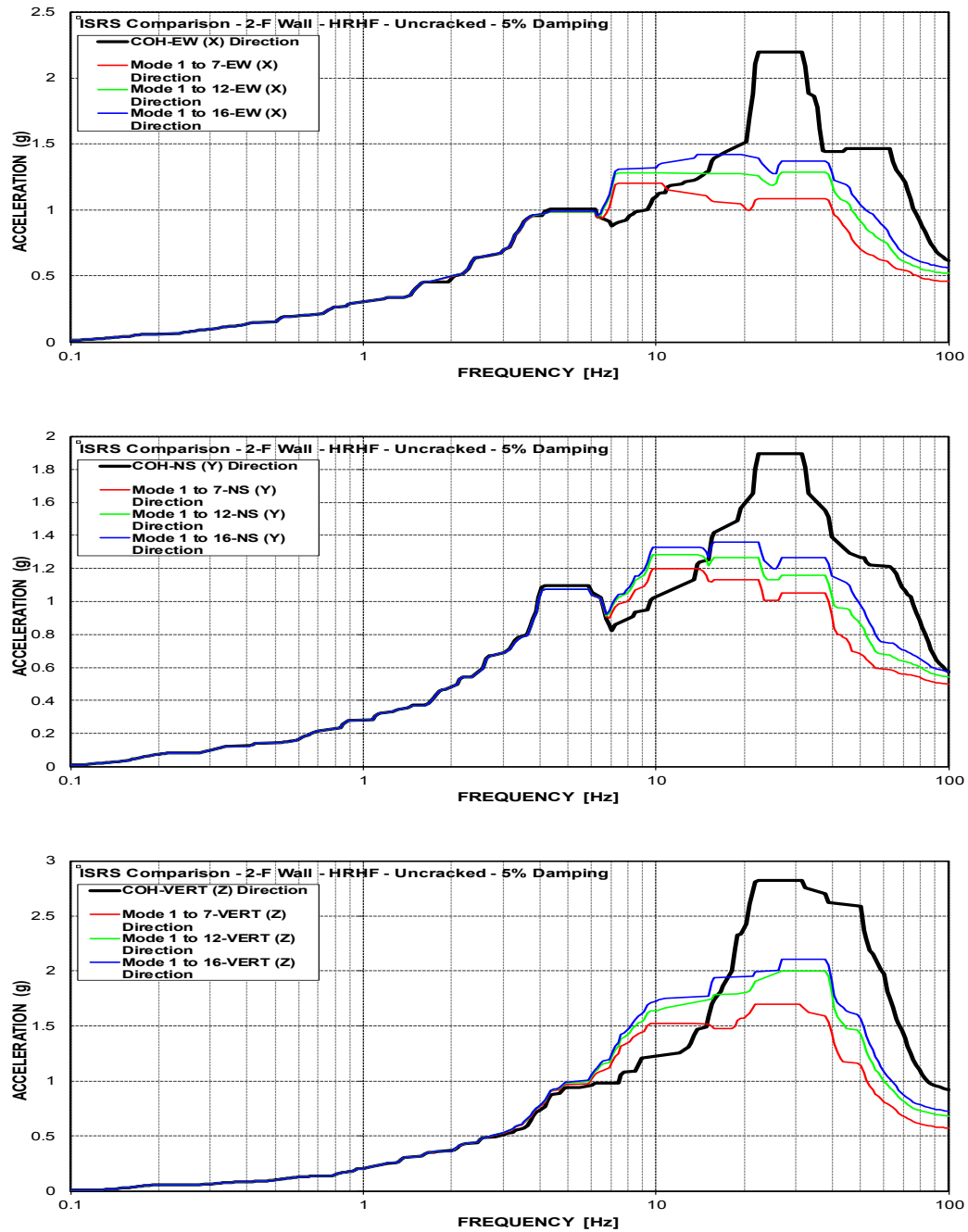


Figure C-249 Mod. Model ISRS– AB Shear Walls (2-F) at El. 78' – HRHF – Uncracked

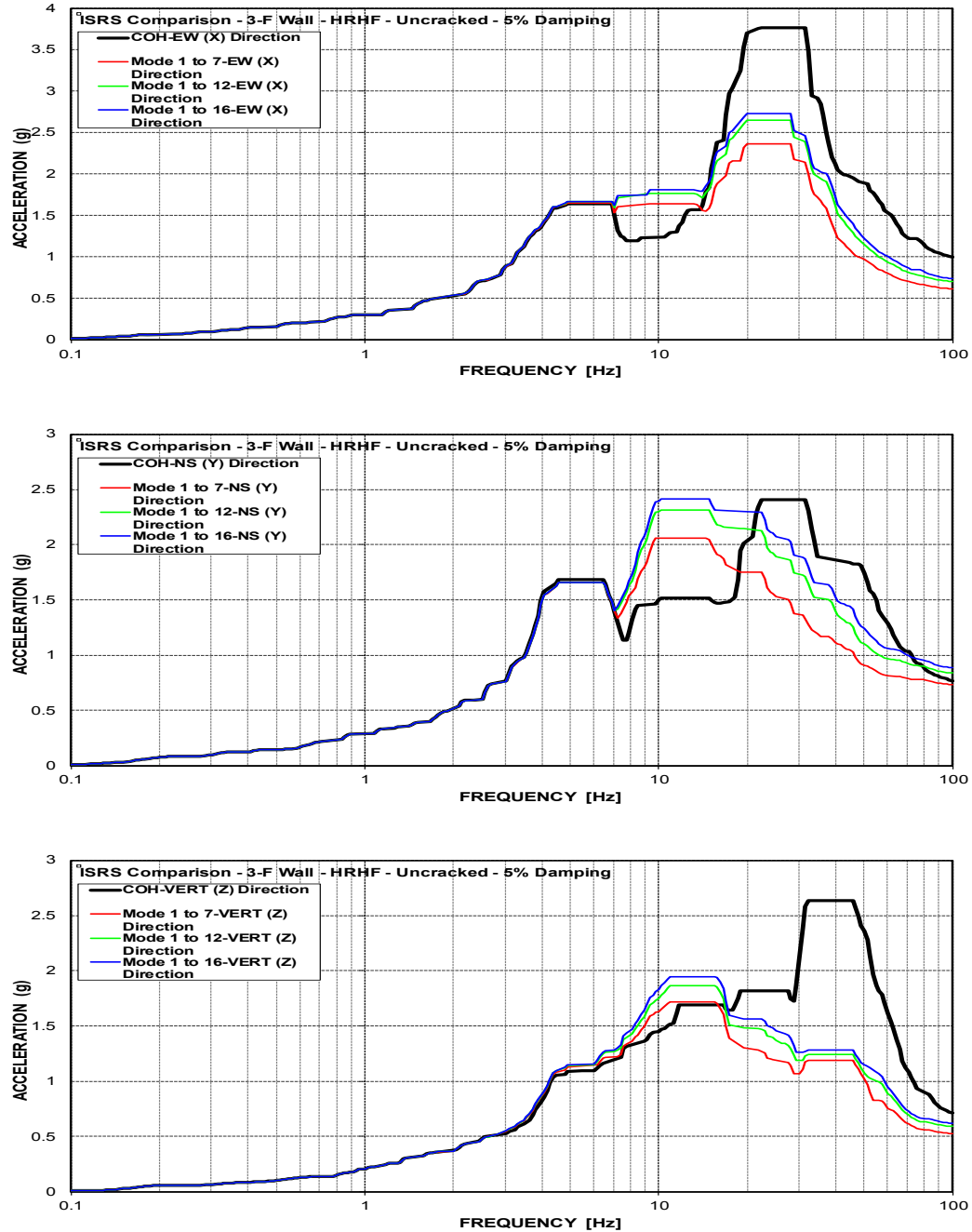


Figure C-250 Mod. Model ISRS– AB Shear Walls (3-F) at El. 100' – HRHF – Uncracked

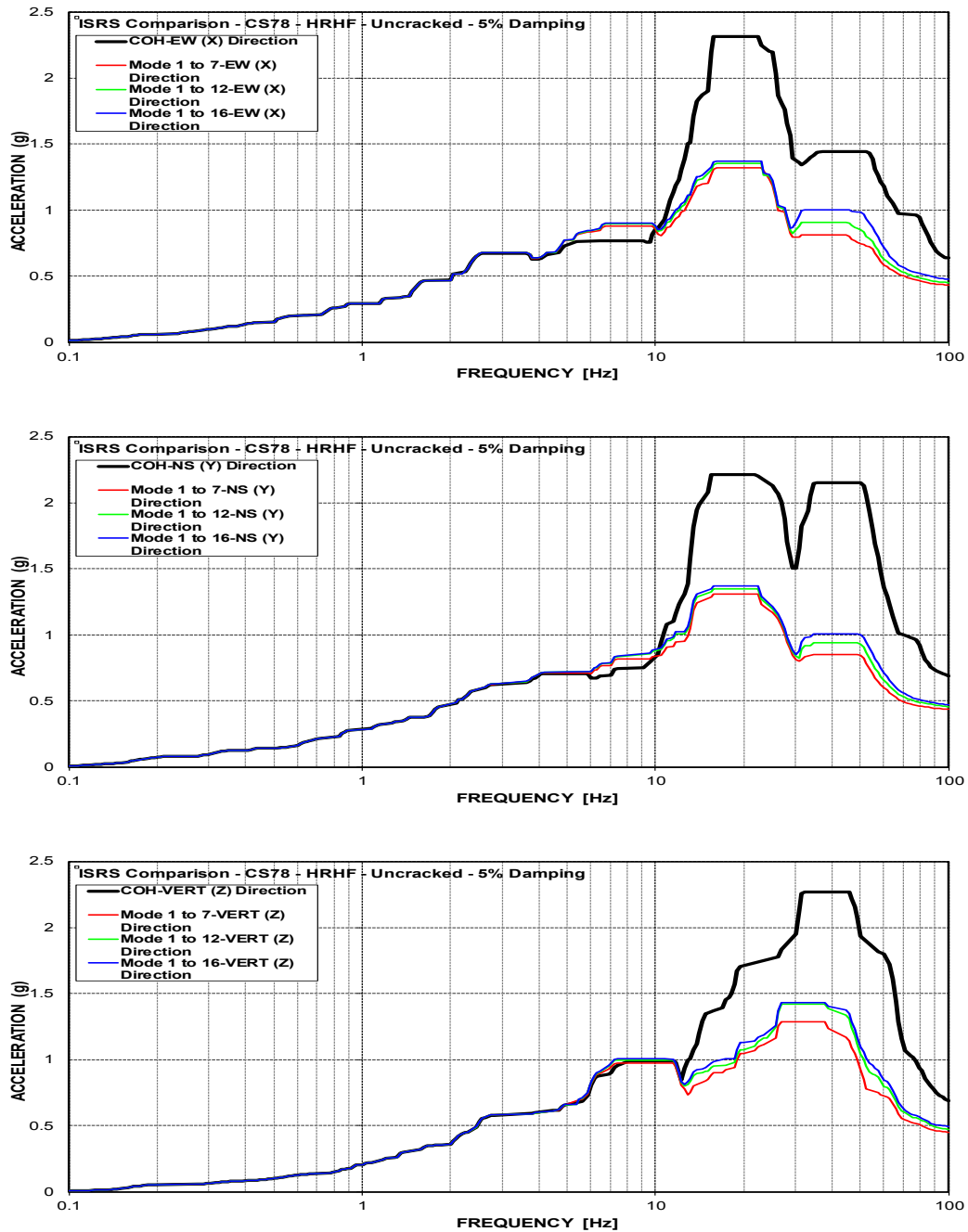


Figure C-251 Mod. Model ISRS– Containment Structure (CS78) at El. 78' – HRHF – Uncracked

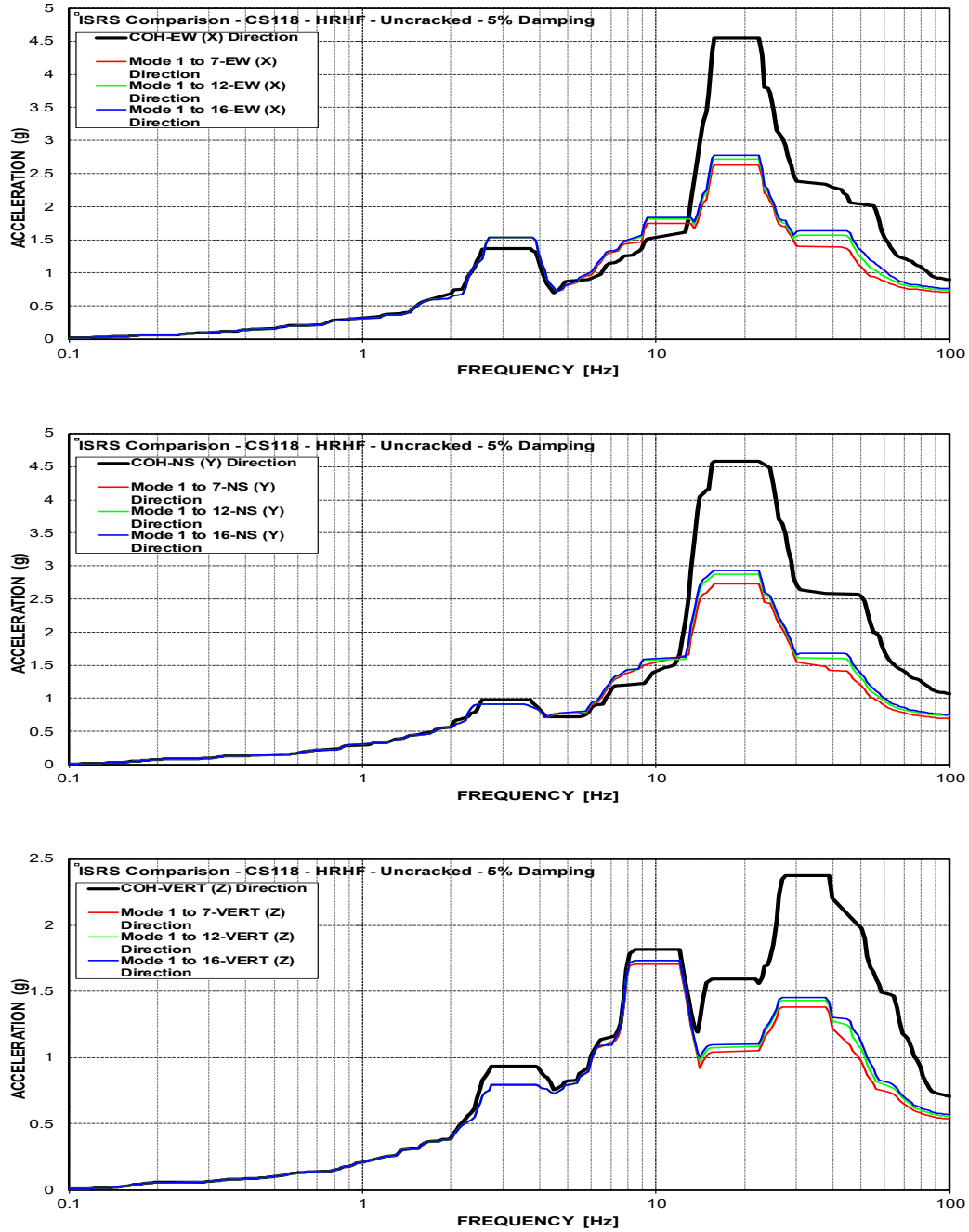


Figure C-252 Mod. Model ISRS– Containment Structure (CS118) at El. 117.75' – HRHF – Uncracked

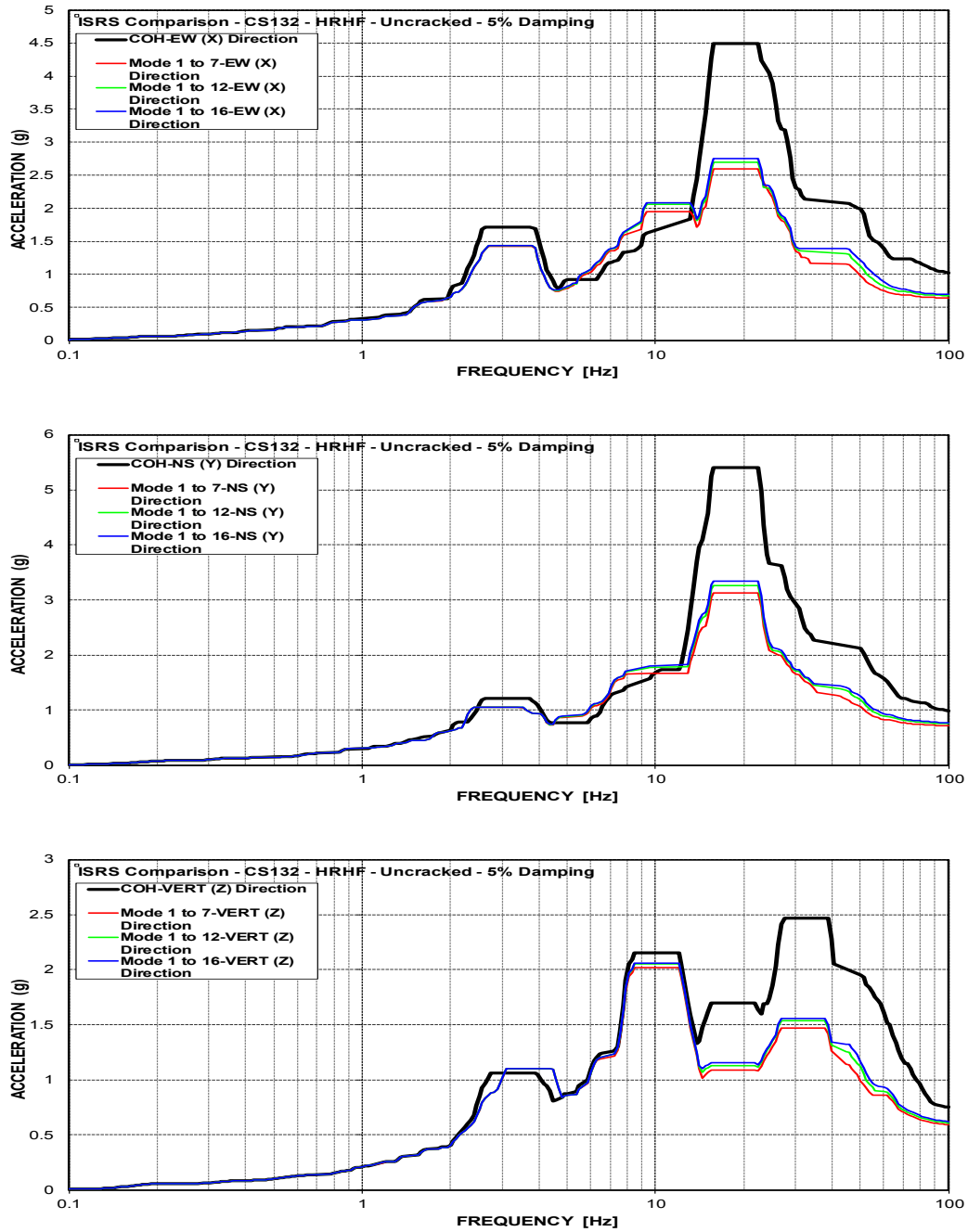


Figure C-253 Mod. Model ISRS– Containment Structure (CS132) at El. 131.56' – HRHF – Uncracked

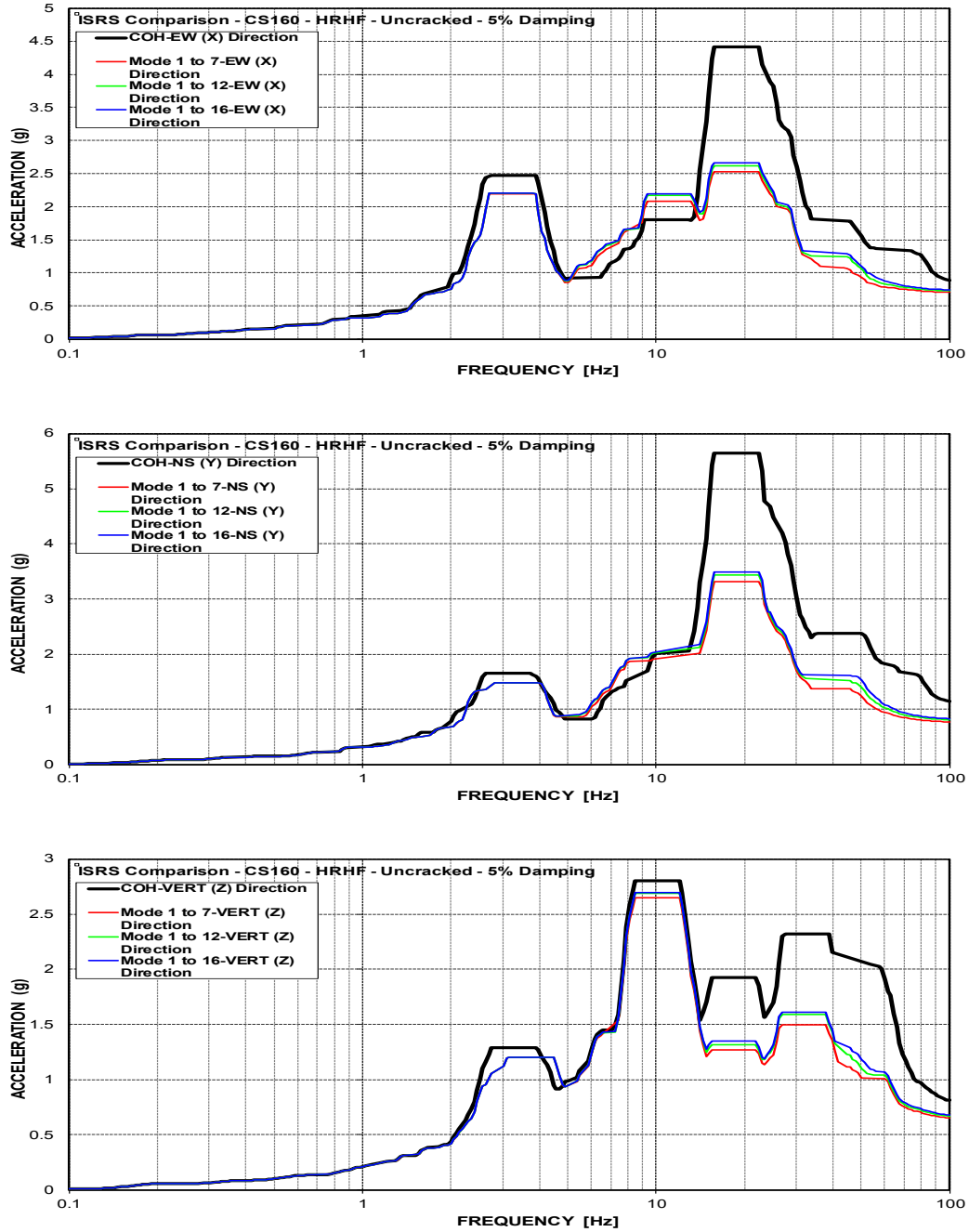


Figure C-254 Mod. Model ISRS– Containment Structure (CS160) at El. 159.75' – HRHF – Uncracked

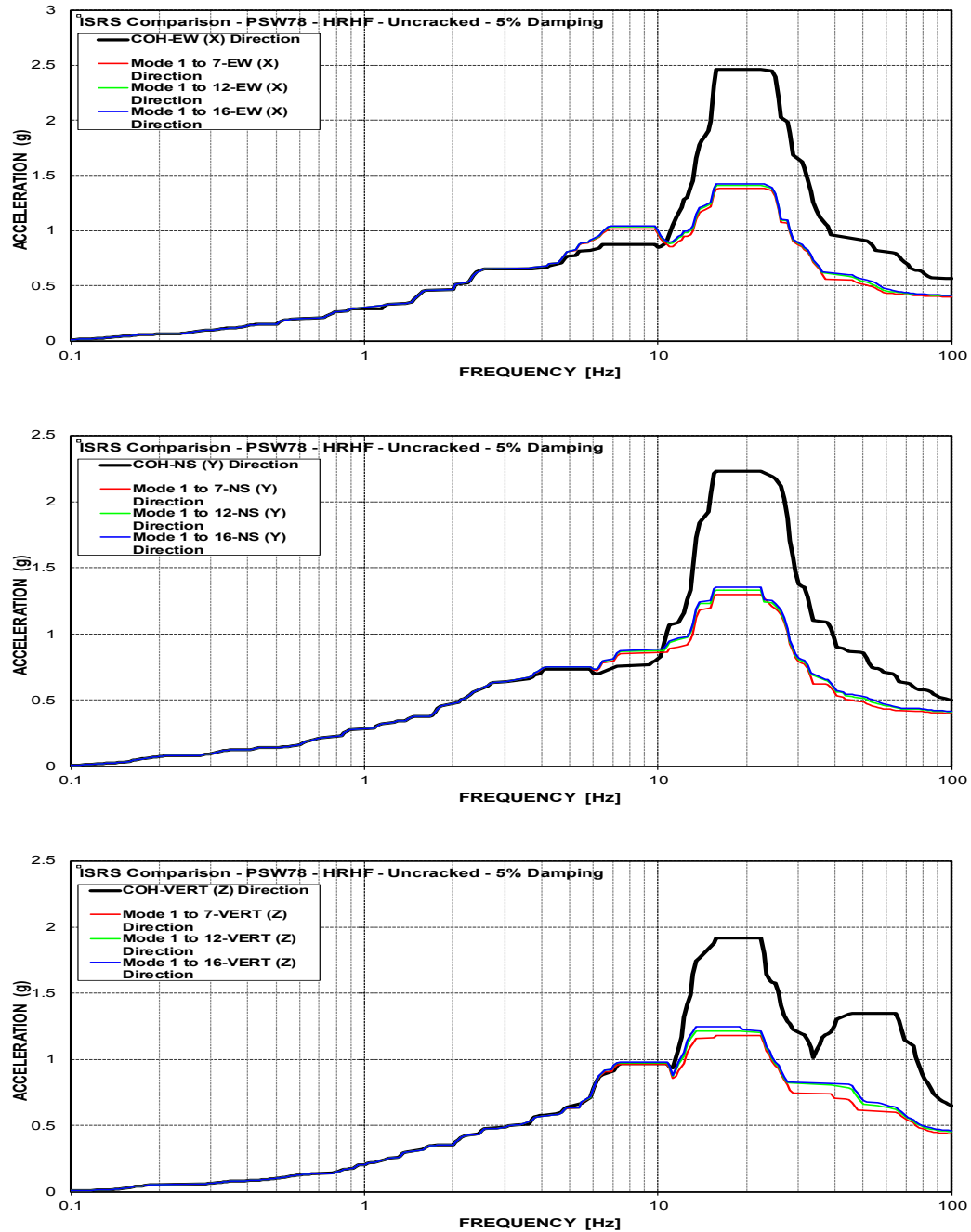


Figure C-255 Mod. Model ISRS– Primary Shield Wall (PSW78) at El. 78' – HRHF – Uncracked

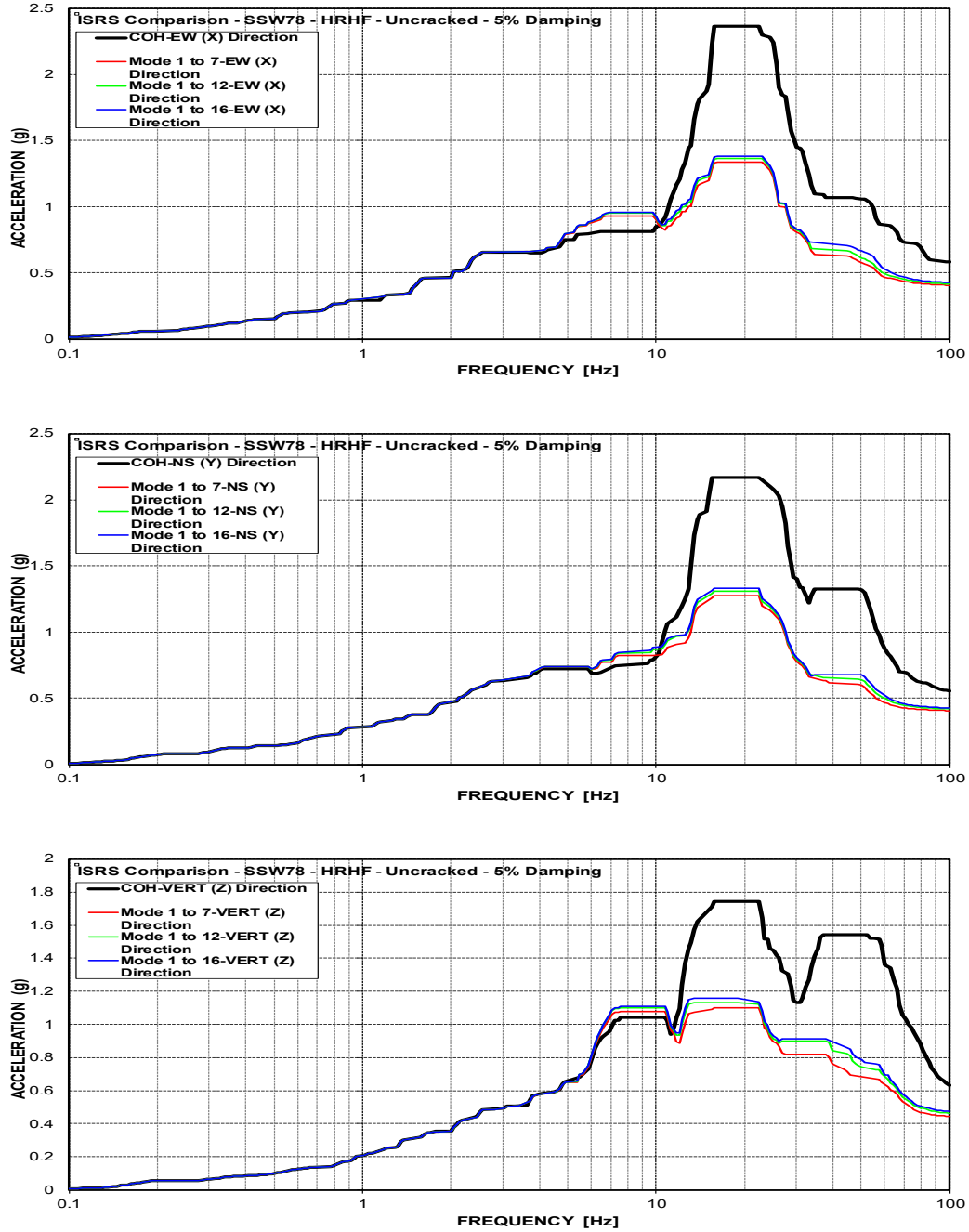


Figure C-256 Mod. Model ISRS– Secondary Shield Wall (SSW78) at El. 78' – HRHF – Uncracked



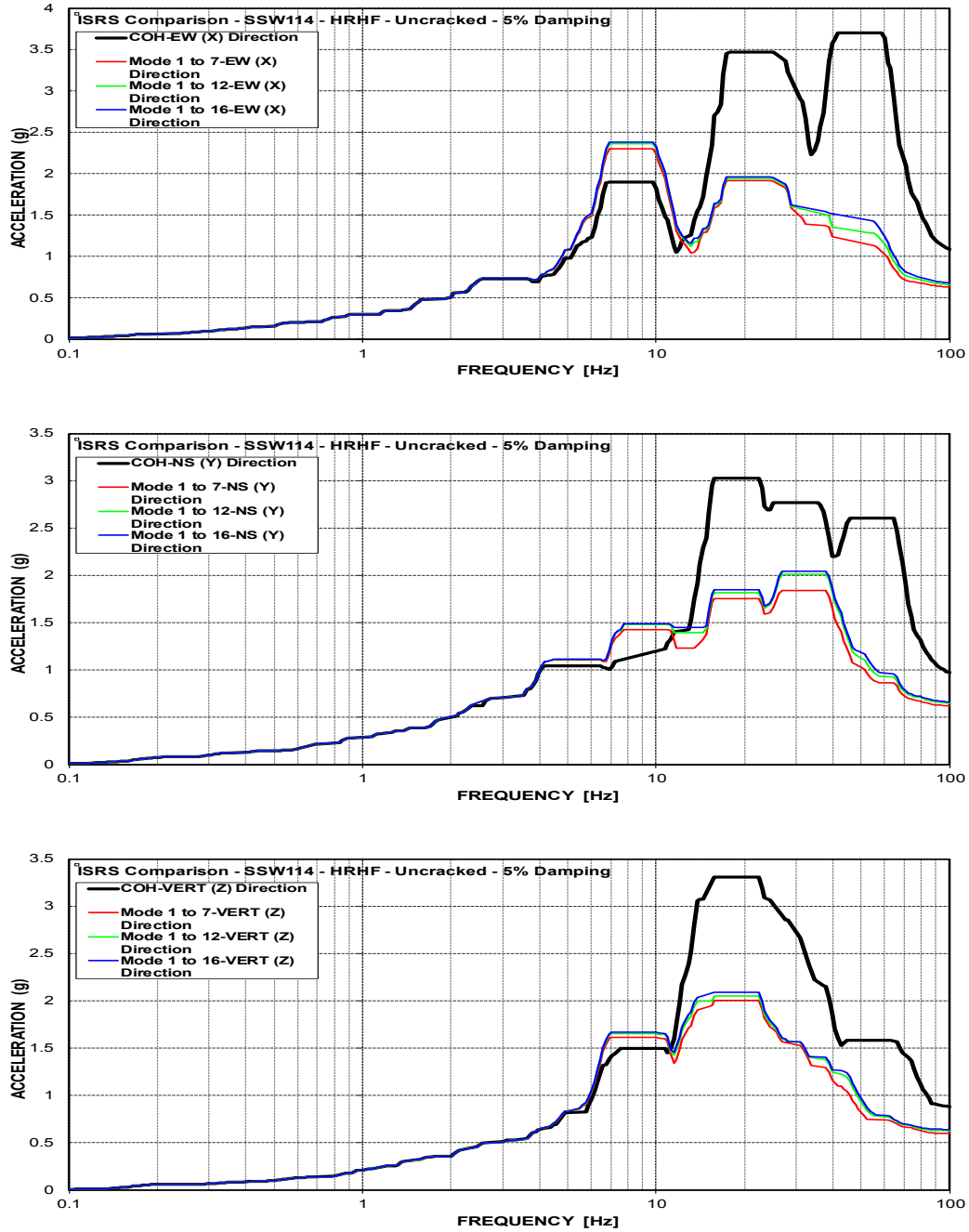


Figure C-257 Mod. Model ISRS– Secondary Shield Wall (SSW114) at El. 114' – HRHF – Uncracked

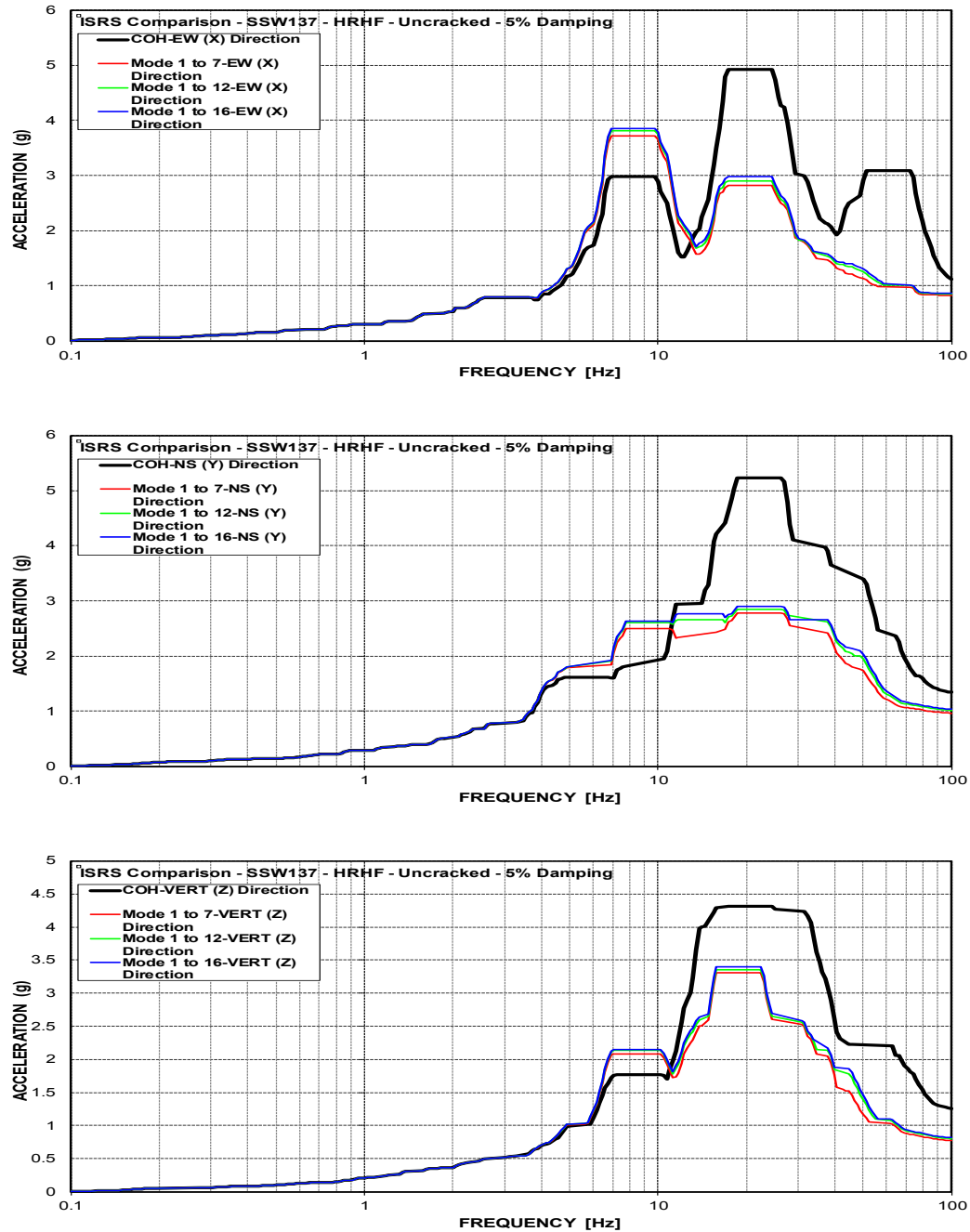


Figure C-258 Mod. Model ISRS– Secondary Shield Wall (SSW137) at El. 136.5' – HRHF – Uncracked

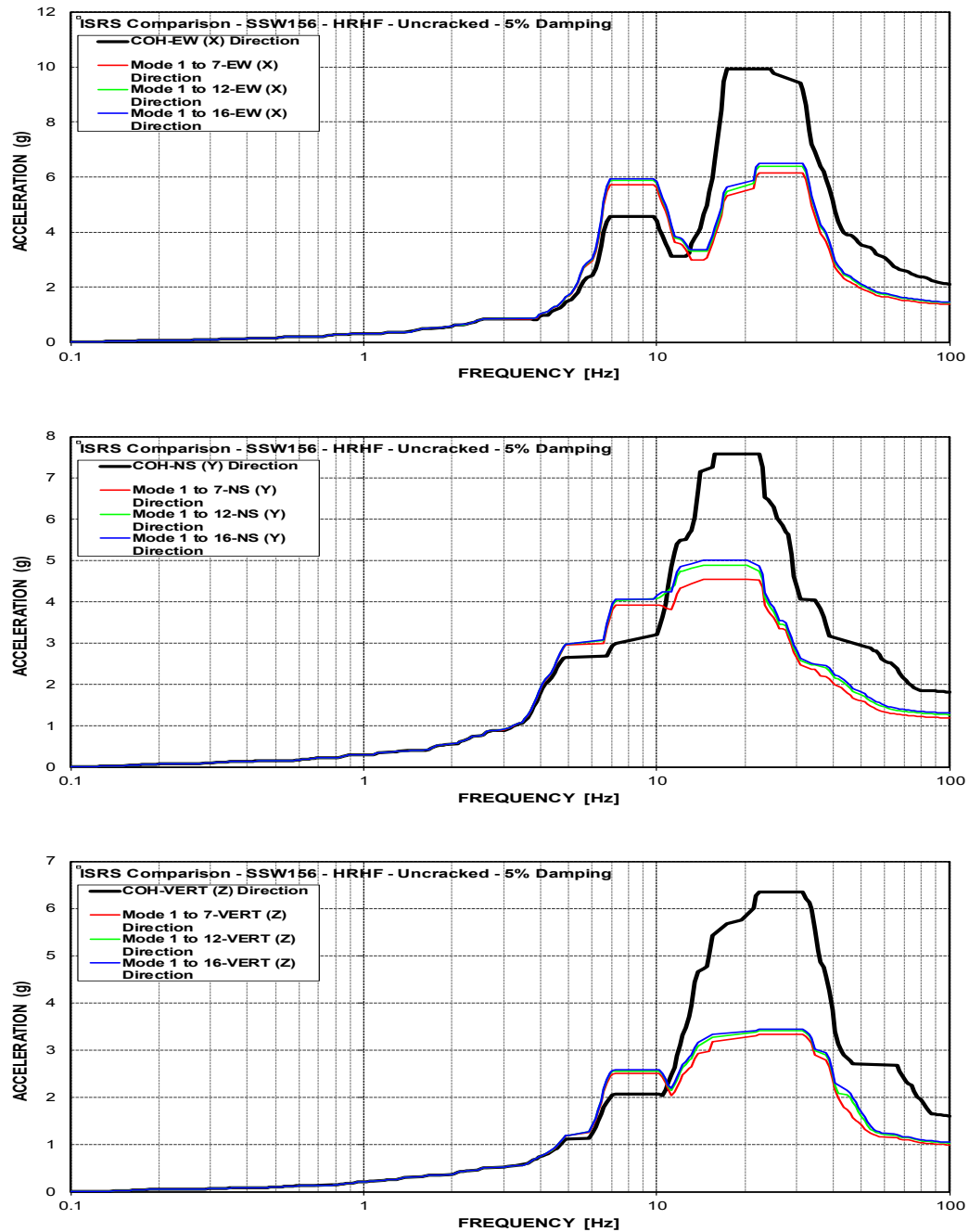


Figure C-259 Mod. Model ISRS– Secondary Shield Wall (SSW156) at El. 156' – HRHF – Uncracked

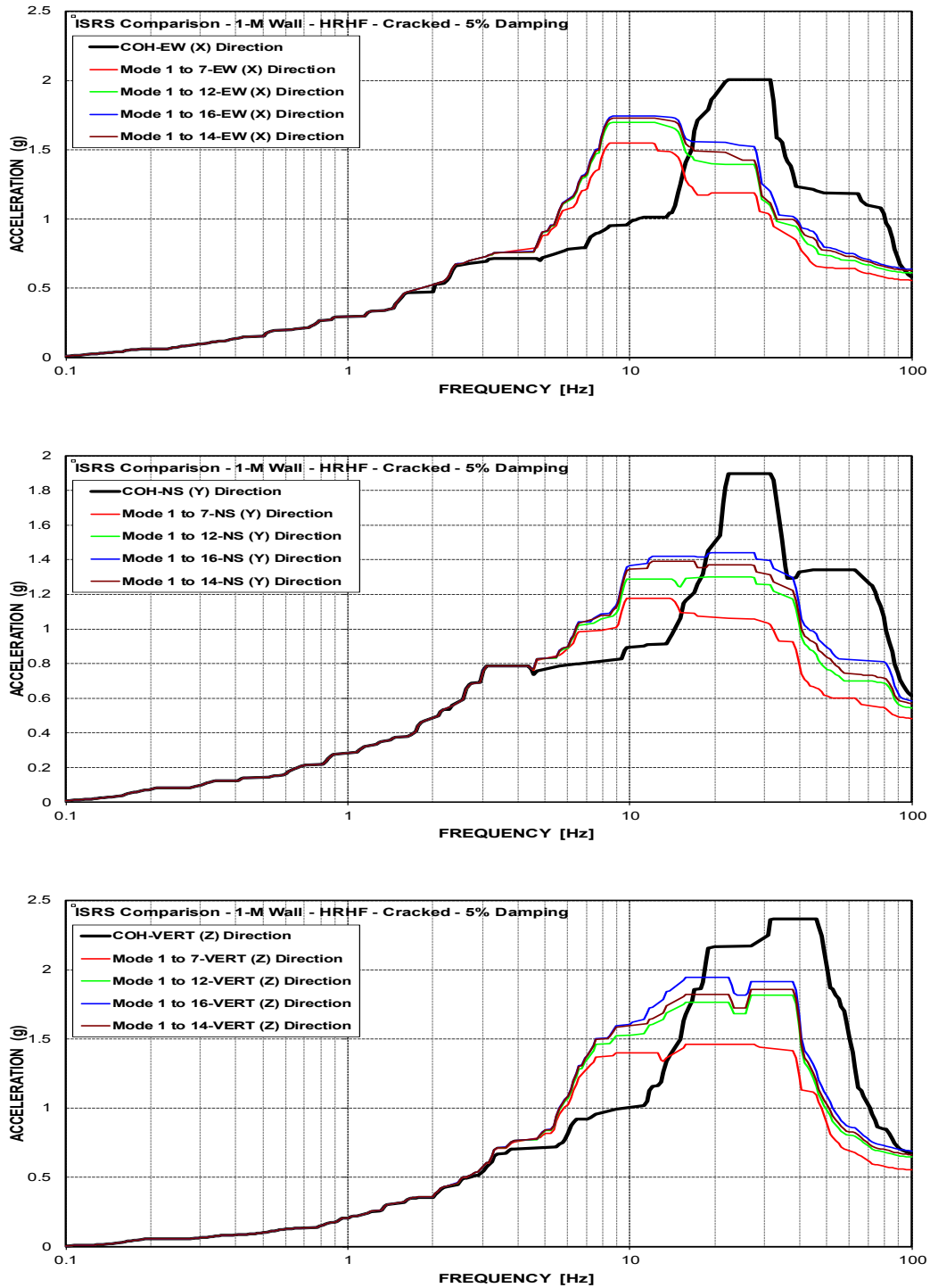


Figure C-260 Mod. Model ISRS– AB Shear Walls (1-M) at El. 68’ – HRHF – Cracked

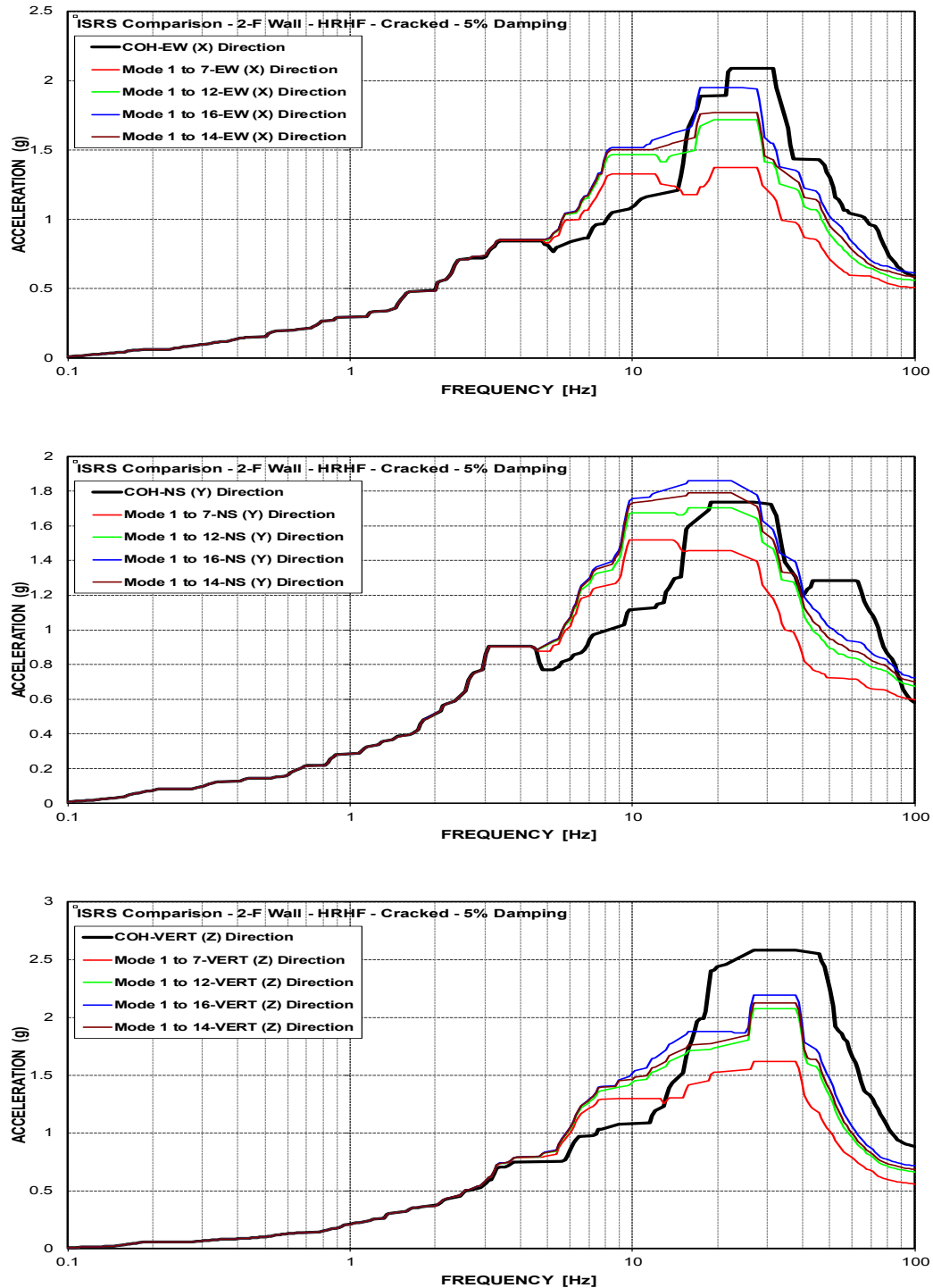


Figure C-261 Mod. Model ISRS- AB Shear Walls (2-F) at El. 78' - HRHF - Cracked

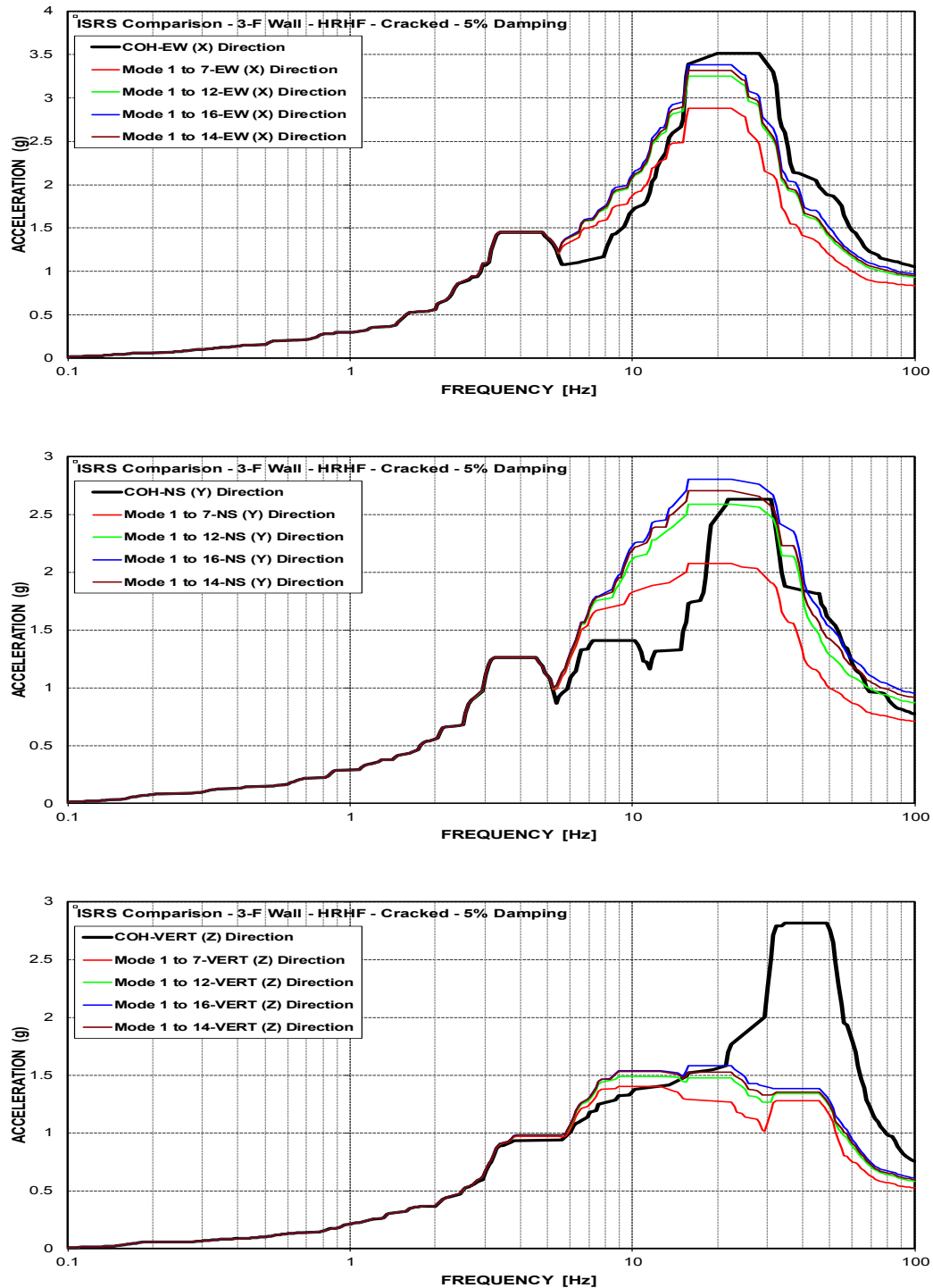


Figure C-262 Mod. Model ISRS- AB Shear Walls (3-F) at El. 100' - HRHF - Cracked

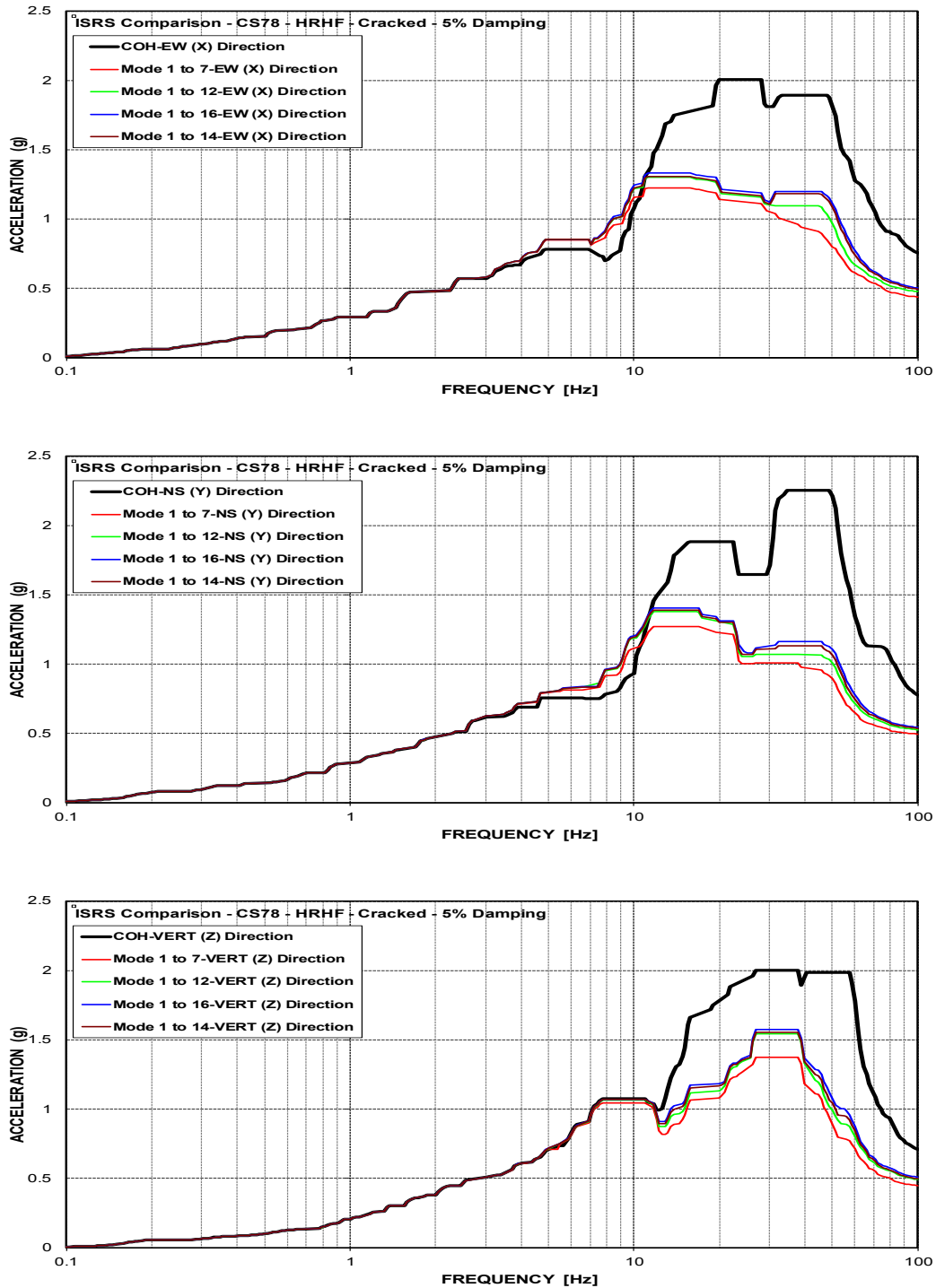


Figure C-263 Mod. Model ISRS– Containment Structure (CS78) at El. 78' – HRHF – Cracked

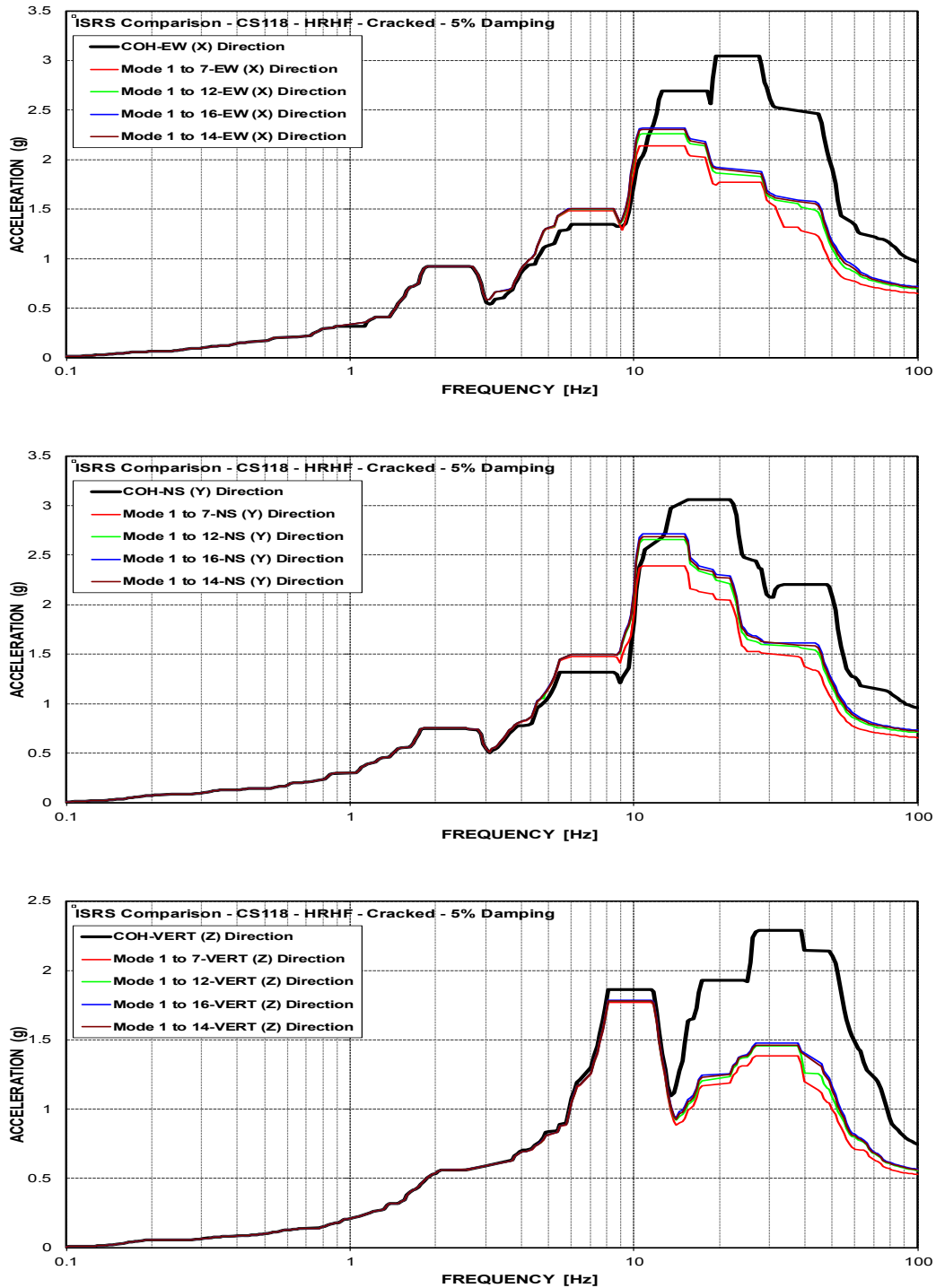


Figure C-264 Mod. Model ISRS– Containment Structure (CS118) at El. 117.75' – HRHF – Cracked



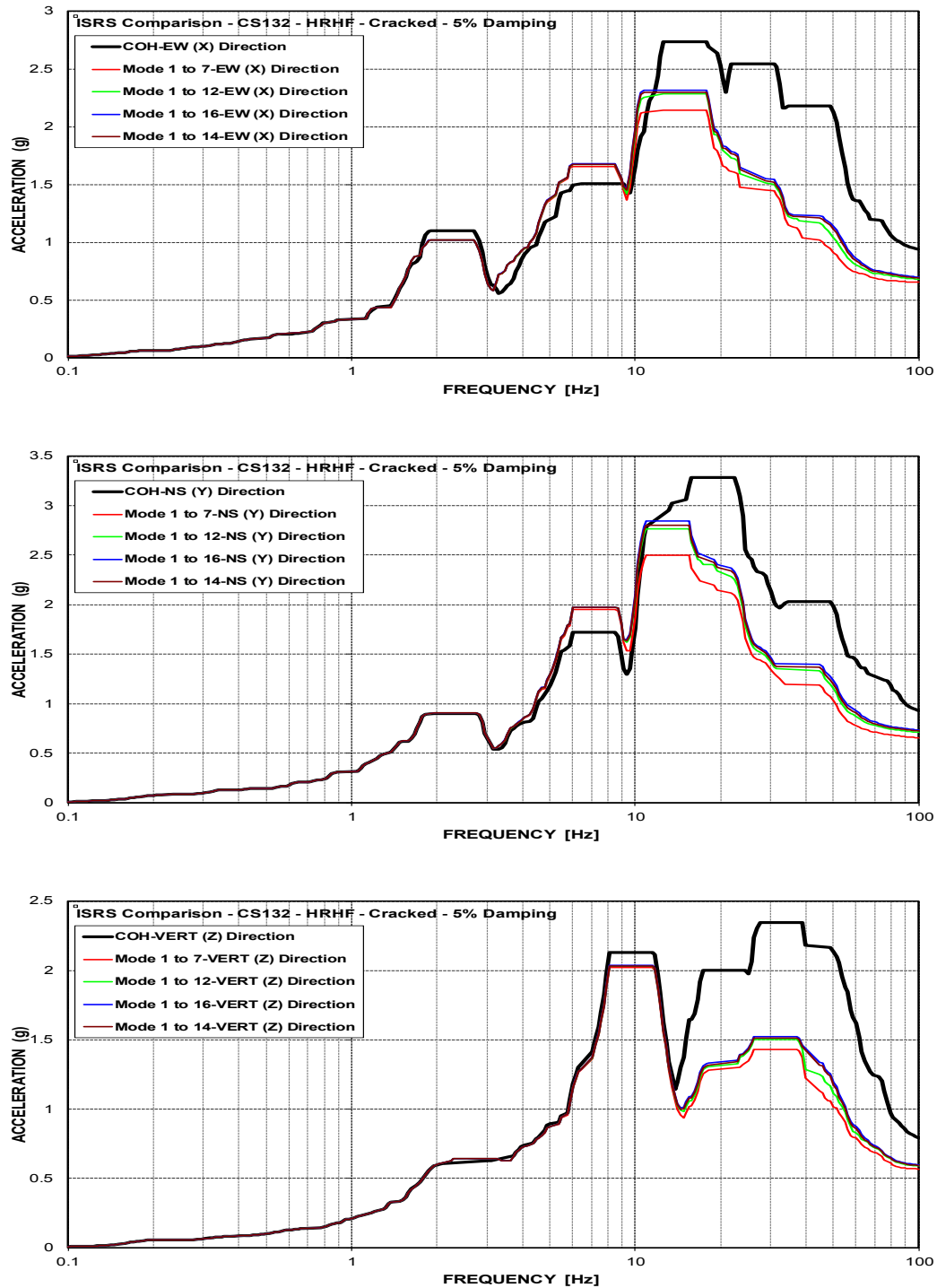


Figure C-265 Mod. Model ISRS– Containment Structure (CS132) at El. 131.56' – HRHF – Cracked

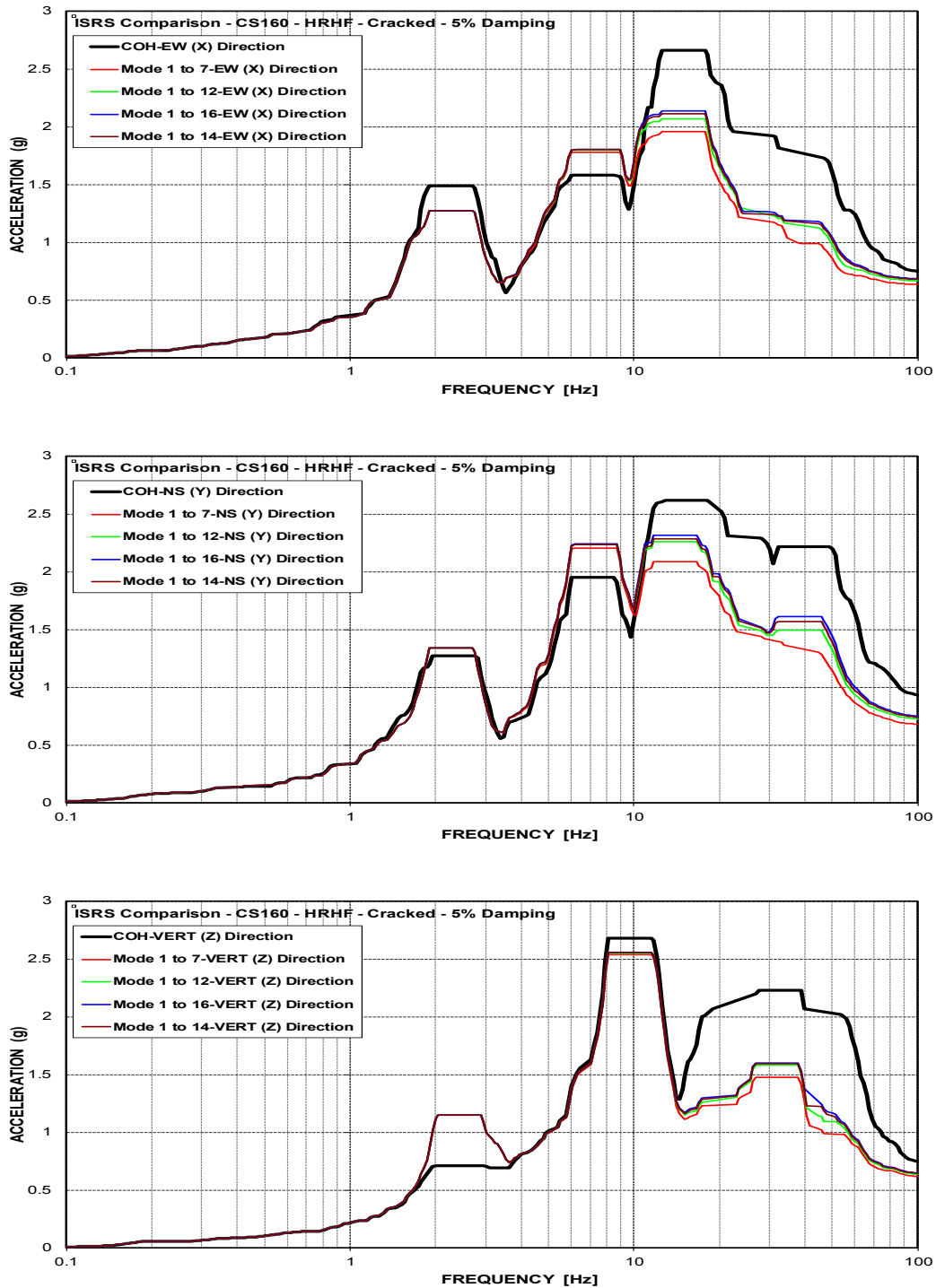


Figure C-266 Mod. Model ISRS– Containment Structure (CS160) at El. 159.75' – HRHF – Cracked

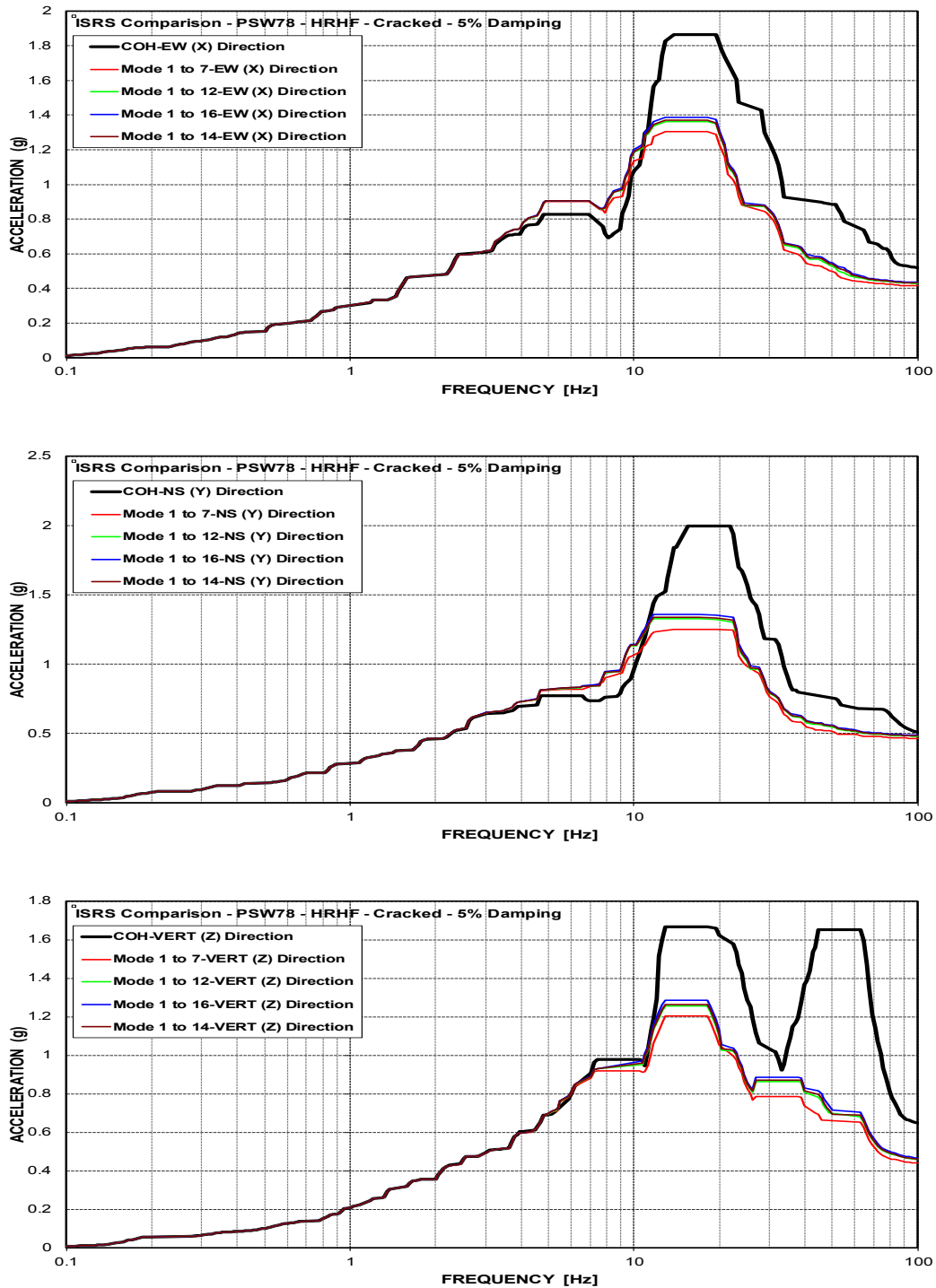


Figure C-267 Mod. Model ISRS– Primary Shield Wall (PSW78) at El. 78' – HRHF – Cracked

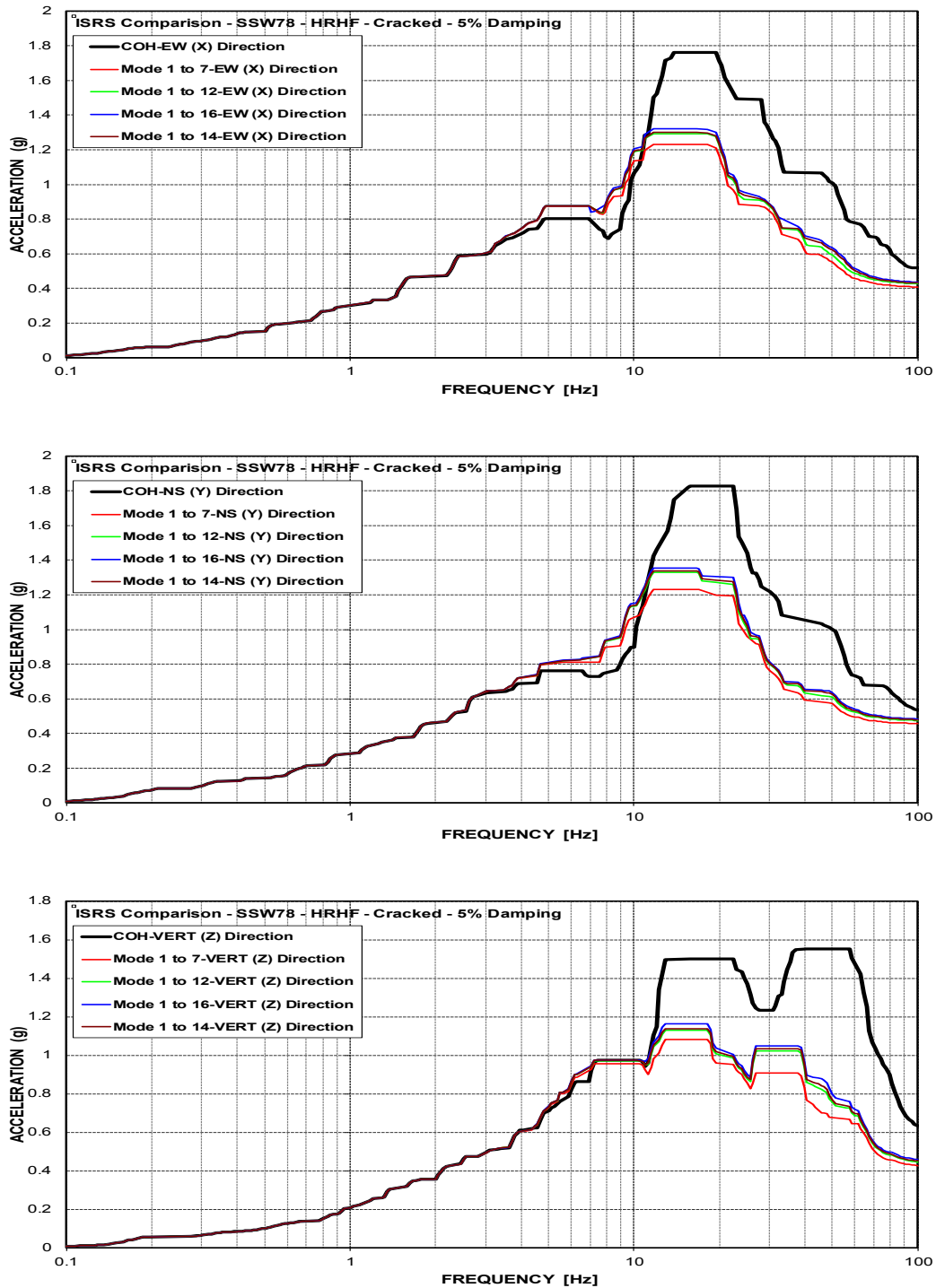


Figure C-268 Mod. Model ISRS– Secondary Shield Wall (SSW78) at El. 78' – HRHF – Cracked

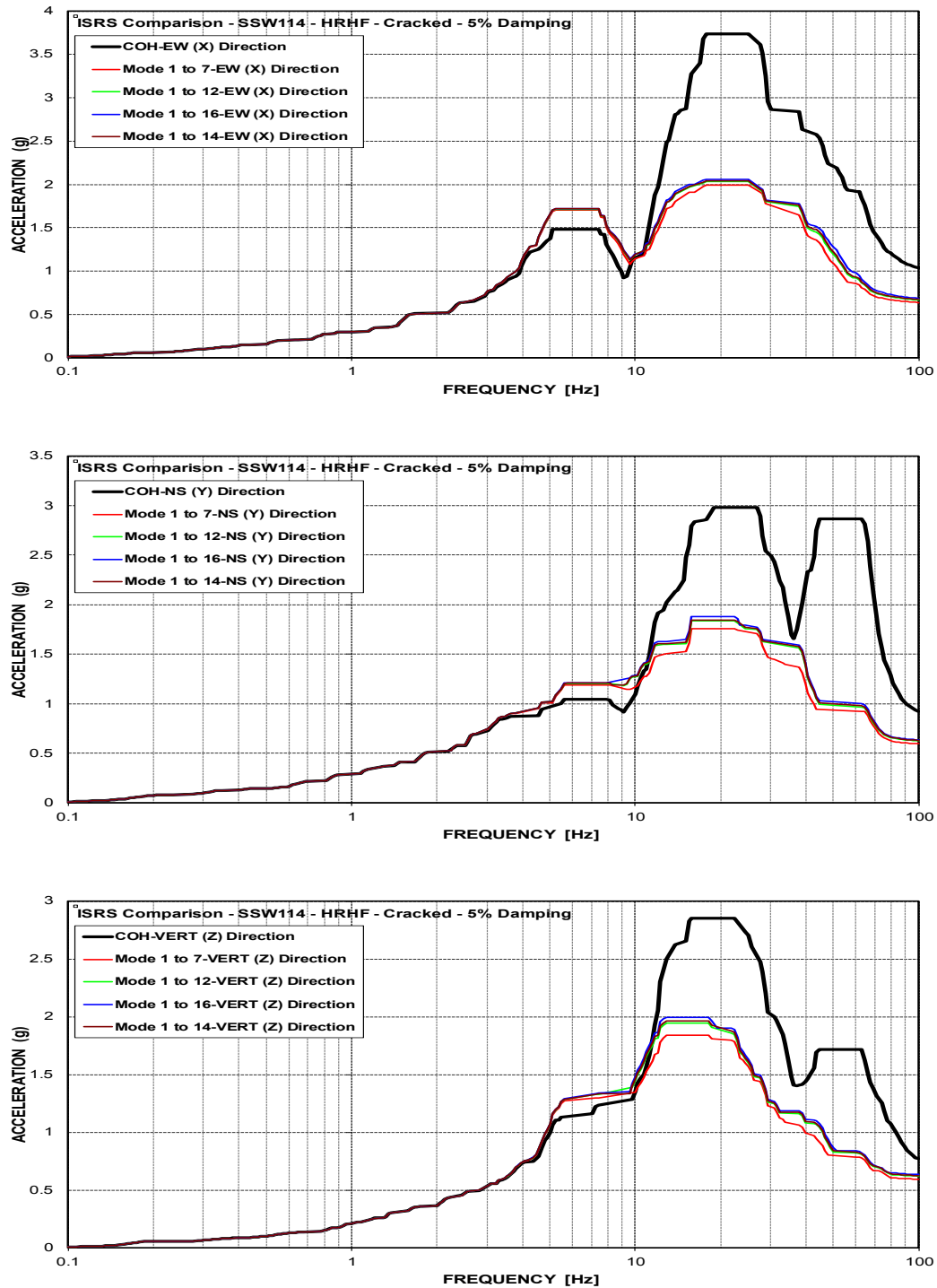


Figure C-269 Mod. Model ISRS– Secondary Shield Wall (SSW114) at El. 114' – HRHF – Cracked

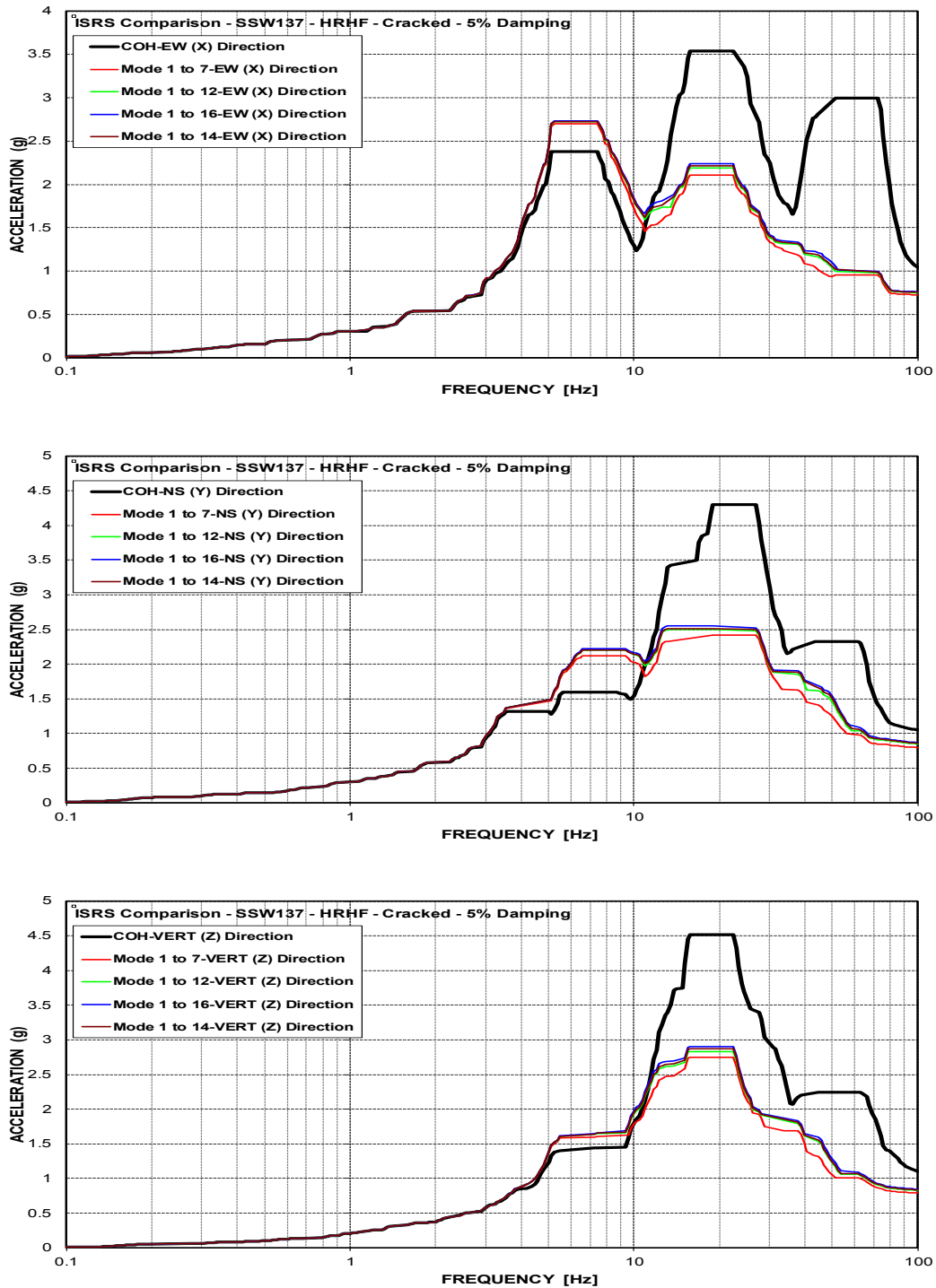


Figure C-270 Mod. Model ISRS– Secondary Shield Wall (SSW137) at El. 136.5’ – HRHF – Cracked

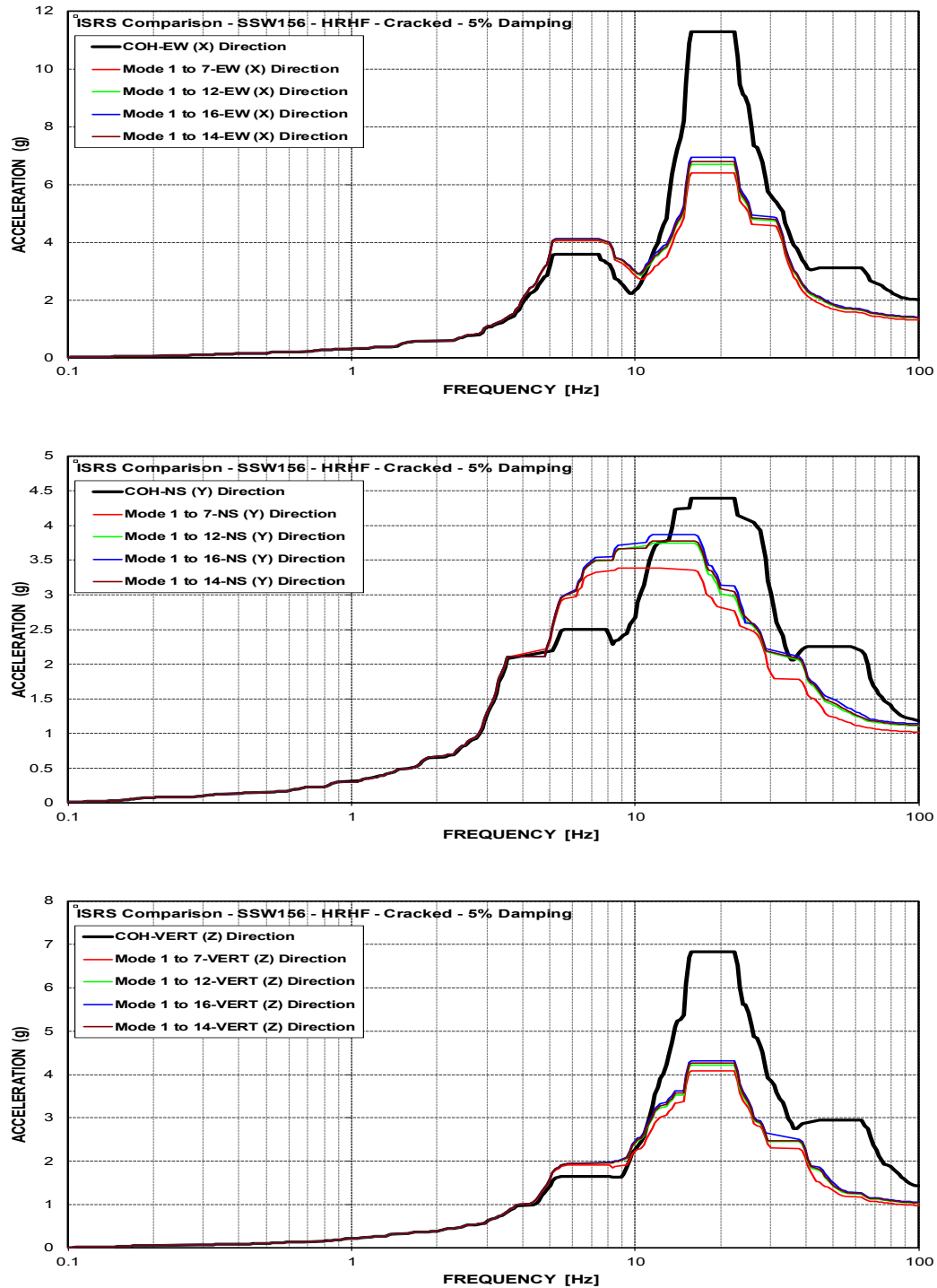


Figure C-271 Mod. Model ISRS– Secondary Shield Wall (SSW156) at El. 156' – HRHF – Cracked

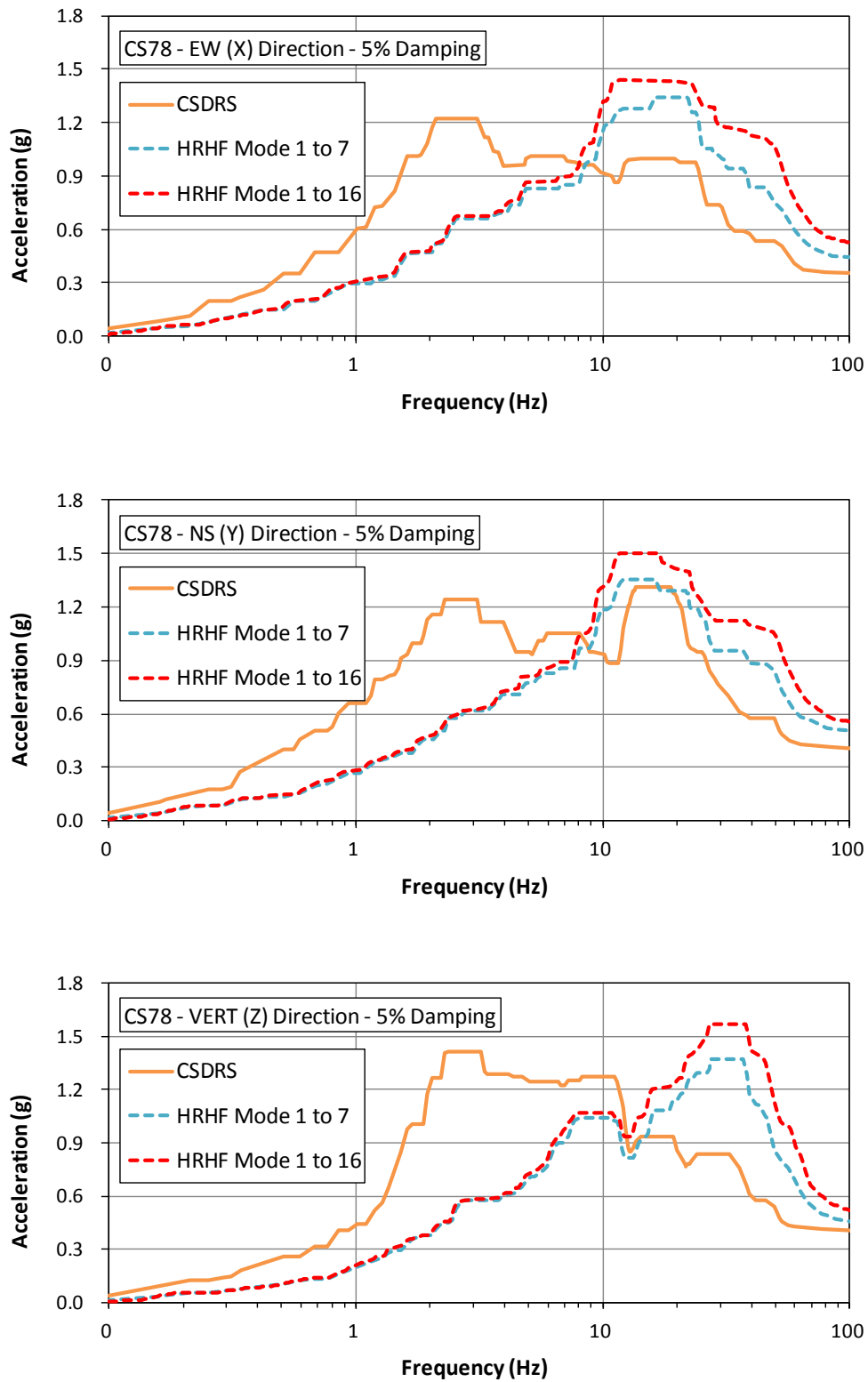


Figure C-272 ISRS Comparison-Containment Structure (CS78) at EL. 78'